AD A091499

# FOREIGN TECHNOLOGY DIVISION

TRANSACTIONS OF THE SECOND ALL-UNION CONFERENCE
ON CHARGED PARTICLE ACCELERATORS

(Moscow, 11-18 November 1970)

Vol. 2

DTIC
SELECTED
NOV 5 1980
C

DDC FILE COPY

80 10 29 101

UNEDITED MACHINE TRANSLATION

FTD-ID(RS)T-0693-80-VOL-2 9 October 1980

MICROFICHE NR: FTD-80-C-001067

TRANSACTIONS OF THE SECOND ALL-UNION CONFERENCE ON CHARGED PARTICLE ACCELERATORS (Moscow, 11-18 November 1970), Vol. 2. Volume 2.

English pages: 1137

Source: Trudy Vtorogo Vsesoyuznogo Soveshchaniya po Uskoritelyam Zaryazhennykh Chastits, Moscow, 1972, pp. 1-282 1972.

Country of origin: USSR
This document is a machine translation
Requester: FTD/TQTD
Approved for public release; distribution unlimited.

TABLE OF CONTENTS

iv

U. S. BOARD ON GEOGRAPHIC NAMES TRANSLITERATION SYSTEM

Block	Italic	Transliteration	Block	Italic	Transliteration
А а	*А а*	A, a	Р р	*Р р*	R, r
Б б	*Б б*	B, b	С с	*С с*	S, s
В в	*В в*	V, v	Т т	*Т т*	T, t
Г г	*Г г*	G, g	У у	*У у*	U, u
Д д	*Д д*	D, d	Ф ф	*Ф ф*	F, f
Е е	*Е е*	Ye, ye; E, e*	Х х	*Х х*	Kh, kh
Ж ж	*Ж ж*	Zh, zh	Ц ц	*Ц ц*	Ts, ts
З з	*З з*	Z, z	Ч ч	*Ч ч*	Ch, ch
И и	*И и*	I, i	Ш ш	*Ш ш*	Sh, sh
Й й	*Й й*	Y, y	Щ щ	*Щ щ*	Shch, shch
К к	*К к*	K, k	Ъ ъ	*Ъ ъ*	"
Л л	*Л л*	L, l	Ы ы	*Ы ы*	Y, y
М м	*М м*	M, m	Ь ь	*Ь ь*	'
Н н	*Н н*	N, n	Э э	*Э э*	E, e
О о	*О о*	O, o	Ю ю	*Ю ю*	Yu, yu
П п	*П п*	P, p	Я я	*Я я*	Ya, ya

*ye initially, after vowels, and after ъ, ь; e elsewhere.
When written as ё in Russian, transliterate as yё or ё.

RUSSIAN AND ENGLISH TRIGONOMETRIC FUNCTIONS

Russian	English	Russian	English	Russian	English
sin	sin	sh	sinh	arc sh	$\sinh^{-1}$
cos	cos	ch	cosh	arc ch	$\cosh^{-1}$
tg	tan	th	tanh	arc th	$\tanh^{-1}$
ctg	cot	cth	coth	arc cth	$\coth^{-1}$
sec	sec	sch	sech	arc sch	sech^{-1}
cosec	csc	csch	csch	arc csch	csch^{-1}

Russian	English
rot	curl
lg	log

ix

TRANSACTIONS OF THE SECOND ALL-UNION CONFERENCE ON CHARGED PARTICLE
ACCELERATORS.

(Moscow, 11-18 November 1970).

Page 2.

Transactions of II All-Union Conference on the charged particle accelerators, Vol. II. Publishing house "science", 1972.

In works of the II All-Union conference on charged particle accelerators are placed the materials, which reflect the contemporary state of theory and of accelerators technique. In Soviet and foreign specialists' reports they are described newest accelerators of different types as well as most important systems and elements/cells of accelerators. The transactions of conference are published in two volumes. The second that are connected questions of particle dynamics, and, in particular, the dynamics of intense beams, radio electronics and radio engineering of accelerators, control of accelerators with the aid of the computers, the transportation of beams and others.

The materials of conference will be useful for specialists, connected with development and operation of charged particle accelerators.

Organizers of conference the Academy of Sciences of the USSR state committee on the use of atomic energy of the USSR.

Responsible editor A. A. Vasil"yev.

Page 3.

From the editor.

To second All-Union Conference on the charged particle accelerators were represented 175 reports, 110 of which were reported at twelve sessions of conference and special seminars.

In the works are published, with some small exceptions, all represented to the conference reports, and also materials of discussion. The transactions of conference are published in two volumes.

Second volume includes reports at the VII-XII sessions of conference.

It is possible to hope that containing in the reports and the discussions useful information will be used by specialists in their daily activity.

A. A. Basil'yev.

Page 4.

Blank.

Page 5.

Session VII.

Particle dynamics in the accelerators, the accumulators~~/storage~~ and
units with ~~clashing~~ *colliding* beams (1).

84. Longitudinal compression of clusters.

I. A. Grishaev, A. N. Dovbnya, V. V. Petrenko.

(Physiotechnical institute of AS UkSSR).

   One of the basic factors, which limit obtaining small energy
spreads in the linear electron accelerators, is the phase width of
the injected cluster. For guaranteeing the energy spreads of beam
$\sim10^{-4}$ it is necessary to create at the output of injector accelerator
clusters with phase sizes/dimensions of $\sim1^\circ$. Obtaining such clusters

is connected with the great difficulties, caused by the action of the forces of space charge in the case of applying klystron type grouping. But if for the formation of short cluster is applied high-frequency punch, then obtaining short clusters is conjugated/combined with the large losses of current.

In this work is proposed the method of the formation of the short clusters, applied also in relativistic region where by the action of space charge with the currents in several amperes it is possible to virtually disregard and, thus, to eliminate limitations to obtaining of supershort clusters. The diagram of method is shown in Fig. 1.

let us examine the case when in HF-separator is propagated with the speed of light the traveling wave with the transverse electric field whose vector lies/rests at the horizontal plane [1, 2]. Then

$$x_c' = \frac{e \delta d}{E} \sin \varphi + x_0' , \qquad (1)$$

$$x_c = \frac{e \delta d^2}{2E} \sin \varphi + x_0' d + x_0 ,$$

where x_0. x_0' - radial- angular characteristics of beam at the entrance into the separator; x_c and x_c' - the same at the output of separator; e - electron charge; δ - amplitude of HF field; φ - phase; d - length of separator and E - energy of particle.

HF-separator creates the relation of the characteristics of beam at the entrance into the solenoid with the phase HF field. After making the appropriate transformations of coordinates of particles [3, 4] and after determining the particle path lengths, it is easy to find expression for the phase on the output of the solenoid:

$$\varphi_{out} = \varphi_{ex} - \frac{\pi s}{\lambda} \left\{ \left(\frac{e\mathcal{E}d}{E}\right)^2 \sin^2\varphi \left[1 + \frac{a^2}{4}\left(\frac{d}{2}+\ell\right)^2\right] + \right.$$

$$+ \frac{e\mathcal{E}d}{E}\left[2x_c' + \left(\frac{a^2 d}{4}+\frac{a^2\ell}{4}\right)(x_0 + x_0'\ell + x_0'd) + ay_0 - ay_0'\left(\frac{d}{2}+\ell\right)\right] +$$

$$+ x_0'^2 + y_0'^2 + \frac{a^2}{4}\left[x_0'^2(\ell+d)^2 + 2x_0'x_0(\ell+d) + x_0^2\right] + \quad (2)$$

$$\left. + a\left[x_e'y_0 - y_0'x_0 - x_0'y_0'(\ell+d)\right]\right\},$$

where s - length of solenoid; λ - wavelength of HF oscillations; $a = \frac{3 \cdot 10^{-4} H}{E}$; H - field of solenoid; ℓ - distance between an HF-separator and the solenoid: y_0 and y_0' - initial characteristics of beam in the vertical plane.

The investigation of this expression shows that the bundle of electrons, after traversing this system, can be reduced. Fig. 2 shows the dependence of the exit phase of particle on the input under the condition: $x_0 = y_0 = 0$, $x_0' = y_0' = 0$, $E = 5$ MeV, $\mathcal{E} = 80$ kV/cm, d=3 cm, λ=10 cm, $\ell = 28$ cm, s=260 cm and H=2000 e. As can be seen from graph/curve, if the beginning of cluster is arranged in region of 20°, then at the output of solenoid its phase width will be about 1° with the initial extent of approximately 50°.

For explaining the "real" picture the process of shortening of cluster with the aid of the specific routine was simulated according to the method of Monte Carlo on computers M-220A. In the parameters: $x_0 = y_0 = \pm 0.1$ cm, $x'_0 = y'_0 = \pm 1.10^{-3}$ rad; $E = 5$ (1+-0.04) MeV; $\delta = 82$ (1+-0.005) kV/cm; $d = 3$ cm; $\lambda = 10$ cm; $\ell = 28$ cm; $s = 260$ cm; $H = 2013$ e and two thousand tests (N=2000) are obtained the following results.
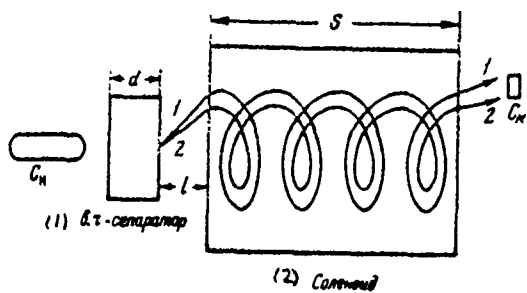
Fig. 1. The diagram of method C_H, C_k - clusters in the initial and in final states; 1 and 2 - particle trajectory, arranged/located respectively in the beginning and at the end of the cluster.

Key: (1). separator. (2). Solenoid.

Page 6.

Fig. 3 gives the histogram of particle distribution according to the phases at the output of solenoid, from which it is evident that into 83o/o of cases the region of exit phases is located in interval of 6°. However, if we consider real particle distributions in the cluster according to the intensity, then the percentage of current in this interval of phases will be still large.

Fig. 4 shows calculated horizontal emittance at the output of the system of phase compression. Since the action of an HF-separator

becomes apparent only into the horizontal of plane, then vertical emittance changes insignificantly. As can be seen from figure, horizontal emittance during the phase compression considerably increases.

The longitudinal compression of cluster can occur also in the fields of another type, for example, in the quadrupole ones, the sector ones, etc. For the quadrupole channel of the type FD with the gradient of 800 Oe/cm and the length of lens 3 cm the solution of the problem of the compression of the cluster was found by simulation in the analog computer MN-7M.

For the beam with the wave energy 5 MeV the dependence of exit phase on the input is shown in Fig. shch. By parameter of the curves is the length of quadrupole channel. From given data it follows that at the length of channel 270 cm and with the appropriate phasing the cluster in initial phase width approximately 45° can be presssed to ~1°.

If for the creation of the required path difference is applied sector magnet, then expression for the phase of particle at the output of the system of compression is represented in the analytical form. And in this case system possesses the property of the compression of cluster similarly how this is obtained in the system

with the solenoid.

The analysis of systems examined here shows that the process of compressing the cluster different factors affect differently. In particular, one group of factors to which they relate the initial geometric characteristics of beam, larger effect exerts to the phase sizes/dimensions; the second group which encompasses energy spread, fluctuations VCh and magnetic field, more greatly it affects the process of changing the effective emittance.

The experimental investigations, conducted from the linear accelerators of PTI of AS UkSSR, showed that the use/application of these methods for obtaining the very short clusters is promising. The decrease of the effective emittance of beam should be, obviously, linked with the search of the systems which would be non-dispersion and at the same time anisochronic.
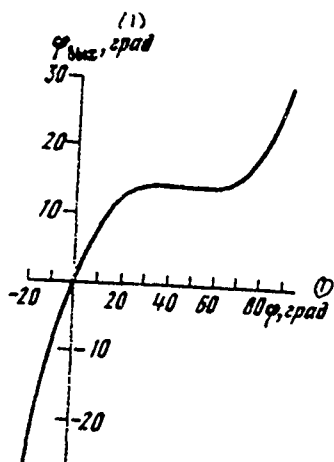
Fig. 2.   Fig. 3.
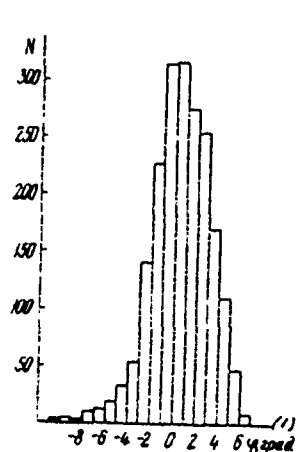
Fig. 2. Dependence of exit phase of particle on input.

Key: (1). deg.

Fig. 3. Particle distribution according to phases.

Key: (1). deg.
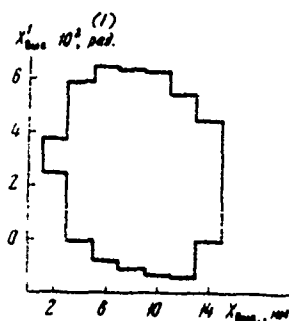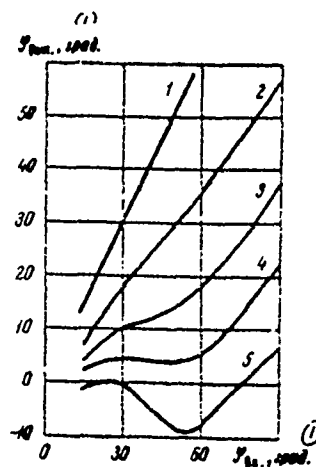
Fig. 4.   Fig. 5.

Fig. 4. Emittance of beam.

Key: (1). rad.

Fig. 5. Phase responses for quadrupole magnetic pipe of length S. 1 -

s=0; 2 - s=120 cm; 3 - s=204 cm; 4 - s=270 cm, 5 - s=360 cm.

Key: (1). deg.

REFERENCES

1. A. A. Bagin, V. I. Kotov, I.V. Semenyushchkin.
    UFN, 1964, 4, 707.

2. V. I. Kotov, V. V. Miller. Focusing and Separation
    by Masses of High-Energy Particles. M., Atomizdat, 1969.

3. J. Hassinski. Nucl. Instrument and Methods, 1967,
    51, N 2, 181.

4. D. Ritson. Experimental Methods in High-Energy Physics.
    M., Izd-vo "Nauka", 1964

Page 7.

85. Use of a high-frequency quadrupole focusing in the linear ion accelerators.

V. A. Teplyakov.

(Institute of high-energy physics).

All contemporary linear accelerators of protons are constructed on the basis of the cylindrical cavity, loaded with the drift tubes, in which are placed magnetic quadrupole lenses. Accelerators of this type are well investigated and structurally/constructurally finished. The attempts to use the focusing of protons by accelerating field in cylindrical cavity [1-4] were not crowned by success, and, possibly ; therefore to the development of accelerators with the focusing by accelerating field it was not given proper attention. However, the diverse variants of focusing by high-frequency field in the accelerating systems with the use of H-resonators are of doubtless practical interest. Therefore, examining in the report only one of the versions of focusing by the accelerating field: focusing by HF quadrupole field, it is necessary to dwell also on the special features/peculiarities of H-resonators as the structural/design basis

of accelerator.

1. Single clearance.

In the description of interaction of ions with HF field of one accelerating gap it is convenient to use the expansion of scalar potential in the series/row in the eigenfunctions of cylindrical coordinate system. During this resolution in the linear approximation/approach by essential ones for interaction prove to be only two components of the field: axially symmetrical and quadrupole. Since a change in the speed of ion in one clearance is small, from the resolution of these components of field in the series/row in terms of z (Z-axis coincides with the axis/axle of accelerator) it suffices to hold down/retain only one harmonic. Thus, for describing that part of the field with which the ion effectively interacts, it suffices to introduce three parameters:

$$u = \frac{2\vartheta U}{\pi} \cos \omega t \left\{ -I_0\left(\frac{k_1 z}{\delta}\right) \sin k_1 z + \cos 2\psi I_2\left(\frac{k_1 z}{\delta}\right) \times \right.$$
$$\left. \times (\sigma' \sin k_1 z + \sigma'' \cos k_1 z) \right\}. \tag{1}$$

Here u - scalar potential; $k_1 z = \frac{2\pi}{\beta\lambda} z$; λ - wavelength; z, ϕ, x - cylindrical coordinate system; $\vartheta, \sigma', \sigma''$ - parameters of clearance.

Time t_0 of passage by the particle of the center of clearance determines the phase of particle $\varphi = -\omega t_0$.

A change in the energy of particle on one clearance is determined by the axisymmetric component

$$\Delta \gamma = \frac{\vartheta U}{\xi} \cos \varphi, \qquad \left(\xi = \frac{\mu_0 c^2}{e} \right). \qquad (2)$$

The parameter ϑ we will call the effectiveness of interaction of particle with the field. A change in the transverse particle momentum is determined by the axially symmetrical, and quadrupole components of the field:

$$\Delta \left(\frac{\dot{x}}{c} \right) = \frac{\pi \vartheta U}{2 N \lambda \beta^2 \gamma^3 \xi} (\sin \varphi \pm \sigma) \approx \frac{\pi \Delta W}{4 N \lambda W} (\sin \varphi \pm \sigma). \quad (3)$$

Here N - multiplicity of the period of acceleration, value, reciprocal to the number of clearances to $\beta \lambda$; $\sigma = \sigma' \sin \varphi + \sigma'' \cos \varphi$ - "quadrupole nature " of clearance.

2. Versions of HF focusings.

It is possible to construct different types of alternating-gradients focusing by accelerating field. In the first half-period of the focusing

$$N \lambda \Delta \left(\frac{\dot{x}}{c} \right) = \eta + \zeta, \qquad (4)$$

but the second

$$N \lambda \Delta \left(\frac{\dot{x}}{c} \right) = \eta - \zeta, \qquad (4b)$$

where η and ζ let us name/call the parameters of focusing.

If it is afterward axially symmetrical, and the phase of particles in the adjacent clearances is determined by expression $\gamma = \dot{\gamma} \pm \theta$, then the parameters of this alternating-phase focusing [2, 5] are equal to:

$$\eta = \frac{\pi N \Delta W}{4W} \sin \varphi' \cos \theta,$$

$$\zeta = \frac{\pi N \Delta W}{4W} \cos \varphi' \sin \theta. \tag{5}$$

With the focusing by HF quadrupole field, if in the adjacent clearances changes only sign φ (FD- focusing), then

$$\eta = \frac{\pi N \Delta W}{4W} \sin \varphi,$$

$$\zeta = \frac{\pi N \Delta W}{4W} (\theta' \sin \varphi + \theta'' \cos \varphi). \tag{6}$$

Focusing by HF field can have more complicated structure, if in the adjacent half-periods changes both the phase of synchronous particle and quadrupole nature of clearances.

3. Fundamental principles.

As for any alternating-gradient focusing, for the focusing by accelerating field there is a zone of stability. Fig. 1 gives the typical diagram of the zone of stability with the plotted/applied on

it lines of permanent phase change of transverse vibrations in the period of focusing (μ) and the lines of minimum frequency (ν - frequency of transverse vibrations to scale of the time of flight of one period of focusing).

From (5) and (6) it is evident that in the process of longitudinal (phase) oscillations the states of particles on the diagram of stability remain in the cut of the ellipse (see Fig. 1).

Page 8.

(With the focusing with the magnetic quadrupole lenses of the state of particles they move over the segment of line, parallel axis of abscissas). Parametric connection/communication of transverse motion with the longitudinal leads to an increase in the emittance of beam [6]. If beam is matched with the channel, all particles of the accelerated cluster are not distinguished on phase change μ, and a change in frequency ν occurs adiabatically slowly, then the emittance of beam will remain constant/invariable. Focusing by HF quadrupole field (6) makes it possible to create conditions with which the emittance of beam will remain almost constant/invariable.

Willows (5) and (6) it is evident that parameter of defocusing η - the low value, proportional to a relative change in the energy

of ion on the clearance. The parameter of focusing ζ, as this follows from the diagram of the stability Fig. 1, must be 5-10 times more. This means that the amplitude of quadrupole component must be in so many once of more than the amplitude of axially symmetrical component.

It is possible to show that the maximum strength of field according to (1) within the cylinder of radius R_a is equal to maximum radial component of the strength of field. Therefore the maximum intensity/strength of the field

$$E_{max} \geqslant \frac{\pi \xi \delta}{\lambda^2} \frac{\Delta W}{W} R_a \left(2 + \delta_{max}\right). \qquad (7)$$

The maximum strength of field on the surface of real electrodes with a radius of aperture of R_a can several times exceed estimation (7).

If we consider that there is a certain maximum strength of field with which it is possible to virtually work, then dependence (7) sets limitation on a radius of aperture and the permissible change in the energy on one clearance. Numerical estimation according to (7) shows that the focusing by HF quadrupole field is in principle attained. It is necessary to only find the structurally/constructurally acceptable electrodes, the strength of field on surface of which it would not strongly exceed estimation according to (7).

A possible large change in the energy per the unit of length
does not succeed in realizing in the cylindrical cavity, since in it
the significant part of the path particle must fly in the drift,
without interacting with accelerating field. So that would increase
the rate of acceleration, it is necessary to increase a number of
clearances on the cutting off $\beta\lambda$. This can be made in the resonators,
in which phase displacement of voltages in the adjacent clearances
less or is equal to π, for example, in H-resonators. Only in such
cases in which the particle interacts with HF field on entire path in
the accelerator, it is possible to attain the high rate of
acceleration and large capacity of the focusing channel.
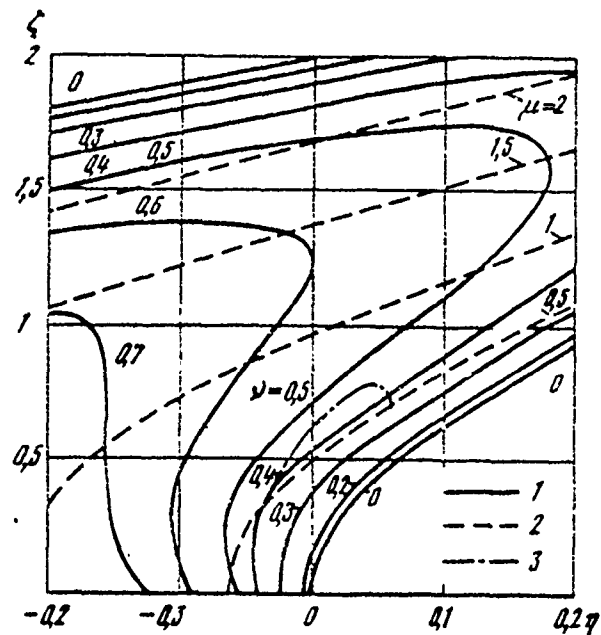
Fig. 1. Diagram of the zone of stability. 1 - ν=const; 2 - μ=const; 3 - curve of state of particles.

4. Electrodes.

By the simplest version of the electrodes by which are created the necessary components of field, are drift tubes with the channel of rectangular cross section [3, 4] (Fig. 1$\overset{a}{k}$, b). These electrodes can be used in the accelerators with the low current and the low speed of ions. They are of doubtless interest in the accelerator with the combined focusing: alternating-phase and by HF quadrupole [8].

Electrodes with the "horns" [1, 9] (Fig. 2c) make it possible to

obtain the quadrupole component of field with the smaller strength of field on surface of electrodes. These electrodes can be applied to the higher speeds of ions, with them is reached the higher linearity of the strength of field on a radius.

$$\rho = \frac{\sin \kappa_1 \theta}{\kappa_1 \theta I_0(\kappa_1 R_{ca})}$$

$$\delta' = 0$$
$$\delta'' = \mathrm{ctg}\,\kappa_1 \theta$$

$$\rho = \frac{\sin \kappa_1 \theta \cdot \cos \kappa_1 l}{\kappa_1 \theta \cdot I_0(\kappa_1 R_0/\gamma)}$$

$$\delta' = 0$$

$$\delta'' = \frac{I_0(\kappa_1 R_0/\gamma)}{2 I_2(\kappa_1 R_0/\gamma)} \mathrm{tg}\,\kappa_1 l$$
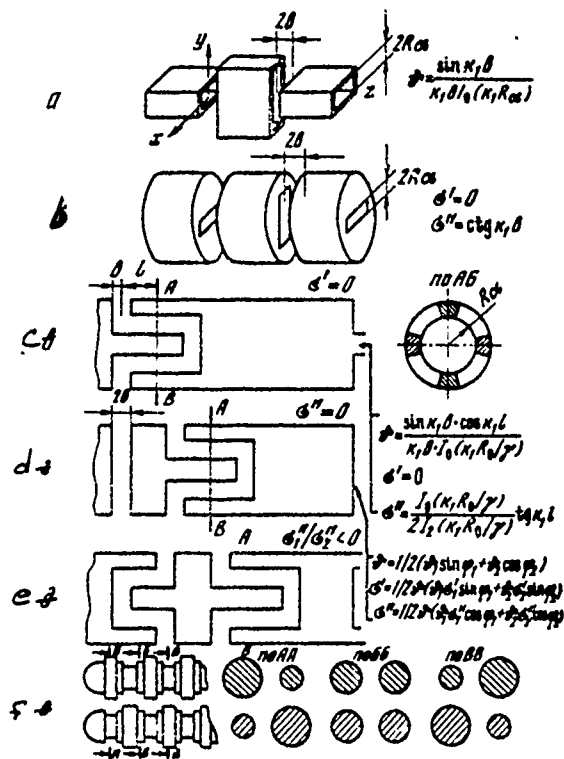
Fig. 2. Forms of electrodes. a, b) with the rectangular channel; c) electrodes with the "horns"; d, e) dual clearance; f) four-wire line.

Page 9.

Both electrodes with the channel of rectangular cross section and electrodes with the "horns" possess the specific symmetry in z relative to the center of clearance; therefore they do not make it possible to obtain necessary phase displacement between the axially symmetrical and quadrupole components. If we introduce in the

clearances supplementary electrode with the intermediate potential (Fig. 2d, e), then will be obtained so-called dual clearance [9]. It it is easy to make asymmetric relative to electrical center and to attain the necessary phasing of the focusing component of field furthermore, in the dual clearance even more greatly descends the strength of field on the surface of electrodes.

Specifically, dual clearance makes it possible to realize the major advantages of focusing by accelerating field.

If synchronous phase lies/rests at interval $20° < \psi_c < 37°$, then in the optimum version of dual clearance the first half clearance is axially symmetrical (Fig. 2d) [7].

At the low speeds of ions and in large synchronous phase $\psi_c > 37°$ the fields of separate clearances near the axis/axle overlap. In the case of a FD-focusing in the resolution of the scalar potential by which is described the field of many clearances, fundamental component of quadrupole component does not depend on z. A field with the scalar potential

$$u = \vartheta U \cos \omega t \left\{ -\frac{2}{\pi} I_0 \left(\frac{k_1 \gamma}{\gamma}\right) \sin k_1 z + \frac{k_1^2}{8} \vartheta'' z^2 \cos 2\psi \right\} \quad (8)$$

can be utilized for focusing and accelerating the beam in the initial part of accelerator [10, 11]. The electrodes, with the aid of which

is created potential (8), are given in Fig. 2f. They form the
four-wire line whose adjacent conductors have a potential difference
+-Ucosωt. Each of the conductors of line is body of revolution with
the radius of envelope, which depends on longitudinal coordinate.
This version of the focusing electrodes makes it possible to begin
acceleration from the very low speeds of ions, since the focusing
properties of uniform along the length of HF quadrupole field depend
neither on the phase nor on the speed of ion. The parameters of
focusing in this case

$$\eta = \frac{\pi \dot{\theta} U}{4 f^{\sim t}} \sin\varphi, \qquad \zeta = \frac{U}{4\pi\xi} \left(\frac{\lambda}{R_\bullet}\right)^2, \qquad (9)$$

where R_0 - average distance from the axis/axle to the nearest point
of electrode.

5. Initial part of accelerator.

A reduction in the energy of injection into the linear
accelerator without the decrease of the intensity of beam is possible
only with a substantial change of the operating mode in the initial
part of the accelerator (NChU). So that the high charge density in
the clusters would not lead to the limitation of the accelerated
current, the sizes/dimensions of cluster (its length and radius) must
remain constant/invariable. The invariability of the length of
cluster is provided with satisfaction of three conditions:

1) is retained along the length the frequency of the small longitudinal oscillations:

$$\Omega_q^2 = \frac{\vartheta U \sin\varphi_c}{\beta^2 \gamma^3 \xi} = \frac{\Delta W}{2W} \sin\varphi_c = \text{const}; \qquad (10)$$

2) is retained the extent of stability region, which occurs, if

$$\beta_c \, tg \, \frac{\varphi_c}{2} = \text{const}; \qquad (11)$$

3) the states of particles at the input of NChU evenly fill entire stability region of axial motion, which to a certain degree is provided with the aid of high-frequency demonochromator of beam.

The motion of synchronous particle in NChГ is described by the equalities

$$\Omega_q^2 ct = \lambda \ln\left(\frac{1+\sin\varphi_0}{\cos\varphi_0} \frac{\cos\varphi_c}{1+\sin\varphi_c}\right);$$

$$\mathcal{z} = \frac{\lambda}{2} \beta_c tg \frac{\varphi_c}{2} \left\{\frac{1}{\Omega_q^2} \ln\frac{\cos\varphi_c(1-\cos\varphi_0)}{\cos\varphi_0(1-\cos\varphi_c)} + \frac{2}{\pi} \ln\frac{\sin\frac{\varphi_c}{2}}{\sin\frac{\varphi_0}{2}}\right\}. \qquad (12)$$

Here φ_0 – synchronous phase at the input of NChU; $\mathcal{z}$ – longitudinal coordinate of the center of clearance.

Acceleration in NChU begins from the synchronous phases, close to 90°. Therefore upon the acceleration of feeble beams the

coefficient of capture is close to 100o/o.

The emittance of beam in NChU grows/rises, but this does not lead to the loss of particles.

6. H-resonator.

The structural basis of linear accelerator with HF focusing compose different modifications of a H-resonator. An H-resonator we named/called [12] such cavity resonators, in which is excited uniform along the length magnetic flux with the vector of magnetic intensity, parallel to the axis/axle of accelerator. The simplest version of an H-resonator is given in Fig. 3. It is the single turn from the very wide strip/film, placed into the screen. Maximum HF voltage acts on the slot of turn. It does not depend on longitudinal coordinates. Accelerating electrodes alternately are connected up first to one, then to another end/lead of the turn they distort the form of field in the manner that this is necessary for the creation by that focusing and that accelerating component.
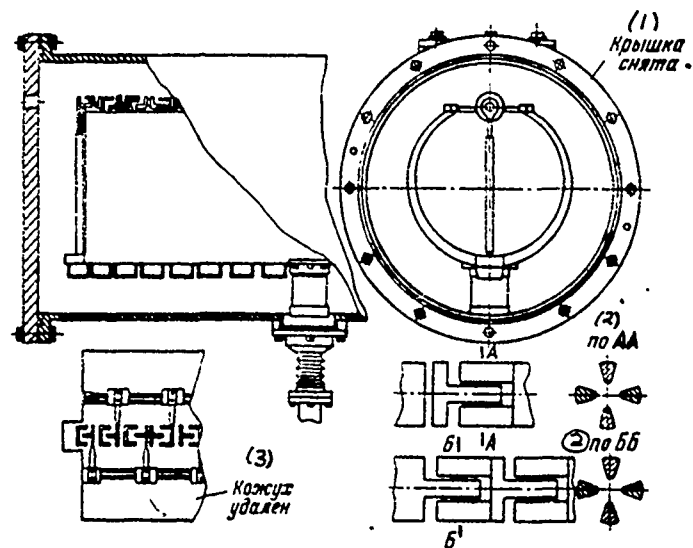
Fig. 3. An H-resonator. Key: (1). Cover/cap is taken/removed. (2). on. (3). Housing removed.

Page 10.

Dynodes are fastened to the legs which intersect turn according to its diameter.

The working wavelength of an H-resonator in essence is determined by an inside radius of turn R_1

$$\lambda = 2\pi R_1 \sqrt{1 - \ell n \frac{\delta_p}{R_1}} \sqrt{1 + \frac{C_g}{C_{u\mu}}}. \qquad (13)$$

Here $2\delta_p$ - width of slot in the turn; C_g - capacity/capacitance,

created by drift tubes; $C_\text{ш}$ - shunt capacity/capacitance of the equivalent diagram of the resonator

$$C_\text{ш} = 1{,}15 \frac{\varepsilon z_p}{\pi} \left\{ \frac{1}{4} + \frac{1}{(k_1 R_1)^2} \right\}. \qquad (14)$$

Shunt resistance of the equivalent diagram of the resonator

$$R_\text{ш} > \frac{1800 \pi^2 (k_1 R_1)^3}{R_\text{s} \left[1 + 2 \left(\frac{R_1}{R_2} \right) \right]} \frac{\lambda}{z_p}, \qquad (15)$$

where z_p - length of resonator; R_s - specific surface/skin ohmage. For copper $R_\text{s} = 0{,}047 \overline{\lambda}^{1/2}$, where λ - wavelength in cm, $2R_2$ - diameter of screen. Usually $R_1/R_2 = 0.6$.

In comparison with the cylindrical cavity, which works on the same wave and with the same linear acceleration, an H-resonator is 3-4 times less in the diameter, in it it reserves itself almost by an order less HF energy, and power loss in copper approximately/exemplarily the same; therefore an H-resonator does not allow/assume large capacitive load and in practice does not make it possible to produce the acceleration of ions with the use of stored energy.

In the well adjusted H-resonator the adjacent in the frequency types of oscillations are sufficiently distant from the basis; therefore the washing of resonator it does not cause any difficulties. The construction/design of an H-resonator makes it

possible to easily suppress HF resonance electronic load by the method of feed to the turn of bias voltage relative to container.

Small transverse sizes/dimensions, simplicity and manufacturability of the entire accelerating system - basic advantages of an H-resonator.

As has already been spoken, for the acceleration and the focusing in NChU is applied a heterogeneous along the length four-wire line, which represents too great a capacitive load for an H-resonator. Therefore in NChU is applied four-chamber resonator [10], which reminds by itself the greatly extended in length resonator of four-chamber magnetron or dual H-resonator.

Dual H-resonator (Fig. 4) consists of the the external of a duct-screen and two ducts with the section/cut on the generatrix, inserted in it. Ducts with the section/cut it is the resounding turns. Magnetic flux in them is cophasal. Capacitive load create electrodes "four-wire lines" (Fig. 2f).

As the illustration of the possibilities of focusing by HF quadrupole field let us give the possible parameters of the linear accelerator of protons [13]:

Energy of injection..... 100 keV.

Output energy .... 30 keV.

Length of accelerator..... 30 m.

Diameter of vacuum container..... 41 cm.

Wavelength..... 2 m.

Normalized acceptance..... 1.6-3 mrad cm.

HF loss in copper of resonator..... 2.3 MW.

Current protons per pulse..... 250 mA.

The use/application of a focusing by HF quadrupole field is possible not only in the accelerator of protons, but also in the accelerator of polyvalent ions.
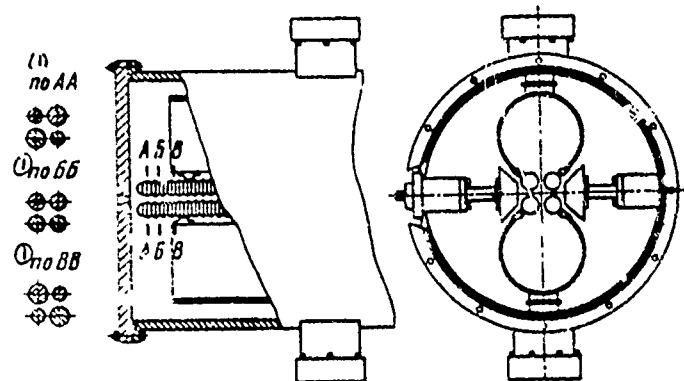
Fig. 4. Dual H-resonator.

Key: (1). on.

REFERENCES

1. V. V. Vladimirskiy. PTE, 1956, No 3, 35.
2. Ya. B. Faynberg, ZHTF, 1959, 29, No 5, 568.
3. D. V. Karetnikov, Linear Ion Accelerators,
   M., Atomizdat, 1962; G. M. Anisimov,
   V. A. Teplyakov. PTE, 1963, no 1, 21.
4. F. Fer dr. International Conference on
   Accelerators. Dubna, 1963, M., Atomizdat,
   1964. str. 513.
5. O. A. Bal'dner, A. D. Blasov, A. V. Shal'nov,
   Linear Accelerators, M., Atomizdat, 1969.
6. V. A. Teplyakov. Preprint IFVE, INZH 69-60,
   Serpukhov, 1969.
7. A. P. Mal'tsev, S. M. Yermakov, V. A. Teplyakov.
   Atomic Energiya, 1967, 23, no 3, 195.
8. A. P. Mal'tsev, E. A. Zotova, V. A. Teplyakov.
   PTE, 1964, no 4, 20.
9. V. A. Teplyakov. PTE, 1964, no 6, 24.
10. I. A. Kapchinskiy, V. A. Teplyakov. Preprint,
    ITEF, No 673, M., 1969.
11. I. A. Kapchinskiy, V. A. Teplyakov. Preprint.
    ITEF, INZH 69-48, Serpukhov, 1969.
12. V. A. Teplyakov, V. B. Stepanov,
    "Radiotekhnika and Elektronika", 1968, 13, No 11, 1965.
13. I. M. Kapchinskiy, A. P. Mal'tsev, V. A. Teplyakov.
    Proceeding of 7th International Conference on
    High-Energy Charged - Particle Accelerators, Vol I.
    Yerevan, Izd-vo AN Arm. SSR, 1970, STR 153.

Page 11.

Discussion.

K. Reich. Is planned/glided the use of a high-frequency quadrupole
focusing in the acting or projected/designed accelerators?

V. A. Teplyakov. Now we study in the mock-ups all necessary technical
and technological questions and carry out first experiment in
acceleration. After accelerator with HF quadrupole focusing will be

investigated under laboratory conditions, it will be possible to examine a question about use and use/application of this form of accelerators.

A. N. Didenko. Was not examined focusing by the high-frequency fields of higher order?

V. A. Teplyakov. If I correctly understood a question, then he requests herself, was not examined focusing by the fields of more high degree of symmetry relative to transverse axes. Such fields are proportional to a radius to the appropriate degree, and the potential of field has components the proportional ones of the 6th and 8th degree of a radius. These fields are very small, in any case they will not have the term, linear on a radius. This means that the beam will complete nonlinear transverse vibrations. We such fields did not in detail examine, considering it their small.

B. I. Polyakov. To what energies it is expedient to utilize HF quadrupole focusing?

V. A. Teplyazhov. HF focusing by quadrupole field can be used to any energies, here there are no limitations. A question can be raised otherwise: it is expedient whether to apply H-resonators to the very high energies? At high energies to more expediently utilize the

resonators, which work on $\pi/2$ - to wave for the purpose of eliminating the sections of the drift where particle does not interact with the high-frequency field.

V. K. Baev. How does differ the rate of acceleration in the accelerator about which you did report, from the rate the accelerations in the accelerators in operation?

V. A. Teplyakov. In that project which we reported at the Yerevan conference, the rate of acceleration was selected by the same as in the linear accelerator (of Alvarez's type) in Serpukhov.

Yu. D. Beznogikh. In the accelerator of Alvarez-Blyuett is assigned sufficiently stringent requirement for the stability of the magnetic focusing fields. In your system the transverse focusing field works over a wide range of values. As you show, this situation does not lead to an increase in the emittance of beam. It is not possible whether in connection with this to lower requirement for stability of focusing fields in the accelerator of Alvarez-Blyuett?

V. A. Teplyakov. I enumerated conditions, with which the emittance of beam will not grow/rise. These conditions are reduced to remove parametric connection/communication between the motion in the transverse direction and the motion lengthwise. This

connection/communication in the first approximation, does not depend
on the amplitude of the focusing high-frequency field. As far as
lenses are concerned magnetic quadrupole, then there such a
connection/communication unavoidably exists, because the line of the
state of particles on the diagram of stability compulsorily the
secants of equal phase change of transverse vibrations, i.e.,
different in the phase particles have different phase change of
transverse vibrations. This effect is significant only at the very
beginning of accelerator. Further phase oscillations strongly
attenuate, and parametric connection/communication of transverse and
axial motion decreases. If changes the amplitude of HF field, then it
decreases synchronous phase and capture region, and all particles of
cluster, although will complete the smaller longitudinal
oscillations, they will be as before located near the line of
permanent phase change. However, channel capacity with the reduction
of the amplitude of HF field somewhat decreases. Therefore with the
reduction of the amplitude of HF field we can lose the part of the
particles either due to the longitudinal or due to the transverse
motion, but not due to the increase of phase volume.

G. Kumpfert. Is there in the method of focusing about which you did
tell, the limitations, connected with the high currents (beam load,
connection/communication of longitudinal and transverse vibrations,
Coulomb limit)?

V. A. Taplyakov. Are prescribed/assigned two questions: about the
beam load and about connection/communication of longitudinal and
transverse motion in the presence of large space charge in the beam.
As far as beam load is concerned, then the resonators with low stored
energy, which it is proposed to utilize for the realization of
focusing HF accelerating field, actually/really they do not make it
possible to produce acceleration on the stored energy. For an example
I will give these numbers: the losses of HF power in the small
resonator are 30 kW. Accelerated in this resonator to the energy 2
MeV beam with current on the order of 1 mA consumes 20 kW. For
accelerating the beam in several ten or hundreds of milliamperes it
is necessary to introduce additionally power. Therefore HF generator
must feed the power, sufficient for accelerating the beam.

With the large space charge certainly will arise the additional
constraint of transverse motion with the longitudinal. It is most
dangerous in the initial part of the accelerator. Therefore we try to
make length of clusters sufficiently large in order to decrease this
connection/communication. Virtually we begin acceleration from the
almost steady beam. The longitudinal component of field from the
space charge in the beginning there is no acceleration. And only when
energy of particles sufficiently will increase (order 1 MeV), it is

possible already to speak about the existence of clusters and about connection/communication of longitudinal and transverse motion. With such binding energy will be of the same order as in usual accelerator, and will lead it to the same effects of the increase of phase volume.

Page 12.

86. Special features/peculiarities of the dynamics of beam in the circular F-M cyclotron in the absence of the similarity of guiding field.

V. N. Kanunnikov, A. A. Kolomenskiy, V. A. Papadichev.

(Physical institute im. P. N. Lebedev of the AS USSR).

The circular F-M cyclotron, for the first time proposed in [1] as is known, it makes it possible to accelerate particles over a wide range of energies in the limits of a comparatively annulus of magnetic system. The constancy of magnetic field in the time contributes to obtaining high average/mean intensity and good time/temporary structure of beam. As examples let us point out to the possibility of obtaining the quasi-continuous electron beams of medium energies upon the inductive acceleration ("betatron with the

stationary guiding field", see, for example, [2]) and to the
prospects of developing the proton circular F-M cyclotrons to the
high energies with superconducting coil electromagnet [3, 4].

In order upon the acceleration in the strongly nonlinear field,
which grows on a radius into ten and hundreds of times, to avoid
dangerous resonances, it is necessary that the frequencies of the
betatron of particles Q_τ, Q_z little would change with a radius; in
the ideal case of the so-called dynamic similarity of orbits the
frequencies must remain unchanged in the entire operating region of
accelerator. As it was shown [5], for satisfaction of this condition
it is sufficient geometric similarity of the shape of orbits and
constancy of field index n, which in turn, leads to the requirement
of the identity of azimuthal field distribution on all radii. This
means that the closed orbits of particles with different
impulse/momentum/pulse differ only in terms of scale by a radius, and
variable/alternating the dependence of magnetic field on a radius and
an azimuth are divided:

$$H(\tau, \theta) = H_0 \left(\frac{\tau}{\tau_0}\right)^n \sum_{k=1}^{\infty} (\mathcal{f}_0 + \mathcal{f}_k \cos k N \theta). \qquad (1)$$

This requirement, however, too strong and is not necessary, since
there is a broad class of fields, which ensure dynamic similarity.
Numerical integration on the computers of equations of motion for the
distributions of the magnetic field of the form

$$H(\tau,\theta) = H_0 \sum_{k=0}^{\infty} f_k \left(\frac{\tau}{\tau_0}\right)^{n_k} \cos kN\theta \qquad (2)$$

showed that scaling of betatron frequency it is possible to achieve by many methods. For example, Fig. 1 show two strongly differing forms of field, for which computed values of frequencies are identical $\Delta Q < \sim 0.01$. The dependence of the harmonics of field on a radius is shown in Fig. 2. From the calculations it follows that for guaranteeing the dynamic similarity is sufficient to maintain constant proportions of azimuthal average of field f_0 to the fundamental harmonic f_1 of the azimuthal distribution of magnetic field and indices n_0, n_1 for them. The values of the higher harmonics and their gradients on a radius weakly change frequencies. For example, for the parameters, close to the operating point of a radial-sector electronic circular F-M cyclotron (KF) of the Lebedev physics inst. ($N=20$, $n=16$, $f_0/f_1 \sim 0.1$, detailed description see [6]) harmonics ($k>1$), which satisfy condition $f_k/f_1 \leqslant 0.05 \div 0.07$, it is possible not to consider, but when $f_k/f_1 \sim 0.3 \div 0.4$ their effect it is possible to compensate for by change f_0/f_1 and n_0, n_1 with a radius. In general the requirement of constancy f_0/f_1 and n_0, n_1 is not necessary; however, fee/pay/board for the failure of this constancy can be the complication of the form of field.
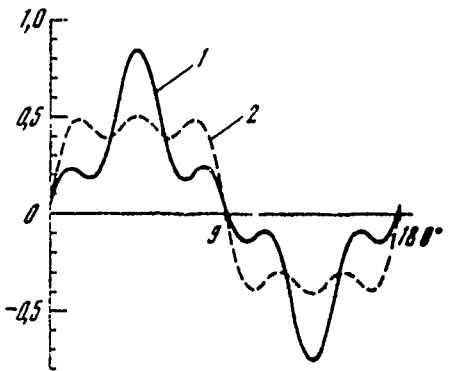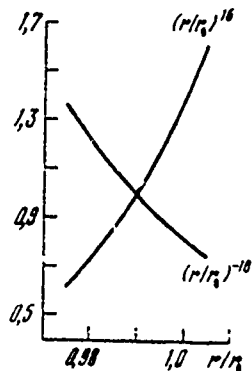
Fig. 1.   Fig. 2.

Fig. 1. Example of two dependences of field, for which particles of betatron oscillations are identical:

$$1 - H_1 = H\left[\left(\frac{r}{r_0}\right)^{16}(0{,}09 + \cos N\theta + 0{,}3\cos 3N\theta + 0{,}3\cos 5N\theta)\right]; 2 - H_2 = H_0\left[0{,}09\left(\frac{r}{r_0}\right)^{16} + \left(\frac{r}{r_0}\right)^{16}\cos N\theta - 0{,}28\left(\frac{r}{r_0}\right)^{-10}\cos 3N\theta + 0{,}2\left(\frac{r}{r_0}\right)^{16}\cos 5N\theta\right].$$ In both cases N = 20, Q_r = 5,81, Q_z = 2,78

Fig. 2. Dependence of harmonics of field H_2, given in Fig. 1 (curve 2) on radius. It is evident that within the limits of the wave-like shape of orbit ($\Delta r \propto \pm 1{,}5$ cm) f_3 decreases 1.4 times, and remaining harmonics increase 1.6 times.

Page 13.

Such approach to the guarantee of dynamic similarity expands the class of magnetic fields, suitable for the acceleration it allows,

for example, during the production to simplify pole-piece
configuration. Specifically, this was used for shaping of the
magnetic field of circular F-M cyclotron the Lebedev physics inst.

As is known, in the region of the low and average/mean values of
magnetic intensity it is formed/shaped with the method, which ensures
a precise similarity. It lies in the fact that all essential
sizes/dimensions of magnet (vertical and azimuthal clearances, width
of sector) vary in proportion to to a radius, and an increase in the
field is reached due to distributed windings. In the high-field
region this method of shaping is unsuitable, since it leads to an
excessive increase in the ampere turns of power of magnet power
supply. Therefore necessary field pattern here (in KP the Lebedev
physics inst. in the region 150 cm $<$ τ $\leq$ 160 cm) it is necessary to
obtain by the shaping of poles. In order to satisfy the condition of
similarity and in this case, it was necessary to expect and to
prepare the pole of intricate shape, with variable/alternating camber
in both sections - azimuthal and radial. However, in practice it is
necessary to considerably deviates from the calculated form of poles,
in particular, to decrease their extent along the azimuth for the
arrangement/position between the units of the magnet of the
accelerating devices/equipment and for reducing the leakage fluxes.
This last goal it serves and the location of the current carrying
conductors is radial at the edge of pole. The existing methods of

calculation of the form of pole (for example, [7]) becoms in this
case badly/poorly applicable and do not make it possible to
rate/estimate the permissible error.

For calculating the form of field and poles in our case was used
adequate to task the method, based on conformal mapping and which
makes it possible also consider the effects of the conductors with
the current, located near operating region of magnet [8]. For
obtaining field distribution, providing assigned values Q_z, Q_x is
varied the width of pole in positive and negative sector. The
vertical clearance between the shaped poles is made decreasing
according to the law τ^n, and the lateral surfaces of poles have plane
shear/sections (Fig. 3) (i.e. the width of pole depends on a radius
linearly). The prescribed/assigned values of frequencies can be
obtained on two selected radii, on the calculated ones and on
intermediate radii. Accelerator KP can work in any of two cells:
$Q_z \approx 5.8$, $Q_x \approx 2.4$ $(f_0/f_1 \approx 0.09)$ and $Q_z \approx 5.6$, $Q_x \approx 1.8$ $(f_0/f_1 \approx 0.11)$. The calculation of
poles is produced for the intermediate position of operating point
$(f_0/f_1 \approx 0.1)$, and the available corrective windings make it possible
to change by several percentages the level of field in the region of
poles and thereby to regulate the position of operating point by a
change in ratio f_0/f_1.

The calculated form of poles was first checked in the magnetic

measurements to four spare units KP, established/installed on the
special measuring bench and connected in series in the power-supply
system of accelerator. Then these results were confirmed in the
measurements of field and frequencies Q_z, Q_z in the accelerator. Fig.
4 shows measured field distributions (coinciding with the calculation
with error $\leqslant 0.1$o/o) on two radii: $z = 137$ cm (the middle part of the
region of a similar field) and $z = 161$ cm (boundary of operating region
of the shaped pole). Fig. 5 shows the motion of operating point in
the process of acceleration according to the measurement data with
the beam. It is evident that within the limits of the significant
part of the shaped pole changes of the frequencies are small (when
151 см $\leqslant z \leqslant 159$ см; $Q_z = 5.63 \pm 0.02$; $Q_z = 182 \pm 0.02$); they it is less than the
displacement of operating point in the limits of entire operating
region due to the effect of different factors (edge effect;
transition region from the distributed windings to the poles where
the calculation is hindered/hampered; a difference in the geometry of
conductors with the current, the error for the absolute values of
coil currents, etc.).

During May 1969 during the starting/launching of KP with the
described shaped poles was obtained the acceleration to 40 MeV at the
intensity more than 10^{11} electrons/s and to repetition frequency 50
Hz. As showed magnetic measurements, induction on a maximum radius of
159.5 cm can be increased to 6 kg which corresponds to maximum energy

DOC = 60069301   PAGE 44

of beam ~50 MeV. In this case the saturations of framework does not occur, and further increase in the field is limited to power-supply system.
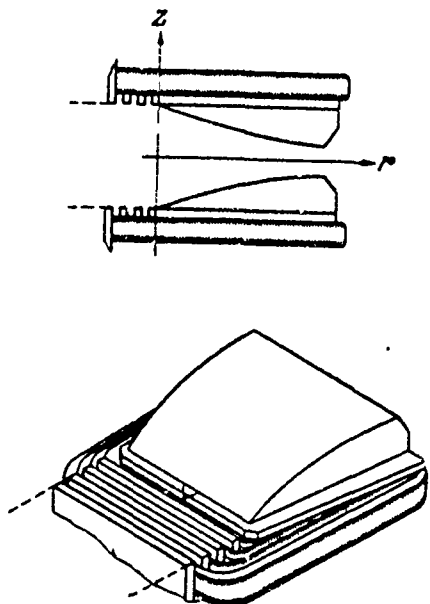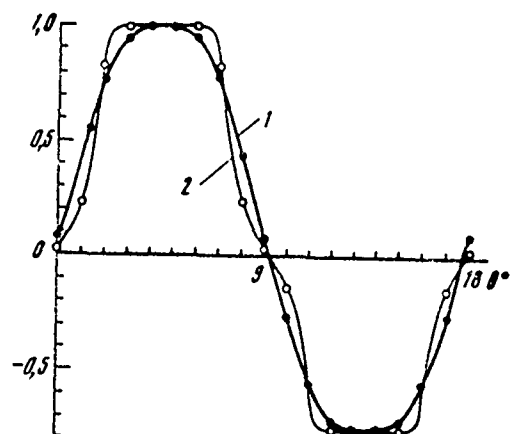
Fig. 3.   Fig. 4.

Fig. 3. Shaped of pole of circular F-M cyclotron Lebedev physics inst. (schematic figure).

Fig. 4. Measured dependences of field on azimuth in circular F-M cyclotron of Lebedev physics inst. 1 - corresponds to the region of distributed windings (ν = 137 cm); 2 - region of shaped pole (ν = 161 cm). The amplitudes of higher harmonics f_k (k = 2, 3, 4, 5) lie/rest within the limits - 0.09 $\leq f_k/f_1 \leq 0.08$

Page 14.

Therefore is possible an increase in the maximum energy by by 10-15o/o more shimmering of poles in positive units for the compensation for the radial edge effect, which decreases f_0/f_1 on the terminal radii.
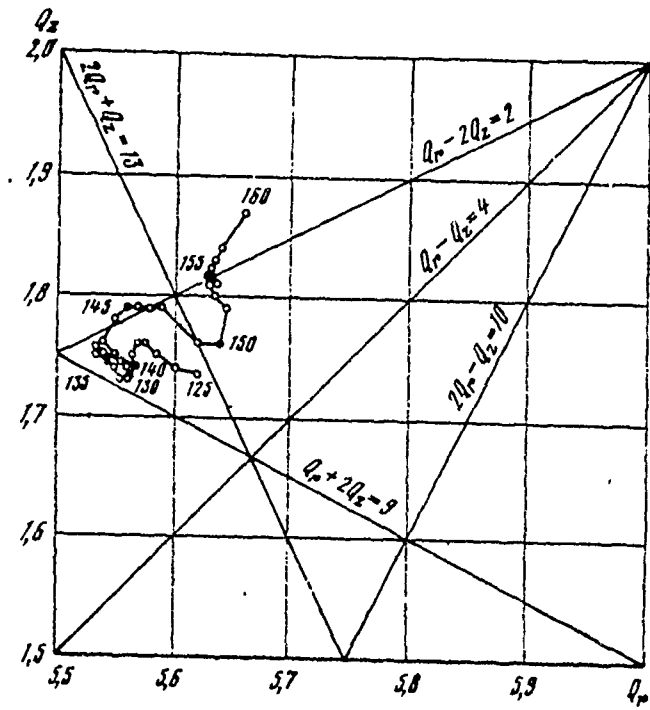
Fig. 5. Change of the frequencies of the betatron in the process of acceleration.

REFERENCES.

REFERENCES

A. A. Kolomenskiy, V. A. Petukhov, M. S. Rabinovich,

REFERENCES

1. A. A. Kolomenskiy, V. A. Petukhov, M. S. Rabinovich,
    Sb. "Some Problems in the Theory of Cyclic Accelerators"
    M., Izd-vo AN SSSR, 1955, str. 7;PTE, 1956, no 2, 26.
2. L. N. Kazanskiy et al, Proceedings of ALL-Union
    Conference on Charged Particle Accelerators. Vol.4.
    M., VINITI, 1970, str. 351
3. V. S. Voronin, V. N. Kanunnikov, A. A. Kolomenskiy,
    A. P. Fateyev, Proceedings of 7th International Conference
    on High-Energy Charged - Particle Accelerators, Vol. II,
    Yerevan, Izd-vo AN arm SSR, 1970, str, 662.
4. G. Parzen. Proc. 1968 Summer Study on Superconduc ting Devices and Accelerators. N.Y., 1969, p. 1052.
5. A. A. Kolomenskiy. Theory of Cyclic Accelerators.Atomnaya Energiya.
    1957, 3, 492; A. A. Kolomenskiy, A. N. Lebedev.
    M., Fizmatigiz, 1962, ftr. 303.
6. V. N. Kanunnikov, A. A. Kolomenskiy, S. N. Lebedev,
    Ye. P. Ovchinnikov, A. P. Fateyev, B. N. Yablokov. PTE,
    1967, No 5, 7.
7. C.C. Iliesen. Nucl. Instrum. and Meth., 1963,21,136.
8. V. A. Papadichev, Brief Reports on Physics, 1970, No 4, 61.

87. Investigation of the longitudinal instability of beam in the accumulator/storage under the effect of the resonances of synchrotron oscillations.

S. G. Kononenko, L. D. Lobzov, L. V. Reprintsev, A. M. Shenderovich.

(Physiotechnical institute of AS UkSSR).

This work is dedicated to the investigation of the effects, which appear during joint action of the induced voltage and resonances of synchrotron oscillations. This question is not examined in the literature, although to the investigation of the longitudinal instability and to the resonances of synchrotron oscillations separately are devoted many works.

Measurements are carried out on the accumulator/storage of electrons with the energy 70 MeV of PTI of AS UkSSR [1]. The full/total/complete block diagram of measuring equipment is shown in Fig. 1. For exciting the instability is used the special passive resonator whose characteristics were thoroughly measured [1].

FOOTNOTE [1]. As showed special theoretical studies, in the majority of

the practical cases physical processes in the system beam - passive
resonator and beam - active resonator were identical. ENDFOOTNOTE.

The same resonator was utilized also for recording the coherent
synchrotron oscillations with the emergence of instability.

The results of the measurements of thresholds of instability in
the absence of resonance disturbances/perturbations are given on Fig.
2. For the comparison the same figure gives the theoretical threshold
values, calculated with the aid of the results of work [2]. From the
figure one can see that on the larger segment of a curve is a good
agreement of theory with the experiment; however, with small detuning
from the resonance is observed essential difference. This difference
especially one can see well in Fig. 3, where is constructed the
contribution of Landau damping in the dependence on the detuning.
Here experimental curve has clearly expressed maximum which is absent
from the theoretical curve. Apparently, it is necessary to consider
that the theory gives the incorrect values of threshold currents with
small detunings.

As showed measurements, during the excitation of the resonances
of synchrotron oscillations is observed the depression of the
longitudinal instability.

Page 15.

Effective depression occurs in the narrow band of frequencies of the resonance disturbance/perturbation smaller than the width of resonance, moreover in the case of parametric resonance this band substantially is narrower than in the case of external resonance. The results of measuring the thresholds of instability depending on the force of resonance disturbances/perturbations and value of accelerating voltage for the cases of external and parametric resonances are given respectively on Figs 4 and 5. From the figures it is evident that already with the very low amounts of disturbance strength is observed the effective depression of instability (into dozens of times on the threshold). In this case strength of resonance is so small that resonance oscillations of beam are not observed.

Maximum values $\frac{J_n}{J_{n_0}}$ in of the curves of Figs 4 and 5 are equal to approximately/exemplarily 50. Experimentally was observed the depression of instability, also, with the high currents. However, with J_n, that exceed J_{n_0} into hundreds of times, instability completely is not suppressed. In this case are observed the oscillations of the type of the play, a precise interpretation of character of which was not conducted.
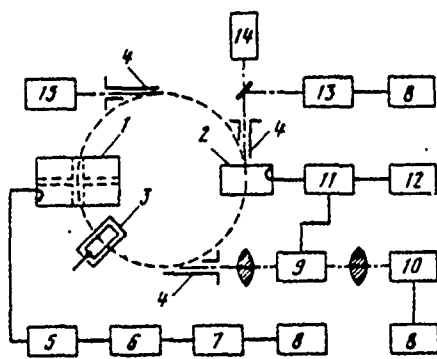
Fig. 1.   Fig. 2.
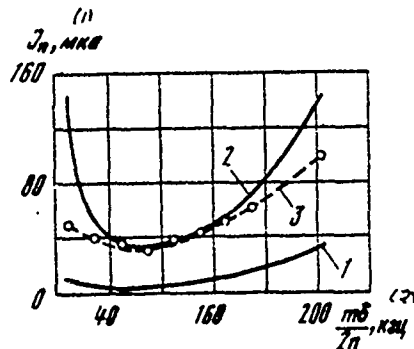
Fig. 1. Block diagram of equipment, used in experiment in investigation of longitudinal instability: 1 - passive resonator, adjusted for 2nd harmonic of frequency of revolution ~104.5 MHz; 2 - accelerating gap; 3 - meter of accumulated current (pick-up-electrode); 4 - window for output of synchrotron radiation; 5 - superheterodyne receiver; 6 - PM discriminator; 7 - selective amplifier; 8 - oscillograph; 9 - EOP; 10 - dissector for measuring longitudinal sizes/dimensions of beam; 11 - high-frequency oscillator of accelerating voltage (frequency 52, 25 MHz); 12 - modulator for exciting resonances of synchrotron oscillations; 13 - dissector for measuring the transverse sizes/dimensions of beam; 14 - television unit; 15 - meter of the accumulated current (photomultiplier).

Fig. 2. Dependence of threshold of instability on detuning relative to resonance with value of accelerating voltage 100 into: 1 -

theoretical curve without taking into account Landau damping; 2 -
theoretical curve taking into account Landau damping; 3 -
experimental curve.

Key: (1). kHz.
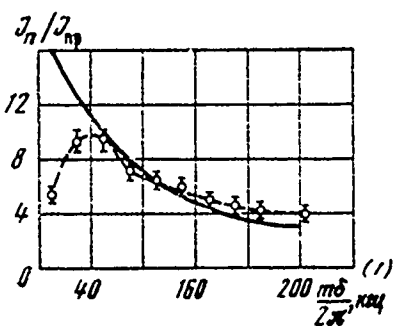
Fig. 3.   Fig. 4.
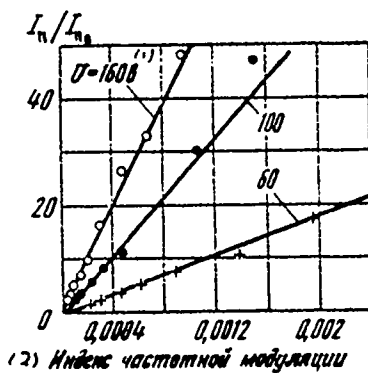
Fig. 3. Dependence of contribution of Landau damping (ratio of real threshold current to his computed value without taking into account Landau damping) on detuning with value of accelerating voltage 100 V.

Unbroken curves - theoretical results, broken - experimental results.

Key: (1). kHz.

Fig. 4. Dependence of threshold of instability on disturbance strength in the presence of external resonance of synchrotron oscillations with different value of accelerating voltage. Along the axis of abscissas are deposited/postponed the values of the index of frequency modulation, along the axis of ordinates - ratio of J_n threshold current J_{n_0} to its value in the absence of resonance

Key: (1). in. (2). Index of frequency modulation.

(1) Глубина амплитудной модуляции
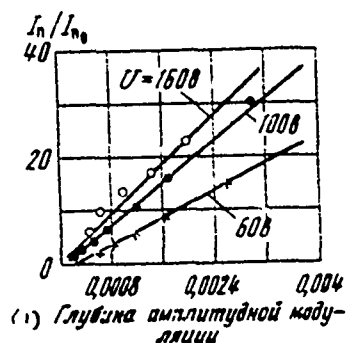
Fig. 5. Dependence of the threshold of instability on disturbance strength in the presence of the parametric resonance of synchrotron oscillations for three values of accelerating voltage. Along the axis of abscissas is deposited/postponed the depth of the amplitude modulation of accelerating voltage (equal to strength of resonance).

Key: (1). Depth of amplitude modulation.

Page 16.

Was experimentally observed also the depression of the longitudinal instability into dozens of times with the aid of synchro-betatron resonance near the resonance of vertical betatron oscillations $v_z = \frac{2}{3}$.

For the theoretical comprehension of the obtained results let us

examine the equation of synchrotron oscillations during joint action
of the induced voltage and parametric resonance of synchrotron
oscillations. We will be restricted to the case when oscillations in
the resonator significantly attenuate during the period of
synchrotron oscillations. In this case, as it follows from the
results of work [3], the equation of synchrotron oscillations in the
cubic approximation/approach takes the form

$$\eta'' - 2(\xi-\zeta)\eta' + \Omega^2\eta = -\frac{\Omega^2}{2}ctg\,\varphi_s\eta^2 + \frac{\Omega^2}{8}\eta^3 +$$
$$+ q\Omega^2\eta\cos(\nu\theta+\chi), \qquad (1)$$

where q - amplitude; ν - frequency of parametric
disturbance/perturbation; ξ - increment of instability; ζ -
decrement of radiation damping; φ_s - synchronous phase; Ω -
frequency of synchrotron oscillations; differentiation is conducted
on dimensionless time $\theta = \omega_s t$; ω_s - the frequency of revolution of
synchronous particle.

    Designating

$$\Delta = \nu - 2\Omega; \quad |\Delta| \ll \nu; \quad \eta = Ae^{i\Omega\theta} + A^*e^{-i\Omega\theta};$$
$$A = ae^{i\psi}; \quad w = \theta\Delta + \chi - 2\psi, \qquad (2)$$

we will obtain how usually ([4]), the following shortened equations:

$$a' = (\xi-\zeta)a + \frac{qa\Omega}{4}\sin w; \quad w' = \Delta + \frac{\Omega}{2}a^2 + \frac{q\Omega}{2}\cos w. \quad (3)$$

From formula (3) it follows that with executing of inequality $4|\xi-\zeta|<q\Omega$ there are steady-state solutions:

$$a_0 = \text{const} = \sqrt{-\frac{2\Delta}{\Omega} \pm q \sqrt{1 - \frac{16(\xi-\zeta)^2}{q^2\Omega^2}}} \; ;$$

$$\sin w_0 = \text{const} = -\frac{4(\xi-\zeta)}{q\Omega} \; ; \qquad (4)$$

moreover stable are the solutions with $\cos w_0 < 0$ that corresponds to positive sign under the root.

From formula (4) it follows that with the the strong instability $(4(\xi-\zeta) > q\Omega)$ or, on the contrary, with strong stability $(\xi-\zeta<0; \; 4|\xi-\zeta|>q\Omega)$ the resonance phenomena do not become apparent. Let us examine now, can arise the reverse situation, when resonance suppresses instability. For this purpose we analyze the equation of cubic approximation/approach for small divergences from steady-state solution $\delta = a - a_0$, which, as it is easy to show, takes the form:

$$\delta'' - \frac{q\Omega^2 a_0^2}{4} \cos w_0 \delta - 2(\xi-\zeta)\delta' = \frac{3q\Omega^2 a_0}{8} \cos w_0 \delta^2 + \\ + \frac{q\Omega^2}{8} \cos w_0 \delta^3 . \qquad (5)$$

From equation (5) it follows that occurs the following dependence of frequency on the amplitude:

$$\Delta\omega = \frac{3}{16} \frac{\delta_{max}^2}{a_0^2} \omega; \quad \omega = \frac{\Omega a_0}{2} \sqrt{q|\cos w_0|} . \qquad (6)$$

If the size/dimension of beam on the phase is equal to $2\delta\varphi$, then greatest amplitude $\delta_{max} = \Delta\varphi$. Consequently, synchrotron oscillation in the presence of the resonance consists of oscillation with frequency $v/2$ and oscillations with the frequencies from $v/2+\omega$ to $\frac{v}{2}+\omega \pm \Delta\omega + \Delta\Omega$ (where $\Delta\Omega$ - scatter of natural frequencies in the beam, $\Delta\Omega = \Omega \frac{\Delta\varphi^2}{16}$). The full/total/complete scatter of frequencies of the synchrotron, which determines the effect of Landau damping on the threshold of instability, is equal to $2\Delta\omega + \Delta\Omega$. In the absence of resonance this scatter is equal to simply $\Delta\Omega$. It is easy to see that with satisfaction of the condition

$$a_0 \ll 3\sqrt{q\cos w_0}$$ (7)

there will be $2\Delta\omega \gg \Delta\Omega$, i.e., in the presence of the resonance the scatter of frequencies and, consequently, also contribution Landau dampings strongly increases.

Thus, the observed effect of the depression of the longitudinal instability is experimentally explained by an increase in the nonlinearity of synchrotron oscillations in the presence of the resonances and as consequence this by an increase of the scatter of frequencies in the beam and by the amplification of the action of Landau damping. Since with the the small a_0 derivative $\frac{da_0}{d\Delta}$ is great (when $a_0 = 0$; $\frac{da_0}{d\Delta} \to \infty$), the effective depression of instability must occur in the narrow frequency band, that also was observed

experimentally. In the case of external resonance are obtained

analogous results, but since in this case $\frac{d\alpha_\varrho}{d\Delta}$ has substantially

smaller value, then the range of effective depression must be

somewhat wider.

REFERENCES
1. Yu. N. Grigor'yev, et al.Atomnay Energiya, 1967,23, No 6, 531.
2. M. M. Karliner, A. I. Skrinskiy, I. A. Shekhtman,
    ZHTF, 1968, 38, No 11, 1945.
3. S. G. Kononenko, A. M. Shenderovich. Atomnaya Energiya,
    1970, 28, No 5, 436.
4. A. A. Kolomenskiy, A. N. Lebedev, Theory of Cyclic Accelerators
    M., Fizmatgiz, 1962.

Discussion.

A. A. Kolomna. External resonances are excited simultaneously with

the parametric ones. You did share them somehow?

A. M. Shenderovich. This not entirely thus. In the case of betatron

oscillations this is actual/real thus. For the synchrotron

oscillations external resonances are excited only on the odd

harmonics, and parametric - only on the even ones. Therefore here

there is a separation.

A. N. Didenko. In what relationship/ratio were located between

themselves the frequency of revolution of particles and the natural

frequency of passive resonance?

A. M. Yaanderovich. These measurements were done as follows. The multiplicity of acceleration was 1, i.e., we accelerated on the fundamental harmonic of frequency of revolution. But the resonator, which excited instability, was adjusted to the second harmonic.

Page 17.

88. INVESTIGATIONS OF THE PASSAGE OF PARAMETRIC RESONANCE IN THE IFVE ACCELERATOR.

Yu. M. Ado, V. I. Balbekov, K. P. Lomov, E. A. Myae.

(Institute of high-energy physics).

Earlier it was established/installed [1], that on the proton synchrotron of IFVE at the intensity of the accelerated beam of 10^{12} proton/pulse and above occur the phenomena, connected with the effect of the proper field of beam. First of all this leads to the displacement of betatron frequencies into the region half integral resonance and, thus, to the limitation of the intensity of accelerator. Therefore increase in the number of injected particles in higher than certain limit does not give a proportional increment in the intensity of the accelerated beam.

There is a series/row of the works (for example, see [2-6]), in which it is indicated the possibility of the passage of parametric

resonance under the condition of the proper correction of resonance band. It is communicated below about the investigations on the origin half integral resonance $2Q=19$, conducted on the accelerator of IFVE [7].

Calculations show [4] that the "natural" intersection of resonance, caused by the Coulomb shift/shear of betatron frequencies, must not lead to the losses of particles, if its half-width $|\dot{p}| \ll 0.5.10^{-3}$ (here and throughout they are utilized the designations, accepted in [8]). According to the data of magnetic measurements, for the accelerator of IFVE upon injection $|P_{n,2}| \approx 5.10^{-3}$. For weakening of the action of resonances was created the system of correction the operating principle of which was presented in [9]. In contrast to the systems, utilized for the same target on other accelerators [5, 6], the system corrects not the harmonic of gradient, but it is direct width of resonance band:

$$p_{n,2} = \mp \frac{i}{4\pi} \int_0^{2\pi} \Delta g \, f_{n,2}^{n_2} \, e^{ik\theta} \, d\theta.$$

The use/application of this system in the accelerators with alternating gradient is more expedient, since besides the fundamental harmonic of disturbance/perturbation $k=2Q$ the considerable ($\sim 30\%$) contribution to width of band of resonance give harmonics $M+-k$, where M - number of elements/cells or periodicity. Corrections only of 19th

harmonic does not allow[1]. in our case to decrease by an order simultaneously of value $|P_1|$ and $|P_2|$.

FOOTNOTE [1]. If in one cycle intersect both resonances, $2Q_1-k$ and $2Q_2-k$, then the total resonance Q_1+Q_2-k intersects also. For its suppression is necessary the correction of the components of magnetic field, that lead to the coupling of oscillations. ENDFOOTNOTE.

For purposes of correction were utilized the supplementary windings of the blocks/modules/units of electromagnet [10], series-connected into four circuits and supplied by direct current from the independent sources. The connection diagram is given in the table.

A quantity of turns is selected in such a way that control P_1 and P_2 occurs independently. This substantially facilitates the selection of the currents of correction experimentally. The realization of the separate control P is possible during the use the minimum of three blocks/modules/units in each circuit. The symmetrical inclusion/connection of three blocks/modules/units on opposite side of accelerator with the field of opposite sign is necessary, since the supplementary windings create identical additions both to the gradient and to the field: $\Delta G/G=\Delta H/H$. In the indicated diagram are not excited even harmonics and, in particular,

most dangerous for the equilibrium orbit 10th harmonic of field. Are
equal to zero also total emf, aimed in the circuit with a change in
the basic magnetic field.

As show calculation, sensitivity of each circuit $\sim 0.02 \frac{1}{a}$.   The
addition into the width of resonance in other direction in this case
is approximately/exemplarily 100 times less.

The adjustment of the system of correction indicated was
conducted in the greatest intensity of the accelerated beam. The
dependence of intensity on a number of injected protons with the
correction and without it is given in Fig. 1. The control of a number
of injected particles was accomplished/realized with the aid of the
grids without a change in the phase volume of beam. During the
introduction to the correction of the width of resonance the
intensity increases in spite of certain deterioration in the
parameters of equilibrium orbit. Orbit distortions in the radial
direction increase with +-1.5 cm to +-(2-2.5) cm due to the odd
harmonics of field and cannot be simply corrected due to the absence
of the circuits of the correction of the 9th and 11th of the
harmonics of field [10]. The correction of parametric resonance leads
also to the expansion of the domain of existence of the accelerated
beam on the diagram of the stability of betatron oscillations.

(1) Коррекция P₁	Блоки(2) 1-й цепи	10	12	17	70	72	77
	Блоки(2) 2-й цепи	40	42	47	100	102	107
	Число(3) витков	44	12	18	-44	-12	-18
(1) Коррекция P₂	Блоки(2) 3-й цепи	2	7	9	62	67	69
	Блоки(2) 4-й цепи	32	37	39	82	97	99
	Число(3) витков	19	13	46	-19	-13	-46

Note. Negative number of turns - contrary start of winding.

Key: (1). Correction. (2). Blocks/modules/units of ... circuit. (3). Number of turns.

Page 18.

The removal/taking diagrams was conducted employing procedure, analogous that described in [11], in the connected system of the correction of the width of resonance and without it. A change in the operating point was conducted with the aid of the direct currents in the system of the correction of the gradient of magnetic field. Intensity was measured 200 ms after the injection when the effect of the currents of the correction of gradient could be disregarded/neglected. Diagrams in coordinates Q_z, Q_x are given in Fig. 2. In the first case (Fig. 2a) the correction of the width of resonance was not conducted. Hence it is apparent that the domain of

existence of beam is limited by region $9.5 < Q < 10.0$. The case of optimum

correction is shown in Fig. 2b. As a result of the fact that the

shift/shear of betatron frequency in η - the direction is less

significant, Q_η does not approach close to value of 9.5; therefore

value P_η proved to be not corrected. For z - direction an evidently

clear difference in the cases (Fig. 2a, b). In the first case (Fig.

2a) entire beam is lost on the resonance during the natural

displacement of the operating point through value $Q_z = 9.5$, in the

second case (Fig. 2b) the part of the beam passes parametric

resonance. The dependence of intensity from the distance of operating

point upon the injection to resonance $Q_z - 9.5$ is shown in Fig. 3; it

is evident that the passage of resonance is accompanied by an

increase in the intensity.

Parametric resonance passed also during the artificial rapid

displacement of the operating point of the accelerator through value

$Q_z = 9.5$. For this into the system of the correction of gradient was

supplied the current pulse in the form of half sinusoid with the

duration in basis/base 7 ms. Within the pulse action time resonance

conditions set in twice. The speed of the passage of resonance

comprised $\frac{dQ_z}{dt} \approx 0.1 \frac{1}{\text{мсек}}$. The oscillograms, which show a change in the

intensity of beam when current pulse is present, and without it, are

given in Fig. 4. Operating point was established/installed both above

and lower than value $Q_z = 9.5$. Each passage of resonance is accompanied

by loss (10-15) o/o of beam and is not very susceptible/critical to
the adjustment of the system of the correction of resonance, in
contrast to the "natural", slower speed of passage (Fig. 3), where
adjustment conditions are more susceptible/critical and losses are
more considerable ($\sim$50 %).

Thus established/installed, which on the accelerator of IFVE is
possible to substantially decrease the width of parametric resonance
with the aid of the developed system of correction. The realization
of correction leads to an increase in the intensity; however,
correction is not full/total/complete (see Fig. 1).
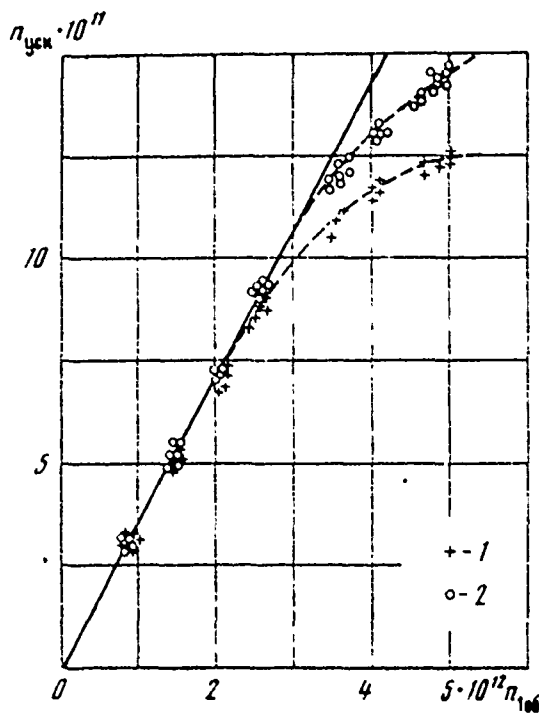
Fig. 1. The dependence of the intensity of the accelerated beam on a number of particles of those injected into accelerator chamber: 1 - the system of the correction of parametric resonance is not connected; 2 - correction are connected.
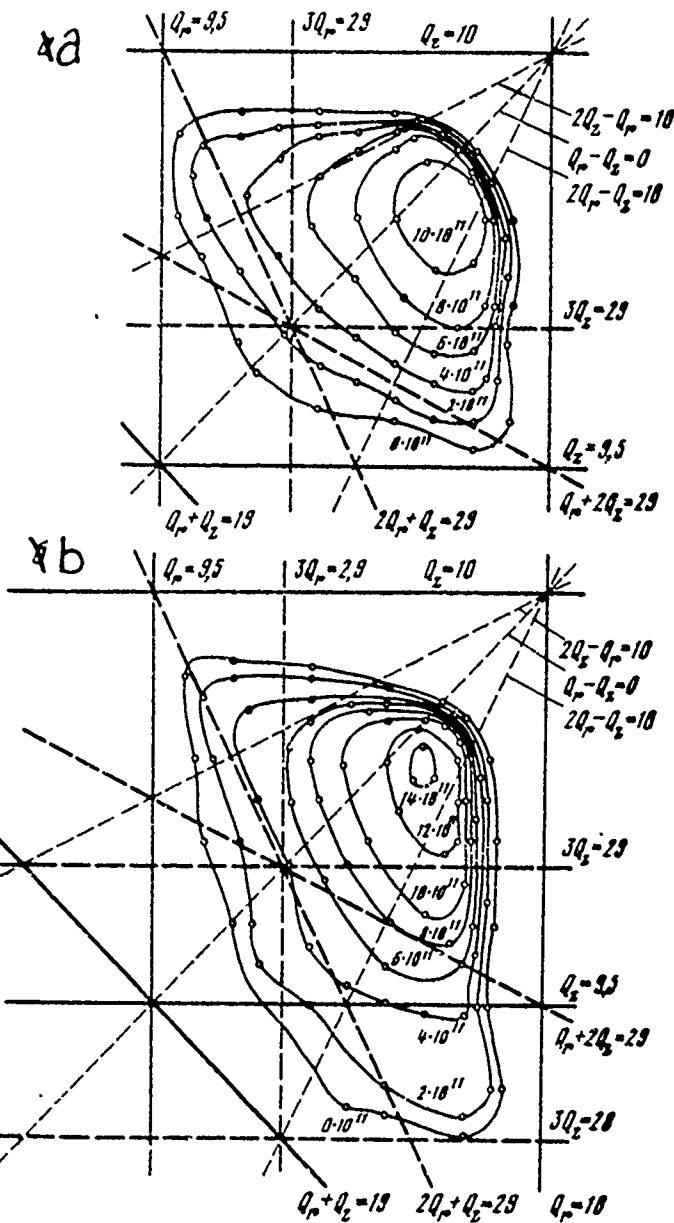
Fig. 2. Maps/charts/cards of intensity of accelerated beam for two cases: a - correction of parametric resonance is not connected; b - is connected correction of resonance $Q_z = 9.5$

Page 19.

The reason for this can consist in the fact that the inclusion/connection of correction is accompanied by certain deterioration in the orbital parameters, can play role other resonances (for example, $Q_x + Q_z = 19$), and also the fact that the correction was accomplished/realized on the direct current. Investigations in this direction will be continued.
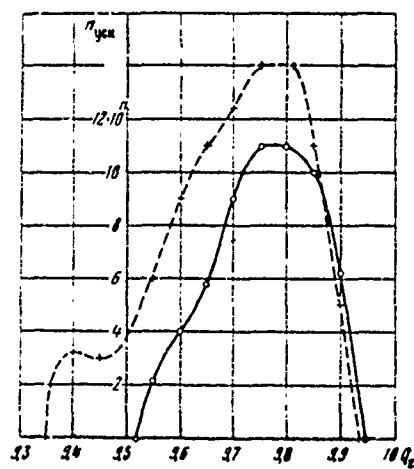
Fig. 3. Intensities of the accelerated beam depending on distance upon the injection to parametric resonance $Q_2 = \overline{9.5}$
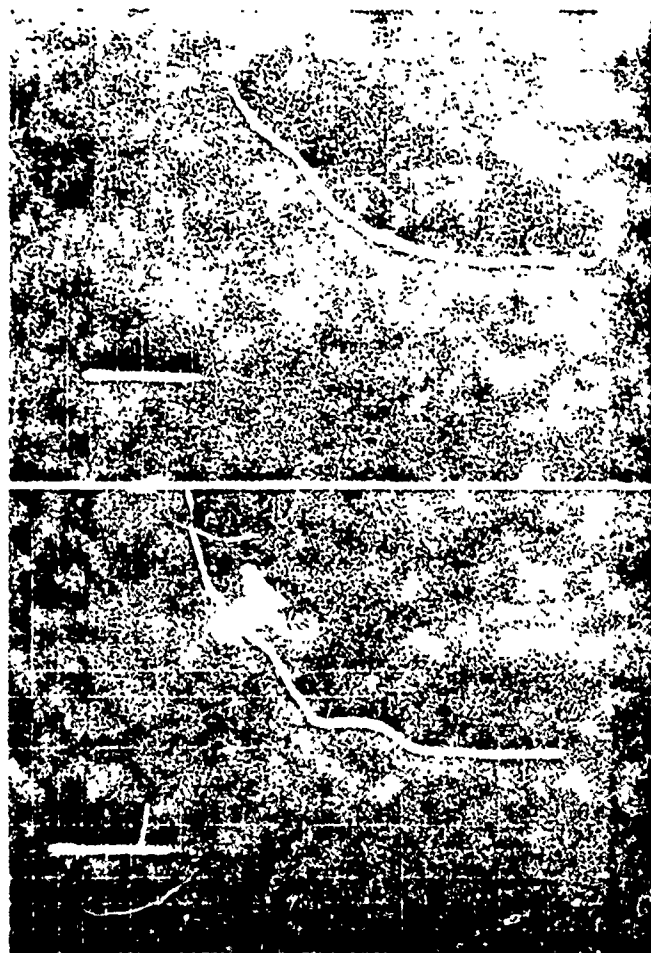
Fig. 4. Oscillograms of intensity of accelerated beam for position of

working point at moment of injection $Q_r = 9.85$ and $Q_3 = 9.60$. Scanning/sweep

1 ms/cm, sensitivity - 5.10^{10} cm^{-1}.

a - natural change in intensity; b - change in intensity with
artificial double passage of resonance   . The marker on the

oscillogram every 5 ms after injection corresponds to the moment of
current pulse feed into the gradient system.

Page 20.

References

1. Yu.M. Ado, E.A. Myae. Proceedings of the international conference
on high-energy charged-particle accelerators, Vol II, izd-vo AN
Arm. SSR. Yerevan, 1970, str. 265.

2. L.Smit. International Conference on Accelerators, Dubna, 1963,
M., Atomizdat, 1964, str. 897.

3. P. Lyapostol'. Tam zhe, str. 900.

4. V.I. Balbekov, I.A. Shukeylo. ZhTF, 39, 1863 (1969).

5. D. Mohl, L. Thorndahl, CERN Report, I JSR-300 (LI/9S) 69-20

6. D. Danby, J. Jackson, et al BNL noate, 2/20/69.

7. Yu.M. Ado et al, Atomnaya energiya, 1970, 28, No. 2, 133.

8. A.A. Kolomenskiy, A.N. Lebedev. Theory of Cyclic Accelerators, M., Fizmatgiz, 1963.

9. V.I. Balbekov, I.A. Shukeylo, Preprint IFVE, SKU-67-65-K, Serpukhov, 1967.

10. V.D. Borisov et al. Proceedings of All-Union Conference on Charged-Particle Accelerators, Vol. I. VINITI, M., 1970, str. 170.

11. Yu.M. Ado, E.A. Myae. Atomnaya energiya, 1969, 27, No. 6, 515.

Discussion.

V. V. Tsygankov. " w was conducted orbital correction maneuver?

E. A. Myae. The adjustment of the systems of correction can be accomplished/realized only according to the data about the beam, since magnetic field we do not know with such precision/accuracy so as to knowingly establish/install the calculated corrective values of currents. The adjustment of the systems of correction is accomplished/realized during the work of the accelerator with the aid of two regulators before obtaining of maximum intensity. Adjustment to the maximum intensity was obtained each time with one and the same

currents of correction. This effect can be explained by the
contraction of the band of parametric resonance.

G. Kumpfert. Do utilize you as the criterion of the passage of
resonance intensity of particles or you do use instruments for
measuring the profile/airfoil of beam? The fact is that an increase
in the emittance of the circulating beam can lead to the series/row
of undesirable effects (for example, with output!), but not only to
the losses of particles on the walls of chamber.

E. A. Myae. To measure inconerent Coulomb frequency shift of betatron
oscillations is very difficult, and we it, naturally, did not
measure. The fact of passage or nonpassage of resonance was
established/installed indirectly according to the data, which I gave.
In our case, since the passage is not full/total/complete, emittance,
probably increases. But we hope that with the supplementary measures
which we intend to accept, with even the more careful correction of
resonance band, it is possible, with the sufficiently rapid passage
of resonance, to almost completely remove the increase of the
emittance of beam.

K. Raykh. The forces of space charge displace Q on the diagram of
frequencies on the straight line the angle of slope of which depends
on beam shape. Do plan/glide you to correct the forbidden band on the

19th harmonic?

E. A. Myae. In the beginning of report I spoke that the created
system makes it possible to produce the independent control of the
width of resonance on z and on r. I explained, why proved to be
uncorrected resonance width on r. We adjusted the system of
correction on the maximum of intensity. Frequency shift in
z-direction according to our calculations is two times more strong
than in r-direction; therefore proved to be compensated band on z.
Concerning correction and resonance on r, then in our possession
later data make it possible to hope that let us be able to correct it
also.

Page 20.

89. ANALYSIS OF STABILITY OF A CLOSED PROTON BEAM IN IONIZED RESIDUAL GAS.

G. I. Dimov, V. G. Shamovskiy, V. Ye. Chupriyanov.

(Institute of nuclear physics of SO AN USSR [CO AH CCCP - Siberian Department of the Academy of Sciences of the USSR]). ·

For the determination of the conditions for space-charge neutralization in the accelerators by us is studied the effect of secondary charged/loaded particles on the beam of the circulating protons.

Experiments are conducted on the circular leading path/track with the magnetostatic field. The mean radius of orbit 100 cm, is working section 5x3.5 cm². Path/track has 4 straight sections, the length of which 2.5 times of more than radius of curvature in the rotary magnets is 100 cm. The introduction of long gaps/intervals made it possible to avoid to the weakly-focusing field of the longitudinal instability of the type of "negative mass' and facilitates the arrangement/position of functional and monitors. With

the aid of the corrective windings it is possible to change over wide
limits of frequency of betatron. We selected operating point with
frequencies $v_x = 1.80$ and $v_x = 0.88$. In this case the bulk factor of orbits
α composes 0.5. The values indicated were measured directly on the
circulating beam. The injection of protons to the path/track is
conducted by recharging method [1]. Time of injection to 1 ms,
current of injection to 1 mA. Energy of protons 1 MeV. The ionizing
losses of the circulating protons in charge-exchange target and on
the residual gas can be compensated by the vortex/eddy electric
field, concentrated in the clearance. Vortex field is induced by the
iron core, which covers one of straight sections. A maximum change of
the magnetic flux in the induction core is 300 volts for the
millisecond. Electric power supply is conducted from the vacuum-tube
modulator, which makes it possible to easily regulate the
temporary/time character of the compensating stress/voltage.

Storage path/track is equipped by the system of puller
electrodes for the removal/distance from the proton beam of secondary
particles all over orbit circumference. Is provided for the
possibility of the disconnection or extraction voltage for the time
of ~1 μs simultaneously on all electrodes. The geometry of the system
of puller electrodes is selected from the condition of the minimum
effect of extraction voltage on the motion of proton beam. Thus,
frequency shift of the betatron oscillations upon the inclusion of

extraction voltage in 2 kV does not exceed 0.01. The measurement of the current of the circulating protons is made by Rogowski loop and by electronic collector/receptacle [2]. Observation of coherent oscillations of beam is conducted with the aid of the system of induction electrodes with the passband to 200 MHz. The potential of proton beam is determined on the spectrum of the large ions, which emerge from the beam across magnetic field [3]. Position, sizes/dimensions and distribution of the losses of proton beam are observed with the aid of the movable sensors of magnetization of secondary electron emission. Fig. 1 depicts the schematic of storage path/track.

The analysis of the accumulation of protons showed that the character of the behavior of proton beam on the path/track, stability and maximum accumulated current depend substantially on the pressure of residual gas in the chamber/camera, and in certain cases and from the type of gas.

At an average/mean residual/remanent pressure in the chamber/camera to $4.6 \cdot 10^{-5}$ the torus and removal/distance from the orbit of all secondary particles the number of protons on the path/track is limited to value $\sim 1.7 \cdot 10^{11}$, which by order of value corresponds to the shift/shear of operating point to resonance $\nu_x = 3/2$. The potential of the space charge of beam, measured according to the

spectrum of large ions, in this case has a value 300 V.

The rapid disconnection of extraction voltage leads to the development of intense bouncing, which sharply increases the losses of protons in the vertical line and is decreased proton current by the path/track (Fig. 2).

The frequency spectrum or the oscillations (Fig. 3) depends on full current on the path/track and with a number of particles ~$1.5 \cdot 10^{11}$ lies/rests in the range 30-50 MHz (14-25 modes of vibration), and with a number ~$1.7 \cdot 10^{11}$ - in the band 10-30 MHz (4-14 modes).

The threshold of the development of this instability depends on the energy spread of the circulating beam and with the spread $5 \cdot 10^{-3}$ comprises $0.9 \cdot 10^{-10}$.

Page 21.

At the pressure of residual gas in the chamber/camera, which exceeds certain critical, which depends on the type of gas, the behavior and the instability of the circulating beam qualitatively are changed. With the connected extraction voltage, on the achievement on the path/track of certain threshold quantity of

current, is developed intense coherent bouncing on the zero mode
(frequency of 1.42 MHz). The threshold of the development of this
instability and its increment depend on residual/remanent pressure in
the chamber/camera and type of gas (Fig. 4). Increment with the
sufficiently good degree of accuracy is proportional to the
ionization cross section of residual gas by protons, density of
residual gas and monotonically it grows/rises with an increase in its
molecular weight.

After the disconnection of extraction voltage coherent
oscillations of proton beam on the zero mode attenuate for the time
of 5 ms.

Further behavior of beam again depends on density and type of
gas in the chamber/camera. There is a second critical pressure of
residual gas, which is determined by certain critical speed of the
formation of large ions, which does not depend on the type of gas.
Critical current of the being born in the entire chamber/camera ions
is approximately/exemplarily equal to the orbital proton current.
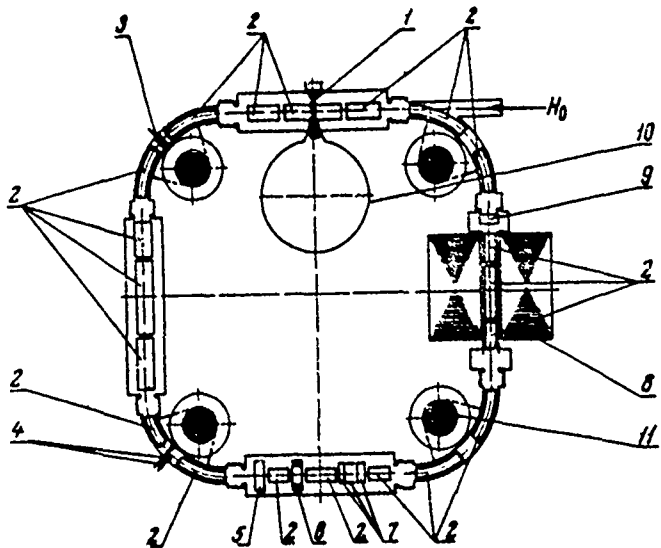
Fig. 1. Schematic of storage path/track. 1 - charge-exchange target; 2 - puller electrodes, 3 - probe of the vertical position of beam; 4 - testers of the radial position of beam; 5 - electronic collector/receptacle; 6 - Rogowski loop; 7 - induction electrodes; 8 - betatron core; 9 - faraday cylinder; 10 - buffer volume; 11 - rotary magnet.

Fig. 2. Current of protons on path/track (a), rectified signal from induction electrodes of vertical position of beam (b), stress/voltage on extracting plates (c). On the horizontal 100 μs/div.
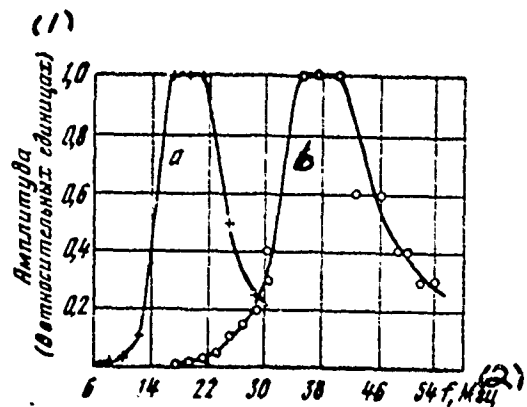
Fig. 3. Spectrum of signal from induction electrodes of vertical position of beam. a — $N = 1.7 \cdot 10^{+10}$ particles; b — $N = 1.5 \cdot 10^{11}$ particles.

Key: (1). Amplitude (in relative units). (2). MHz.
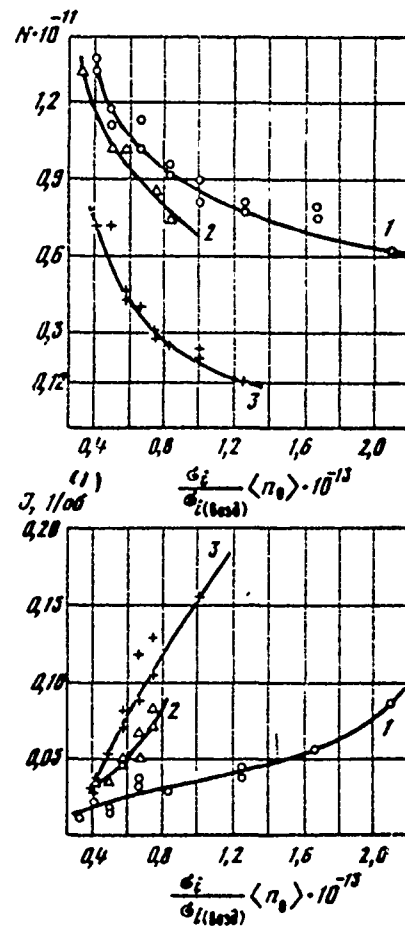
Fig. 4. Dependence of increment (γ) and threshold (N) of development of instability on pressure and kind of residual gas: 1 - hydrogen; 2 - helium; 3 - air.

Key: (1) rev.

Page 22.

At the rate of formation of the large ions of the smaller critical oscillations on the zero mode they convert/transfer in the described above high-frequency bouncing. But if the rate of formation of large ions exceeds this critical value, that, in particular, for the air corresponds to mean pressure in the chamber/camera $3.2 \cdot 10^{-4}$ torr, then with the disconnection of extraction voltage after the sufficiently rapid damping of oscillations on the zero mode the circulating proton beam proves to be completely stable. This sharply decreases the losses of particles in the vertical line and increases the coefficient of capture to the value, close to unity (Fig. 5). The storage time of protons in this case is determined in essence by the lifetime of proton on multiple scattering.

A change of the potential of beam in this case shows that the degree of space-charge neutralization of proton beam by secondary electrons close to 100o/o with its full/total/complete stability and number of particles on the path/track $\sim 1.5 \cdot 10^{11}$.

One should especially emphasize that without the operation/process of the removal/distance of secondary charged/loaded particles at the initial stage of the injection of protons on the path/track it is possible to accumulate not more than $1.5 \cdot 10^{10}$ protons as a result of the development of the coherent high-frequency instability of beam, described above.

The achievement of stable space-charge neutralization of proton beam at the intensity of the order of maximum on the space charge makes it possible to hope to overcome this limit.

As can be seen from preceding/previous, interaction of the beam of the circulating protons with secondary charged/loaded particles leads to the series row of effects. The qualitative behavior of the coherent bouncing of protons on the high modes will agree sufficiently well with the representations about the two-bundle lateral instability of system proton beam - electronic cord [3-5].

The observed with rough vacuum bouncing of proton beam on the zero mode can be, apparently identified with the instability, caused by interaction of the circulating proton beam with their trace, formed from the heavy large ions, by for the first time examined by Hereward. The experimental dependence of the increment of oscillations on the zero mode on kind and density of gas will agree with the behavior of the increment of Hereward. At the air pressure .2.3•10⁻⁴ torus and with connected extraction voltage 800 into the increment of the observed zero point oscillations composed 0.12 reverse revolutions. Calculation under these conditions gives close value. Taking into account that the expression for the increment was

obtained under the very simplified assumptions, the coincidence of increments can be considered satisfactory. In [6] was not examined the effect of any mechanisms of fading on this instability. The threshold character of the development of the observed by us instability on the zero mode, apparently, can be explained by the effect of any of these mechanisms.

Stability it is sufficient intense, completely compensated proton beam, that was being observed by us at a sufficiently high pressure in the chamber/camera it is possible, apparently, to explain as follows. Let us consider the effect of large ions in the beam only as the supplementary focusing force, which acts on the compensating electrons (frequency shift of the coherent betatron oscillations of proton beam we will disregard/neglect). The dispersion equation of this system takes the form

$$F = \frac{\rho \frac{n_e}{n}}{(k-f)^2 - \nu^2} + \frac{\rho \frac{M}{m}}{f^2 - \rho \frac{M}{m} \frac{n_L}{n}} = 1,$$

where $\rho = \frac{n}{n^*}, n^* = \frac{M \omega_0^2}{2 \pi e^2}$; ω_0 - frequency of revolution of protons; n_e, n_L, n - electron density, large ions and protons respectively; k - number of mode; M and m - mass of proton and electron. From the dispersion equation it follows that this system is stable on the modes

$$k < \nu + \sqrt{\frac{M}{m} \frac{n_L}{n^*}}.$$

As can be seen from this expression, the stability of system depends on the absolute density of large ions. This, in particular, is

explained the positive effect of cleaning secondary particles of initial stage of accumulation from beam. At the low density of protons in orbit the degree of ionization of residual gas is low and does not provide stability At an average/mean residual/remanent pressure in chamber/camera ~4.10⁻⁵ torr (air) ionic density in beam $n_i \sim 2n^*$, which corresponds to the stability of proton beam on the modes to k~60. The fact that the instability is not developed on the very high modes, can be, apparently, explained by weakening the effective field of interaction of proton and electron beams for the short-wave disturbances/perturbations. Furthermore, for the short-wave oscillations considerably is amplified that stabilizing: the effect of the energy spread of protons in the beam.

Fig. 5. Current of protons on the path/track (a), detected signal from the induction electrodes or the vertical position of beam (b), stress/voltage on the extracting plates (c). On the horizontal 50 µs/div.

REFERENCES

1. G.I. Dimov. Charge-Exchange Method ofor Injection of Protons into Accumulators. Doktorskaya dissert., Novosibirsk, 1967.

2. GI. I. Budker, G.I. Dimov, V.G. Dudnikov, Atomnaya energiya, 1967, 22, 348.

3. G.I. Dimov, V.G. Dudnikov, A.A. Sokolov, V.G. Shamovskiy. Experimental study of Protons Accumulators on Annular Track in Betatron Mode. Preprint IYaF SO AN SSSR, 1969.

4. G.I. Budker. Atomnaya energiya, 1956, 1, No. 5, 9.

5. B.V. Chirikov. Atomnaya energiya, 1956, 19, 239.

6. N.G. Hereward. The Instability of Radial Betatron Oscillations in the GPS. Preprint CERN, 1964.

Page 23.

Discussion.

A. A. Kolomenskiy. Which the final goal of your investigations?

V. G. Shamovskiy. Purpose of our investigations - to decrease the
limitations on the space charge in the initial part of the
accelerator and to move into the region of smaller energies.

90. SYNCHROTRON MOTION IN A STRONG-FOCUSING PROTON SYNCHROTRON IN THE PRESENCE OF A SPATIAL CHARGE.

I. Gumovskya, K. Raykh.

(CERN)

1. Introduction.

If synchrotron motion in the case of the negligible forces, connected with the space charges, is well known [1], then this not entirely then for the beams of the large intensity when the forces, connected with the space charges, no longer are small in comparison with the external focusing force. We investigated the static case (decision of the equation of Poisson with the introduction of relativistic correction) for four particle distributions: 1) permanent density in longitudinal phase space [2-4], 2) distribution according to the parabolic law in geometric space [5, 6], 3) distribution according to the law of $\cos^2$ in geometric space [7] and 4) permanent bulk density within the ellipsoid in the geometric space. Results are expressed through the areas of high-frequency capture regions (or "benches"), the coefficients of grouping and synchrotron frequencies as the functions

of a number of circulating particles.

Under the assumption of the sinusoidal form of radio-frequency
voltage and absence in the frequency of the errors for accelerating
field synchrotron motion when field $E_{s\gamma}$ of longitudinal space charge
is present, can be expressed by equation [1-6][1]

$$\frac{2\pi R^2 E_0}{hc^2} \frac{d}{dt}\left(\frac{\gamma^3}{\alpha\gamma^2-1} \frac{d\varphi}{dt}\right) =$$

$$= eV_{RF}\begin{cases} \sin\varphi - \sin\varphi_0, & \alpha\gamma^2 < 1 \\ -\sin(\varphi - 2\varphi_0) - \sin\varphi_0, & \alpha\gamma^2 > 1 \end{cases} + 2\pi R e E_{s\gamma}(\varphi - \varphi_0), \tag{1}$$

where R - the mean radius of the chamber/camera of synchrotron; E_0 -
rest energy of particles; n - harmonic order of accelerating field; c
- speed of light; γ - Lorenz factor; e - elementary charge; V_{RF} -
amplitude of radio-frequency voltage, and angle φ - is counted off
from zero this stress/voltage.

FOOTNOTE [1]. More detailed data are given in the internal report of
CERN [8]. ENDFOOTNOTE.

Higher than transition point is accepted convenient for the
calculation form [9] of equation (1): in this case the values φ
always lie/rest at the interval - $\pi \leqslant \varphi \leqslant \pi$ (for the stable motion), and
value φ_0 remains constant.

For simplicity it is accepted that: 1) $E_{s\gamma}$ depends only on the longitudinal coordinate s, 2) beam and vacuum chamber have circular cross sections and 3) this chamber/camera is uniform, deprived of losses and is coaxial with the beam.

In order to determine field distribution, clearly or implicitly is accepted certain linear charge distribution $\lambda(s)$ per the unit of length s and is calculated the corresponding static potential, utilizing a formula for the capacity/capacitance of coaxial (which does not consider effects at the ends/leads of the cluster[2]

$$V(s) = \lambda(s)/C(s), \qquad (2)$$

where $C(s)$ - capacitance per unit length s between the beam of radius $a_\delta(s)$ and the vacuum chamber of radius a_v.)

FOOTNOTE [2]. The admissibility of this simplification is shown in Appendix. ENDFOOTNOTE.

Then the longitudinal component of electrical field on the axis of bundle can be written in the form

$$E_{s0} = dV(s)/ds. \qquad (3)$$

In order to introduce in (3) relativistic correction, replace all lengths l measured along axis/axle s by γl, and the density of charge $\lambda(s)$ on $\gamma^{-1}\lambda(s)$. In the majority of the cases in question this is equivalent to the replacement

$$E_{s\gamma} = \gamma^{-2} E_{s0}.$$

If we disregard/neglect change γ in the course of time, equation (1) can be integrated over ϕ [3].

$$\frac{2\pi R^2 E_g}{2hc^2} \frac{\gamma^3}{\alpha\gamma^2-1} \left(\frac{d\varphi}{dt}\right)^2 + C_0 =$$

$$= -eV_{RF} \left\{ \begin{array}{ll} \cos\varphi + \varphi\sin\varphi_0, & \alpha\gamma^2 < 1 \\ -\cos(\varphi - 2\varphi_0) + \varphi\sin\varphi_0, & \alpha\gamma^2 > 1 \end{array} \right\} + \quad (4)$$

$$+ 2\pi Re V(\varphi)/\gamma^2,$$

where c_0 - integration constant, and $V(\phi)$ - the prescribed/assigned function; ϕ - potential function (2), expressed as function ϕ.

FOOTNOTE [3]. In many practical cases it is necessary to rate/estimate space-charge effect after occurred adiabatic fading of any type. For this it is necessary to solve equation (1), taking into account that $E_{sf}(\varphi-\varphi_0)$ depends on γ. ENDFOOTNOTE.

Page 24.

The comparison of different distributions is accomplished/realized as follows. In all cases this comparison relates to one and the same parameters φ_0, V_{RF}, N, where N - number of circulating particles. For the filled capture region the length of cluster is determined from equation (4) for each distribution. For

the partially filled capture region is accepted one and the same
length of cluster in the case of negligible space charge for all
distributions. It is obvious that the latter/last assumption is not
completely correct, but it is convenient for the calculations.

2. Area and height of capture region (cluster), coefficient of
grouping and frequency of synchrotron.

Assuming/setting $y = d\varphi/d\tau = \dot{\varphi}$ and introducing standardization
$y_n = y\sqrt{\cos\varphi_0/(2\Omega_0^2)}$, which was being utilized earlier [9] (where Ω_0 - the
angular frequency of small synchrotron oscillations for $N = 1$), we will
obtain equation separatrices in the form

$$y_n(\varphi) = C_0(N) + \left[\left\{ \begin{array}{c} \cos\varphi - \cos\varphi_2 \\ \cos(\varphi - 2\varphi_0) - \cos(\varphi_2 - 2\varphi_0) \end{array} \right\} + (\varphi - \varphi_2)\sin\varphi_0^{\pm} \right. \tag{5}$$
$$\left. \pm C_1(N) f_1(\varphi) \right]^{1/2},$$

where $C_0(N)$ and $C_1(N) f_1(\varphi)$ - the functions, which depend on the
charge distribution; φ_2 - abscissa, which is determining to
separatrix (point of unstable equilibrium), and upper and lower terms
and signs relate respectively to the regions below and higher than
transition energy. If φ_1 - another value φ, for which $y_n = 0$, then the
normalized area of capture region is determined by the expression
(for the brevity subsequently is everywhere examined only the region
lower than transition energy)

$$\alpha(N)_n = \frac{\sqrt{2}}{\delta} \int_{\varphi_1}^{\varphi_2} \psi_n(\varphi)\, d\varphi. \qquad (8)$$

The half-height of capture region is equal to

$$\psi(N)_{n\,max} = \psi_n(\varphi_0). \qquad (7)$$

If is required to determine the sizes/dimensions of the cluster, which stretches from φ_{1e} to φ_{2e} in the partially filled capture region or the coefficient of grouping V, then it is possible to use with the same equation (5), after replacing $\psi_n, \varphi_1, \varphi_2$, by $\psi_{ne}, \varphi_{1e}, \varphi_{2e}$. The coefficient of grouping is determined by the relationship/ratio

$$B = \frac{Ne}{2\pi R \lambda(s)_{max}}. \qquad (8)$$

In order to find frequency of syncrotron, it is necessary to have an equation for the particle trajectory within the cluster. It was obtained, on the basis of the fact that potential well was identical for all trajectories. Then

$$\psi_{ni}(\varphi) = \sqrt{\cos\varphi - \cos\varphi_{2i} + (\varphi - \varphi_{2i})\sin\varphi_0 \pm C_2(N) f_2(\varphi)}. \qquad (9)$$

The angular frequency of synchrotron oscillations is equal to

$$\Omega(N) = \pi \sqrt{\frac{2\Omega_0^2}{\cos\varphi_0}} \left[\int_{\varphi_{1i}}^{\varphi_{2i}} \frac{d\varphi}{\psi_{ni}(\varphi)} \right]^{-1}. \qquad (10)$$

Expressions for $E_{si}, E_s f(\varphi)(1), C_0$ and $C_1 f_1$ (5) and $C_2 f_2$ (9) are given in Table 1, and value $\lambda(s)$ and B (8) - 2.

Let us make several final observations [8].

Due to the neglect of dependence E_{so} on the transverse coordinates in (3) all utilized fields are electrostatically mismatched.

Only distribution σ=const in the space (ϕ, $\dot{\phi}$) is stationary according to Kapchinskiy. In other distributions "external" trajectory and envelope of charge do not coincide in the precision/accuracy.

At points ϕ_1 and ϕ_2 the distribution σ=const leads to the interruption/discontinuity in y' lower than transition energy and to the interruption/discontinuity into y - higher than transition energy. Discontinuity can be removed, for example, by the introduction to special function [5, 8], which affects in essence the ends/leads of the cluster. Ellipsoidal distribution it leads also to the special feature/peculiarity, if it are are utilized together with the formula for the capacity/capacitance. This difficulty can be removed, selecting $C_0=R(\phi_0-\phi_1)/h$, i.e., combining one end/lead of the ellipse with ϕ_1.

In prescribed/assigned accelerating field the forces of space charge do not change the length of capture region in the case of

distributions according to the law σ=const and cos². In the case of parabolic and ellipsoidal distributions these forces shorten the capture regions lower than transition energy. For all distributions of area and height of capture regions decrease below transition energies and grow/rise above transition energies.

3. Numerical results and conclusion/output.

Figure gives the results of calculating the area of capture region for booster [10] of proton synchrotron of CERN (PSB), undertaken as an example. The values of the coefficient of grouping are given in Table 3. For the parameters in question the area of capture region and its height decrease to 10-35%.

[Page 25.] Table 1. Expressions for $E_s f(\varphi)$, $C_0(N)$, $C_1(N) f_1(\phi)$ and $C_2(N) f_2(\varphi)$.

(1) Распределение	$E_s f(\varphi)$ (в/м)	$C_0(N)$	$C_1(N) f_1(\varphi)$	$C_2(N) f_2(\varphi)$
(2) $\sigma = \dfrac{e\sqrt{\cos\varphi_0}}{16h\Omega_0}\dfrac{N}{\alpha(N)_n} =$ const в пространстве $(\varphi \dot{\varphi})$	$\dfrac{h^2 \dot{\varphi}_0 \sigma}{2\pi\varepsilon_0 R^2 \gamma^2}\dfrac{\ddot{\varphi}}{\dot{\varphi}}$	$-\dfrac{\sqrt{2}\,ehq_0 N}{32\varepsilon_0 R\gamma^2 V_{RF}\alpha(N)_n}$	$+C_0^2 =$ const	$2C_0\left[y_{n\Theta}(\varphi)-y_{n\Theta}(\varphi_{2\iota})\right]$
(3) Параболическое $\varphi_0 \leqslant \varphi \leqslant \varphi_2$ (или $\varphi_{2\iota}$) (3a) φ_1 (или $\varphi_{1\iota}) \leqslant \varphi \leqslant \varphi_0$	$-\dfrac{3ehq_0 N}{4\pi\varepsilon_0 R^2\gamma^2(\varphi_2-\varphi_1)}\left\{\begin{array}{c}\dfrac{\varphi-\varphi_0}{(\varphi_2-\varphi_0)^2} \\[2mm] \dfrac{\varphi-\varphi_0}{(\varphi_1-\varphi_0)^2}\end{array}\right.$	0	$-\dfrac{\pi R E_s}{V_{RF}}\left\{\begin{array}{c}\left(\dfrac{\varphi-\varphi_0}{\varphi_2-\varphi_0}\right)^2-1 \\[2mm] \left(\dfrac{\varphi-\varphi_0}{\varphi_1-\varphi_0}\right)^2-1\end{array}\right.$	$\dfrac{C_1}{(\varphi_{2a}-\varphi_0)^2}\left\{\begin{array}{c}(\varphi-\varphi_0)^2-(\varphi_{2\iota}-\varphi_0)^2 \\[2mm] \dfrac{\varphi_{2\varepsilon}\varphi_0}{\varphi_{1\Theta}-\varphi_0}(\varphi-\varphi_0)^2-(\varphi_{2\iota}-\varphi_0)^2\end{array}\right.$
$\cos^2$ (3a) $\varphi_0 \leqslant \varphi \leqslant \varphi_2$ (или $\varphi_{2\iota}$) (3a) φ_1 (или $\varphi_{1\iota}) \leqslant \varphi \leqslant \varphi_0$	$-\dfrac{ehq_0 N}{4\pi\varepsilon_0 R^2\gamma^2(\varphi_2-\varphi_1)}\left\{\begin{array}{c}\dfrac{\pi}{\varphi_2-\varphi_0}\sin\pi\dfrac{\varphi-\varphi_0}{\varphi_2-\varphi_0} \\[2mm] \dfrac{\pi}{\varphi_1-\varphi_0}\sin\pi\dfrac{\varphi-\varphi_0}{\varphi_1-\varphi_0}\end{array}\right.$	0	$+\dfrac{2\pi R E_s}{V_{RF}}\left\{\begin{array}{c}\cos\pi\dfrac{\varphi-\varphi_0}{\varphi_2-\varphi_0}+1 \\[2mm] \cos\pi\dfrac{\varphi-\varphi_0}{\varphi_1-\varphi_0}+1\end{array}\right.$	$C_1\left\{\begin{array}{c}\cos\pi\dfrac{\varphi-\varphi_0}{\varphi_{2a}-\varphi_0}-\cos\pi\dfrac{\varphi_{2\iota}-\varphi_0}{\varphi_{2\varepsilon}-\varphi_0} \\[2mm] \cos\pi\dfrac{\varphi-\varphi_0}{\varphi_{1\varepsilon}-\varphi_0}-\cos\pi\dfrac{\varphi_{2\iota}-\varphi_0}{\varphi_{2\varepsilon}-\varphi_0}\end{array}\right.$
(4) Эллипсоидальное $\rho = \dfrac{3eN}{4\pi ha^2 c_0} =$ const[**] $2\varphi_0-\varphi_1 \leqslant \varphi \leqslant \varphi_2$ $\varphi_1 \leqslant \varphi \leqslant 2\varphi_0-\varphi_1$	$-\dfrac{3e\kappa N}{8\pi\varepsilon_0 h^2 c_0^3\gamma^2}\left[(\varphi-\varphi_0)\times\right.$ $\left.\times\left\{q_0-1-\ell n\left[1-\left(\dfrac{\varphi-\varphi_0}{\varphi_0-\varphi_1}\right)^2\right]\right\}\right]$	0	$-\dfrac{\pi R E_s}{V_{RF}}\left\{\begin{array}{c}0 \\[2mm] q_0(\varphi-\varphi_0)^2-q_0(\varphi_1-\varphi_0)^2+f_3(\varphi)\end{array}\right.$	$f_3(\varphi)=(\varphi_0-\varphi_1)^2\times$ $\times\left[1-\left(\dfrac{\varphi-\varphi_0}{\varphi_0-\varphi_1}\right)^2\right]\times$ $\times\ell n\left[1-\left(\dfrac{\varphi-\varphi_0}{\varphi_0-\varphi_1}\right)^2\right]$

* Formulas   is not possible to directly utilize above transition energies [8]; $\ddot{\varphi}/\dot{\varphi}$ it relates to the boundary of cluster;

$$q_0 = 1 + 2\ell n(a_v/a_\varepsilon)$$

** Principal axes/axles $a, a, c_0\left[=R(\varphi_0-\varphi_1)/h\right]$, $E_s f(\varphi)$ is based on (2), $q_0 = 1+2\ell n(a_v/a)$. For the partially filled capture regions $C_2=0$ when $\varphi_1 \leqslant \varphi \leqslant \varphi_{1\Theta}$

Key: (1). Distribution. (2). in the space. (3). Parabolic. (3a). or. (4). Ellipsoidal.

Table 2. Expressions for $\lambda(s)$ and B.

(1) Распределение	$\lambda(s)$	B	(2) Примечание
(3) $\sigma = \frac{e\sqrt{\cos\varphi_0}}{16 h \Omega_0}\frac{N}{\alpha(N)_n} = const$ в пространстве $(\psi,\dot\varphi)$	$\frac{2\sigma h}{R}\dot\varphi$	$\frac{2\sqrt{2}}{\pi}\frac{\alpha(N)ne}{\psi_{n\,max}}$	(4) Простого выражения для B нет
(5) Параболическое	$\frac{3eN}{2h(s_2-s_1)}\left\{\begin{array}{l}1-\left(\frac{s}{s_2}\right)^2,\ 0\le s\le s_2\\[4pt]1-\left(\frac{s}{s_1}\right)^2,\ s_1\le s\le 0\end{array}\right.$	$\frac{\varphi_2-\varphi_1}{3\pi}$	(6) B слабо зависит от N (через φ_1 и φ_2)
$\cos^2$	$\frac{2eN}{h(s_2-s_1)}\left\{\begin{array}{l}\cos^2\frac{\pi s}{2s_2},\ 0\le s\le s_2\\[4pt]\cos^2\frac{\pi s}{2s_1},\ s_1\le s\le 0\end{array}\right.$	$\frac{\varphi_2-\varphi_1}{4\pi}$	(7) B не зависит от N
(8) Эллиптическое $\rho = 3Ne/(4\pi h a^2 c_0) = const$	$\pi\rho a^2\left[1-\left(\frac{s}{c_0}\right)^2\right] = \frac{3eN}{4hc_0}\left[1-\left(\frac{s}{c_0}\right)^2\right]$	$\frac{2hc_0}{3\pi R} = \frac{\varphi_2-\varphi_1}{3\pi}$	(9) Непригодно в случае асимметричных сгустков

Key: (1). Distribution. (2). Note. (3) in the space. (4). There is no simple expression for B. (5). Parabolic. (6) B weakly depends on N (through ϕ_1 and ϕ_2). (7). B does not depend on N. (8). Elliptical. (9). It is unsuitable in the case of asymmetric clusters.

Page 16.

It is evident that the distribution according to the law of $\cos^2$ leads to the values of the coefficients of grouping, approximately/exemplarily for 30 o/o smaller than in the case of distribution $\sigma = const$.

Analogous results were obtained for present and projected/designed parameters [8] of proton synchrotron of CERN (CPS). Relative (in comparison with the zero intensity) frequencies of synchrotron into CPS, that correspond to small and large amplitudes, are given in Tables 4 and 5.

For large amplitudes φ_e is equal

$$\varphi_e = \varphi_0 + \begin{cases} \frac{1}{3}(\varphi_{2e} - \varphi_{1e}) & \sigma\text{-const, параболическое} \\ & \text{распределение,} \quad (11) \\ \frac{1}{4}(\varphi_{2e} - \varphi_{1e}) & \text{распределение } \cos^2 \end{cases}$$

Key: (1) parabolic distribution. (2) distribution cos².

As can be seen from the given below tables, the dominant role of the forces of space charge is reduced to the fact that they decrease the synchrotron frequency lower than transition energy and increase its above transition energies. The change of frequency of small synchrotion oscillations, depending on the number of circulating particles, is roughly proportional to the curvature of distribution of charge density with $\varphi - \varphi_0$.

Of four calculated values it is most convenient for the direct measurement B and Ω. Since the frequency of synchrotron depends both on particle distribution and on intensity, it is the most adequate/approaching value for the experimental check.

Unfortunately, until there exists instrument for its direct measurements. The estimation of frequencies of the synchrotron in CPS

was obtained during the latter/last several years by observing the oscillations of the maximum charge density in the process of work of the accelerator. The frequency of these oscillations does not depend [11] in the limits of the measuring error, equal to approximately 2o/o, from the intensity of proton beam in the range from 0.07 to $1.8 \cdot 10^{12}$ protons per pulse.
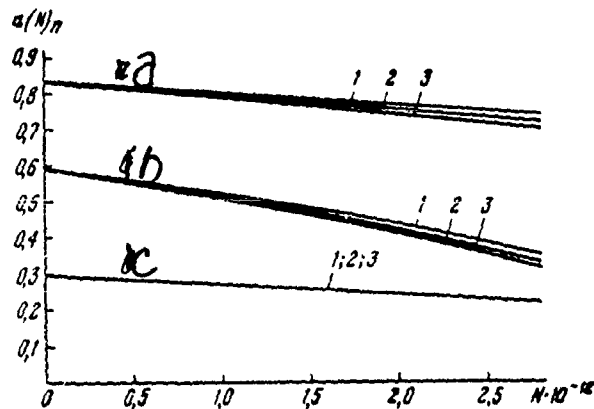
Area of cluster, included by standardized/normalized envelope of charge for the booster of CERN, $a_y=0.03$ m. Curves for 50 MeV correspond to the filled capture region $\Delta\varphi=\varphi_{2e}-\varphi_{1e}$: a - T=50 MeV; $V_{RF}=12$ kV, $\phi_0=4.8$; $a_b=0.02$ м; в - T=800 MeV, $V_{RF}=3$ kV, $\phi_0=0.1°$, $\Delta\phi=220°$, $a_b=0.01$ м; B-T=800 MeV, $V_{RF}=12$ kV, $\phi_0=4.8°$, $\Delta\phi=147°$, $a_b=0.01$ м; 1 - σ=const in the space (ϕ, $\dot\phi$); 2 - parabolic distribution; 3 - distribution according to the law of $\cos^2$.

Table 3. Coefficients of grouping for $N=2.5\cdot10^{12}$ to the ring.

(2) Распределение	(1) Параметры ускоряющей системы	T = 50 МэВ $V_{RF}=12$ кв $\varphi_0=4,8°$	T = 800 МэВ (3)	
			$V_{RF}=12$ кв $\varphi_0=4,8°$	$V_{RF}=3$ кв $\varphi_0=0,1°$
(4) σ = const		0,55	0,30	0,425
Параболическое (эллипсоидальное)		0,54	0,27	0,41
$\cos^2$		0,41	0,20	0,30

Key: (1). Parameters of the accelerating system. (2). Distribution. (3). MeV. (3a) kV. (4). Parabolic (ellipsoidal).

Table 4. Relative frequency of synchrotron in CPS for small
amplitudes with different energies V_{RF} =130 kV, ϕ_0=30°).

γ	Длина сгустка (1)	(2) σ=const в пространстве ($\varphi-\dot\varphi$)		(3) Параболическое		$\cos^2$	
		$N = 10^{12}$	$N = 2.10^{12}$	$N = 10^{12}$	$N = 2.10^{12}$	$N = 10^{12}$	$N = 2.10^{12}$
1,053	Вся область (4) захвата	0,996	0,982	0,994	0,986	0,980	0,956
5,6	33°	0,96	0,92	0,92	0,83	0,68	<0,2
7	29° *	1,03	1,06	1,08	1,16	1,22	1,42
	54° **	1,0	1,01	1,01	1,03	1,04	1,08
12	24° *	1,03	1,04	1,06	1,11	1,10	1,31
	84° **	1,00	1,00	1,00	1,01	1,01	1,01

* Ideal adiabatic value.

** Measured value.

Key: (1). Length of cluster. (2) in the space. (3). Parabolic. (4).
Entire/all capture region.

Page 27.

In order to match this result with this work, it would be possible,
for example, to consider that (1) real distribution has with $\phi=\phi_0$ the
smaller curvature than any one of the investigated distributions, or
that (2) the observed oscillations are not the oscillations of single

particles, as it was accepted above, but by the oscillations of
envelope, for which the shift/shear is 4 times less [5, 12].

Application/appendix.

Comparison of the exact solution of the equation of Poisson with
the formula for the capacity/capacitance in the case of ellipsoid
with the permanent bulk density of inside cylindrical uniform coaxial
vacuum chamber/camera without the losses.

Let us examine the evenly charged/loaded ellipsoid

$$\frac{\xi^2}{a^2} + \frac{\zeta^2}{\beta^2} + \frac{\eta^2}{c_0^2} = 1, \qquad c_0 > \beta \geqslant a \qquad (A1)$$

with bulk density $\rho = \frac{Ne}{h} \frac{3}{4\pi a \beta c_0}$.

P(x, z, s) - point inside or out of surface (A1). It is known
[for 13], that for the isolated/insulated ellipsoid the potential at
point P takes the form within

inside
$$V_{Pi} = \frac{\rho a \beta c}{4\varepsilon_0} \left(M_0(0) - M_x(0)x^2 - M_z(0)z^2 - M_s(0)s^2 \right),$$
$$(A2)$$

outside
$$V_{Pe} = \frac{\rho a \beta c}{4\varepsilon_0} \left(M_0(k) - M_x(k)x^2 - M_z(k)z^2 - M_s(k)s^2 \right),$$

where M - form factors of ellipsoid. Let $a \cdot \beta$ and the ellipsoid be
surrounded by the coaxial ideally conducting cylinder of radius a_v.
Then parameter k in (A2) is equal to

$$k = \frac{s^2 - c_0^2 - a^2 - a_v^2}{2} +$$

$$+ \sqrt{\left(\frac{s^2 - c_0^2 - a^2 - a_v^2}{2}\right)^2 + a^2 s^2 + c_0^2 (a_v^2 - a^2)} \qquad (A3)$$

and potential on the surface of cylinder takes the form

$$V_{P\theta}(s) = \frac{\rho a \delta c}{4 \varepsilon_0} (M_0(k) - M_x(k) a_v^2 - M_s(k) s^2), \quad (A4)$$

where

$$M_0(k) = \frac{1}{\Delta^2} \ell n \frac{\sqrt{c_0^2 + k} + \Delta}{\sqrt{c_0^2 + k} - \Delta}, \qquad \Delta = \sqrt{c_0^2 - a^2},$$

$$M_x(k) = \frac{1}{\Delta^2} \frac{\sqrt{c_0^2 + k}}{a^2 + k} + \frac{1}{2\Delta^3} \ell n \frac{\sqrt{c_0^2 + k} - \Delta}{\sqrt{c_0^2 + k} + \Delta},$$

$$M_s(k) = \Delta^{-3} \left[\ell n \frac{\sqrt{c_0^2 + k} + \Delta}{\sqrt{c_0^2 + k} - \Delta} - \frac{2\Delta}{\sqrt{c_0^2 + k}} \right].$$

Let us examine the boundary-value problem

$$\Delta V(s, \tau) = \frac{1}{\tau} \frac{\partial}{\partial \tau} \left(\tau \frac{\partial V}{\partial \tau} \right) + \frac{\partial^2 V}{\partial s^2} = 0, \quad 0 \leqslant \tau \leqslant a_v; \ -\infty < s < +\infty$$

$$(A5)$$

$$V(s, s_v) = V_{P\theta}(s), \quad \text{determined from (A4)}.$$

With the aid of the Fourier transform it is possible to show that decision (A5) is written/recorded in the form

$$V(s, \tau) = 2 \int_0^\infty \frac{I_0(\tau \tau)}{I_0(a_v \tau)} F_v(\tau) \cos s\tau \, d\tau,$$

$$(A6)$$

$$F_v(\tau) = \frac{1}{\pi} \int_0^\infty V_{P\theta}(s) \cos \tau s \, ds.$$

Thus, the potential distribution, created uniform by the charged/loaded ellipsoid is inside of the ideally conducting coaxial vacuum chamber/camera can be presented in the form

$$V_i(s,z) = \frac{\rho a^2 c_0^2}{4\varepsilon_0} \left(M(0) - M_x(0)z^2 - M_s(0)s^2 \right) - V(s,z),$$

$$V_e(s,z) = \frac{\rho a^2 c_0^2}{4\varepsilon_0} \left(M_0(k) - M_x(k)z^2 - M_s(k)s^2 \right) - V(s,z).$$

$$(A7)$$

Table 5. Relative frequency of synchrotron in CPS for the large amplitudes with different energies V_{RF} =130 kV, ϕ_0=30°).

γ	Длина сгуст-ка (1)	Смеще-ние час-тоты * (2)	σ=const в пространстве $(\gamma \cdot \gamma)$ (3)		Параболическое (4)		$\cos^2$	
			$N = 10^{12}$	$N = 2 \cdot 10^{12}$	$N = 10^{12}$	$N = 2 \cdot 10^{12}$	$N = 10^{12}$	$N = 2 \cdot 10^{12}$
1,053	Вся область захвата (5)	0,896	0,994	0,989	0,994	0,988	0,988	0,974
5,6	33°	0,99	0,957	0,901	0,917	0,826	0,770	0,450
7	29°	0,99	1,04	1,08	1,08	1,15	1,14	1,26
	54°	0,99	1,00	1,01	1,01	1,02	1,02	1,05
12	24°	0,99	1,04	1,05	1,05	1.11	1,10	1,18
	84°	0,96	1,00	1,00	1,00	1,00	1,00	1,01

* Frequency switch in comparison with small amplitudes for N=1.

Key: (1). Length of cluster. (2). Frequency switch *. (3) σ=const in the space. (4). Parabolic. (5). Entire/all capture region.

Page 28.

Introducing the usual relativistic correction $s \rightarrow \gamma s$, $c_0 \rightarrow \gamma c_0$, we obtain an electric field within vacuum chamber

$$E_{s\gamma}(s,\tau) = -\frac{3Ne\gamma M_s(k)}{8\pi h \varepsilon_0} s +$$

$$+2\int_0^\infty \frac{I_0(\eta\tau)}{I_0(\alpha_\gamma\tau)} F_\nu(\tau)\tau \sin \gamma s\tau d\tau . \qquad (A8)$$

Then, if we disregard/neglect adiabatic fading, the equation of

synchrotron oscillations with the energies lower than critical will take the form

$$2\pi \frac{R^2 E_0}{hc^2} \frac{\gamma^3}{a\gamma^2-1} \frac{d^2\varphi}{dt^2} = eV_{RF}(\sin\varphi - \sin\varphi_0) - $$

(A9)

$$-2\pi Re E'_{s\gamma}\left(\frac{\gamma R}{h}(\varphi-\varphi_0),\tau\right).$$

If we assume first in (A9) $\tau=0$ and to examine linear component $E_{s\gamma}$, then

$$-\frac{\cos\varphi_0}{\Omega_0^2} \frac{d^2\varphi}{dt^2} = \sin\varphi - \sin\varphi_0 - S_c \frac{M_s(k)-M_v}{M_s(0)-M_v}(\varphi-\varphi_0),$$ (A10)

where

$$M_v = \frac{8\pi\varepsilon_0 h}{3Ne} 2\int_0^\infty \frac{\tau^2}{I_0(a_\gamma\tau)} F_v(\tau)d\tau,$$

$$S_c = \frac{3Ne\gamma R^2[M_s(0)-M_v]}{4\varepsilon_0 h^2 V_{RF}}.$$

If we integrate[1] (A10) and to analyze for that fixed/recorded S_c (in parameters PSB and CPS) that results will differ from the appropriate results, obtained with use $E_{s\gamma}$ from capacitive formula (3) only by third significant digit.

FOOTNOTE [1]. Integrals in (A6), (A8) and (A10) with difficulty are calculated, since in them the integrands are, since in them the integrands are rapidly oscillating. Utilizing asymptotic expansions [8], it is possible to convert integrals in such a way that in the integrands it would not be the oscillating terms. Then the

calculation of integrals of type (A8) and (A10) occupies about 5 s in electronic computer CDC 6600. ENDFOOTNOTE.

If the same procedure is fulfilled for equation (A9), again assuming/setting r=0, then results will differ per unit in second significant digit, which is completely acceptable for purposes of this investigation.

REFERENCES

1. H.G. Hereward. What are the equations for the phase oscillations in a synchrotron? CERN 66-6, 1966.
2. C.F. Nielsen, A.M.Sessler. Rev. Scient. Instrum., 1959, 30, 80.
3. V.K.Neil, A.M. Sessler. Rev. Scient. Instrum., 32, 1961, 256.
4. A.N. Lebedev, E.A. Shilkov. Nucl. Instrum. and Meth., 1966, 45, 238.
5. H.G. Hereward. UCRL Internal Report BeV 515(1960); CERN Internal Report, MPS/DL66-3, 1966.
6. CERN Internal Report, AR/SG/64-15, 1964.
7. CERN Internal Report, SI/EL 68-2, 1968.
8. I. Gumowski, K.H. Reich. CERN Internal Report, SI/DL 70-6, 1970.
9. I. Gumowski. CERN Internal Reports MPS" RF 67-1 and 67-4. 1967.
10. Bigliani et al. Proceedings of the International Conference on High-Energy Charged-Particle Accelerators, Vol. I, Yerevan, izd-vo AN Arm. SSR, 1970, str. 433.
11. H.H. Umstätter. CERN Internal report. MPS/SR-Note, 70-29, 1970.
12. H.G. Hereward, A.Sörenssen. Private communication.
13. W.D.MacMillan. The theory of the potential. Dover, 1958.

Discussion.

V. A. Kolomenskiy. Synchrotron frequency in your explanation depends

on time. But you are close approach the transition energy, and how I do understand, you do not have data about the behavior of frequencies near the transition energy?

K. Reich. It is very difficult to measure the frequencies when you are located near the transition energy. However, it is possible more or less accurately to assume according to the results of measurement, and also by extrapolation, as will behave these frequencies. We fulfilled some extrapolation, since the direct measurements with the transition energy cannot be directly taken. According to these data it is possible to arrive at the conclusion that there is a steady transition of frequency, but not that jump which was by us obtained during calculations.

Page 29.

91. INTERACTION OF BEAM WITH INSTALLATION. ELECTRODYNAMICS OF RELATIVISTIC BEAMS IN VACUUM CHAMBERS OF VARIABLE CROSS SECTION.

Ye. Keyl, B. Tsotter.

(CERN).

The longitudinal stability of the beam of ungrouped drifting particles can be determined, comparing the impedance of connection/communication, caused by the surrounding vacuum chamber/camera, from the curved zero rate of growth in the plane of complex impedance. The character of this curve depends on energy distribution in the beam, but usually it is completely satisfactorily it is possible to approximate by the circumference of the normalized radius $2/\pi$. Then stability criterion can be written in the form [1]

$$\left| \frac{Z}{n} \right| \leqslant \frac{E_0}{e} \frac{|\eta|}{\Gamma L_0} \left(\frac{\Delta p}{m_0 c} \right), \qquad (1)$$

where z - impedance of connection/communication; n - number of the mode of disturbance/perturbation (number of wavelengths on the

perimeter); E_0 - rest energy, e - charge m_0 - rest mass of
particles; $\eta = -\frac{\omega}{\delta p} \times \frac{p}{\pi} = \gamma^{-2} - \gamma_\tau^{-2}$ (γ_τ - critical energy); γ - Lorenz
factor; I_0 - beam current; $2\Delta p$ - full/total/complete spread of
impulses/momenta/pulses. Substituting the value of the parameters for
the rings of CERN (ISR), we will obtain that the strictest
limitations are superimposed in the beginning of the process of the
accumulation when must be z/n<10 ohm. For the full/total/complete
accumulation the limit exceeds 1 kiloohm. These criteria are valid
for the slight disturbances of beam and give only the threshold and
the initial velocity of increase.

During the last few years is carried out the estimation of the
contributions of different elements/cells of vacuum chamber ISR.
Contribution from resistance of wall is 5 (1+j) ohm for the lowest
mode and it is considerably less for all higher modes. The impedance
of connection/communication of high-frequency resonators is reduced
to several ohms by strong feedback [2]. The contribution of the
suction electrodes is determined by their characteristic impedance
and for the lowest mode is approximately 3 j ohm. Bellows and other
changes in the cross section give mainly inductive additions. At the
low frequencies capacitive addition is created only by instability of
the type of "negative mass" and corresponds to the impedance of
connection/communication inedeal of the conducting vacuum
chamb r/camera. The active part or the full/total/complete impedance

remains less than 10 ohms, but inductive grows/rises to 20 ohms. Taking into account the severe limitations, which lead to the criterion 10 ohms (for example, utilizing design density in the phase space not yet achieved/reached in the injector), it is possible to see that the situation at the low frequencies is not ideal, but it can be considered acceptable.

Picture sharply is changed at the more high frequencies when the resonance effects of changes in the cross section can increase the impedance of connection/communication z/n several orders. Although the resonance frequencies on the whole are not multiple to frequency of revolution, resonance peak usually is sufficiently wide in order to overlap several modes. Furthermore, real frequency shift can prove to be sufficient in order to move resonance for the integral number of mode.

In order to rate/estimate the resonance impedances of connection/communication, we investigated [3] the simplified model, shown in Fig. 1. Disregarding the curvature of ring, we replaced vacuum chamber with the infinitely long straight cylinder of radius B. Periodically - with the period $2\pi R$, which corresponds to the perimeter of ring, divided into a number of equidistant elements/cells - a radius or chamber/camera grows/rises to value d at length g (" gap length), forming resonators. The concentric

cylindrical beam of particles of the radius and moves along the axis/axle of chamber/camera with speed βC. It is accepted that the undisturbed beam has uniform density with a small longitudinal divergence, which corresponds to the number of mode n (in this stage it is not compulsory whole). This disturbance/perturbation generates electromagnetic fields which, in turn, act on the moving/driving charged/loaded particles. Fields are found from the decision of wave equation with the appropriate boundary conditions on the metallic walls. For regions I and II corresponding to beam and chamber/camera, is found the infinite set of the three-dimensional/space harmonics which must be matched on E_z and H_φ with the infinite set of standing waves in the resonators (region III). The coefficients A of three-dimensional/space harmonics in the beam region are determined from the infinite system of equations with an infinite number of unknowns which can be compactly written in the matrix form

$$(U - \alpha NRN^{+} I) A = \alpha NRN^{+} B, \qquad (2)$$

where A - vector of the coefficients of three-dimensional/space harmonics in the beam region; B - vector with unique nonzero component $B_n \approx -\frac{\beta^2}{2\beta^2}$　U - unit matrix; $\alpha = q/2\pi R$; R and I - diagonal matrices/dies, which contain the relations of Bessel functions; N^{+} - hermitian is conjugated/combined with N;

$$N_{ps} = \frac{\pi \alpha p}{(\pi \alpha p)^2 - (\frac{\pi s}{2})^2} \begin{cases} \sin \pi \alpha p, \text{ при s четном}, \\ -i \cos \pi \alpha p, \text{ при s нечетном,} \end{cases}$$

Key: (1). with. (2). even. (3). odd.

where N_{ps} is obtained by the resolution by Fourier of the s mode on the boundary of resonator in terms of the period $2\pi R$; $U - \alpha N R N$ $I -$ "nucleus" of matrix equation.
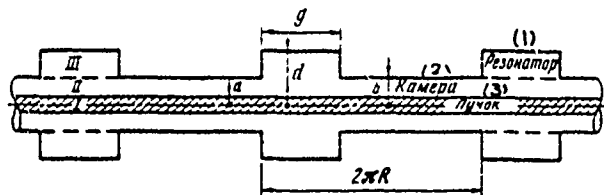
Fig. 1. Diagram of calculated geometry.

Key: (1). Resonator. (2). Chamber/camera. (3). Beam.

Page 30.

The impedance of connection/communication can be defined as (negative) ratio of stress/voltage to the current of disturbance/perturbation, moreover stress/voltage is obtained by the integration of the retarding electric field along the trajectory during one period. During the integration all three-dimensional/space harmonics, with exception of harmonic with the same number of mode, that also in disturbance/perturbation, they disappear and the impedance of connection/communication it takes the form

$$\frac{Z}{n} = -i \frac{2\beta Z_0}{\left(\frac{\omega a}{c}\right)^2} (A_n - 1). \quad (3)$$

Coefficient A_n is found from the decision of matrix equation (2). The direct decision or equation with the aid of the electronic

computer for parameters ISR is unrealizable, since for this are

necessary the matrices/dies whose dimensionality exceed a number of

resonance modes (this number usually on the order of several

thousands for the decimeter resonators on the circumference by length

on the order of 1 km). The artificial decrease of the length of

period leads to the yielding to working/treatment dimensionality of

matrices/dies and not must not considerably change results, if period

remains large in comparison with the sizes/dimensions of resonators.

Resonance frequencies are determined from the condition for

inversion into zero real parts of the determinant of the nucleus of

matrix equation.

Let us find by other now method approximations for the resonance

impedances. Converting/transferring to the new unknown

variable/alternating $A^1=N^+IA$, we will obtain the matrix equation

$$(U+\alpha N^+INR)A^1=\alpha N^+NRN^+B, \qquad (4)$$

which for the form it is similar to initial equation for A, but the

order of matrices/dies N and N^+ in the nucleus is changed by the

reverse. This completely changes convergence properties; now it is

necessary to transpose only very small matrices/dies. Furthermore,

nucleus becomes almost diagonal, and in the approximation/approach of

the smallness of the arguments of the Bessel functions of substances

to matrix/die I we obtain analytical decision. From the condition for

inversion into zero real parts of the denominator let us find the
resonance frequencies

$$\omega_{pq} = c\sqrt{\left(\frac{x_q}{b}\right)^2 + \left(\frac{\pi p}{q}\right)^2} \ , \quad (5)$$

where x_q - decision of the transcendental equation

$$x\frac{F_0(x)}{F_1(x)} = 2 ,$$

moreover $F_i(x) = Y_0(\lambda x)J_i(x) - J_0(\lambda x)Y_i(x), \ i=0,1.$

Values x_q depend only on geometric parameter $\lambda = d/B$. Index $p \geqslant 0$
can be defined as the number of axial mode in the resonator, and $q \geqslant 1$
- number of radial mode. For the lossless resonator the impedance of
connection/communication of the lowest axial mode

$$\left(\frac{z}{n}\right)_{0q} = \frac{8Z_0}{\pi} \ \frac{\beta^3 b^3}{Rq\delta} \ \frac{F_1^2(x_q)}{x^2} \sin^2\frac{x_q q}{2\beta b} \ . \quad (6)$$

For the practical targets it is possible to rewrite these
formulas (and formula for quality Q) in the form

$$\omega_{01} = 2,405\frac{c}{d}X_1(\lambda),$$

$$\left(\frac{z}{n}\right)_{01} = 200\beta\sqrt[3]{\sigma} \ \frac{(2d)^{5/2}}{qR}\Phi_1(\lambda)\sin^2\frac{\omega q}{2\beta c} ,$$

$$Q_{01} = 15\sqrt{(2d)\sigma} \ \Psi_1(\lambda),$$

where X_1, Φ_1 and Ψ_1 - functions, which depend only on λ and given in
Fig. 2. All these functions approach unity with the large ones λ,
this corresponds to the case of closed resonator (B=0), when these

formulas convert/transfer into the known expressions.

More detailed investigation snows that this
approximation/approach is correct only when along the duct, which
connects resonators, are not propagated waves. Usually this occurs
for the low modes.

Most obvious variation in the cross section in vacuum chamber
ISR - the frequently repeating transition from the circular to the
elliptical duct. Replacing elliptical chamber/camera by circular
chamber/camera with the equal cross-sectional area, we will obtain
the impedance of connection/communication $z/n=3.5$ ohm in the presence
of the lowest resonance near 1430 MHz, which corresponds to quality Q
on the order of 4900. The following higher resonance lies/rests only
scarcely higher in the frequency and has almost doubly larger
impedance (with the same quality). Subsequently the impedance drops
approximately as $\omega^{-3/2}$. Since the ring contains about 150 resonators,
the full/total/complete impedance of connection/communication is
almost 1 kiloohm. It is expected that the real value Q is somewhat
below due to the imperfection or the metallic surface of negligible
resistance of the end walls and other heterogeneities. Presence in
the majority of these chambers/cameras of cleaning electrodes
decreases the quality approximately from 1000 to 800. This still
corresponds to the impedance of connection/communication of more than
150 ohms. Therefore was initiated installation of extinguishing
resistances.
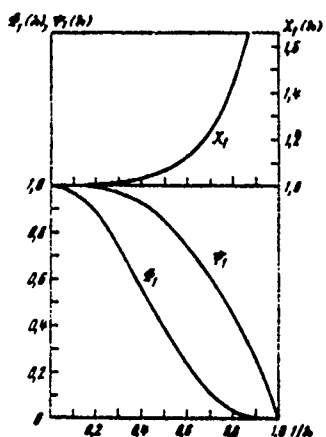
Fig. 2. Plotted function $X_1(\lambda), \Phi_1(\lambda)$ and $\Psi_1(\lambda)$

Page 31.

The series/row of other elements/cells of vacuum chamber ISR creates in the presence of the resonance the large impedances of connection/communication. Such elements/cells are, for example, large chambers/cameras, arranged/located for the experimental targets near the sections of intersection. Therefore inauguration of accelerator will occur with the use of simple X-shaped sections of intersection. Subsequently it is planned/glided to electrically separate/liberate large experimental chambers/cameras from the beam with the thin-walled extensions, which continue the geometry of vacuum chamber. These extensions must be the thickness the only of the order of the depth of skin-layer at the lowest resonance frequency (usually

several microns), but it is necessary to take measures against an
excessive increase in the role of the final conductivity of walls at
the low frequencies.

REFERENCES
1. E. Keil, W. Schnell. CERN Divisional Report, CERN-
   ISR-TII-RF/69-48, Geneva, 1969; К.Йонсен.
Proceedings of 7th International Conference on High-Energy
Charged-Particle Accelerators Vol II, Erezan. Izd. An Arm. SSSR,
1970, str. 131.
2. F. Ferger. This collection, t. II.
3. E. Keil, B. Zotter. CERN Divisional Reports,
   CERN-ISR-TII/70-30 and 70-33, Geneva, 1970.

Discussion.

A. A. Kolomenskiy. Was conducted any experimental check of effect,
which does exert ceramic coating?

B. Tsotter. Experimental measurements it was not carried out, but was
observed a change in quality and a change in the frequency band.

92. STUDY OF THE FLUCTUATIONS OF THE DIMENSIONS OF A BEAM IN CIRCULAR ACCELERATORS CONSIDERING THE SPATIAL CHARGE.

P. R. Zenkevich.

(Institute of theoretical and experimental physics).

Basic effect, which limits the intensity of beam in the circular accelerators of protons, the decrease of the frequency of transverse vibrations due to the pushing apart, which leads to the intersection of parametric and summation resonances. In the majority of works [1-3], in which was examined this effect, was applied the model of the "monochromatic" beam, which does not have spread along the betatron frequencies. With the aid of this model it was shown that besides classical parametric resonance there exists and the "coherent" parametric resonance, on which are swung coherent oscillations of the size/dimension of beam. Purpose of this work - investigation of the effect of dispersion in the frequencies on free and induced coherent oscillations envelope of particles. The solution of this problem makes it possible to also give the simple treatment of the effect of a change in the harmonic of gradient near the incoherent resonance in the presence of dispersion in the

frequencies, considered earlier in A. G. Stadnikov's work [4].

We will be restricted subsequently to the account to the dispersion of beam in the betatron frequencies, connected with the spread along the impulses/momenta/pulses (effect of the dispersion in the frequencies, connected with the nonlinearity of gradient, leads to the qualitatively similar results). Let us examine first free coherent oscillations envelope of particles. In the presence of the dispersion of beam for the frequencies the equation of V. V. Vladimirskiy and I. M. Kapchinskiy in the "smooth" approximation/approach can be written in following form [5]:

$$q''_r + v_r^2 q_r - \frac{1}{q_r^3} = q_r \, 4 \left| \Delta v_k \right| \left\langle \frac{1}{q_r(q_r + q_z)} \right\rangle, \quad (1)$$

where $q_v = v_{max}/\sqrt{V_\phi}$; v and z - two transverse coordinates; V_ϕ - phase volume; sign $\langle \rangle$ indicates averaging on the ensemble; Δv_k - Coulomb shift/shear of betatron frequency. Converting/transferring from g to Δg and linearizing on $\Delta y/y$, we will obtain the equation

$$\Delta q'' + (4 v^2 - 8v|\Delta v_k|) \, \Delta q = -3v \, |\Delta v_k| \langle \Delta q \rangle. \quad (2)$$

Let us present $\langle \Delta g \rangle$ in the form: $\langle \Delta g \rangle = c \exp (i \omega \theta)$. Substituting this expression in (2), we will obtain for ω the following dispersion equation:

$$1 = 0,375 \, |\Delta v_k| \int_{v_0 - \Delta v}^{v_0 + \Delta v} \frac{f(v) dv}{\frac{\omega}{2} - v + |\Delta v_k|}, \quad (3)$$

where

$$\int_{\nu_0-\Delta\nu}^{\nu_0+\Delta\nu} f(\nu)d\nu = 1.$$

During the calculation of integral in (3) should be considered the following fact: if the pole of integrand falls into the range of integration ($|\frac{\omega}{2}-\nu_0 +|\Delta\nu_k||\le\Delta\nu$), then the linearization of equation for the envelope, strictly speaking, is wrong. Actually/really, in this case will be located the particles (with ν_0, the close ones to $\omega/2$), which possess the infinite amplitude of oscillations.

This difficulty can be removed, after assuming that in the system is a fading whose value is more than the width of the parametric resonance, created by coherent oscillations of envelope.

Page 32.

Then the deviations of envelope it is everywhere final, and dispersion equation acquires following form [6]:

$$1-0{,}375\,|\Delta\nu_k|\left[i\pi f\left(\frac{\omega}{2}+|\Delta\nu_k|\right)+ \right.$$
$$\left. + \mathcal{P}\int_{\nu_0-\Delta\nu}^{\nu_0+\Delta\nu} \frac{f(\nu)d\nu}{\frac{\omega}{2}-\nu+|\Delta\nu_k|}\right], \qquad (4)$$

where P before the integral means that is taken its principal value.

The analysis of this dispersion equation shows that its decision

exists only when is satisfied the following condition:

$$\Delta\nu \leq |\Delta\nu_k| \cdot 0,6. \qquad (5)$$

Let us examine now forced oscillations of envelope. When the resonance harmonic of gradient is present, the linearized equation for the envelope takes the form

$$\Delta q'' + 4\nu^2 \Delta q - 8|\Delta\nu_k|\Delta q = -3|\Delta\nu_k|\langle\Delta q\rangle + \tau q_0 \cos k\theta \quad (6)$$

Decision of equation (6)

$$\frac{\Delta q}{q_0} = \frac{\tau \cos k\theta}{8\nu} \frac{\left\langle \dfrac{1}{k/2 - \nu + |\Delta\nu_k|} \right\rangle}{1 - 0,375|\Delta\nu_k|\left\langle \dfrac{1}{k/2 - \nu + |\Delta\nu_k|} \right\rangle} . \quad (7)$$

Zero denominators in [7] determine the frequencies of free coherent oscillations. Hence it follows that the condition for existence of the coherent free oscillations (inequality (5)) it is simultaneously the condition for existence of the resonance of coherent oscillations of envelope.

Let us rewrite equation (7) in the form

$$\left|\frac{\Delta q}{q_0} \middle/ \frac{\tau\cos k\theta}{8\nu(\nu - k/2)}\right| = \left|\frac{\varphi(\alpha,\beta)}{1 - 0,375\alpha\varphi(\alpha,\beta)}\right| = F(\alpha,\beta), \quad (8)$$

where

$$\varphi(\alpha,\beta) = \int_{-1}^{+1} \frac{f_1(x)dx}{\dfrac{\alpha - 1}{\beta} - x} ; \qquad (9)$$

$$\alpha = \frac{|\Delta\nu_k|}{\nu - k/2}, \quad \beta = \frac{\Delta\nu}{\nu - k/2}, \quad f(\nu)d\nu = f_1(x)dx. \quad (10)$$

As can be seen from the plotted function $F(\alpha, \beta)$ of that shown

in Fig. 1, an infinite increase in the amplitude of coherent oscillations at point $\alpha \sim 1.6\,(k/2 - \nu - 0.625\,|\Delta\nu_k|)$ occurs only with $\beta < 0.6$. For the high values β coherent resonance is crowded of large ones α.

Upon transfer of incoherent resonance ($\alpha=1$, $k/2 = \nu - |\Delta\nu_k|$) the amplitude of coherent oscillations always remains final. In spite of this for the polychromatic beam is possible the death of particles, since the amplitudes of the oscillations of particles, close to the resonance, can be swung to the very high values. If the width of resonance $\Delta\nu_p \ll \Delta\nu$ (usually this requirement it is made), then particles with different ν in the turn transfer incoherent resonance, moving in the joint field, formed by applied field and the field of remaining beam. In this case the coherent play envelope of particles leads to the emergence of the resonance harmonic of the gradient of coulomb field. The ratio of the amplitude of the sum of the external and Coulomb harmonics of gradient to the amplitude of external harmonic is expressed by the formula

$$\frac{\Gamma'}{\Gamma} = \frac{1}{|1 - 0.375\,\alpha\,\varphi(\alpha,\beta)|} = F_1(\alpha,\beta). \quad (11)$$

Plotted function $F_1(\alpha,\beta)$ when β as the parameter is shown in Fig. 2.
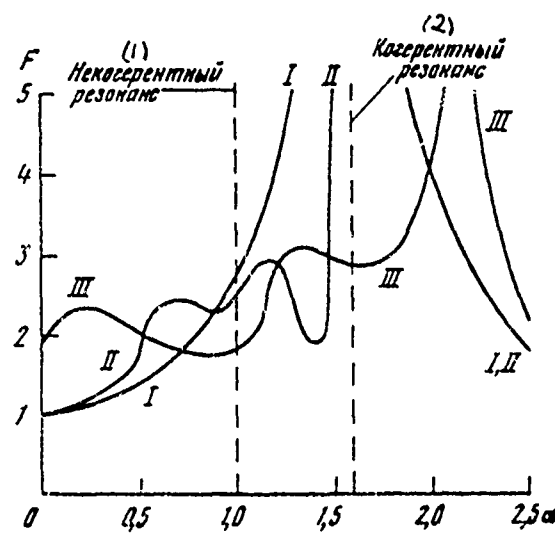
Fig. 1. Plotted function $F(\alpha, \beta)$ when β as the parameter. I - $\beta=0$; II - $\beta=0.5$; III - $\beta=1.2$.

Key: (1). Incoherent resonance. (2). Coherent resonance.
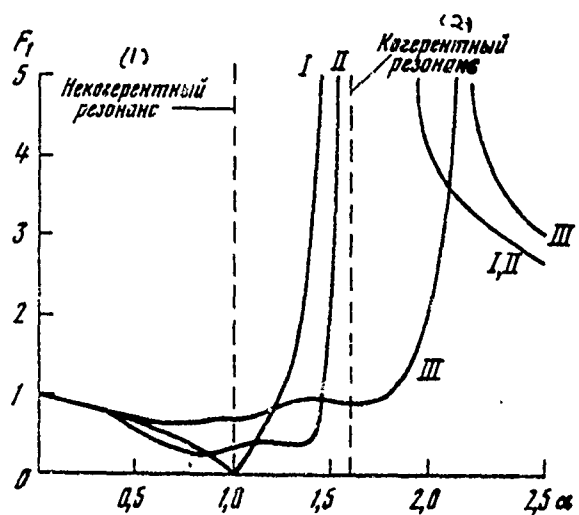
Fig. 2. Plotted function $F_1(\alpha, \beta)$ when β as the parameter. Designations the same as in Fig. 1.

Key: (1). Incoherent resonance. (2). Coherent resonance.

Page 33.

In conclusion let us formulate the basic special features/peculiarities of the effect in question, which follow from the analysis of the obtained formulas:

1) the basic effect, which appears during free and forced oscillations of envelope, creation of the resonance "Coulomb" harmonic of gradient; 2) the betatron frequency of single particles

(at least, in the first order on $\Delta g/g$) does not depend on the oscillations of envelope[1]); 3) the action of the Coulomb harmonic of gradient leads to the appearance of coherent parametric resonance and to a change in the width or incoherent parametric resonance; 4) upon the large dispersion of beam in frequencies $(\Delta \nu \geq \alpha_6 |\Delta \nu_k|)$ "coherent" parametric resonance disappears; 5) upon a small dispersion of beam in the frequencies, on the contrary, disappears incoherent parametric resonance, since the appearing Coulomb harmonic of gradient compensates external harmonic.

FOOTNOTE [1]. A. A. Kolomenskiy and A. G. Polukhin [7] obtained another result: Coulomb shift/smear decreases in the first order on $\Delta g/g$. This result, apparently, is incorrect, moreover the reason for error - incorrect use of a method of averaging. This question will be in detail discussed in the more extensive article, which is prepared for print. ENDFOOTNOTE.

REFERENCES.
1. L. Smit. Proceedings of International Conference on Accelerators.
2. L. Lyapostol'. Tam. Zhe, str. 900.
3. P. Lapostolle, L. Torndalle. ISR/300-LIN/66-27, 1966.
4. A. G. Stadnikov. PTE, 1968, No. 3, 22.
5. I.M. Kapchinski, V.V. Vladimirski. Proc. Internat. Conf. on High Energy Accelerators and Instrumentation. CERN, 1959, P, 274.
6. Yu.G. Globenko, D. G. Koshkarev. PTE, 1968, No. 6, 17.
7. A.A. Kolmenskiy, A.G. Polukhin. Journal of Moscow University, un-ta, 1968, No. 5, 81.

93. DEPENDENCE OF THE MAXIMUM INTENSITY OF PROTON ACCELERATORS ON THE CHARGE DISTRIBUTION IN THE CLUSTERS.

Yu. M. Tereshkin, Yu. A. Khlestkov.

(Moscow physical engineering institute).

In the accelerators of protons the upper limit in the intensity is limited to the disturbance/breakdown of the mechanism of phase stability under the action of the space charge of clusters. There is a series/row of models for describing the stationary axial motion. In tne work of A. D. Vlasov is examined the representation of clusters in the form of evenly charged/loaded ellipsoids [1], in I. M. Kapchinskiy's works the clusters are represented in the form of cylinders with density distribution of charge, repeating course separatrices [2]. Problem in the approximation/approach of the shielded beam is solved in the work of A. N. Lebedev [3]. The case of neutral equilibrium is examined in works [3, 4].

In this work are presented the results of the investigation of the qualitative dependence of estimation on the model taking into account the incomplete shielding of the field of clusters by walls.

Task is examined in known assumptions [1-3], which make it
possible to bring together it to the one-dimensional. In this case
the axial motion is described by the equation of oscillator and for
the cyclic and linear accelerators is characterized by only
expression for effective mass [5]. Clusters are represented in the
form of the cylinders of a radius a and by length $2b = 2\frac{v_s}{\omega}\psi_m$ with the
self-consistent charge distribution, which are the exponential
function of the potential of the "pit" of $V(\phi)$:

$$\rho(\phi) = \frac{e\,N\omega}{2\pi a^2 v_s \psi_m}\left[\frac{V(\phi)}{V(\phi_s)}\right]^{n+\frac{1}{2}},\ \left(n = -\frac{1}{2}, 0, \frac{1}{2}\ldots\right) (1)$$

where N - number of particles in the cluster. With $n=-1/2$ we obtain
evenly - the charged/loaded cylinder (Q_1) when $n=0$ - cylinder with
the distribution, repeating course separatrices (ϕ_2), when $n=1/2$ -
cylinder with the distribution, repeating the form of potential well
(ϕ_3), when $n=3/2$ - cylinder with the distribution, repeating the
course of the square of potential well (ϕ_4). Data of distribution
cover the basic interesting cases. All noted one-dimensional
distributions in the principle are "almost" self-consistent. However,
their examination makes sense in the approximation/approach of
strongly elongated on ϕ clusters or strong relativity. Furthermore,
as showed numerical calculations, small divergences in the form of
distribution $\rho(\phi)$ weakly affect estimation N_{max}.

The canonical potential $V(\phi)$ was located by the method of Green's function. The task about the stability of oscillations was reduced to the integral equation whose nucleus both for the cylindrical chamber/camera and upon the approximation of chamber/camera by two parallel to infinite ones planes is described well by exponential curve [5]. The decision of integral equation is found in the first approximation,; is obtained expression for a maximum number of particles in the cluster:

$$N_{max} = 10^6 \varepsilon_0 \tau_s^2 \beta_s^2 \lambda^2 \varphi_6^4 F^i(\mu), \qquad (2)$$

where ε_0 - average/mean intensity/strength of field on the axis of accelerator; λ - wavelength of generator; $F^i(\mu)$ - form factor; depending on the means of distribution $\rho(\phi)$:

$$F^i(\mu) = \begin{cases} 31{,}4\, x_M^3\, (1 - \tfrac{2}{3}\, x_M)\mu - u_1, \\ 42{,}3\, \mu & - u_2, \quad (3) \\ 6{,}6 & - u_3, \\ 2{,}54 & - u_4, \end{cases}$$

where

$$x_M = \frac{\varphi_M}{\varphi_3}, \quad \mu = \frac{a}{\tau_s b} \ll 1.$$

Page 34.

Are explained the following laws. For the even distribution (also for the ellipsoid) steady states are possible with any

size/dimension of cluster. In this case $N=0$ both when $\Psi_M = -\frac{3}{2}\varphi_S$

(undisturbed separatrix) and with the contraction of cluster into

point $\Phi_M = 0$. Phase density nowhere goes to infinity. Maximum charge is

reached at certain intermediate size/dimension of cluster $0 < x_M < \frac{3}{2}$.

For the remaining collapsible/dropped to the edges of cluster

distributions $\rho(\phi)$ the cluster virtually does not have the

capability to be compressed on the phase with increase in N due to

the appearance of the local minimum $V(\phi)$ on the left boundary of

cluster (distribution $\overset{T_S}{\phi_2}$), or maximum $V(\phi)$ in the synchronous phase

(distribution $\overset{T_S}{\phi_4}$) which disrupts stability. It is interesting that

$$N_{max} = \begin{cases} T_S \, a\, \alpha\, \varphi_S^3 \; - u_1, \, u_2, \\ T_S^2 \, x^2 \, \varphi_S^4 \; - u_3, \, u_4, \end{cases}$$

i.e., a maximum number of particles in the cluster for the sharply

collapsible/dropped distributions more strongly depends on energy,

the wavelengths and synchronous phase does not depend on a radius of

cluster.

A maximally possible intensity is achieved by the distribution,

repeating the course of potential well $(\overset{T_S}{\phi_3})$. This case corresponds to

the neutral equilibrium when longitudinal field within the cluster is

constant, potential well is converted into the line and phase density

approaches infinity. The same conclusion/output is obtained in works

[3, 4].

The displacement of synchronous phase under the action of the field of beam is negligibly small for all distributions, with exception of the ellipsoid for which maximum increase v_8 composes the value of order 15o/o from quiescent value [1]. This can be explained by the fact that the electrostatic center of gravity where the field of cluster is equal to zero, is close to the synchronous phase.

Model examined here of the incompletely shielded bundle occupies the intermediate position between the free beam (walls are absent) and shielded beam [3]. For these limiting cases the corresponding form factors take form [5]

$$
F_0^{(i)} = \begin{cases} 23.5\, x_M^3 (1 - \frac{2}{3} x_M)\, \mu - u_1, \\ 15.8\, \mu & \cdots u_2, \\ \dfrac{9.92}{\ln\frac{4}{\mu} - 2} & - u_3, \\ \dfrac{3.8}{\ln\frac{4}{\mu} - 2} & - u_4, \end{cases}
\qquad
F_{3\mu p}^{i} = \begin{cases} \infty & - u_1, \\ 42.3 & - u_2, \\ 8.6 & - u_3, \\ 2.54 & - u_4 \end{cases}
$$

$$(4)$$

Hence it is possible to draw the conclusion that the account of walls increases the maximum intensity (for ϕ_3 with $\mu \sim 10^{-3} \sqrt{4}$ times), for the steady distributions approximation/approach of the shielded beam gives the high results, and during the sharply collapsible/dropped distributions beam is virtually completely

shielded. During the calculation of the maximum intensity of accelerator it is necessary to consider the concrete/specific/actual means of distribution $\rho(\phi)$. Thus, for instance, with $\mu \sim 10^{-3}$ estimations can differ to two orders, which is substantial.

Table gives the estimates of the magnitude of a maximum number of particles in orbit (ellipsoid, $\ell_1 - \phi_4$) for the acting and projected/designed proton synchrotrons for the high energy. Results are compared with the value of maximum intensity due to permissible Coulomb frequency shift of betatron oscillations, which was calculated from the formula

$$q N_{max}^{\delta} = \frac{5 \pi \epsilon_0 E_0}{e^2 c^2} \nu_{x0} r_s \omega_s^2 a^2 \delta \phi. \qquad (5)$$

During conclusion/output (5) is taken into consideration the wall effect of chamber/camera and magnet poles, moreover it is placed $\alpha/h = 1/2$ $\alpha/g = 1/3$ (h - radius of chamber/camera, 2g - distance between the magnet poles). Table gives the comparison of the maximum intensity of accelerators on the betatron (N_{max}^{δ}) and synchrotron (N_{max}^{c}) oscillations with the achieved/reached or calculated values.

(1) Ускоритель	$E_{max},$ ГэВ (1a)	$eV_s,$ МэВ (1b)	$R,$ км	γ_i	$\lambda,$ м	$\varphi_s,$ град (2)	q	$\mu \cdot 10^{-3}$
(3a) ЦЕРН	28	0,054	0,1	1	100	30	20	4,5
(4) Брукхейвен	33	0,1	0,13	1	214	30	12	1,8
(5) Серпухов	76	0,38	0,24	1,1	115	49	30	2,5
(6) Беркли	(200)	0,35	1	8	5,75	47	758	1,4
(3a) ЦЕРН	(300)	1	1,2	8	1,64	45	4500	6
(6a) СССР	(500)	12	2,4	18	2,8	45	6000	1,1
(6a) СССР	(1000)	52	–	–	–	–	–	–

y_{x0}	$N_{факт},$ част/имп (3)	$N_{max},$ част/имп (b)	$N^c_{max},$ част/имп (4)				
			3	$Ц_1$	$Ц_2$	$Ц_3$	$Ц_4$
6,3	10^{12}	$6\cdot10^{11}$	10^{11}	$8\cdot10^9$	$3\cdot10^{10}$	10^{12}	$4\cdot10^{11}$
8,8	10^{12}	$5\cdot10^{11}$	$4\cdot10^{11}$	10^{10}	$5\cdot10^{10}$	$4\cdot10^{12}$	$2\cdot10^{12}$
8,3	$1,5\cdot10^{12}$	$3,5\cdot10^{12}$	10^{13}	$6\cdot10^{11}$	$2\cdot10^{12}$	10^{14}	$5\cdot10^{13}$
16,8	$3\cdot10^{13}$	$3\cdot10^{13}$	$3\cdot10^{14}$	$8\cdot10^{12}$	$3\cdot10^{13}$	$4\cdot10^{15}$	10^{15}
28,3	$3,3\cdot10^{13}$	$8\cdot10^{13}$	$4\cdot10^{14}$	$4\cdot10^{13}$	10^{14}	$3\cdot10^{15}$	10^{15}
33,3	$3\cdot10^{13}$	$5\cdot10^{13}$	$3\cdot10^{15}$	$7\cdot10^{13}$	$3\cdot10^{14}$	$4\cdot10^{16}$	10^{16}
–	–	–	10^{18}	$3\cdot10^{14}$	10^{15}	$2\cdot10^{17}$	$7\cdot10^{16}$

Key: (1). Accelerator. (1a). GeV. (1b). MeV. (2). deg. (3). part./pulse. (3a). CERN. (4). Brunkheyven. (5). Serpukhov. (6). Berkeley. (6a). USSR.

REFERENCES

1. A.D. Vlasov. All-Union Conference on Charged-Particle Accelerators, tom 2, izd. VINITI, 1968, str. 404.

2. I.M. Kapchinskiy. Dynamics of Particles in Linear Resonance accelerators, M., Atomizdat, 1966.

3. A.N. Lebedev. Doctoral dissertation, FIAN, 1968.

4. A.D. Vlasov, Proceedings of 7th International Conference on Hihg-Energy Charged-Particles Accelerators, Vol II, Yerevan, izd-vo AN Arm. SSR, 1970, str. 376.

5. Yu.A. Khlestkov, Yu.M. Tereshkin, ZhTF, 1971, 41, No. 2, 339.

Page 35.

94. METHOD OF GAUSSIAN BRACKETS IN THE THEORY OF ACCELERATORS.

A. D. Dymnikov.

As is known, the analysis of particle motion in the cyclic and linear accelerators, and also in any long channels, which consist of the set of discrete/digital lenses, requires the solution of the equations of Mathieu-Hill of form [1, 2]

$$u'' - q(s)u = 0, \quad q(s+L) = q(s). \quad (1)$$

Here S - arc length of orbit (in the cyclic accelerators) or longitudinal coordinate or time (in the linear accelerators); u - transverse divergence of particle, $q(s)$ - the periodic function, which describes structure accelerating - focusing of system; L - length of the element/cell of periodicity, measured along s; primes indicate differentiation with respect to s.

The standardized/normalized decision of equation (1) in the case of the arbitrary function $q(s)$ let us write in the matrix form

$$\begin{pmatrix} u \\ u' \end{pmatrix} = R_{s_0}^s \begin{pmatrix} u_0 \\ u'_0 \end{pmatrix}, \quad (2)$$

where u_0 and u'_0 - values u and u' at the initial fiducial mark s_0.

Matrix/die $R_{s_0}^s$ is calibrated in such a way that

$$R_{s_0}^{s_0} = \begin{pmatrix} 1 & 0 \\ 0 & 1 \end{pmatrix} = E, \qquad (3)$$

but its Wronskian is equal to 1 with all s.

In many practical applications of theory of periodic focusing function $g(s)$ they approximate by stepped, or piecewise constant function. Therefore let us examine the case when the period of focusing has such structure, that

$$g(s) = g_j = const, \; s_{j-1} \leq s < s_j \; (j = 1, 2 \ldots n) \qquad (4)$$

Whereas it is shown in works [3, 4], if we introduce into the examination of the bracket of Gauss, determined according to recurrence formulae

$$[a_1 \ldots a_n] = a_n [a_1 \ldots a_{n-1}] + [a_1 \ldots a_{n-2}], [\;] = 1, [a_1] = a_1, \tag{5}$$

then for the matrix elements $R_{s_0}^{s_0+L}$ we will obtain

$$\left(R_{s_0}^{s_0+L}\right)_{11} = \left[c_1 t_2 \ldots t_j c_j t_{j+1} \ldots c_n t_{n+1}\right]_{s_0}^{s_0+L},$$

$$\left(R_{s_0}^{s_0+L}\right)_{12} = \left[t_1 c_1 \ldots t_j c_j t_{j+1} \ldots c_n t_{n+1}\right]_{s_0}^{s_0+L}, \tag{6}$$

$$\left(R_{s_0}^{s_0+L}\right)_{21} = \left[c_1 t_2 \ldots t_j c_j t_{j+1} \ldots t_{n-1} c_n\right]_{s_0}^{s_0+L},$$

$$\left(R_{s_0}^{s_0+L}\right)_{22} = \left[t_1 c_1 \ldots t_j c_j t_{j+1} \ldots t_{n-1} c_n\right]_{s_0}^{s_0+L}.$$

Here

$$t_j = t_{j-1}^0 + t_j^0, \; t_0^0 = t_{n+1}^0 = 0 \, (j = 1, 2 \ldots n+1) \tag{7}$$

If we assume

$$s_n = s_0 + L, \; \Delta s_j = s_j - s_{j-1} \; (j = 1,2, \ldots n), \quad (8)$$

then the form of the function c_j and t_j^o can be determined on the table.

In the examination of the fluctuations of particles in the accelerators important value has the matrix/die of period $R_s^{s+L}[1,2,5]$ through which it is determined the series/row of basic characteristics of oscillations. Since during the conclusion/output of expressions (6) it did not nave value, is the subscript of matrix/die R permanent or variable value, then the matrix/die of period will take the form

$$(R_s^{s+L})_{11} = \left[c_k t_{k+1} \cdots t_j c_j t_{j+1} \cdots c_{k+n} t_{k+n+1} \right]_s^{s+L},$$

$$(R_s^{s+L})_{12} = \left[t_k c_k \cdots t_j c_j t_{j+1} \cdots c_{k+n} t_{k+n+1} \right]_s^{s+L}, \quad (9)$$

$$(R_s^{s+L})_{21} = \left[c_k t_{k+1} \cdots t_j c_j t_{j+1} \cdots t_{k+n} c_{k+n} \right]_s^{s+L},$$

$$(R_s^{s+L})_{22} = \left[t_k c_k \cdots t_j c_j t_{j+1} \cdots t_{k+n} c_{k+n} \right]_s^{s+L}, \; .$$

where are used the designations

$$t_j = t_{j-1}^o + t_j^o, \; t_{k-1}^o = 0, \; t_{k+n+1} = t_{k+n}^o \; (j = k, k+1, \ldots k+n)(10)$$

(1) Функция	$q_j > 0$	$q_j < 0$	$q_j = 0$
c_j	$\sqrt{q_j}\ \mathrm{sh}(\Delta s_j \sqrt{q_j})$	$-\sqrt{q_j}\sin(\Delta s_j\sqrt{q_j})$	0
t_j^o	$\dfrac{1}{\sqrt{q_j}}\mathrm{th}(\tfrac{1}{2}\Delta s_j\sqrt{q_j})$	$\dfrac{1}{\sqrt{q_j}}\mathrm{tg}(\tfrac{1}{2}\Delta s_j\sqrt{q_j})$	$\tfrac{1}{2}\Delta s_j$

Key: (1). Function.

Page 36.

In view of periodicity $q(s)$ we have

$$q_{n+\tau} = q_\tau \quad (\tau = 1, 2, \ldots k).\qquad (11)$$

Taking into account expressions (10)-(11) functions c_j and t_j^o can be determined on the table where Δs_j are determined by the following expressions:

$$\Delta s_j = s_j - s_{j-1} \quad (j = k+1, k+2, \ldots n)$$

$$\Delta s_{n+l} = s_l - s_{l-1} \quad (l = 1, 2, \ldots k-1)\qquad (12)$$

$$\Delta s_k = s_k - s, \quad \Delta s_{k+n} = s - s_{k-1}.$$

Let us find now, substituting expressions for the matrix elements in the form of the brackets of Gauss, value $\cos \mu$, where μ - known in the theory floquet the characteristic index

$$\cos\mu = \frac{1}{2}\left\{\left(R_s^{s+L}\right)_{11} + \left(R_s^{s+L}\right)_{22}\right\} = \left\{\left(R_0^L\right)_{11} + \left(R_0^L\right)_{22}\right\} =$$

$$= \frac{1}{2}\left\{\left[c_1 t_2 \ldots c_n t_{n+1}\right]_0^L + \left[t_1 c_1 \ldots t_n c_n\right]_0^L\right\}.\qquad (13)$$

Here c_i and t_i are determined by table taking into account

expressions (7)-(8) for $s_0=0$.

Expression for $\cos \mu$ can be presented as expansion in the

series/row in terms of the particular brackets of Gauss for the

periodic structure from even and odd number of elements/cells:

$$\cos \mu = \frac{1}{2}\left\{(t_1+t_{n+1})[c_1\cdots c_n]+(c_1+c_n)(t_2\cdots t_n)+ \right.$$
$$+(t_2+t_n)[c_2\cdots c_{n-1}]+$$
$$\left. +\ldots+(c_{n/2}+c_{n/2+1})[t_{n/2+1}]\right\}+1, \quad n=2m\,(m=1,2,\ldots); \tag{14}$$

$$\cos \mu = \frac{1}{2}\left\{(t_1+t_{n+1})[c_1\cdots c_n]+(c_1+c_n)[t_2\cdots t_n]+ \right.$$
$$\left. +(t_2+t_n)[c_2\cdots c_{n-1}]+\ldots+(t_{\frac{n+1}{2}}+t_{\frac{n+3}{2}})[c_{\frac{n+1}{2}}]\right\}+1,$$
$$n=2m+1\,(m=0,1,2,\ldots).$$

Expressions (14) are highly useful, when the structure of period

has any symmetry.

The stability condition of oscillations will be written in the

form

$$-1<\cos \mu<1, \tag{15}$$

where $\cos \mu$ is determined by expressions (13) or (14).

The general solution equation (1), or equation of individual

trajectory, can be written through modulus/module and phase of the

function of Floquet:

$$u = B\rho \cos\left(\int_0^s \frac{ds}{\rho^2} + \theta\right),$$

$$u' = B\frac{d\rho}{ds}\cos\left(\int_0^s \frac{ds}{\rho^2} + \theta\right) - B\frac{1}{\rho}\sin\left(\int_0^s \frac{ds}{\rho^2} + \theta\right), \quad (16)$$

where B and θ - the constants, which depend on initial conditions, ρ^2 - square modulus of the function of Floquet, it is determined by the expression

$$\rho^2 = \frac{1}{\sin\mu}\left[t_1 c_1 \cdots c_n t_{n+1}\right]_s^{s+L}. \quad (17)$$

Eliminating sin and cos of expressions (16), we will ~~ in the equation of the ellipse of Floquet or projection of t. phase volume of the beam:

$$\frac{1}{\rho^2}u^2 + \rho^2(\gamma u + u')^2 = B^2, \quad (18)$$

where ρ^2 it is determined according to (17), and function γ takes the form

$$\gamma = \frac{\left[c_1 t_2 \cdots c_n t_{n+1}\right]_s^{s+L} - \left[t_1 c_1 \cdots t_n c_n\right]_s^{s+L}}{2\left[t_1 c_1 \cdots c_n t_{n+1}\right]_s^{s+L}} \quad (19)$$

Here $B^2 = S/\pi$ where S - area of the ellipse over which moves the point, which depicts oscillations on the phase plane u, u'.

The method of the brackets of Gauss can be used also in the arbitrary structure of periodic function $g(s)$ for the approximate determination of matrices/dies R_s^{s+L} and $R_{s_0}^{s_0+L}$. For determination R_s^{s+L} it

suffices to break the interval of the variation s from s to s+L on r

sufficiently small intervals $\Delta s_j (j=1,2,...r)$ so that in each subinterval

would be fulfilled the inequality

$$\sqrt{g_j}\, \Delta s_j \ll 1. \qquad (20)$$

Then the approximation formulas for the matrix elements of the

matrix/die of period are written as follows:

$$\left(R_{s}^{s+L} \right)_{ik} \approx \left[a_{3-k} a_{3-k+1} \cdots a_{2r+2-i} \right]_{s}^{s+L}, \qquad (21)$$

$$(i, k = 1,2),$$

where

$$a_{2j-1} = \frac{1}{2}(\Delta s_{j-1} + \Delta s_j),\quad a_{2j} = g_j \Delta s_j (j=1,2...r+1),$$
$$(22)$$
$$\Delta s_0 = 0,\quad \Delta s_j = s_j - s_{j-1},\quad s_0 = s,\quad s_r \equiv s+L.$$

Analogously will be written matrix/die $R_{s_0}^{s_0+L}$, which is obtained from

the matrix/die of period by replacement s on s_0.

REFERENCES

1. A. A. Kolomenskiy, A.N. Lebedev, Theory of Cyclic Accelerators, M., 1962.

2. I.M. Kapchinskiy. Dynamics of Particles in Linear Resonance Accelerators, M., izd-vo "Nauka", 1966.

3. A.D. Dymnikov. ZhTF, 1968, 38, 1120.

4. P.W. Hawkes, Brit. J. Appl. Phys., 1967, 18, 545.

5. Yu.Ya. Lembra. ZhTF, 1965, 35, 574.

Page 37.

Session VIII.

PARTICLE DYNAMICS IN ACCELERATORS, ACCUMULATORS, AND INSTALLATIONS
WITH OPPOSING BEAMS (2).

95. SOME FEATURES OF PARTICLE DYNAMICS IN A SPECTROMETRIC CYCLOTRON.

A. A. Kolomenskiy, A. F. Pateyev.

(Physical institute im. P. N. Lebedev of the AS USSR).

The special feature/peculiarity of spectrometric cyclotron (STs)
- high intensity (~100 μA) and energy homogeneity (~10^{-4}) of the
accelerated beam which is achieved by the proper identification of
parameters of STs and their maintenance in the prescribed/assigned
limits. The selection of these parameters and allowances is conducted
on the basis of the results of the investigation of particle dynamics
in the cyclotron.

We investigated two "modes/conditions": static and dynamic.
Static behavior corresponds to the free particle motion which occurs

in the absence of accelerating field. Dynamic, mode/conditions characterize the process of particle acceleration.

1. Static behavior.

In the static state or motion of particle in STs is described by the system of nonlinear equations whose exact solution can be found only with numerical integration. However, for the estimations it suffices to be restricted to linear approximation/approach. In this approximation/approach the equations of motion can be solved analytically. Analytical calculation is especially useful in the initial stage of design of STs, when it is necessary "to look over" a large number of versions. However, the selection of final (working) version must be conducted on the basis of the results of numerical calculation.

As the calculated version of STs was undertaken the version with the following basic parameters[1]:

Maximum energy (protons) ... 80 MeV.

Energy of the injection ... 1 MeV.

Average/mean value of magnetic field in the central region ...

4970 Oe.

Cyclotron radius ... 626 cm.

An azimuthal variation in the magnetic field - sinusoidal ...

$H = H_0 [f_0(r) + f_1(r) \cos N\theta]$.

FOOTNOTE [1]. I. Ya. Barit et al. Preprint Lebedev physics inst. No 15, M., 1969. ENDFOOTNOTE.

A number of sectors N, "flutter" and a radial dependence of magnetic field were varied.

Dependence of frequency of betatron on N.

Fig. 1 gives the graph/diagrams of dependence $\nu(r)$ for different N at one and the same value of flutter, which corresponds $f_0 = f_1$. From the graphs/curves it is evident that the version with N=3 must be excluded from the examination, since ν_r in this version too closely it approaches stability limit.

Dependence ν on the azimuthal form of field is illustrated by graphs/curves in Fig. 2. This dependence is different for the radial and bouncing. If for the radial oscillations the harmonics of field

weakly affect frequency, then for the vertical ones they are determining.

Isochronism. Sufficient condition, which ensures the isochronism of particle motion in the cyclotron, the constancy of the harmonics of a variation in the field and the special law of a change in the middle field. In the first approximation, this law takes the form

$$\langle H \rangle \sim \frac{1}{\sqrt{1 - \left(\frac{v}{v_c}\right)^2}}.$$

However, for STs this approximation/approach proves to be too rough. Actually/really, as it follows from the graph/curve, given in Fig. 3, nonisochronicity of this "isocaronal" field reaches on terminal radii 10^{-3}, which exceeds the limits of that permitted.

In order to find the necessary law of a change in the middle field, it was necessary to rate/estimate its effect, and also effect of the fundamental harmonic of a variation in the field for the period of revolution of particles. For this purpose were calculated dependences $T_0(v)$ for different laws of $f_0(v)$ and $f_1(v)$. The obtained results (Fig. 3) show, as one should change $f_0(v)$ with the given one $f_1(v)$ in order to attain constancy T_0 with the necessary degree of accuracy.

Effect of betatron oscillations on the isochronism. The

requirement of isochronism, which was discussed above it related to
the particles, which move along the orbit. The period of revolution
of such "equilibrium" particles is determined only by the
configuration of magnetic field. However, for the particles, which
accomplish betatron oscillations, the revolution period will depend
not only on magnetic field, but also on amplitude and phase of
oscillations. Calculation shows that this dependence carries an
oscillatory nature, moreover the amplitude of these oscillations
decreases with an increase in the radius. Assuming that $\rho \approx 2.5-3$ mm,
then $(\Delta T/T)_{max} \approx 3.10^{-4}$. The corresponding broadening of cluster (in the
degrees) will be $+-0.1$ q, where q - multiplicity of acceleration.

Page 38.

The acceptance of spectrometric cyclotron proves to be small:
for example, for the version $\delta_{\gamma} \approx 7\pi$ mm. mrad in question. With the
high currents this sets very severe limitations on the parameters of
the injected beam.

Effect of the nonlinearity of magnetic field. The requirement of
the separation of orbits sets natural limitation on the amplitude of
radial betatron oscillations in STs. In particular, in the
examined/considered by us version the permissible amplitude of
oscillations <3 mm. It is obvious that with such small amplitudes the

nonlinear effects[1] must not become apparent.

FOOTNOTE [1]. Here have in mind the effects, caused by the "ideal" nonlinearity (resonances N/3, N/4 and the like). ENDFOOTNOTE.

For checking this confirmation was investigated the dependence of phase particle trajectories on the amplitude. As it was expected, the form of phase trajectories and frequency ω_y are not changed even with the amplitudes, which noticeably exceed value indicated above.
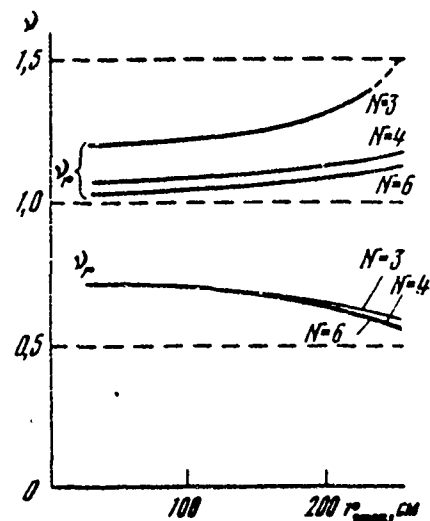
Fig. 1. Dependence of "frequency" of betatron ν on N with the sine flutter in field ($\tau_{0\,max}$ a maximum radius of orbit).
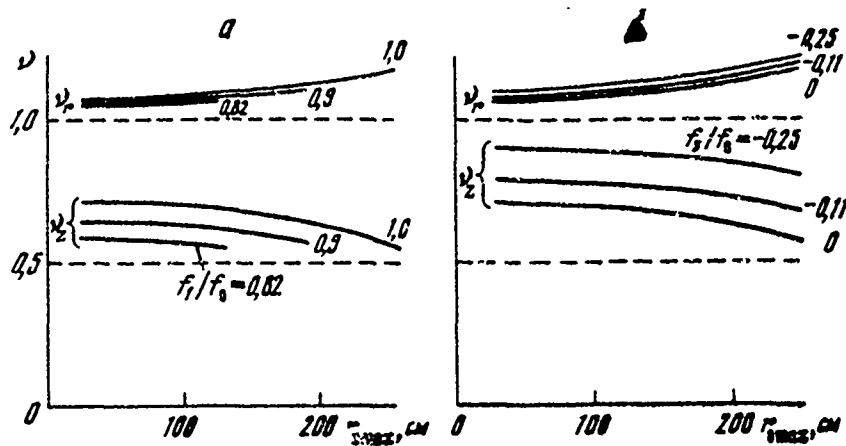
Fig. 2. Dependence ν on azimuthal variation in magnetic field: a) effect of depth of variation, $H = H_0(f_0 + f_1 \cos 4\theta)$, $f \sim \frac{1}{\sqrt{1-(\frac{\tau}{\tau_c})^2}}$. Standardization: $H_{max} = 2H_0$, $H_0 = 4{,}97$ kOe; b) the effect of the "form" of variation, $H = H_c(f_1\cos 4\theta + f_3 \cos 12\theta)$, $f \sim \frac{1}{\sqrt{1-(\frac{\tau}{\tau_c})^2}}$. Standardization $H_{max} = 2H_0$, $H_{min} = 0$
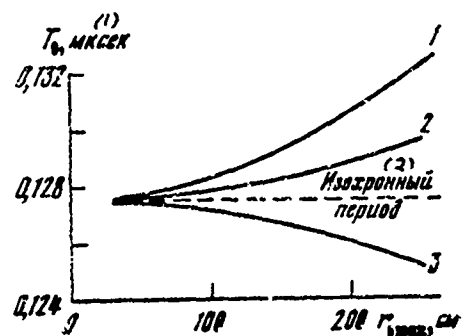
Fig. 3. Dependence of the period of conversion of particles in the cyclotron on the "middle" field

1 - r_{oc} = 710 cм; 2 - r_{oc} = r_{ic}; 3 - r_{oc} = 550 cм;

$H = H_o (f_0 + f_1 \cos 4\theta)$,

$f_0 = \dfrac{1}{\sqrt{1-\left(\frac{r}{r_{oc}}\right)^2}}$, $f_1 = \dfrac{1}{\sqrt{1-\left(\frac{r}{r_{ic}}\right)^2}}$, H_o=4,97кэ, r_{ic}=628см

Key: (1). µs. (2). Isochronal period.
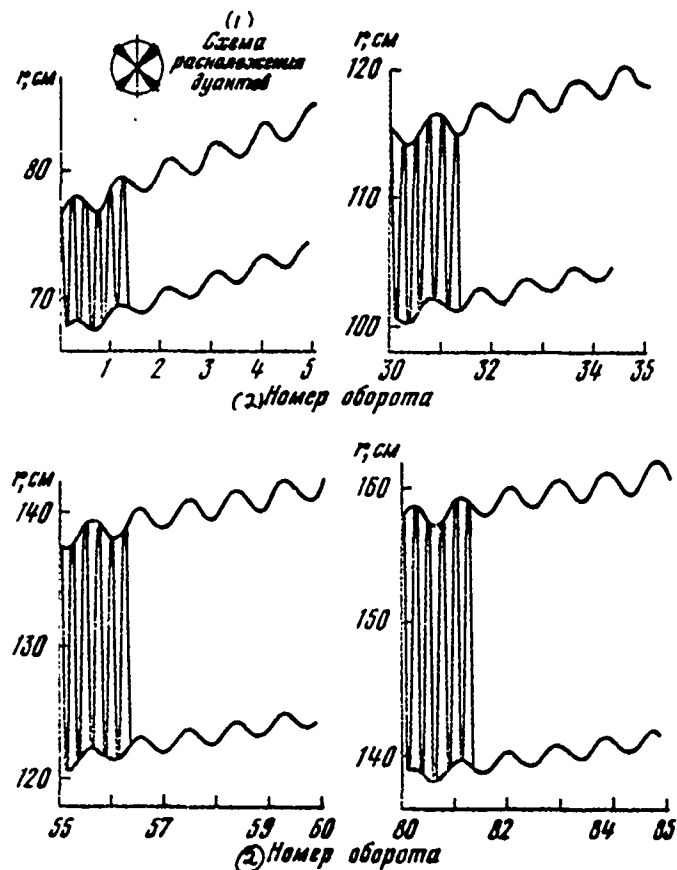
Fig. 4. Particle trajectory, accelerated in STs.

Key: (1). Diagram of the layout of dees. (2). Number of revolution.

Page 39.

2. Dynamic mode.

Special feature/peculiarity or dynamic behavior in the cyclotron

- discrete/digital character or the set of energy. During the
discrete/digital set of energy the orbit abruptlyly changes its
position, as a result of which are excited the induced, so-called
"slotted" oscillations with the frequency of external force (in this
case with the frequency, to multiple of accelerating slots). The
presence of radial and vertical components of HF-field will also lead
to the excitation of oscillations; however in contrast to the slotted
oscillations particle momentum in this case virtually is not changed.
It is obvious that these oscillations do not represent large danger,
since they are equivalent to the distortion of equilibrium orbit.
Dangerous can be the oscillations, excited with the frequency, close
to the frequency of betatron. In order to exclude them, the
accelerating slots must be arranged/located perpendicularly to orbit.

For checking the expressed considerations were calculated
several versions of STs, which are characterized by a number and an
angular extent of dees. Calculation was performed under the
assumption of the infinitesimally narrow accelerating slots and
precise isochronism. Fig. 4 gives the typical particle trajectory
which shows that the amplitude of oscillations in the process of
acceleration does not grow/rise.

3. Effects of space charge in the spectrometric cyclotron.

In the spectrometric cyclotron the effects of space charge have a series/row of special features/peculiarities. First of all, the nearness of resonances which sets limitation on the value of "transverse" charge in the clusters. In the second place, the close tolerance for the spread of particles on the energy leads to the need for considering the effect of the "longitudinal" charge of clusters, since this charge can substantially increase the energy spread of particles in the cluster.

In the version in question "transverse" charge does not exert a substantial influence on particle dynamics up to the currents 200-300 μA. Danger can represent "longitudinal" charge. Actually/really, if one assumes that particle distribution in the clusters uniform, then the fraction/portion of particles which will obtain a supplementary energy gain, which exceeds that permitted (in our case of 10^{-4}), it will compose 60-70 o/o. To decrease this effect is possible by an increase in the radius of STs, and also by the appropriate selection of the form of accelerating voltage.

96. ANALYSIS OF PARTICLE MOTION IN A PROTON SYNCHROTRON WITH MAGNETS, WHICH HAVE A VERTICAL PLANE OF SYMMETRY.

A. I. Dzergach.

(Radio engineering institute of the AS USSR).

Gradient magnets with the vertical plane of symmetry for the proton synchrotron with the the strong focusing [1-4] make it possible in certain cases to obtain gain in the value of field on 30 o/o in comparison with the usual magnets. Gain is obtained because of the vectorial addition of dipole and quadrupole the component of field in operating region, which leads to the relatively smaller values of induction in the poles of iron magnets or to the decrease of the density of ampere turns for the iron free (superconducting) magnets. This makes it possible under prescribed/assigned focusing strength to increase bending field or in the prescribed/assigned field to raise focusing strength.

The effect of disturbances/perturbations (error for field and gradient, the shifts/shears of magnets, etc.) on stability of motion of particles proves to be virtually the same as in the usual magnets with the horizontal (median) plane of symmetry.

The linearized equations of the excited betatron oscillations in the magnetic field with the indices of the decrease

$$n_0 = -\frac{r_0}{B_0}\frac{\partial B_z}{\partial x}\bigg|_{\substack{x=0\\z=0}}; \quad m_0 = -\frac{r_0}{B_0}\frac{\partial B_z}{\partial z}\bigg|_{\substack{x=0\\z=0}}$$

take the form

$$x'' = n_0 x + m_0 z - x - 2(m_0 x - n_0 z)\varepsilon - (r_0 + n_0 x + m_0 z) \times$$

$$\times \frac{\delta p}{p_0} - (r_0 + x)\frac{\delta B_z}{B_0} - n_0 \xi - m_0 \zeta + x\delta n_0 + z\delta m_0, \quad (1)$$

$$z'' = -n_0 z + m_0 x - \left[r_0 - 2(n_0 x + m_0 z)\right]\varepsilon -$$

$$- (-n_0 z + m_0 x)\frac{\delta p}{p_0} - m_0 \xi + n_0 \zeta - z\delta n_0 + x\delta m_0.$$

Accepting further $n_0 = 1/2$, we will obtain equations in coordinates u, v, which correspond to the axes/axles, turned on 45° relative to axes/axles x, y:

$$u'' - \left(m_0 - \frac{1}{2}\right)u = \left(\frac{r_0}{\sqrt{2}} + \frac{1}{2}v - m_0 u\right)\frac{\delta p}{p_0} - \left(\frac{r_0}{\sqrt{2}} + \frac{u-v}{2}\right) \times$$

$$\times \frac{\delta B_z}{B_0} - \left(\frac{r_0}{\sqrt{2}} - 2m_0 v - u\right)\varepsilon + \frac{1}{2}\delta v - m_0 \delta u + u\delta m_0 - v\delta n_0;$$

$$v'' + \left(m_0 + \frac{1}{2}\right)v = -\left(\frac{r_0}{\sqrt{2}} - \frac{1}{2}u - m_0 v\right)\frac{\delta p}{p_0} + \left(\frac{r_0}{\sqrt{2}} + \right.$$

$$\left. + \frac{u-v}{2}\right)\frac{\delta B_z}{B_0} - \left(\frac{r_0}{\sqrt{2}} - 2m_0 u - v\right)\varepsilon + \frac{1}{2}\delta u + m_0 \delta v -$$

$$- u\delta n_0 - v\delta m_0.$$

Page 40.

The effect of momentum errors, according to (2), is described by the equations

$$u^{2}-(m_{p}-\tfrac{1}{2})u=\left(\tfrac{\tau_{0}}{\sqrt{2}}+\tfrac{1}{2}v\right)\frac{\delta p}{P_{0}}\approx\frac{\tau_{0}}{\sqrt{2}}\ \frac{\delta p}{P_{0}},$$

$$v^{n}+(m_{p}+\tfrac{1}{2})v=-\left(\tfrac{\tau_{0}}{\sqrt{2}}-\tfrac{1}{2}u\right)\frac{\delta p}{P_{0}}\approx-\frac{\tau_{0}}{\sqrt{2}}\ \frac{\delta p}{P_{0}},$$

(3)

where $m_{p}=m_{0}\left(1-\frac{\delta p}{P_{0}}\right)$, i.e. it leads to a usual change in the frequencies of betatron $\Delta Q/Q=-\frac{\delta p}{P_{0}}$ and to the expansion of equilibrium orbit $\overline{\Delta\tau}=\frac{\tau_{0}}{Q^{2}}\ \frac{\delta p}{P_{0}}$. Furthermore, are as in the usual system, oscillations with the frequency of alternation F- and D- magnets and the same amplitude as in the usual system. The components of these oscillations are directed along the axes u, v, so that for the particles near x axis the resulting oscillation is oriented along the axis z, for the particles near axes/axles u, v - respectively along the axes u, v, and for the particles near z-axis - along the axis x. The effect of errors δB_{z} for field, according to (2), is described by the equations

$$u^{n}-(m_{0}-\tfrac{1}{2})u=-\frac{\tau_{0}+x}{\sqrt{2}}\ \frac{\delta B_{z}}{B_{0}},$$

$$v^{n}+(m_{0}+\tfrac{1}{2})v=\frac{\tau_{0}+x}{\sqrt{2}}\ \frac{\delta B_{z}}{B_{0}},$$

(4)

showing that the errors for field produce in orbit the same action as in the usual system.

The effect of errors δm_{0} gradient is described by the equations

$$u'' - (m_0 + \delta m_0 - \tfrac{1}{2})u = 0, \quad v'' + (m_0 + \delta m_0 + \tfrac{1}{2})v = 0, \quad (5)$$

i.e., has the usual character (effect δn_0 is taken into consideration below). The effect of the shifts/shears of magnets ε, ζ on the horizontal and the vertical line or corresponding shifts/shears $\delta u = (\zeta + \xi)/\sqrt{2}$, $\delta v = (\zeta - \xi)/\sqrt{2}$ along the axes u, v according to (2), is described by the equations

$$u'' - (m_0 - \tfrac{1}{2})u = \tfrac{1}{2}\delta v - m_0 \delta u \approx -m_0 \delta u,$$
$$v'' + (m_0 + \tfrac{1}{2})v = \tfrac{1}{2}\delta u + m_0 \delta v \approx m_0 \delta v, \quad (6)$$

i.e. virtually the same as usually. Finally, the effect of inclinations/slopes ε of magnets relative to orbit, according to (2), is described by the equations

$$u'' - (m_0 - \tfrac{1}{2})u = \left[m_0 v - (\tfrac{n_0}{\sqrt{2}} - 2m_0 v - u) \right]\varepsilon \approx \left(-\tfrac{n_0}{\sqrt{2}} + 3m_0 v\right)\varepsilon,$$
$$v'' + (m_0 + \tfrac{1}{2})v = \left[m_0 u - (\tfrac{n_0}{\sqrt{2}} - 2m_0 u - v) \right]\varepsilon \approx \left(-\tfrac{n_0}{\sqrt{2}} + 3m_0 u\right)\varepsilon, \quad (7)$$

where it is accepted $\delta n_0 = -m_0 \varepsilon$. The comparison of the low-frequency components of equations (7) and equations [5]

$$\bar{x}'' + Q^2 \bar{x} = 2n\bar{z}\varepsilon;$$
$$\bar{z}'' + Q^2 \bar{z} = -\bar{z}_0 \varepsilon + 2n\varepsilon\bar{x} \quad (8)$$

for the usual system shows that the effect of the inclinations/slopes of magnets in both systems approximately/exemplarily identical.

Thus, to linear system with the vertical plane of symmetry are

not characteristic any specific unpleasant effects: allowances have

usual order of magnitude. It is possible to assume that the

allowances on the nonlinearity will also have usual values.

The author is grateful to E. L. Burshteyn and A. A. Vasil'yev

for the attention to this work.

REFERENCES

1. J.C. Jacobsen. Lectures on the theory and design of
   an alternating-gradient proton synchrotron. Geneva,
   CERN, 1953, p. 133.
2. В.Н. Мелехин. Письма в ЖЭТФ, 1969, № 9,552.
3. А.И. Дзергач. Сверхпроводящий электромагнит
   синхротрона. Авторск. свидет. № 300137. Бюл-
   летень изобретений и товарных знаков, 1971,№ 19.
4. В.Н. Мелехин. Труды УII Международной конфе-
   ренции по ускорителям заряженных частиц высо-
   ких энергий; том. II. Ереван, Изд-во АН Арм.
   ССР, 1970, стр. 288.
5. A. Schoch. CERN Report 57-21. Geneve, 1958.

Discussion.

Yu. G. Basargin. What advantages does have the structure examined in

comparison with the structure with the divided functions?

A. I. Dzergach. The advantage: it consists, first of all, of the fact

that it is possible to obtain a somewhat larger value of middle

field. For example, for the accepted in the report structure for the

accelerator on 1000 GeV field by approximately 5o/o is more than in

the analogous accelerator with the divided functions. This gives the

possibility to reduce a radius of accelerator
approximately/exemplarily in the same sense.

V. G. Davidovskiy. We examined magnets of this type in 1965-1968 when
selecting of the version of accumulator/storage VEPP-3. It turned out
that such systems from the point of view of the particle motion and
allowances possess no advantages in comparison with the usual
systems. The model of magnet was prepared and investigated by B.
Levichev. It was explained that in the strong fields appear the very
essential nonlinearity, so that is required considerable correction.
As a result of gain in the value of middle field in comparison with
the compactly carried out systems with the divided and semidivided
functions it is not obtained, but appear inconveniences with the
commutation it is such.

In the case of electronic synchrotrons and accumulators/storage
the quantum fluctuations of radiation/emission lead to the fact that
the beam becomes not flat/plane, but it is thickened, as a result of
which the luminous density with clashing beams falls. It is necessary
to introduce special lenses for thinning the frequencies on both
inclined axes/axles.

Page 41.

97. STUDY OF THE STABILITY OF ACCELERATION OF AN INTENSE BEAM IN A MICROTRON.

Ye. L. Kosarev, L. B. Iuganskiy, V. N. Melekhin.

(Institute of the physical problems of the AS USSR).

At those values of the currents which are achieved/reached in the microtrons, the field, aimed by clusters with the flight/span through the accelerating cavity, is compared with full/total/complete accelerating field. Interaction beam - resonator is conveniently estimated with the aid of the parameter of high current η_e, of equal to the ratio of power accelerated beam $\overset{\smallfrown}{P}_e$ to the power of the excitation of resonator P_ν. In practice this parameter attains values $\eta_e \sim 1 \div 3$ and interaction beam - resonator is substantial.

In our works [1-3] are theoretically and experimentally investigated two mechanisms of high-current instability in the microtron. One of them is connected with the fact that at the

specific values of equilibrium phase in the microtron occurs the
driving of phase oscillations, caused by the nonlinearity of phase
equations. This driving leads to the fact that on the "volt-ampere"
characteristic of microtron, i.e., to the curve, that is determining
the dependence of the accelerated current on the amplitude of
accelerating voltage, appear failures/dips/troughs and sections with
the large negative slope/transconductance. In such sections appears
the high-current instability, caused by the negative differential
conductivity of beam.

Another mechanism is caused by the detuning of resonator,
introduced by beam, and which leads to the development of
instability, if the frequency of resonator with the beam is lower
than the frequency of the exciting generator. The physical sense of
this instability consists of the following. Electron beam in the
microtron increases the natural frequency of resonator. With the
random decrease (or an increase) of the power of beam the frequency
of resonator decreases (or increases). If in this case oscillator
frequency is selected above frequency of resonator with the beam,
then the change in the detuning of resonator, caused by a change in
the power of beam, will cause further increase (respectively
decrease) in the detuning. Due to this the amplitude of accelerating
field and the power of beam decrease (respectively they increase). As
a result of the development of this process with the sufficiently

large initial beam current appears the instability.

The experimental analyses of stability of acceleration were carried out on the microtron of the IPP of the AS USSR with 30 orbits with the energy of beam to 30 MeV and the current to 80 mA in impulse/momentum/pulse [4].

The first mechanism of instability is investigated in work [2]. Fig. 1, depicts the dependence of the accelerated current on the eighth, the 15th and 28th orbits on the equilibrium phase, taken with currents less than critical ones, and an energy gain per revolution 0.6 MeV. As is evident in the figure, for the data of orbits the curves have sharply pronounced nonmonotonic character. The reason for the appearance of failures/dips/troughs is shown above, and the supplementary lift of curve in 8th orbit with the large amplitudes of field is connected with the existence of the new regions of phase stability [5]. In the sections of the drop of the volt-ampere characteristic of microtron stationary acceleration mode is impossible, if current is more than critical, since occurs the disruption/separation of acceleration mode, caused by instability.

Critical current, with which begins the disruption/separation of acceleration mode, was measured in different orbits. In the measurements the resonator, loaded with beam, it was adjusted

accurately for the frequency of the exciting generator. The results of measurements are shown in Fig. 2, where curves 1 and 2 correspond to sections of 1 and 2 curves of Fig. 1. The emergence of instability was fixed/recorded on the oscillograph. As can be seen from Fig. 2, critical currents decrease with an increase in the number of orbits:, once in 10th orbit, they are small (about 50 mA), and in the 28th orbit compose a total of several milliamperes.
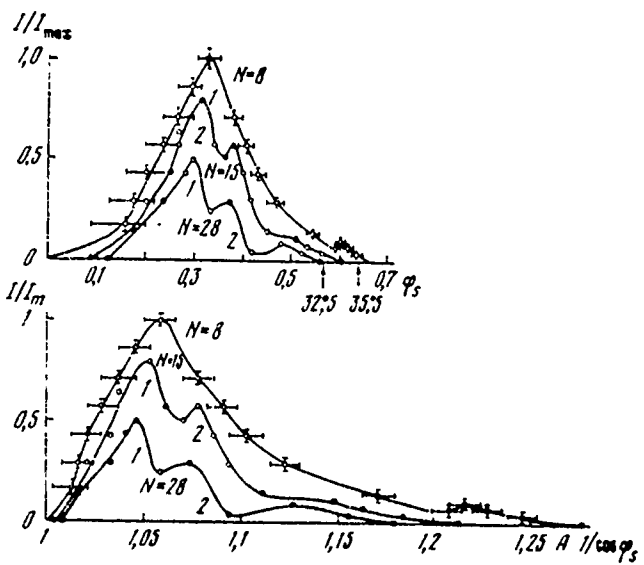
Fig. 1.   Fig. 2.
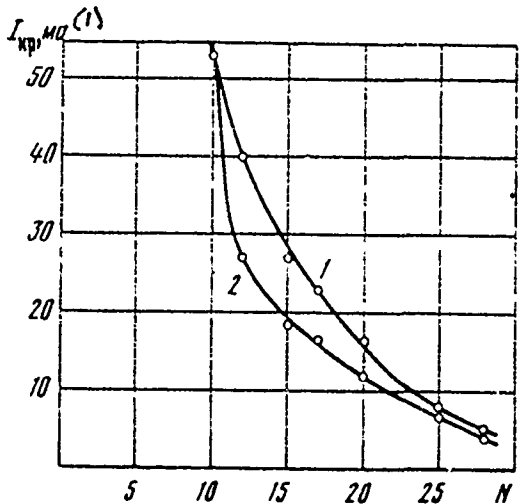
Fig. 1. Dependence of accelerated current on equilibrium phase.

Fig. 2. Dependence of critical current on number of orbit.

Key: (1). mA.

Page 42.

The instability, caused by the negative differential conductivity of beam, directly does not limit the accelerated current, since it is absent from the left slopes of volt-ampere

characteristics (sections with the positive slope/transconductance in Fig. 1). With the large accelerated currents the work of microtrons in the pulsed operation is possible only in equilibrium phases φ_{6}, of those corresponding to the left-most slope (to the first maximum), since whereas in the first collapsible/dropped section occurs the disruption/separation cf acceleration mode and large equilibrium phases cannot be realized. This leads to the contraction approximately/exemplarily 2 times of the region of the equilibrium phases, in which is possible the acceleration of high currents. The obtained result is essential for the microtrons with a large number of orbits, for the sectional microtrons with a large energy gain per revolution, and also for continuous microtrons with the superconducting resonator.

The high-current effects, connected with the detuning of resonator, introduced by beam, are calculated in work [1] and are experimentally investigated in work [3]. Fig. 3 gives the results of the static measurements cf the amplitude of field in the resonator (lower curve) and accelerated current with a change in the adjustment of resonator. The double-humped character of curves is connected with the fact that was utilized the eccentric mechanism of adjustment, which has two operating positions. Lower curve is taken with the switched-off injector. The following curves (down-up) show the dependence of beam current in 20th orbit with the energy 18 MeV on a

change in the adjustment of resonator at different maximum values of
the accelerated current - 13, 27, 33 and 40 mA. From the given
records it is evident that the domain of existence of stable
acceleration mode in accordance with theory [1], is arranged/located
with the negative detuning of resonator (when its frequency higher
than frequency of magnetron), moreover the width of this region
increases to the side of negative detuning with an increase in the
current. These measurements show that the effectiveness of
stabilization increases with an increase in the power of the
accelerated beam.

For conducting the dynamic measurements was applied the
following procedure. Was studied the reaction of the beam of
microtron to the artificially created slight disturbance of the
falling/incident power. The impulses/momenta/pulses of the
disturbance/perturbation with duration about 0.25 μs were included
with the accurately known and controlled delay relative to the front
of the basic boosting impulse during each second main impulse. This
method gave the possibility to differ the reaction of beam for the
supplied disturbance/perturbation from different focusings/inductions
and interferences, which act during the impulse/momentum/pulse.

In the equilibrium phase smaller than the optimum (left slope of
volt-ampere characteristics in Fig. 1), interaction of beam with the

resonator must lead to the stabilization of acceleration mode on the
left slope of resonance curve. And actually/really, on the shown in
Fig. 4 and 5 oscillograms of the reaction of beam to the
impulse/momentum/pulse of disturbance/perturbation, taken at the
value of equilibrium phase $\varphi_8 = 0.23$ and with the beam current 27 mA
for two values of the frequency of adjustment $f_{pe3.} = f_{Mar\text{Ã}.} + 0.8$ by MHz
and $f_{pe3} = f_{Mar\text{Ã}.}$ is evident that in the second case of the stability
of beam less, steady state is established oscillatorily with a small
decrement. The corresponding oscillations/vibrations in the detuned
cavity on the left slope of resonance curve are overdamped.

The obtained results lead to the following conclusions. At the
values of equilibrium phase, which correspond to the falling/incident
sections of volt-ampere characteristic (Fig. 1), the work of
microtron with the sufficiently high currents is unstable with any
adjustment of resonator. This leads to the contraction
approximately/exemplarily two times of the region of the permissible
equilibrium phases. If equilibrium phases correspond to the
increasing section of volt-ampere characteristic, then the work of
microtron with the high currents is stable only on the left slope of
resonance curve.

With satisfaction of the stability conditions (left slope of
volt-ampere characteristic and left slope of resonance curve)

indicated the investigated by us high-current effects do not lead to the limitation of the accelerated current in the acting pulse ricrotrons.

For the continuous microtrons with the superconducting resonator are necessary supplementary both theoretical and experimental studies, in view of the very high values of their own quality in comparison with the usual resonators.
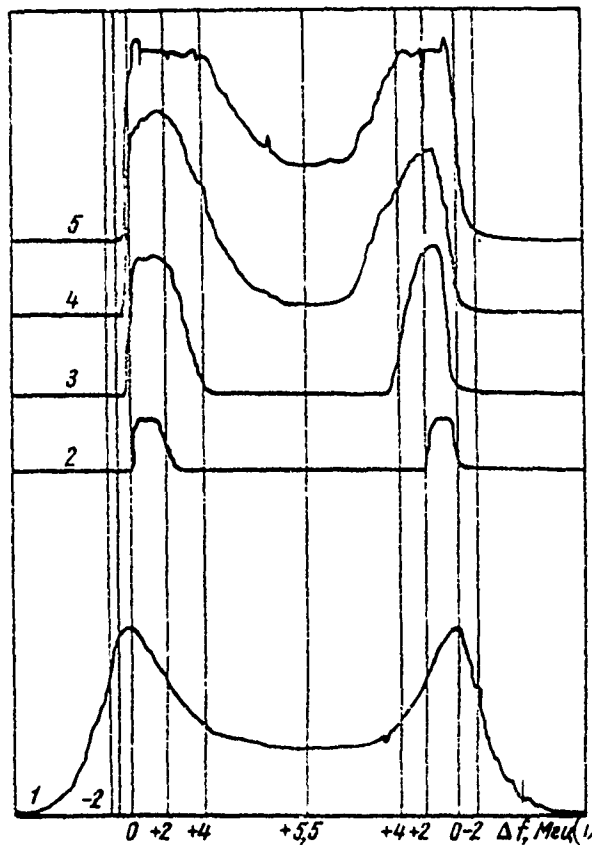
Fig. 3. Domains of existence of stable mode/conditions in the microtron with the hi_n current of beam. Detuning of resonator $\Delta f = f_{pea} - f_{maн}$. 1 - recording of the amplitude of accelerating field in the empty resonator with a change in its adjustment; 2 - change in the current strength of beam with a change in the frequency of resonator. Maximum current 13 mA; 3 - maximum current 27 mA; 4 - maximum current 33 mA (left maximum) and 27 mA (right maximum); 5 - maximum current 40 mA.

Key: (1). MHz.

Page 43.
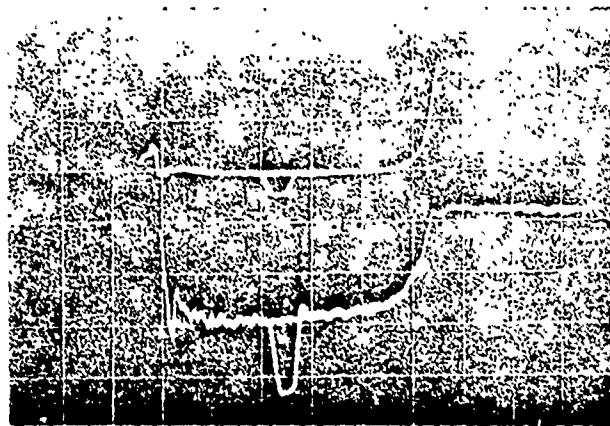
Fig. 4. Reaction of beam to the impulse/momentum/pulse of disturbance/perturbation, frequency $f_{pe3.} = f_{Mazn.} + 0.8$ MHz, beam current 27 mA (lower ray/beam). Upper ray/beam - falling/incident power. Scanning speed 0.5 μs/div.
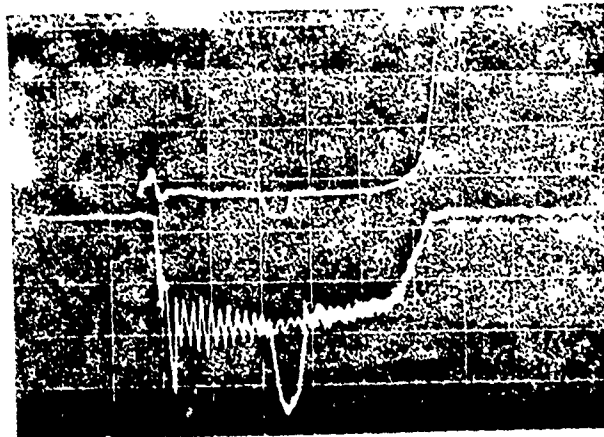
Fig. 5. Reaction of beam to impulse/momentum/pulse of compensation $f_{pe3} = f_{Mazn}$ beam current 27 mA.

REFERENCES

1. Ye. L. Kosarev. Coll.: Electronics of large powers, iss. 5. M., publishing house "science", 1968, page 283.

2. V. N. Melekhin, L. B. Luganskiy. ZhTF, 1970, 40, No 11, 2465.

3. Ye. L. Kosarev. ZhTF, 1971, 41, No 7, 1452.

4. S. P. Kapitsa, V. N. Melekhin. Microtron. M., publishing house "science", 1969.

5. L. B. Luganskiy. Coll.: Electronics of large powers, iss. 6, M., publishing house "science", 1969, page 130.

Discussion.

A. K. Belovintsev. How is determined the form of the volt-ampere characteristic of this microtron?

Ye. L. Kosarev. The form of volt-ampere characteristic is determined by dependence of the size/dimension of phase stability region on the equilibrium phase and by filling of this stability region upon the injection.

A. M. Shenderovich. Is it possible to in greater detail explain the physical mechanism of the instability, connected with falling characteristic I=f(ϕ)?

Ye. L. Kosarev. Mechanism does not differ from the mechanism of the excitation of radio-frequency generators on negative resistance.

N. I. Mocheshnikov. What it is possible to speak about a change in the energy spectrum of beam during the development of instability?

Ye. L. Kosarev. Energy spectrum does not change with the current of less than the critical.

98. INSTABILITIES OF THE BEAM OF THE BROOKHAVEN PROTON SYNCHROTRON CAUSED BY INTERACTION WITH A HIGH-FREQUENCY SYSTEM.

M. K. Barton, Ye. K. Rak.

(Brookhaven national laboratory, Upton, New York).

In accordance with the program of the alteration of Brookhaven synchrotron the high-frequency s. em of neck ring underwent considerable changes. The purpose of these changes was the carrying out of power amplifiers from the ring. They were transferred into the central building, and a supply of 12 individual resonators they began to accomplish/realize with the aid of the coaxial lines.

After the setting up of this system were soon discovered the instabilities of beam. These instabilities best anything are described as coherent phase oscillations in the modes for which different clusters have different phases. Fig. 1 gives the oscillogram of radial signal on one of the signal electrodes, obtained soon after the emergence of instability. In proportion to the development of instability becomes noticeable also its effect on the form of the cluster (see Fig. 2 and 3). This instability has the

distinct threshold (about 5×10^{11} the protons).

Page 44.

Scarcely higher this threshold was observed build-up/growth far beyond phase transition. At the higher intensities the build-up/growth occurred at the earlier moment/torque in the cycle of acceleration. At the intensities of the order of 10^{12} protons the build-up/growth was observed to the phase transition, but further increase in the intensity did not lead to noticeably the earlier emergence of instability. After the achievement of amplitudes of approximately 1 cm the build-up/growth ceased and was not observed the noticeable losses of particles. The effective width of beam, determined by this instability, grew/rose to the value, too great for the channel rapid a conclusion/output and leading to the series/row of difficulties during the introduction of targets and the slow conclusion/output.

In order to understand the mechanism of this instability, should be first examined the geometry of the resonator, shown in Fig. 4. The capacity/capacitance, utilized for obtaining the resonance on ferrite, is displaced from the real position of clearance toward the introduction/input of the feeding coaxial lines. In this position these capacities/capacitances serve as coupling transformer, which

agrees impedance of resonator with the impedance of line. However, in this case is introduced the stray inductance of the busbars/tires between the trimmer capacitors and the accelerating gaps. As a result in each accelerating gap appears the impedance, as can be seen from equivalent diagram in Fig. 5. When cluster passes through the accelerating gap, it induces the stress/voltage

$$V = \frac{q}{c} e^{-t/\tau} e^{-i\omega_s t} F(\omega_s, \sigma), \qquad (1)$$

received by the following cluster at the moment of time t. Here q — charge of cluster; ω_s — the resonance frequency of idle mode; c — its shunting speed, and τ is connected with its quality Q with expression $\tau = 2Q/\omega_s$. $F(\omega_s, \sigma)$ — the function which describes, is how effectively the cluster of width σ excites resonance. For example, assuming that the cluster has Gaussian form, then $F = e^{-\omega_s^2 \sigma^2/2}$. As the proof of the fact that such stresses/voltages exist, can serve oscillograms in Fig. 6. From the figure one can see that in the signal, induced by beam on the separate resonator (adjusted to the resonance with ~4.4 MHz), is present the large fifth harmonic. Measurements with the spectrum analyzer show that the amplitude of fifth harmonic is approximately/exemplarily on 10 dB lower than the amplitude of the fundamental frequency of ~4.4 MHz.
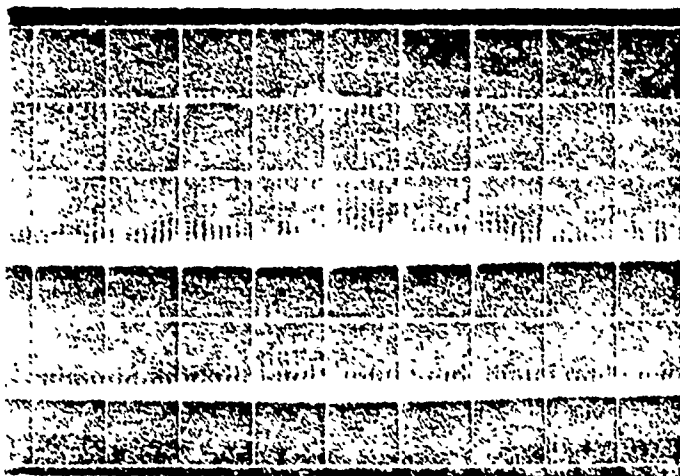
DOC = 80069304   PAGE

Fig. 1. The oscillograms of the signals of pick-up-electrodes, which measure the beam current (it is above) and the radial position (below).

Scale value - 2 μs. Photograph is made after the establishment of instability.
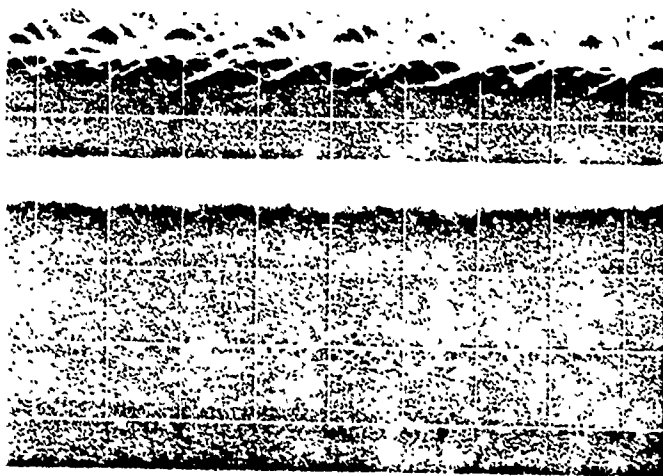
Fig. 2. the same as in Fig. 1, not with very slow sweep.

Scale value - 2 μs.

DOC = 80069304   PAGE 20
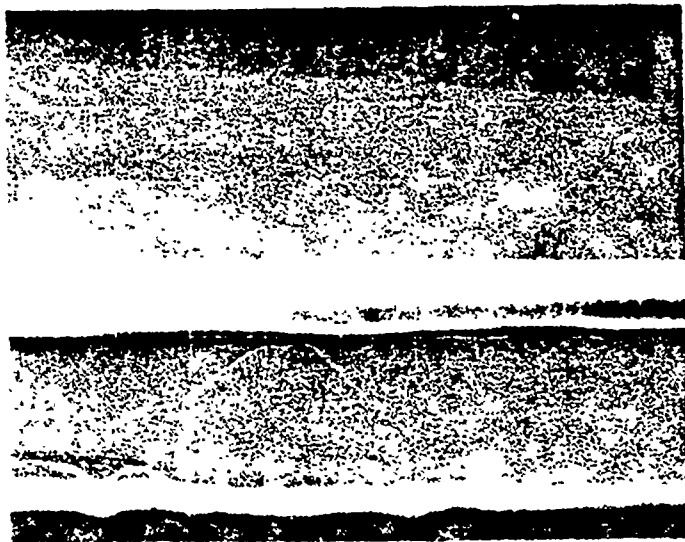
Fig. 3. The oscillogram, analogous Fig. 2 with that difference, that the signal of a pick-up-electrode was gated, so that was observed only one cluster of twelve. Clearly evidently radial motion with the frequency of phase. In all cases is essential modulation of difference signal; modulation of total signal indicates oscillations of the form of cluster, caused, apparently, by nonlinearity.

Page 45.

Equation of motion for the centers of mass 12 clusters is in this case the connected equations

$$\ddot{\varphi}_I + \Omega_0^2 \varphi_I = \sum_{J=1}^{12} A_{IJ} \varphi_J,$$

where A_{IJ} is determined by the stresses/voltages, described by equation (1) and corresponding dynamic coefficients

$$A_{IJ} = -\frac{\Omega_0^2 N}{V \cos\varphi_s} \frac{\partial V_{IJ}}{\partial \varphi_J}.$$

Here V - incremental stress in one revolution; φ_s - equilibrium phase angle, and V_{IJ} - stress/voltage on cluster I, created by cluster J in accordance with equation (1): N - number of resonators, and Ω_0 - frequency of small phase oscillations. It should be noted that if the clusters are identical, then coefficients A_{IJ} depend only on I-J so that system it is cyclic and normal modes are the roots of the twelfth degree of unit. The solutions we search for in the form

$$\varphi_I = e^{i\Omega_M t}, \quad \varphi_J = \varphi_I e^{i(M)(J-I)(2\pi/12)}$$

for mode M, $1 \leqslant M \leqslant 12$,

$$\Omega_M = \Omega_0 + \delta\Omega_M$$

Solving equations of motion relatively $\delta\Omega_M$, we will obtain

$$\delta\Omega_M \approx -\frac{1}{2\Omega} \sum A_{JI} e^{iM(J-1)\pi/6}.$$
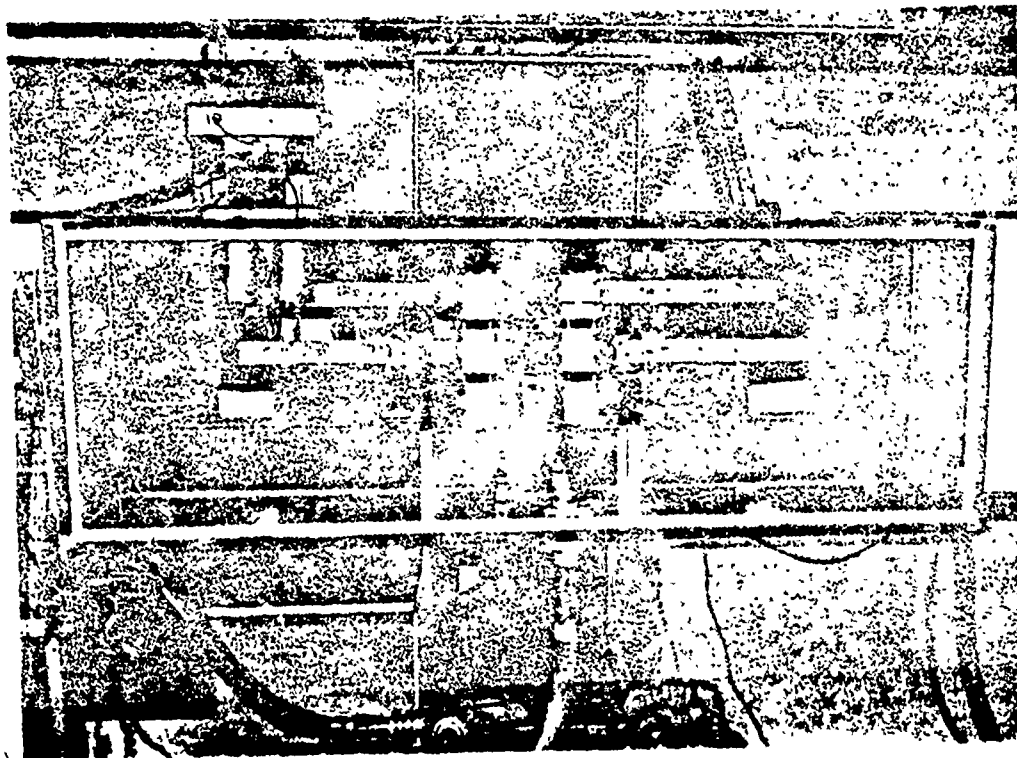
Fig. 4. Photograph of the resonator, modified for the target washing by coaxial line from the distant amplifier. Washing it is introduced into the capacity/capacitance in the center of figure. The converted stress/voltage is supplied on the busbars/tires into the real clearances along the sides.

184
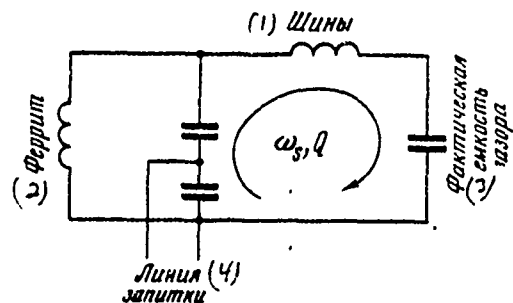
Fig. 5. Diagram of equivalent contour/outline for the resonator clearance.

Key: (1). Busbars/tires. (2). Ferrite. (3). Actual gap capacitance. (4). Line washing.
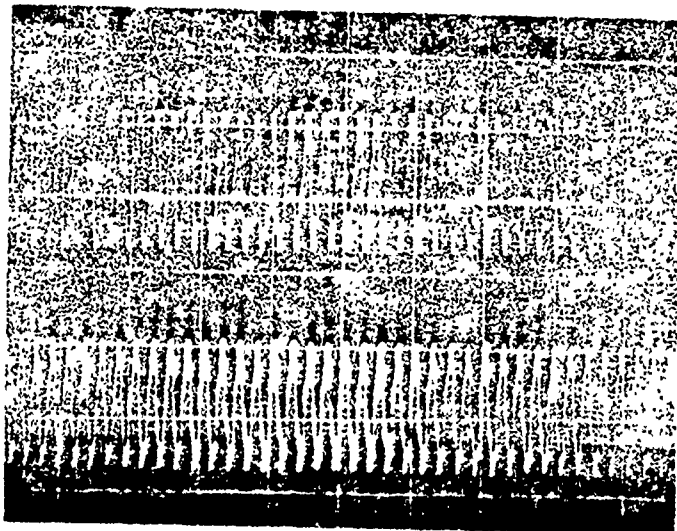
Fig. 6. Voltage oscillogram on resonator, adjusted for nominal frequency, but beam induced only. In the upper oscillogram the fifth harmonic is distant by filter.

Page 46.

The real part of the frequency shift/shear is connected with the threshold. The analysis of dispersion equation shows that if this frequency shift/shear is compared with the scatter of the frequency of phase oscillations in the beam (about 1o/o) or exceeds it, then must occur instability. The alleged part of the scatter of frequency gives the rate of growth in the presence of instability. Are given below the corresponding parameters for the Brookhaven synchrotron:

intensity ... of 10^{12} protons.

Number of harmonics ... 12.

Frequency of phase oscillations $(\Omega_0/2\pi)$ ... 300 Hz.

Energy, acquired for one revolution ... 200 keV.

Equilibrium phase angle ... 150°.

Number of accelerating gaps ... 24.

Capacity/capacitance of the accelerating gap ... 50 pF.

Frequency of idle mode ... 4.8.

Quality of idle mode ... 30.

Width of the cluster ... ⎯ 15 ns.

Мода (1)	Частотный сдвиг гц (2)	Время нараста- ния, мсек (3)
1	10,5	∞
2	11,1	35,9
3	7,9	11,0
4	−7,2	13,3
5	−7,7	40,9
6	−6,3	127,8
7	−5,86	∞
8	−6,3	−127,8
9	−7,7	−40,9
10	−7,2	−13,3
11	7,9	−11,0
12	11,1	−35,9

Key: (1). Maud. (2). Frequency shift/shear Hz. (3). Rise time, ns.

Parameters these are determined very approximately; however, it
is clear that there are unstable modes with the properties, analogous
observed at times of the build-up cf the order of several
milliseconds.

In order to eliminate this instability, it is necessary either
to decrease the coupling coefficients A_{ij}, or to increase the scatter
of the frequency of phase oscillations in the beam. The first
possibility can be realized, after changing coefficient of P in
equation (1). Resonators were modified, as shown in Fig. 7. At

present the resonance frequency of the idle mode of resonators is increased to ~50 MHz, and its quality is lowered to ~12. The expected improvements in the parameters of accelerator are given below.

Frequency of idle mode ... 11.6.

Quality of idle mcde ... 12.

All remaining parameters did not change.

Мода (1)	Частотный сдвиг гц (2)	Время нараста- ния, мсек (3)
1	0,19	∞
2	0,17	1788
3	0,11	977
4	0,02	784
5	−0,09	836
6	−0,18	1366
7	−0,22	∞
8	−0,18	−1366
9	−0,09	−836
10	−0,02	−784
11	0,11	−977
12	0,17	−1788

Key: (1). Mode. (2). Frequency shift/shear Hz. (3). Rise time, ms.
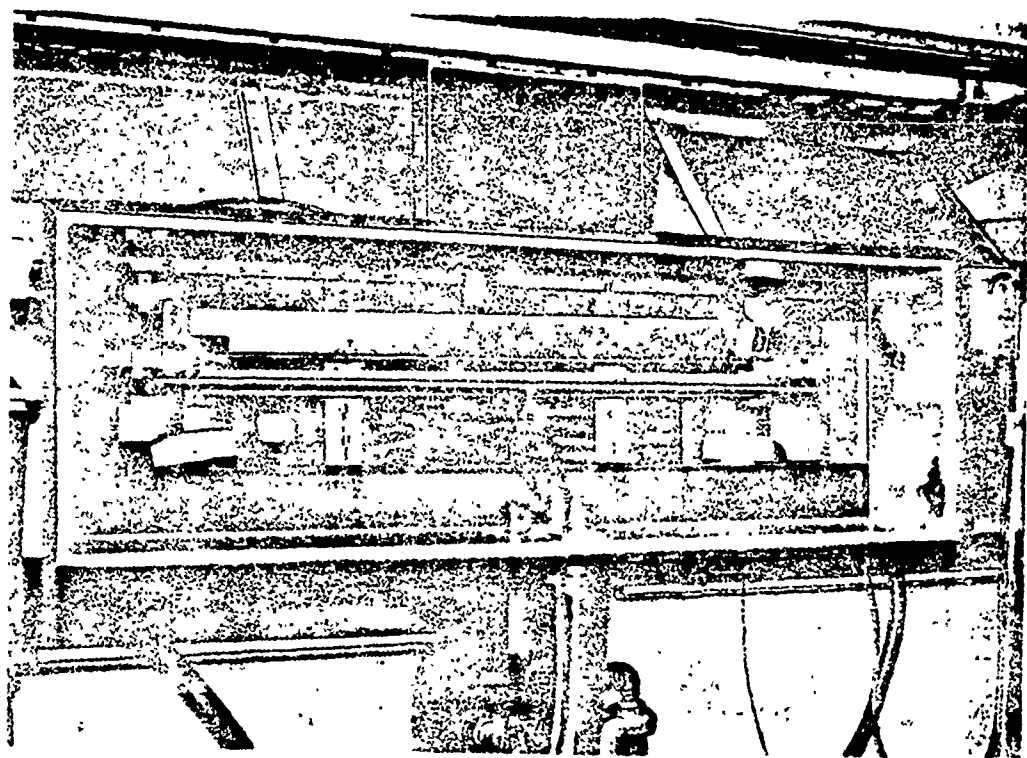
Fig. 7. One of the rescnators, modified for the purpose of the depression of instability. The capacities/capacitances of connection/communication are displaced nearer to the real clearances, which leads to a reduction in the inductance between the clearances and the trimmer capacitors.

Page 47.

After the realization of these modifications in the Brookhaven synchrotron the instability disappeared. It is possible to assume

that this solution is useful up to intensities 10^{13} protons per pulse.

A similar instability was observed also on the accumulator ring "Adone" in Frascati.

We are grateful to K. Pellegrini for the granting to us of the unpublished data on "Adone", and also to E. K. Kurant and to A. S. Sessler for the useful discussions.

Discussion.

V. B. Stepanov. There are any special features/peculiarities and changes in the diagram of the final stage of the hf supplies, connected with the strong beam load?

M. Barton. No changes, besides those which were connected with the carrying out of the final stage into the separate building, it was not made.

K. reich. Me it would like to add that the analogous instability was observed in the proton synchrotron of CERN and was suppressed by a somewhat different method.

99. INVESTIGATIONS OF PARTICLE DYNAMICS IN A STRONG-FOCUSING SYSTEM
BY THE METHOD OF SIMULATION ON COMPUTERS.

V. N. Sidel'nikov, N. A. Sozon, N. L. Sosenskiy.

(Radio engineering institute of the AS USSR).

1. Introduction.

The study of particle motion, accelerated in the proton
synchrotron, on computer presents difficulties, connected, first of
all, with the considerable machine time, necessary for such
investigations. Thus, the integration of system of equations, which
describe the betatron oscillations/vibrations of one particle in the
imperfect strong-focusing system, by Runge-Kutta's method on computer
BESM-6 requires on the average several seconds of machine time for
the revolution of particle. Thus, during the study of particle motion
during the cycle of acceleration are required times on the order of
hundreds of hours. The necessary machine time becomes completely
fantastic during the investigation of the more complicated phenomena,
such as the effect of the proper field of beam, etc.

However, after turing from the examination of the studied system to precision/accuracy, and replacing by certain its model, it is possible to 2 orders) tc substantially (more than reduce the required machine time. In this case it is important so that the model, generally speaking, which differs from the studied system (beam of particles, which move in the strong-focusing field), would not differ from a precise system in terms cf those its properties for investigation of which this model was intended.

In the report are briefly examined two versions of the digital model of bundle, intended for the study of nonlinear transverse vibrations of particles in the proton strong-focusing synchrotron - varsion for the study cf the motion of the noninteracting particles (single-particle model) and version for study of particle motion taking into account the effect of their interaction (multiparticle model). Furthermore, are given scme results of simulation.

2. Single-particle model.

The need for long machine time during the integration of the system of the differential equations, which describe particle motion in the proton synchrotron, is caused, first of all, by the fact that the particle is subject to the influence of forces from the side of magnetic field virtually for entire elongation/extent of its motion.

It is reasonable to assume that the replacement of real forces by the forces, which act at the separate chosen points, could give essential savings in the machine time.

Let us examine the model of bundle, based on the replacement of the real focusing structure of accelerator by the structure which consists of thin magnets arranged/located in the centers of the symmetry of the focusing and defocusing sections of real magnet blocks. From the point of view of simulation it is important to determine the parameters of the focusing structure of model, in which the fundamental characteristics of the transverse nonlinear vibrations of particle in the accelerator and the model maximally coincide, and to also rate/estimate the errors, which appear as a result of replacing the structure.

Simple analysis makes it possible to make following conclusions. For the case of magnetic field without the disturbances/perturbations the parameters of the focusing structure of model and the initial conditions of injection can be selected by such that the frequencies of horizontal and vertical betatron oscillation/vibrations, and also amplitude of smoothed transverse vibrations in the accelerator and the model would be equal with any prescribed/assigned degree of accuracy. In this case a maximally possible difference between the form factors of accelerator and model composes ~7.7o/o¹.

FOOTNOTE [1]. Ye. Kurant, Kh. Snyder. PSP, 1958. No 4, 91. ENDFOOTNOTE.

Page 48.

For the case of the magnetic field, agitated by multipole components in the form of uncorrelated random functions of azimuth, the functions, which are determining the dependence of the amplitudes of smoothed transverse vibrations on the azimuth, for the accelerator and the model can have the quantitative differences not exceeding 0.1o/o for the purely dipole disturbances/perturbations, 0.2o/o for quadrupole, 8o/o for sextupole, and 10o/o for the octupole disturbances/perturbations.

3. Multifrequency model.

Let us examine the model of an unbunched bundle, which considers incoherent interaction of particles. Model is constructed on the following positions, which differ it from the real bundle: 1) the real focusing structure is replaced by the structure, which consists of the thin magnets; 2) real bundle is replaced by the system, which consists of the finite number (not more than thousand) of linear currents; 3) the account of the effect of the forces of

electromagnetic field of bundle to the linear currents it is
conducted in the center of each interval between two adjacent thin
magnets; 4) for calculating the forces of electromagnetic field of
the system of linear currents is conducted its approximation at the
first and second moments/torques by elliptical cylinder with the
continuous current distribution.

Analytical estimation of error, caused by the replacement of
real bundle by its multiparticle model, is very complicated.
Therefore this estimation was carried out experimentally on the
computers.

4. Some results of simulation.

In RTI of the AS USSR were created and fixed the programs in the
language FORTRAN, that correspond to the single-particle and
multiparticle models of bundle. Work with these programs on computer
BESM-6 showed that the machine time, necessary for the simulation of
the motion of particle in one revolution, does not exceed 0.04 s,
which to two orders is less than during the use of a routine of
integration for Runge-Kutta's method. The simulation of the motion of
beam taking into account interaction of particles requires not more
than 3.5 s machine time for the revolution with the approximation of
bundle 100 by linear currents.

Were solved tasks, for which is known the precise analytical
solution: free oscillations/vibrations, forced oscillations far from
the resonance and at the resonance values of frequencies of the
betatron for the different type of disturbances/perturbations. A
difference in the results of simulation from the exact solutions did
not exceed 10o/o in the amplitudes and 0.1o/o in the frequencies.

For the purpose of the estimation of error in the simulation of
interaction was carried out the solution of one and the same problems
for a different quantity of linear currents into which is
divided/marked off real bundle, and for a different number of points,
at which are considered the forces of electromagnetic field of
bundle. It turned out that the results of simulation virtually depend
neither on a number of linear currents, if their quantity exceeds
value on the order of 100 nor from a number of points, at which is
considered the effect of electromagnetic field of bundle, if a number
of these points is not less than one to the interval between two
adjacent thin magnets.

On the multiparticle model was carried out the study of the
process of passage through the whole resonance under the effect of
the space charge of bundle for different means of the random

disturbances of the magnetic field of the proton synchrotron of the RTI of the AS USSR. In the figure as an example are given the dependences of the maximum values of the first and second moments/torques of bundle from the speed. The integration of equations of motion was conducted in the interval of the variation in the frequencies of the particles from 5.9 to 6.1 with the random disturbances of field with which the rms value of excursion of closed orbit is equal to 20/o from the semiaperture, and the rms values of width of resonance bands were equal to 0.01. The curves of figure correspond to average/mean values on 10 realizations of random functions.

The authors hope that this work will draw specialists' attention in particle accelerators to the great possibilities which open/disclose digital simulation in the accelerative technology.
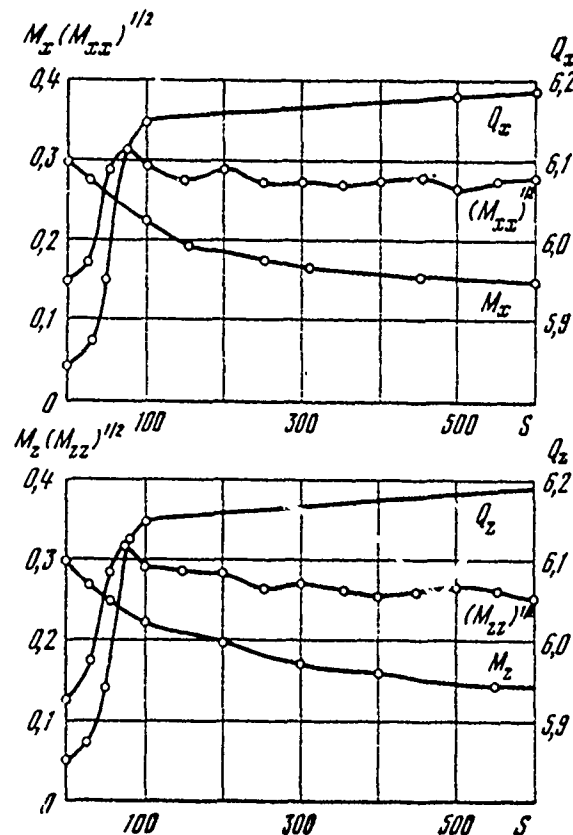
Passage through the whole resonance in the presence of dipole, quadrupole and sextupole disturbances/perturbations M_x, M_z - the first moments/torques of bundle in the fractions of semiaperture; M_{xx}, M_{zz} - central second moments/torques of bundle; Q_x, Q_z - frequency of betatron; S - speed of bundle.

Page 49.

Discussion.

A. N. Didenko. In the real accelerators there are resonances, distant to value $\Delta\nu$, compared with the precision/accuracy of your method. It is possible whether, utilizing your method of simulation, to obtain the results, which characterize the effect of such resonances on the particle motion?

N. L. Sosenskiy. It is possible. In these cases it is necessary to use the approximation cf real magnet by a large number of thin magnets (two, three, etc.). In this case, however, increases the necessary machine time.

V. V. Tsygankov. In what there was the purpose of the work? Which order of magnitude of nonlinearity and is substantial their effect?

N. L. Sosenskiy. The basic purpose of the work consisted of the investigation of allowances on the nonlinear disturbances/perturbations of magnetic field in the accelerator of the RTI of the AS USSR tc the energy 1 GeV, which is necessary for developing the systems cf nonlinear correction.

The effect of nonlinearity was essential.

V. G. Davidovskiy. How many revolutions were outlined?

N. L. Sosenskiy. For purposes of our investigations it was simulated the order of several thousand revolutions.

Ye. L. Kosarev. How machine time of the calculation of one revolution in the single-particle approximation/approach?

N. L. Sosenskiy. Count time on the computers BESM-6 of ~0.03 s for one revolution of particle motion with a number of magnets 100.

Ye. Regenshtreyf. How far it is possible to use the extrapolation of your low-energy into the region program and under what conditions?

N. L. Sosenskiy. Investigations were conducted for the energy of injection, equal to 1 MeV. For lower energies the estimations were not conducted.

100. ELECTRON ANALOG OF THE CIRCULAR CYCLOTRON.

A. A. Glazov, V. P. Dzhelepov, V. P. Dmitriyevskiy, B. I.
Zamolodchikov, V. V. Kol'y, D. L. Novikov, L. M. Onishchenko.

(Joint Institute for Nuclear Research).

The constantly growing requirements for the precision/accuracy
of physical experiment cause the need for the creation of
accelerators with all by aigh currents and stimulate the theoretical
and experimental studies of the possibility of designing of such
accelerators.

In the laboratory of nuclear problems in the beginning of 1968
was put into operation electron analogue of new type accelerator -
relativistic circular cyclotron with strong focusing [1].

Model has an identical to the proton accelerator being simulated
final energy and a set of energy per revolution (in the energy units
of rest), and also frequency of betatron and phase width of cluster.

If we proceed from the assumption that the current strength in

the accelerator is limited to weakening transverse focusing due to
the action of space charge, then under conditions indicated above
current in the proton machine being simulated is connected with the
current of electron analogue with the relationship/ratio

$$\frac{i_p}{i_e} = \frac{eV_p}{eV_e} \frac{\omega_p}{\omega_e} \frac{\Delta z_p}{\Delta z_e} = \frac{M_{0p}}{m_{0e}} \frac{\omega_p}{\omega_e} \frac{\Delta z_p}{\Delta z_e} = \frac{B_{0p}}{B_{0e}} \frac{\Delta z_p}{\Delta z_e} \quad (1)$$

where ω and Δz - frequency of revolution and height of bundle; M_0 -
mass of particle, B_0 - magnetic field, eV - set of energy; index p -
relates to the protons, e - to the electrons. Magnetic field in the
model on a radius of injection is equal to 14 G; if we accept for the
proton machine $B_0 = 4200$ G and $\Delta z_p/\Delta z_e = 2$, then the coefficient of
simulation in current $i_p/i_e = 800$.

Basic parameters of electron analogue following:

Energy of the injection ... 6 keV.

Radius of the injection ... 18 cm.

Final energy ... 409 keV.

The terminal radius ... 100.7 cm.

Frequency of revolution ... f=39.475 kHz; λ_e-
-121.2 cm; Q_r= 1,045+2; Q_z-
- 1,15 + 1,32.

The system of injection into electron analogue [2] provides on a radius of injection current in the form of microclusters in amplitude to 20 mA and by duration of 2.0 ns.

Model has besides continuous also pulsed operation mode, which is reached by modulation of injector or accelerating voltage or that, etc. simultaneously.

Is at present on the terminal radius of accelerator obtained average/mean current 600 μA, which corresponds to the current of protons 300-400 mA. The dependence of current on a radius is shown on Fig. 1A, b.

Fig. 1c shows the dependence of the electron density on a radius (curve 1), defined as [3]

$$n = \gamma^3 \frac{E_0}{eV} \frac{i}{f\gamma^2_\infty \Delta z \Delta \varphi_e} . \qquad (2)$$

In the same figure (curve 2) is shown the dependence on a radius of the maximum density, determined from the condition

$$Q_x^2(\imath) - 4\pi \frac{n(\imath)\gamma^2_\infty \gamma_e}{\gamma^3(\imath)} = 1 , \qquad (3)$$

where $\gamma_e = e^2/4\pi e_0 m_0 c^2 \approx 2{,}82 \cdot 10^{-13}$ [см] - classical radius of electron. During conclusion/output (3), and also (1) it was assumed that the space charge, concentrated in the "infinite" layer by thickness Δz

reduces the frequency cf bouncing Q_z to the unit.

Page 50.

During the determination of density from (2) it is necessary besides the current strength to know also the set of energy per revolution eV, vertical Δz and azimuthal $\Delta\phi$ the sizes/dimensions of bundle.

The vertical size/dimension of bundle was determined according to the current distribution on the nine-segment target, which was written/recorded to the automatic recorder (or it was observed on the five-beam oscillograph). Dependence $\Delta^x(v)$ is shown in Fig. 2a (full/total/complete width on the half-height of distribution). On the larger part of the radii Δz do not exceed 5 mm.

The set of energy per revolution was determined by the time of the acceleration of bundle to the fixed/recorded radius in the pulsed operation

$$eV = \frac{W(v_2) - W(v_1)}{t(v_2) - t(v_1)} T, \qquad (4)$$

where $W(v)$ - energy on a radius v; $t(v)$ - the time of acceleration to this radius; T - revolution period. Fig. 2, in shows the averaged for the selected interval cf radii value of the set of energy depending on a radius with accelerating voltage 1.2 kV. This picture gives also

representation about the motion of the phase of the accelerated

bundle. Fig. 2d shows the behavicr of the phase of bundle along a

radius, changed directly with the aid of the phasemeter. It is

evident that the full/tctal/complete deviation of phase does not

exceed 25°.

The azimuthal size/dimension of the cluster of the accelerated

particles was measured with the aid of shielded target signal with

which with the matched cable was supplied to the entrance of the

stroboscopic oscillograph (simultaneously was determined the

amplitude of current). The results of this measurement are shown in

Fig. 2b, from which it is evident that $\Delta\phi$ not not greatly strongly it

is not changed along a radius and close to 0.5 rad.

Besides the measured characteristics of bundle whose knowledge

is necessary for determining the particle density in the accelerated

bundle, were experimentally determined the values of frequencies of

the betatron on different radii. Oscillations/vibrations (center of

gravity of bundle) were swung by the high-frequency field which was

created by the electrodes of the corresponding configuration (by two

horizontal plates, supplied antiphase - for oscillation of bouncing;

by vertical plate and by claddings of chamber/camera - for the

driving of bouncing; by vertical plate and by claddings of

chamber/camera - for the building up of radial oscillations). The

supplying to the plates radio-frequency voltage cables terminated by the matched loads, which provided constant (with an accuracy to 20o/o) stress of driving over a wide range of frequencies. The reconstructed in the range 45-105 MHz oscillator operated on a pulsed basis. Resonance was fixed/recorded on reduction in current on the target.
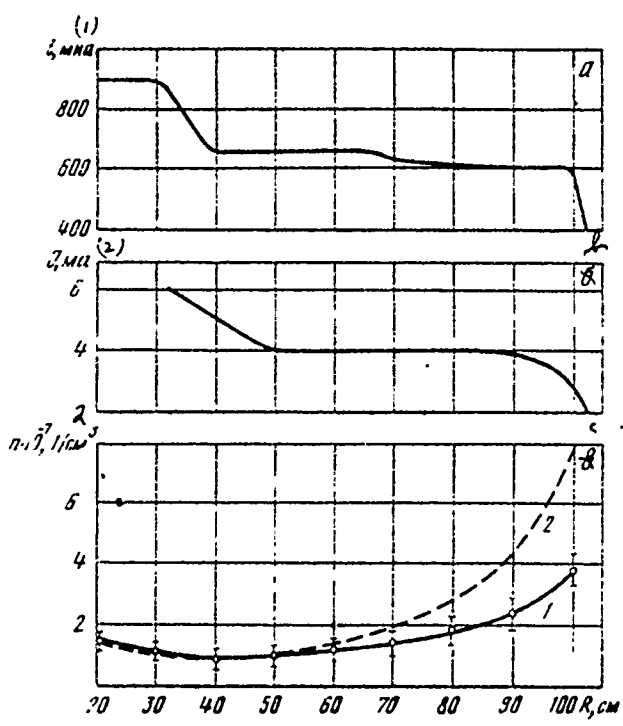
Fig. 1.
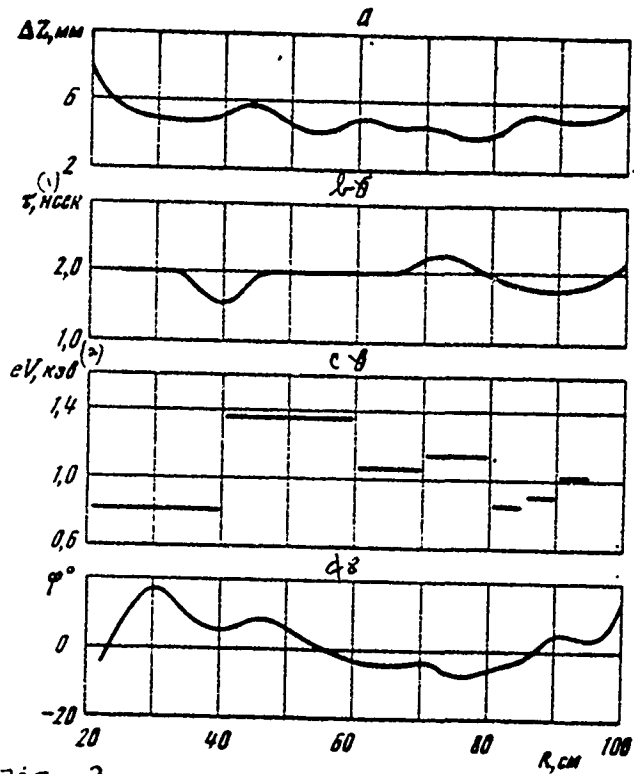
Fig. 2.

Fig. 1. Dependence on radius of average/mean current (a), amplitude of current in cluster (b), electron density (c).

Key: (1). μA. (2). mA.

Fig. 2. Dependence on radius of height of bundle (a), phase width (duration) of cluster (b), set of energy per revolution (c); phase position of cluster (d).

Key: (1). ns. (2). keV.

Page 51.

The results of measurement Q_r and Q_z are represented in Fig. 3a and 3b together with the theoretical dependences of these values from a radius, obtained from relationships/ratios [4]

$$Q_z^2 = -n + \frac{\varepsilon^2 N^2}{2(N^2-1-n)} + \frac{\varepsilon^2 R^2}{2\lambda^2(N^2-1-n)} + \frac{\varepsilon^2 R^2}{2\lambda^2 N^2},$$

$$(5)$$

$$Q_r^2 = (1+n)\left[1 + \frac{3}{2N^2}\left(\frac{\varepsilon R}{N\lambda}\right)^2\right] + \frac{\varepsilon^2}{2(N^2-4-4n)}\left(2 - \frac{N}{N^2-1-n} + n\right)^2 + 0.7\frac{\varepsilon^2}{N^2-1-n},$$

where n - index of an increase in the magnetic field; ε - depth; $\lambda = 8$ cm - spiral pitch; N=8 - number of spirals.

Resonance frequency was fixed/recorded with the precision/accuracy not worse than 200 kHz, so that the precision/accuracy of measurement Q is determined in essence by final radial extent of plates (4 cm). Described measurements give sufficiently complete information about the characteristics of bundle and they make it possible to define as particle density in the accelerated bundle (maximum density, achieved/reached on the terminal

radius, is 4.10^7 $1/cm^3$), so also expected frequency shift of bouncing under the action of space charge.

According to theoretical representations [5] the space charge must have an effect on the incoherent frequency (frequency of particles relative to the center of gravity of bundle) of betatron, while coherent frequency must remain constant with the high degree of accuracy. This latter/last confirmation was subjected to experimental check. Frequency bouncing the center of gravity of bundle was determined on the fixed/recorded radius with a change in the current from 10 to 620 μA, which corresponds to density change from $2.5 \cdot 10^5$ $1/cm^3$ to $1.6 \cdot 10^7$ $1/cm^3$. The relative precision/accuracy of measurement Q composed 0.005. Within this precision/accuracy it was not noted dependence Q_z on the strength of current (Fig. 3c).

For measuring the frequency of incoherent was made the attempt excite parametric resonance by high-frequency field, close one in form to the field of quadrupole, which, however, proved to be unsuccessful. This, apparently, it is possible to explain by the insufficient speed of the accelerated bundle in the zone of action of the exciting field. In order to overcome this difficulty, was realized the mode/conditions of the circulating bundle. Bundle remained in the zone of action of exciting fields due to modulation accelerating voltage. In this case due to finite time of the life of

electrons and deliquescence of the circulating bundle in the azimuth
bearing the charge density decreases in the time. Fig. 4a shows the
oscillogram of the signal, aimed at a pick-up-electrode by the
circulating bundle, while in Fig. 4b the same during the excitation
of external resonance (duration of the pulse of the exciting field of
approximately 15 μs). At present this experiment continues.
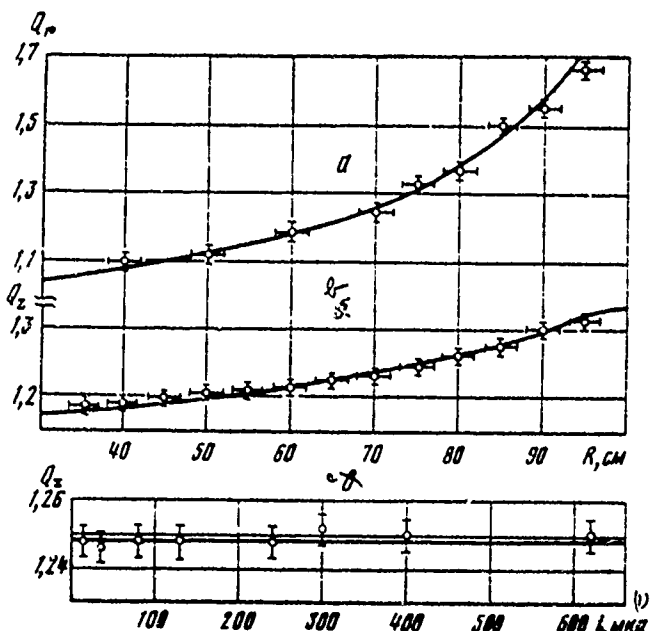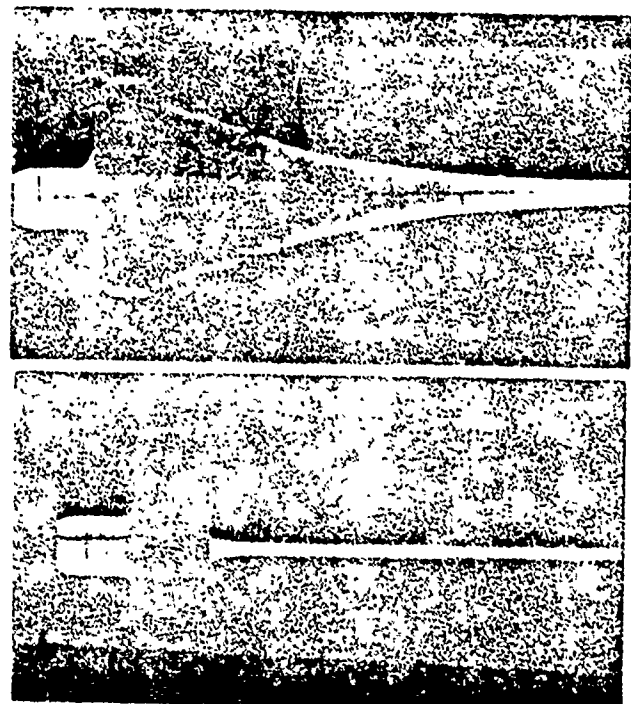
Fig. 3.   Fig. 4.

Fig. 3. Dependence Q_τ on radius (a), Q_x from radius (b), Q_z from strength of average/mean current (c).

Key: (1). μA.

Fig. 4. Oscillograms of signal on pick-up-electrode, aimed by circulating bundle (scanning/sweep 50 $\mu s/cm$). a) in the absence of exciting field; b) during the excitation of external resonance.

REFERENCES

1. V. N. Anosov et al. Atomic energy, 1968, 25, No 6, 539.

2. A. A. Glazov, D. L. Novikov, L. M. Onishenko. Transactions of
All-Union conference on the charged particle accelerators, Vol. 1.
M., VINITI, 1970, page 485.

3. V. P. Dmitriyevskiy, B. I. Zamolodchikov, V. V. Kol'g. On the
minimum amplitude of accelerating voltage in the relativistic
cyclotrons. Transactions of conference on the cyclotrons, Krakow,
1961.

4. V. P. Dzhelepov, B. P. Dmitriyevskiy, B. I. Zamolodchikov, V.
V. Kol'g. UFN, 35, 1965, No 4, 651.

5. L.J.Laslett. Proc. 1963. Summer Study on Storage
Rings, Accelerators and Experimentation at Super-
High Energies. BNL-7534, 324-367.

Page 52.

101. SOME EFFECTS OF A SPACE CHARGE IN THE BOOSTER AND MAIN ACCELERATOR OF THE INSTITUTE OF HIGH-ENERGY PHYSICS [IFVE].

V. I. Balbekov.

(Institute of high-energy physics).

I. A. Shukeylo.

(Scientific research institute of the electrophysical equipment im. D. V. Yefremov).

The projected/designed increase in the intensity of proton synchrotron of the IFVE [1] requires the detailed analysis of the phenomena, connected with the effect of space charge. In this work is examined the repeated intersection of resonances due to the Coulomb shift/shear of betatron frequencies. Is usually dangerous the intersection of linear resonances; however, in booster and in main accelerator of the IFVE are established/installed severe limitations

for the permissible increments in the amplitudes. Furthermore, in main accelerator is provided for prolonged - to 1.2 s - the circulation of beam in the magnetostatic field. Under such conditions proves to be dangerous the intersection of resonances to the 4th order, which makes it necessary attentively to relate to the selection of the position of operating point and the work of the systems of correction.

The repeated intersection of one-dimensional resonances was examined in the series/row of works [2] however a strict solution of this problem sufficiently complicatedly and leads to the bulky results. The target of this article consists in the fact that, on the basis of some simplifying assumptions obtaining of the formulas, suitable for the rapid evaluations of the effect of any resonance.

Examining accelerator with high intensity, it is possible to disregard the dependence of betatron frequencies on the impulse/momentum/pulse and to consider only Coulomb shift/shear. From the following it will be evident that when spread along the impulses/momenta/pulses proves to be essential, its effect it is not difficult to rate/estimate. We will not also examine coherent Coulomb shift/shear, since it usually is considerably less than the incoherent. During the calculation of the l·tter it is possible to disregard wall effect which give relatively small contribution.

In these propositions the shifts/shears of the betatron frequencies from rating values Q_{r0}, Q_{x0} are connected with the relationship/ratio

$$\Delta Q_r = \xi \Delta Q_x \qquad (1)$$

with the constant ξ and ΔQ_x oscillating with the double frequency of the synchrotron oscillations/vibrations between the extreme values:

$$(\Delta Q_x)_{max} = \Delta Q, \quad (\Delta Q_x)_{min} = \Delta Q(1-\alpha^2)^{1/2}, \quad (2)$$

where α - relative amplitude of the synchrotron oscillations (it is assumed that the phase density is permanent, and synchrotron oscillations they are linear).

An increment in the amplitude during the single intersection of resonance is determined by the speed of intersection, for which is obtained the estimation:

$$\left| \frac{d(\Delta Q_x)}{ds} \right| \simeq \frac{(\Delta Q_x)_{max} - (\Delta Q_x)_{min}}{\Delta s} = \qquad (3)$$

$$= \frac{\Delta Q}{\Delta s}\left[1 - (1-\alpha^2)^{1/2}\right],$$

where s - arc, measured along the equilibrium orbit; Δs - path, passed by particle for fourth of period of synchrotron oscillations, i.e., during the mean time between two intersections of resonance.

The radial and verticals deflection of particles from the

axis/axle let us write in the form

$$(\tau,z) = \left(\frac{b_0}{p}\right)^{1/2}\left(a_{\tau,z}\,\varphi_{\tau,z} + a^*_{\tau,z}\,\varphi^*_{\tau,z}\right) \qquad (4)$$

with the function of floquet, calibrated according to the condition:

$$\varphi\varphi^{*\prime} - \varphi^\prime\varphi^* = -i\,w, \qquad (5)$$

where p - impulse/momentum/pulse; $w = 2\,m$ - Wronskian determinant, prime indicates differentiation with respect to s.

As is known (see for example, [3]), near the resonance the amplitudes of betatron oscillations satisfy system of equations:

$$a^\prime_{\tau,z} = a_{\tau,z}\,\frac{\mathcal{P}_{\tau,z}}{R_0}\left(\frac{b_0}{p}\right)^{\frac{n}{2}-1} e^{\pm\frac{i}{R_0}\int e\,ds},$$

where $e = n_\tau Q_\tau + n_z Q_z - k$ - detuning; R_0 - the mean radius of equilibrium orbit; $n = |n_\tau| + |n_z|$ - order of resonance; $\mathcal{P}_{\tau,z}$ - its width. The sign of the index of exponential curve depends on the signs of integers n_τ, n_z and it does not affect results. Furthermore, further it will be necessary to know only moduli/modules $\mathcal{P}_{\tau,z}$ which with a sufficient precision/accuracy can be written in the form

$$|\mathcal{P}_{\tau,z}| \propto \frac{(n-1)!}{(|n_{\tau,z}|-1)!\,|n_{\tau,z}|!}\,\frac{R_0\,b\,\Gamma_{n_\tau n_z}}{R\,w\,|a_{\tau,z}|^2}\left(\frac{|a_\tau|^2}{b^2}\right)^{\frac{|n_\tau|}{2}} \times \quad (7)$$

$$\times \left(\frac{|a_z|^2}{b^2}\right)^{\frac{|n_z|}{2}}.$$

$$\Gamma_{n_\tau n_z} = \left|\frac{1}{2\pi R_0}\int_0^{2\pi R_0}\tau_{n-1}\,|\varphi_\tau|^{|n_\tau|}\,|\varphi_z|^{|n_z|}\,e^{-i\frac{ks}{R_0}}\,ds\right|, \quad (8)$$

$$\tau_{n-1} = \frac{b^{n-1}}{(n-1)!\,H}\,\frac{b^{n-1}(\Delta H)}{\partial \tau^{n-1}}\bigg|_{\tau=z=0} \quad (9)$$

where R - radius of curvature in the magnetic field; τ_{n-1} - nonlinear

addition to the magnetic field at a distance δ from the axis/axle; δ
- half-width of the chamber/camera: $\Delta H(\imath,z)/H$ - the relative deflection
of magnetic field from computed value, moreover $\Delta H = \Delta H_z$ with even $|n_z|$
and $\Delta H_\imath$ - with the odd.

Page 53.

For solving system (6) we will use the method, which were being
applied earlier in work [4] where shown that with an accuracy down to
the terms $\sim|\varphi_{\imath,z}|$ a relative increment in the amplitude $\Delta|a|/|a|$ is
random function with the zero average/mean value, and is found
dispersion. In order to find the expansion of beam, for example
according to $\imath$, the distribution, examined/considered with maximum
initial amplitude $|a_\imath|$, one should average in the amplitudes of
synchrotron and vertical betatron oscillations. Then, considering
that the phase density is permanent in all projections, and utilizing
(1), (3), (7), we will obtain the following expression for a
root-mean-square increment in the sizes/dimensions of the beam:

$$\left\langle\frac{\Delta|a_{\imath,z}|}{|a_{\imath,z}|}\right\rangle \approx \left[\frac{2\pi^2\Delta Q_0^2\,|\varphi_{\imath,z}|^2}{|n_z+\xi n_\imath|(2|n_{z,\imath}|+1)}\int\left(\frac{p_0}{p}\right)^{n-2}\right._{\times(10)}$$

$$\left.\frac{f\,dt}{\Delta Q^3}\right]^{1/2},$$

where f - frequency of revolution; $\bar{\varphi}_{\imath,z}$ are taken with the maximum
amplitudes; integration is conducted according to the region in which
$\Delta Q > \Delta Q_0$, ΔQ_0 - vertical Coulomb shift/shear with which the operating

point reaches the resonance line

$$\Delta Q_0 = \frac{n_\gamma Q_{\gamma 0} + n_z Q_{z 0} - k}{n_z + \xi\, n_\gamma}.$$ (11)

Applying formula (10) to main accelerator, let us examine the period of injection, which represents the maximum danger. In this case $p=p_0$; $f=1.86\cdot 10^5$ s^{-1}, $t=1.2$ s, $\Delta Q_0=0.12$, $\xi=0.5$. Coulomb shifts/shears are found on the assumption that the chamber/camera of booster is utilized completely ($E_\gamma = 44$ cm$\cdot$mrad, $E_z = 10$ cm$\cdot$mrad), and subsequently the sizes/dimensions of beam change adiabatically, since upon the injection into main accelerator $E_\gamma = 5.3$ cm$\cdot$mrad, $E_z = 1.2$ cm$\cdot$mrad. The permissible increase of the sizes/dimensions of beam takes as the equal to 0.15 on a radius and 0.30 on the vertical line.

Thus, are obtained limitations to the width of the resonance:

$$|\mathcal{P}_\gamma| < \frac{2\cdot 10^{-6}}{\Delta Q_0} \left[|2n_z + n_\gamma|(2|n_z|+1) \right]^{1/2}$$ (12)

$$|\mathcal{P}_z| < \frac{4\cdot 10^{-4}}{\Delta Q_0} \left[|2n_z + n_\gamma|(2|n_\gamma|+1) \right]^{1/2}.$$ (13)

In the most adverse case when $\Delta Q_0=\Delta Q=0.12$, allowances for the width of resonance in limits of $10^{-5}-10^{-4}$.

Let us note that $\mathcal{P}_{\gamma,z} = 0$, if $2n_z + n_\gamma = 0$, i.e. when the operating point is moved along the resonance line. In reality, here it is necessary to consider the dependence of betatron frequencies on the impulse/momentum/pulse, which will lead to a change in the parameter ξ. Analysis shows that in this case should be taken $\xi \approx 1$, i.e., the

limitations for the resonance of the third order $n_x = -1$, $n_v = 2$
approximately/exemplarily the same as to the others: $|\varphi_v| < 5 \cdot 10^{-5}$;
$|\varphi_x| < 1 \cdot 10^{-4}$.

According to the data of magnetic measurements the
root-mean-square spread of the nonlinearity of the field of main
accelerator is evaluated with n=2-5 at $(1-5) \cdot 10^{-4}$ at a distance of
8.5 cm from the axis/axle. Hence it is possible to rate/estimate
harmonics of field and then actual width of resonance bands.
Comparison with allowances (12)-(13) makes it possible to conclude
that the resonances of the second and third order undoubtedly are
dangerous: their width exceeds that permitted into ten or hundreds of
times. The width of the resonances of the fourth order somewhat more
than permitted, but not so that it would be possible to make the
single-valued conclusion about their danger, since, apparently,
difference is within the limits of the errors for magnetic
measurements and calculations. The resonances of the fifth order have
a width, mismachined undersize, but when $|n_v| \geq 3$ the precision/accuracy
again is insufficient for the confident conclusion about their
safety.

After considering all dangerous and doubtful resonances, it is
possible to conclude that optimum frequencies are $Q_{r0} = 9.9$, $Q_{z0} = 9.87$,
linearity correction $\tau_v^{(v)}$ of that calling resonance ? $r Q_x = 10$, to

$1 \cdot 10^{-5}$ making it possible substantial to facilitate the conditions for particle motion.

Analogous calculations were made for the booster, Coulomb shift/shear in which grows/rises during 1.5 ms, after injection from 0.05 to 0.1, and then smoothly it decreases, reaching at the end of cycle -0.01. The permissible increments in the sizes/dimensions of beam were accepted equal to 0.15. It turned out that from the resonances of the third order are most dangerous the following: $3Q_\tau = 10$; $2Q_\tau + Q_x = 10$; $2Q_\tau - Q_x = 3$. From intersection possibly, if the spread of quadratic nonlinearity at a distance of 8 cm from axis/axle $\tau_2^{(\tau,x)} < 5 \cdot 10^{-5}$. The intersection of the remaining resonances of the third order is possible, if $\tau_2^{(x)} < 1 \cdot 10^{-4}$, $\tau_2^{(\tau)} < 5.10^{-4}$. All resonances of the fourth order are safe when $\delta_3^{(\tau,x)} < 5 \cdot 10^{-4}$, which, apparently, is easily feasible. Therefore the selection of betatron frequencies in region $Q_{\tau 0} = 3.26$, $Q_{x0} = 3.38$ seems sufficiently to those substantiated, although they are not excluded and other regions, for example, $Q_{\tau 2} = 3.42$, $Q_{x0} = 3.38$.

In conclusion let us note that increments in the amplitudes sufficiently weakly are changed with the change ΔQ so that, if the actual displacement of operating point will differ somewhat from the calculated, this little will influence the permissible value of the scatter of the parameters of blocks/modules/units.

REFERENCES

1.   Yu. M. Ado, et al. Increase in Intensity of Proton Synchrotron
      of Energy of 70 GeV by Increasing Injection Energy.
      This collection. Vol. II.
2.   A. L. Artemov, et al, Fast Booster - Injector of Proton
      Synchrotron of IFVE [Institure of High-Energy Physics]
      This collection, Vol. II.   Atomnaya Energiya, 1965, 18, 636,
      PTE, 1967, 1, 24.
3.   A. A. Kolomenskiy, A. N. Lebedev, Theory of Cyclic Accelerators,
      Chapter III, Section 8. M., Fizmatgiz, 1962.
4.   B. I. Balbekov, I. A. Shukeylo. ZhTF, 1969, 39, 1863.

Page 54.

102. ALIGNMENT AND ADJUSTMENT OF BEAMS OF SECONDARY PARTICLES. THE USE OF COMPUTERS FOR INVESTIGATION OF THE PROCEDURE OF ADJUSTMENT.

V. V. Miller.

(Institute of theoretical and experimental physics).

During the calculation of displacement tolerances of the magnetic elements/cells (see references in [1]) they always accept, that the value of the central particle momentum p_0 of band $\Delta p/p_0$ is determined at the input into the system. However, in the secondary beams the isolation/liberation of momentum range occurs in system itself, and the transverse shift/shear of lenses not only displaces beam at the end of the system, but also changes value of p_0.

In work [1] it is shown that the transverse shift/shear of the i lens to value δ_x in the linear approximation/approach causes the displacement of source of the image, created by the j element/cell, on

$$\Delta x_j = \varepsilon_x \left(M_{ij} - M_{(i-1)j} \right) \qquad (1)$$

where M_{ij} - coefficient of linear magnification from the i-th to the

j image. Let at the point of the j image be placed the collimator for the isolation/liberation of band $\Delta p/p_0$ (pulse collimator). Then through the center of this collimator pass particles with $\delta = \Delta p/p_0 = \varepsilon_x (M_{(i-1)j} M_{ij})/D_{0j}$, where D_{0j} - dispersion in pulse collimator, and beam displacement at the end of the system (in the k image)

$$\Delta x_k = \varepsilon_x D_{jk} (M_{(i-1)j} - M_{ij})/D_{0j} .$$
(2)

For nondisperse systems $D_{0j} M_{jk} + D_{jk} = 0$ and latter/last formula takes the same form, as (1).

For the isolation/liberation of the band of impulses/momenta/pulses is important also fine adjustment along the axis of the system of internal target of accelerator and all collimators. With the adjustment the target locations usually establish/install minimum clearances in aperture (AK) and pulse (IK) collimators (Fig. 1) and in the switched-off lenses and the nominal field in magnet B_2 is changed current in magnet B_1. If target offset $x_M \neq 0$, then the maximum of the count of small counter at the end of the system reaches at the field in B_1 different from the the nominal H_0, $\gamma_M = \Delta H/H_0 \stackrel{\cdot}{\cdot} 0$. Target location is corrected until γ_M is equal to 0.

The sensitivity of method in the linear approximation/approach is equal to

$$d\gamma_M/dx_M = [\alpha_1(L_3+L_4)L_1 + \alpha_2(L_1+L_2)L_4]/[\alpha_1(L_3+L_4)L_1 \times$$
$$\times (T_{12} T_{23} - T_{22} T_{13}) - \alpha_1\alpha_2 L_2 L_4 T_{12}],$$

where T_{ij} - coefficients of the matrix/die of transition from the

target to the collimator AK. If target is located out of the magnetic

field, then $T_{23} = T_{13} = 0$, $T_{12} = L_0$. Then in the parameters of channel,

designated in Fig. 1, $d\tau_M / dx_M = -0.48\% \cdot cm^{-1}$. Sensitivity increases, if

counter C approaches magnet B_2.

Formula (3) is obtained in the assumption that there is no focusing

in magnets, and dimensions of the target, counter C

        and clearances in the collimators they are negligible.

Counter C single although actually is applicable telescope of

counters. In the real cases, especially when a larger number of

magnets is present, it is possible to resort to the aid of computers.

Fig. 2 reflects dependence on γ the intensity, recorded by counter C

of finite dimensions (curve of adjustment) with the final clearances

in the collimators and the finite dimensions of target for the

channel, shown in Fig. 1. Calculations are carried out according to

the program "Focus"[1].

FOOTNOTE [1]. Program "Focus" for the optimization of the magnetic

systems (see references in [1]) is substantially modified. Are added

the new operators of optimization, for example, is introduced the

operator of the generalized focusing, who makes the divergence of

sine-like trajectory with the given x'_0 (or y'_0) equal to the given

one (taking into account the sign). In particular, this divergence

can be equal to zero (image). Is possible the optimization of the

axial extent of bunch of particles and isochronization of system, the

optimization of chromatic aberration, agreement of phase ellipses,

etc. Program allows the calculation of all aberrations of the 2nd

order and most important aberrations of the 3rd and 5th orders. In

the program are provided for check, diagnostics, and sometimes also the correction of the errors in input data and the convenient form of readout, in particular, most automatic possible obtaining of the charts of separate trajectories, and also pulse spectra of particles, passing through the system, which switches on collimators and counters, and also the total "profile/airfoil" of beam for entire set of particle momenta. Program calculates the aperture ratio of system taking into account the dependence of the output of secondary particles on their mass, the impulse/momentum/pulse and the angle of emission, and also energy of protons. ENDFOOTNOTE.

Sensitivity $d\tau_M/d\tau_M$ calculated from the shift of the maximum of curve of adjustment, will agree with the value, obtained from formula (2). Analogously it is possible to examine the effect of the shift of collimators.
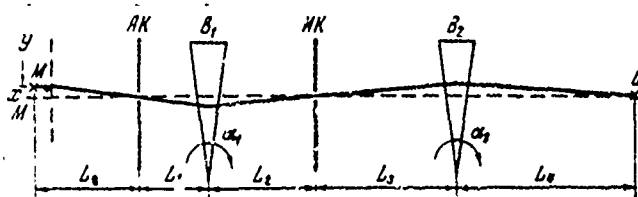
Fig. 1. System of magnets and collimators. M - target; AK and IK -
aperture and pulse collimators; Y - region of the field of
accelerator; B_1 and B_2 - magnets; C - counter; angles of rotation
$\alpha_1 = \alpha_2 = +0.1$ rad; L_0-L_4 are equal to with respect 6, 4, 6, 8 and 10 m.
Unbroken curve - trajectory, passing through centers AK, IK and S.

Page 55.

Let us pause even at the use/application of computers to the
investigation of the procedure of the adjustment of horizontal
focusing in the first objective. The first results are described in
[1]. Is sufficiently propagated the following method of adjustment.
At the end the systems place counter C (large size/dimension on the
vertical line) and consider that the correct adjustment to the pulse
collimator corresponds to the maximum of readings. Frequently as a
result of this procedure system proves to be in the completely
unlikely mode/conditions.

Alignment procedure it is convenient to simulate on the

computers. As the first example let us examine the achromatic system,
shown in Fig. 3. Fig. 4 shows the dependence of the intensity,
recorded by counter from the mode/conditions of the first and second
objectives. As the criterion of the defocusing of the first objective
is accepted the distance δ_1 from the center of IK to the source of
the image, created by the first objective. Along curves 1-6 δ_1 is
constant, and varies δ_2 - distance from IK to that point on the
axis/axle of system, that is focused by the second objective to the
center of counter C.

From Fig. 4a it is evident that curve 3, which corresponds to a
precise focusing on IK, is separated/liberated in no way: if we focus
beam on 0.5 m nearer than IK, then it is possible to obtain the large
intensity (curve 2). With the large defocusing (curves 5, 6) the
curves become double-humped; this phenomenon is accompanied by the
appearance of the second maximums in the pulse spectrum of particles.

If at the output of the system (it is direct after lens Q_Φ) to
supply magnet B_3, which turns beam on the angle of $\alpha_3 = 0.1$ rad (in the
other direction, than B_1 and B_2), then curves 1-6 strongly will be
drawn together, and their maximums will increase (Fig. 4b). In this
case is observed an increase in the band $\Delta p/p$ by the passed system
due to the compensating action of rotation in B_3. With sign change α_3
the curves strongly are separated/expanded, their height and band

$\Delta p/p$ decrease.

Fig. 5 shows the calculated curved adjustments for the real system - beam 2A on the accelerator of the IFVE. The structure of channel is analogous shown in Fig. 3, but doublet Q_4Q_5 is replaced to the quartet, within which is created parallel beam. At the end again is conducted magnetic analysis. Evidently strong change in the form with a change in the size/dimension of counter C. Upon the achromatic inclusion/connection, on the other hand, curve of ideal adjustment prove to be maximum for the small counter and somewhat less than adjacent curves for the case of large counter.
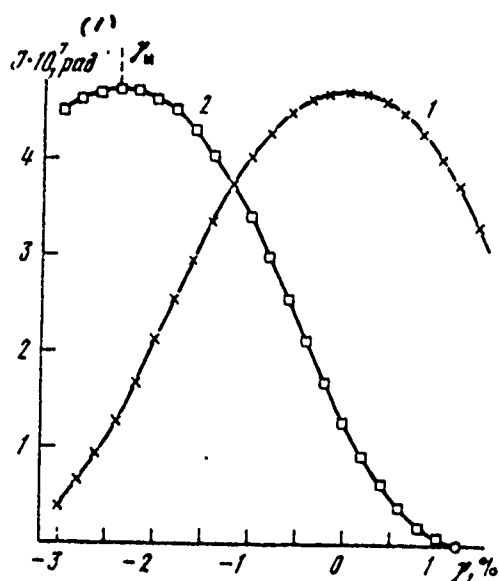
Fig. 2.
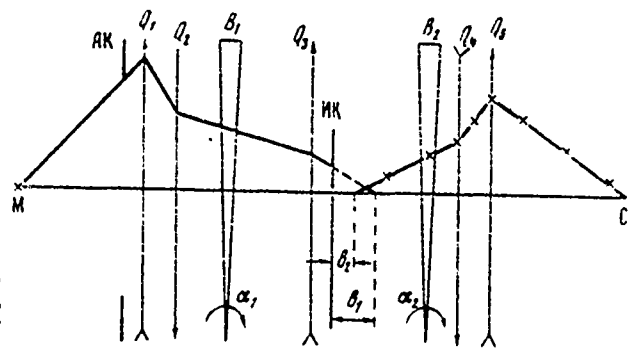
Fig. 3.

Fig. 2. Dependence of intensity $\Im$, of that recorded by counter C, on field in magnet B_1. Target out of the field of accelerator. Clearances in AK and IK are equal to ± 2 mm, target ± 1.5 mm, on the horizontal, counter C – 4 mm. 1 – target on the axis/axle of system; 2 – target are displaced by $X_M = +5$ мм; $\Im = \int \varphi_{x}(\vartheta) d\vartheta$, φ_{x} – acceptance angle.

Key: (1). rad.

Fig. 3. Achromatic magnetic system. On the vertical line the beam is always focused on 2 m for IR and to counter C $\alpha_1 = +0.25$ rad, $\alpha_2 = +0.1825$ rad, clearance in AK of ± 5 cm, in IK – ± 1.5 mm, counter C

- 3 mm. The length of channel is 29 m, all lenses ML15, $\beta_{эфф} \sim$ 96 cm.
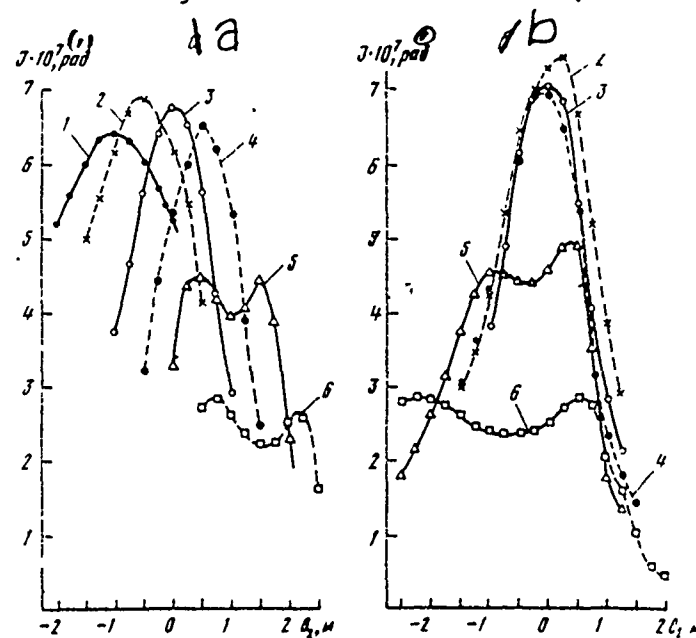
Fig. 4. Setup curves for system in Fig. 3. a) achromatic mode/conditions; b) with magnet B_3 after Q_5; 1-6 - correspond to the constant duty of the first objective; $B_1=1$, -0.5, 0, +0.5, +1.0, +1.5 m.

Key: (1). rad.

Page 56.

Is created impression, that on the basis of qualitative concepts it cannot be indicated applicability conditions for the described method of adjustment. However, it is possible that with the method of the comparison experimental setup curved from those calculated for of the given conditions it is possible it will be obtain satisfaction sufficiently precise conclusions about the adjustment of system.
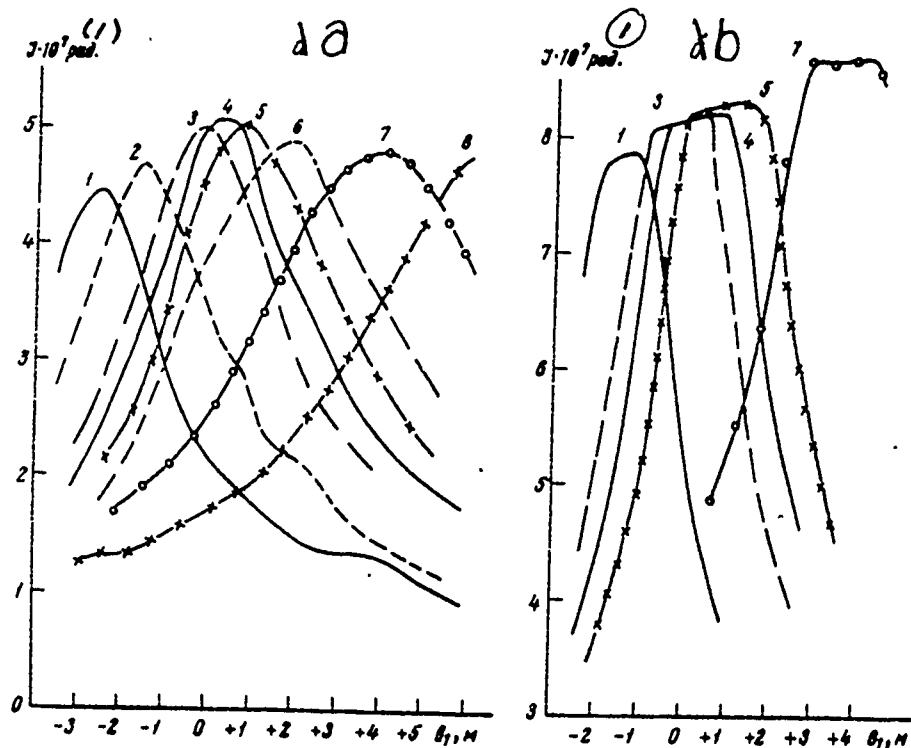
Fig. 5. Setup curves for beam No 2A of the IFVE. Target - 1 mm a) counter 2 cm; b) counter 3 mm. 1-8 correspond to the constant duty of tail piece of the system; θ_2=+4.5, +2.0, +0.5, 0, -0.5 -1, -2, -3 m.

REFERENCES

1. V. I. Kotov, V. V. Miller, Focusing and Separation by Masses of High-Energy Particles. M., Atomizdat 1969.

103. COMPUTER SIMULATICN OF A SYSTEM FOR THE SUPPRESSION OF THE PHASE OSCILLATIONS OF THE CENTERS OF CLUSTERS.

B. I. Bondaryev, B. P. Murin, L. Yu. Solovyev.

(Radio engineering institute of the AS USSR).

An increase in energy and intensity of particles at the output of linear accelerators and the increased requirements for the parameters beam caused the need of applying the new principles of the automatic control of amplitudes and hf phases in the resonators. The proposed by B. P. Murin and by I. Kh. Nevyazhskiy and developed/processed in the radio engineering institute AS USSR the system of the automatic correction of hf accelerating fields according to the data about the phase of the centers of clusters (ARF-P) makes it possible to remove also the coherent phase (longitudinal) oscillaticns of clusters in beam [1].

For the explanation of the corrective action of system ARF-P let us examine the phase plane where along the axes of abscissas and ordinates is plotted/deposited the shifts of the center of cluster relative to synchronous particle on the phase and the

impulse/momentum/pulse respectively. Let us assume that to the specific place of accelerator, let us say, at the N resonator, the center of cluster arrived with some disturbances/perturbations of phase $\delta\varphi$ and speed $\delta\rho/\rho_s$. Phase sensor measures value $\delta\varphi$ and is changed the phase of hf field in the resonator to value $-\delta\varphi$. The length of resonator is equal to $(2n+1)\ \lambda_{\varphi}/4$, where λ_{φ} - length of phase oscillations, $n=0,\ 1,\ 2:$. We will consider that the resonator is the ideal accelerating structure.

Page 57.

Through fourth of period of phase oscillations the representative point, moving over the phase trajectory (ellipse in the case of small phase oscillations), will be displaced after flight/span by the cluster of latter/last resonator into the point, arranged/located on the axis/axle of abscissas. The second phase sensor measures at this moment shift $\delta\varphi'$ and is changed phase in $(N+1)$ resonator to value $-\delta\varphi'$. As a result of the second correction the representative point falls into the origin of coordinates and the motion of the center of cluster ceases. Virtually, since the resonator is not the ideal accelerating system, the speed of the center of cluster will differ somewhat from ideal computed value.

The system of the depression of the phase oscillations of the

centers of clusters can improve the monochromaticity of the exit beam of linear accelerator in such a case when the basic reason for deterioration in the monochromaticity are coherent beam displacements. However, the nonlinearity of longitudinal oscillations can lead to a change in the configuration of clusters and to an increase in its effective phase area. In this case the use/application of systems of the depression of the phase oscillations of the centers of the clusters was barely effective and unsuitable.

In connection with the fact that the linear theory does not make it possible to determine the distortion of the form of cluster on the phase plane, the investigation of this effect was carried out by the method of a probability-statistical simulation of the accelerating channel.

The mathematical model of the accelerating channel of the linear accelerator of protons allows (taking into account nonlinearity and nonconservatism of longitudinal oscillations) to determine particle trajectory with any origin coordinates in the accelerating channel whose ideal structure, and also amplitudes and phases of accelerating fields are subjected to random disturbances. With the aid of this model it is possible to determine the trajectories of the sufficiently large collective of particles and to calculate the

sizes/dimensions of cluster, the scatter of speeds, the shift of the
center of cluster, particle distribution according to the phases and
speeds, etc. Interaction of particles with each other is not
considered.

For the statistical-probability simulation of the accelerating
channel is utilized the method of Monte Carlo. On computers is
simulated the accelerating channel and with the aid of the
random-number transducers are imitated the fluctuations of the
parameters of HF fields and error both production and to arrangement
of the elements/cells of the accelerating channel. So "is reproduced"
one of the possible realizations of channel, which then with the aid
of the simulating program "accelerates particles". With the aid of
the new set of random numbers is reproduced another realization of
channel which also "accelerates particles" and, etc. Particle
distribution at the output of many accelerating channels
statistically is processed.

For the simulation was selected the long-wave part of the linear
injector-accelerator of cybernetic proton synchrotron [2]. Model
consists of seven resonators with the drift tubes, which work on the
wavelength 1.5 m, and which accelerate protons to the energy 200 MeV.
Computed value of synchronous phase is selected with 26°, specific
acceleration $2.7 \cdot 10^{-3}$.

During the simulation were considered the errors in the
accelerating channel, given in the table.

Root-mean-square magnitudes of error in the production, installation
and adjustment of the accelerating channel.

№ п/п (a)	Наименование погрешности (b)	Величина (c)
1.	Погрешность длины резонатора, %	$1{,}5 \cdot 10^{-2}$
2.	Погрешность длины трубки дрейфа, %	$7 \cdot 10^{-2}$
3.	Погрешность измерения длины трубки дрейфа, %	$3 \cdot 10^{-2}$
4.	Погрешность установки трубки дрейфа, м	$3 \cdot 10^{-5}$
5.	Масштабная ошибка установочной рулетки, %	$2 \cdot 10^{-4}$
6.	Погрешность амплитуды среднего поля в резонаторе, %	1
7	Неравномерность в.ч. поля в резонаторе, %	1
8.	Наклон поля вдоль резонатора, %	1
9.	Погрешность установки фаз в.ч. поля между резонаторами, град	1

Key: (a). in sequence. (b). Designation of error. (c). Value. (1).
Error in length of resonator, o/o. (2). Error in length of drift
tube, o/o. (3). Error of measurement of length of drift tube, o/o.
(4). Error in setting up of drift tube, m. (5). Scale error for
adjusting tape measure, o/o. (6). Error in amplitude of middle field
in resonator, o/o. (7). Nonuniformity of hf field in resonator, o/o.
(8). Inclination/slope of field along resonator, o/o. (9). Error in
setting up of phases of hf field between resonators, deg.
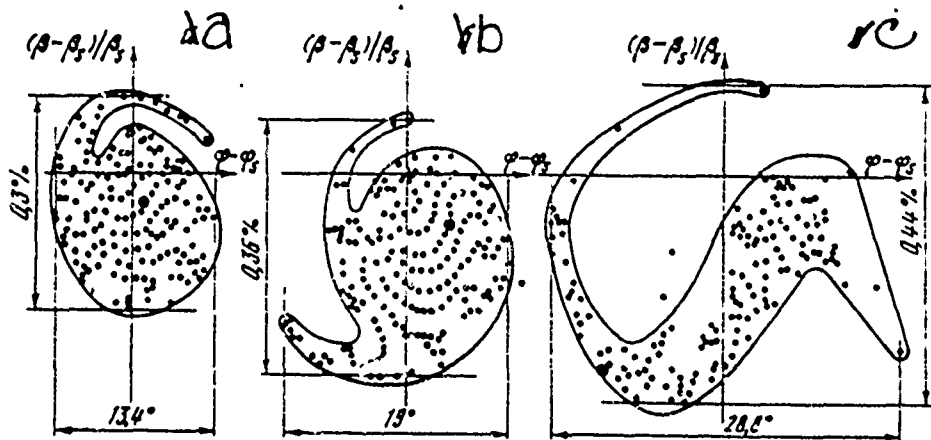
Fig. 1. Configurations of clusters on phase plane at output of accelerator a) value of errors correspond to data, given in table; b) error increased two times; c) error increased four times; small circle showed synchronous particle.

Page 58.

These tolerances are accepted by the Soviet strong-focusing accelerators. Furthermore, were investigated the random realizations in which the amplitudes of the errors increased into two or three and even four times.

Simulation showed that with the allowances, equal or it is twice more than as the allowances, given in the table, the form of clusters on the phase plane differed little from the elliptical, and their

centers of gravity were arranged/located near from the synchronous particle. With further increase in the allowances the form of cluster on the phase plane increasingly less resembled ellipse, but sometimes cluster was no longer compact formation/education. Thus, fear apropos of the smearing of clusters is substantiated, but with the existing allowances these effects do not appear, and system ARP-P can effectively work. Fig. 1 for an example gives several characteristic configurations of cluster with different allowances.

For the evaluation of effectiveness in the work of the system of the depression of the phase oscillations of the centers of clusters the latter was connected with the model of the accelerating channel. The simulating program imitated the action of this system, and at the output of accelerator were obtained particle distributions according to the phases and the speeds which were compared with particle distributions in the absence of system ARP-P. The comparison of given in Fig. 2 and 3 particle distributions shows that with generally accepted tolerances the system ARP-P removes 50o/o of increase in the size/dimension of cluster in the impulses/momenta/pulses and 80o/o of increase in its phase width. Simulation also showed that an increase of the allowances 1.5-2 times with the work of system ARP-P virtually does not make the parameters worse of exit beam.
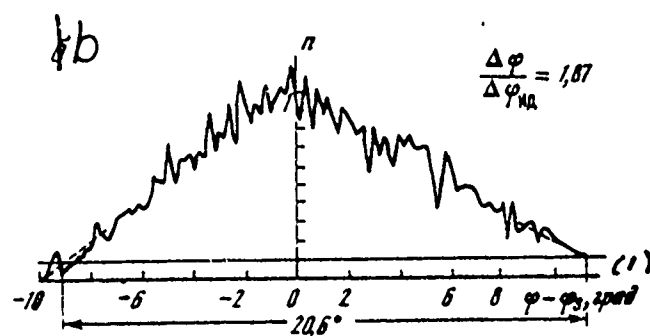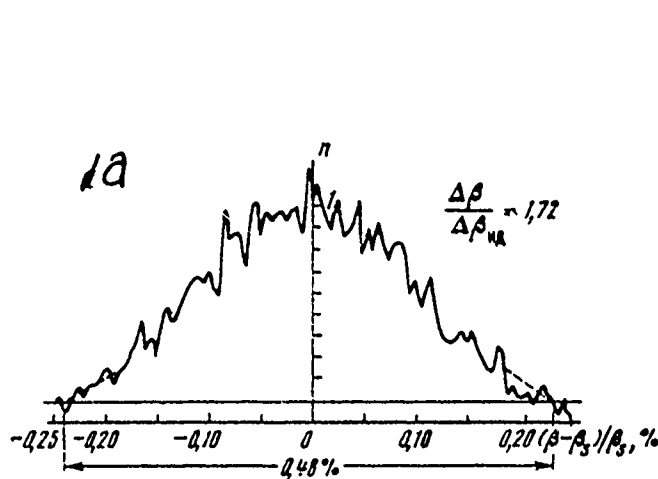
Fig. 2.
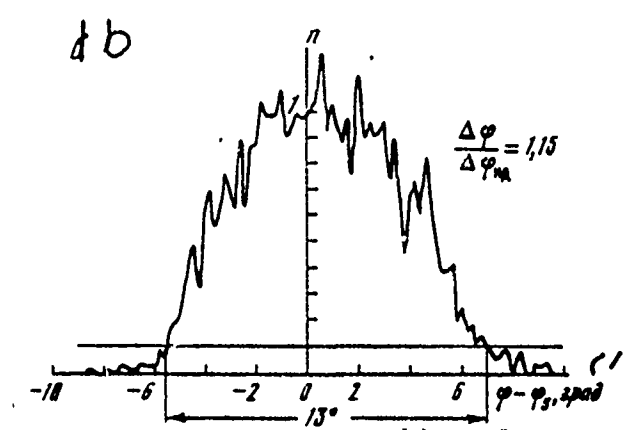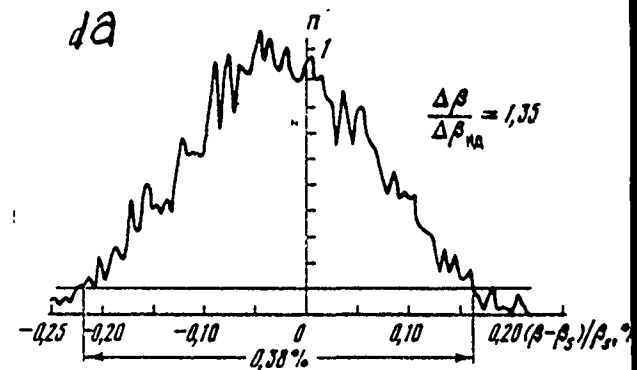
Fig. 3.

Fig. 2. Particle-velocity distributions (a) and phases (b) at output of accelerator without use of system ARF-P, $\varphi - \varphi_s$, $(\rho - \rho_s)/\rho_s$ - deviation of phase and particle speed from phase and speed of synchronous particle; $\Delta\varphi_{HA}$, $\Delta\rho_{HA}$ - phase width of cluster and velocity spread in it in accelerating channel without errors. The sizes/dimensions of cluster ($\Delta\varphi$ and $\Delta\rho/\rho_s$) are determined on the points where the

particle density is equal to 10c/o of the maximum value of density.

Key: (1). deg.

Fig. 3. Particle-velocity distributions (a) and phases (b) at output of accelerator during use of system ARF-P. Designations the same as in Fig. 2.

Key: (1). deg.

REFERENCES

1. B. P. Murin, Preprint RAIAN, HT-8266-136, M., 1966.
2. Cybernetic Proton Accelerator for Energy of 1000GeV. Edited by A. A. Vasil'yev. Preprint RAIAN, HT-9267-148, M., 1967.

Page 59.

104. SOME QUESTIONS OF THE OPTICS OF A BEAM IN THE MULTISECTION
LINEAR 2-GeV ELECTRON ACCELERATOR

V. I. Artemov, I. A. Grishayev, A. N. Dovbnya, N. I. Mocheshnikov, V.
V. Petrenko.

(Physiotechnical institute of AS UkSSR).

At present one of the basic tasks of the development of
accelerators, including linear electron accelerators, is an
improvement in the quality of the accelerated beams. For this is
necessary the solution of number of questions among which the
significant role play questions of optics of beams both in the
accelerating channel and in different systems of formation and
transportation of particles on the target. The optical properties of
the accelerating channel of linear electron accelerator to a high
degree depend on different perturbing forces, which exist on the
accelerator, from the properties of the systems of focusing and
transportation of the beam through the accelerator, from the quality
of the injected beam, etc.

As is shown analysis, on these reasons in the linear
multisection electron accelerator appears connection/communication
between the phase and transverse motion of beam. For the analysis of
the dynamics of beam is developed the program emittance", which makes
it possible to obtain the results of the investigation by the method
of the numerical solution of the equations of electrons, and also by
the method of the setting of "mathematical experiments" on the
computers M-220 A.

In the accelerator to the energy 2 GeV [1] there are transverse
electric fields, which are caused by the dissymmetry of the
introduction/input of high-frequency power into the accelerating
section. Structurally/constructurally the introduction/input of power
is accomplished/realized in the horizontal plane; therefore the
action of cross fields in essence becomes apparent in this plane.

Cross field in the matchers out of phase on 90° reaches 0.13
amplitude values of accelerating field [2]. These fields exist only
in the short sections (to 3 cm), but with a large quantity of
matchers in multisection accelerator the action of cross fields
proves to be essential.

For the calculations the emittance of the injected beam in both
planes is accepted in the form of rectangle with the sides 1 cm and

$1 \cdot 10^{-2}$ rad whose area encompasses real emittance. At the input into the accelerator the emittance for different phases in the cluster is accepted identical.

Fig. 1 shows a change in the partial emittances on the output of accelerator in the value and the form for the particles with the different phases. Dotted line snowed that part of the cluster which is lost in the process of acceleration as a result of the fact that the coordinates of particles obtain the values, which exceed the aperture of accelerator. Depending on phase partial emittance at the output of accelerator is displaced from the optical axis of accelerator, which leads to an increase in the effective emittance

$$V = k V_0 - \frac{E_0}{E_k} , \qquad (1)$$

where V_0, V - values of emittance at input and output of accelerator, E_0, E_k - respectively initial and final values of energy; k - coefficient of an increase, which appears as a result of the separation of particles on the phases.

In our case of $k=3$. This expression allows with the assigned magnitude of the emittance of beam at output of accelerator to determine requirements for the beam of injector, and by the rational selection of collimators it is possible to substantially improve the parameters of beam.

Tha analysis of a radial-phase motion shows that the intense decrease of the phase width of cluster Δ⏀ occurs to the 20th section, which is connected with an increase in the energy of the accelerating beam. The full/total/complete width of phase channel does not exceed 30.

Trajectory calculation in a x- plane for the particles with the different values of phase and the initial conditions x=0 and $\ddot{x}_0^{\prime}$=0 shows that under our conditions the trajectories are well divided in the region of the 20th accelerating section. Here the dependence of the sizes/dimensions of beam with different initial conditions on the phase takes the form, shown in Fig. 2. This can be utilized for the shortening of the phase width of cluster, and therefore for the monochromatization by a method of the irising of beam in the horizontal plane.
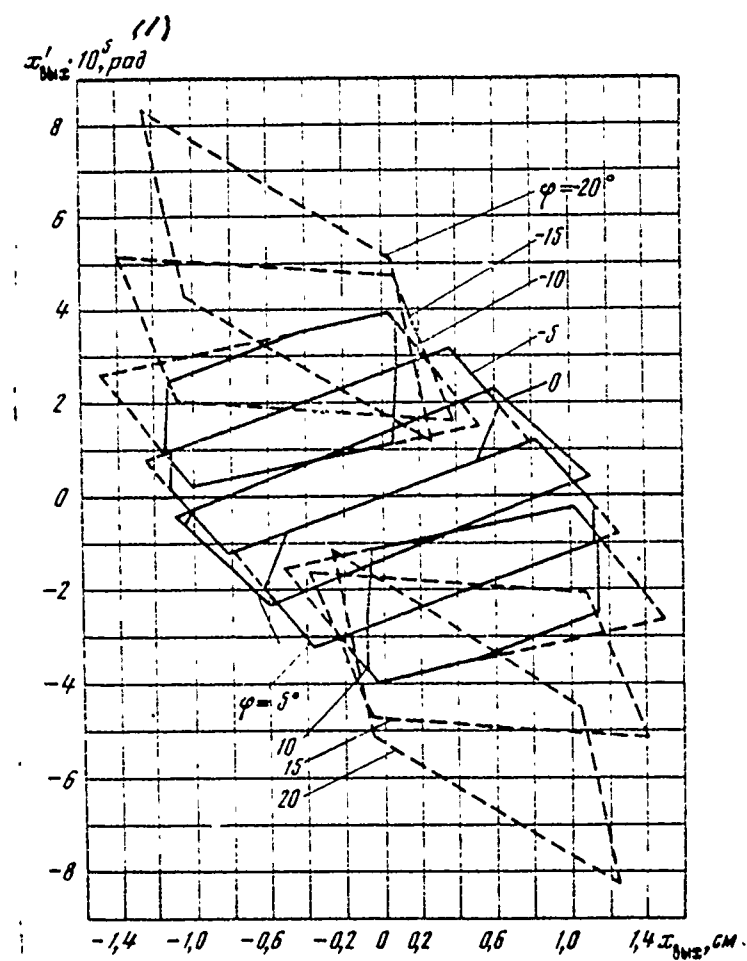
Fig. 1. Emittances of beams at output of accelerator.

Key: (1). rad.

Page 60.

For example, the setting up of the diaphragm with a diameter of 0.5 cm makes it possible to reduce the phase width of cluster to 5°.

Having artificially enforced the effect of separation, it is possible to create conditions, with which the irising proves to be possible to carry out with the smaller energies in order at the very beginning of accelerator to already have "pure/clean" beam with a small phase width of cluster.   .

The searches of the accelerating channel, in which would be accelerated "pure/clean" beam with small phase duration of cluster, led us to the diagram which was shown in Fig. 3. this figure shows envelope of particles in the horizontal (x) and vertical (y) planes, and also arrangement of magnetic quadrupole lenses and collimators k_1, k_2, k_3.

The electron beam of injector with the short magnetic lens is focused to the input into the first accelerating section where is established/installed collimator k_1 in width of slot 0.26 cm. Then in the horizontal plane by the first two quadrupole lenses beam is again focused. Is here established/installed collimator k_2 in width of slot 0.3 cm. The third collimator in width of slot 0.3 cm is established/installed in the 20th accelerating section. Characteristic feature of this channel consists in the fact that for the separation of particles on the phases, besides cross fields, are

utilized the lenses. Separation by lenses is the consequence of chromatic aberration and certain relation of energy of particle with its phase in the cluster.

Practical creation of the accelerating channel with the properties examined allowed to obtain beams with a small energy scatter. Fig. 4 shows the energy spectrum of the accelerated electrons. As can be seen from figure, energy scatter at the level 0.5 of intensity does not exceed $1.5 \cdot 10^{-3}$. Characteristic for the shown spectrum is the absence of low-energy tail, which considerably decreased the background on the targets and the activation of the parts of accelerator.

The given spectrum is obtained with the average/mean output current of accelerator 0.33 μA, which is 2 times less than the current with the work of the accelerator in the existed previously standard mode/conditions. It would seem, reduction in current must occur proportional to the decrease of the width of the spectrum. However, current falls more slowly than the width of the spectrum. However, current falls more slowly than the width of the spectrum. Is explained this by the phase compression which occurs as a result of the close coupling of transverse motion with the phase.

The measurement of emittance at the output of accelerator was

made at the zero level of tne density of distribution of particles on the phase plane and at the level of 0.1 maximum densities. In the first case the value of emittance characterizes 100o/o of particles in the beam, in the second case - 90o/o. The results of measurements showed that the value of the horizontal emittance of beam in the standard mode/conditions comprised $14.4 \cdot 10^{-} $ m$\cdot$rad at the zero level and $4.7 \cdot 10^{-7}$ m$\cdot$rad at the level 0.1. After the setting up of collimators and channel checkup - respectively $5.8 \cdot 10^{-7}$ and $1.75 \cdot 10^{-7}$ m$\cdot$rad.

In the real accelerator there are fluctuations of amplitude, phase of hf field and current of the accelerated electrons. Their effect on characteristics of beam can be essential.
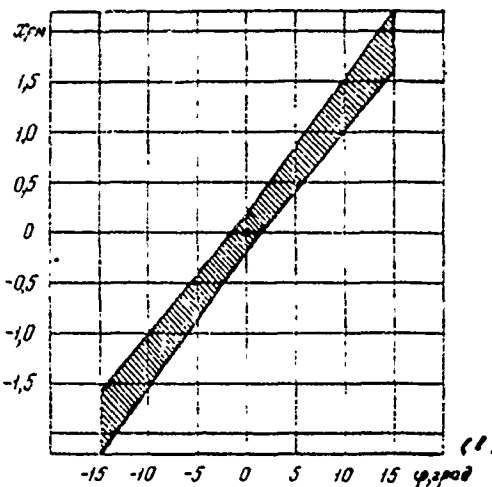
Fig. 2.   Fig. 3.
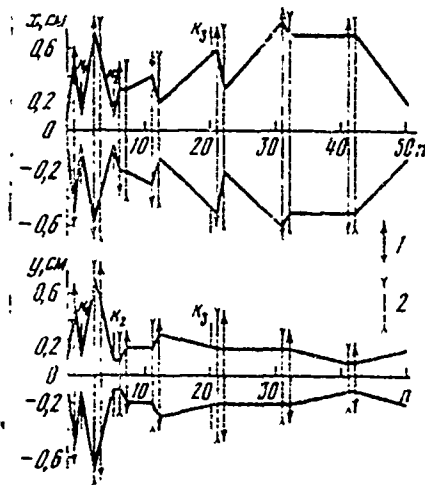
Fig. 2. Dependence on sizes/dimensions of beam in horizontal plane from phase of particle.

Key: (1). deg.

Fig. 3. Optical diagram and envelope of particles in accelerator. n - number of section; k_1, k_2, k_3 - collimators; 1, 2 - quadrupole doublets.
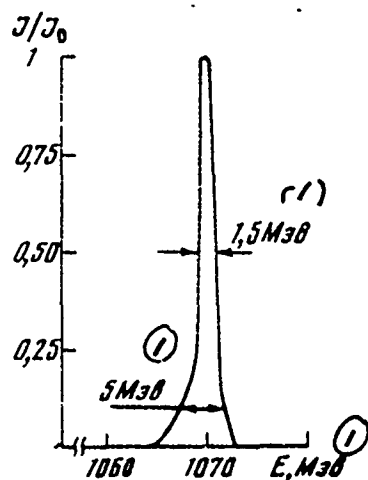
Fig. 4. Energy spectrum of electrons.

Key: (1). MeV.

Page 61.

Fig. 5 shows the calculated energy spectra of electrons at the output of accelerator for the cluster with extent of 10°. Along the axis of ordinates is deposited/postponed a number of realizations with this energy (axis/axle of abscissas). Solid lines showed the "spectrum" without taking into account fluctuations, broken - taking into account the fluctuations. As can be seen from figure, fluctuations affect the spectrum in a two-fold manner. On one hand, the spectrum is widened. Thus, width in basis/base increases 3 times.

On the other hand, the energy in the maximum of the spectrum
decreases.

Besides effect on the energy characteristics of beam,
fluctuation they affect also its optical characteristics. Calculation
shows that in the idealized case the horizontal emittance of beam is
equal to $5.5 \cdot 10^{-7}$ m·rad, and in the presence of fluctuations
$12.3 \cdot 10^{-7}$ m·rad.

Creation on the accelerator of narrow phase channel contributed
to improvement in spectrum and optical characteristics of beam, and
also to development/detection, and then to the elimination of the
series/row of fluctuations.
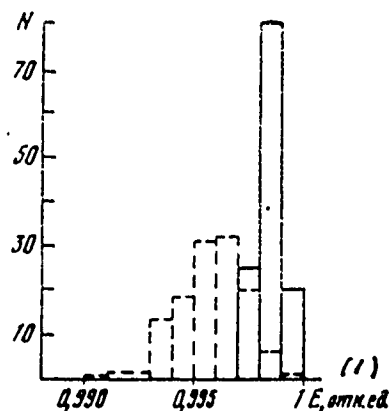
Fig. 5. Calculated energy spectra of electrons.

Key: (1). rel. un.

REFERENCES

1. V. I. Beloglazov. et al. Atomnaya Energiya, 1968,
    24, no 6, 540.
2. I. A. Grishayev, G. K. Dem'yanenko, K. S. Rubtsov,
    ZhTF. 1970. 40, No 1.

105. OPTIMUM INJECTION OF RELATIVISTIC PARTICLES INTO A SYNCHROTRON.

D. G. Borisov, P. V. Bukayev, A. I. Gryzlov, V. M. Levin, Yu. P.
Shchepin.

(Scientific research institute of electrophysical equipment im. D. V.
Yefremov).

It is known that the best results upon the particle injection
into the circular accelerator can be obtained, when energy of the
injected particles changes synchronously with the building up in the
time field of circular accelerator [1]. In the region of the
nonralativistic values of energy of injection this problem is solved
[2, 3]. However, for the particles with the relativistic energy task
until recently was not solved.

At the VI conference of the physiotechnical institute of AN
UkrSSR [4] was reported the method of modulation of energy of the
relativistically accelerated particles by the method of the
transmission of the clusters through the section of the septate
waveguide, in which were excited the electromagnetic vibrations with
the period, different from the repetition period of clusters. With

the small difference of periods occurs the steady change in the
energy of particles from one cluster to the next, which carries
sinusoidal character. Thus, in the principle is possible the
generation of beam with energy that increases from one cluster to the
next, i.e., in the course of time.

However, the use/application of the septate waveguide for
modulation of energy of clusters leads in the interesting us case to
contradictory results.

Thus, for instance, upon the injection of electrons into the
Yerevan synchrotron on 6 GeV and during the use as the modulating
energy of particles section, calculated on 50 MeV, it is possible to
modulate energy on the section of cosine curve in the region of
phases, which corresponds to the character of a change in the
magnetic field for the time of particle momentum (2 μs), only on 20
keV at the necessary value of 600 keV. The attempt to modulate energy
to 600 keV in 2 μs due to a change in phase change will lead to the
fact that the modulation curve and acceptance are radiated in the
middle part, coinciding only at the ends/leads.

However, it is possible to utilize for modulation of energy of
the particles of the section of linear induction accelerator [5] in
inductor of which is excited vortex/eddy electric field with the

building up during the passage of particles amplitude. This makes it possible to preserve optimum conditions for the capture of relativistic particles during entire interval of injection.

For obtaining building up in the time accelerating voltage in the interaction space of field with the beam it is possible to utilize pulse modulators with heterogeneous forming lines. Figure shows the oscillogram of the building up impulse/momentum/pulse of accelerating voltage and the oscillogram of the current, flowing through the winding of inductor.

Page 62.

According to our calculations, grouped into the clusters and accelerated in the septate waveguide to the energy 50 MeV electrons it is necessary to introduce into the induction accelerator by length 1.5 m of 24 inductors, connected to eight pulse modulators in thickness 30 kW. With the strength of field at the end of the impulse/momentum/pulse $0.4 \cdot 10^6$ V/m can be obtained an energy gain 600 keV, which corresponds to the character of the build-up of magnetic field in the synchrotron in 2 μs.

Building up impulse/momentum/pulse of accelerating voltage and
current, flowing through the winding of inductor.

REFERENCES

1. M.H. Blewett et al. Rev. Sci. Instr. 24, No 9,
   861, 1953.
2. D. Kenneth Wells et al. Rev. Sci. Instr. 31, No 9,
   942, 1960.
3. F.E. Mills et al., Rev. Sci. Instr, 35, No 11, 1451,

4.   D. G. Borisovi, et al. Collection "Linear Accelerators"
      Materials of 6th Final Conference of KhFTI 69/13,
      Khar'kov, 1969, 69.
5.   A. I. Anatskiy, P. V. Bukayev, E. P. Khal'chitskiy,
      Proceedinga of All-Union Conference or Charged - Particle
      Accelerators, M., VINITI, 1970, 231.

106. THE SUM OF THE DECREMENTS OF COHERENT OSCILLATIONS OF A BEAM IN AN ACCUMULATOR

Ya. S. Derbenev, N. S. Dikanskiy, D. V. Pestrikov.

(Institute of nuclear physics of SO AN USSR [Siberian Department of the Academy of Sciences of the USSR]).

1. As is known, collective interaction of beam with external system (v.s.) can lead to development in beam of instabilities, impeding thereby to accumulation of high currents. Is known series/row the method of attenuating the collective oscillations. In this case the damping devices can be conditionally divided into the narrow-band ones (are suppressed the separate modes of collective motion) and the broadband ones (the so-called systems "without the memory"), with the aid of which it is possible to simultaneously damp many modes. The concrete/specific/actual methods of attenuating the collective oscillations of bunched beams by broadband systems were proposed in works [1-4].

In this communication/report are discussed some general/common/total aspects of interaction of beams with v.s. in connection with the tasks of attenuating the collective oscillations.

Basic conclusion is the possibility in principle of the simultaneous depression of oscillations according to all oscillator degrees of freedom, which is based on the obtained in the work theorem about the sum of the decrements[1] of coherent motion.

FOOTNOTE [1]. By decrement we will understand value $\delta = -\mathfrak{Im}\,\omega$, when the time dependence of excitation $\exp(-i\omega t)$. ENDFOOTNOTE.

2. During analysis of stability of small collective oscillations of beam, which weakly interacts with v.s., it is convenient to present its function of distribution $f(\mu, p, t)$ in the form

$$f = f_0(\mathfrak{J}) + \tilde{f}(\mathfrak{J}, \varphi, t) = f_0(\mathfrak{J}) + \sum_{m=0} f_m(\mathfrak{J}, t) e^{im_i \varphi_i}, \quad (1)$$

where $\mathfrak{J}$ and φ - variable/alternating action-phase of unperturbed motion. By definition, in the absence of collective oscillations $f = f_0(\mathfrak{J})$, and are described the coherent excitations of arbitrary form.

Far from the machine resonances normal oscillatory mode $\tilde{f}$ takes the form

$$\tilde{f} = \tilde{f}_m(\mathfrak{J}) e^{im_i \varphi_i - i\omega t}, \quad (2)$$

where $m_i \varphi_i = \sum_{i=1}^{3} m_i \varphi_i$. The smallness of interaction assumes that $|\omega - m_i \omega_i| \ll |m_i \omega_i|$, where $\bar{\omega}_i = Q_i \omega_0$ - frequencies of the undisturbed, and ω_0 - frequency of revolution. Applying csfourier analysis to the system of equations of Vlasov, in the first approximation, of the method of averaging it is possible to obtain equation for $f_m(\mathfrak{J})$ ([2,5]):

$$(\omega - m_i\omega_i)f_m = e^2 m_i \frac{\partial f_0}{\partial J_i} \sum_{n,k} \frac{(\vec{v}\,\overline{A}_k)_{m,n} \int d\Gamma (v A_k)^*_{m,n} \tilde{f}_m}{\omega_k^2 - (\omega + n\omega_0 + i\lambda_k)^2}. \quad (3)$$

Here

$$(v A_k)_{m,n} = \frac{\omega_0}{2\pi} \int\limits_0^{2\pi/\omega_0} dt \int\limits_0^{2\pi} \frac{d^3\varphi}{(2\pi)^3}\, v A_k\, e^{-in\omega_0 t - im_i\varphi_i},$$

$A_k(v)$ - the eigenfunctions of v.s., which satisfy equation
$\Delta A_k + (\omega_k^2/c^2) A_k = 0$ and gauging condition $\mathrm{div}\, A_k = 0$.

Page 63.

The energy absorption of field we will consider phenomenologically by
the introduction of the internal friction of the oscillations of
field λ_k. This simplified introduction to dissipation is done here
exclusively for the clarity of the presentation (in more detail see
in [5]).

3. System of equations (3) determines spectrum of normal
oscillatory mode of system beam field. It is not difficult to show
that the sum of the decrements of full/total/complete system is equal
to the sum of the decrements of the oscillations of field in the
absence of interaction. However, physical interest is of the sum of
the decrements not of all normal modes, but only those in which is
contained basic part of the energy of collective particle motion ($\omega \approx$

$m_i \omega_i$). Far from resonances $\omega_k - m_i \omega_i = n \omega_0$ (in the sense that partial

frequency shifts $|\Omega_{m,n}|$ much less than the detuning $|\omega_k - m_i \omega_i - n \omega_0|$) of

sum on n and k (3) weakly depend on a precise value ω. Therefore in

the nonresonant case, in the first order on interaction, ω in right

side (3) it is possible to replace by $m_i \omega_i$. Then from (3), according

to the known theorem about the sum of characteristic roots, we obtain

the sum of decrements in the form

$$\Delta = \sum_{\alpha} \delta_{\alpha} = e^2 N \mathfrak{I}_m \left\{ \sum_{m,n} \sum_{k} \frac{\left\langle m_i \frac{\partial}{\partial \mathfrak{I}_i} \left| (v A_k)_{mn} \right|^2 \right\rangle}{\omega_k^2 - (m_i \omega_i + n \omega_0 + i \lambda_k)^2} \right\}, (4)$$

where N — number of particles, brackets <> indicate averaging on the

ensemble. If the oscillation spectrum of field is continuous, then

summation over k in (4) must be replaced with integration, while λ_k

at $\delta \rightarrow +0$.

From (4) follows that for high-Q systems $(\lambda_k \ll \omega_k, \lambda_k \ll \omega_0)$ the sum

of decrements Δ can strongly depend on detuning $|\omega_k - m_i \omega_i - n \omega_0|$, then, as

during interaction with low-quality v.s. $(\lambda_k \gg \omega_0)$ both the sum of

decrements and partial decrements weakly they depend on frequencies.

By direct calculation it is possible to be convinced of the fact

that the sum of the decrements of coherent oscillations (4) coincides

with the sum of the decrements of the single particles, which

interact with v.s. independantly of each other. Of this, strictly,

and consists the confirmation about the sum of the decrements of

collective oscillations.

In connection with the tasks of attenuation by broadband systems $(\omega_{k} \sim m_{i}\dot{\omega}_{i} + n\omega_{0})$ of the low-frequency oscillations, not suppressing by scatter[1] it is possible to formulate theorem in the narrower and more concrete/more specific/more actual sense, after leaving in right side (4) only those oscillations which effectively interact with the low-frequency oscillations of beam.

FOOTNOTE [1]. In this theorem the effect of scatter is not considered, since during the conclusion of theorem actually was utilized assumption about the discreteness of the undisturbed oscillation spectrum of beam. ENDFOOTNOTE.

The usefulness of the formulated above confirmation consists in the fact that, as in the case of noncoherent radiation, for the calculation Δ are required only single-particle characteristics.

The sum of decrements (4) can be written also in the form

$$\Delta = -N\langle \overline{\frac{\partial J_{i}}{\partial J_{i}}} \rangle = -\overline{N\langle \operatorname{div}_{p} F(\tau, p, t) \rangle} \; , \qquad (5)$$

where F - force of interaction of particles with the induced by it field, feature indicates averaging along the trajectory.

4. Let us especially emphasize that sum of decrements as partial decrements, they are nct proportional to total power of losses, as it takes place, for example, for incoherent synchrotron radiation $F_c = -Pv/c^2$. Moreover, it is possible to give the examples when the sum of decrements is obliged to the excitation of v.s. only by transverse vibrations of beam ([2, 3, 5]). Physically this is connected with the fact that during the cclective interaction indused fields are determined not only particle trajectory, but also by geometric properties of v.s.

5. In this connection let us briefly discuss possibility of effective attenuation by broad-band v.s. of synchrotron oscillations simultaneously with betatron ones. The nontriviality of this question is connected with the fact that the instantaneous power of coherent losses weakly depends, or completely it does not depend on energy (in this case for the low-quality systems the sum of decrements is mainly obliged to transverse motion). The depression of phase oscillations can be ensured with the aid of a radial-longitudinal connection/communication, utilizing the system in which the energy losses depend on the radial position of particle. In this case unavoidably the decrease of the radial decrement (it is analogous with the case of noncoherent radiation, the sum of decrements (4) for the broadband system, but linear approximation/approach, does not depend on radial-longitudinal connection/communication [5]). This

decrease can be compensated by the special broadband system, which does not contribute decrement into the axial motion. A specific example of this method of attenuation with the aid of the systems of the type of the matched lines was examined in [3].

REFERENCES

1. N. S. Dikanskiy, et al Atomnaya Energiya, 1967, 22, 188.
2. Ya. S. Derbenev, N. S. Dikanskiy, Preprint No. 315, Institute of Nuclear Physics, Siberian Branch, Academy of Sciences USSR.
3. Ya. S. Derbenev, N. S. Dikanskiy. Preprint, No. 318, Instutute of Nuclear Physics, Siberian Branch, Academy of Sciences USSR, 1969.
4. Ya. S. Derbenev, N. S. Dikanskiy. Preprint No. 326, Institute of Nuclear Physics, Siberian Branch, Academy of Sciences USSR. 1969.
5. Ya. S. Derbenev, N. S. Dikanskiy, D. V. Pestrikov. Preprint 34-70, Institute of Nuclear Physics, Siberian Branch, Academy of Sciences USSR, 1970.

Page 64.

107. Dynamics of particle acceleration in the spectrometric cyclotron.

Yu. K. Khokhlov.

(Physical institute im. P. N. Lebedev of the AS USSR).

Under the theory of trajectories in the cyclotron usually is implied the theory of the closed orbits, which exist only in the absence of electric field. Meanwhile there is a series/row of the urgent questions for solving which is necessary the more full/totaler/more complete dynamic theory, which considers both the properties of trajectories in the magnetic field and the main effects, connected with those accelerating for slots. One of the possible ways of the construction of this theory consists of the description of slots by means of the effective boundary conditions, assigned on the middle vertical plane of slot. In the lowest approximation/approach the slots are assumed/set infinite-narrow,

i.e., particle motion is determined by the equation of the form

$$\frac{d}{dt}\vec{p} = \frac{e}{c}\left[\vec{v} \times \vec{H}\right] \qquad (1)$$

out of the slots and by boundary conditions of the type

$$\Delta p_{\tau} = 0, \quad \Delta p_{\theta} = \sqrt{(p+\Delta p)^2 - p_{\tau}^2} - \sqrt{p^2 - p_{\tau}^2}, \quad \Delta p_{z} = 0 \ (1a)$$

on the slots. (It is assumed that the slots are arranged/located radially; τ, θ, z - cylindrical coordinates).

Some results, which relate to the particle trajectories in the isochronal cyclotron with sectioned magnetic system can be obtained from system (1) and (1a) on the basis of following approach [1-3].

First of all, is introduced the concept of the ideal trajectory, which plays the role of natural reference point for others. This trajectory is the evenly turned/run up spiral - its step/pitch along any radius, considered as the function of speed, does not have usual oscillations/vibrations with frequency $\mu = 2\pi(\nu_{x}-1)$. Among many trajectories $t=t(\theta)$, $\tau=\tau(\theta)$, differing from each other only by initial values τ_0, τ_0' is always one ideal $t_{uq}(\theta)$, $\tau_{uq}(\theta)$. (We select θ as the independent variable and we are limited cases $z=0$.)

Further is fulfilled transition from the equation for $t(\theta)$, $\tau(\theta)$ to the equations for the small differences

$$\tau(\vartheta) = t(\theta) - t_{uq}(\theta), \quad x(\vartheta) = \left[\tau(\theta) - \tau_{uq}(\theta)\right]\cos\psi(\theta),$$

where $\vartheta = \vartheta(\theta)$ - the generalized azimuth; $\psi(\vartheta)$ - the angle, determined from $tg\,\psi(\vartheta) = v'_{uq}(\theta)/v_{uq}(\theta)$. (Ideal trajectory it here belongs to the same energy, as examined/considered). The obtained in the linear approximation/approach equations and boundary conditions take the form:

$$\frac{d}{d\vartheta}X(\vartheta) = G(\vartheta)X(\vartheta), \quad \Delta X(\vartheta_j) = -\frac{(\Delta\dot{W})_j}{\omega_u p_j}\Gamma(\vartheta)X(\vartheta), \quad (2)$$

where $x(\vartheta)$ - the column, comprised of $r(\vartheta)$, $x(\vartheta)$, $x'(\vartheta)$; $G(\vartheta)$, $\Gamma(\vartheta)$ - three-dimensional matrices/dies, determined by magnetic field; elements/cells $G_{12}(\vartheta)$ and $G_{13}(\vartheta)$ are proportional v^{-1}; j - number of slot; ω_u - frequency of revolution of particle; ΔW - energy gain on the slot; point indicates time derivative.

The developed in [2] adiabatic method of solving system (2) makes it possible to express $x(\vartheta)$ through amplitude and phase of the three-dimensional representation of floquet. The latter can be found with the aid of any of the known approximation methods. Can be used the stepped model, which gives the responses/answers in the form of simple analytical formulas.

Let us pause at some results, which relate to energy distribution in the bundle of projected/designed spectrometric

cyclotron [4]. This cyclotron has four 45-degree dees, arranged/located in the opposite gaps/intervals between the magnetic sectors. We will assume that the central particle of cluster moves over the ideal trajectory and that this trajectory absolutely is isochronous both in the "small" and in the "large" (in this case the closed equilibrium orbits it goes without saying are not fully isochronous).

The potential of dee is written/recorded in the form $U(t) = U_0(\sin q_0 \omega_u t - \eta \sin q_1 \omega_u t)$; or phase they are selected so that U=0 at the moment of the passage of the central particle of the cluster through the bisector of dee; q_0, q_1 - multiplicity of fundamental and supplementary harmonics. By substituting in $U(t)$ $t(\theta) = t_{uq}(\theta) + \tau(\vartheta)$ and by taking into account the angular size/dimension of dee, we will obtain

$$\Delta W_{I,II} = \Delta V'[1 \mp \lambda q_0 \omega_u \tau(\vartheta_{I,II})]; \quad (\Delta \dot{W})_{I,II} = \mp \Delta W \lambda q_0 \omega_u;$$

$$(3)$$

$$\Delta W = U_0\left(1 - \frac{q_0^2}{q_1^2}\right)\sin\frac{\pi q_0}{8}; \quad \lambda = \left(1 - \frac{q_0^2}{q_1^2}\right)^{-1}\left(ctg\frac{\pi q_0}{8} - \frac{q_0}{q_1}ctg\frac{\pi q_1}{8}\right),$$

where I, II - numbers of input and exit slits; ΔW - nominal energy gain on the slot.

An energy gain per revolution comprises for one particle $4\Delta W\{1 + \frac{1}{2}\lambda q_0 \omega_u[\tau(\vartheta_{II}) - \tau(\vartheta_I)]\}$; consequently after summation over revolutions we will have

$$W_k = W_{uq,k} + \delta W_k; \quad \delta W_k = 2\Delta W \lambda q_0 \omega_u \sum_{\ell - k_0}^{k}\left[\tau_\ell(\vartheta_{II}) - \tau_\ell(\vartheta_I)\right]. \quad (4)$$

The use/application of the theory presented makes it possible to find values $\bar{\tau}_\ell(\vartheta_\ell)$ as the function of the speed ℓ and to perform summation over ℓ. Finally is obtained the expression, which defines δW_k as the function of initial values $\tau_{k_0}, x_{k_0}, x'_{k_0}$, of the given ones on the bisector of adjacent free intermediate sector. The explicit form of this expression without taking into account the difference between the values τ in the free and in the occupied with dee intermediate sectors, is given in [2].

Page 65.

It proves to be that δW_k contains following components/terms/addends: 1) growing in the absolute value as $\ell n(W_k/W_0)$; 2) decreasing approximately as $k^{-1}/2$; 3) oscillating with frequency $\mu = 2\pi(\nu_x - 1)$; 4) constant.

In the stepped model with $x = H_2/H_1 = 0.25$ ($\nu_x = 1.039$) taking into account the mentioned difference between the free and occupied intermediate sectors, logarithmic growing component/term/addend is equal to

$$\delta W_{k,nor} = \frac{1}{8} q_0 \lambda^2 \cdot 4\Delta W \cdot 0.203 q_0 \omega_u (\tau_{k_0} + \tag{5}$$
$$+ 0.938 v_{k_0}^{-1} x'_{k_0}) \ell n \frac{W_k}{W_0}.$$

With $W_k = 80$ MeV, $W_{k_0} = 1$ MeV, $4\Delta W = 305$ keV, $x'_{k_0} = 0$, $q_0 \omega_u \tau_{k_0} = +-5°$ we will have in two basic versions

(A) $q_0 = 2$; $q_1 = 6$; $\lambda = \frac{3}{2}$; $\delta W_{nor} = \pm 1.34 k_3 \delta$; (1)

(B) $q_0 = 3$; $q_1 = 6$; $\lambda = \frac{4}{3}(\sqrt{2}-1)$; $\delta W_{nor} = \pm 1.325 k_3 \delta$. (6)

Key: (1). keV.

Calculation on computers, made for the version (V) in work [5] gives $\delta W = +-3.5$ keV, while the permissible variations, which corresponds $\delta W/W = +-0.5 \cdot 10^{-4}$, composes $\delta W = +-4$ keV.

The swept aside effect (let us name/call its logarithmic) actually limits the theoretically attainable degree of the monochromaticity of bundle. The role of other effects, also connected with the initial sizes/dimensions of cluster, under the made assumptions is not so/such great. The fact that during calculations on the computers theoretical limit (6) was not achieved/reached, can be explained both by the inaccuracy in estimations (6), introduced by stepped model and by some factors, which differ calculation [5] (not absolute isochronism, three-dimensional/space separation of basic and supplementary dees, etc.).

269

REFERENCES

1. Yu. K. Khokhlov.   Atomic Energy, 1970, 29, Nr. 1, 39.
2. Yu. K. Khokhlov.   Atomic Energy, 1971, 30, Nr. 5, 451.
3. Yu. K. Khokhlov.   Atomic Energy, 1971, 31, Nr. 6, 626.
4. I. Ya. Barit and others.   Preprint FIAN, 1969, Nr. 15,
5. R. N. Litunovsky, O. A. Minajev, Some details of orbit
   parameter calculation in ring isochronous cuclotron.
   Report at International Conference on Cyclotrons,
   Oxford, 1969

108. Dependence of energy scatter at the output of linear electron accelerator on stochastic instabilities of its parameters.

G. P. Aver'yanov, A. V. Nesterovich, A. V. Shal'nov.

(Moscow physical engineering institute).

The energy spectra of linear electron accelerators (LEU) are determined by a number of factors: by the instability of parameters of the source of high-frequency power, by a change in the temperature of the accelerating waveguide, by the phase width of cluster, by particle distribution according to the density, etc.

One of the most essential factors, which cause the scatter of particles on the energies, are the frequency-phase instabilities of the sources of high-frequency power. Usually their contribution to the general/common/total energy scatter of bundle is evaluated according to formulas, analogous those given in [1]. Such estimations have a number of the deficiencies/lacks: is estimated the deficit of energy, but not a change in the energy spectrum, and so it is not the possible to rate/estimate the contribution of the frequency-phase instabilities, which are changed during the impulse/momentum/pulse.

The latter is especially important, since in a number of cases [2] the intrapulse instabilities consicerably exceed slow frequency drifts.

In this work are given and are discussed the results of the simulation of the fast-changing frequency-phase instabilities by ETsVM   [digital computer]. During the simulation it was assumed that in the accelerator are not applied the special measures for an improvement in the energy spectrum of bundle. As the calculated ones were utilized the parameters of the sections LEU UFTI   [Ukrainian Scientific Research Physicotechnical Institute] on 2 GeV, since the supplies of power, the diagram of phasing and synchronization, and also parameters of the accelerating sections which they are applied on this accelerator, are typical for this class of installations.

Let us assume that into multisection LEU during the time interval τ (duration of high-frequency pulse) is injected the sequence of the clusters, which have the specific phase width and following after each other through the identical time intervals T. To the entrance of each section is supplied the high-frequency power whose frequency changes in the time randomly; however, its mathematical expectation is equal to the frequency of bunches, and dispersion $(\sigma_{\delta f})^2 = (\frac{1}{3}\delta f)^2$ (δf - allowance for a change in the

frequency).

Page 66.

Energy, which gathers the particle, which is located in the cluster, which flies at moment of time t (0<t<τ) in the n - section LEU, in the presence of frequency-phase instabilities it is convenient to write in the following form:

$$W_{nt} = \int_0^L \left\{ \mathcal{E}e^{-sz}\cos\left[\varphi_0 + \psi_n + \varphi(t) + \psi(\_\_) - IR_{w}(1-e^{-sz})\right] \right\} dz. \tag{1}$$

Are here introduced the following designations: I - current of particles per pulse, R_{w} - shunt resistance; L - length of the accelerating waveguide; s - attenuation factor; z - current longitudinal coordinate; φ_0 - phase of particle in the cluster; ψ_n - phase displacement due to an inaccuracy in the phasing; y(t) - slip of particle relative to wave, determined by the deviation of frequency f from its nominal value f_0 at the moment of time t;

$$\varphi(t) = 2\pi \int_0^t \left[f_0 - f(t) \right] dt$$

phase change along the length of impulse/momentum/pulse due to changes in the frequency. This factor during the investigation of frequency-phase instabilities usually is not considered, since is not examined the sequence of clusters. For the short durations of pulse (1-2 μs) it actually/really has a weak effect. However, with an increase in the duration the contribution of this factor increases. Subsequently it will be shown that in this case phase change can

prove to be such large that the particles can hit the region of negative half-wave. In view of random character of frequency instabilities the analytical determination of the energy spectra of bundle is difficult; therefore investigation was conducted numerically. Simulation was conducted under the simplifying assumptions. Thus, it was considered that the sections of accelerator are ideally phased ($\psi_n = 0$), and the disturbances/perturbations of frequency are spread with the particle speed. In view of a larger quantity of clusters in the impulse/momentum/pulse, and also since the time of flight of particles in the waveguide is considerably less than the period of frequency fluctuations, the results of simulation weakly depend on the assumption indicated.

The procedure of statistical simulation is described in sufficient detail in the literature [3]. Let us note that for the realization of simulation is necessary the a priori knowledge of the laws of the distribution of instabilities. As it follows from the investigation of the intrapulse instabilities of frequency of klystrons [2], the frequency-time dependence $f(t)$ can be considered as stationary normal ergodic random function with the mathematical expectation, equal to the nominal value of oscillator frequency. In this case the function $\varphi(t)$ is random unsteady ergodic function [4] with the mathematical expectation, equal to zero and by the dispersion: $D_\varphi = 2 \int_0^t (t-\tau) \cdot k_{\Delta f}(t)\, dt,$ where $K_{\Delta f}(t)$ - coefficient of

correlation of function $r^o(t)$. Its definition does not cause fundamental difficulties, since for this purpose they can be used both special analyzing instrument-correlators [5] and different calculated methods [4].

In Fig. 1 it is shown, as changes σ_y along the length c inpulse/momentum/pulse with $\sigma_{\Delta f} = 0.1$ MHz (parameters $f(t)$ - experimental [2]). As can be seen from figure, with an increase in the pulse duration it is more than 20 ms, the part of the particles can fall into the decelerating field. But also in the smaller pulse durations: as the consequence of this effect should be expected essential deterioration in the spectrum of particles. Are represented below the results of the simulation both of point and extended clusters. Density distribution along the length of cluster was taken from the experimental data [6].

Fig. 2 depicts energy spectra during the impulse/momentum/pulse at the output of one section for different frequency instabilities (cluster was considered point).
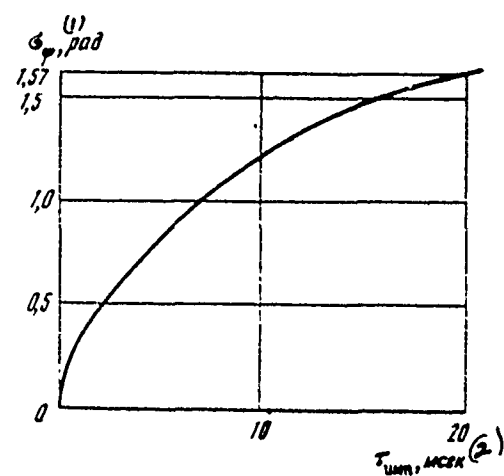
Fig. 1. Increase σ_φ with an increase in the duration of pulse ($\sigma_{\Delta f}$ =0.1 MHz).

Key: (1). rad. (2). ms.
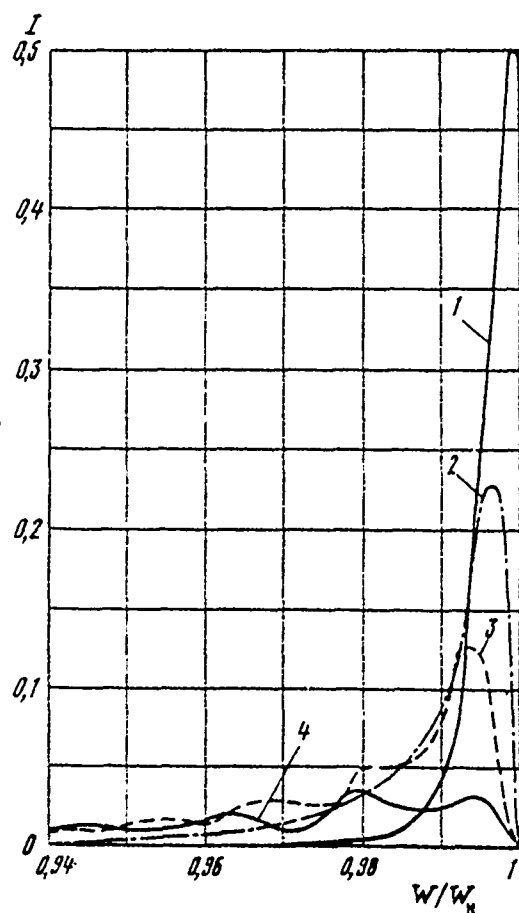
Fig. 2. Dependence of energy spectrum on the degree of frequency fixing (clusters point)

$1-\sigma_{\Delta f}=0.03\text{МГц}(\sigma_{\Delta f}=10^{-6})$; $2-\sigma_{\Delta f}=0.05\text{МГц}(\sigma_{\Delta f}=1.7\cdot10^{-6})$; $3-\sigma_{\Delta f}=0.1\text{МГц}(\sigma_{\Delta f}=3.3\cdot10^{-6})$; $4-\sigma_{\Delta f}=0.2\text{МГц}(1)$ $(\sigma_{\Delta f}=6.6\cdot10^{-6})$

Key: (1). MHz.

Page 67.

Attention is drawn to the presence of long "low-energy" in the region tails, and also the strong dependence of the form of the spectrum on the value of frequency instabilities.

Fig. 3 depicts the comparison of the spectra during the impulse/momentum/pulse for the case of point (unbroken curves) and extended (+-15°) clusters with different frequency instabilities. From the figure it follows that the noticeable difference in the spectra begins to appear only with instability of supply of power $\frac{\delta f}{f}$ =10^{-6} and it is less. Were investigated also the spectra of multisection accelerators. Fig. 4 gives the spectra of the accelerators, which consist of different quantity of sections with the different values of frequency instabilities. Clusters were considered point. From the figure one can see that with an increase in the number of sections the spectrum becomes narrower and more symmetrical. The average/mean value of the collected/composed energy is shifted/sheared relative to the nominal value into the region of lower energies. These phenomena will agree well with the general considerations of the probability theory and the mechanism of simulation.

Thus according to the results of simulation it is possible to make the following conclusions:

1) frequency-phase instabilities are the determining factor, which leads to deterioration in output characteristics of bundle;

2) the shortening of clusters for the purpose of an improvement in output characteristics of bundle is expedient only upon reaching of the certain degree of frequency fixing;

3) an increase in the duration of high-frequency pulse (with the constancy of the parameters of frequency instability) leads to an increase in the energy scatter of particles.
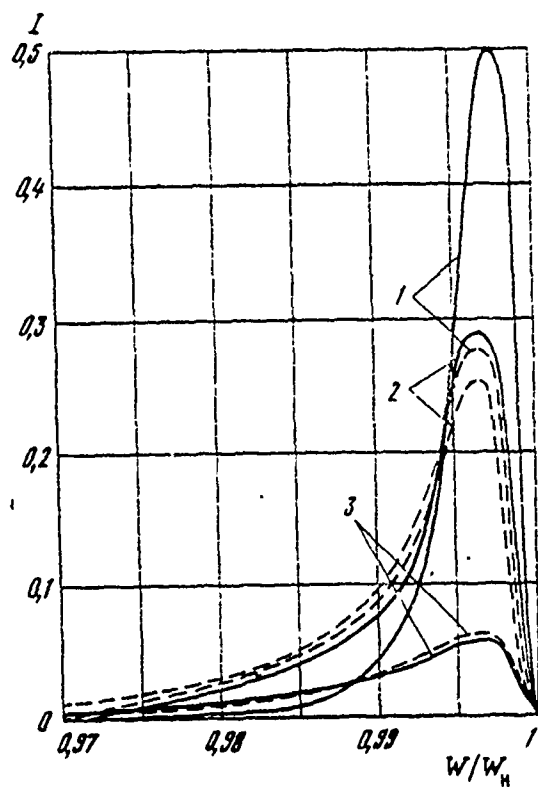
Fig. 3.

Fig. 3. Comparison of spectra of point (solid lines) and extended
(dotted lines) clusters. Designations the same as in Fig. 2.

Fig. 4. Spectra of multisection accelerators dotted line - $\sigma_{\Delta f}$ =0.1
MHz; solid line - $\sigma_{\Delta f}$ =0.03 MHz: 1 - one section; 2 - ten sections; 3
- 50 sections.

280
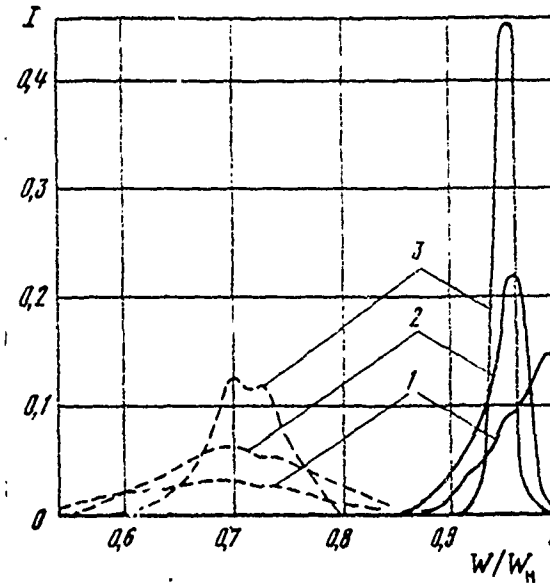
REFERENCES

1. G. P. Aver'yanov, A. V. Shal'mov. Collection "Accelerators", Issue XI, Moscow, Atomizdat, 1969, pp. 146

2. I. A. Grishayev, V. B. Mufel', T. F. Nikitina, ZHTF, 1969, 39, Nr. 7, 1237.

3. N. P. Buslenko, Yu. A. Shreyder. Method of Statistical Tests (Monte Carlo) and its Realization os a Computer, Moscow, Fizmatgiz, 1961.

4. A. A. Sveshnikov, Applied Methods of Random Functions Theory, Moscow, Izd-vo "Nauka", 1968.

5. F. Lenge. Correlation Electronics, Leningrad, Fizmatgiz, 1963.

6. A. I. Zykov and others. ZHTF, 39, Nr. 6, 1007 (1969).

Page 68.

109. Calculation of waveguide bunchers with the increased
requirements for the characteristics of the bundle of high-current
linear electron accelerators.

V. N. Golovin, V. N. Podsaivalov, N. P. Sobenin, E. Ya. Shkol'nikov.

(Moscow physical engineering institute).

Waveguide bunchers without the supplementary devices/equipment
for the initial formation of clusters are simple in the production
and in the adjustment and have high reliability in operation [1].
However, the calculation or such bunchers with the high coefficient
of capture and with the necessary phase-energy distribution presents
considerable difficulties. Task even more becomes complicated, if
waveguide buncher is intended for the formation of high-current
bundles, since questions of the account of load by the current also
of space charge in the region of intense phase motion did not obtain
a sufficient development.

In the present work are given the basic conclusion/output,
obtained during the solution of questions indicated above in

connection with the creation of waveguide bunchers for the
high-current accelerators.

Extreme method of calculation of longitudinal dynamics. The
use/application of extreme calculation methods to the waveguide
bunchers makes it possible to considerably reduce time of the search
of version with the required characteristics of bundle. Let us
restrict the examination by the case of the minimization of exit
energy scatter $\Delta\gamma_k$(γ - energy of electron, in reference to its rest
energy)

$$F(\vec{X}) = \Delta\gamma_k = \gamma_{i_k max} - \gamma_{j_k min}; \quad (i,j = 1,2,\ldots,n), (1)$$

where n - quantity of "enlarged molecules". Scatter is the function
of the independent variables β_0, β_1, β_2, m, entering the expression
of phase wave velocity (referred to the speed of light):

$$\beta_\varphi(\xi) = \beta_0 - \beta_1 exp(-\beta_2 \xi^m). \qquad (2)$$

Expression (2) converts function $\beta_\varphi(\xi)$ into the finite-dimensional.
Here ξ - dimensionless length of accelerator.

This assignment $\beta_\varphi(\xi)$ simplifies checking the limitations,
superimposed on the function and substantially decreases a quantity
of varied independent variables. A quantity of input "enlarged
molecules" of n is determined by the coefficient of capture, by
requirements for the output parameters and by calculation procedure.

Let us define extremum as function $\beta_\varphi(\xi)$ with the prescribed/assigned function of the intensity/strength of accelerating field $\varepsilon(\xi)$ and at fixed/recorded length ξ_K. The analytical expression of the function of response is unknown; therefore is necessary to be restricted to its expression in the form of polynomials [2]. According to the results of experiment on the computers are determined the selective regression coefficients which after standardization are utilized for determining the direction of the motion of search. The block diagram of the algorithm of the solution of problem is represented in Fig. 1.

On the strength of the fact that the form of the function of responce is unknown, this algorithm utilizes for the acceleration of the speed of convergence gradiant method. The obtained vector of the direction of the fastest descent is standardized, which makes it possible to rapidly pass the regions, distant from the extremum. This search procedure in this task converges fast enough (for 30-60 iterations). Thus, in the case $\xi_K = 12, \varepsilon_{Hav} = 20$ kV/cm, $\varepsilon_{max} = 100$ kV/cm, coefficient of capture $\kappa_3 = 20$o/o is obtained an improvement in the energy spectrum 8 times. In this case the coefficients of formula (1) are equal to: $B_0 = 0.95462$; $\beta_1 = -0.34684$; $B_2 = 0.055446$; $m = 3.00213$.

Account of load by current. The calculation of longitudinal dynamics taking into account the load by current is conducted

numerically. Initial bundle is divided/marked off into n of the elementary bundles each of which consists of the well grouped clusters, which follow after each other with the frequency of accelerating field ω.
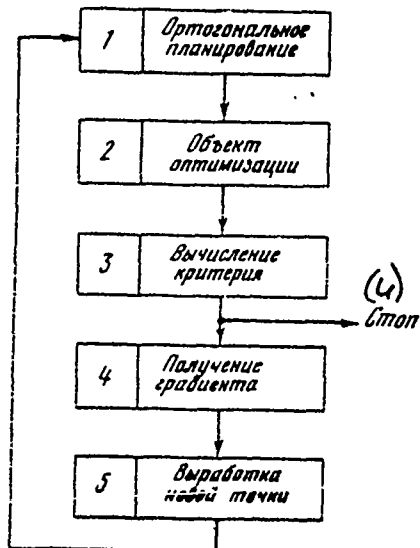
Fig. 1. Block diagram of algorithm.

Key: (1). Orthogonal planning/gliding. (2). Object of optimization. (3). Calculation of criterion. (4). Obtaining gradient. (5). Consumption/production/generation of new point. (6). Stop.

Page 69.

Is solved system from 3n the differential equations of the type:

$$\frac{d\varepsilon_{0i}}{d\ell} = -\left(\alpha - \frac{1}{R}\frac{dR}{d\ell}\right) + I_{0i} R \cos\varphi_i ,$$

$$\frac{d\varphi_i}{d\ell} = \frac{2\pi}{\lambda}\left(\frac{1}{\beta_\varphi} - \frac{\gamma_i}{\sqrt{\gamma_i^2 - 1}}\right) , \tag{3}$$

$$\frac{d\gamma_i}{d\ell} = \frac{e}{m_0 c^2}\left(\varepsilon_r \cos\varphi_i - \sum_{q=1}^{n} \varepsilon_{0q} \cos(\varphi_q - \varphi_i)\right),$$

where $\delta_{oi.q}$ - longitudinal components of radiation of elementary

beam; α - fading, R - series resistance of waveguide, I_{oi} - the

average/mean current of the i elementary beam; φ_i - phase of i-

beam; λ - wavelength of accelerating field in the free space; -

relative energy of the i beam; δ_i - relative energy of the i beam;

δ_r - accelerating field or outside oscillator; ℓ - longitudinal

coordinate.

System (1) differs from the usual equations of dynamics in terms

of the fact that is considered the field of the study of beam. In

connection with this the equations of motion of separate clusters are

not divided.

Fig. 2 gives phase-energy distributions for the buncher RTI of

the AS USSR.

For the comparison the same figure gives the distribution,

calculated from the equation of the balance of power for beam [3].

Space-charge effect. In the presence of the forces of space

charge the particle motion is described by system of N equations (see

[1]), where N - number of separations of cluster. Cluster was

divided/marked off either into the series/row of the charged/loaded

spheres with the centers on the axis/axle of accelerator or to the

series/row of the charged/loaded cylinders. A number of separations,
the sizes/dimensions of spheres or cylinders and their charge be
determined by the form of cluster, by its length in the coordinate
system, connected with the beam, and with the variable/alternating
bulk density of charge. During this simulation of cluster the
strength of the field of each element/cell was determined from the
electrostatic task.
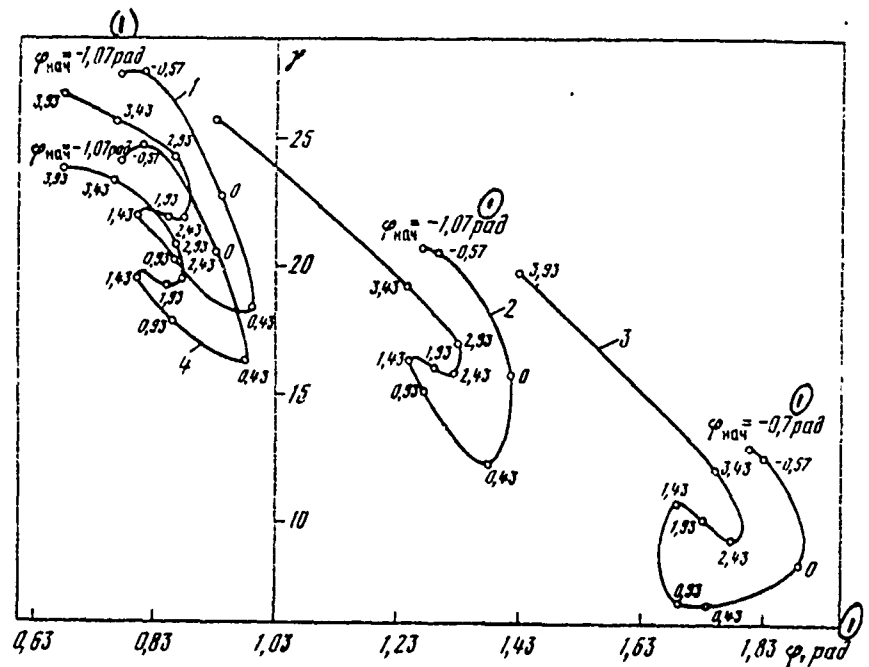
Fig. 2. Phase-energy distribution for the buncher RTI of the AS USSR:
1 - I_0 = 0; 2 - I_0 = 1 a; 3 - I_0 = 1.8 a; 4 - calculation according to the equation
of the balance of power for I_0=1a.

Key: (1). rad.

Basic parameters of bunchers RTI of AS USSR and FTI of AS UkSSR are given in table.

	(1) Им-пульс-ный ток, а	(2) Энер-гия, Мэв	(3) К.п.д., %	(4) Дли-на волны см	(5) Дли-на груп-пиро-вате-ля, м	(6) В.ч. мощ-ность, Мвт	(7) Напря-жение инжек-ции, кэв	(8) Коэф-фици-ент за-хвата, %	(9) Фазовая протя-женность сгустка на выхо-де, град
РТИ АН СССР	1	11,2	55	16,5	2,22	20	120	90	15
ФТИ АН УССР	1	11	52	10,7	1,6	18	80	100	8

Key: (1). Pulse current, A. (2). Energy, MeV. (3). Efficiencies. (4). Wavelength cm. (5). Length of buncher, m. (6). V. h. power MW. (7). Stress/voltage of injection, keV. (8). Coefficient of capture, %. (9). Phase width of cluster on output, deg.

Page 70.

For the first model (clusters in the form of spheres)

$$\varepsilon_{ij} = \begin{cases} \pm \dfrac{q_i}{(\ell_i - \ell_j)^2}(1 - \beta_j^2) & |\ell_i - \ell_j| > \tau_i\sqrt{1 - \beta_j^2} \\[2mm] \pm \dfrac{q_i}{\tau_i^3}|\ell_i - \ell_j|(1 - \beta_j^2) & |\ell_i - \ell_j| < \tau_i\sqrt{1 - \beta_j^2} \end{cases}, \quad (4)$$

where ε_{ij} - intensity/strength of field j - element/cell in the location of i-element/cell; ℓ_i, ℓ_j - longitudinal coordinates of elements/cells; τ_i, L_i - radii and lengths of elements/cells:

$\beta_{i,j}, q_{i,j}$ - speed and charges of elements/cells. Positive sign corresponds $\ell_i > \ell_j$, "minus" - corresponds $\ell_i < \ell_j$.

System of 3N equations was realized according to Runge-Kutta's method on the computers M-20. A number of separations and a model were established/installed separately for each case.

In Fig. 3 dotted lines depicted the phase-energy spectra for the bunchers RTI of the AS USSR and FTI of AS UkSSR with current 1 and taking into account the space charge (solid line - without the account). With calculation were selected N=30, the first model and τ =3 and 5 mm respectively. It is obvious, the account of space charge with the current into 1 and little affects the characteristics of beam, since the forces of interaction in the buncher are weakened by factor $1-\beta^2$.

DOC = 80069306   PAGE 291
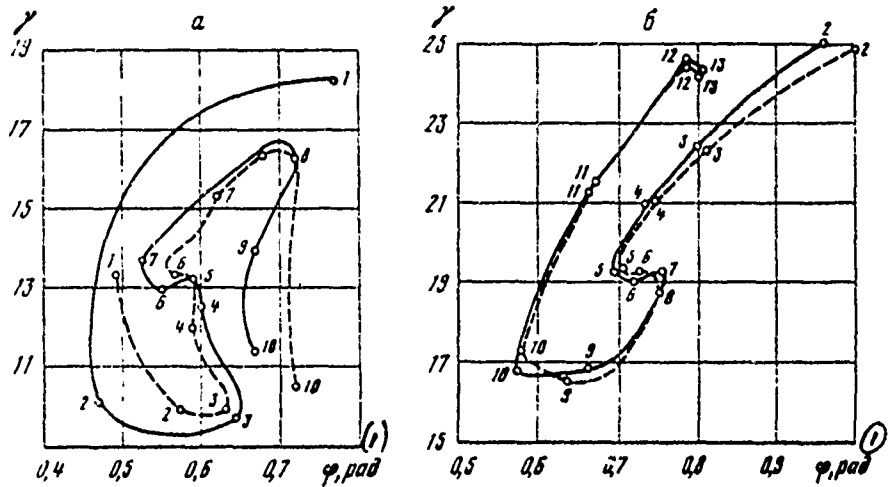
Fig. 3. Phase-energy distribution for the bunchers of FTI of AS UkSSR (a), RTI of the AS USSR (b).

Key: (1). rad.

REFERENCES

1. O. A. Bal'dner. Linear Electron Accelerators, Moscow, Atomizdat, 1966.

2. V. V. Nelimov and N. A. Chernova. Statistical Methods for Planning Experiments, Moscow, Izd-vo "Nauka", 1965.

3. R. B. Neal, J. Appl. Phys., 1958, 29, 1019.

110. Effect of the high-frequency field of the waveguide accelerating systems by the particle motion in the accelerators to the superhigh energies.

A. N. Didenko, V. K. Conan, G. P. Fomenko.

(Scientific research institute of nuclear physics with by Tomsk polytechnic institute).

Recently widely is investigated a question about the possibility of applying the waveguide accelerating sections in the cyclic accelerators to the superhigh energies. Thus, in [1] it is proposed to utilize waveguide sections as the accelerating systems of electron-positron accelerator on 100 GeV. It is proposed to use to waveguide section, also, in one of the versions of the accelerating system of the cybernetic accelerator of protons to the energy 1000 GeV [2].

The special feature/peculiarity of the use of waveguide sections in this case is the fact that the frequency of accelerating field must be modulated in the process of acceleration. This leads to the slip of field relative to particles in the process of acceleration.

The consequence of this is the fact that the optimum accelerating sections will be such, in which the HF field has in general all 6 components of field. As it was shown in [3], such fields lead to connection/communication of betatron oscillations both between themselves and to connection/communication with the phase oscillations. Appearing in this case additions to the betatron oscillations will be inversely proportional to energy of particles, and, thus, they change in the time according to the specific law. This leads to the fact that in the process of acceleration the operating point completes motion on the diagram of resonances and in view of this can pass through some of them.

Page 71.

Therefore it is of interest to examine particle motion in the accelerator, as the accelerating element/cell in which serves waveguide section, and to investigate the effect of HF field for this motion. We will solve problem, writing/recording separately equations of motion in the straight portion with a length of L, where is arranged/located the accelerating section, and in the sections of the element/cell of the periodicity where there is no HF field. In [4.5] it is shown that the structure, close to the optimum, will be a system of the type of double-row stairs in the circular waveguide. We showed that approximately the components of the field of the cophasal

symmetrical wave which they are only and of interest, in the rectangular coordinate system (y is directed along the axis of waveguide) they take the following form:

$$E_y = E_m \cos \frac{2\pi}{\lambda} z \, \text{ch} \frac{2\pi}{\lambda} x \cos \left(\omega t - \frac{2\pi}{\lambda} y \right),$$

$$E_x = - E_m \cos \frac{2\pi}{\lambda} z \, \text{sh} \frac{2\pi}{\lambda} x \sin \left(\omega t - \frac{2\pi}{\lambda} y \right),$$

$$H_y = E_m \sin \frac{2\pi}{\lambda} z \, \text{sh} \frac{2\pi}{\lambda} x \cos \left(\omega t - \frac{2\pi}{\lambda} y \right),$$

$$H_x = - E_m \sin \frac{2\pi}{\lambda} z \, \text{ch} \frac{2\pi}{\lambda} x \sin \left(\omega t - \frac{2\pi}{\lambda} y \right),$$

$$E_z = H_z = 0.$$

(1)

Equations of motion in these fields in the linear approximation/approach are divided on x and y. For the magnetic structure, selected in the radio engineering institute of the AS USSR for the synchrotron to 1000 GeV, equations of motion for any section of the element/cell of periodicity it is possible now to present in the following form:

$$\frac{d^2 X(y)}{dy^2} + k(y) X(y) = 0, \qquad (2)$$

where X(y) represents either radial or vertical displacement, and k(y) satisfies periodicity condition and equally respectively:

$$k = \begin{cases} 0 & \text{— на прямолинейном участке,} \quad (1) \\ \pm \dfrac{\theta}{B\rho} & \text{— в квадрупольных линзах,} \quad (2) \\ \dfrac{1}{\rho^2} & \text{— в заворачивающих магнитах,} \quad (3) \\ \pm \dfrac{e E_m \sin \varphi_z}{\delta_c} \dfrac{2\pi}{\lambda} & \text{— в волноводных секциях.} \quad (4) \end{cases}$$

Key: (1). in the straight portion. (2). in quadrupole lenses. (3). in

turning up magnets. (4). in waveguide sections.

Here G - gradient of magnetic field in the lenses; ρ - radius of curvature of orbit; B - maximum induction of magnetic field; Ψ_s and δ_s - equilibrium phase and energy of particle. Solving equations (2), we will obtain the matrices/dies, which describe particle motion in any section of the element/cell or periodicity. The general/common/total matrix/die of transition will be the product of these matrices/dies and it it is possible to represent in the form [6]

$$M_{x,z} = \begin{pmatrix} \cos\mu_{x,z} + \alpha_{x,z}\sin\mu_{x,z} & \beta_{x,z}\sin\mu_{x,z} \\ -\gamma_{x,z}\sin\mu_{x,z} & \cos\mu_{x,z} - \alpha_{x,z}\sin\mu_{x,z} \end{pmatrix},$$

where α, β, μ and γ - known characteristics of betatron oscillations. We examined 2 versions of the location of the magnetic periods:

1) magnetic periods with the waveguide accelerating sections evenly distributed in the circumference of accelerator. Matrices/dies M in this case take the form:

$$M_x = \left\{ O(\tfrac{\ell}{2})T_F\left[O(\ell_5)T_5\right]^6 O(\ell_5)T_D O(\ell)T_D\left[O(\ell_5)T_5\right]^6 O(\ell_5)T_F O(\tfrac{\ell}{2}) \right\}^7 \times$$
$$\times \left\{ O(\tfrac{\ell}{2})T_F\left[O(\ell_5)T_5\right]^6 O(\ell_5)T_D O(\ell)T_D B_x T_F O(\tfrac{\ell}{2}) \right\}.$$

$$M_z = \left\{ O(\tfrac{\ell}{2})T_D O(L)T_F O(\ell)T_F O(L)T_D O(\tfrac{\ell}{2}) \right\}^7 \times$$
$$\times \left\{ O(\tfrac{\ell}{2})T_D O(L)T_F O(\ell)T_F B_z T_D O(\tfrac{\ell}{2}) \right\}.$$

Here T_F, T_D, T_6, B, O(y) — matrix/die of focusing and defocusing lenses, turning up magnet, waveguide section and straight section length y respectively:

2) magnetic periods with the waveguide sections are located in a row in one place for circumference. In this case

$$M_x = \left\{ O\left(\tfrac{\ell}{2}\right) T_F \left[O(\ell_6) T_6\right]^6 O(\ell_6) T_D O(\ell) T_D \left[O(\ell_6) T_6\right]^6 O(\ell_6) T_F O\left(\tfrac{\ell}{2}\right) \right\}^{147} \times$$
$$\times \left\{ O\left(\tfrac{\ell}{2}\right) T_F \left[O(\ell_6) T_6\right]^6 O(\ell_6) T_D O(\ell) T_D B_x T_F O\left(\tfrac{\ell}{2}\right) \right\}^{21},$$

$$M_x = \left\{ O\left(\tfrac{\ell}{2}\right) T_D O(L) T_F O(\ell) T_F O(L) T_D O\left(\tfrac{\ell}{2}\right) \right\}^{147} \times$$
$$\times \left\{ O\left(\tfrac{\ell}{2}\right) T_D O(L) T_F O(\ell) T_F B_x T_D O\left(\tfrac{\ell}{2}\right) \right\}^{21}.$$

Calculation α, β, γ, and μ followed method itself, proposed in [7], on the computers BESM-4 for the following values of the parameters of synchrotron on 1000 GeV: $\rho=1736$ m, B=19.2 kg, G=3.045 kgf/cm, L=39.52 m, $L_F = L_D = 1.5$ м, ℓ = 2 м, ℓ_6 = 0.7 м, L_6 = 5.77 м, $\psi_6 = \tfrac{3L}{4}$, f = 235.44 MHz, $eE_m \sin\psi_5 = 51.99136$ MeV.
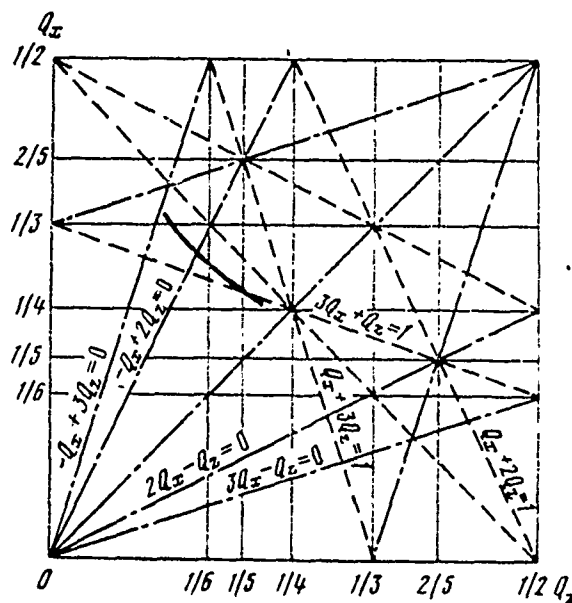
Fig. 1. Diagram of resonances and motion of the operating point of accelerator.

Page 72.

The results of calculation are given in Fig. 1.2. Fig. 1 depicts the
diagram of resonances and is shown the motion of operating point in
the accelerator. From the figure one can see that with a change in
the energy the operating point the secants of the resonances of the
3rd, 4th and higher order and with the high energies (~500-1000 GeV)
it approaches its position without the waveguide section. Fig. 2
shows divergences α, β, γ (solid lines) from the appropriate values
without the waveguide section (broken). For the illustration are

given only the characteristics of radial oscillations for one section of the element/cell of periodicity. Calculations show that the waveguide sections change maximum value β approximately/exemplarily on 7-8o/o for the bouncing and about 5o/o for the radial ones. The same picture is observed also in the case of the nonuniform location of the magnetic periods with the waveguide sections.

Additions to α, β, γ and μ are the functions of time and, apparently, any changes in the magnetic system cannot compensate those effects which introduces the waveguide structure. Therefore we examined the possibility of eliminating these effects due to the location of waveguide sections. If we arrange waveguide sections so as to adjacent sections would be turned friend from carrier the friend on 90° (system of the type "waveguide quadrupole"), then the appearing supplementary resonances have very high order (the 5th and more), which are not dangerous, but additions to values α, β, and γ do not exceed 1-2o/o.

REFERENCES

1. A. I. Alikhanyan and others. Summaries of Reports
    at the 7th International Conference on High-Energy
    Charged-Particle Accelerators. Yerevan, 1959.

2. Cybernetics Accelerator of Protons for an Energy
    of 1000 GeV. Edited by A. A. Vasil'yev. Preprint
    9267-148, Moscow, 1967.

3. A. A. Vorob'yev and others. Waveguide Synchrotrons.
    Atomizdat, Moscow, 1966.

4. W. Schnell. Proc. V Internat. Cong. on High Energy
    Accelerators, Frascati, 1965, Roma, 1966, p. 38.

5. Yu. A. Khlestkov, A. V. Shel'nov. In Collection
    "Accelerators", Issue XI., Moscow, Atomizdat,
    1969, p. 155

6. E. D. Courant, H. Snyder, Ann. Phys. 1958, 3, 1;
    sm. Ttakzhe PSF, 1958, Nr. 4, 91.

7. E. L. Burshteyn, L. S. Solov'yev, Preprint.
    Radio Technology Institute of Academy of Sciences
    USSR, NT-2260-27, 1960.
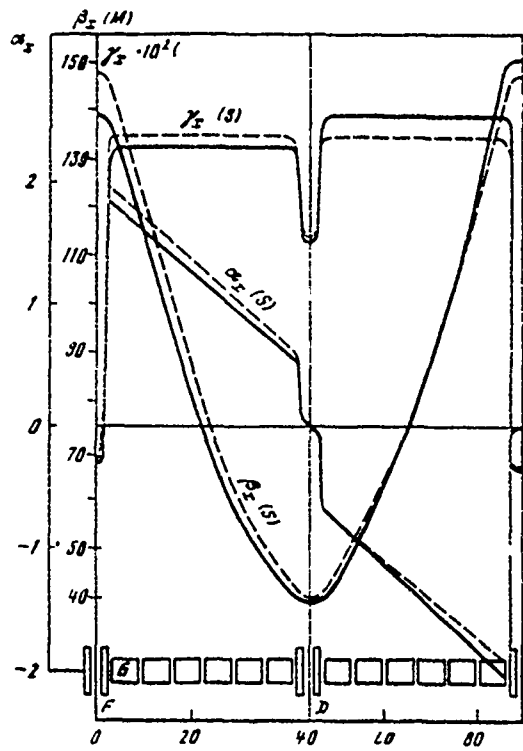
Fig. 2. Functions α, β, γ for the radial ones of oscillation.

111. Interaction of beam with the transverse waves in the periodic structures of high-current linear electron accelerators.

I. A. Grishaev, G. D. Kramskoy, A. I. Zykov, G. L. Fursov.

(Physicotechnical institute of the AS USSR).

To the investigation of the "shortening" of make pulse in the linear electron accelerators are dedicated experimental [1-9] and theoretical works [10-15], in which it is established/installed, that the reason for this effect is the excitation by beam in the periodic structure of accelerator, besides wave E_{01}, hybrid (transverse) waves, in particular waves EH_{11}, which act on beam, deflecting/diverting it in the transverse direction.

Critical (threshold or maximum) current $I_{\kappa p}$ is inversely proportional to the duration of make pulse and to the length of accelerator, and also it depends on the geometry of waveguide, quality at the defocusing mode, the group velocity, the focusing field. As shown in [3, 4] $I_{\kappa p}$ in the multisection accelerators substantially less than in the accelerators, which consist of one section, the mechanism of the development of the lateral instability

with the high energies and the pulse currents several ten

milliamperes carries cumulative character [5], while in

single-section medium-energys accelerator and currents in several

hundred milliamperes instability has regenerative character.

Page 73.

In [10-12] it is assumed that the amplitude of the excited by

the grouped electron beam is axial-asymmetric wave EH_{11} with

$v_\phi \approx v_e = c$ is proportional to the radial displacement of part or

clusters. The field of this wave is represented by the superposition

of radiation fields all earlier flown clusters and builds up in the

time.

As the final result, the solution of equations of motion,

accordingly [10-12] leads to the exponential expression for the

transverse displacement of clusters at the output of linear

accelerator, which applicably both in the case of cumulative and

regenerative instability takes the form

$$x_n(x,t) = x_0 e^F, \tag{1}$$

where x_n - the transverse displacement of n-th cluster; which

corresponds to the moment/torque of time t from the beginning of

injection, x_0 - initial divergence, F - coefficient characterizing

structure both the parameters of accelerator and that expressing, in

particular, accordingly [11] in the form

$$F = 1.64(CI_0 t)^{1/3} \left(\int_{z_0}^{z} \frac{dz}{[\gamma(z)]^{1/2}} \right)^{2/3} - \frac{w}{2Q} t - \frac{1}{4} \ell q \frac{\gamma}{\gamma_0} ,$$

where $C = \frac{e}{m_0 c^2} \frac{c z_t \ell_1}{LQ} \frac{w^2}{2c^2}$; z_t – transverse shunt resistance; ℓ_1 –
effective length of interaction of beam with wave L – the distance
between the interaction regions; I_0 – beam current; Q – quality of
structure; $w = 2\pi f_{11}$ – frequency; t – time; x – longitudinal
coordinate; γ_0, γ – initial and final energy of electron in unity
$m_0 c^2$; e – electron charge; c – speed of light.

Expression (1) in work [11] is obtained, on the basis of the
model, on which multisection accelerator with the sections of
variable/alternating structure, represented by the sequence of the
single resonators, beam induced at the frequency of hybrid mode f_{11},
moreover the excited level of resonators is proportional to the
transverse coordinate of particle or cluster x and as a result of
effect on the beam of the excited resonator in beam appears certain
structure in the transverse direction, so that x will be modulated
with the frequency, close to f_{11}.

The source of initial disturbances (particle displacements from
the axis/axle) can be snot noises in the beam, collision excitation
due to inaccuracies in the setting up, thermal noises in the
sections, noise or parasitic signals from the klystrons, electrical

discharges in the strong SHF fields, etc.

Available experimental data on make it possible to make a single-valued conclusion about which of the sources of initial driving is more important.

Thus, as the basis of theoretical examination in the mentioned works they are placed two assumption:

1) the proportionality of tne amplitude of the induced by beam signals on wave EH_{11} to the transverse displacement of particles or clusters and

2) the need for initial disturbance/perturbation or transverse displacement of particles (cluster) x for the development of instability when the remaining parameters of accelerator are such, that it can be developed. One should emphasize that the validity of these positions did not directly undergo experimental check.

In the present work was undertaken the attempt measure the parameters of instability at tne varied conditions for passage and interaction of beam witn the periodic structure of accelerator.

Were investigated dependences $I_{КР}$, of amplitude and frequency of

the induced by beam signals on wave EH_{11} and EH_{21}, the coefficients of cluster amplification on a change in the following parameters:

1) the initial transverse displacement of beam as whole relative to the axis/axle of the septate waveguide;

2) the quality of the septate waveguide on wave EH_{11};

3) the longitudinal focusing magnetic field of solenoid;

4) the diameter of the injected into the accelerator beam;

5) the agreement of the end devices/equipment of the septate waveguide.

Experimental setting up and procedure.

The schematic of experimental installation is shown in Fig. 1. Electron beam from the injector with the energy in the maximum of the spectrum 5.5 MeV was carried out through the septate waveguide with a length of 2.5 m without the introduction/input into it of power at the operating frequency $f_{01}=2797$ MHz, i.e., without the acceleration.
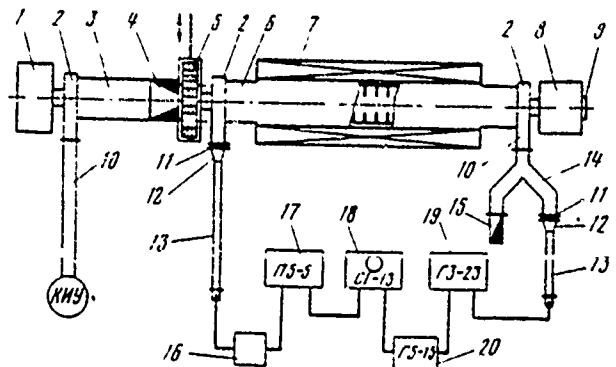
Fig. 1. Schematic of experimental installation. 1 - electron gun; 2 - matching transitions, 3 - injector section; 4 - load; 5 - interchangeable collimator; 6- investigated septate waveguide; 7 - focusing solenoid; 8 - faraday cylinder; 9 - the glass plate; 10 - waveguide transition from 72x34 mm to 48x24 mm; 13 - waveguide 48-24 mm; 14 - waveguide T-joint 72x34 mm; 15 - load; 16 - calibrated attenuators; 17 - measuring receiver; 18 - oscillograph; 19 - SHF oscillator; 20 - Generator of impulses/momenta/pulses; KIU - klystron pulse amplifier.

Page 74.

Structurally the diaphragm waveguide was carried out dismountable and consisted of 5 subsections with the flange joints and rubber seals on the ends/leads of the subsections.

At the output of electron conductor (after the exit matcher of the diaphragm waveguide) was established/installed the faraday cylinder with the the measuring screen-flag for the survey of form and position of beam with the aid of the television camera, which terminates by steel cap with the turning in the center section in diameter of 40 mm and thickness of walls 0.15 mm, which made it possible to obtain the impressions of beam shape with the aid of the glass plates, adjusted on the external wall of cap.

At the input and outlet ends of the diaphragm waveguide they were established/installed matching junctions to rectangular waveguiles 72x34 mm, on which entered the HF signals, induced by beam and supplied from the external oscillator. Input rectangular waveguide 72x34 mm concluded with transition section by the waveguide 48x24 of mm whose designation/purpose consisted of the filtration of the signal, induced by beam at the fundamental frequency of 2797 MHz.

Exit rectangular waveguide 72x34 mm concluded with the specially matched T-joint, to one of arms of which was connected the load for absorbing the signal of fundamental wave, and to the other - rectangular waveguide by the sizes/dimensions 48x24 of mm. The vacuum seals between the basic waveguide channels and the septate waveguide with the matchers it was accomplished/realized with the aid of the teflon partitions with a thickness of 4 mm, established/installed in

the choke flanged joints.

The septate waveguide and the focusing solenoid were established/installed on frame and they were adjusted independently with the aid of the regulating devices. The adjustment of solenoid and section relative to the axis/axle of the injected into the section bundle from the injector was checked with the aid of television camera and fixing of the impressions of beam on the glass plates. The adjustment of solenoid was considered finished, when the departure/attendance of center with an increase in the field from 0 to 400 e did not exceed +-3 mm. These beam displacements in the measurements were compensated for each of the values of magnetic field by the system of the correction, arranged/located on the septate waveguide. The alignment accuracy of beam on the axis/axle of waveguide was +-0.5 mm.

At the entrance of the septate waveguide was established/installed the remotely/distance adjustable collimator with the set of openings/apertures (precision/accuracy of their setting up to the axis/axle +-0.2 mm).

Signal from beam at frequency f_{11} came from the entrance of section into the measuring receiver P5-5 and was observed on the oscilloscope face S1-13. Signal f_{01} did not fall into the receiver,

being reflected from the filter - the long section of waveguide 48x24 mm.

The measurement of signal amplitude was achieved with the aid of the calibrated attenuators at the entrance of receiver. High-frequency oscillator G3-23, connected to the output of section, served as the external source of excitation in the septate waveguide of oscillations in the range 3700-4100 MHz. The passed through the section signal from G3-23 also came on P5-5 and was observed on S1-13.

Pulse generator G5-15 made it possible to smoothly regulate the moment/torque of starting/launching G3-23 and to see on oscillograph the combined or displaced in the time signals from the beam and G3-23.

The beginning of "shortening" was determined on the oscillogram of current pulse from the faraday cylinder and in form and amplitude of the oscillogram of the signal, induced by beam at frequency f_{11}.

Initial beam displacement.

The axis/axle of the bundle, injected into the septate waveguide, was displaced relative to the axis/axle of the latter in

the horizontal and vertical directions in the limits +-(12+-0.5) mm
by displacing the frame, rigidly connected with the waveguide. The
obtained displacement was fixed/recorded on the impressions of beam
on the glass plates. The diameter of the injected bundle was
regulated by remote/distance collimator at the entrance and comprised
in these measurements 1 and 2 mm.

Full/total/complete input divergence of beam from the injector
composed $3 \cdot 10^{-3}$ for 100o/o of particles; however, the diameter of
beam at output in which it is contained by 80o/o of particles, it did
not exceed 8 mm with the diameter at the entrance 1 mm, so that
maximum divergence for 80o/o of particles did not exceed $1 \cdot 10^{-3}$.

Were measured dependences $I_{кр}$, of the amplitudes of the induced by
bundle signals on waves EH_{11} and EH_{21} and the amplification factors
by the bundle of the signals of external oscillator on the
displacement of the axis/axle of bundle relative to waveguide in the
horizontal and vertical directions.
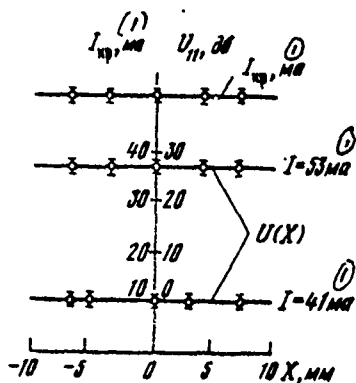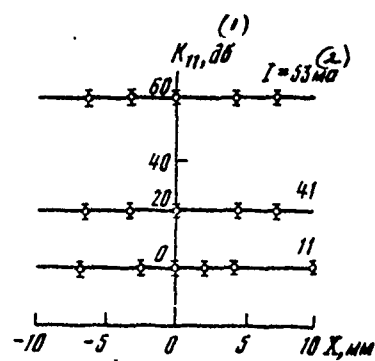
Fig. 2.   Fig. 3.

Fig. 2. Dependence $I_{кр}$ and amplitude of induced signal U on wave EH_{11} on beam displacement relative to axis/axle of waveguide. Diameter of collimator 2 mm.

Key: (1). mA.

Fig. 3. Dependence of coefficient of cluster amplification k_{11} on wave EH_{11} with coincidence of beam bursts and generator on beam displacement relative to axis/axle of waveguide.

Key: (1). dB. (2). mA.

Page 75.

Fig. 2 shows the results of measurement $I_{кр}$ and of the induced

signal level on wave EH_{11} in decibels u(x) with different currents,
relative to signal level with the current I=41 mA from the
displacement of the axis/axle of the injected into the waveguide
bundle.

Fig. 3 shows the analogous dependence of the factor of
amplification of the signal of oscillator on wave EH_{11} with the
coincidence of the beam bursts and oscillator.

As can be seen from Fig. 2, 3, correct within error limits for
measurement (+-2 mA), critical current, level of the induced signal
and coefficient of cluster amplification do not depend on the
position of bundle.

Measurements were made both for the waveguide without the
sections/cuts of diaphragms and for the waveguide with the
sections/cuts of diaphragms, and also with the beam displacement not
only in the horizontal, but also in the vertical directions, with the
introduction/input of beam at angle to the axis/axle of waveguide and
the beam displacement with the aid of the system of the magnetic
correction (latter was done for the waveguide with the sections/cuts
of diaphragms). In these all cases during the repeated repetition in
limits of accuracy of measurements it was not fixed any dependence of
the measured parameters of instability on wave E_{11} on the position of

th~ axis/axle of bundle relative to the axis/axle of waveguide.

Fig. 4 shows the dependences of the build-up/growth of cluster signal on wave EH_{21} (frequency $f_{21}=5520$ MHz; $(u_\varphi)_{21} = c$) on the displacement of the axis/axle of bundle in the horizontal direction with the different current strengths.

As far as dependence is concerned the induced by bundle signal level on wave EH_{21} with the displacement of the axis/axle of bundle in the vertical direction (it is perpendicular to the plane of the axis/axle of rectangular waveguide of input coupler), then in this case it did not change.

Quality of the septate waveguide.

As it was shown in [6, 7] the decrease of the quality of the septate waveguide it can be achieved/reached by the introduction of radial sections into the diaphragms. This method was utilized in the present work during the determination of dependence $I_{кр}$ on the quality. The results of measurements and calculations are given in Fig. 5.

Fig. 6 shows the dependences of the frequency of the hybrid wave EH_{11}, which correspond to value $(\bar{v}_\varphi)_{11} = c$ from length and type of

radial sections in width of section/cut 0.4 mm, determined from resonance measurements [6] and are plotted/applied the experimental points, obtained as a result of measuring the frequency of the induced by bundle signals.
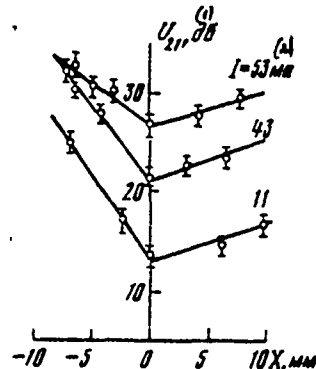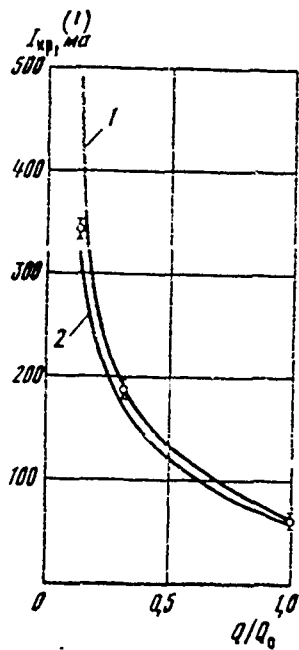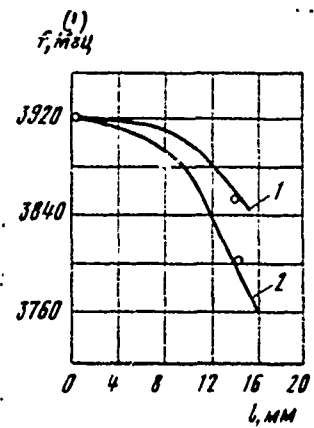
Fig. 4.   Fig. 5.   Fig. 6.

Fig. 4. Dependence of amplitude of cluster signal U_{21} on wave EH_{21} on beam displacement relative to axis/axle of waveguide.

Key: (1). dB. (2). mA.

Fig. 5. Dependence $I_{кр}$ on relative quality of structure Q/Q_0 1 - result of calculation (without taking into account energy losses by bundle to radiation/emission on fundamental wave) according to work [12] and data about quality at different length of sections/cuts [6]; 2 - result of analogous calculation taking into account losses not radiation/emission [16] with the use of averaged value of energy;

points - result of measurement. Along the axis of abscissas is deposited/postponed the ratio or quality Q to value of Q_0 without the sections/cuts.

Key: (1). mA.

Fig. 6. Dependence of frequency of hybrid wave EH_{11} $(v_\phi)_{\eta}=c)$ on length and type of radial sections in width of slot 0.4 mm. Points - value of signal frequency, induced by bundle; 1 - rectangular section/cut; 2 - cross-shaped.

Key: (1). MHz.

Page 76.

Diameter of the injected bundle.

There was a vagueness regarding the effect of the diameter of the injected into the accelerator bundle to the value of critical current. On one hand, this question in practice was not examined in the investigations on the cluster instability, with exception of work [13], where it was indicated that the threshold current at the permanent electron density must grow/rise with an increase in the working wavelength, or at wave length constant and density with an

increase in the sizes/dimensions of bundle, while on the other hand,

there was an opinion that for increasing critical currents it is

necessary to utilize dense bundles of small sizes/dimensions with the

sharply outlined boundaries. We carried out the measurements of

dependence I_{kp} on the diameter of the injected into the septate

waveguide bundle. The diameter of bundle changed with the aid of the

remote/distance collimator at the permanent mold and the density of

beam at the entrance into the collimator.

The results of measurements are represented in Fig. 7 (as

parameter serves the value of the quality of waveguide). From the

curves it is evident that critical current not only does not descend

with an increase in the diameter of bundle at the entrance, but also

grows/rises approximately/exemplarily 1.4 times with an increase of

the diameter of opening/aperture in the collimator from 2 to 24 mm.

With the full/total/complete input current of collimator 800 mA 80o/o

current it is concentrated in the diameter of 8 mm.

Dependence $\dot{I}_{kp}$ and of the induced by bundle on wave EH_{11} signal

on value of the focusing magnetic field of solenoid.

The use/application of a focusing field of solenoid for

increasing the limiting current was examined theoretically in works

[10, 14] and it was investigated experimentally in [8]; however in

[8] they were not given dependence $I_{КР}$ on the magnetic field strength.

Since this question is insufficiently studied and is of practical interest, were carried out the measurements of the dependence of the value of critical current from the magnetic field at the different values of the quality of waveguide, and also of the induced signal level on wave EH_{11} in the case of waveguide without the sections/cuts. Magnetic field was created with the aid of three focusing coils with a total length of 160 cm at the overall length of section 250 cm. The maximum magnetic field (averaged along the length) composed 400 e.

Fig. 8 depicts the dependences of cluster signal level at frequency EH_{11} of wave on the values of focus current, measured for the waveguide without the sections/cuts of diaphragms. It is evident that the imposition of magnetic field sharply decreases the generatable signal level.

Fig. 9 depicts the dependences of critical current on the magnetic field strength. With field change from 0 to 400 e critical current increases approximately/exemplarily 2 times at all values of quality; it should be noted that calculations according to the formulas of work [10, 14] give a considerably smaller increase in critical current: according to calculation, field into 400 e at the overall length of waveguide (2.5 m), gives increase of critical current only 1.4 times.
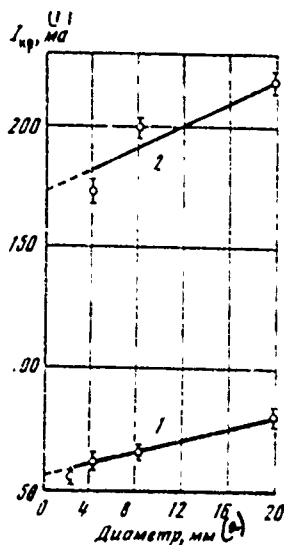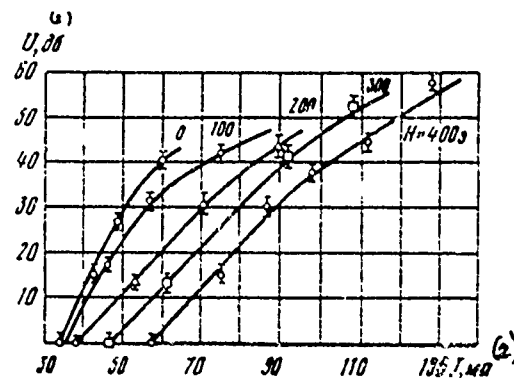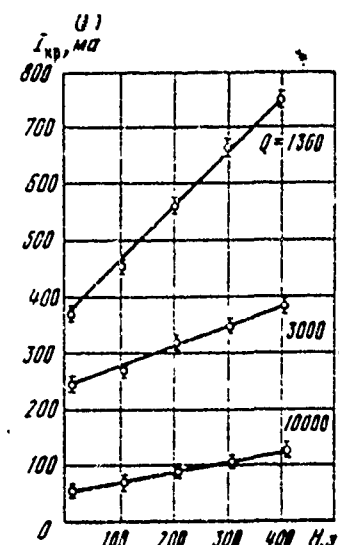
Fig. 7   Fig. 8   Fig. 9.

Fig. 7. Dependence of critical current on diameter of collimeter with quality of waveguide Q=10000 (1) and Q=3000 (2).

Key: (1). mA. (2). Diameter, mm.

Fig. 8. Dependences of cluster signal level at frequency EH_{11} of wave on current at different values of magnetic field.

Key: (1). dB. (2). mA.

Fig. 9. Dependences of critical current on focusing magnetic field. Q-factor of waveguide.

Key: (1). mA.

Page 77.

With the imposition of magnetic field and currents more than 400 mA was discovered nonlinear (apparently, plasma origin) effect- was observed the peculiar "aftereffect" of electron beam, which consists in the fact that the impulse/momentum/pulse from the external oscillator was distorted in form and changed in the amplitude, being it was arranged/located in the time considerably later than the cluster impulse/momentum/pulse, moreover this temporary/time brace varied from 2 to 20 μ s depending on the frequency of external oscillator and value of beam current.

Fig. 10 shows the dependence of the time of the brace of interaction of the signal of oscillator with the "residual medium" in the waveguide (remaining after the passage of beam) on the oscillator frequency with the current 520 mA and the field 400 e.

Unfortunately, effect is difficult to reproduce and was not in detail studied.

Agreement of the end devices/equipment of the septate waveguide and the frequency dependence of the factor of amplification of the hybrid wave EH_{11}.

As indicated in [15], threshold current in the section of linear accelerator it must depend on the degree of the agreement of the septate waveguide with the end transitions at the frequency of hybrid mode with $V_\Phi = c$, descending with an increase in the reflections.

The virtually always matching transitions, which do not reflect in the fundamental frequency f_{01}, introduce large reflections (k.s.v.~5-6) at frequency r_{11}. Attempt to experimentally determine the effect of mismatch on the level of critical current was

undertaken in [9]. Where it was established on a short section of the waveguide that the level of the induced signal decreased three-fold with the matching of the waveguide output.

As indicated in [9], this result little which gives for the multisection accelerators with the permanent gradient.

We carried out the measurements of the dependence of the induced signal and critical current on the agreement of end transitions. It turned out that the amplitude of the induced by bundle signal in the waveguide without the sections/cuts varied approximately/exemplarily 2 times with a change of disagreeing/mismatching the input transition from SWR on the order of 1.3 to SWR, it is equal to infinity. However, a substantial change in critical current in this case it was not discovered.

Let us note one additional fact, which concerns the behavior of the coefficient of the cluster amplification of signal from the external oscillator at the different values of current and signal frequency. such dependences are given in Fig. 11. From the figure one can see that with the specific currents and at the frequencies the bundle can not only amplify the supplied to the system signals, but also weaken/attenuate them.

Conclusion/output.

1. Measurements conducted concerned case of single section of accelerator with permanent structure, i.e., case of regenerative instability. Therefore not all of the obtained conclusion/output can be valid for the case of cumulative or combined instability, i.e., in connection with multisection accelerator.

2. It is experimentally shown that constant values in time (of equilibrium) initial displacement and angle of entry of beam relative to axis/axle of periodic structure do not affect parameters of instability. These data contradict the given in [3] dependence of signal level, induced by bundle in one of the sections of accelerator on 2 GeV, obtained with the beam displacement with the aid of the

magnetic system of correction, established/installed in the
preceding/previous section. As yet there is no satisfactory
explanation to this fact and it is possible to only assume that in
expression (1), which describes the increase of the sizes/dimensions
of bundle during the advance of it along the accelerator, by x_0
should be understood variable component of origin coordinate, i.e.,
initial transverse modulation of the bundle of noise origin. In this
case the results of similar type experiments on the single-section
and multisection accelerators can not be single-valued.

3. Critical current in the first approximation, is inversely
proportional to quality of structure, which satisfactorily will agree
with calculations according to data [12].

4. Critical current in investigated interval of values of
focusing magnetic field linearly grows/rises with increase in field.
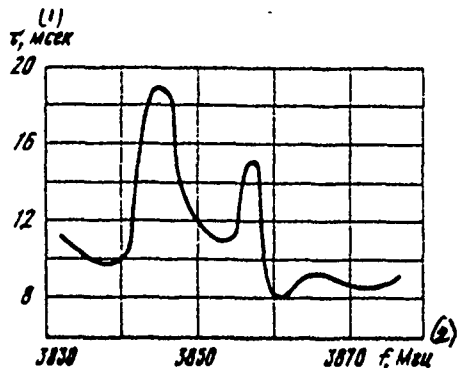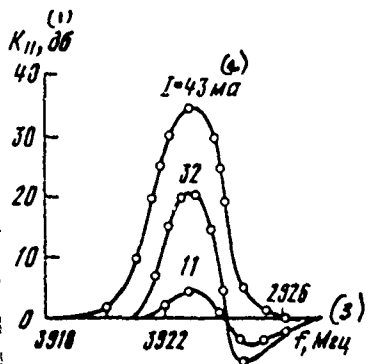
Fig. 10.   Fig. 11.

Fig. 10. Dependence of time of brace of interaction of signal of oscillator with "residual" medium in waveguide on oscillator frequency with current $I=520$ mA and field 400 e.

Key: (1). ms. (2). MHz.

Fig. 11. Dependences of coefficient of cluster amplification on wave EH_{11} on frequency. Parameter - beam current.

Key: (1). dB. (2). mA. (3). MHz.

Page 78.

REFERENCES

1. M. C. Growley - Milling. "Nature", 1961, 191,
    N 4787, 483.

2. V. A. Bishnyakov, A. I. Zykov, V. M. Grizhko and
    I. A. Grishayev, ZHTF, 1968, 38, Nr. 1, 133.

3. A. I. Zykov, I. A. Grishayev, V. A. Vishnyakov,
    N. I. Mocheshnikov, G. D. Kramskoy, ZHTF, 1968,
    Nr. 1, 129.

4. W. K. H. Panofsky, Report TU-66-27, LINAC, 1960.

5. Loew, IEEE Trans. on Nucl. Sci, 1967, NS-14, N 3, 529.

6. G. D. Kramskoy and others, ZHTF, 39, Nr.1, 2054
    (1969).

7. V. M. Levin, V. L. Smirnov, Author's certificate.
    Nr. 197786. Bulletin of Inventions and Trade Marks,
    Nr. 13, 1967.

8. T. R. Jarvis, G. Saxon, M. C. Growley-Milling, Proc.
    IEE, 112, N 9, 1795 (1965).

9. O. H. Altenmueller et al. SLAC-Pub-224, Los Alamos,
    1966.

10. G. V. Voskresenskiy, Yu. N. Serebryakov, Collection
    "Accelerators", Issue X, Atomizdat, 1968, p. 130.

11. W. K. Panofsky, M. Bander, Rev. Scient. Instrum.,
    39, N 3, 206 (1968).

12. V. I. Kurilko, A. P. Tolstoluzhskiy, Atomnaya
    Energiya, 1970, 28, Nr. 6

13. H. Hirakawa, Japan J. Appl. Phys, 1964, 3, N. 1, 27.

14. Yu. N. Serebryakov, Candidate Dissertation, Moscow,
    MIFI, 1969.

15. V. I. Kurilko, 1968, ZHTF, 38, Nr. 1, 118.

16. R. B. Neal, J. Appl. Phys., 1958, 29 N 7, 1019.

Page 79.

Session IX.

RADIO ELECTRONICS OF ACCELERATORS. Measuring systems of the parameters of beam.

112. Systems and methods of beam display on the accumulator/storage of FTI of AS UkSSR.

N. I. Mocheshnikov, L. V. Reprinetsv.

Physicotechnical Institute AS UkSSR).

The implementation of the program of studies on the dynamics of beam on the accumulator/storage requires the creation of the complex of diverse equipment for diagnostics of beam. On the accumulator/storage N-100 [1] is provided: a) the measurement of the parameters of the injected beam; b) characteristic measurement of stacked beam on its synchrotron radiation; c) the study of the

harmonic composition of stored current.

Fig. 1q. shows the schematic of injection measuring
equipment. Beam from the linear electron accelerator (LUE) passes two
rotary magnets (PM) and it falls into the working clearance of the
inflector, arranged/located in straight section. With the aid of the
magnetic-induction sensors D_1 and D_2 is measured envelope and the
coordinate of the current pulse of accelerator at the input in PM_1.
Sensors work in the aperiodic mode/conditions, their signals are
amplified by the wideband amplifiers (USh). the accuracy of the
measurement of angle water in PM_1 is $+-10^{-3}$ rad for the currents
10-100 mA in the impulse/momentum/pulse. With the aid of the
magnetic-induction sensor D_3 is made the measurement by the envelope
of current pulse after PM_1, a number of electrons or positrons in one
message, and also the measurement of energy with precision/accuracy
$+-1o/o$ with the aid of collimation of beam (K). Sensor works together
with the operational amplifier (UO), that makes it possible
considerably to weaken/attenuate the effect of instability on the
output signal. In the measurement of current the operational
amplifier provides the aperiodic mode/conditions of the work of
sensor, while in the measurement of charge - resonance [2].
Sensitivity of sensor in the measurement of current and charge of 50
mV/mA and $1.6 \cdot 10^{-8}$ V/particle respectively, operating speed - 40 ns.

With aid of the meter of the spectrum (IS) measurements are made
of the pulse energy characteristics of the injected beam with energy
resolution +-$2 \cdot 10^{-3}$. Sensor is movable ionization chamber, situated
in the focus of magnet PM_1. Collecting anode of the chamber/camera of
sectional, width of bands is 1 mm, the gap/interval between them of
0.2 mm. Signals from the separate bands through the delay unit (LZ)
are supplied to the oscillograph on screen of which the image of the
spectrum is obtained in the form or histogram.

. Parameters of beam at its injection into the ring are measured
by the system of two-dimensional ionizing chamber of sensors (ID_1,
ID_2, ID_3), established/installed directly before the inflector, after
it and through 1/2 revolutions of beam in the ring. They make it
possible to measure the magnitude of the charge, its distribution
over cross section and location of the center of gravity of the
injected beam. The aperture of each sensor comprises 60x40 mm²,
three-dimensional/space resolution 5 mm. With the aid of the relay
assembly (BR) they by choice can be connected to the system of the
electronic switches (EP_1, EP_2), which make it possible to obtain
charge distribution according to two coordinates for one injection
impulse/momentum/pulse on the screen of dual-trace oscillograph.

Fig. 1b shows the schematic of equipment for measuring the
parameters of stacked beam on its synchrotron radiation/emission.

Azimuthal particle distribution is measured with the aid of single-chamber image converter tube (EOP) whose scanning/sweep is conducted by sine voltage with synchronous frequency f_s. With the sizes/dimensions of cluster, small about to comparison with the orbit circumference, is utilized the horizontal sweep. Image on the screen EOP, corresponding to the azimuthal distribution of electrons in the cluster, in this case is analyzed by camera tube "dissector" (DIS_2) and is oscillogramed. Gauging signal is obtained in this case by scanning/sweeping the point-source image. With image sizes, compared with the period of scanning/sweep (for example, in the presence of the synchrotron resonance), in ZOP is utilized the circular sweep. With aid of the diagram of strobing (S) from the sequence of the videosignals of television camera (TK) it is separated/liberated the signal of one lines whose image simultaneously is extinguished on the screen of kinescope. In the measurements is selected the row, which coincides with the diameter of scanning/sweep EOP. For the reading of the amplitude of synchrotron oscillations the image is moved with the aid of phase converter (FV) on the scanning/sweep EOP so that its edge consecutively/serially they would be combined with the gated row.

Page 80.

The resolution in the measurements with the dissector composes value $\sim 10^{-10}$ of s and is limited to the final duration of the light pulse, emitted by exact cluster into the solid angle EOP, and also other next factors [3, 4]. At the sweep frequency of the dissector 50 Hz of the measurement of azimuthal extent it is possible to carry out in the range of energies 50-100 MeV for the accumulated currents >1 mA.

Recording the center-of-gravity location of cluster in the accumulator/storage, it is possible to measure a change in its synchronous phase in the presence of coherent losses. This is achieved by differentiation of signal from the dissector DIS_2 and by fixing the moment/torque or its passage through zero on the oscilloscope face. The accuracy of measurements composes value of $+-0.5^\circ$ for the currents >1 mA and is limited to instabilities in the sweep circuits EOP and HF generator.

For measuring particle distribution in the cross section of stacked beam is utilized the dissector DIS_1. It analyzes the light cross-sectional view of beam, which is created by the synchrotron radiation/emission. Resolution besides the factors of technical character is limited by the "diffuseness" of the light image of beam, which is caused by the properties of quite synchrotron radiation. For

the installation N-100 it is estimated by a value of ~0.1 mm during

the image transmission to the dissector with optical multiplicity 1ˣ.

The measurement of the coordinates of equilibrium orbit is made

by the interruption of beam by the introduced into vacuum chamber

probes (3, Fig. 1b). In all are 5 radial and 3 vertical measuring

points. Coordinates are counted off on the screen of electron-beam

afterglow tube. To its horizontally deflecting plates is supplied the

stress/voltage from the linear potentiometer (PL), mechanically

connected with the probe, while to those vertically deflecting -

signal from FEU, recording moment/torque interruption of beam. The

accuracy of measurements depends on vacuum and is equal to ~1 mm for

$P < 10^{-7}$ torus.

Fig. 1c   shows the schematic of equipment for studying the

harmonic composition of current in the accumulator/storage with aid

of resonance receivers, adjusted to the harmonics of the frequency of

revolution of cluster in the accumulator/storage.

The strength of accumulated current is measured with the aid of

a pick-up-electrode (PE) and the measuring superheterodyne receiver

(IP₂), adjusted to the second harmonic of frequency of revolution

≈104.5 MHz. Signal from it is detected by linear detector and is

recorded by indicators (I). The minimum measured current is equal to

50 μA and is limited to interference from HF generator. Entire
circuit was calibrated with the aid of the Rogowski loop, which
recorded signal with the discharge/break of stacked beam by
inflector. The precision/accuracy of absolute calibration composes
+-10o/o, if necessary is considered supplementary error due to a
change in the longitudinal sizes/dimensions of cluster.

For studying the processes of the self-excitation of the
longitudinal instability and angular damping is conducted recording
the frequency and amplitude-modulated signals, induced by cluster on
the resonator and a pick-up-electrode. Resonator (R) represents the
specially prepared passive resonator which permits rearrangement to
the second third and fourth of the harmonic of frequency of
revolution and has characteristics close to the characteristics of
ideal contour/outline. During the study of the processes of the
self-excitation of longitudinal coherent instability it was utilized
both for its excitation and recording the threshold of instability.
For this the frequency modulated signal, induced in it by beam, is
recorded by receiver IP_1 in width of band 100 kHz; the result of
frequency detection (Det_1) is amplified by the selective amplifier
(UI), tuned to a frequency of coherent phase of oscillations (15-35
kHz), in this case width of band of entire circuit comprises several
kHz, equipment makes it possible to carry out the measurements of
minimum threshold currents ~5 μA and amplitude of phase oscillations
~0.5°.
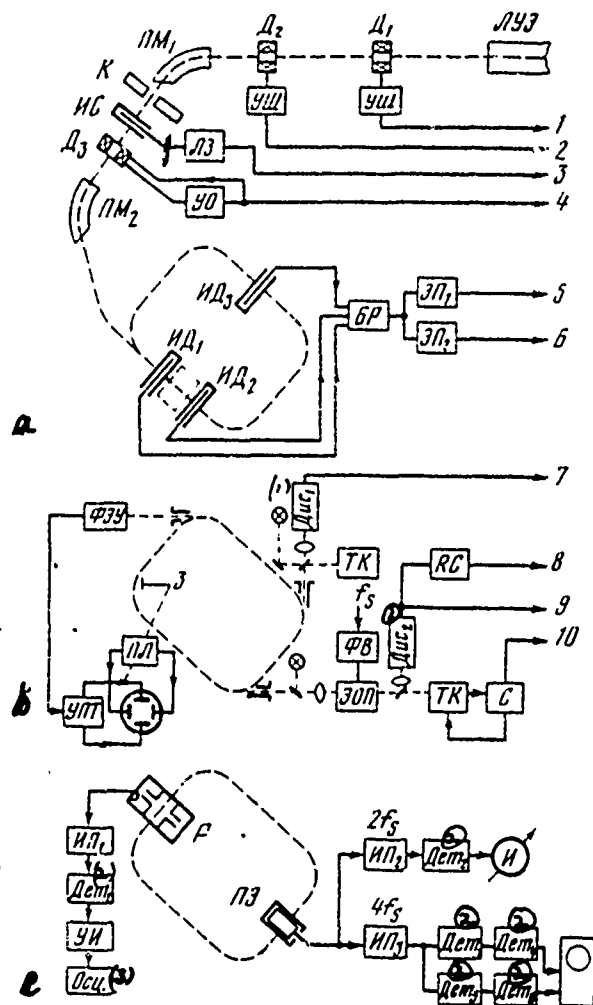
Fig. 1. Schematic of measuring equipment on the accumulator/storage.
a) apparatus for measuring the parameters of the injected beam.
Outputs of signals. 1, 2 - envelope and coordinate of the current
pulse of linear accelerator; 3 - energy spectrum; 4 - envelope of
current pulse after rotary magnet, number of electrons or positrons,
5, 6 - profile/airfoil and coordinates of the bundle, injected into

the ring; b) equipment for characteristic measurement of stacked beam
on the synchrotron radiation. The outputs of signals; 7 - particle
distribution in the stacked beam according to two coordinates; 8 -
synchronous phase; 9, 10 - azimuthal particle distribution in the
accumulator/storage; c) equipment for studying the harmonic
composition of the accumulated current.

Key: (1). Dis_2. (2). Det_2. (3). Oscillograph.

Page 81.

The study of the processes of fading coherent phase of
oscillations of large amplitude is conducted with the aid of of
wideband receiver IP_3, adjusted to the fourth harmonic of the
frequency of revolution. Width of its band is 1 Mhz, which makes it
possible to measure the amplitudes of phase oscillations to value of
~150°. Detectors Det_3 and Det_5 separate/liberate the form of the
frequency and amplitude modulation of signal from pick-up electrode,
and Det_4 and Det_6 - respectively their envelope.

Fig. 2, 3, 4 give some oscillograms of signals, which illustrate
the work of equipment.

Fig. 2. Charge distribution in the cross section of the injected beam. Oscillogram of signal from the sensor ID_2: upper ray/beam - distribution according to the horizontal, the lower ray/beam - on the vertical line; the step/pitch of histograms 5 mm.
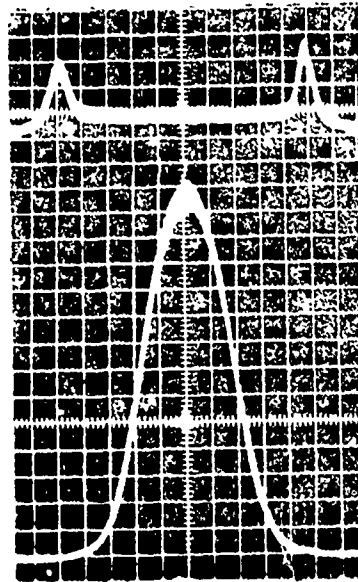
Fig. 3. Azimuthal distribution of particles in the accumulator/storage. Above - the oscillogram of gauging signal, the distance between the markers 3 ns; below - the oscillogram of signal from the dissector DIS_2.

DOC = 80069307   PAGE   336

Fig. 4. Displacement of the synchronous phase of cluster when in chamber/camera the accumulator/storage of passive resonator is present,. Oscillogram of signal from the detector DIS_2 after the differentiation: above - the accumulated current 4 mA, below - 1 mA, scale of 1° deg/div.

REFERENCES

1. Yu. N. Grigor'yev, et al, Atomnaya Energiya, 1967, 23, issue 6, 531.

2. N. I. Mocheshnikov, Proceedings of International Conference on accelerators.

3. Ye. K. Zavoyskiy, S. D. Fanchenko, DAN[Doklady Akadamii Nauk] SSSR, 1956, 108, 218.

4. O. D. Dmitriyevskiy, B. S. Neporent, B. A. Nikitin, UFN [Uspekhi Fizicheskikh Nauk, 1968, issue 3, 445.

Discussion.

V. A. Kochagurov. Sensors D_2 and D_3 do measure the boundaries of beam or the envelope of current pulse?

L. V. Reprintsev. Envelope of current pulse.

V. G. Davidovskiy. Usually photocathode sensitivity EOP is strongly heterogeneous in the surface. Did carry out you the calibration of this sensitivity during the investigation of charge distribution according to the cross section of beam?

L. V. Reprintsev. In the measurements it was utilized only the insignificant region of photoelectric cathode. The heterogeneity of sensitivity was checked by preliminary measurements.

Page 82.

113. Methods of measuring the parameters of beam.

V. Agoritsas, S. Battistik, K. D. Dzhnoson, G. Shnayder.

(CERN, Switzerland).   ∩ 1. Introduction.

According to the program of the European organization of nuclear research at present they will foresee themselves the work on the improvement of synchrophasotron, target of which is an increase in the intensity of beam and optimization of the operational conditions of synchrophasotron as injector into the rings with clashing beams. The need of conducting the large volume of calculations in the digital computer at present and in the future and also the need for the creation of effective control system up to that moment/torque when is intended to introduce into the action complex linear accelerator - injector-accelerator - rings with clashing beams, led to the reasonable decision to conduct the detailed investigation of the contemporary possibilities of diagnostics of beam and collection and storage of data with the aid of the digital computer.

In the report is made the attempt to present the contemporary

state of metrology in this region, and to also illuminate the

contemporary developments of equipment, intended for measuring the

parameters of external and internal beams of synchrophasotron. In

many respects this equipment is analogous to the technical equipment,

developed/processed at present for injector-accelerators and channels

of the transportation of beams. In the report are not examined the

monitors using targets, since their construction it changed

insignificantly from the moment/torque of issuing preceding/previous

reports [1, 2] and in many instances these monitors were not intended

for the direct measurement of the parameters of beam.

2. Characteristics of beam.

As a rule, during the development of measuring equipment for

control of the parameters of accelerators is necessary to have matter

concerning the beams of average/mean and high intensity; usually the

instantaneous density of flow ranges from 10^{11} to 10^{20} proton x cm^{-2}

x s^{-1} and the time-averaged density of flow - from 10^{10} to 10^{13}

proton x cm^{-2} x s^{-1}.

The flash durations of external ray/beam it comprises: 10 ns

(one cluster) - 2 μs (20 clusters) during the rapid beam deflection;

100 - 400 ms during the slow beam extraction. Equipment must measure

the parameters of beams with the time structure (internal grouped and

rapidly emitted beams) and beams which in the ideal case do not possess the time structure (internal grouped and slowly emitted beams). In the latter case there is very frequently undesirable time structure of beam, which is measured by equipment for the purpose of its elimination during the subsequent adjustment; as a result there is the possibility to determine the index of quality of beam [3]. It is necessary to also measure the position of the center of mass of proton beams, the sizes/dimensions of these beams, intensity and change of the parameters with time.

3. Sensors of beam.

For the latter several years appeared many new types of the sensors of the parameters of the beams, some of which are specially adapted for the work together with the digital computers. Some sensors were subsequently modified, while some non-current. Table 1 gives the enumeration of the available today types of the sensors of beam, used in the proton syncarctron of CERN, that corresponds to framework indicated above of present report. In the table are enumerated the essential features of each type sensor, and the more detailed description of these sensors is given below. The more full/totaler/more complete enumeration of the selected methods of the monitoring of the parameters of beams is given at the end of the present report. In the report are utilized the following reductions:

CODD - digital representation of the closed orbit;

IBS - scanning device/equipment for beam measurement;

SEC - chamber/camera of the secondary emission;

SEPD - detector of the position of the beam of slow
conclusion/output;

toposcope - sensor of the profile/airfoil of beam on the basis of the
use of the secondary emission from fitting strips;   ·

miniscanner - sensor of the profile/airfoil of beam, which uses the
small target, scanned through the beam.

4. Observations apropos of the methods of beam monitoring, enumerated
in the table.

    4.1. Current transformers [2, 4]. It is possible to name/call
three types of current transformers of the circulating beam. Passband
for each of these types is shown in the table. Slow transformer
provides the precision/accuracy of order 0.1o/o, the
precision/accuracy of intervening transformer composes 1o/o, the
precision/accuracy of rapid transformer ranges from 2 to 3o/o for the

middle of the frequency band. The utilized previously system of the
addition of the output signals of rapid and slow transformers is at
present demounted, since with this method are not utilized the
precision characteristics of slow transformer.

Current transformer in the rapidly emitted beam has circuit of
transmission, which is self-actuated from the current pulse with the
duration of 2 μs which serves for decreasing the effect of noise.

Page 83.

Some experiments carried out earlier with current transformers
in the slowly emitted beams made it possible to establish that due to
a small signal-to-noise ratio such transformers cannot be utilized as
the sensors of the intensity of beam [2]. Are later investigations in
which were applied the methods of statistical averaging, distance
encouraging results [5]. The authors continue to work on the
possibility of using the mentioned above transformers for purposes of
the check of the absolute intensity of the slowly emitted beams.

4.2. Electron emission from targets or plates [6]. This simple
and convenient method of the check of the intensity of external beams
is in practice extruded/excluded by more expensive, but by the more
stable on precision/accuracy and reproducibility method of intensity

measurements with the use of a chamber/camera of secondary emission
[7]. The emission of charge still is utilized for the sensors with
the targets in intensity measurements of the rapidly emitted beams.
In the development of investigations on by the calibration methods of
the chamber/camera of secondary emission recently were carried out
the experiments, in which was accomplished/realized the crossed
calibration of the chamber/camera of the secondary emission with aid
of current transformer in the rapidly emitted beam and the activation
of aluminum foil [8]. Between the measured absolute values of the
intensity of beam still are observed the differences from 5 to 10o/o.
The utilized now in CERN procedure is reduced to use the
chamber/camera of the secondary emission, calibrated with the aid of
current transformer in the rapidly emitted beam, as the standard of
intensity in the measurements into slowly derived beam.

4.3. Electrostatic measuring sensors. Compact electrostatic
measuring sensors [9], establishment in 40 straight sections of
synchrotron, are at present united into one system which was called
the digital indicator or the closed orbit of beam (CODD). This system
[10] measures the closed orbit, tracking the trajectory of one
cluster around the synchrotron and furthermore it makes it possible
to observe coherent betatron oscillations.

(1) Параметр пучка	(2) Метод измерения		
	(3) Циркулирующий пучок	(4) Пучок при быстром выводе	(5) Пучок при медленном выводе
(6) Интенсивность пучка	(7) Трансформатор тока (10) быстрый, 100 кгц—100 мгц (11) (12) (13) средний, 0,3 гц—3 мгц (14) (15) медленный, 10^{-4} гц—10 кгц (16) (19)	(8) Трансформатор тока Фронт — 5 нсек (16) SEC, откалиброванная с помощью трансформатора тока	(9) SEC, откалиброванная в пучке быстрого вывода или при помощи активации фольги
	(17) электростатические электроды (будут отсоединены)	(18) Активация фольги	(14) трансформатор тока (20) Электронная эмиссия из мишеней или пластин (21) Активация фольги
(22) Положение центра пучка	(23) Система CODD с электростатическими датчиками (26) Электромагнитные датчики (начаты испытания)	(24) Электростатические электроды (пока еще не в работе) (27) Электромагнитный датчик (предложен)	(25) SEPD, использующий вторичную эмиссию и/или ионизацию газа
(28) Положение пучка и размеры	(29) Специальные мишени дают размеры пучка только на "плато" магнитного поля. (31) IBS — измерение параметров пучка в течение всего цикла.	(30) Топоскопы (32) Минискэннер на входе в канал эжекции (34) Флюоресцентные экраны	(6) Топоскопы (33) Минискэннер на входе в канал эжекции (35) Флюоресцентные экраны IBS —сканирование при 50 гц
(36) Азимутальные параметры	(37) Широкополосные электростатические датчики с фронтом 400 псек (39) Электромагнитный датчик с фронтом 1 нсек		(38) Мишенные датчики дают временную структуру (40) Рубиновый сцинтиллятор

Key: (1). Parameter of beam. (2). Method of measurement. (3).
Circulating beam. (4). Beam during rapid conclusion/output. (5). Beam
during slow conclusion/output. (6). Intensity of beam. (7). Current

transformer. (8). Current transformer front - 5 ns. (9). SEC, calibrated in beam of rapid conclusion/output or with the aid of activation of foil. (10). rapid. (11). kHz. (12). MHz. (13). average/mean. (14). Hz. (15). slow. (16). SEC, calibrated with the aid of current transformer. (17). electrostatic electrodes (they will be disconnected). (18). Activation of foil. (19). current transformer. (20). Electron emission from targets or plates. (21). Activation of foil. (22). Position of center of beam. (23). System CODD with electrostatic pickups. (24). Electrostatic electrodes (thus far yet off-duty). (25). SEPD, that uses secondary emission and/or ionization of gas. (26). Electromagnetic sensors (are initiated tests). (27). Electromagnetic sensor (it is proposed). (28). Position of beam and sizes/dimensions. (29). Special targets give sizes/dimensions of beam only in "plateau" of magnetic field. (30). Toposcopes. (31). IBS - measurement of parameters of beam during entire cycle. (32). Miniscanner at duct inlet of ejection. (33). Miniscanner at duct inlet of ejection. (34). Fluorescent screens. (35). Fluorescent screens IBS - scanning with 50 Hz. (36). Azimuthal parameters. (37). Broadband electrostatic pickups with front 400 ps. (38). Target sensors give time structure. (39). Electromagnetic sensor with front 1 ns. (40). Ruby oscillator.

Page 84.

Rapid measurements cr frequency of betatron on small energy levels [11] are carried out via the comparison of the frequency spectrum of the output signal of electrostatic pickup before and after the excitation of betatron oscillations with the aid of special kickers. This principle cr measurements at present applies to higher level of energy.

Was recently established/installed new type broadband electrostatic measuring sensor [12]. Resonance oscillations, characteristic to old system, were removed due to a change in the vacuum chamber design. New measuring sensor is based on the use of an old structure of electrodes, it has capacitive coupling with the very good cable and in the range of low frequencies for expanding the passband is utilized cathode rollower. The measured bandwidth of this sensor is 120- kgq - 880 MHz.

The creation of electrostatic pickups for the monitoring of the parameters of the rapidly emitted beams is complicated technical problem, since the normal vacuum of external beam composes approximately 10^{-1} torus, and at this pressure due to the phenomenon of the ionization of gas usual electrostatic pickups become unsuitable. Electrostatic pickups were utilized at atmospheric pressure [13]; however, this decision hardly was more convenient for the majority of external beams. Was expressed opinion relative to

promise of the use of electromagnetic sensors; however, such sensors are not thus far yet developed.

4.4. Fluorescent screens. Recently for measuring the parameters of the slowly emitted beam of synchrophasotron was used experimental sample/specimen of resistant to the radiation scintillator with oxide of aluminum, activated by chromium. This scintillator is developed by R. J. Allison and colleagues from the institute of Berkeley [14]. The authors consider promising the use of this material in future for the monitoring of the parameters of the beam of high intensity, since its sensitivity proved to be sufficiently high for the majority of practical tasks. Was also tested the special television indicator in which to y - coordinate of raster x-y was added scintillating indicating light. Thus is realized exploded view [15], in which are more clearly visible the nonlinearity, inherent in television system.

4.5. Special targets [16] and miniscanner [17]. The sizes/dimensions of beam in the vertical and radial planes of synchrotron are measured on "areas" of magnetic cycle with different energies by the installation of forked target on the path of the propagation of beam. After the thorough control of target is made the measurement of current in the circulating beam before and after the depression of target, which gives the possibility to determine the current strength in the beam inside, also, out of the fork. Being

assigned by any concrete/specific/actual law of density distribution
of protons, for example by Gaussian, it is possible then to calculate
the width of beam. To a certain degree is analogous to this method
the method of measurement of the parameters of beam with the use of a
target with the variable distance between the teeth. In this case
teeth are installed separately on two targets, arranged/located in
one housing. By changing the distance between the teeth and by
recording the strength of circulating current before and after
alignment of target, it is possible to determine the sizes/dimensions
of beam, moreover in this case there is no need for accepting any
hypotheses about the character of the distribution of protons.

Miniscanner is thin foil target. This target is utilized for the
scanning of beam over its section at the entrance into the septum of
the channel of beam extraction, and also on the external channels.
Electronic emission from the foil is utilized for control of the flow
of the protons, passing through foil. In order to minimize the
effects of auto-polarization, the ionization of gas and idle magnetic
and electric fields, foil is surrounded by the thin copper
polarization screen. As insulation/isolation between the foil and the
screen are utilized the strips of oxide of aluminum,
deposited/postponed chemically. The use/application of this screen
leads to certain decrease of the three-dimensional/space resolution;
however, experiment shows that this is the necessary measure,

especially in the case of rough vacuum (is less 10^{-6} torus).

4.6. Toposcopes [19]. These devices/equipment, which are actually the bands of foil with the secondary emission, scanned by the high speed analog multiplexer or the digital quantizing diagram together with the multiplexer, find ever increasing use for the control of external beams. In the very near future it is proposed to utilize toposcopes for the measurements of the emittance of the slowly emitted beams. The three-dimensional/space resolution is at present limited to several millimeters; however, for its increase it is necessary to only modify mechanical design.

4.7. Electromagnetic sensors of beam. Were up to now spent only insignificant efforts/forces for introducing the electromagnetic sensors of beam. By arrangement with the scientists, who operate German electronic synchrotron, device/equipment of such type it passes tests on synchrotron [20], while prototype of electromagnetic measuring sensor is developed by Mank [21]. In this sample/specimen is utilized the transformer coupling between the walls of vacuum chamber and the high-quality cable. Signal levels are sufficiently low (between 10 mV and 0.9 V in the injector-accelerator with 2.5×10^{12} protons, which circulate in each ring); however, it was possible to ensure passband from 100 kHz to 400 MHz and more. Was very recently accepted decision continue further work in this

direction for the purpose of the use of electromagnetic sensors for measurements in the injector-accelerator of synchrotron.

5. Use of digital computer for collection of measurable data.

For collection and data processing increasingly more widely is utilized the controlling digital computer of model IBM of 1800.

Page 35.

As the example below are enumerated the operations/processes for executing which is utilized the digital computer: data collection from current transformers in the beam, numerical indication of the closed orbit of beam, determination of the effectiveness of beam extraction on the basis measurements of the intensity of beam with the aid of the sensors, check and data collection from miniscanner.

The first of the enumerated uses/applications is most effective, especially when the character of work requires the periodic measurements of the current strength in the beam at different moments of time during the operating cycle. The program of the analysis of capture mode makes it possible to investigate the capture efficiency of particles immediately after injection; with the high energy the same system of data collection is utilized for determining of the

dimensions of beam according to the results of the measurements, obtained with the aid of the forked targets about which it went speech in section 4.5. In the latter case the final part of the calculations is conducted not during the measurements.

The position of miniscanner is checked with the aid of the digital computer, and information about the density of the flow of protons is started in the form of feedback signal, so that, utilizing special accessory equipment, it is possible to construct the curves of the distribution of intensity over beam section. Miniscanner of the described type at present is utilized for measurement of the emittance of slowly emitted beams [22].

6. Electronics for the sensors of beam.

This question is located out of the basic content of report. However, we will point out basic direction of the developments, which have as a goal to derive active elements/cells from the devices/equipment of the sensors of beam, which are located near vacuum chamber/camera. This is connected with an overall increase in the radiation danger of proton synchrotron. An example of this elimination of active elements/cells are the new methods of the transmission of signals, proposed by G. Shnayder [23] and S. Battisti [24]. In both propositions are removed the cathode followers which

recently were arranged/located near vacuum chamber.

In the first system is utilized coaxial cable for
connection/communication with electrostatic pickups. Due to the use
of matching systems of filtration it is possible to ensure
sufficiently wide passband. In the second system there is a
transformer coupling with the preamplifiers, arranged/located in
several meters from vacuum chamber of synchrotron.

7. The intercalibration of current transformers.

7.1. Effects being investigated. In the process of these
investigations were used two current transformers of the circulating
beam, established/installed in different straight sections of
synchrotron. The target of investigations consisted of confirming of
the expected high accuracy of the measurement of the absolute values
of current in the beam. This problem was solved via the comparison of
readings of two transformers for the varied conditions for the work
of synchrotron and in different parameters of beam.

Was investigated the effect of the following parameters of beam
[25]: a) the radial position of beam in vacuum chamber; b) the time
structure of the circulating beam; c) the impulse/momentum/pulse of
protons; d) the loss of protons in the region of the location of

transformer.

7.2. Results. At present the precision/accuracy of the
calibration of transformer composes 1o/o. In the process of tests was
conducted thorough intercalibration of transformers under the
following conditions: a) a change in the average/mean radial position
of beam on 40 mm; b) transition from the bunched beam to that
grouped; c) a change in the impulse/momentum/pulse from 6 to 24
GeV/s; d) an increase of the losses of intensity in the circulating
beam to 50o/o during 30 ms on internal target, located at a distance
of 50 cm before one of the transformers.

Thus, it was possible to establish that the precision/accuracy
of calibration lies/rests within the limits of one percent. Further
checking consisted of the comparison of readings of two
structurally/constructurally different transformers - current
transformer of the circulating beam and current transformer for the
channel of rapid conclusion/output. These measurements were carried
out during the rapid conclusion/output with the very low losses.
Results coincided with the precision/accuracy better than 1o/o (Fig.
1).
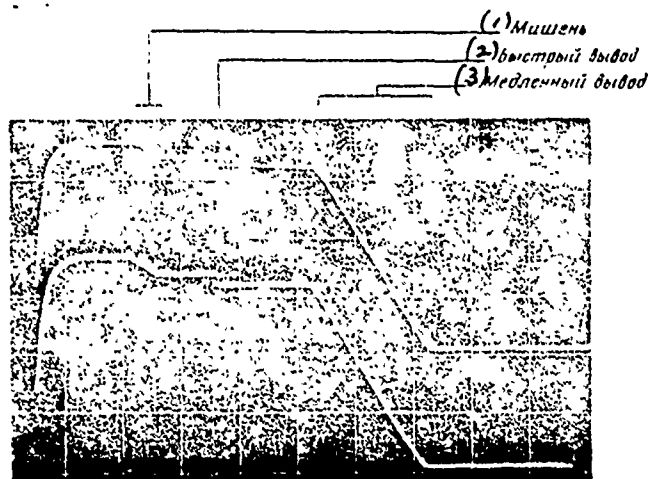
Fig. 1. Photograph of signals from the outputs of current transformers, mixed in straight sections No No 42 and 72, during entire cycle of accelerator. Both signals coincide with the accuracy of 1o/o; the scale: x axis - 200 ms/div; axis/axle y (channels 1 and 2) - 2 V/div.

Key: (1). Target. (2). Rapid conclusion/output. (3). Slow conclusion/output.

8. Detector of the position of the beam of slow conclusion/output (SEPD) [26].

8.1. Operating principle. According to the operating principle this detector is analogous to the detector, developed by Hornstrom for the accelerator in Arjonne [27]. Proton beam ionizes residual gas

along trajectory; in those places where beam of protons passes

through thin screens within vacuum chamber, it frees electrons due to

the secondary emission.

The electron stream, caused by both factors, is amplified due to

the reignition and is derived/concluded with the aid of the electric

field to cut off along the line differential electrodes (Fig. 2).

Page 86.

Amplification factor can be regulated due to a change in the

stress/voltage of the electric intensity and pressure in the gas.

3.2. Technical characteristics: range of measurements +-50 mm;

resolution 0.1 mm; range of intensity of beam from 10^{11} to 10^{13}

protons per pulse; passband from 0.001 Hz to 1 kHz and and higher:

no-flow length of beam 300 mm.

8.3. Construction/design. a) detector. Measuring and

high-voltage electrodes are shown in Fig. 3. Beam falls into the

sensor to the left.

Measuring electrodes are arranged/located symmetrically relative

to beam so, that did not appear mixing of zero. voltage on the

high-voltage electrode can be led to the value of 25 kV.

b) The description of the possibilities of sensor. Fig. 4 depicts completely the measuring system: in the right angle the detector, established/installed on the mounting base, from the left side is shown the control panel and above it is depicted high-voltage power supply. The preamplifier (it is shown in the center) is connected with the detector with the aid of the differential cable with a length of 5 m. The differential and total signals, which enter from the output of preamplifier, are converted analog type by divider into the signal of position. The signals of intensity and position of beam enter the display unit in the analog form. Further these signals can be measured and be reproduced in the digital form at any moment of operating cycle.

The calibration of detector is accomplished/realized between two consecutive cycles with the aid of the special test signal. Adjustment and calibration of preamplifier can be accomplished/realized remote/distance by means.

The automatic control of leakage with the aid of the system of servostabilization in the detector makes it possible to remotely/distance support the operating pressures of order 10^{-3} - 760 torr.

8.4. Results. Fig. 5 shows the signals of intensity and position (upper curve) for the beam of slow conclusion/output. Intended badly/poorly controlled automatic beam spill to the target was the reason for modulation of the signal of intensity at the end. The signal of position which do not affect modulations of the signal of intensity, makes it possible to make the conclusion that the divider functioned exactly.
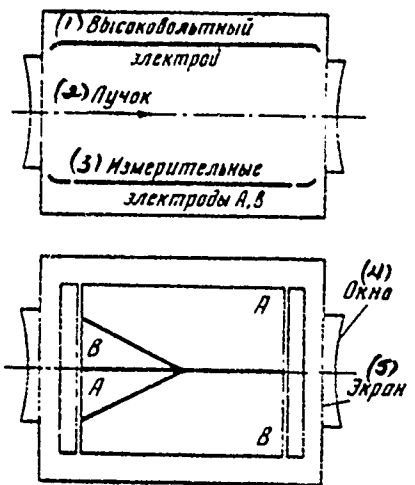
Fig. 2. Location of electrodes into SEPD.

Key: (1). High-voltage. (2). Beam. (3). Measuring electrodes. (4). Window. (5). Screen.
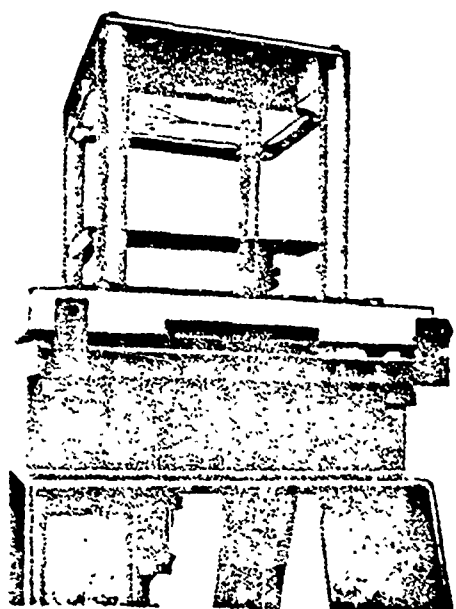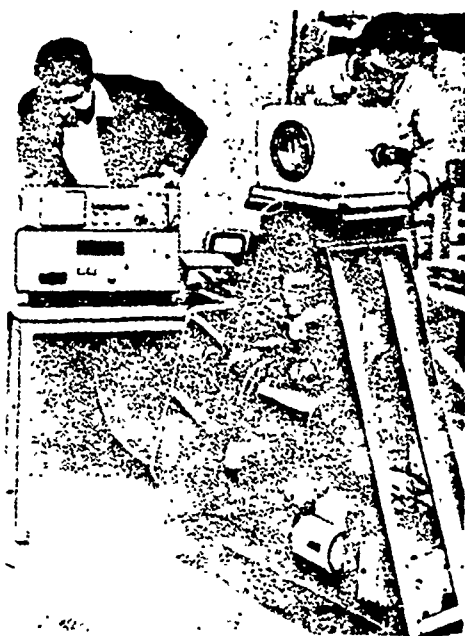
Fig. 3.   Fig. 4.

Fig. 3. View of high-voltage and measuring electrodes SEPD.

Fig. 4. General view of detector of position of beam of slow
conclusion/output (SEPD).

Page 87.

Fig. 6 gives results for spill on the target of signal in depth
of modulation 100o/o. At the end of each cluster is observed certain
displacement of the signal of position. Calibration coefficient was
equal to 1 V/cm beam displacement.

The resolution of recording the position of beam with the interference effect and pulsations was 0.1 mm (signal of intensity lay/rested in the range 10-1000/o of the peak signal for divider).

9. Ionizing device/equipment for scanning of beam (IBS).

IBS relates to those not destroying beam to the sensors which are intended for measuring the projection of density distribution of protons in external or internal beams of synchrotron. On these projections can be established/installed the sizes/dimensions of beam and is obtained information relative to distribution of density of protons.

9.1. Operating principle. The principle of operation IBS is in sufficient detail described in the internal reports of CERN [28, 29] and in the works of American national conference of 1969 on the particle accelerators [30].

In short, the principle of operation IBS consists of the measurement of the signal, proportional to a number of electrons, freed/released with the ionization by beam of the protons of residual gas in vacuum chamber. For steering of electrons along the cycloidal

trajectory of a small radius in the electrical equipotential planes

are utilized mutually perpendicular electrical and magnetic fields.

These equipotential surfaces in operating region of the pass·ge of

proton beam are uniform and parallel to the direction of beam. Under

these conditions spatial distribution of the electrons, which move

along equipotential surfaces of electric field, being the orthogonal

projection of density distribution of protons in the beam. Fig. 7

will help to better clarify this process.

One additional special feature/peculiarity IBS lies in the fact

that electron stream, emitted by proton beam, it is measured with aid

one detector with the high three-dimensional/space resolution and the

characteristic time of the order of one microsecond. This

mode/conditions of scanning is reached because the detector is under

the potential of the earth, while to the pair of electrodes, which

generates the basic electric field IBS, simultaneously are supplied

the symmetrical triangular impulses/momenta/pulses of high voltage.

Equipotential surface with the zero potential which under normal

conditions passes through the center of the scanning

device/equipment, during the supplying of the signal of triangular

form will be mixed to the right and to the left in that region where

is passed proton beam. Since the detector can recover only those

electrons which move along or near equipotential surface with the

zero potential, to it will alternately supply the electrons from each

part of the beam, through which passes equipotential surface with the zero potential. Fig. 8 shows the series of diagrams IBS and configuration of electric field in the process of one cycle of the scanning of beam.
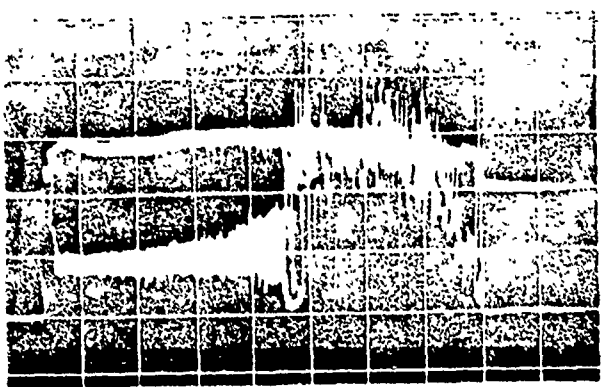
Fig. 5. Photographs of signals from SEPD during the slow beam extraction. Upper curve - signal or position (Δ/Σ)-5 V/div.; lower - intensity (total signal, Σ), 2 V/div.; x-axis - one large division - 50 m/s.
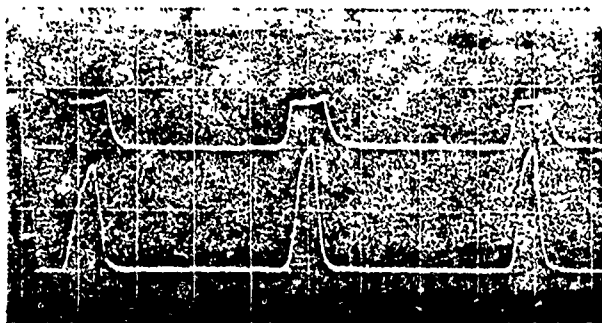
Fig. 6. Photographs of signals from SEPD for the conclusion/output with 100o/o modulation of intensity. Upper curve - Δ/Σ, 5 V/div.; lower curve Σ, 5 of V/div.; x-axis - one large division - 50 m/s.
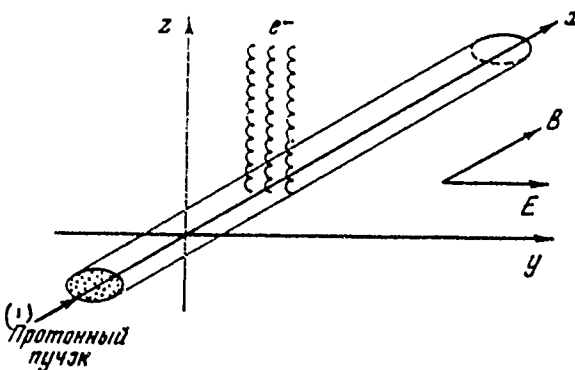
Fig. 7. Extraction of the electrons of their of that ioni ed by the proton beam of gas with the use of the lattice-type electrical and magnetic fields. The drift velocity of electrons $V=E/B$, a radius of cycloid $R=[y_0^2+(\dot{z}_0 E/B)^2]^{1/2}(\frac{e}{m}B)^{-1}$; e - the electron charge, t - mass of electron; E, B - intensity/strength of electrical and magnetic fields; y_0 - component of the initial velocity of electron in the direction of electric field; $\dot{z}_0$ - the same, but in the direction, perpendicular to electrical and magnetic field.

Page 88.

The basic nodes/units of detector are two closely spaced electrodes, that are located under constant voltage +30 V and -30 into relatively the earth/ground. These electrodes serve for generation of electric field which guides electrons into the neck/throat of detector and forces them to move over the cycloid to the first dynode of electron multiplier. These electrodes fulfill the

functions of collimator for those electrons with the large energy, which move over the cycloid of a large radius, and also for those electrons which move along equipotential surfaces with the potential beyond the limits +-30 V. The distinctive special feature/peculiarity IBS lies in the fact that the three-dimensional/space resolution, i.e., the width of the zone of beam, which falls in the field of the scanning of detector, depends on the potential difference of +-30 V; within certain limits this difference can be varied very simply due to a change of voltages on the working electrodes of detector.

9.2. Uses/applications. At present are developed/processed and are applied in practice several modification IBS: a) vertical or radial scanning of the circulating beam of the synchrotron (it is operated), range of scanning from 100 Hz to 10 kHz, pressure from 3×10^{-7} to 5×10^{-6} Torr ; the vertical or radial scanning of the circulating beam of synchrotron (for the investigations), the range of scanning from 10 Hz to 500 kHz, pressure from 3×10^{-7} to 5×10^{-6} torus; c) the beam of slow conclusion/output, the range of scanning 50 Hz, pressure by 10^{-1} Torr; d) the scanning device/equipment which will be utilized as the detector of scatter of particles on the energy in 50 MeV spectrometer, the range of scanning 400 kHz, pressure 10^{-5} torus; e) four pairs in the injector-accelerator of synchrophasotron, the scanning of each of four rings in the radial and vertical planes. Range of scanning from 100 Hz to 300 kHz,

pressure from $3 \cdot 10^{-7}$ to $3 \cdot 10^{-6}$ torus.

The length of the phase of trajectory of the proton beam, on
which occurs the extraction of electrons, usually is from 3 to 10 cm.
The three-dimensional/space resolution can be higher than 1 mm.
Frequency range of scanning can reach 500 kHz, although it must be
noted that modulation of intensity due to the time structure of beam
limits the use of high frequencies of the scanning by in practice
those cases when beam has the grouped structure, for example
immediately after injection into the ring of synchrotron. The
operating range of pressure depending on requirements can be from
$3 \cdot 10^{-7}$ to $5 \cdot 10^{-6}$ torus.

9.3. Calibration IBS in circulating beam of synchrotron was
conducted with the aid of measurement of sizes/dimensions of beam
with use of forked targets (section 4.5). The comparison of results
can be carried out only for the beams with the
impulses/momenta/pulses from 8 to 20 GeV/s. In this range for the
beams by size/dimension from 3 to 15 mm (95o/o of the maximum
altitude) the results of calibration coincided with an accuracy to
several tenths of millimeter [31].

Important condition of correct determination of the
sizes/dimensions of beam on the signals of the scanning

device/equipment - knowledge or the characteristics of the
instrument/tool expansion of the cross sections of beam due to the
final three-dimensional/space resolution of instrument. These
characteristics it is very difficult to calculate; however, they were
determined experimentally by the high-precision measurement of the
cross sections of the collimated circulating beam in the synchrotron.
These measurements were conducted for several different adjustments
of the three-dimensional/space resolution (voltage on the working
electrodes of detector) of the scanning device/equipment (Fig. 9).
The dependence of the sizes/dimensions of beam on the electrode
voltage proves to be rectilinear, as shown in Fig. 10. The
extrapolation of the linear dependence indicated to the zero voltage
allows to determine the actual sizes of beam. Furthermore on the
inclination/slope of straight line it is possible to correct
experimental results taking into account the expansion of beam over
the section for those cases when is fixed/recorded only the
adjustment of the three-dimensional/space resolution.
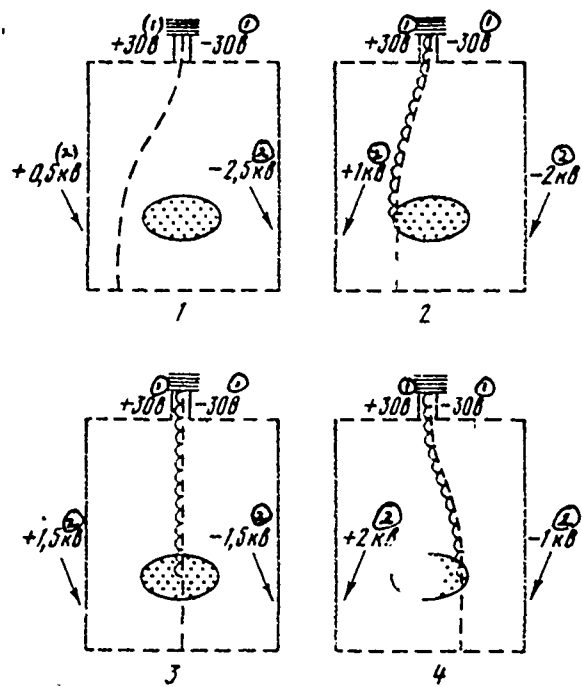
Fig. 3. Different configurations of electric field in IBS during the scanning.

Key: (1). V. (2). kV.
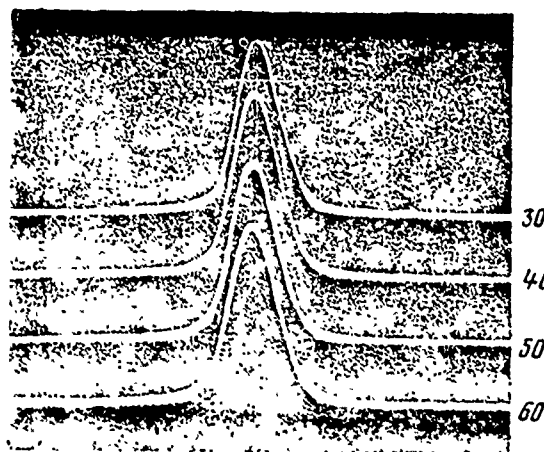
Fig. 9. Obtained with the aid of IBS elevation profile at the different values of instrument/toci broadening (voltage on the detector electrodes).

Page 89.

9.4. Results. For lack of space in this article there is no possibility to give the detailed description of the results, obtained with the aid of (IBS).

In the given figures (Fig. 11-19) are clarified the basic special features/peculiarities of beam. Raster images are always scanned in the direction on top in the direction downward. The pilot signal of the scanning voltage, taken/removed directly with IBS, was utilized as the horizontally deflecting voltage of raster image, which thereby could be calibrated in accordance with the position of beam within the meter.
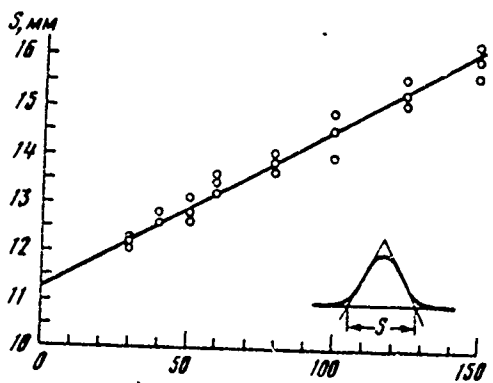
Fig. 10 dependence of the sizes/dimensions of beam on the voltage on the detector electrodes IBS.
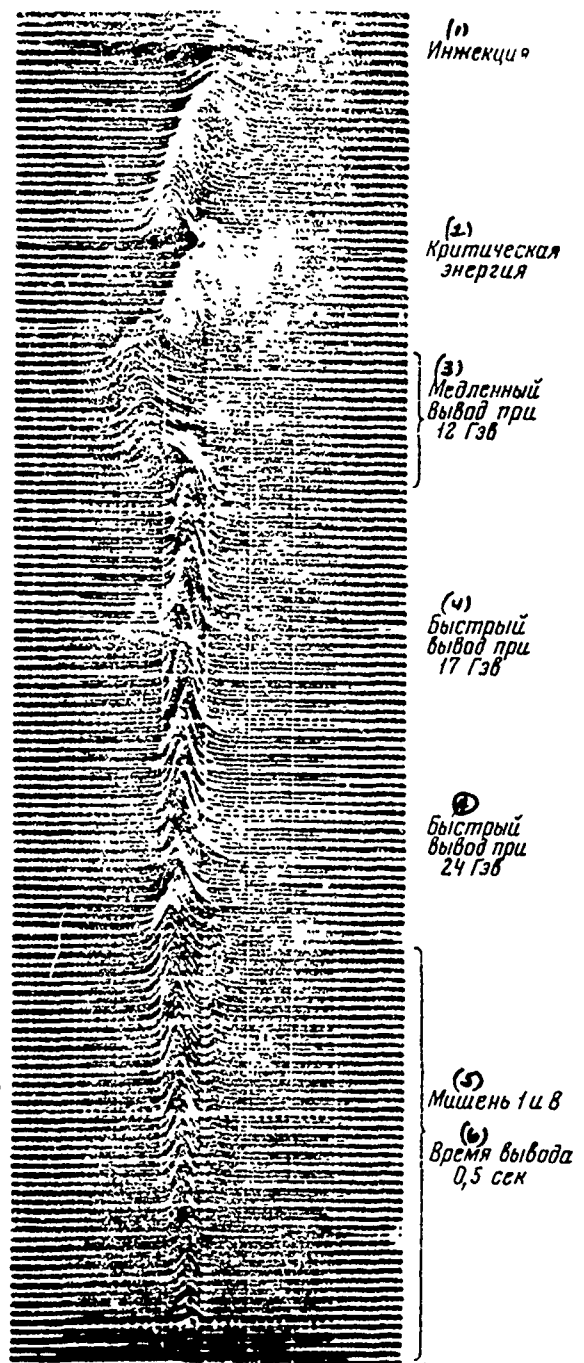
Fig. 11. Obtained with the aid of IBS profile/airfoil of beam for complete cycle of acceleration. June 1970. Vertical scale: One large

division - 50 ms; the horizontal scale: one large division - 15 mm.

Key: (1). Injection. (2). Critical energy. (3). Slow
conclusion/output with 12 GeV. (4). Rapid conclusion/output with 17
GeV. (5). Target 1 and 8. (6). Time of conclusion/output 0.5 s.
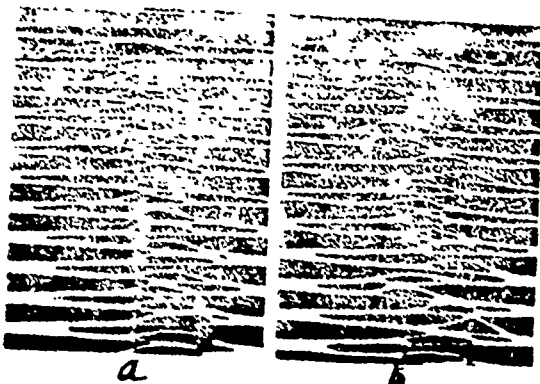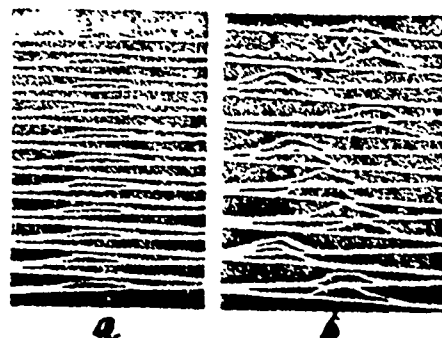
Fig. 12.   Fig. 13.

Fig. 12. Rapid scanning   (3.3 μs) of profile/airfoil with the aid
of IBS in radial plane (right after injection). Accelerating voltage
is not switched off. a) beam is displaced to inside chamber wall; b)
the same, but in the presence of coherent oscillations. Horizontal
scale; one large division or ≈3.3 cm.

Fig. 13. Rapid (3.3 μs) scanning of elevation profile of beam with
switched-off accelerating voltage. a) protons filled only the half
the perimeter of accelerator; therefore each second scanning ray/beam
passes along the horizontal axis; b) scanning is
accomplished/realized with the completely filled accelerator, but are
present coherent betatron oscillations. Horizontal scale; one large
division - 2 cm.

Page 90.
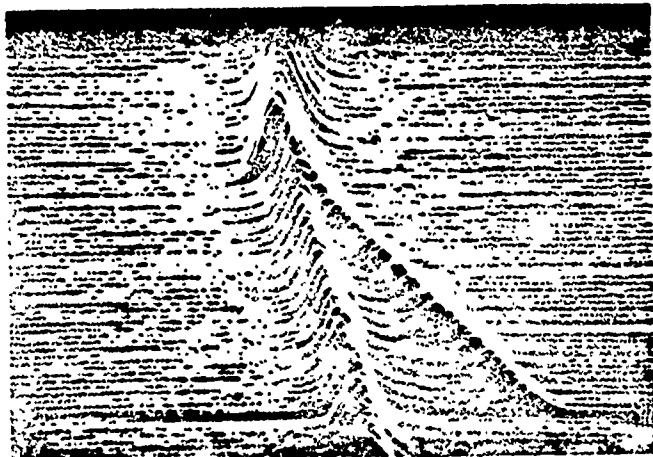
Fig. 14.

Fig. 15.

Fig. 14. Elevation profile of beam of large energy (it is obtained with the aid of IBS), circulating in proton synchrotron in "plateau" of magnetic cycle. In the lower three curves is shown the beam after its collimation with the aid of the fork target (distance between the teeth - 3.5 mm). Instrument/tool broadening - 2.2 mm. Horizontal scale: one large division of 5.0 mm.

Fig. 15. Dual beam in radial plane, which is formed during debunching (energy 27 GeV) in "plateau" of magnetic cycle. Vertical scale: one large division - 100 ms; the horizontal scale: one large division - 15 mm.
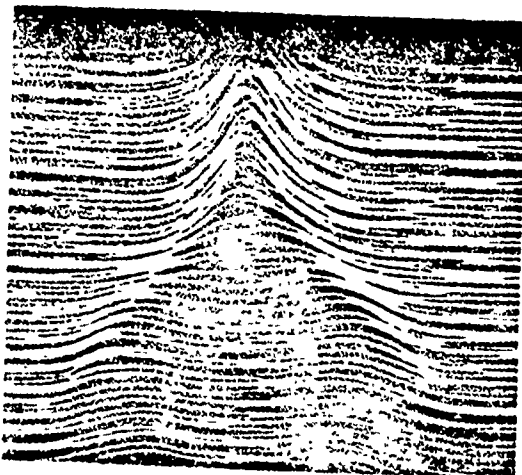
Fig. 16.

Fig. 17.

Fig. 16. Dual beam in vertical plane, formed due to instability, which is observed on energy 10 GeV. This instability normally is eliminated; photogrph is obtained in the process of executing the study program of accelerator.

Vertical scale; one large division - 8 ms the horizontal scale; one large division - 10 mm.

Fig. 17. Obtained with the aid of IBS elevation profile of beam vo.vrem4 and right after injection. Modulation of intensity is connected with the formation of separate clusters. Time of one scanning - 50 µs. The horizontal scale: the sizes/dimensions of photograph correspond to approximately/exemplarily 8 cm of the aperture of synchrotron.

Key: (1). Injection.
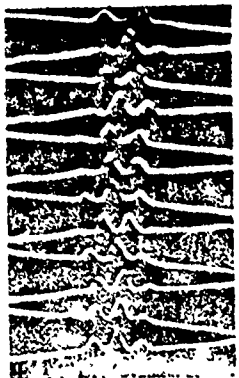
Fig. 18.
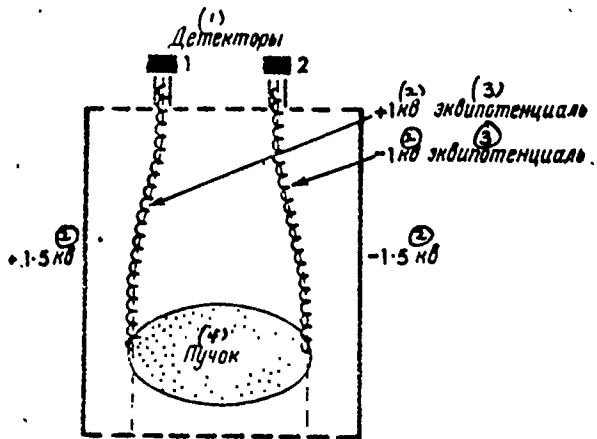
Fig. 19.

Fig. 18. This photograph depicts just as Fig. 17, elevation profile of beam in time after injection, but with very rapid scanning.

The sizes/dimensions of photograph in the horizontal direction correspond to 8 cm of the aperture of synchrotron.

Fig. 19. System IBS proposed with two collectors/receptacles for simultaneous detection of electrons from two edges of beam. With the aid of this device/equipment, studying phase relationships/ratios at the outputs of two detectors, it is possible to distinguish the coherent and incoherent oscillations envelope of particles.

Key: (1). Detectors. (2). kV. (3). equipotential.

Page 91.

Present article is partially survey work; therefore we want to note works whose those, names they are mentioned in the bibliography. For the participation in the development of devices described in the second part of the report, we are grateful to A. Barlet, and also to colleagues of the vacuum section of the division of proton synchrotron for the permanent aid in the development and testing SEPD and IBS, we are also grateful to V. Sent Albert for the the technical assistance and to the operators of the hall of the control of proton synchrotron for the support. G. Dems and T. Dorenbos proposed the series/row of improvements IBS for proton synchrotron and booster of proton synchrotron. L. Ternaal' participated partially in the work, described in section 9.

Finally, we want to thank Jean Eddison for her aid in the preparation of this article.

REFERENCES

1. V. Agoritsas, S. Battisti, C.Bovet, D.Dekkers, L. Henny, L.Hoffmann, K.H.Reich, W.Riezler, J.Robert, M.van Rooy. Proceedings of U.S.National Particle Accelerator Conference. Nuclear Sci., 1967, 14, 1155–1159.
2. V.Agoritsas, S.Battisti, C.D.Johnson. Proc. Daresbury Sympos. on Beam Intensity Measurement, 1968, 58–67.
3. D.Blcess, D.Dekkers, G.Shering. CERN Internal. Report, MPS/SR, 69–9, 1969.
4. S. Battisti. CERN Internal. Report, MPS/CO, 69–15, 1969.
5. G.Shering.Unpublished Work.
6. K.Budal. CERN Yellow Report, 67–17. 1967.
7. V. Agoritsas. Proc. Daresbury Sympos. on Beam Intensity Measurement, 1968, 117–151.
8. V. Agoritsas, S. Battisti, L.Henny, B.Nicolai. Unpublished work.

378

DOC = 30069307   PAGE

9. G.Schneider. CERN Internal Report, MPS/SR 69–10, 1969.
10. J.Boucheron, D. Boussard, F. Ollenhauer. CERN Internal Report, MPS/SR 69–7, 1969.
11. G.Schneider. CERN Internal Report, MPS/SR 69–10, 1969.
12. H.H. Umstatter. CERN Internal Report, MPS/SR 70–1, 1970.
13. H.Pflumm. Unpublished work.
14. R.W. Allison, R.W. Brokloff, R.L.Mc Laughlin, R.M. Richter, Marsh Tekawa, J.R. Woodyard. LRL (UCRL–19270).
15. R. Cappi. Unpublished work.
16. E. Brouzet. CERN Internal Report, MPS/CO 68–21 and 68–21/ add., 1968.
17. J. Comte, M.van Rooy, Ch. Serre CERN Internal Report, MPS/CO 69–19, 1969.
18. Y.Baconnier. Unpublished work.
19. V.Agoritsas.CERN Internal Note, MPS/CO, Note 70–5.
20. G.Rosset. To be published 1970.
21. J. Manca. CERN Internal Report, SI (Int. El), 70–3, 1970.
22. A. Millich. Unpublished work.
23. G.Schneider. CERN Internal Note, MPS/SR/Note 70–5, 1970.
24. S.Battisti. CERN Internal Report, MPS/CO. Electronique, 70–1, 1970.
25. V.Agoritsas, S.Battisti, J.H.B.Madsen. To be published, 1970.
26. G.Schneider. CERN Internal Note, MPS/SR. Note 70–13, 1970.
27. F.Hornstra. ZGS Quarterly Report, QU 68–2,1968.
28. C.D.Johnson, L.Thorndahl. CERN Internal Report, MPS/CO 68–8, 1968.
29. C.D.Johnson, L. Thorndahl. CERN Internal Report, MPS/CO, 68–13, 1968.
30. C.D.Johnson, L.Thorndahl. Proceedings U.S. National particle Accelerator Conference. Nuclear Sci., 1969, 16, 909–913.
31. E.Brouzet, C.D.Johnson, P.Lefevre. To be published 1970.

Discussion.

I. P. Karabekov. Which energy of electrons in scanning beam?

K. D. Johnson. Energy of electrons 100 eV. All electrons with the energy, which exceeds this value, are collimated off.

Page 92.

114. STRUCTURAL SOLUTICNS FOR COMPLEXES CONSISTING OF POWER-SUPPLY SYSTEMS AND EQUIPMENT FOR CENTRALIZED DIGITAL MONITORING AND CONTROL FOR SYNCHROTRONS AND BEAM-TRANSPORT CHANNELS

V. P. Gerasim, O. A. Gusev, S. Ya. Kolesov, S. S. Reshin, A. A. Tunkin.

(Scientific research institute of the electrophysical equipment im. D. V. Yefremov).

To the contemporary multiunit ones of the complex of the systems of power of accelerators and channels of conclusion/output from the accelerators are presented the following basic requirements.

1. Output parameters of systems must have lasting stability in view of complexity of current adjustment of drift by hand.

2. Must be provided possibility of remote/distance setting of output parameters of all systems, including codes from programmers or

ETsVM [digital computer].

3. Complex must be equipped with equipment for precision check
of all forms of electrical parameters with data extraction in digital
form (by printed digital output, memory, and ETsVM).

4. In complex of systems of pulse supply must be provided for
system of branched step by step check of nominal values (+-
allowance) of parameters of each power-supply system, which analyzes
state of complex in all stages of its functioning and which controls
keys/wrenches of stages in synchronizer (timer) of complex - system
of dynamic blockings (DB).

In connection with the systems of beam extraction from the
accelerators system DB must exclude functioning the systems of orbit
perturbation with the inadmissible divergences from the nominal
current strengths in the magnets of the channels of beam transport
and thereby - incidence/impingement of beam for the walls of channel
and its activation. Requirements on paragraphs 1 and 2 entirely
answer digital regulating circuits (SAR) with the discretely
controlled regulator, the digital supports, the error amplifiers and
(for multiple-contour SAR) the calculators of the resulting code of
error.

The construction of digital SAR is especially expedient in cases when the output parameter easily is led to the time characteristics, with the how conveniently high precision/accuracy which are represented in the digital form, for example, during the stabilization of the relation of constant and variable/alternating components of the current of the electromagnet of synchrotron.

In this case the task is reduced to the stabilization of the time interval between the impulses/momenta/pulses from the ferromagnetic probes in the clearance of electromagnet (Fig. 1). Fig. 2 gives the block diagram of digital SAR, solving this task with the precision/accuracy $2 \cdot 10^{-*}$: system has redundant mesh of the control on the stress/voltage selecting the temperature instabilities of the circuit elements of synchrotron.

The advantages of digital SAR are retained also for the stabilization systems of direct currents and stresses/voltages, if available precision analog-to-digital converters (ATsP) for the given parameters. Fig. 3 show the diagram of digital SAR of the direct current (unit Ka) of electromagnet, the ensuring precision/accuracy of stabilization $5 \cdot 10^{-*}$. ATsP, which consists of DT (current-sensing device - comparison circuit) and IPT (source of saw-tooth current), is realized on one of the base diagrams, shown in Fig. 4.

With the required precision/accuracy of stabilization not better
than 10^{-3} is expedient the use/application of analog SAR with the
program reference-voltage sources (PION) of the type of
digital-analog converters (TsAP) - Fig. 5.
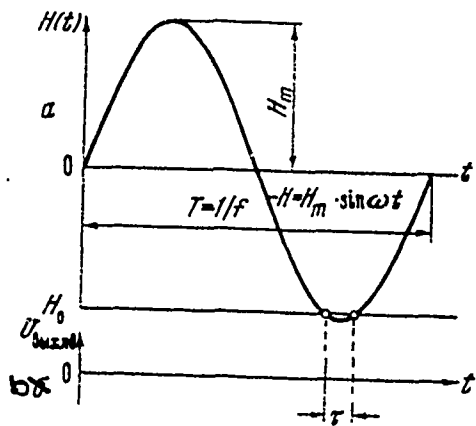
Fig. 1. The time graph of the components of the current of the electromagnet of the synchrotron. a) the curve of field change in the clearance. Electromagnet of syncnrotron; b) the impulses/momenta/pulses of output potential of Permalloy sensor.
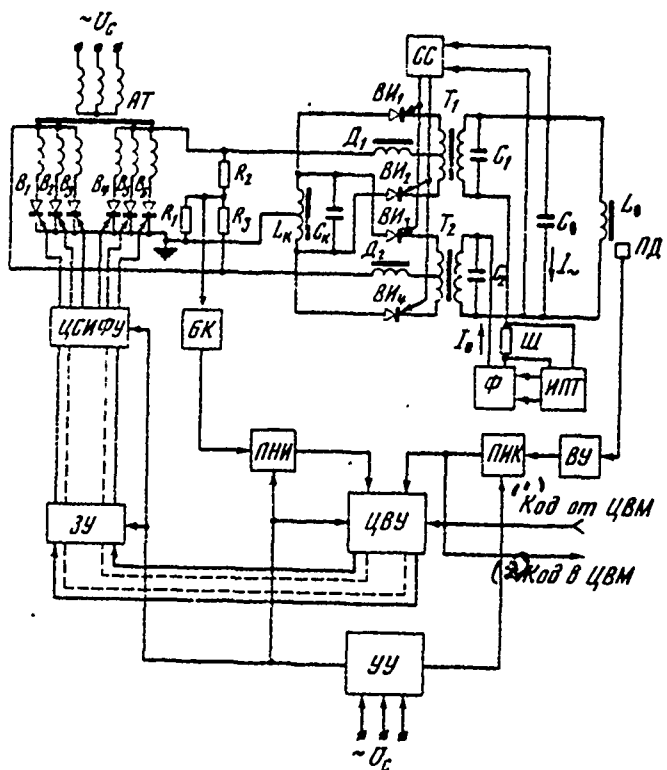
Fig. 2. Functional diagram of digital SAR of stabilization of field of electromagnet of synchrotron. PIK - converter interval-code; TsVU - digital computer (summator); PNI - converter voltage-interval; UU - control unit; ZU - memory unit; TsSIFU - digital system of the pulse-phase control.

Key: (1). Code from. (2). Code to.
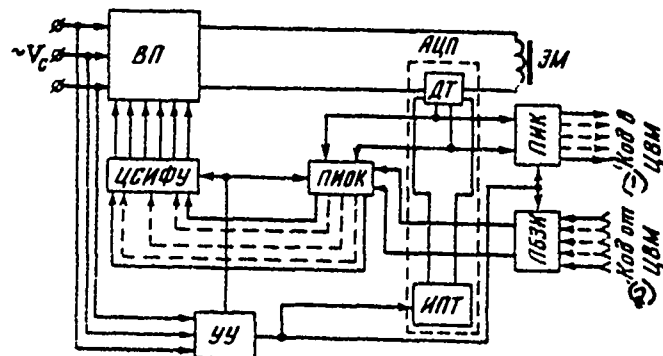
Fig. 3. Functional diagram of digital SAR of the stabilization of direct current in the electromagnet.

Key: (1). Code to. (2)0. Code from.

Page 93.

At present there are industrial TsAP with the precision/accuracy of order 10^{-3} with the delay of exit stress/voltage from the moment/torque of the admission of the code not more than 20 μs, in NIIEFA are developed TsAP on the magneto controlled contacts with the appropriate parameters 10^{-4} and 10^{-3} s. Digital-analog SAR in view of the in principle high freedom from interference of numerical controls are promising on the objects, unattainable for the control for communication along wires.

Equipment KEP and DE let us examine in connection with the complex of the power-supply systems of the channels of conclusion/output from the synchrotron of IFVE. Observation and measurement of all electrical signals in the systems (current pulses and stresses/voltages by duration from hundreds of μs to units s and constant values) are performed by system KEP of the following composition:

1) pulse digital voltmeter of the instantaneous values ITsVM3-4 (development of NIIEFA) with precision/accuracy +-0.03o/o for the duration of selection 3 μs in the assembly with timer and block/module/unit of the lasting memory;

2) the digital voltmeter of direct current V2-19 with the precision/accuracy +-5*10^{-4};

3) dual-trace oscillograph with the memory S1-51 in the assembly with the block/module/unit of the automatic compensator of the larger part of the input signal for the observation on the large/coarse scale of pulse apex.

The given instruments are connected to the sensors of the control values by pushbutton commutator simultaneously with control knobs of the settings of the same values.

Fig. 6 shows the generalized block diagram of DB of the complex of the power-supply systems of the channels of the conclusion/output of proton synchrotron of the IFVE.

System DB is controlled by sync pulses of the devices/equipment of the channels of conclusion/output. Blocking is accomplished/realized into three stages. Sources of the information: a) the total contacts of static blocking (I stage); b) the two-threshold discriminators of stress/voltage (II stage); c) the two-threshold discriminators of current (III stage). During the disturbance/breakdown of the operating mode is blocked trigger pulse and is supplied signal to the discharge/break of the already connected devices/equipment. Indicator indicates address and stage of the emergence of malfunction.
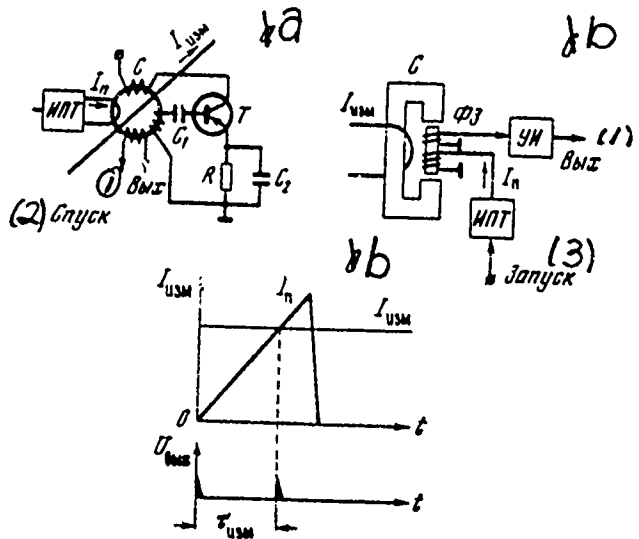
Fig. 4. Base diagrams of ATsP of direct current. Functional diagrams of current-sensing devices. a) cn the blocking oscillator; b) on the ferromagnetic probe; c) time graphs; PBEI - program block/module/unit of standard interval; FIOK - converter interval error-code.

Key: (1). Output. (2). Discharge. (3). Starting/launching.
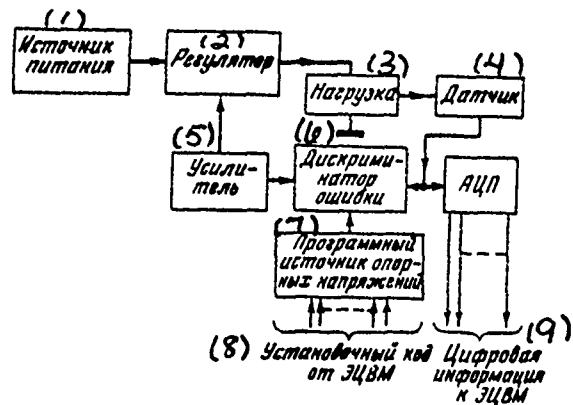
Fig. 5. Block diagram of analog SAB with the program reference-voltage source.

Key: (1). Power supply. (2). Regulator. (3). Load. (4). Sensor. (5). Amplifier. (6). Error detector. (7). Program reference-voltage source. (8). Adjusting code from ETsVM. (9). Digital information to ETsVM.
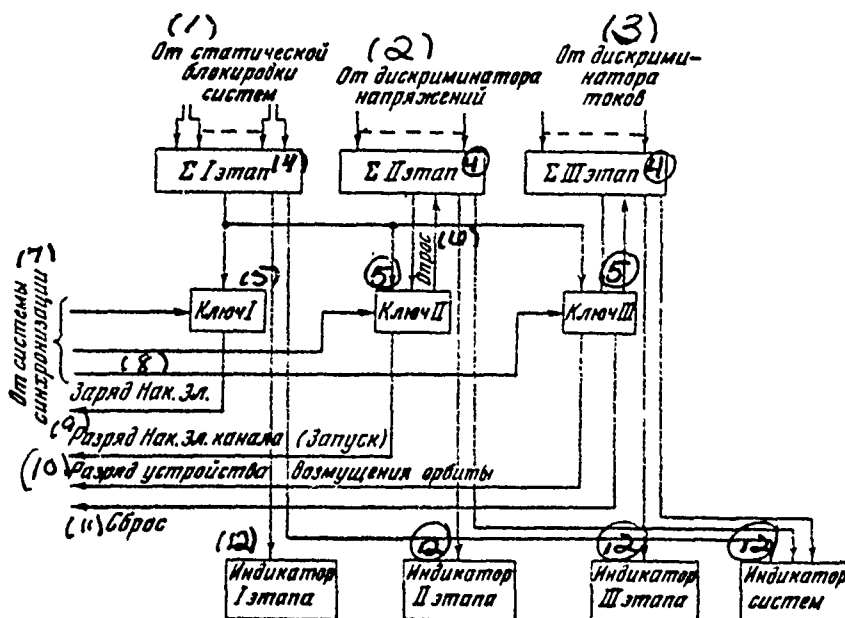
Fig. 6. Generalized block diagram of system LB of the channels of conclusion/output.

Key: (1). From static blocking of systems. (2). From discriminator of stresses/voltages. (3). From discriminator of currents. (4). stage. (5). Key/wrench. (6). Request. (7). From timing mechanism. (8). Charge Nak. El. (9). Discharge Nak. El. of channel (starting/launching). (10). Discharge device/equipment of orbit perturbation. (11). Discharge/break. (12). Indicator of ... stage.

Page 94.

REFERENCES.

LITERATURE

1. L. L. Gol'din et. al. Magnetic Measurements in Accelerators of Charged Particles. Gosatomizdat, 1962.

2. E. Dzhuri. Automatic Control Impulse Systems, Moscow, Fizmatgiz, 1963.

3. A. A. Kuznetsov, O. A. Kuznetsov. Elements of High-speed Analog-digital Converters, Izd-vo "Energiya", 1969.

4. Ye. K. Krug, C. N. Dilichenskiy. Principles of Construction of Single-channel and Digital Regulators. Moscow, Soviet Radio, 1969.

Discussion.

V. V. Tsygankov. In what state is the developed/processed system?

O. A. Gusev. System is developed for the Yerevan synchrotron and it will be soon put into operation. Were conducted the investigations of system in the mock-up cf the power-supply system of Yerevan accelerator in NIIEFA. Are developed, tested and are made systems for extraction channels of Serpukhov accelerator.

115. INVESTIGATION OF THE PERIODIC INSTABILITIES OF THE INTENSITY OF THE ACCELERATED BEAM ON THE YEREVAN ELECTRON SYNCHROTRON AND THEIR ELIMINATION.

S. K. Yesin, K. A. Sadoyan, A. R. Tumanyan.

(Yerevan physical institute).

The investigations cf the modes of operation of Yerevan electronic synchrotron at the initial stage of its operation made it possible to reveal/detect the considerable fluctuations of the intensity of the accelerated beam from one cycle to the next. The typical character of such fluctuations is shown on the lower ray/beam of oscillogram (Fig. 1A). With the aid of computers "Nairi" was produced a harmonic analysis of these fluctuations at the length of the interval of 1.49 s (69 cycles of acceleration). The table gives the obtained values of Fourier coefficients for the harmonic components, who correspond to the frequencies indicated.

The presence of the sharply pronounced harmonics with frequencies ~2.6; ~5.2; ~7.8 Hz made it possible to make the assumption that the basic contribution to the fluctuations of

intensity introduces the play at frequencies, multiple $\omega_c - \omega_k$ and $\omega_u - \omega_k$:

$$\mathfrak{I} = \mathfrak{I}_0 + \sum_{n=1}^{\infty} \left[\beta'_n \sin n(\omega_c - \omega_k)t + c'_n \cos n(\omega_c - \omega_k)t \right] +$$
$$+ \sum_{k=1}^{\infty} \left[\beta'_k \sin k(\omega_u - \omega_k)t + c'_k \cos k(\omega_u - \omega_k)t \right], \quad (1)$$

where ω_c, ω_u and ω_k - respectively angular frequencies of industrial network/grid, autonomous stable source, feeding injector, and resonant circuit of electromagnet.
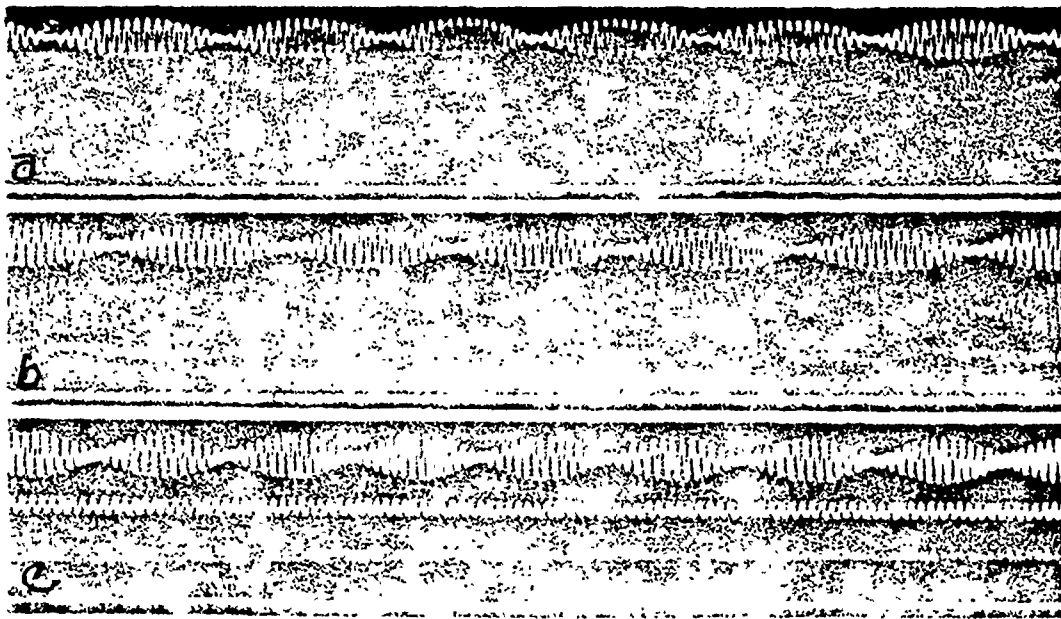
Fig. 1. Oscillograms of the intensity of the accelerated beam, play of stresses/voltages network-contour/outline, injector-contour/outline.

Page 95.

Since ω_c and ω_u are very close in the value, then for the determination of the basic source of instability was recorded the play of stress/voltage at frequencies $\omega_u - \omega_\kappa$ (upper ray/beam in Fig. 1A) and $\omega_c - \omega_\kappa$ (average/mean ray/beam of the same figure). Then was constructed the character of a change in the intensity of beam in the cycles, which correspond to the identical phase of play at frequency $\omega_u - \omega_\kappa$ (curve 1, Fig. 2) and in the cycles in which is retained

constant the phase of play at frequency $\omega_c - \omega_k$ (curve 2, Fig. 2). From Fig. 2 it is evident that the basic contribution to the fluctuations of intensity gives play between the frequency of resonant circuit and the oscillator frequency of the stable stress/voltage, which feeds injector.

It should be noted that the frequency of most strong harmonic will agree with the frequency of the aggregate/unit of the stable supply of injector.

The majorities of the nodes/units of injector are supplied from the single-phase full-wave rectifiers. In this case the operational characteristics of these nodes/units fluctuate with the frequency, equal to the double frequency of the feeding source.

As a result of a difference in the frequencies of resonant circuit of electromagnet and the generator, which feeds injector, occurs the "slip" of the moment/torque of injection along the phase of the pulsations of power supply. If the optimum value of the parameter is selected so that it lies/rests at the middle of the interval of pulsations, then the frequency of intensity can be determined according to formula $\omega_2 = 4(\omega_u - \omega_k)$. But if the optimum value of the parameter is located beyond range of oscillations, then intensity will be changed with frequency $\omega_1 = 2(\omega_u - \omega_k)$.

Respectively the nodes/units, supplied from the three-phase full-wave rectifiers, can be the reason for fluctuations at frequencies $\omega_u = 12(\omega_u - \omega_k)$ and $\omega_s = 6(\omega_u - \omega_k)$.

If energy storage in the storage element of supply power of this node/unit occurs during the series/row of the consecutive cycles (but not in the separate cycle), then the depth of modulation of intensity will be inversely proportional $\omega_u - \omega_k$. From the table it is evident that the basic contribution to the fluctuations of intensity introduce harmonics $4(\omega_u - \omega_k)$ and $2(\omega_u - \omega_k)$.

On the basis of described analysis was produced the translation/conversion into the synchronous with the current generator of the focusing coils of injector, since the currents into the bottom with difficulty yield to filtration due to the low apparent resistance of coils. As a result of fluctuation the intensities of the accelerated beam decreased to +-15o/o (Fig. 1b).

The coefficients of expansion in the Fourier series of the fluctuations of intensity from one cycle to the next.

(1) Номер	(2) Частота неста- бильности, гц	A sin	B cos
1	0,6711	-1,28285	2,91631
2	1,3422	0,95088	-1,11612
3	2,0133	0,11408	-1,68135
4	2,6844	1,10002	-8,50192
5	3,3555	0,09614	1,15188
6	4,0266	-0,31994	1,64249
7	4,6977	0,72566	0,49897
8	5,3688	9,38379	-5,47806
9	6,0399	1,70594	2,40725
10	6,7110	-0,86134	2,53218
11	7,3821	-0,64826	1,60085
12	8,0532	-1,05547	2,43629
13	8,7243	-0,46696	0,69324
14	9,3954	-0,57558	2,34195
15	10,0665	-0,72198	1,03617
16	10,7376	0,52924	-0,52151
17	11,4087	0,48443	1,63172
18	12,0798	-0,60476	0,61265
19	12,7509	-0,55062	1,68013
20	13,4220	-1,12302	0,69577
21	14,0931	-0,10295	1,62518
22	14,7642	0,48742	1,65026
23	15,4353	-0,43231	0,69572
24	16,1064	0,27081	2,03027

Key: (1). Number. (2). Frequency of instability, Hz.
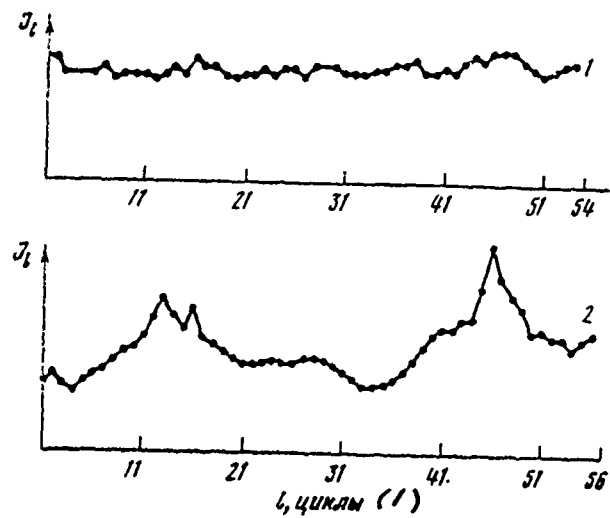
Fig. 2. Dependence of the intensity of the accelerated beam on the phases of the play of stress/voltage network-contour/outline, injector-contour/outline $1-(\omega_{v}-\omega_{k})t=2n\ell$, $\ell=0$, 1, 2, ..., 54:

$2-(\omega_{c}-\omega_{k})t=2n\ell$, $\ell=0$, 1, 2, ..., 56.

Key: (1). cycles.
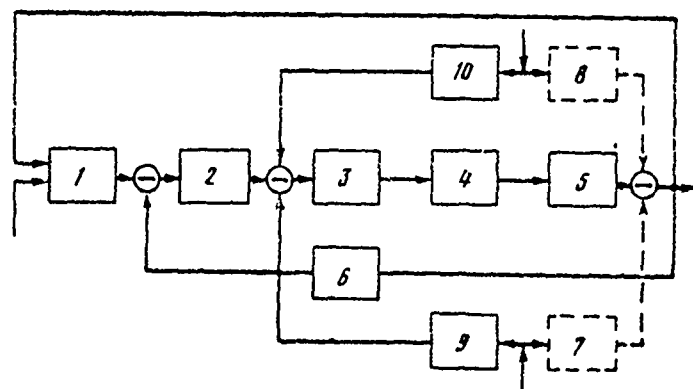
Fig. 3. Block diagram of timing mechanism of voltages of feeding generator of injector. 1 - synchronizing block/module/unit; 2 -

amplifier with correcting components/links; 3 - magnetic amplifier; 4
- direct-current motor; 5 - induction motor with the phase rotor; 6 -
meter of frequency; 7, 8 - blocks of the substitution of induction
motor on the perturbing effects; 9, 10 - compensating
components/links.

Page 96.

Was further developed the diagram of the supply of entire basic
equopment of injector from the generator, synchronized with the
contour/outline (Fig. 3). Timing mechanism provides the stabilization
of time interval from the moment of the transition of voltage of one
of the phases of the synchronous generator through 0 to the
moment/torque of the achievement by the magnetic field of the
accelerator of field level of injection with the precision/accuracy
+-10 μs. Timing mechanism is created on the basis of the principle of
invariance with respect to the basic external
disturbances/perturbations: the instability of voltage and frequency
of power line. The transfer functions of blocks 9, 10 (Fig. 3), which
ensure the invariance of system with an accuracy to $\varepsilon = 0.1$, are
respectively equal to:

$$W_0(p) = 0.23 \frac{(0.14p+1)(0.32p+1)}{(0.01p+1)(0.02p+1)} ;$$

$$W_{10}(p) = 0.14 \frac{(0.21p+1)(0.32p+1)}{(0.01p+1)(0.02p+1)} ,$$

where p=dx/dt and x - cutput parameter of blocks.

As a result of applying the diagram of power of injector indicated was provided the stability of the intensity from one cycle to the next not worse than +-5o/o. The corresponding oscillogram is shown in Fig. 1c. It is evident that the play on a difference in the frequencies is absent (average/mean ray/beam).

116. NONCONTACT MEASUREMENT OF BEAM CURRENTS OF CHARGED PARTICLES WITH THE AID OF THE HALL EFFECT.

G. I. Razin, V. G. Savenko, A. P. Shchelkin.

(Scientific research institute of the electrophysical equipment im. D. V. Yefremov).

1. Introduction.

The noncontact Hall meter of the beam currents of the charged/loaded particles is torcidal concentrator, encompassing the beam, in clearance (or clearances) of which are placed one or several Hall pickups. Sensors are supplied from source of alternating current, and emf of Hall, proportional to the intensity/strength of

the field, created by team current, it is amplified with the aid of the selective amplifier and is measured by dial instrument 1 (Fig. 1).

The basic difficulties, which appear during the creation of measuring meters of such type, consist in the guarantee of the necessary precision/accuracy of measurement and threshold of response, determined by the relationship/ratio of sensitivity and additive error. Is given below the analysis of the factors, which are determining the parameters indicated.

2. Sensitivity of Hall meters of currents.

The sensitivity of the meter of the beam currents of the charged/loaded particles to a considerable degree depends on the correct selection of sizes/dimensions and material of concentrator. After simple mathematical conversions it is possible to find the following expression for the sensitivity of meter to current S_i [2]:

$$S_i = k \frac{1/D}{1/\mu + d/\pi D} ,$$

where $k = \frac{1}{\pi} R_x I_n$; R_x - Hall constant; I_n - feed current for the Hall pickup; μ - magnetic permeability of the substance of concentrator; D - diameter of the center line of concentrator; d - width gap. With small clearances when $d/\pi D \ll 1/\mu$, $S_i \approx k \frac{\mu}{D}$. With the ample clearances

even larger μ, when $1/\mu \ll d/\pi D$, the sensitivity of measuring device virtually does not depend on the diameter of concentrator and is determined only by width gap $S_l = S_{l\,max} = \frac{\pi}{D}$, $S_l/S_{l\,max} = \frac{1}{1+\pi D/\mu D}$, whence magnetic permeability of substance, required for guaranteeing the prescribed/assigned relation $S_l/S_{l\,max}$ with known d and D, is equal to

$$\mu = \frac{\pi D}{d} = \frac{1}{S_l/S_{l\,max}-1}.$$

Fig. 2 shows family of curves $\mu = f(S_l/S_{l\,max})$, ratio $\pi D/d$ is undertaken as the parameter.
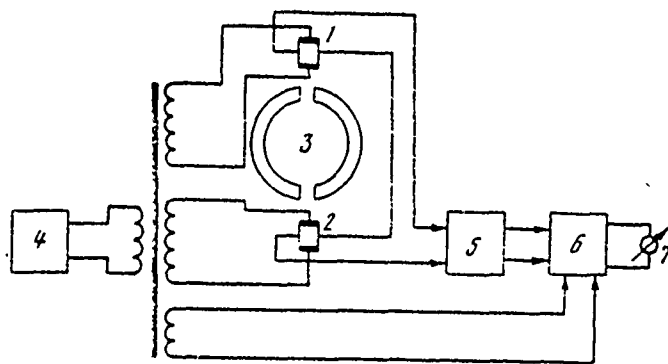
Fig. 1. Block diagram of the noncontact meter of the beam currents of the charged/loaded particles. 1 and 2 Hall pickups; 3 - concentrator; 4 - source of alternating current; 5 - amplifier; 6 - the phase-sensitive rectifier; 7 - dial instrument.

Page 97.

Using this graph/curve, it is possible to determine the minimum value μ, at which $S_i/S_{i\,max}$ will compose the desired value. The selection of the material of concentrator more than this value does not lead to noticeable increase S_i.

For considerable sensitization of device/equipment by the method of the selection of material with the higher magnetic permeability of substance it is necessary to increase $S_{i\,max}$: It is impossible to make this due to the decrease of width gap d, as a rule, since clearance

is limited by the thickness of the Hall pickup. Taking into account
this, in certain cases it is expedient to perform concentrator in the
form of spiral with closed ends/leads [3]. It is not difficult to
show that magnetic permeability cf body and sensitivity $S_{i max}$ of this
concentrator with $\mu \rightarrow \infty$ grow/rise in n of times where n - number of
turns of spiral.

3. Multiplicative errors of measurement.

Multiplicative errors in the noncontact Hall meters of currents
have all those components which characterize contact meters. Besides
this in a multiplicative error in the analyzed instruments is
included the series/row specific component, inherent only in Hall
meters of the beam currents of the charged/loaded particles: errors
due to a change in the position of beam in the ion guide due to the
final sectional area and nonuniform particle distribution according
to the beam section, these components of basic multiplicative error
having the greatest specific gravity/weight. Fig. 3a and b gives the
experimental dependance of an error of measurement from the beam
displacement on a radius with the permanent azimuth and along the
azimuth with constantly a radius. Experiment was carried out by the
method of displacement within the concentrator of conductor with the
current with a diameter of 0.2 mm. Curves with the prime correspond
to concentrator with two Hall pickups, curves without the prime - to

concentrator with one sensor. In the first case an error of measurement reaches 10o/c, the secondly - 3o/o. With four Hall pickups, arranged/located according to two mutually perpendicular diameters, this compcnent of errcr is equal cnly 0.5o/o.

As can be seen frcm Fig. 3a in the case of two Hall pickups the sign of error does not change with any mixings of the center of gravity of beam. Hence it follows that a multiplicative error of measurement must be determined not only by the position of beam, but also by the form of section and by the law of particle distribution in the space.

Let us break the sectional area of beam into the surface elements (Fig. 4), to each of which corresponds the elementary current dI, measured with the error

$$\delta' = f(\varphi, \, \tau/R),$$

where φ and τ - the coordinate of area/site ds, R - a radius of concentrator.
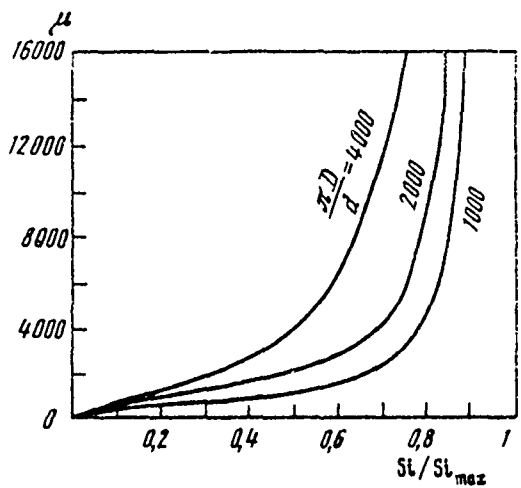
Fig. 2. Graph/curve of family of curves $\mu = f(St/St_{max})$ at the different values $\pi D/d$.
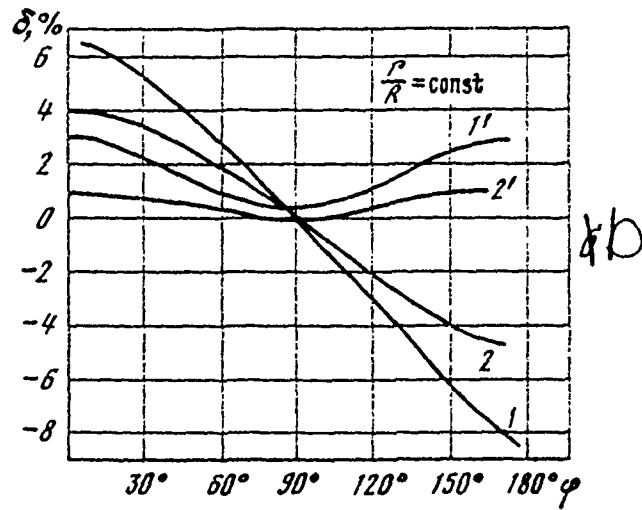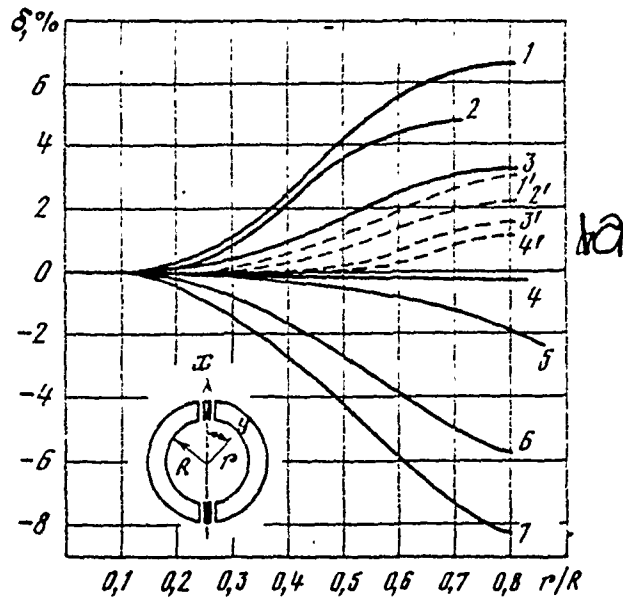
Fig. 3. Dependence of error of measurement from the beam displacement on a radius with azimuth φ=const (a) and along azimuth φ with r=const (b): a) with the azimuth φ const: 1-φ=0°, 2=φ=30°, 3-φ=60°, 4-φ=90°, 5-φ=120°, 6-φ=150°; 7-φ=180°;

b) along azimuth φ when $\tau =$ const: $1,1' - \dfrac{\tau}{R} = 0,75$, $2,2' - 0,5$

Page 93.

If beam is arranged/located in the center of concentrator, then the multiplicative error of measurement, which considers the finite dimension of the area of its section, can be determined with the aid of the expression:

$$\delta = \frac{I - I'}{I} = \frac{\displaystyle\int_{0}^{\pi/2}\int_{0}^{\tau/R} \delta'(\varphi, \tau/R)\,\tau\,d\tau\,d\varphi}{\displaystyle\int_{0}^{\pi/2}\int_{0}^{\tau/R} \tau\,d\tau\,d\varphi}, \qquad (2)$$

where I and I' - real and measured value of beam current respectively.

The functionals of curves, depicted in Fig. 3a and b determined with the aid of the procedure, presented in [4], take the form

$$\delta = k\left(\frac{\tau}{R}\right)\varphi, \quad k = 3,3\left(\frac{\tau}{R}\right)^2 - 0,4\left(\frac{\tau}{R}\right)^3. \qquad (3)$$

Being limited to term $k = 3.3)(\tau/R)^2$ and substituting (3) in (2), we will obtain

$$\delta = 1,15\left(\frac{\tau}{R}\right)^2 (\%).$$

Further it is possible to show that under the normal (Gaussian) law of the distribution of particles over beam section

$$\delta \simeq \int_0^1 1,15\, x^2 e^{-2,3x^2}\, dx \ (\%).$$

4. Additive errors in meter.

In the additive error in the meter, which limits its threshold of response, are included the errors, determined by noises within and at the output of the Hall pickup, and also by the temporary/time and temperature drift of his zero signal, latter/last component cf error in the overwhelming majority of the cases playing the decisive role.

The authors proposed several devices/equipment, which make it possible to eliminate the effect of the temperature drift of zero signal on the additive error and the threshold of response of meter [5, 6]. Diagram of one cf such devices/equipment is shown in Fig. 5. Sensor is supplied from the source of direct current. Concentrator in the circumference comes into contact with modulating magnetic circuit 3 in to slot/groove of which is placed modulating winding by 4. By the selection of the value of the current of the modulating winding they attain the periodic saturation of concentrator that it leads to the pulse modulation of the direct flow, created by the measured current. Obtained thus variable/alternating Hall emf can be easily isolated from the constant in the direction of emf of nonequipotentiality.

The authors prepared one of the versions of the meter of the
direct beam currents of the charged/loaded particles. Basic given
error of instrument does not exceed 5o/.o in the range 0-10 mA.
Further perfection of instrument will be conducted in the direction
of an increase in precision/accuracy and reduction in the threshold
of response, which can be achieved/reached by the method of the
introduction of the corresponding corrections, which decrease the
multiplicative error, and due to further reduction in the additive
error.
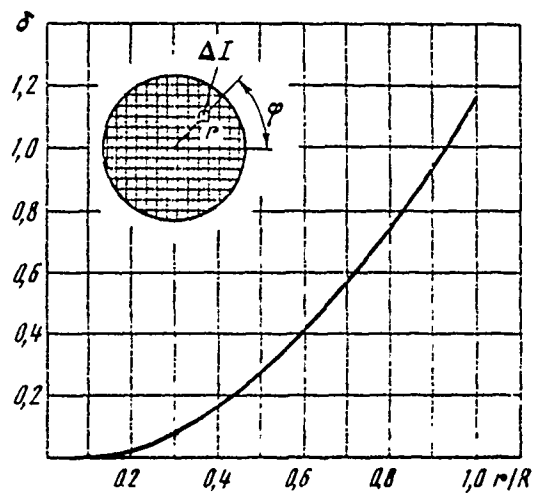
Fig. 4. Dependence of error on the sizes/dimensions of beam.
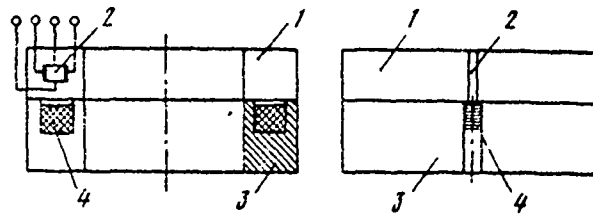
Fig. 5. Sensor with modulation of permeability μ concentrator.

REFERENCES.

DOC = 80069308   PAGE 412

LITERATURE

1. V. I. Pogodin, A. P. Shchelkin, G. A. Yur'yeva. Improvement of contactless Hall transducers of the intensity of beams of charged particles. PTE, 1967, No. 3.

2. V. G. Savenko, A. P. Shchelkin. Contactless measurement of currents by means of the Hall effect. Materialy Nauchno-tekhnicheskoy Konferentsii LEIS [Data of the Scientific and Technical Conference of LEIS], Issue 5, 1968.

3. V. N. Bogomolov, V. I. Pogodin, A. P. Shchelkin. Device for contactless measurement of currents. Author's certificate 21 ye, 36/01, No. 213972. Byull. izobret, i tov. znakov, 1968, No. 11.

4. K. M. Kudelin. Method of approximation of experimental curves by power polynomials "Izmeritel'naya tekhnika" [Measuring Technology], 1969, No. 4.
A. P. Shchelkin

5. Device for measuring weak magnetic fields. Author's certificate 21ye, 12, No. 203762. Byull. izobret. i tov. znakov [Bulletin of inventions and trade marks], 1967, No. 35.

6. G. I. Razin, A. P. Shchelkin. Device for measuring weak constant circular fields. Author's certificate. 21 ye, K No. 256851. Byull. izobret. i tov. znakov, [Bulletin of inventions and trade marks] 1969, No. 35.

Discussion.

K. D. Johnson. Is how the effect of radiation on the Hall pickups?

G. I. Razin. With the room temperature and with the beam currents on the order of 10-100 mA the effect of radiation insignificantly and little affects the accuracy of measurement. Sensors are made from indium antimonide.

N. S. Medvedko. What are sensitivity and threshold sensitivity of your sensor?

G. I. Razin. The sensitivity of sensor composes 10 μV on 1 mA of the measured current. Threshold sensitivity 100-200 μA.

I. M. Bolotin. Which the upper band edge of the transmission of sensor and the necessary screening constant of sensor?

G. I. Razin. The time constant of the Hall pickup is $10^{-11} - 10^{-13}$ s. Thus band depends in essence on current frequency, which feeds sensor. In our case this frequency composes several kilohertz.

The threshold sensitivity of sensor is determined by the effect of external magnetic fields, in particular, the field of the Earth. With the beam current 1-10 mA the screening constant must be not less several thousand.

A. A. Kuz'min. Was utilized your sensor for measuring the currents of real beams?

G. I. Razin. Yes, such measurements were conducted on the neutron generator. Factor of merit was approximately 0.5 mA. It is possible to measure the currents from 100 μA.

A. A. Kuz'min. Are such the sizes/dimensions of concentrator?

G. I. Razin. Bore of 60 mm, external - 80-90 mm. Material - Permalloy, ferrite.

Page 99.

117. SPACE-CHARGE EFFECT ON THE EFFECTIVENESS OF THE IONIZING METHOD OF MEASURING THE PROFILE OF A PROTON BEAM IN ACCELERATORS.

V. V. Yelyan

(Radiotechnical Institute AN USSR)

The devices/equipment, used for measuring the transverse parameters of beam without its destruction on annular proton accelerators are based on the phenomenon of the ionization of residual gas. Using the method the extractions of ionizing charge for the purpose of further working these devices are characterized by the extracting systems in which are applied either only electric field or combination of electrical and magnetic fields. Magnetic field is utilized for the focusing of "image" during the high requirements for the resolution, determined by the essential (several ten electronvolt) wave energy of ions in the transverse with respect to the extraction direction.

By effectiveness of ionizing method are implied two characteristics: the resolution and the speed of the extraction of

ions, determined by the type of the extracting system.

The decisive factor when selecting of the type of the extracting system proves to be the proper field of beam as a result of low wave energy of ions. With the achievement on the proton synchrotron of the IFVE (Serpukhov) with working intensity $1 \cdot 10^{12}$ protons/pulse the intensity/strength of its own electric field of beam reaches several tens of volts per centimeter. The project of the reconstruction of synchrotron of the IFVE is designed for obtaining of the intensity $5 \cdot 10^{13}$ protons/pulse, in this case in the project there are reserves, so that in the future could be solved task the achievements of intensity to $3 \cdot 10^{14}$ protons/pulse. With this proper field of beam it will increase to several hundred and thousands of V/cm. Obtaining the high resolution (about 1 mm) with the aid of the ionizing profilometers under these conditions sets practical limitations on the selection of the type of extracting system, connected with the value of the extracting voltage.

With the identical time of the extraction of ions and identical resolution were compared the extracting systems with crossed and parallel fields.

It is easy to show that in this case and without taking into account the proper field of the beam of the value of the

intensity/strength of the extracting electric field for the systems with crossed $(\varepsilon_\perp)$ and parallel $(\varepsilon_{\parallel})$ fields are located in the relation

$$\varepsilon_\perp / \varepsilon_{\parallel} \approxeq d / \Delta , \qquad (1)$$

where Δ - resolution,

d - diameter of beam.

At the beginning of the cycle of acceleration this relation maximally and in the accelerator of the IFVE can reach several ten. Thus, for obtaining in the Serpukhov accelerator of the time of extraction 10 ns it is necessary to have the extracting voltages 1 kV for parallel fields and 50 kV for crossed fields.

The proper field of beam affects the resolution of these extracting systems differently. In the case of parallel fields appears supplementary defocusing of ionic image, caused by the transverse component of the proper field of beam and which is compensated by the appropriate increase in the intensity/strength of the focusing magnetic field.

In the case of crossed fields the effectiveness of the extracting system is determined by the behavior of the equipotentials, along which is accomplished/realized the extraction of ions.

Page 100.

Its own potential of beam causes the distortion of equipotentials, in consequence of which they appear, in the first place, blur with respect to the real position of beam, and in the second place, the strain of image. The amount of displacement in the center of beam is determined by the relationship/ratio

$$x \cong \frac{e}{4\pi\varepsilon}\ \frac{N\ell}{uL\delta}\left(1 + 2\ell n\ \frac{\ell}{d}\right), \qquad (2)$$

where N - intensity of beam, protons/pulse; u - extracting voltage, in; L - orbit circumference: m; B - duty factor of orbit; ℓ - distance between extracting electrodes, m; d - diameter of beam, m; e - electron charge, Coulomb; ε - dielectric constant, F/m.

This relationship/ratio was obtained analytically for the cylindrical beam during its central location in the extracting system. For the check is carried out the decision of the equation of Poisson by the net point method on the computers for a special case of the geometry of the extracting system. During the displacement of equipotentials to 10 mm relative to ideal position numerical and analytical results coincide with the precision/accuracy of better than 10o/o.

Relationship/ratic (2) makes it possible to introduce as the criterion critical value the extracting voltages u_{kp}, lower than which displacement equipotentials will exceed permissible value x_{gon}:

$$u_{kp} = 2,9 \cdot 10^{-9} \frac{N\ell}{x_{gon} L b} \left(1 + 2 \ln \frac{\ell}{d}\right). \qquad (3)$$

Let us rate/estimate the value of retarded potential for the accelerator of the IFVE for the energy of 70 GeV.

Let us assume: $L = 1.5 \cdot 10^3$ m, $\ell = 0.2$ m, $x_{gon} = 10^{-3}$ m, $B = 10^{-1}$, $d = 10^{-2}$ m. For $N_1 = 5 \cdot 10^{11}$, $N_2 = 5 \cdot 10^{12}$ and $N_3 = 5 \cdot 10^{13}$ value u_{kp} are equal to with respect $u_{1kp} = 13,5$ to kV, $u_{2kp} = 135$ kV, $u_{3kp} = 1350$ kV.

If we disregard/neglect the displacement of image and as the criterion to select the strain of image (change in the second moment/torque of distribution tc 10o/o), these values can be decreased by approximately one order.

At the achieved/reached and planned/glide intensities of Serpukhov accelerator the requirements for the value of the extracting voltage in the case of crossed fields prove to be in practice impracticable, and must be used parallel fields.

If we utilize for the focusing a longitudinal magnetic field with the induction to 1 kg, then practical limit in the intensity for the extracting system with the parallel fields will compose $10^{14}-10^{15}$ protons/pulse.

118. A TWENTY-CHANNEL HIGH-SPEED METER FOR THE POSITION OF A BEAM IN AN ACCELERATOR.

V. A. Skuratov.

(Radio engineering institute of the AS USSR).

For observing the orbit of the motion of beam with the work of the accelerator in the mode/conditions of the first revolution and circulation it is important to have an information about the position of beam in the points/items, evenly distributed on the ring of accelerator chamber.

With the aid of 20-channel high speed meter of the position of beam the observation of orbit is accomplished/realized visually on the oscilloscope face. The voltages, which correspond to the position of orbit in the points/items of measurement, are fixed/recorded consecutively/serially on scanning/sweep of oscillograph for the time, which does not exceed 50 μs.

During the development of 20-channel high speed meter of the position of beam in the accelerator as the basis was accepted the

equipment for display system. Display system encompasses twenty
channels, which record the position of beam by sum-and-difference
method by the method of isolation/liberation with the output of the
channel of voltage, which corresponds to the divergence of beam from
the center of chamber/camera. Output potentials of display system
vary within the limits of 0.3-8 V of any polarity.

The block diagram of device/equipment is shown in Fig. 1. The
measured voltages through the matching cathode followers are fed to
the normally-closed keys/wrenches. Keys/wrenches are commutated by
control voltages, taken from the triggers. The sequence of the start
of keys/wrenches is assigned by the counter, comprised of the
controlling triggers. The recalculation of the sequence of the start
of the triggers of counter is assigned by the impulses/momenta/pulses
of the waiting blocking oscillator. The operating time of blocking
oscillator is determined by the interval between the spin of the
beginning of measurements and by the impulse/momentum/pulse, which
are formed upon the inclusion/connection of the latter/last code.
Commutated such by form voltages are united on summing amplifier
whose output is connected to the oscillograph.

The elements/cells, which are determining the quality of the
work of device/equipment, are keys/wrenches. All keys/wrenches are
uniform. The schematic of key/wrench is represented in Fig. 2. In the

key/wrench are used two transistors of the type 1T311 and 1T313.

Transistors are connected in series by means of the association of

emitter circuits. Normally transistors are in the open state. The

measured voltage through resistance equal to 5 kiloohm, is connected

to the general/common/total emitter circuit. Consequently, low output

resistance of emitter circuits shunt input currents from the channels

of display system.

Page 101.

In the presence of strobe pulses from the controlling trigger

the transistors of key/wrench are closed and the current,

prescribed/assigned by the measured voltage, enters summing

amplifier, to which it separates/liberates the voltage pulses, which

correspond in the amplitude to measured voltage, and in the duration

- to strobe pulse. Due to the difference of the fronts of strobe

pulses and difference in the transistors at the output of

keys/wrenches appear pulse currents which create false

impulses/momenta/pulses, which do not exceed in the duration of 0.7

µs, but in the amplitude, equivalent to the measured voltage into 1

V. Nevertheless these impulses/momenta/pulses do not interfere to

measure the voltage according to the residual/remanent pedestal with

the precision/accuracy 200-300 mV of any polarity.

Fig. 3 shows oscillogram of the recording voltage at the meter output in the absence of input voltage.

For agreement and increase of input resistance of device/equipment are used dual emitter followers. Schematic diagram is depicted in Fig. 4.

Variable resistances in the basis of the first transistor and the emitter of the second transistor give the possibility of the control of "zero".
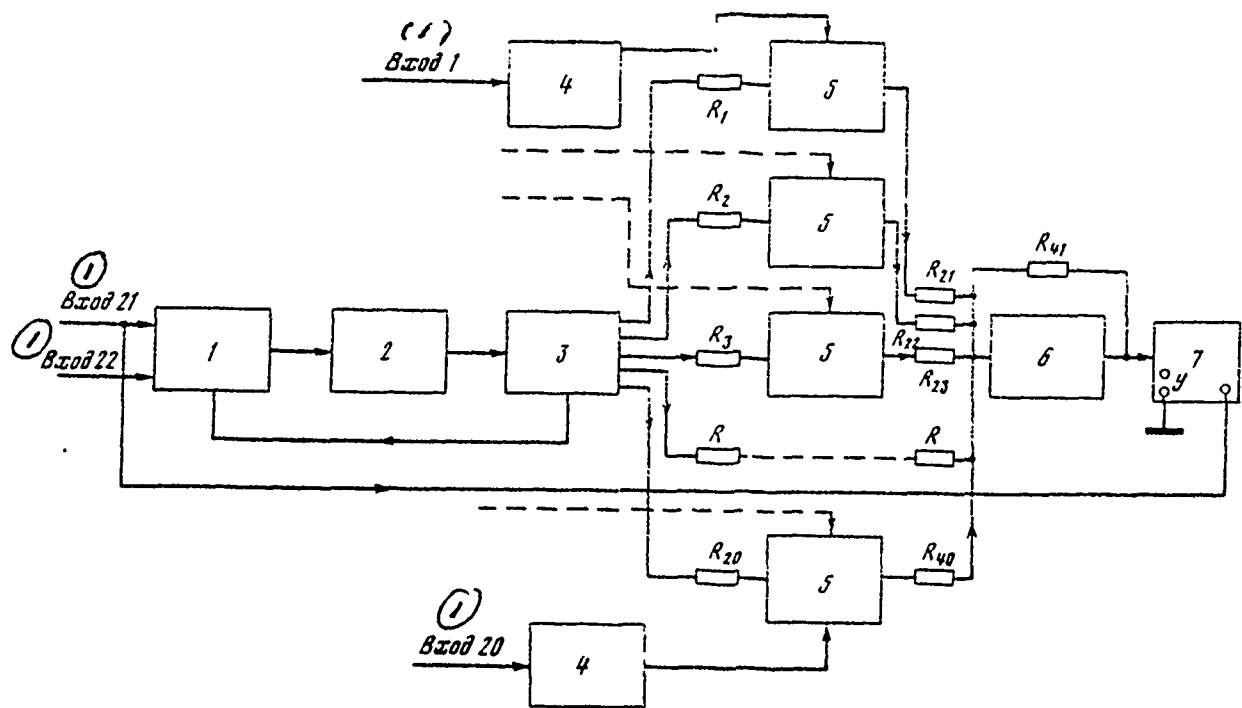
Fig. 1. Block diagram of the 20-channel high speed meter of the position of beam in the accelerator. 1 - trigger; 2 - waiting blocking oscillator; 3 - shaper of sequence of driving pulses; 4 - the emitter follower; 5 - key/wrench; 6 - summing amplifier; 7 - oscillograph.

Key: (1). Input.
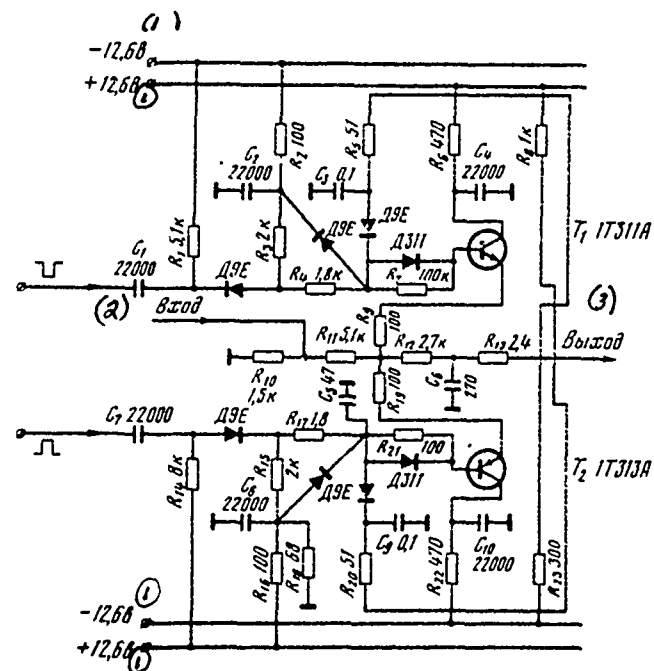
Fig. 2. Schematic diagram of key/wrench.

Key: (1). V. (2). input.
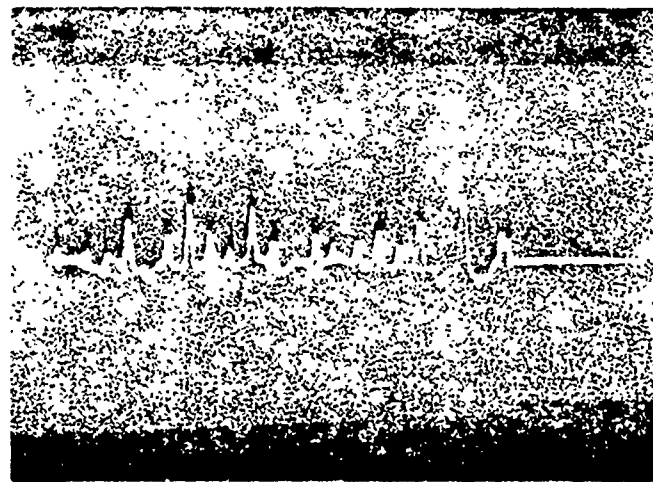
Fig. 3. Palse impulses at output of device/equipment. 1 cm in the

amplitude corresponds to voltage on the input of 0.5 V.

Page 102.

Summing amplifier of the direct current is made of two
differential cascades/stages, included by negative feedback. Gear
ratio is equal to 0.5. The highest limit of frequency characteristic
corresponds to 4 MHz.

The mock-up of the 20-channel high speed meter of the position
of beam in the accelerator was used with the final adjustment of the
initial conditions for the introduction/input of beam during
inauguration of accelerator. The correctness of the
introduction/input of beam was estimated during the observation of
the orbit of the first revolution. Another use/application occurred
during the final adjustment of the program of the correction of
magnetic field both by nand and with the aid of computers of the type
"Dniepr". The device/equipment of the rapid measurement of orbit in
the mode/conditions of circulation on the oscillograms clearly came
to light/detected/exposed the results of acting the correction of
magnetic field.

Fig. 5a - in gives respectively the oscillograms of the orbits
of the first revolution, mode/conditions of circulation without the

correction of magnetic field and mode/conditions of circulation with the introduction to correction of magnetic field.
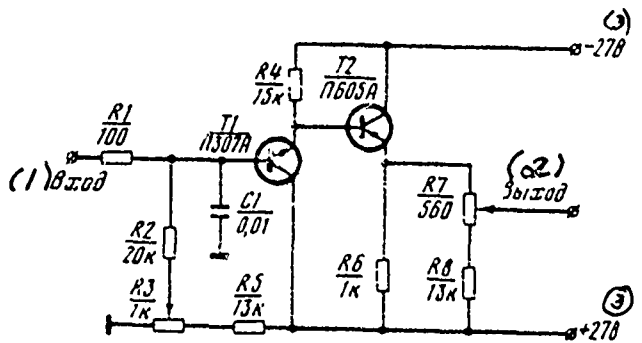
Fig. 4. Schematic diagram of the emitter follower.

Key: (1). input. (2). output. (3). V.

Fig. 5. the oscillogram of orbits. a) exit voltage in the mode/conditions of the first revolution; b) exit voltage in mode of circulation without the correction of magnetic field; c) exit voltage in the mode/conditions of circulation with the manual control of the correction of magnetic field. On 14 channels is brought out the voltage of the intensity of beam, which corresponds to divergence

with respect to the orbit on 6 sm.

Discussion.

N. S. Medvedko. For equilibrium orbital correction maneuver is necessary the measurement of the center-of-gravity location of cluster for many revolutions. What speed is averaged in your system?

V. A. Skuratov. Order of 10-15 revolutions in the mode/conditions of circulation.

119. NEW DIGITAL INSTRUMENTS FOR INVESTIGATION OF THE AMPLITUDE AND
ENERGY PARAMETERS OF PULSE PROCESSES IN ELECTROPHYSICAL
INSTALLATIONS.

V. P. Gerasimov, O. A. Gusev, S. S. Repin, V. A. Skosarev.

(Scientific research institute of the electrophysical equipment im.
D. V. Yefremov).

Development of accelerative and thermonuclear technology in the
contemporary stage advances new requirements for the instruments for
investigation of pulse processes, in connection with which in NIIEFA
are developed the new digital measuring meters, which differ from
those previously developed by the class of precision and by ultimate
purpose. Are examined below the principles of construction and the
circuit decisions of digital instruments for the automatic
investigation of the form of pulses and measurement of the energy,
isolated by single electric pulse in the resistive load.

Page 103.

1. Pulse digital voltmeter of instantaneous values ITsVM3-4.

Instrument provides the measurement of the instantaneous values
of surge voltages with the random error not more than +-0.03o/o for
the duration of selections 2 μs and the cyclic recurrence of
measurements to 500 Hz. The code of each selection is
written/recorded in ZU on the magnetic elements/cells and is
reproduced on the indicator with the subsequent survey with the
simultaneous output to the printed digital output.

The block diagram of instrument (Fig. 1) realizes the method of
two-step the time of pulse conversion with the compensation basic
part of input voltage signal, proportional to the result of the first
step/pitch of conversion, by the developed digital-analog converter.
Under the condition of executing the inequality

$$\varepsilon_{gon} = \sqrt{\varepsilon_{чАп}^2 + \varepsilon_{cAB}} \ll \varepsilon_{ччвмз},\qquad (1)$$

(where ε_{gon} - relative integral error in the supplementary schematics
of two-step converter, $\varepsilon_{чАп}$ - a relative random error in the first
step/pitch ATs and TsA of conversion, ε_{cAB} - a relative random error
in the diagram of analog subtraction) is correct the
relationship/ratio:

$$\varepsilon_{ччвмз} = \frac{\varepsilon_{ш}}{n},\qquad (2)$$

where $\varepsilon_{ччвмз}$ - integral random error of measurement of instrument; $\varepsilon_{ш}$

- the random error in the steps/pitches of conversion; n - quantity of discrete/digital levels of the compensating voltage, developed by TsAP. In [1] is shown the possibility of obtaining $\varepsilon_{w} \leqslant \pm 0,1\%$, which when selecting n=10 in principle provides value $\varepsilon_{uu\text{вмз}}$ of order ⊢0.01o/o. Of interest is the circuit realization of input amplifier (Fig. 2a), device of analog memory of SAP (Fig. 2b) and SAV (Fig. 2c), carried out with the use/application of field-effect transistors and the additionally ensured increased reliability and high input resistance of instrument (not less than 10 aΩ for the signals with highest harmonic component of 1 MHz).

2. Digital oscillograph with memory TsOP-1.

Utilized in the oscillographs with the memory memory/memorizing cathode-ray tubes (ZELT) in principle allow simultaneously with the visual observation of signal to realize the automatic three-dimensional/space coding of its amplitude, instantaneous values, duration, value of front and shear/section. In this case should be utilized an internal reading by the method of the inclusion into the circuit of the collector/receptacle of ZELT of resistor and the digital measurement of the intervals between the pulses of the intersection of the charge patterns of the signal being investigated and calibrated sweep (scale-time conversion [2]). In principle can be processed with the nominal precision/accuracy the single

impulse/momentum/pulse cf any duration, which satisfies the condition:

$$\frac{\ell_p}{t_u} < (V_3)_{max},\qquad (3)$$

where ℓ_p - length of the line of the image of signal, written in the limits of the working part of the target of the ZELT; t_u - pulse duration; $(V_3)_{max}$ - the maximum speed of the recording ZELT used.
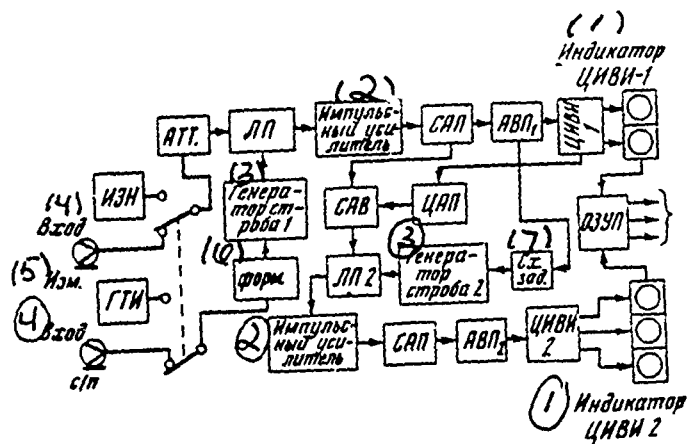
Fig. 1. Block diagram of ITsVM3-4.

Key: (1). Indicator. (2). Pulse amplifier. (3). Generator of gate/strobe. (4). input. (5). Meas. (6). Forms. (7). Delay circuit.
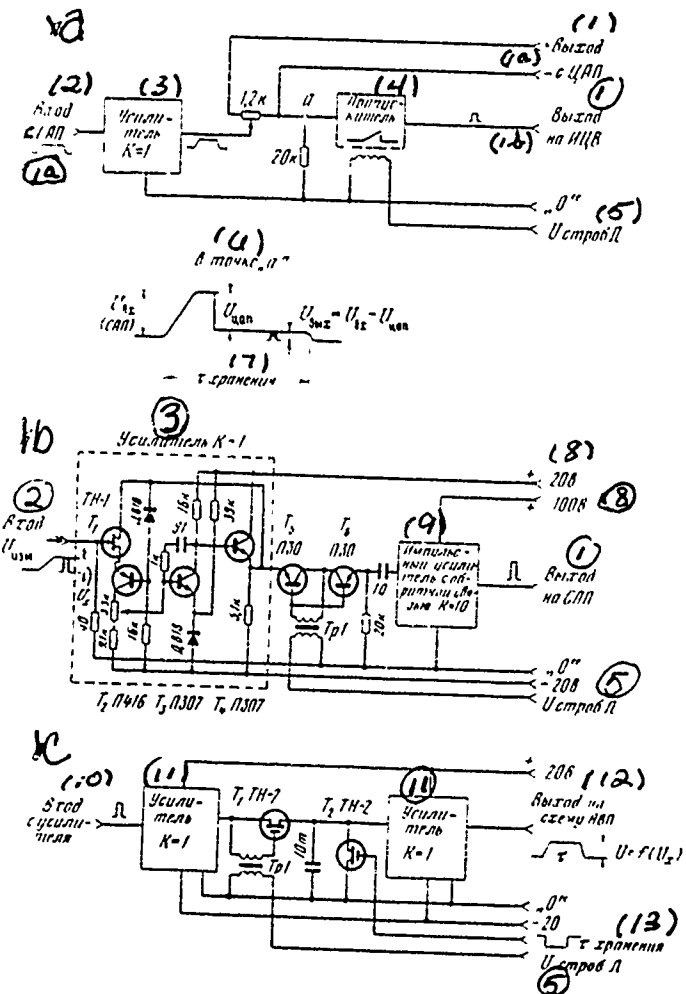
Fig. 2. Input amplifiers with the linear bandpass filter (a), schematic of the device of analog memory (b) and diagram of analog subtraction (c).

Key: (1). output. (2). from TsAP. (3). Amplifier. (4). Bandpass filter. (5). gate/strobe. (6). At point ... (7). storage. (8). V. (9). Pulse amplifier with feedback. (10). Input from amplifier. (11).

Amplifier. (12). Output to circuit. (13). storage.

Page 104.

Fig. 3 gives not requiring special explanations the generalized block diagram of instrument in tne mode/conditions of the measurement of instantaneous values. Fcr measuring the instantaneous values with the high precision/accuracy is utilized the differential method, which expediently combines the advantages of time-pulse (precision/accuracy) and scale-time coding (operating speed). In this case the measured instantaneous value is represented by the sum of two components/terms/addends

$$u_{\text{вх}} = u_{\text{оп}} + u_{\text{вых.огр}} \text{,}$$

where $u_{\text{оп}}$ - voltage of supporting/reference source (limitation level), measured by time-pulse converter: $u_{\text{вых.огр}}$ - instantaneous value at the output of limiter.

The resulting methodological error in the diagram is described by the expression

$$\varepsilon_{\Sigma} = \sqrt{\left[\left(\frac{1}{1+\frac{1}{n}}\right)\varepsilon_{\text{оип}}\right]^2 + \left[\left(\frac{1}{n+1}\right)\varepsilon_{\text{элт}}\right]^2} \text{,} \qquad (4)$$

from which evident that an error in the three-dimensional/space coding of CRT can be reduced in (n+1) once where n - relationship/ratio of signals at input and output of limiter. The

digital equivalent of the measured instantaneous value takes form $N = K f_{uueu} u_{sx}$, where

$$K = \left(\frac{n-1}{n} K_{sun} + \frac{1}{n} K_{snt} \right), \qquad (5)$$

where K_{sun} and K_{snt} - gear ratios of the time-pulsed and scale-time coding converters respectively.

It is evident that under condition $K_{sun} = K_{snt}$ the result of conversions does not depend on n. Furthermore it is apparent that systematic errors in the schematics of instrument average out during the supplying of signal and calibrated scanning/sweep through the general/common/total circuit of vertical deflection, and in mode of the measurement of time parameters - with the combination of the functions GOR and GKR (operating now on the horizontal deflection) in one device/equipment. A real random error of measurement of instrument composed +- 1o/o.

3. Meter of energy of single electric pulse in the resistive load TsIIE.

Instrument is the specialized computer, which realizes the operation/process

$$E = \int_{0}^{t} u i \, dt, \qquad (6)$$

led to the form

$$E = \sum_{i=1}^{n} (u_u)_i (u_i)_i \ \text{with} \ n \to \infty \quad (7)$$

and having built-in analog-digital converters ATsP for obtaining the digital equivalents of the instantaneous values of the pulse of voltage $(u_u)_i$ and current $(u_i)_i$. ATsP are selected in such a way that the operation/process of multiplication is performed in the process of conversion. If we carry out a time-pulse conversion, for example, of values $(u_u)_i$ and pulse-frequency $(u_i)_i$, and then to code interval $T_i = \mathfrak{G}_T (u_u)_i$ by filling on the valve/gate and by the counting of the pulses of frequency $f_i = \mathfrak{G}_f (u_i)_i$, then digital result will be:

$$N_i = (u_u)_i \, \mathfrak{G}_T (u_i)_i \, \mathfrak{G}_f = T_i f_i . \quad (8)$$

In the resulting expressions: $\mathfrak{G}_T$ - conversion factor $(u_u)_i \to T_i$; $\mathfrak{G}_f$ - conversion factor $(u_i)_i \to f_i$. Results on (8) can be further summed up in the recording counter, in this case the indicator of the latter will show the number

$$N = \sum_{i=1}^{n} (u_u)_i \, \mathfrak{G}_T (u_i)_i \, \mathfrak{G}_f , \quad (9)$$

which with sufficiently large n is identical (6).

Block diagram of TsIIE is shown in Fig. 4. The applicability of structure for the construction of TsIIE of narrow pulses (unit ms) is completely determined by the presence of circuit GUCh that corresponds to the following requirements: 1) frequency range

DOC = 80069308 PAGE 440

(0.35-3.5) MHz; 2) instrument error - is not more than +-0.5o/o in the range of temperatures (20+-10) $^\circ$C; 3) $\sigma_f \geqslant 350$ kHz/V.
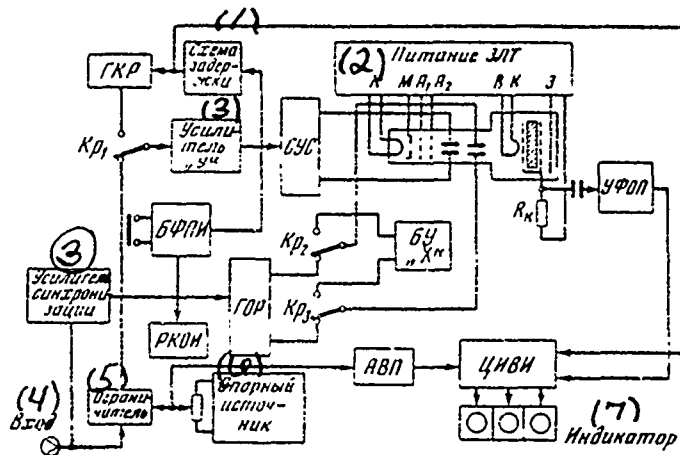
Fig. 3. Block diagram of TsOP-1. GKR - generator of calibrated scan; SUS - balanced amplifier; GOR - generator of oscillograph scanning/sweep; RKOI - relay of commutation oscillograph-measurement; UFOP - amplifier-shaper of the marks of intersection; BU "X" - the block of the setting up of the abscissa of the measurement of instantaneous values; TsIVI - digital meter of time intervals.

Key: (1). Delay circuit. (2). Supply. (3). Amplifier. (4). Input. (5). Limiter. (6). Supporting/reference source. (7). Indicator.
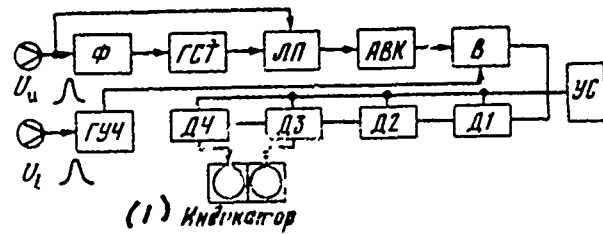
Fig. 4. Block diagram of TsIIE. f - shaper; GST - generator of gate/strobe; LP - linear bandpass filter; V - valve/gate; D -

decade/ten-day period; GUCh - generator of the controlled frequency; US - device/equipment of discharge/break.

Key: (1). Indicator.

Page 105.

The authors proposed use/application as GUCh the diagram of relaxation oscillator on a transistor-tunnel diode relay with the supplementary current amplifier (T_3) in the feedback loop (Fig. 5). When selecting of frequency range is taken in the attention the statistical processing of the results of the coding of intervals T_i with the addition of the large quantity n=100 of their numerical equivalents $N_i = T_i f_i$ in the recording counter, in connection with which this resulting error in the discreteness it is determined by the expression

$$\varepsilon_q \cong \frac{\varepsilon_{q\,max}}{3} . \qquad (10)$$

All instruments examined have an output of standard binary decimal code 1-2-4-8 by printed digital output and ETsVM.
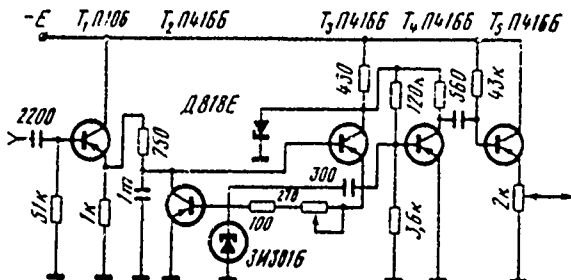
Fig. 5. GUCh circuit.

REFERENCES.

1. V. P. Germaimov, et. al. Precision pulse digital voltmeters
for checking the operation of systems of pulse feed of accelerators
and magnetic measurements. Doklad na I. Bcecoyuznom cofeshchanii
po uskopitelyam [Report to the First All-Union Converence on
Accelerators], 1968.

2. A. I. Petrenko, S. V. Denbnovetskiy. Time-scale converters of
pulse signals]. Kiev, Izd-vo "Tekhnika", 1965.

3. N. V. Malygina. Method of construction of digital wattmeters *tekhnika,*
of dc and ac current collection: "Tsifrovaya elektroizmeritel'naya*,
[Digital electrical measuring technology, Part II, Moscow. Pul.
House of State Committee on instrument building, means of automation
and control systems affiliated with the Gosplan of the USSR, 1966.

Discussion.

L. V. Reprintsev. Are such the advantages of the diagram of the

analog memory with the field-effect transistors in comparison with

the standard by detectors?

V. P. Gerasimov. Advantage consists in the larger time of the

retention/preservation/maintaining information. This is correct for

small amplitudes of input signal, since instead of the nonlinear element/cell is utilized field-effect transistor in the key mode/conditions (relay element/cell).

120. MEASUREMENT OF THE PARAMETERS OF THE ELECTRON BEAM IN CYCLIC
ACCELERATORS USING SYNCHROTRON RADIATION

A. A. Vorobyev, A. N. Didenko, A. V. Kozhevnikov, N. M. Nikitin, V.
P. Tsipilev.

(NII nuclear physics at Tomsk polytechnic institute).   Upon the
acceleration of electrons in the cyclic accelerators to energies on
the order of 100 MeV and above is observed the strong
radiation/emission of electromagnetic vibrations. As is known, the
spectral composition of this radiation/emission is changed with the
energy of electrons E, with E~~100 MeV lies/rests at the visible or
ultraviolet region. Theoretically experimentally this phenomenon is
studied sufficiently in detail [1-3].

On the electronic synchrotron TPI to the energy 1.5 GeV the
synchrotron radiation was utilized for measuring the number of
accelerated electrons, ard also transverse and azimuthal
sizes/dimensions of electron beam during the cycle of acceleration.
Are given below methods, on which were conducted the measurements of
each of the parameters cf the electron beam cf synchrotron enumerated
above.

a) The measurement of a number of particles.

The procedure of the determination of a quantity of accelerated particles is based on the comparison of the measured by optical method intensity of the synchrotron radiation of beam of particles with the calculated intensity of the radiation/emission of single particle in the specific spectral interval. In this case it is necessary to have a radiation detector, calibrated completely with the aid of the standard illuminant. The block diagram of this installation is depicted in Fig. 1. Total luminous flux from the cluster is recorded with the aid of FEU (11, 12). The light/world, by emitted electrons, falls to mirror 4 and through the glass plate of 6 lateral branch pipes is derived/concluded outside. Diaphragm 7 makes it possible to record light/world from the limited section of orbit. Prism 19 makes it possible to divide light/world in the space. With the aid of interference filters 9, 10 of the spectrum of synchrotron radiation/emission are cut out narrow sections at wavelengths 4610 and 8520 $\overset{o}{A}$ respectively. As the standard illuminant was utilized tungsten lamp SI8-200, calibrated completely according to the bright temperature. Its emissivity with respect to the blackbody was taken from work [4]. In view of the various polarizational characteristics of sources from straight/direct comparison is impossible. Therefore

the effect of the optical elements of the installation to the passage
of light/world with different forms of polarization was considered by
Mueller's method [5].

Page 106.

Experiment showed that this monitor of current makes it possible
to define the quantity of particles with precision/accuracy 5-10o/o.
This 2-3 times higher than that precision/accuracy, which provide the
induction sensors. A deficiency/lack in this method is the fact that
in proportion to work deteriorates the sensitivity of the
installation due to the darkening of mirror. The same was noted in
work [6]. Therefore this monitor can be used in conjunction with
other sensors as the control room.

b) The measurement of the transverse sizes/dimensions of beam.

The transverse sizes/dimensions of electron beam were measured
by several methods: by the method of high-speed filming,
electron-optical converter, by photoelectronic conversion and by
method of mechanical scanning with the photoelectronic conversion
(method of rotary disk).

By the method of high-speed filming were carried out the

measurements of the root-mean-square amplitudes of vertical and
radial oscillations beam. Photographing the cross section of electron
beam was conducted by rcvie camera SKS-1M in a rate of 2000
frame(s)/s. The kinograms of the cycle of acceleration contain 75-77
frames/personnel (for the duration of the cycle of acceleration 40
ms). The distribution cf the intensity of radiation/emission over the
section of the image of beam on the kinogram was measured on the
microphotometer MF-4. According to work [7] the half-width of the
obtained microphotograms at the level 0.368 from maximum I_{max} is equal
to the root-mean-square amplitude of the oscillations of electrons.

Density distribution of electrons according to the transverse
section was measured alsc by the photomultiplier FEU-13 by the method
of the mechanical scanning of the image of bundle of electrons with
the aid of the rotary disk with the gashes. In contrast to the method
of high-speed filming, the sizes/dimensions of beam are measured
directly on the oscilloscope face during the work of the accelerator.

With the aid of the photomultiplier and the neutral light filter
of variable/alternating density was determined also the contribution
to the cross section, caused by the fluctuations of the center of
gravity of beam. Depending on the orientation of light filter was
measured a change in the orbit of electrons during the cycle of
acceleration in the vertical and radial directions. This made

possible to consider amplitude and frequency of the center of gravity
of electron beam.

The diagram of experiment with the use of FEU for determining
density distribution of electrons according to section and amplitudes
and frequencies of the center of gravity of beam is depicted in Fig.
2. Fig. 3 depicts the results of this experiment.

c) The measurement of the azimuthal sizes/dimensions of beam.

The instantaneous azimuthal sizes/dimensions of electron beam
were measured by the method of image converter tube. Fig. 4 depicts
the diagram of this experiment. Optical image from the screen of
high-speed gate enters the amplifier of light/world 6, two pairs of
deflector plates of which is supplied hf voltage from the hf
generator of the system of accelerator with a phase difference of
90°.
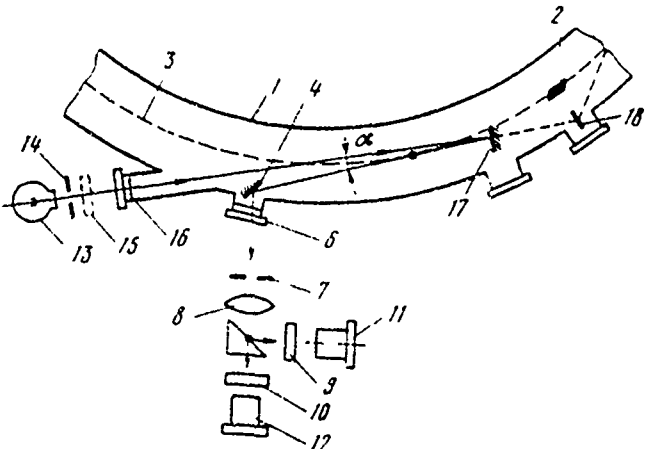
Fig. 1. Measuring circuit of a quantity of accelerated electrons. 1 - vacuum accelerator chamber; 2 - beam of the accelerated electrons; 3 - orbit of electrons; 4, 17 - mirror; 6 - branch pipe; 7, 14 - diaphragm; 8 - objective; 9, 10 - interference light filters; 11, 12 - photomultipliers; 13 - standard illuminant; 15 - light polarizing filter; 16 - glass plane-parallel plate; 18 - screen; 19 - prism.

Fig. 2.

Fig. 3.
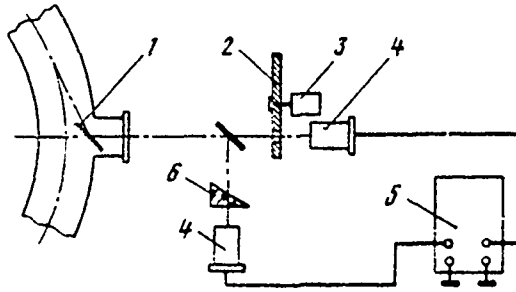
Fig. 2. Installation diagram for measuring of transverse
sizes/dimensions and fluctuation of the center of gravity of electron
beam. 1 - mirror; 2 - disk with the gashes; 3 - electric motor; 4 -
photomultiplier; 5 - oscillograph; 6 - the neutral light filter of
variable/alternating density.
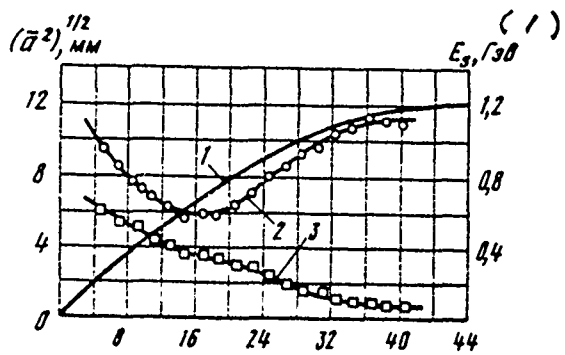
Fig. 3. Change in amplitudes of radial and bouncing of electrons. 1 -
energy of the accelerated electrons; 2 - curve of a change in the
amplitude of radial oscillations; 3 - curve of a change in the
amplitude of bouncing.

Key: (1), GeV.

Page 107.

That obtained in this case on the screen of circular scan corresponds
on the specific scale to the orbit of electrons in accelerator

chamber. The use/application of cascades/stages of the amplification
of light/world is caused by the fact that, in contrast to [8], in the
synchrotron the length of beam must be measured during the short time
interval when energy can be considered constant.

By the method of electron-optical conversion were measured also
the transverse sizes/dimensions of electron beam. Because of the high
speed operation of gate it was possible to obtain the "instantaneous"
cross-sectional view of one bundle of electrons, but not averaged, as
this was in other named above methods.

The measurement of the azimuthal sizes/dimensions of each
individually of bundle of electrons was conducted also with the aid
of the temporary/time photomultiplier of FEU-30 with the resolving
time of 2 ns, which made it possible to determine the length of bunch
of particles without supplementary processing of the results of
experiment.

The given above methods of measuring the parameters of beam
during the cycle of acceleration make it possible to determine effect
on the sizes/dimensions of the beam of the separately betatron and
phase oscillations of electrons. Experimental data are in a good
agreement with the theoretical calculations about the effect of
different factors on the transverse and longitudinal sizes/dimensions
of clusters.

DOC = 80069308   PAGE *453*
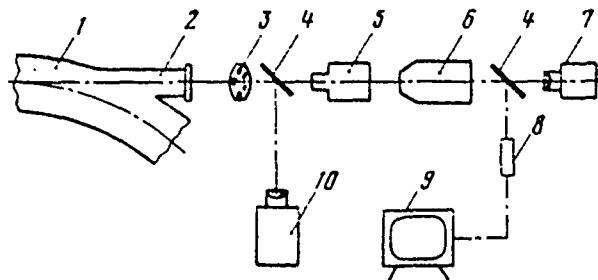
Fig 4. Installaticn diagram for measuring the azimuthal and transverse sizes/dimensicns of electron beam. 1 - vacuum accelerator chamber; 2 - tangential branch pipe; 3 - objective; 4 - semitransparent mirror; 5 - high-speed gate; 6 - amplifier of light/world; 7 - camera RKF-5; 8 - transmitting television camera; 9 - television set; 10 - high-speed/high-velocity movie camera SKS-1.

REFERENCES.

1. Synchrotron Emission. Collection edited by A. A. Sokolova and I. M. Ternova, Izd-vo "Nauka", 1969.

2. F. A. Korolev, A. G. Yershov, O. F. Kulikov, Dokl. AN USSR, [Reports of AS of USSR], 1960, 134, 314.

3. A. A. Vorob'yev, A. N. Didenko, A. V. Koshevnikov. Atomnaya energiya, [Atomic Energy], 1970, 28, 260.

4. V. D. Dmitriyev, G. K. Khlopkov, ZhPS, 1967, 6, 425.

5. U. Sherkliff. Polyarizovannyy svet. [Polarized light.] Izd-vo "Mir", (World), 1965.

6. R. Haensel, B. Sonntag. Appl. Optik, 1967, 38, 3031.

7. A. G. Yershov. ZhETF, 1962, 42, 606.

8. E. I. Zinin, et. al. System of Control and Checking of Parameters of Electron beams in the Electro Electron storage element **Discussion.**   VEP-1. Preprint of IYaF, Siverian Branch of AS of USSR, 1965.

K. A. Belovintsev. Could not you report the data about a change of the longitudinal sizes/dimensions of beam in the process of acceleration?

A. N. Didenko. There are the data, which make it possible to judge beam measurement in the process of acceleration and which make it possible to determine how affect quantum fluctuation separately the radial betatron oscillations and phase oscillations. The method of high-speed filming, which gives total sizes/dimensions, makes it possible to conduct this working. It was, in particular, it is shown that the quantum fluctuations begin to earlier affect phase motion. Later was obtained the more general formula from which it follows that this conclusion is quotient, but general/common/total, since between the energies with which it becomes apparent the effect of quantum fluctuations on the phase and betatron oscillations, there exists this relationship/ratio:

$$E_\phi \simeq \left(\frac{\Omega}{\omega_0}\right)^{1/5} E_\delta ,$$

where E_ϕ - energy with which the quantum fluctuations of radiation/emission begin to strongly affect phase oscillations, Ω - the frequency of phase oscillations, ω_0 - frequency of revolution, E_δ - energy with which quantum fluctuations affect betatron oscillations.

Since always the frequency of phase oscillations is lower than the frequency of revolution, follows conclusion about the universality of confirmation about the fact that the quantum fluctuations first of all affect phase oscillations.

Page 108.

121. Instruments and methods of measurement and check of the three-dimensional characteristics of external beams ARUS.

G. A. Arakelyan, G. S. Vartanyan, S. K. Yesin, I. P. Karabekov, A. M. Kotsinyan, M. A. Martiresyan, Yu. R. Nazaryan.

(Yerevan physical institute).

Monitoring external photon bundles on the Yerevan synchrotron was conducted for the purpose both of determining a number of equivalent γ-quanta, which fall to the target of experimental installations per unit time and determining the effectiveness of the conclusion/output of particles to internal target.

For this was preliminarily determined the constant of Wilson's quantameter (α) with the aid of calorimeter [1], which proved to be equal to $4.55 \cdot 10^{18}$ MeV/coulomb and in the range of energies from 1.5 to 5 GeV it remains constant/invariable with precision/accuracy

+-2o/o, with the filling of quantameter with mixture 80o/o $A_z \div 20\%\ CO_2$.

The effectiveness of the conclusion/output of particles to internal target is determined by the relationship/ratio

$$\frac{Q_M}{I_q \tau} = \xi, \qquad (1)$$

where Q_M - quantity of charge, concluded to internal target for time τ, I_q - the averaged beam current, measured by inductive-type pickup for the same time. Value Q_M can be determined with the aid of bette-Heitler's formula, if we check by quantameter the total flux of energy of bremsstrahlung ε_γ with known thickness of internal target t_0 (in radiation unity) and kinetic energy of electrons at the moment of conclusion/output T_0. However, setting up and introduction of quantameter under the bundle in immediate proximity of internal target is operationally difficultly attained. Therefore for the continuous monitoring of the effectiveness of exit into the annular chamber was established/installed the monitor of the secondary emission (MVE), structurally/constructurally combined with the target as this is shown in Fig. 1a. The calibration of sensitivity MVE was conducted with the aid of the quantameter, established/installed in the direction of the output of γ-beam at a distance of ~18 of m from internal target. Sensitivity of MVE is determined by the formula

$$K = \frac{T_0 \, t_0}{\alpha \, e} \, \frac{Q_{MB3}}{Q_{K8}} \,, \qquad (2)$$

where Q_{MB3} and Q_{K8} - the charges, assembled from MVE and quantameter for time t respectively, e - electron charge.

This value proved to be equal to 0.455 and it remains constant with precision/accuracy +-10o/o in the range of energies 1.5-5 GeV.

The divergence of the characteristic of conversion MVE with respect to the current from the linear law, in entire range of the currents reached, lies/rests at limits of accuracy of measurement.

As can be seen from Fig. 1a, besides MVE of intensity, before the target are established/installed the two additional monitors of the secondary emission, which make it possible to determine the vertical position of bundle in the place of conclusion/output and the stability of this parameter in the time. Actually/really, a change in vertical position from one cycle to the next must lead to an increase in the vertical size/dimension γ - bundle, which must decrease the effectiveness of the transportation of bundle by the experimental targets. Fig. 1b shows the characteristic of the transformation of this sensor.

Measurements showed that the effectiveness of conclusion/output is changed in the considerable limits depending on the adjustment of the deriving/concluding devices/equipment, state of magnetic system and from the configuration of the real relief of vacuum chamber. Here has in mind the setting up of one or the other devices/equipment into vacuum chamber, in particular, the output units of electron beam, etc. Therefore for an improvement in conditions of conclusion is necessary information about density distribution of the precipitation of particles according to the perimeter of accelerator at the moment of conclusion/output. For this purpose on the perimeter the rings in the places, close to the maximum of the function of floquet |F|, are established/installed the sensor of the bremsstrahlung, which measure the intensity of the high-energy part of it spectrum.
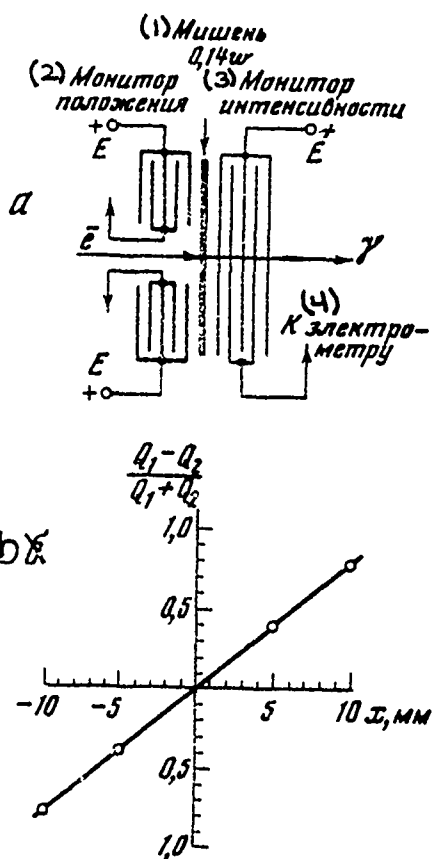
Fig. 1. Draft of the monitor, combined with internal target (a), and the characteristic of the transformation of the monitor of vertical displacement (b).

Key: (1). Target. (2). Monitor of position. (3). Monitor of intensity. (4). To electrometer.

Page 109.

As the same were tested thick-walled ionization chambers. These chamber design is determined by the configuration of site of installation, and wall thickness is determined by maximum energy of the accelerated particles.

After conducting of a comparative calibration of sensitivity of the camera the obtaining and information processing from them must be conducted as follows. During brought-out internal target and taken excitation of output units at the moment of achieving the prescribed/assigned energy is turned off/disconnected accelerating voltage. Asymmetry of readings of the sensors of bremsstrahlung informs about the presence of the extreme points where first of all is satisfied the condition

$$\tau_0(\theta) + \psi(\theta)\frac{n\Delta T}{T_0} = A(\theta), \qquad (3)$$

where as is known (for example, see [2]), $\psi(\theta) = |F_\tau|\frac{\bar{\rho}\sqrt{\nu_\tau}}{(M\nu_\tau)^2}$, $\tau_0(\theta)$ — the coordinate of equilibrium orbit at point at the moment of conclusion/output, ΔT — energy gain per revolution; n — speed, during which the bundle is displaced into vacuum chamber; $\bar{\rho}$ — the mean radius of ring; F_τ — modulus/module of the function of floquet; ν_τ — radial frequency of betatron; M — number of periods of gradient.

Further with connected accelerating field and brought-out target is conducted the excitation of the deriving/concluding

devices/equipment. If for a period of time of excitation sensors do
not show the appearance of radiation/emission on the perimeter, then
orbit distortions, created by the deriving/concluding settings up,
lie/rest within the limits of allowances.

For increasing the precision/accuracy of the laying out of
bundles γ - quanta, combination of the axis/axle of bundle with the
principal axis/axle of experimental installations, decrease of
cluster time for the setting up of collimators and correct
determination of the coefficients of collimation, and also for the
continuous monitoring of the position of the axis/axle of bundle, is
utilized the instrument for measuring the center of gravity γ -
bundle. Instrument is ionization chamber with the symmetrically cut
collecting anode, as shown schematically in Fig. 2a. Fig. 2b shows
the set of characteristics of the transformation of sensor in the
coordinates of displacement x and ratio Q_1-Q_2/Q_1+Q_2, where Q_1 and Q_2
- charges, measured from the individual parts of collecting anode,
for the different values of radii of bundles ($R_{пуч}$). Is remarkable the
fact that in the thickness of front/leading chamber wall h, equal to
2 mm, the achievement of relationship/ratio $\frac{Q_1-Q_2}{Q_1+Q_2} = 0,78$ corresponds
to the displacement, equal to a radius the knob/arm/handle. The
precision/accuracy of the determination of the center of gravity γ -
bundle is limited by the accuracy of the measurements of values of Q_1
and Q_2 and in the experiment composes ~2-3o/o of the diameter of

bundle.

Fig. 2c shows the set of characteristics of transformation, obtained at constant value $d_{nyq} = 19$ mm, but at the different values of the thicknesses of front/leading wall (h). From these curves it is evident that mutual conductance of transformation increases proportional to h. So proportionally increases contrast during the determination of the diameter of bundle.

The described methods of the detection of the position of internal and external bundles, and also the possibility of continuous monitoring of the effectiveness of conclusion/output make it possible to construct the logic of the stabilization systems of external beams ARUS.

Fig. 3 shows the system of the location of sensors circuit γ - bundle and the block diagram of processing obtained information, which makes it possible to stabilize the position of the axis/axle of bundle, and to also automatically change its intensity from the counting rate of basic experimental installation. Here DI - the sensors of intensity, DP - the position detectors γ of bundle, KV - quantameter, MVE - monitor of the secondary emission of intensity, K_1, K_2 and K_3 - collimators, 1 - the block/module/unit of the continuous determination of ratios $\frac{Q_{MK_1}}{Q_{K6}}$ and $\frac{Q_{MK_2}}{Q_{K6}}$. In the case of the

divergence of these relations from the assigned magnitudes at the output of block/module/unit 1 will appear the signal, which comes simultaneously 3 and 5. Block/module/unit 2 come the signals from the position detectors of the center of gravity δ of bundle. In the presence of signal at the output of block/module/unit 2 block/module/unit 3 develops the signal which enters the entrance of block/module/unit 4, which controls angle of slope γ - bundle. Block/module/unit 6 determines relation ξ.
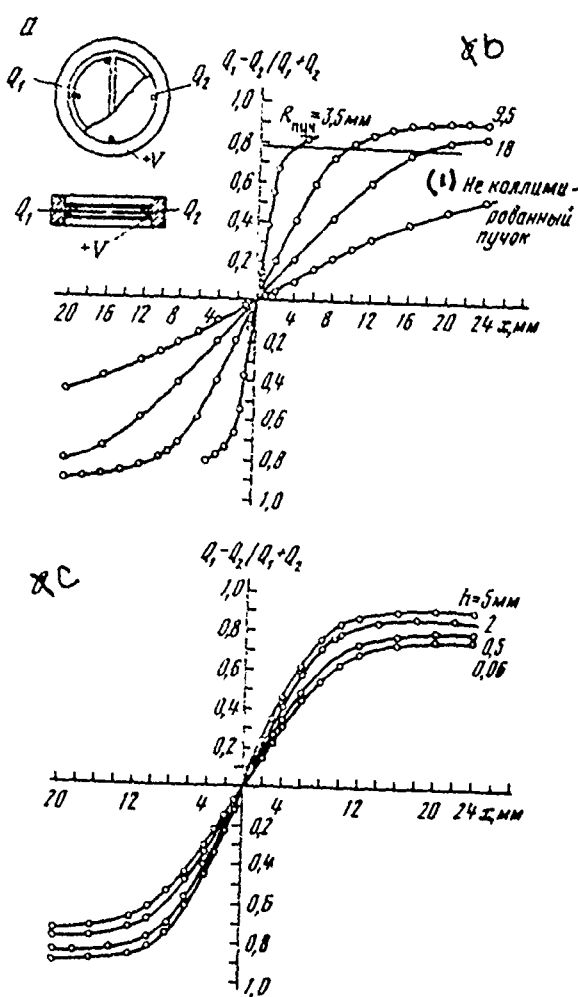
Fig. 2. Monitor of the position or axis/axle γ of bundle (a) and its characteristic of transformation (b, c).

Page 110.

If this value changed with a simultaneous change in ratios $\frac{Q_{uk_1}}{Q_{k6}}$ and

$\frac{Q_{uk2}}{Q_{x6}}$, then is developed the signal at the entrance of

block/module/unit 7, starting device of the final adjustment of the

position of internal beam according to the described above method.

Block/module/unit 8 records the average/mean counting rate of useful

events and with its change puts out signal to block/module/unit 9,

which controls the redistribution of a number of cycles per s   d,

concluded along this channel.
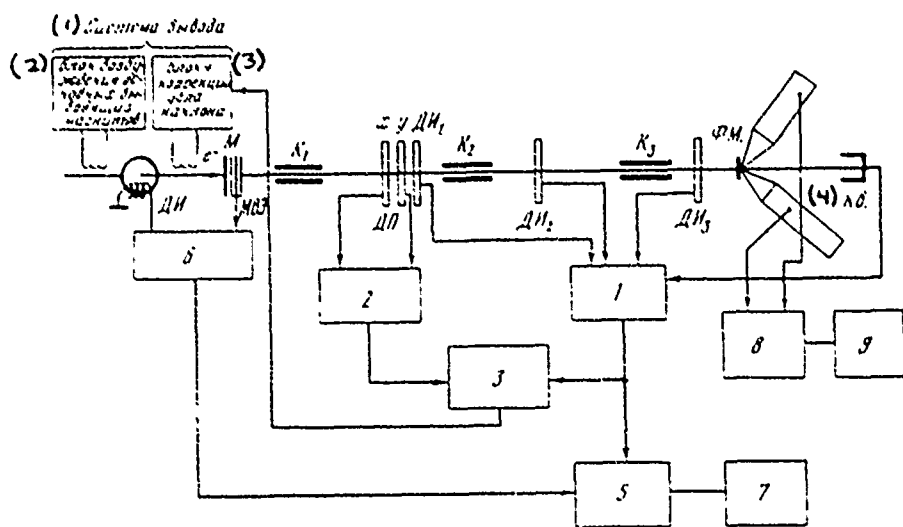
Fig. 3. Distribution of sensors according to the circuit and system

block diagram of the automatic stabilization of the space-time

characteristics of external ones γ - bundles.

Key: (1). System of conclusion/output. (2). Block/module/unit of

exciting permanent deriving/concluding magnets. (3).

Block/module/unit of 4 corrections of angle of incidence. (4). kV.

REFERENCES.
1. S. P. Kruglov, et al. Determination of sensitivity of a Gauss
    quantum meter and Wilson quantum meter in an energy range of
    1 to 4.75 GeV on an Accelerator beam of gamma quanta of the
    accelerator of Yerevan. Physics Institute PTE, 1970, No. 6,216.
2. S. A. Kheyfets. Electronic Synchrotrons. Yerevan. Publishing
    House of Academy of Sciences of Armenian SSR. 1963.

Discussion.

A. V. Kochegurov. What system of control of photon bundles is utilized in your diagram: according to the divergence or extreme?

I. P. Karabekov. For the correction of position and angle of photon bundle are utilized the devices/equipment of the type of servo systems. By presetting is established/installed the necessary mode/conditions of bundle, and then are switched on the devices/equipment of stabilization according to the divergence.

K. A. Belovintsev. Which the accuracy of the measurement of the center of photon bundle with the aid of sector ionization chambers?

I. P. Karabekov. Precision/accuracy depends on the diameter of bundle and with the available electrometers comprises not more than 1/30 this diameter.

A. Ya. Belyak. Which the stability of bundle in the prescribed/assigned by conclus.on/output channel?

I. P. Karabekov. With the stable work of the accelerator the stability of the intensity of bundle in the channel is not worse than +-15o/o.

K. D. Johnson. What gas is utilized in ionization chamber?

I. P. Karabekov. Air.

G. V. Bagdalyan. In the control system has the capability of the
control of the angle of the incidence/impingement of electron beam to
the target in the horizontal plane. This is reached with the aid of
the supplementary windings on the blocks/modules/units of
electromagnet which give the possibility to regulate this angle in
the limits of +-0.5 mrad. The system of correction is based on
current control in these windings.

   Prolonged observations showed that the route of bundle is
sufficiently stable, and its divergences on the basis 30-40 m do not
exceed several millimeters (to 5-6 mm). Large divergences it was not.

   On the vertical line were observed the departures/attendance of
bundle because in the section of the conclusion/output where is
arranged/located physical equipment, are located massive shielding
blocks, and the shrinkage of foundation led to the slant of magnet
blocks and to the divergence with respect to the apexes/vertexes (on
the basis 40-50 m) on 8-10 mm. In order to remove these divergences,
it was necessary to restore/reduce the position of magnet blocks.

Page 111.

122. Automatic measurement of phase volume on the Yerevan synchrotron.

V. N. Arutyunyan, G. V. Badalyan, P. G. Vasilenko, S. K. Yesin, V. K. Krol', V. L. Serov.

(Yerevan physical institute).

Is known the series/row of the methods of the automatic measurement of the phase volumes or bundles, injected into high-energy accelerators [1-3]; however, they all provide for work in the mode/conditions of the rarely repeating and comparatively long impulses/momenta/pulses and in connection with this they are unsuitable for measuring the phase volume of the injector of the Yerevan synchrotron, which gives current pulses with the duration of 1.5 μs with the frequency of 50 Hz, the energy 50 MeV and the currents in the impulse/momentum/pulse 150 mA. Is known method [4] for the analogous accelerator (DESY in Hamburg), deficiency/lack in which is the fact that the scanning on the coordinate is conducted by the mechanical displacement of the collimating shutter in the vacuum, and scanning on the angle is accomplished/realized with the aid of HF

capacitor/condenser, adjusted within electron conductor.

In the present work is described the method, which makes it
possible to fully automate these measurements without the mechanical
displacement of shutters in the process of measurement. The essence
of method consists of the following. All displacements of beam are
accomplished/realized with the aid of the magnetic deflecting system,
established/installed out of the vacuum volume of electron conductor.
By the parallel displacement of the beam of particles relative to
first motionless collimator slots are cut out the consecutive
sections of beam section and then are determined the critical angles
of the disagreement of each cut out part of the bundle by their
divergence relative to the second fixed slit. The determination of
the critical angles of disagreement is accomplished/realized by means
of the established/installed after the second slot sensor of
intensity signals from which modulate the brightness swellling of
oscillograph. In this case the ncrizontal sweep swellling of
oscillograph it is synchronized with the parallel displacement of
beam of particles, and the vertical deflection of the light beam of
oscillograph is synchronized with the divergence of the cut out part
of the bundle relative to the second slot. This synchronization makes
it possible to reproduce on the cscilloscope face the phase volume of
bundle on the specific scale.

The block diagram of device/equipment for the automatic measurement of phase volume is given in Fig. 1. Dual deflecting magnet 1 is supplied from the sawtooth current generator 6 with rise time of saw 20 s and currents 0-500 mA, and provides the parallel beam displacement of electrons with the energy 50 MeV on 0.1 mm on 1 mA of current in the magnet. Single deflecting magnet 3 is supplied from the sawtooth current generator 7 with rise time of saw 0.5 s and currents 0-750 mA and provides the rotation of bundle at an   angle of 0.03 mrad on 1 mA of current in the magnet. As the meter of beam current 6 serves toroidal ferrite sensor with the sensitivity of 1 mV/mA, signals from which through the amplifier with the amplification factor by 1000 are supplied to the special modulator of the brightness of the light beam of oscillograph.

The width of slots is selected as being equal to 1 mm in order to have the capability to sufficiently thinly investigate the structure of bundle and to obtain in this case the signals from the meter of current, which exceed interference level.

Minimum speed of the displacement of the beam before the first slot determines the time (order 20 s), necessary for obtaining of one full/total/complete frame on oscilloscope face. A decrease in the velocity of the displacement of beam although raises the accuracy of measurement, impedes the observation of the form of phase ellipse due

to the insufficient time of the screen afterglow of oscillograph.

The scanning time of the cut out part of the bundle before the second slot is selected equal to 0.5 s from the compromise considerations, since, on one hand, this time must be much less than the time of the displacement of the beam before first slot (in contrary case is reduced the accuracy of the measurement of the coordinate of the cut cut part of the bundle), on the other hand, this time must be much more than the repetition period of current of the bundle being investigated (otherwise is reduced the accuracy of the measurement of the critical angles of disagreement).

The final selection of the width of slots and time of scanning on the coordinate and the angle is accomplished/realized taking into account the concrete/specific/actual parameters of the bundle being investigated and sensitivity of equipment for measuring the beam current.

in this article is examined only the measurement of phase ellipse in the horizontal plane. The measurements of vertical phase ellipse are made analogously.
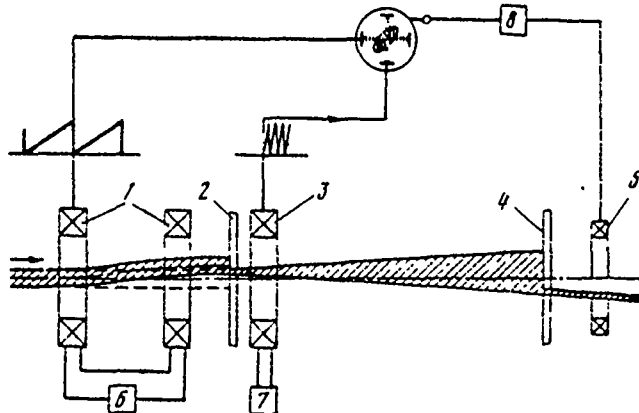
Fig. 1. Block diagram of device/equipment for the automatic measurement phase volume. 1 - dual deflecting magnet; 2 - first collimating slot; 3 - single deflecting magnet; 4 - second collimating slot; 5 - meter of beam current; 6, 7 - sawtooth current generators; 8 - modulator of the light intensity of oscillograph.

Page 112.

Fig. 2 depicts the horizontal emittance, obtained by the method of the mechanical scanning of bundle with the aid of two movable collimating slots.

The horizontal emittance, constructed on the basis of the measurement of coordinates and angles via the discrete/digital scanning of bundle the magnetic field of the relative to motionless slot is given in Fig. 3.

From the examination of Fig. 2 and 3 it is evident that the ellipses, obtained by these methods, greatly insignificantly differ one from another.

The ellipse, observed on the oscilloscope face (Fig. 4), is analogous given in Fig. 2 and 3.

Error of measurement of the phase volume of order 20o/o.
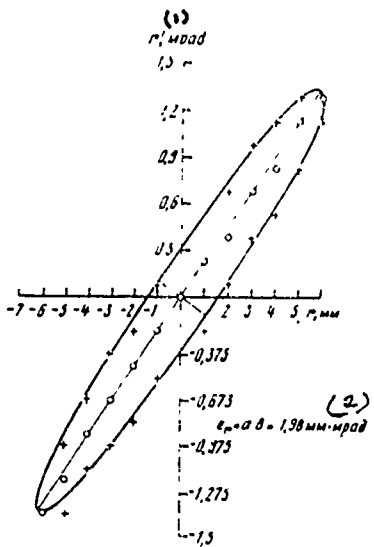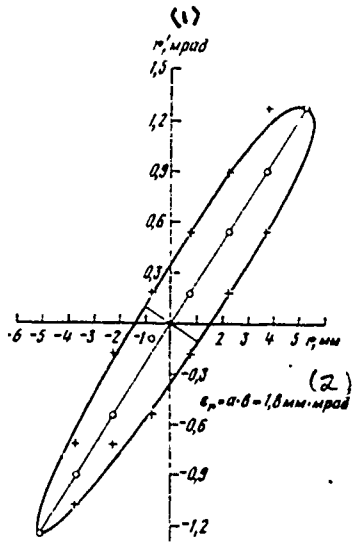
Fig. 2.

Fig. 3.

Fig. 2. Horizontal emittance, obtained by "method of two slots".

Key: (1). mrad. (2). mm•mrad.

Fig. 3. Horizontal emittance, obtained via scanning of bundle by magnetic field relative to fixed slits.

Key: (1). mrad. (2). mm•mrad.
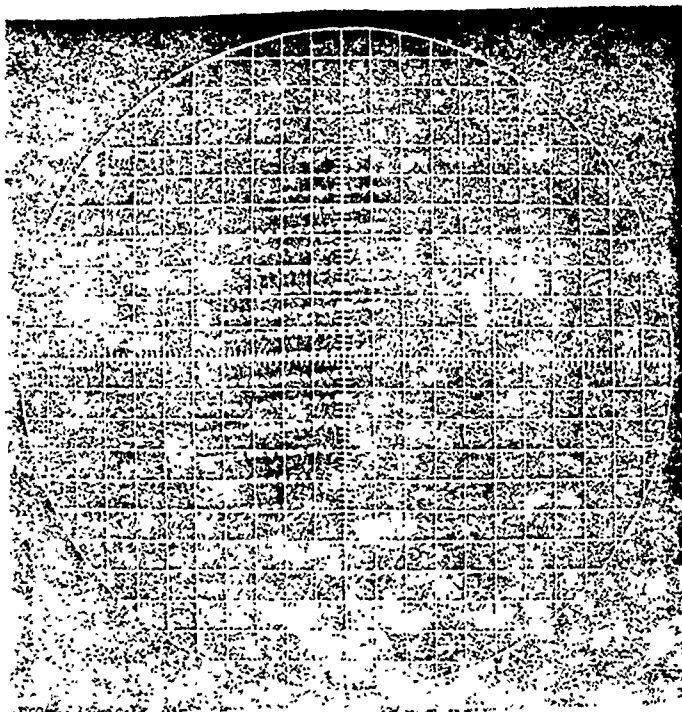
Fig. 4. Horizontal emmitance. obtained by automatic method on the

oscilloscope face.

REFERENCES.

1. V. A. Batalin, V, Yu. Moguchev. Measurements of the phase current
   density of the pulse beam of protons. PTE, 1966, No. 5, p. 26.

2. Th. Sluyters, et al., JEEE Trans on Nuclear Sci., 1967, v.NS-14,
   N 3, p. 1143-1150.

3. D. A. Demichousky, E. F. Trojanov. Proc. Sympos. on Beam Intensity.
   Measurement, 1968, p. 244-251.

4. W. Gentschke, et al. Atom wirtschaft, 1964, N 7, S.304-307.

Page 113.

123. Device/equipment for the resonance excitation and measuring the betatron oscillations of proton synchrotron IFVE.

A. M. Gudkov, A. A. Kuz'min, V. Ye. Pisarevskiy, G. F. Senatorov, I. I. Sulygin.

(Institute of high-energy physics; the radio engineering institute of the AS USSR).

For the investigation of the dynamics of the particle motion, position of operating point in the cage/cell of frequencies of the betatron in the process of acceleration in entire range of energies on the proton synchrotron IFVE was developed and realized the special device/equipment, which maximally uses the available on the accelerator equipment.

In works [1-3] are in detail described the methods of measuring the betatron oscillations. All these methods are connected either with the measurement of the distortions of the equilibrium orbit which appear upon the inclusion/connection of permanent disturbance/perturbation on certain azimuth of the ring of

accelerator into the interesting researchers cycle time or with the measurement of period of coherent betatron oscillations. In work [1] it is proposed to plot the amplitude-phase curve of the response of bundle to the resonance excitation and of it to reduce the function of particle distribution in the bundle according to the frequencies of betatron.

The authors stopped at the resonance method of exciting the betatron oscillations. The estimations, carried out on the basis of works [1, 3], showed that if we assign the amplitude of steady-state oscillations, equal to 1 mm, and by the scatter of frequencies of the betatron $\delta Q=0.01$, then on the maximum energy in 70 GeV it is necessary to create in the straight portion with a length of 1.5 m variable resonance field with the stress/voltage $\sim 8 \cdot 10^{-3}$ V. If we consider it possible that the frequency of betatron Q during entire cycle of acceleration can be changed in the limits from 9.55 to 9.95 f_0 (where f_0 - frequency of revolution of particles), then the band of the generating device/equipment must be order 80-90 kHz. During calculations it was assumed that the bundle is not monoenergetic; the width of the resonance frequencies of the bundle is determined only by the scatter of particles by the frequencies of the betatron of frequency of vertical and radial are sufficiently spread.

Calculations showed the possibility of using as the

high-frequency power amplifier any of the accelerating stations of
proton synchrotron IFVE [4] with the minimum, undemanding essential
expenditures of forces, resources and time, alterations.

The block diagram of exciter is shown in Fig. 1. Signal from the
master oscillator of syncnrotron with the frequency $30f_0$ through the
key/wrench, which is determining beginning and duration of
high-frequency "packet" and phase inverter, comes the entrance of the
accelerating station, it is amplified and is supplied to the
actuating element/cell - exciting plates. The given above value of
maximum stress/voltage - 8.0 sq. ampl. - was obtained with the
geometry of plates, which is optimally entered in the overall design
of the end devices of station. The supplementary
capacity/capacitance, introduced by plates into the resonance system
of the final stage of station, is compensated by the decrease of the
value of the fine-adjustment (shortening) capacitors/condensers of
resonator.

Input signal $30f_0$ is supplied also to the divider, which has
exit frequency $30f_0/K$, where K - can take any value in the limits
from 60 do 300 with the step/pitch through unity. Stress/voltage from
the divider enters the control grid of the second cascade/stage of
the station where is accomplished/realized a deep (to 100o/o)
amplitude modulation of the carrier frequency. During the preliminary

search of resonance frequencies the modulating stress/voltage can be supplied from the usual audiofrequency oscillator.

The exit stress/voltage or device/equipment is correspondingly phased with accelerating voltage of the entire system of stations.

The system of the automatic frequency control (APCh) of station works according to the principle of the continuous, monotonic rearrangement of resonator from the low frequency to the high. So that the pulse signal or "packet" (with the work on the average/mean and high energies) would prove to be within pull-in range of system APCh and the fronts of the increase of output potential would be minimum, was used the special system of the preliminary magnetic biasing of ferrite and adjustment of resonator in the required signal frequency.

For the possibility of the operational changeover of the system of driving with R to Z of oscillation and vice versa was realized special switching circuit. Diagram makes it possible to also carry out switching on of all four plates for the creation of quadrupole field. As the commutating elements/cells are used vacuum switches with electromagnetic control.
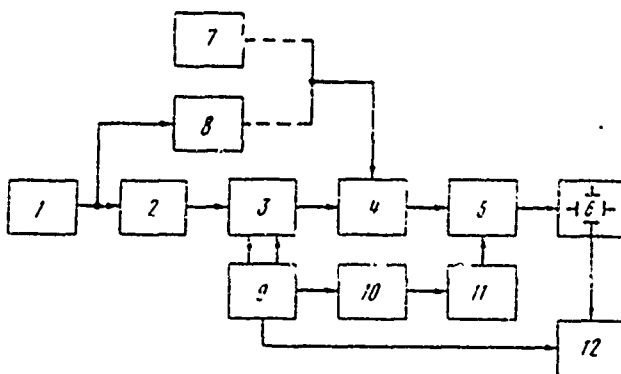
Fig. 1. Block diagram of the exciter of betatron oscillations. 1 - master oscillator; 2 - phase inverter; 3 - key/wrench; 4 - power amplifier; 5 - resonator; 6 - exciting plates; 7 - oscillator of low frequency; 8 - synchronous divider; 9 - timer; 10 - waiting multivibrator; 11 - dc amplifier; 12 - oscillograph.

Page 114.

The procedure of the adjustment of the exciter of betatron oscillations consists of the following: 1) at the moment of the cycle of the acceleration, which interests researcher, is switched on and is adjusted high-frequency packet. Its amplitude and form are checked on the oscillograph. Amplitude is established/installed in accordance with the energy of protons; 2) from the frequency divider or from the audio signal generator is supplied the modulating signal and simultaneously is checked the filtered and amplified differential signal from the sensitive signal electrodes. Selecting frequency and

depth of modulation, operator attains the maximum amplitude of response.

Fig. 2 shows the characteristic oscillograms of the adjustment of the mode/conditions of excitation and measurement. The block diagram of observation and measurement of frequencies of the betatron is shown in Fig. 3.

Observing the process of the building up of oscillations and their fading after the disconnection of the signal of excitation, it is possible to evaluate the scatter of particles in the bundle in the frequencies of betatron and to determine with the high precision/accuracy the supplement of frequency of betatron to the nearest integer.   Frequency of betatron can be determined in the modulation frequency, but this procedure does not give the required precision/accuracy because from one cycle to the next due to the instabilities of the parameters of accelerator somewhat are changed excitation condition. Therefore the precise measurement of frequency of betatron was carried out with the aid of the device/equipment, which measures the period of free oscillations after the disconnection of excitation. Device/equipment makes it possible to isolate at will of operator from one to seven periods of free oscillations and with the aid of the counter to conduct the count of a number of impulses/momenta/pulses, which follow with the frequency $30f_0$ and which fill the chosen interval.
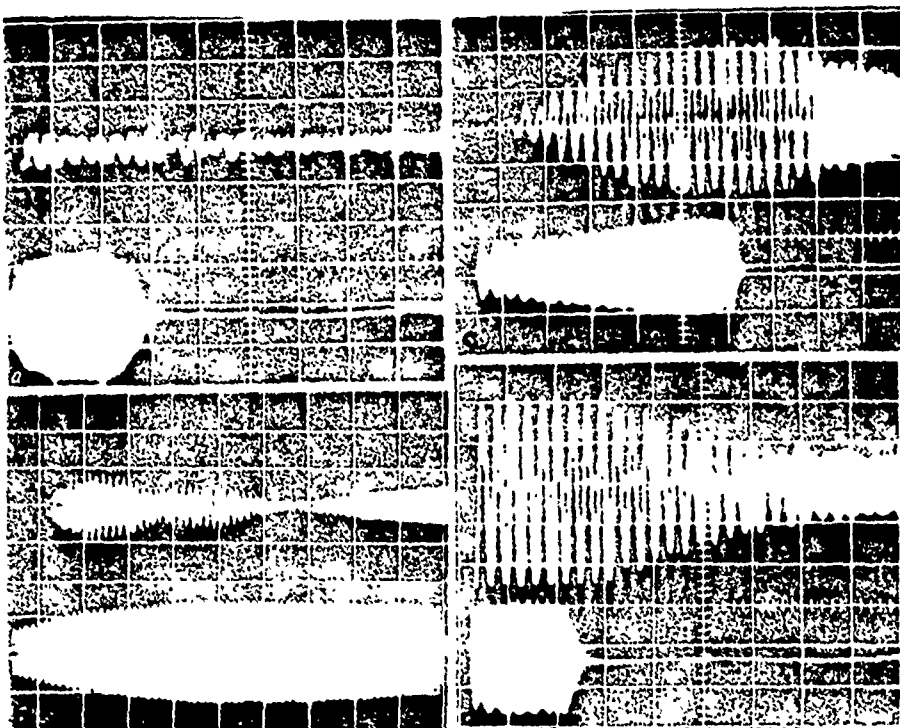
Fig. 2. The oscillograms of the mode/conditions of the adjustment of the excitation of the betatron oscillations: a) the frequency of excitation is distant from the resonance. Scanning/sweep 0.05 ms/cm. Sensitivity 10 and 0.25 V/cm; b) the frequency of excitation close to the resonance. Scanning/sweep 100 µs/cm. Sensitivity 10 and 0.25 V/cm; c) a precise resonance. Scanning/sweep 0.5 µs/cm. Sensitivity 10 and 0.5 V/cm; d) the end/lead of the excitation. Scanning/sweep 50 µs/cm. Sensitivity 10 and 0.5 V/cm. In all oscillograms upper ray/beam - the signal or response, lower ray/beam - excitation.
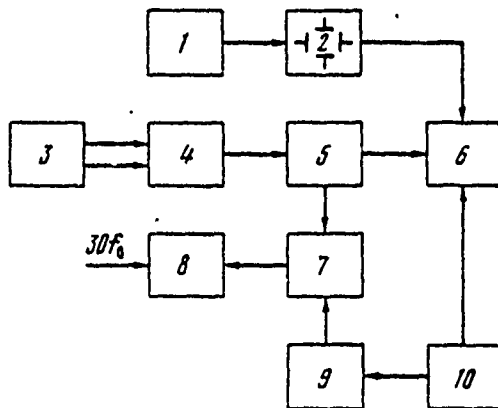
Fig. 3. The block diagram of excitation and measurement of frequencies of the betatron: 1 - system of the resonant step-up; 2 - exciting plates; 3 - signal electrodes; 4 - differential amplifier; 5 - filters of low frequencies; 6 - oscillograph; 7 - device/equipment for isolation/liberation 1, 3, 5, 7 - periods; 8 - counter; 9 - controlled delay; 10 - timer.

Page 115.

The error in measurement in this case can be calculated according to the following formula

$$\Delta q_n = \pm \frac{1}{30n} q^2,$$

where Δq_n the error in interval measurement in p - periods; n - number of measured periods; q - supplement Q to the nearest integer.

Is possible to easily ascertain that the maximum error is obtained with q=0.5 and n=1 comprises ~+-8.3•10⁻³.

In the measurement of seven periods and q=0.1 the error does not exceed +-5•10⁻⁵. Under the actual conditions for the measurements, which were being carried out on the synchrotron, the error did not exceed 5•10⁻⁴.

Thus, on the accelerator IFVE to the energy 70 GeV were carried out the measurements of frequencies of the betatron in entire range of energies. Measurements were conducted without the interferences with physical experiments, since the amplitude of the building up of oscillations in entire cycle of acceleration did not exceed 1 mm.

The results of the measurements of frequencies of the betatron employing the described procedure on the high energies were utilized for calculating the systems of conclusion/output; on the low energies - for the selection of optimum correction and preliminary investigations of work of the accelerator with the high currents.

The authors express appreciation to G. G. Gurov, K. F. Gertsev, A. A. Rukin, who rendered great assistance in the adjustment of equipment and conducting of measurements.

REFERENCES.

1. V. A. Uvarov, G. F. Senatorov. Change in frequency of betatron oscillations by the method of resonant excitation. Instruments and technique of experiment. 1968, No 6, p. 20.

2. S. A. Kheyfets, S. K. Yesin. Simple method of measuring the frequency of free transverse oscillations in a synchrotron. Atomic Energy, 1965, 18, issue 1, p. 60.

3. G. Schneider. Fast Q-measurement at the CPS. CERN/MPS"SR/69-10, 1969.

4. B. M. Gutner, et al. Accelerating resonators and powerful high-frequency equipment for their excitations of the proton synchrotron at 70 GeV, IFVE. Transactions of All-Union Conference on accelerators of charged particles. Vol II. 1970, p.101.

124. Reconstruction of the accelerating stations of proton synchrotron IFVE.

B. M. Gutner, V. Ye. Pisarevskiy, V. V. Polyarkov, I. I. Sulygin, V. A. Sichev, B. K. Shembel'.

(Institute of high-energy physics).

With design and modernization of contemporary accelerators is logical the tendency to arrange/locate a maximum quantity of technological equipment beyond the limits of radiation-hazardous zone [1, 2]. This raises the reliability of the work of systems, increases the service life of parts and assemblies of equipment due to the elimination of the effect of radiation, facilitates maintenance/servicing, gives the possibility of conducting repair work without stopping of accelerator. Special importance this principle of the arrangement/position of equipment acquires with the contemporary tendencies toward a considerable increase in the intensity of accelerators and duration of the performances of their continuous work. On the basis of these considerations, in IFVE was developed the project of the reconstruction of the accelerating stations, after actualization of which in the circular hall of

accelerator remain only the resonator, the output stage and the system of their cooling. Block diagram and location of the equipment of existing station [3] are shown in Fig. 1 of that reconstructed - in Fig. 2.

Project allows for the possibility of simultaneous operation of the existing and reconstructed stations, which makes it possible to realize it gradually, without special accelerator shutdown.

It is given below the analysis of the diagram of the HF supply of the output stage on the cable and the basic results of experiment.

Agreement of HF cable in the range of frequencies.

At present signal from the master oscillator is opened to the separate stations on the matched HF cables at the level 3 V. With the carrying out of prefinal cascade/stage appears the problem of the agreement of cable with input circuit of lamp GU-47B in the range of the frequencies of 2.5-6.1 MHz at the level 150-200 V.

In the broadband diagram of agreement the power of penultimate cascade/stage proves to be equal to several hundred watts. In this case is required the use/application of a 2- kilowatt lamp with the forced cooling and appear difficulties with the arrangement/position

of preliminary HF circuit.

The economical diagram, which ensures satisfactory agreement, can be realized by the use/application of the reconstructed in the range contours/outlines (Fig. 3). For this diagram: $\frac{u_2}{u_o} = \frac{(1+P_2)\,e^{-\gamma\ell}}{1-P_1 P_2\,e^{-2\gamma\ell}}$. Here $u_o = I_1 \frac{z_1 \cdot W}{z_1 + W}$ - amplitude of the incident wave; P_1, P_2 - reflection coefficients from the oscillator and from the load; $\gamma = \alpha + jm$ - propagation constant; α - decay constant; m - phase constant.

Page 116.

Diagram assumes obtaining the linear phase shift between u_2 and I_1. If the first (anodic) contour/outline is accurately adjusted into the resonance, and KSB in the feeder is different from 1, then obtaining linear phase shift is possible only due to the complexity of the input resistance of the second (grid) contour/outline, i.e., due to its detuning. The angle of this detuning is determined from the relationship/ratio

$$tg\,\varphi = \frac{2a\,tg\,m\ell}{6 + d\,tg^2 m\ell} ,$$

where $a = (K_1 - 1)(K_2 - 1)e^{-2\alpha\ell}$; $6 = (K_1 + 1) + (K_1 - 1)e^{-2\alpha\ell}$;
$d = (K_1 + 1) - (K_1 - 1)e^{-2\alpha\ell}$; a $K_1 = \frac{R_1}{W}$ and $K_2 = \frac{R_2}{W}$.

- KSV in the direction to the oscillator and in the direction to the load. Maximum detuning $tg\,\psi_{max} = \frac{a}{\pm\sqrt{3}d}$ is obtained when $tg\,m\ell = \pm\sqrt{\frac{\delta}{d}}$.

Rate of change in the phase of contour/outline

$$\frac{d\varphi}{d(m\ell)} = \frac{2a(1+tg^2 m\ell)(\delta-d\cdot tg^2 m\ell)}{(\delta+d\cdot tg^2 m\ell)^2 + 4a^2 tg^2 m\ell}$$ has maximum $\left.\frac{d\varphi}{d(m\ell)}\right|_{max} = -\frac{2a}{d}$ when $tg\,m\ell = \infty$.

The change in the phase angle of contour/outline, necessary for obtaining of linear phase shift in the feeder, presents supplementary requirements to the speed of the rearrangement of the frequency of the contour/outline

$$\dot{f}_\kappa = \dot{f}_\iota\left(1 + \frac{d\varphi}{d(m\ell)}\,\frac{\pi f_\iota \tau_\varphi}{Q}\right).$$

Here $\tau_\varphi = \frac{\ell_\varphi}{c}$ - delay time in the feeder; $\dot{f}_\iota$ and $\dot{f}_\kappa$ - rate of change in the frequency of the master oscillator and frequency of contour/outline.

The given analysis is made on the assumption that the first contour/outline is adjusted into the resonance, i.e., $Z_1 = R_1$. The parameters of circuit, used in the project, virtually satisfy this requirement. Both contours/outlines are wound on the identical ferrite rings, has an identical quantity of turns of magnetic biasing and they are reconstructed by one current. Energy factor of the loaded plate circuit $Q_1 = 1-1.5$; grid $Q_2 = 7-10$; $K_2 \leq 2$; $K_1 \leq 5$ taking into account the internal impedance of oscillator; $e^{-ia\ell} = 0,5$. To these data

corresponds comparatively small angle $\varphi_{max} = 20°$. In this case the detuning of plate circuit does not exceed 2-3°, i.e., contour/outline is virtually adjusted and initial assumption is correct.

Contour/outline are reconstructed by the static system of self-alignment the phases (APF_1) of oscillations on the grid of output tube under the phase of the input signal, which passed through the cable of delay (Fig. 2). With a comparatively low coefficient of the control of system $K=25$ the static error does not exceed 20°.
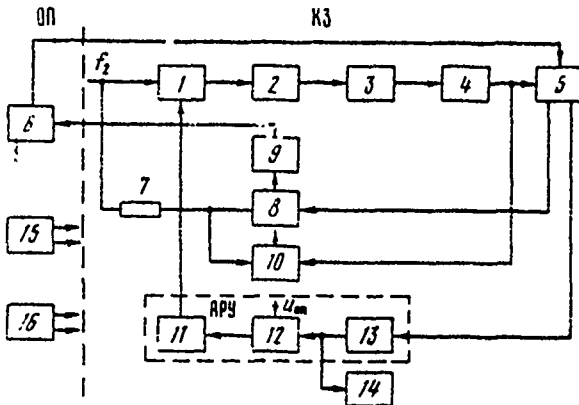
Fig. 1.   Fig. 2.
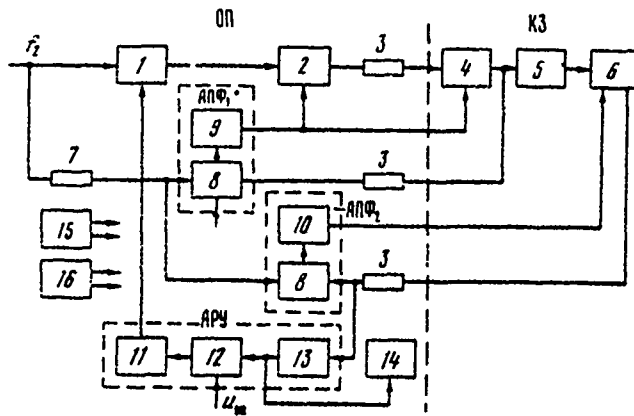
Fig. 1. Block diagram of accelerating station; OP - serviced

locations; KZ - circular nall; 1 - preliminary HF circuit; 2 -

penultimate lamp GU-40B, 3 - device/equipment of interstage

connection/communication; 4 - output tube GU-47B; 5 - resonator; 6 -

powerful/thick semiconductor dc amplifier; 7 - delay line; 8 - phase

discriminator; 9, 11 - electron-tube dc amplifiers; 10 -

block/module/unit of phase checking; 12 - power supplies; 16 - system

of control, blocking and signaling; U_{OH} - reference voltage.

Fig. 2. Block diagram of reconstructed accelerating station. OP -

serviced locations; KZ - circular nall; 1 - preliminary HF circuit; 2

- contour/outline of the penultimate cascade/stage; 3 - cables with a

length of 200 m; 4 - grid circuit; 5 - output tube GU-47B; 6 -

resonator; 7 - delay line; 8 - phase discriminators; 9, 10, 11 - dc amplifiers; 12 - circuit of comparison; 13 - detector; 14 - block/module/unit of the inspection of amplitude; 15 - power supplies; 16 - system of control, blocking and signaling; U_{OM} - reference voltage.
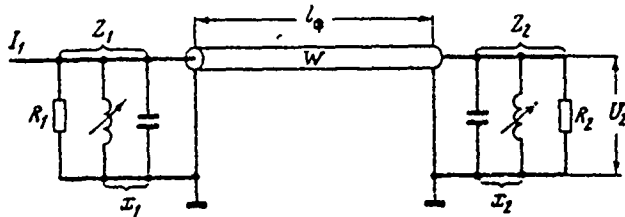
Fig. 3. The equivalent diagram or the grid circuit of final stage R_1, X_1, Z_1 - the equivalent parameters of the plate circuit of penultimate cascade/stage; R_2, X_2, Z_2 - equivalent parameters of grid circuit; W - wave impedance of cable; I - input current; U_2 - grid voltage.

Page 117.

The total time constant of field windings is 2 μs. Dynamic error taking into account an increase in the necessary for speed rearrangement of contour/outline in this case does not exceed 2°, i.e., virtually it is absent.

To decrease the static error is not expedient, since the system of the self-alignment of resonator (APF_2) has approximately the same error. With their precise equality the output tube will feel only the dynamic detuning of resonator.

Construction/design and results of experiment.

Because of the use/application of the reconstructed
contours/outlines the output stage of preliminary HF circuit it was
possible to construct on two connected in parallel lamps with the
natural cooling of the type GU-29. Prefinal broadband cascade/stage
is carried out on two lamps 6E5P with the correction. It is
controlling in the system ARU. At the entrance of amplifier will cost
cathode follower n lamp 6S15P.

The diagrams of the self-alignment of phase and ARU are carried
out on the semiconductors in the general/common/total
block/module/unit of autotuning.

The extensible blocks/modules/units of preliminary HF amplifier
and autotuning are constructed on the basis of standard
chassis/landing gear and are placed in the cabinet of the supply of
station.

The output stage remains in the extensible unit of the
accelerating device/equipment. Fig. 4 and 5 show the layout of the
existing and new r-f units. It must be noted, that in the new unit
there is a place for distribution of more powerful/thicker output
tube that gives the possibility of further development of system.

The developed diagram of reconstruction was investigated experimentally on the special bench. The nonuniformity of amplitude on the grid of output tube with $f_t = 200$ MHz/s does not exceed +-10o/o, but the divergence of phase, caused by the disagreement/mismatch of cable, lies/rests within limits of +-2°.

During August 1969 diagram were introduced on one of the stations of accelerator and it works under actual conditions for 3.8 thousand hours. Within this time it was not one case of failure of equipment, arranged/located in the circular hall, and the units of preliminary HF amplifier and autotuning.

The estimated time of the mean time between failures of the equipment of station, which remains in the circular hall, is 10 thousand hours, that 3 times than higher existing.
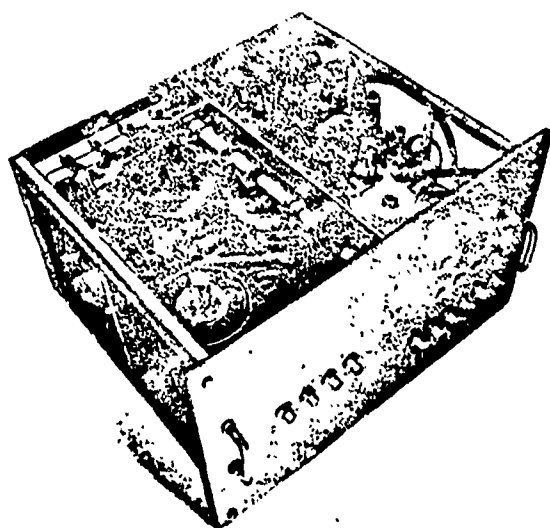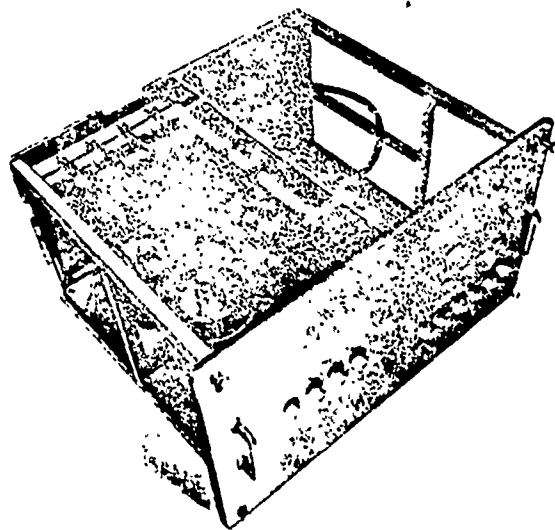
Fig. 4.   Fig. 5.

Fig. 4. R-f unit of accelerating station.

Fig. 5. R-f unit after reconstruction.

REFERENCES.

1. M. Plotkin. Folded ferrite boaded cavities for impedance matching in the AGS. — IEEE Trans. on Nuclear Sci., 1967, v. N S—14, N 3.
2. The second stage CPS improvement study 800 Mev Booster synchrotron. — MPS/Int. DL/B67—19, 3 rd October, 1967.
3. B. M. Gutner, et al. Accelerating resonators and powerful high-frequency equipment for their excitations of the proton synchrotron at 70GeV, IFVE. Transactions of All-Union Conference on accelerators of charged particles. Vol II. 1970, p. 101.

Page 118.

125. Equipment for the syncaronization of the systems of the output
of Yerevan synchrotron.

V. G. Ivkin, V. N. MInyaev, I. V. Mozin, Ye. Ye. Trifon.

(Scientific research institute of the electrophysical equipment im.
D. V. Efremov).

Equipment for the synchronization of the systems of the
conclusion/output of Yerevan synchrotron is intended for the central
control of the work of the elements/cells of the conclusion/output of
electron beam into accelerator chambers and beam spill to internal
targets, and also for the synchronization of equipment for physical
experiment.

The output pulses of equipment for synchronization control the
work of the following systems of conclusion/output: a) the systems of
local orbit perturbation; b) the power-supply system of

septum-magnet; c) the power-supply system of the deflecting magnet; d) the power-supply systems of quadrupole and sextupole lenses; e) the equipment, which disconnects HF generator; f) equipment for physical experiment.

Fig. 1 shows the block diagram of equipment for the synchronization of the systems of conclusion/output.

Equipment encompasses integrator with four comparators and four diagrams of electronic delay and provides the work of four channels of conclusion/output.

Impulses/momenta/pulses for the starting/launching of experimental equipment are developed with the aid of the integrator with the comparators and correspond to the specific value of the building up magnetic field in the clearance of the measuring unit of electromagnet.

Impulses/momenta/pulses for the starting/launching of output units are developed with the aid of the precision variable delay lines relative to the reference pulse, created at the moment/torque when magnetic intensity in the clearance of measuring unit is equal to zero.

Job priority and duration of the work of each channel of conclusion/output are determined by programmer, while the job priority of the elements/cells of conclusion/output is determined by the value of the established/installed delays.

All sensors of equipment for synchronization are located in the location of measuring units, and programmer, diagrams of controlled delays and output stages of equipment, and also equipment for check - in the location of main accelerator frequency.

1. Integrator and comparators.

The voltage from the induction coil, proportional by the derivative of magnetic field, arranged/located in the clearance of measuring unit, on coaxial cable is supplied to the electronic integrator with the commutator from output of which is removed/taken the signal, proportional to magnetic field only during its build-up. To the output of integrator are connected four diode-regenerative comparators, the moments of operation of which are determined by the levels of reference voltage. A quantity of points of reference voltage is selected as being equal to thousand. The value of reference voltage is established/installed on the programmer. The instability of the output pulses of comparators relative to the rating value of magnetic field in the range from 1000 to 8000 oersteds does not exceed 0.1o/o.
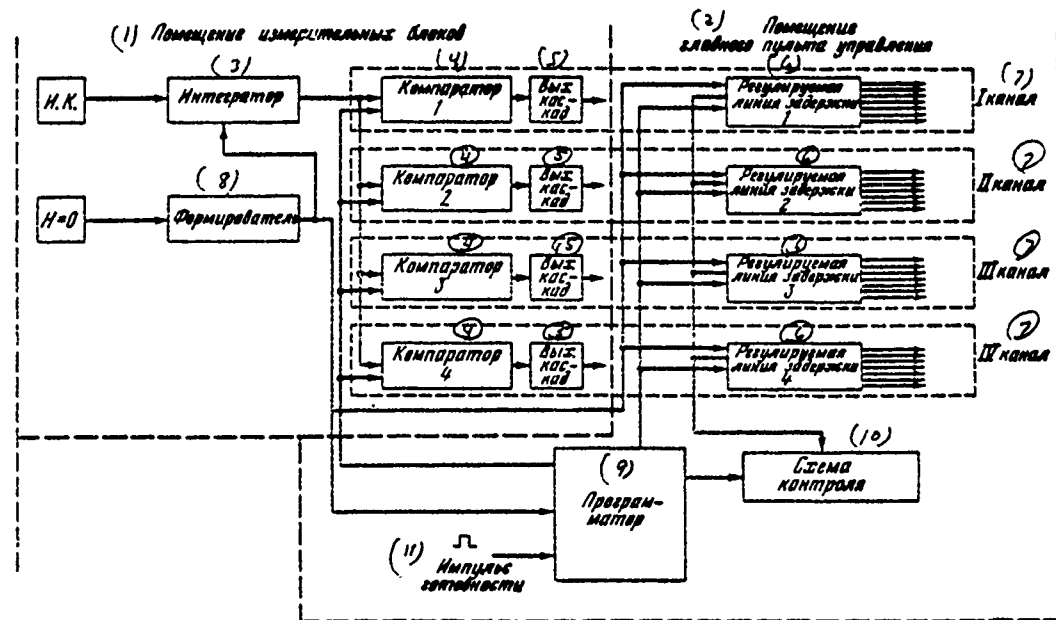
Block diagram of equipment for the synchronization of the systems of conclusion/output.

Key: (1). Location of measuring units. (2). Location of main control panel. (3). Integrator. (4). Comparator. (5). VYKh cascade/stage. (6). Variable delay line. (7). channel. (8). Shaper. (9). Programmer. (10). Diagram of check. (11). Impulse/momentum/pulse of readiness.

Page 119.

2. Diagram of controlled delay.

The diagram of controlled delay consists of crystal oscillator with the frequency of 1 MHz, four decimal counters with a capacity/capacitance of 10* each and 28 diagrams of the formation of output pulses, on seven - of each channel of equipment.

From the signal of crystal oscillator are formed/shaped the square pulses, which enter one of four counters, in the dependence on the state of programmer. General/common/total duration of delay 10 ms. The selection of delay factors of each of seven output pulses is accomplished/realized via the connection of the corresponding coincidence circuits to the outputs of the decoders of two latter/last decades/ten-day periods. Delay factor is established/installed by switches; the discreteness of installation 100 μs.

The diagram of the formation of output pulses contains the continuously-adjustable delay line and the exit blocking oscillator, which ensures at the output of hundred-meter cable with the wave impedance of 75 ohms positive pulse with an amplitude of 5 V and with duration of 5 μs.

The stability of delay factors of output pulses relative to reference pulse is better than 10 μs.

3. Programmer.

Programmer consists of the counter of a number of cycles of acceleration and whole series of the logic circuits, which allow the providing of order and duration of the operation of each of four channels of conclusion/output.

The operating cycle of programmer is selected either by 50 c· 1000 cycles of acceleration.

Programmer provides the following operating modes: a) continuous operation of any of the channels of conclusion/output; b) the work of two any channels alternately; c) the work of two channels alternately, moreover one channel works two times of more than another, d) the work of two channels, moreover one channel works by n cycles of acceleration, and another - 50 (100)-n cycles; e) the work of one channel during the n cycles of acceleration, and the work of two any others during 50(100)-n cycles in accordance with paragraphs b and c.

In all operating modes one of the channels is found in the waiting mode/conditions, i.e., begins to work with the arrival of the impulse/momentum/pulse of the readiness of experimental equipment, in this case in this cycle of acceleration all remaining channels are

DOC = 80069310   PAGE 505

blocked.

The moment of operation of the "waiting channel" can be detained relative to the impulse/momentum/pulse of readiness for 1-5 cycles of acceleration.

4. Diagram of check.

Equipment for synchronization encompasses the diagram of check, which makes it possible to operationally check the correctness of the work of equipment. The diagram of check provides measurement by choice of delay factor of any of 28 output pulses, measurement of the duration of the work of any of the channels, expressed by a number of cycles of acceleration during the operating cycle of programmer. The diagram of check provides also visual control of the established/installed program.

Equipment for the synchronization of the systems of the conclusion/output of Yerevan synchrotron is carried out in the form of two standard struts. For the purpose of an increase in the reliability in the equipment is widely used the slipping redundancy is provided for cold reserve of all basic building blocks of equipment.

The operation of equipment during two years confirmed its high reliability.

126. Precision wide-range thyristor-transistor stabilizer of high currents.

Yu. N. Denisov, V. V. Kalinichenko, V. A. Perezhogin.

(Joint Institute for Nuclear Research).

Transistor compensative current regulators are used extensively in the power-supply systems or the electromagnets of physical installations [1-5]. Such stabilizers provide the prolonged stability of field current by 0.01-0.001o/o and the suppression of pulsations to the appropriate level. In the wide-range transistor compensative stabilizers of high currents is commonly used the system of dual control, which consists of the contour/outline of precise and contour/outline of coarse control. With the aid of the transistor regulator and the system or feedback with the high factor of amplification and the stable reference voltage (contour/outline of a precise control) the current of load is supported by constant with a high degree of accuracy. At the same time output potential of the source of the direct current, which feeds stabilizer, with the aid of the feedback loop is regulated so (contour/outline of coarse control) so that the voltage drop across gap/interval the emitter-collector of the controlling transistors would remain in effect permanent and

would not exceed several volts.

Regulating rectified voltage can be conducted by a change in the amplitude of the alternating voltage, applied to the rectifier, by changing the transformation ratio of power transformer. A change in the transformation ratio is achieved by means of the commutations of the windings of power transformer. A regulator of this type provides a stepped variation in permanent output potential of rectifier. At the specific value of the quantity of the steps of voltages this method can be successfully used in combination with a precise transistor compensative regulator. A commutation of windings it is expedient to accomplish/realize with the aid of the thyristor switches of alternating current.

Page 120.

The block diagram of the stabilized current source with thyristor-transformer regulator in the contour/outline of coarse control is shown in Fig. 1A. The power transformer of rectifier (Fig. 1.b) has n of commutated secondary windings a number of turns of which (and respectively load voltage) are proportional 2^{i-1}, where i - the reference number of the corresponding winding. If proportionality factor is equal to k of volt (value of the step of regulating), then voltage on the secondary side of power transformer by the

corresponding changeovers of windings can be regulated in the range

of values $u_q \div [u_q + (2^n - 1) k]$ volt. Supplementary, not compensated

winding U provides the initial stress level of the compensating loss

on the rectifier and precise regulator $u_{k \ni min}$. The use/application of

this winding makes it possible to also decrease a number of

commutated windings, or a value of the step/pitch of regulating

voltage.

The main doubtless advantages of this version of

thyristor-transformer regulator are: the high value efficiency and

factor of power cos ϕ; the insignificant distortions of the

sinusoidal form of voltage and output current of regulator, since the

commutations are accomplished/realized at the moments of the

transition of the current through zero, and the time of the

inclusion/connection of thyristors, as already mentioned, little.

Although for the discussed regulator is required a relatively large

number of thyristors, however in the majority of the cases can be

used the thyristors with a small inverse voltage, which have low

cost/value.

Fig. 2 and 3 give the schematic diagrams of the block of control

of thyristor switches. The block/module/unit of generation of

commands (Fig. 2) encompasses: the device/equipment of the

isolation/liberation of timing pulses, threshold device/equipment and

bidirectional counter.

The device/equipment of the isolation/liberation of timing pulses serves for the formation of the command impulses whose temporary situation provides the changeover of thyristor keys/wrenches at that moment/torque when voltage on the anode of thyristor approaches a zero value. This makes it possible to avoid the simultaneous starting/launching of two thyristor switches and short circuit of windings. The temporary situation of timing pulse relative to the reference sine voltage, removed from winding of the VI power transformer, is determined by the value of resistance R1. The conversion of sine voltage into pulse is accomplished by the schematic of asymmetric trigger and frequency divider of five triggers, assembled on triodes T1-T17. Frequency division is necessary for an increase in the repetition period of command impulses. The repetition period of command impulses must be somewhat more than the time, occupied by transient processes in the nodes/units of entire stabilizer. Threshold device/equipment consists of two asymmetric triggers, which have the different levels of functioning on the input voltage and two keys/wrenches, controlled by these triggers. Trigger (T20-T21) must operate/wear at value $U_{k9} < U_{k9\,min}$, trigger (T18-T19) - when $U_{k9} > U_{k9\,max}$. The exit voltages of triggers control keys/wrenches (T23 and T24). With the aid of these keys/wrenches is accomplished/realized the commutation of timing

pulses on the entrances of bidirectional counter.

Bidirectional counter contains four bits (T29-T47). The
potential levels of triggers are commands for inclusion/connection
and disconnection of thyristor switches. The initial state of the
triggers of counter, which corresponds to "zero" commands, i.e., to
the minimum rectified voltage, is established by the short-term
closing of contacts of relay R1 during the supplying of the voltage
of supply of counter. For eliminating the possibility of the
transition of counter from the "zero" state is direct into the
"single" and reverse (in such a case if they will continue to enter
command impulse on further increase or decrease in the rectified
voltage with the depleted possibilities of key control) serve
keys/wrenches T25-T26 and T27-T28.

The transmission of the commands, prescribed/assigned in the
form of the potential levels of triggers, to the thyristor
keys/wrenches is accomplished/realized with the aid of eight
identical controlled voltage converters. (On Fig. 3 it is shown the
diagram of one block/module/unit, which contains 4 voltage
converters).

In the contour/outline of precise current control in the load
enter: transistor regulator, reference-voltage source, modulator,

low-frequency amplifier, phase discriminator, and also series/row of auxiliary.

By reference-voltage source in the diagram of comparison (Fig. 4) serves three-circuit voltage regulator (T12-T13, D7-D9, D3-D6, D2). General/common/total stabilization factor with a change in the line voltage is ~10⁴.
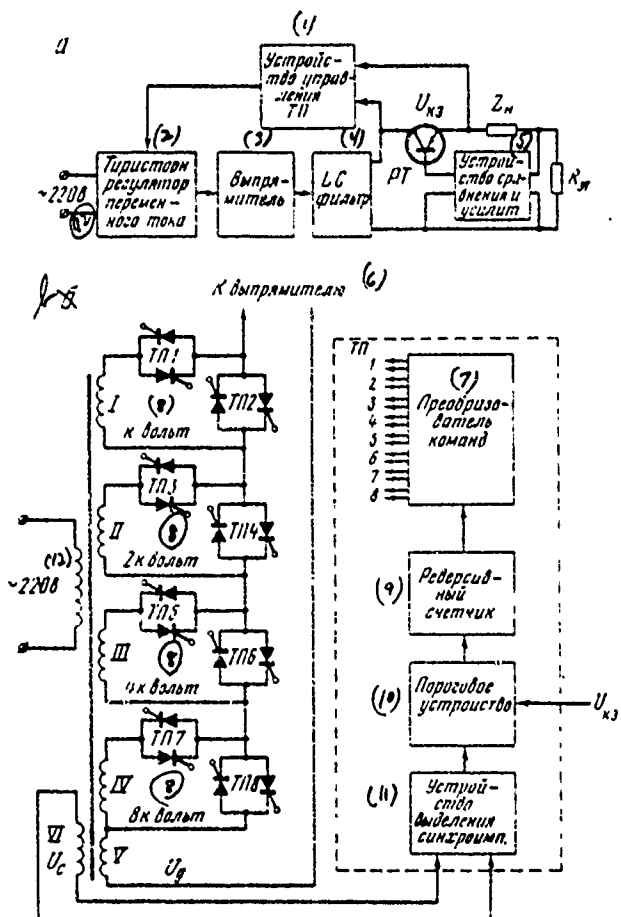
Fig. 1. Block diagram of thyristor-transistor current regulator (a), block diagram of rough control loop (b). TP - thyristor switch; k - value of step.

Key: (1). Control unit. (2). Is thyristor. regulator of alternating current. (3). Rectifier. (4). filter. (5). Device/equipment of comparison will enforce. (6). To rectifier. (7). Converter of commands. (8). volt. (9). Bidirectional counter. (10). Threshold device/equipment. (11). Device/equipment of isolation/liberation of synchro pulse. (12). V.

Page 121.
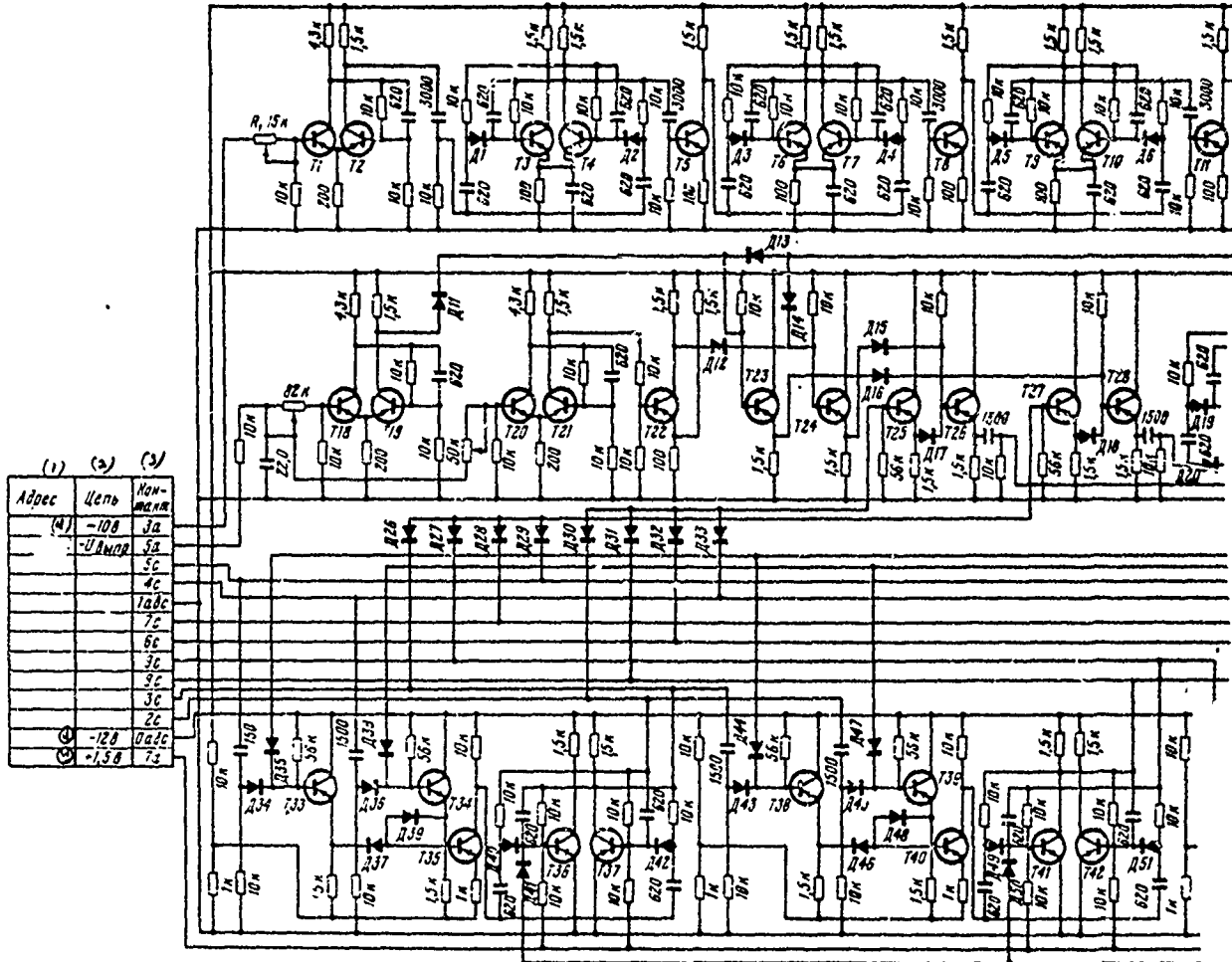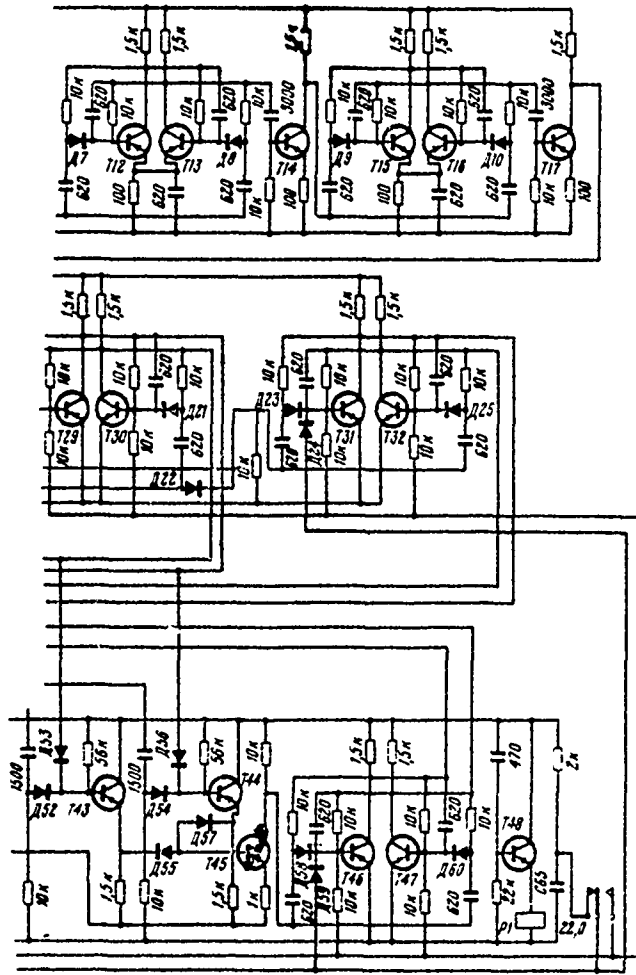
Fig. 2. The schematic diagram of the unit of generation of commands of control.

Key: (1). Address. (2). Circuit. (3). Contact. (4). V.

Page 122.
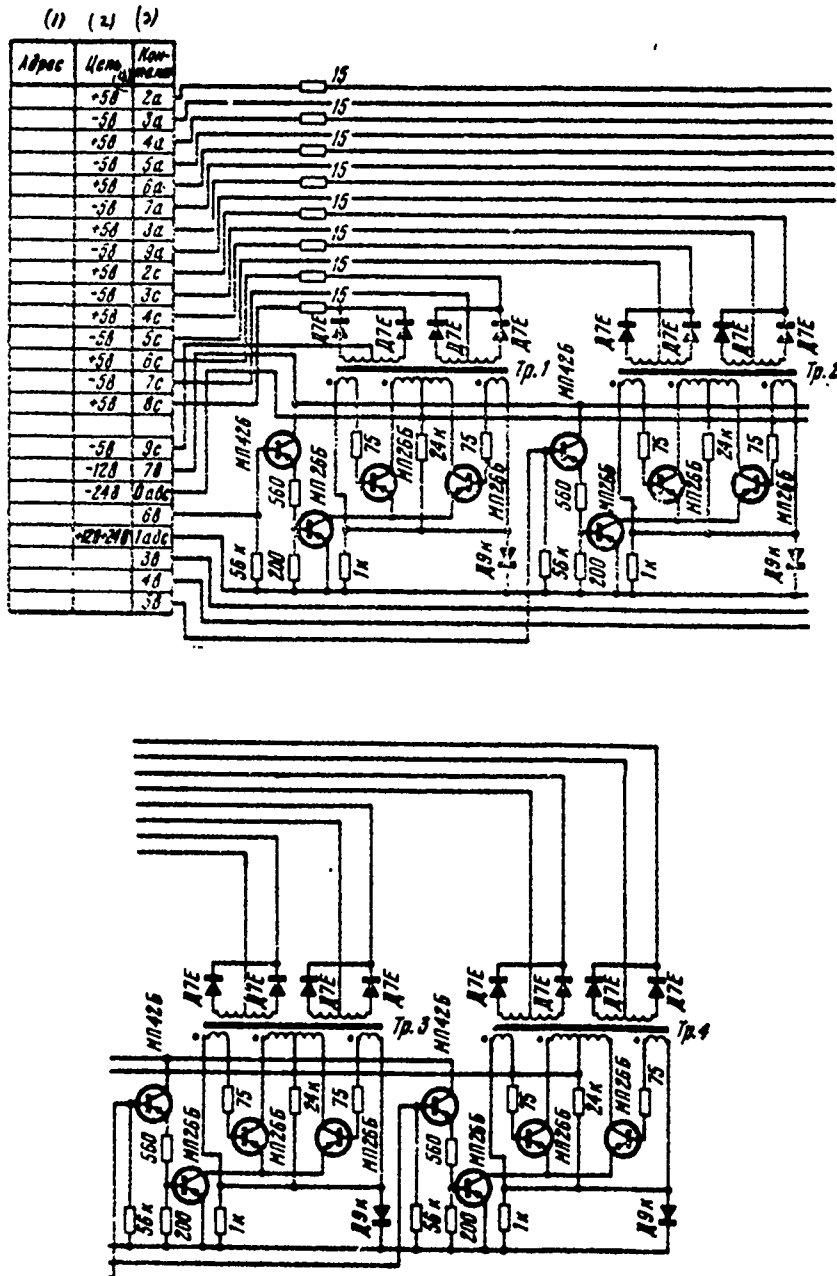
Fig. 3. Schematic diagram of the block of converter of commands.

Key: (1). Address. (2). Circuit. (3). Contact. (4). V.

(2)	(3)	(4)
Кон-такт	Цепь	Адрес
3a	-12в	
6a	Выx. УПТ	(5)
9a	$-U_{R_{эт}}$	
10a	$+U_{R_{эт}}$	
4в	~50в	
5в	~50в	
1c	+12в	
2c	+12в	
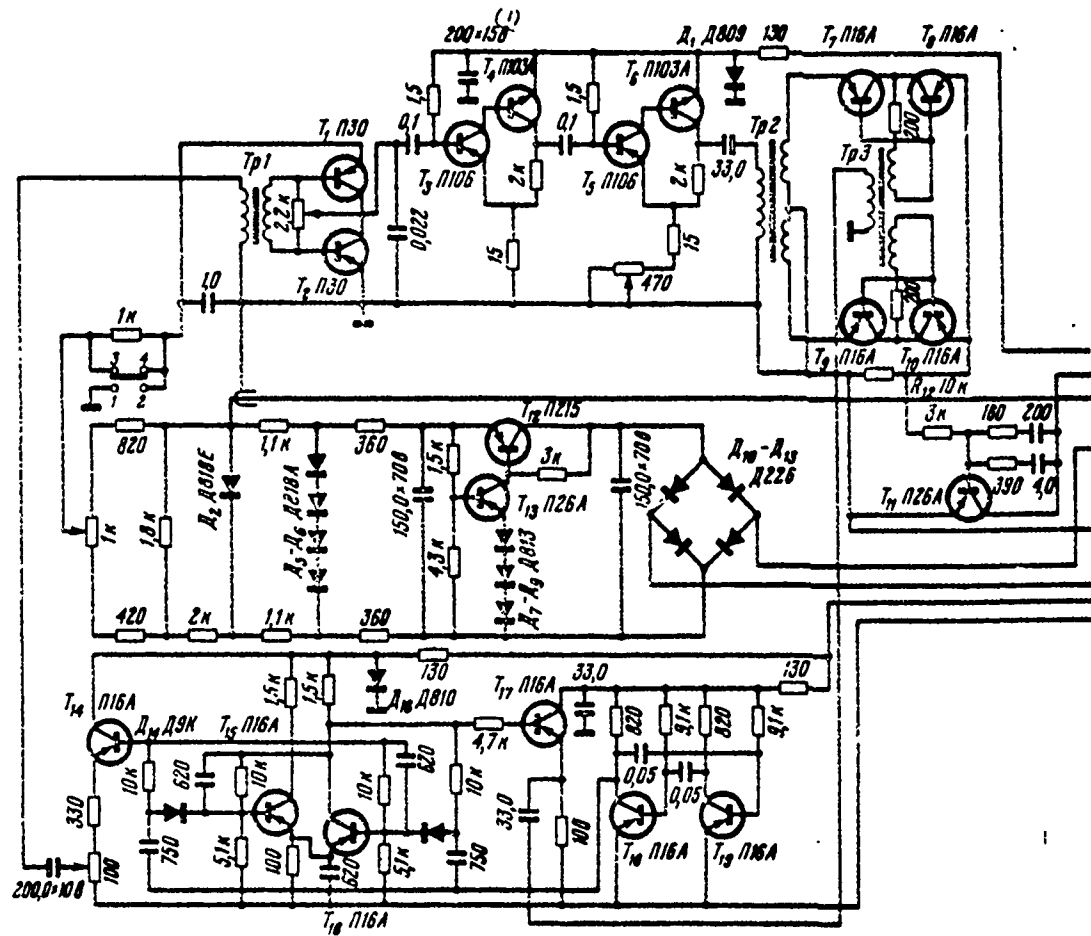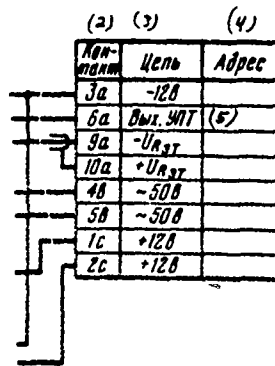
Fig. 4. The schematic diagram of the block of comparison and amplifying the error signal.

Key: (1). V. (2). Contact. (3). circuit. (4). Address. (5). VYKh.

Page 123.

The difference between a voltage drop across the standard resistance (connected in the circuit of the stabilized current) and the adjustable part of the reference voltage enters the entrance of the transistor modulator T1-T2, where it is converted into right-angled alternating voltage - error signal. Modulator is carried

out on transistors T30 on the schematic of parallel-series transistor key [6].

The amplification of the error signal is accomplished/realized by a transistor low-frequency amplifier T3-T6. Then the voltage of the error signal is straightened/rectified by phase-sensitive detector (T7-T10) and enters the entrance UPT (T11). Exit voltage UPT through the matching cascades/stages controls transistor regulator. Maximum value of gear ratio from the entrance of modulator to the output of the phase discriminator to equal ~1200. Transistor UPT T11 (type P26A or P21A) is selected with the low value of current Temperature stability UPT can be increased by the I_{ko}. inclusion/connection of small resistance (200 ohms) into the emitter circuit T11.

The described stabilized current source supplies magnet windings, used for calibrating the magnetometers. Range of current control 0.7-34 A.

Fig. 5 depicts the curve of the drift of current, written with the aid of the meter of an instability of the type V2-13. Stabilizer is connected in 40 minutes prior to the beginning of recording. Mode/conditions of the work of the stabilizer: I_H = 10 a, U_H = 22   V, U_{ks} =10 V. The maximum cutoff/disconnection of current in the load from initially fixture does not exceed $8 \cdot 10^{-3}\%$. On the graph/curve are noted the oscillations of the temperature in the location where is established/installed the stabilized source and electromagnet.
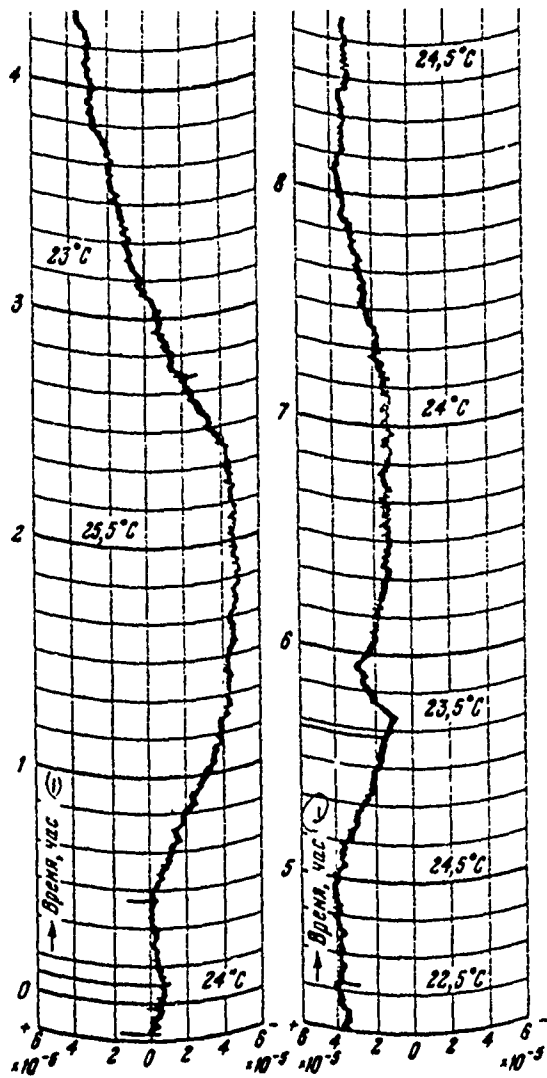
Fig. 5. Curve of the drift of current.

Key: (1). Time, hour.

REFERENCES.

1. R.L. Garvin. Rev. Scient. Instr., 1958, v. 29, p.223.
2. M.H.N. Potok. Electr.   Engng., 1959, v. 31, p. 745.
3. I. Lutz, Ch. Pike. Rev. Scient. Instr., 1959, v. 30,
   p. 841.
4. J.C.Richard. Electr. Engng, 1960, v. 32,p. 22.
5. Yu. N. Denisov, V. V. Kalinichesko, A. G. Komissarov, Yu. I.
   Sulov, Preprint. OIYaI, 13-5068. 1970.
6. I. I. Akulov, V. Ya. Barkhin, R. A. Balitov, et al.
   Theory and Calculation of Basic Radio Engineering Transistorized
   Circuits. IZD VO "Svyaz'" 1964.

Page 124.

127. Device/equipment of high-frequency synchronization of particle injection in accumulator/storage VEPP-3.

M. N. Zakhvatkin, E. A. Kuper, V. I. Nifontov.

(Institute of nuclear physics of SO AN USSR).

In the work is described the device/equipment of high-frequency synchronization for the particle injection into accumulator/storage VEPP-3.

The resonator of accumulator/storage works on the 19th harmonic (76 MHz) of frequency of revolution. Device/equipment provides for program control of injection into different separatrices of accumulator/storage. The output pulse, which is determining the moment/torque of injection, is phased with the high-frequency resonator voltage. Precision/accuracy of fixation of phase of 10-15° (0.3-0.5 ns).

Device/equipment has two operating modes: 1) work in the presence of two rigidly phased radio-frequency voltages 76 and 4 MHz

(frequency of revolution); 2) work in the mode/conditions of the
internal frequency discrimination of inversion with the aid of the
divider on 19.

The block diagram of device/equipment (Fig. 1) is functionally
divided into 3 nodes/units - diagram of fixation of phase 76 MHz (I),
synchronizing circuit for observation and measuring the parameters of
beam (II), diagram of control or filling of the separatrices of
accumulator/storage (III).

The diagram of fixation of phase 76 MHz works as follows (Fig.
2).

Entering entrance B radio-frequency voltage 4 MHz is limited, is
amplified (T_{5-8}) and is supplied on the entrance of the shaper of
narrow pulses $T_9, _{10}$). Impulses/momenta/pulses from the first arm of
shaper (T_{10}) are amplified ($T_{15, 16}$) and through the
block/module/unit of variable/alternating delay enter the coincidence
circuit, carried out on diodes D_1, D_2 and tunnel diode TD_3.
Simultaneously to the coincidence circuit are fallen the
impulses/momenta/pulses, capled to the phase of HF voltage 76 MHz by
amplifier by shaper ($T_{3,4}$).

The impulses/momenta/pulses of amplifier (T_9, T_{10}) through the

switch ($T_{17, 18}$), which controls the work of the diagram of preliminary joining (TD_2, T_{22}), support TD_2 at the diffusion branch.

The impulse/momentum/pulse "start 1" readjusts trigger (TD_2) to the tunnel branch, and the next impulse/momentum/pulse of shaper (T_{19}) returns T_1D_2 to the initial state. Positive drop/jump after amplification. (T_{22}) it enters the trigger (TD_3) and prepares it to the work.

Coincidence pulse returns TD_3 to the diffusion branch, starting univibrator (TD_4) and amplifier (T_{23}, T_{24}).

Output pulse (40 V, fronts 8 ns) enters the power amplifier with the continuously adjustable delay in limits of one period of 76 MHz.

Synchronizing circuit for observation and measuring the parameters of beam cables the trigger pulses of recorders to the specific phase of the frequency of revolution of particles in the accumulator/storage. maximum launching rate 10 kHz. The temporary/time performance records of diagram are given in Fig. 3.

Block/module/unit of variable/alternating delay (Fig. 4).

Delay is accomplished/realized by a shorting of cable by diodes

(D311), controlled by commutator. Input pulse after being reflected from the connected with the given moment/torque diode, it appears at the entrance of line after the time, equal to the doubled electrical length of cable.

The capacity/capacitance of diodes in the closed state is less than 2 pF, dynamic resistance with the current 15mA is equal to 4-5 ohms, that provides in the case of the pulse delay on 250 ns the fading not more than 20o/o. Since particles are injected simultaneously into 2 adjacent separatrices, overall delay is collected of 9 segments of cable in electrical length 13.05 ns in each.

The working detuning of the frequency of resonator 76 MHz composes +-0.3o/o with respect to T=13.052+-0.4 ns. Temperature instability of delay in the range of temperatures from +20 to +40°C comprises $1.2 \cdot 10^{-3}$% [1].
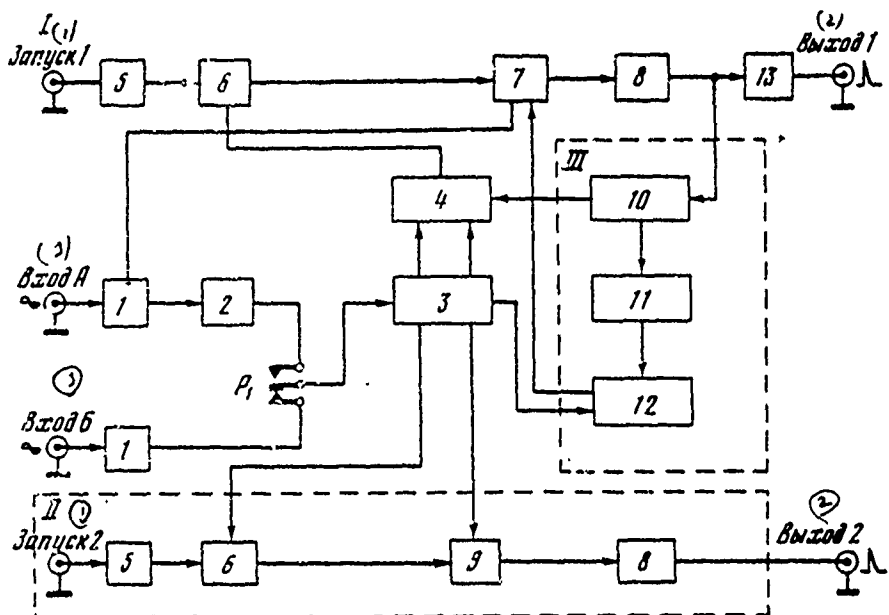
Fig. 1. Block diagram of the device/equipment of high-frequency synchronization. 1 - diagram of fixation of phase 75 MHz; II - synchronizing circuit; III - diagram of control of filling of the separatrices of accumulator/storage; 1 - amplifier limiter; 2 - circuit of frequency division; 3 - amplifier-shaper; 4 - electronic relay; 5 - shaper; 6 - diagram of preliminary joining to 4 MHz; 7 - coincidence circuit in the channel 76 MHz; 8 - exit shaper; 9 - coincidence circuit in the channel 4 MHz; 10 - diagram of control; 11 - commutator; 12 - block/module/unit of variable/alternating delay; 13 - amplifier of power with the controlled delay.

Key: (1). Starting/launching. (2). output. (3). input.

Page 125.
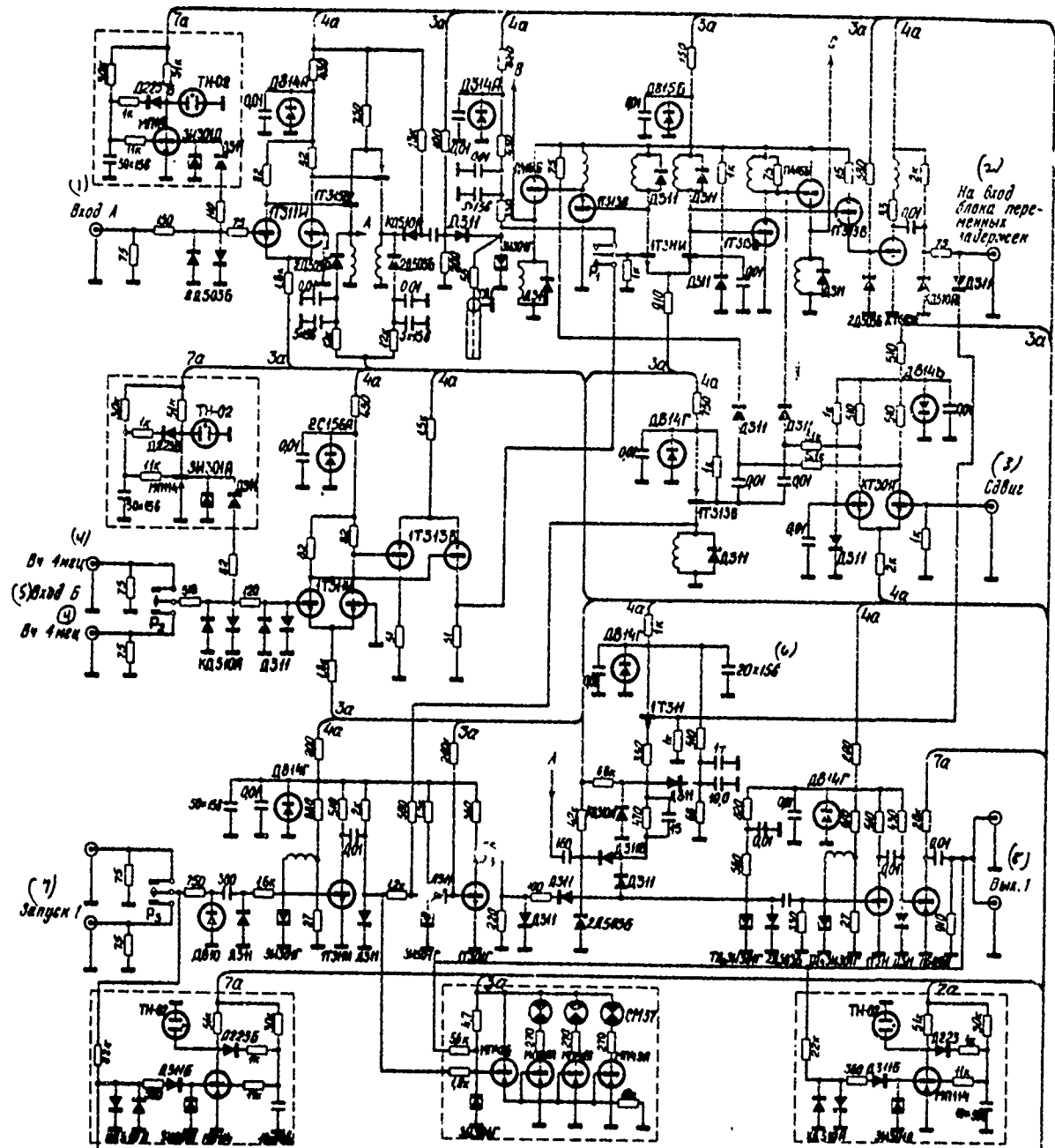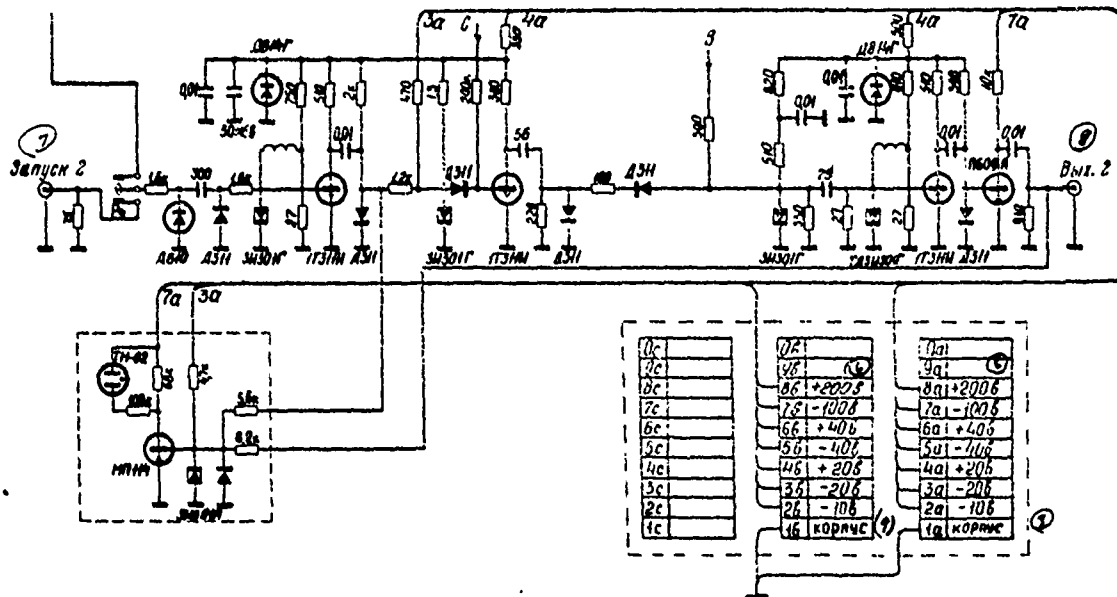
Fig. 2. Diagram of fixation of the phase of the high frequency of 76 MHz and synchronizations on the phase 4 MHz.

Key: (1). Input. (2). To Entrance of block/module/unit of variable/alternating delays. (3). shift/shear. (4). MHz. (5). Input. (6). V. (7). Starting/launching. (8). Out. (9). Housing.

Page 126.
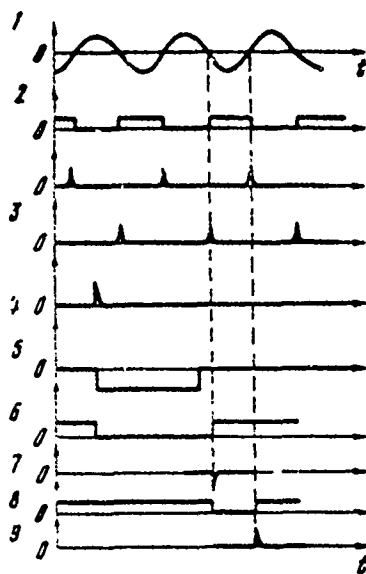
Fig. 3. Time graphs of synchronizing circuit 4 MHz. 1 - HF voltage 4 MHz; 2 - output pulse of amplifier-limiter T_7, T_8; 3 - the output pulses of amplifier-shaper T_{11}, T_{12}; 4 - trigger pulse; 5 - output pulse from the shaper TD_6; 6 - impulse/momentum/pulse of the diagram of preliminary joining TD_6; 7 - output pulse from the diagram of preliminary joining; 8 - impulse/momentum/pulse in the diagram of coincidences TD_7; 9 - output pulse (T_{28}).
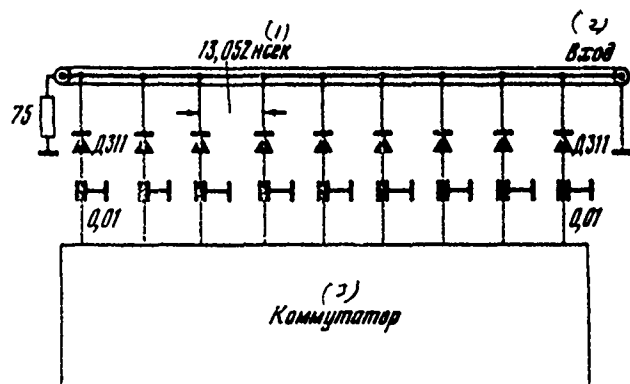
Fig. 4. Diagram of variable/alternating delay.

Key: (1). ns. (2). Input. (3). commutator.

REFERENCES.

1. A. A. Kurashov. "Generation of Series of Pulses in Systems with Delaying Feedback." Proceeding of 6th Conference on Nuclear Radio Electronics. Vol I, p. 179. Atomizdat, 1964.

Page 127.

Session X.

Powerful radio engineering devices/equipment and accelerating systems.

128. Injector of the booster of proton synchrotron IFVE.

A. L. Mints, B. P. Murin, I. Kh. Nevyazhskiy, V. G. Kuhlmann, B. I. Polyakov, L. G. Lomize, A. V. Mishenko, B. I. Bondaryev, A. D. Belov, V. V. Kushin, A. A. Dzhanko, A. P. Fedotov, E. A. Mirochnik, N. L. Sosensiy, V. V. Kurasov, Yu. S. Cherkashin.

(Radio engineering institute of the AS USSR).

V. A. Alekseyev, G. A. Grau, A. I. Gryzov, A. V. Popov, A. I. Solnyshkov.

(Scientific research institute of the electrophysical equipment im. D. V. Efremov).

S. A. Il'yevskiy.

(Institute of high-energy physics).

Projected/designed accelerator - the injector of the booster of synchrotron IFVE - single-cavity linear accelerator with the preinjector, the buncher and the debuncher. Its basic parameters are given below:

exit energy ... of 37.8 MeV.

Energy of the injection ... of 700 keV.

Frequency of the accelerating dF field ... of 148.5 MHz.

Average/mean rate of acceleration ... 1.24 MeV/m.

Design beam current at the output ... 100-150 mA.

Spread of particle momenta at the output (after debuncher) ... +-0.3o/o.

Duration of the pulse or the proton current ... of 1.5-20 μs.

Duration of HF pulse ... 250 µs.

Stability of the amplitude of accelerating field ... +-1o/o.

Power of losses in copper or resonator, buncher and debuncher ... of 3 MW.

Power of beam with the current 150 mA ... of 5.7 MW.

Length of the resonator ... of 29.9 m.

Diameter of the resonator ... or 1327 mm.

Number of drift tubes ... 1/2+94+1/2.

Diameter of the drift tubes ... of 23.2-10 cm.

Diameter of the aperture ... of 2-3.5 cm.

Length of the period of focusing ... 2.

Gradients of magnetic fields in the lenses ... of 6-0.6 kgf/cm.

The capacity of the focusing channel ... of 1.2 cm•mrad.

The mode/conditions of work of the accelerator is packaged-pulse. Pulse repetition frequency in the package 25 Hz, while repetition frequency of packages 0.1 or 0.2 Hz.

As the accelerating structure is utilized the resonator with the drift tubes, which is the copy of the first resonator of accelerator I-100 [1]. Particle focusing is accomplished/realized by the magnetic quadrupole lenses with the pulse supply, placed one in each drift tube. In the construction/design of drift tubes in comparison with the drift tubes of accelerator I-100 is provided for an improvement in the heat withdrawal from the coils of lenses. Resonator and drift tubes are cooled by the water, thermostatically controlled with precision/accuracy of $+-0.1°C$.

The vacuum system of resonator - is two-chamber. For the high-vacuum evacuation will be used titanium pumps.

As the buncher and the debuncher are utilized single-gap resonators. Construction/design of buncher the same as on the linear accelerator I-100 [1], and debuncher - as on accelerator I-2 [2]. The amplitude of the voltage of debuncher composes 700 kV, drift spaces -14 m. The system of HF supply is constructed analogously justified

itself on accelerator I-100 in Serpukhov. Large average/mean powers
and beam current to 150 mA they were necessary to increase a number
of terminal amplifiers (on triodes GI-27A) to three. They are
arranged/located along the resonator so as to avoid the noticeable
excitation of the overtones of working mode of vibration.

The block diagram of HF system is given in Fig. 1. Exciter V and
setting device ZU differ little from those utilized on accelerator
I-100. For adding the powers of three terminal amplifiers OU in one
resonator besides the coupling adjustment is provided for the
automatic control of the phase relationships/ratios between them by
means of the phase shifters fie.

Page 128.

The HF supply of buncher B and debuncher D is intended to carry out
from the resonator R, where will be supported the stable amplitude of
accelerating field. The anodic supply of terminal amplifiers will be
conducted from the modulator M with the rigid discharger/gap and the
partial discharge of capacitive accumulator/storage without the peak
transformer, which will ensure the necessary operating speed of the
system of program regulating with anode voltage for the stabilization
of the level of accelerating field. For the circuit of the charge of
modulator it is possible to utilize a rectifier of the type KVTM with

thyristor voltage regulator. The same modulator can be utilized for the excitation.

The stabilization of the adjustment of the frequency of resonator to the maximum or accelerating field is accomplished/realized by a system ARF-Ch, analogous that utilized on the second resonator I-100 [1]. Analogous devices/equipment AFR-Ch will ensure the stabilization of a phase difference between resonator-buncher and resonator-debuncher. The actuating elements of system ARF-Ch will be the plates of the adjustment of resonator, buncher and debuncher.

Trigger pulses on the preinjector and the timer device/equipment of linear accelerator are supplied directly from the booster. The control of trigger pulses on the linear accelerator is conducted on its timer device/equipment.

For the measurement of the parameters of beam are utilized mainly traditional methods and devices/equipment: the induction current-sensing devices and position of beam at input and output of injector, magnetic spectrum analyzer, system of slots and collectors/receptacles for the check of emittance characteristics, system of screens for the observation of the form of the cross section of beam. Furthermore it is proposed to utilize the noncontact

method of measurement of the average speed (energy) of protons in the cluster at the output of injector on a phase difference between two small resonators which are excited by beam on the second harmonic of the frequency of bunches.

The approximate estimate of the width of the spectrum with the beam currents, which exceed approximately/exemplarily 20-30 mA, it is proposed to produce also with noncontact method. For this it is planned/glided to measure durations and forms of proton clusters at the output of injector and before the debuncher.

For the optimization of the process of injection into the booster 's provided for the system of the correction of the basic parameters of beam according to the information about the position in the phase space of the injected into the booster particles.
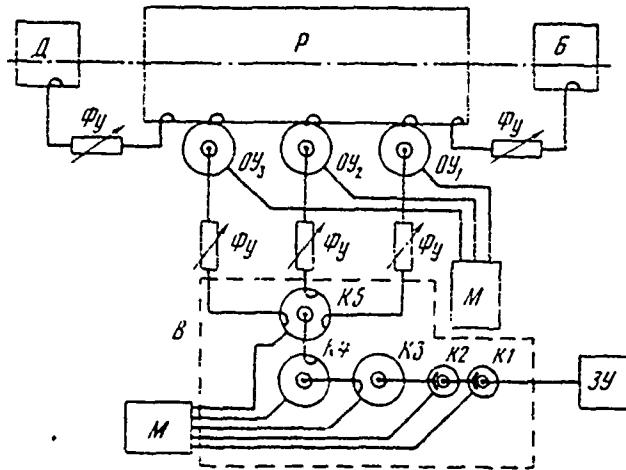
System block diagram of HF supply of accelerator.

REFERENCES.

1. I. M. Kanchinskiy, et al. Proceedings of International Conference on Accelerators, Dubna, 1963. M., Atomizdat. т. 462.

2. V. G. Andreyev, et al. PTE, 1967, No. 5, 71.

129. Powerful part of HF system of the intersecting rings CERN.

P. Ferger, U. Shnel.

(CERN).

1. Introduction.

In the literature [1, 2] have already been examined the
questions, connected with the rings. In the proposed report the
attention is accentuated on some special features/peculiarities,
which relate to the determination of the parameters of the equipment
of the powerful/thick part of the HF system of the intersecting
rings.

2. Comparison of parameters of injector-accelerator (proton
synchrotron) and rings.

As the injector of rings serves the acting proton synchrotron of
CERN on 28 GeV; therefore, being based on the real parameters of
proton synchrotron, it is possible to make basic propositions
relative to the high-frequency system of rings.

First, it is desirable to accomplish/realize one complete cycle
of acceleration for the time interval smaller than the
full/total/complete cycle time of proton synchrotron, which is 1.5-2
s [3].

To this condition corresponds work of both rings on the
alternating impulses/momenta/pulses of proton synchrotron.

Page 129.

In the second place, the brought-out from the proton synchrotron
beam is bunched and is transferred/translated into the intersecting
rings by already bunched, which provides reliable capture by bunch
with synchronous separatrices. For fulfillment of this condition it
is required so that the frequency of rings would be equal to the
frequency of proton synchrotron during the ejection, which is 9.536
MHz with the energy 28 GeV. Proton synchrotron works on the 20th
harmonic of high frequency, and rings - to their 30th, since mean
radius are one and a half times more.

This means that after one impulse/momentum/pulse of injection,
which consists of 20 bunches, in the ring will remain ten empty

separatrices. If we do not take special measures, then, naturally,
the effectiveness of accumulation not to exceed 2/3. For an
improvement in the effectiveness of accumulation the authors of
present report examined saveral versions. In first version [4] it was
proposed to hold down/retain the first impulse/momentum/pulse,
injected by synchrotron and puncned by high frequency, in orbit of
injection and to fill empty separatrices with the part of the second
impulse/momentum/pulse. As the second was examined the version of
absent separatrices [5], with which the HF voltage is turned
off/disconnected after each complete revolution of particles to the
period, during which not one particle passes through resonators.

The first diagram involves the close tolerances; therefore the
authors dwelled on the second diagram.

Finally, by the most important parameter which determines the
quality of proton synchrotron, is the area of separatrix in the phase
space. The area of separatrix must be not more than the area of
bunch, otherwise will occur rapid beam blowup in the phase space.

3. Characteristics of rings and their effect on the powerful/thick
part of HF system.

With accumulation of beams in the longitudinal phase space are

possible two methods of filling of separatrices, that lead to the
varied conditions for the work of the accelerating sections.

The diagram of repeated accumulation is simplest, moreover in
this case it is possible to carry out the mode/conditions during
which the voltage and rate of change in the frequency are retained
constants during entire storage time at the end of which high
frequency is always connected. In this method the area of separatrix
is accurately matched with the area of the bunches of proton
synchrotron, which makes it possible to utilize a sufficiently low
voltage or value $\sin\phi_s = r$, close to unity (for example, 1.5 kV for one
revolution with $r=0.84$ and the energy, equal to 25 GeV). In this case
small change r entails a sufficient large change in the area of
separatrices, which requires the appropriate change in the voltage,
and rate of change in the frequency, if it is desirable to avoid beam
blowup in the phase space.

The calculations of the effectiveness of accumulation, carried
out by the authors [6, 7], showed that high value of r (>0.5) leads
to the low effectiveness of accumulation, if we do not increase a
number of impulses/momenta/pulses. However, low value r leads to the
very long time of the acceleration of beam.

Diagram of single accumulation. The basic goal of development is

obtaining high effectiveness in the accumulation at the low value Γ.
This it indicates actually that the process must be produced on the
diagram of single accumulation which consists of three parts.

Bunches are seized into the wide ones of separatrices, and after
the appropriate equalization in the phase space beam is accelerated
at high values $\frac{dp}{dt}$. Then the area of separatrix decreases so, that is
compared with area of bunch; in the final analysis of separatrix they
have also sizes/dimensions, as in the case of the liagram of repeated
accumulation. After this high frequency is turned off/disconnected.

The total time of acceleration (corresponding to $\Delta p/p = 4o/o$)
depends in essence on initial voltage. Therefore it is desirable to
select sufficiently high voltage; the upper limit is limited to
economic considerations. With selected high voltage is facilitated
the equalization of the parameters of the bunches of proton
synchrotron and intersecting rings.

The compromise decision of a question leads to the value of
maximum voltage 20 kV on one revolution.

Both the methods presented nigher than of accumulation require
during certain part of the period of the acceleration of
comparatively small voltages. The diagram of single accumulation

makes it possible to exercise rigid control over a decrease in the
voltage from the maximum of up to the minimum. The typical values of
maximum voltage compose 20 κV, minimum -75 V and values of dynamic
range ~300:1.

By heaviest problem for power stage and accelerating cavity is
load current during the use of extremely low voltages in the process
of accumulation. At present the current of proton synchrotron is 150
mA or $2 \cdot 10^{12}$ protons per pulse. The high-frequency component of
current, caused by short bunches, comprises in the first
approximation, 300 mA. In combination with the usual impedance of
resonator this current will immediately cause in it very high
voltage. Thus, it is necessary to take special measures in order not
to lose check of the beam in the resonator due to stress by current
at the nominal frequency.

Interaction beam- resonator sets severe limitations on the
impedance of resonator.

Works [8-11] examine a question about the criterion of the
longitudinal stability of uniform beam. Simplest and useful for
recommendation for the development of equipment of rings are
represented by E. Keyl and U. Snell [12]. Investigating the
parameters of the intersecting rings, they derived the condition of

the stability

$$\left| \frac{Z}{n} \right| \leq 10 \text{ ohm}$$

where Z - general/common/total impedance [9], and n - number of mode. This limit barely depends on the phase angle of impedance. Consequently, the detuning of resonator with the permanent shunt impedance is barely effective.

After using stability condition to the accelerating section, which works on the 30th harmonic of frequency, we will obtain limitation to the general/common/total impedance

$$|Z| \leq 300 \text{ ohm.}$$

Stability condition shows, besides the fact that the dependence of the general/common/total impedance of the accelerating section on the frequency can be essential over a wide range of frequencies, beginning from the frequency of revolution to the higher harmonics.

Page 130.

4. Accelerating cavities, their connections with the power amplifier. Questions, connected with the load with current and interaction beam-

resonator.

In the ring are utilized seven accelerating cavities, placed in the separate octant each. Six of them actually are intended for the accumulation, and by the seventh for the experimentation.

In this circuit maximum voltage 20 kV is divided into six equal parts according to 3.3 kV to the resonator. Since amplifier must provide work in the wide dynamic range, more advantageously utilize it in the mode/conditions of class A. For a period of time of accumulation total variation of the frequency is very small: it is less than 10^{-3}. For changing the average/mean value of energy of ring is required a larger change in the frequency. With a decrease in the energy of beam to 3.5 GeV it is necessary to change frequency to 3o/o. Therefore quality Q of accelerating cavity is selected as being equal to 180. In this case the adjustment of resonator with the aid of the mechanical capacitor/condenser with the remote control becomes not very complex problem.

By most serious problem is strong load current. According to condition of stability $\left|\frac{Z}{n}\right|$ the maximum permissible impedance, determined by the effect of beam on the resonator, must be 50 ohms. On the other hand, shunt impedance must be possible higher in order to ensure the optimum energy consumption from the source of HF power.

Consequently, the introduction or strong fading to resonator does not remove stress by current.

Coaxial cavity is adjusted capacitor constant with the total capacitance of 1000 pF, placed across the accelerative slot (see Fig. 4), and variable/alternating capacitor. Each resonator is supplied from the power amplifier, loaded on the shunt impedance 3 kiloohm (Fig. 1 and 2). For the supply of six resonators with the voltage 20 kV on the revolution require 11 kW of power. In this case the efficiency is less than 22o/o. As the output tube of power stage serves tetrode 4CW10000AEl$_{max}$. The driver stage consists of six connected with the parallel power tetrods 4SKh350A; the seventh lamp 4SKh350A is utilized for the compensation for beam current and in the cathode of output tube.

The low value of common impedance is achieved by the introduction of strong negative feedback over entire range (Fig. 2). This determines the work or amplifier in the class A, since the low value of the impedance of source must be ensured with a small voltage of high frequency. Fig. 3a-c gives the experimental dependences of impedance on frequency Z=F(f).

The system of feedback makes it possible to obtain the necessary threshold value of the stability of beam. For guaranteeing the reliability into the system is added the sufficiently complicated element of the compensation for beam current.
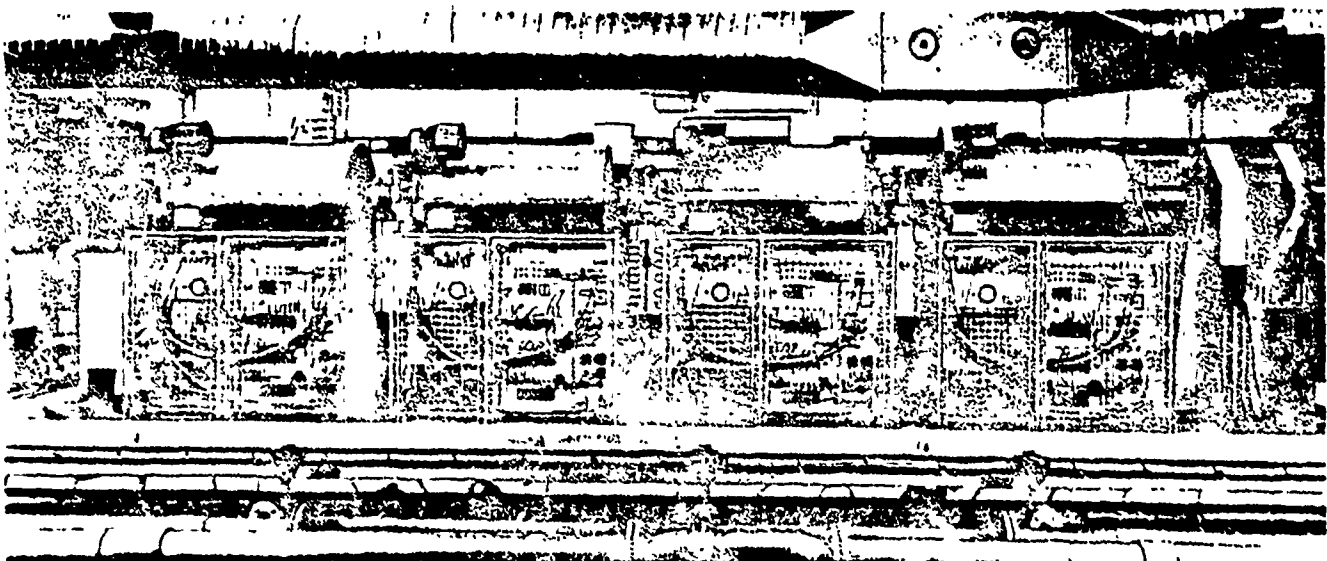
Fig. 1. The general view of four generators in the first octant.
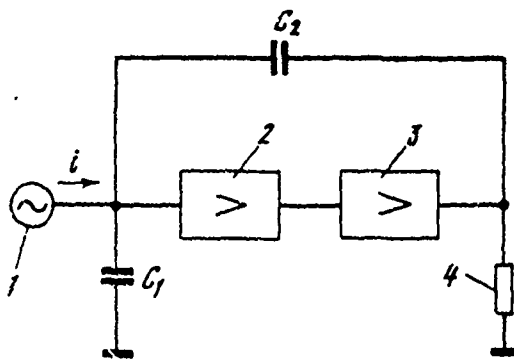
Fig. 2. Equivalent amplifier circuit of power and resonator. 1 -
current source; 2 - preamplifier; 3 - cascade circuit; 4 - equivalent
impedance of resonator.

Page 131.

In this case signal, hely from the beam by broadband sensor, fall
with proper phase and amplitude into the driver stage of high-power
tube. The value of equivalent impedance is $|Z| < 5$ ohm to the resonator.

Although the resonators must not possess too high a resistance
at frequencies higher than frequency of acceleration, nevertheless
the higher harmonics it is necessary to damp with ferrite rings which
form the integrating part capacitor constant on 1000 pF (Fig. 4).
Since the quality of resonator Q on the ferrite sharply falls at the
frequency of higher than the dual frequency of acceleration, these
frequencies substantially affect the operation of resonator. On the
other hand, the attenuation is necessary for the stabilization of
feedback loop.

The construction/design of resonator and power amplifier they
are developed on the modularized circuit. Power amplifier simply is
detached from the resonator and consists of several sections of
plunger type.

Resonator is made dismountable/release lengthwise and can be
opened for the access to vacuum chamber without the deterioration in
vacuum.

а

2 б
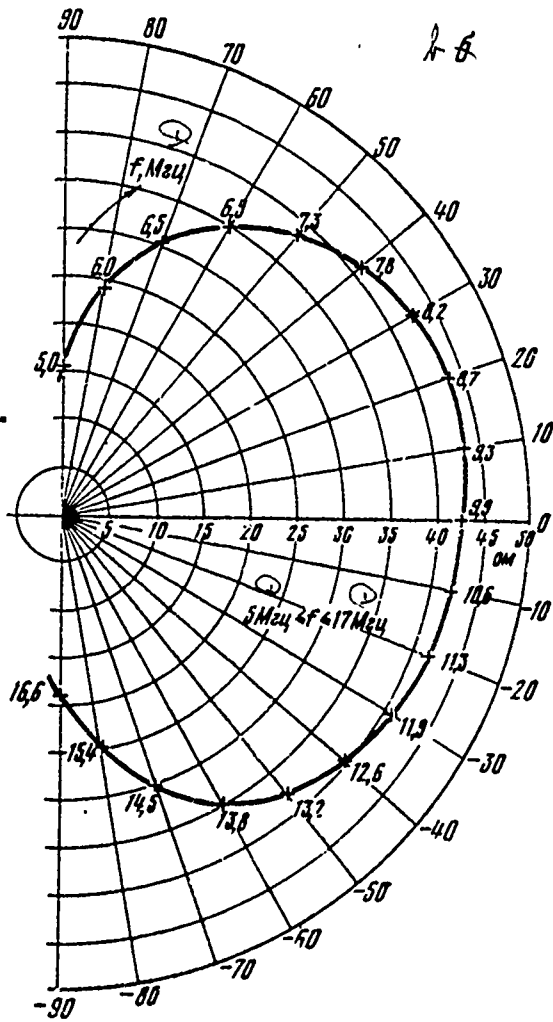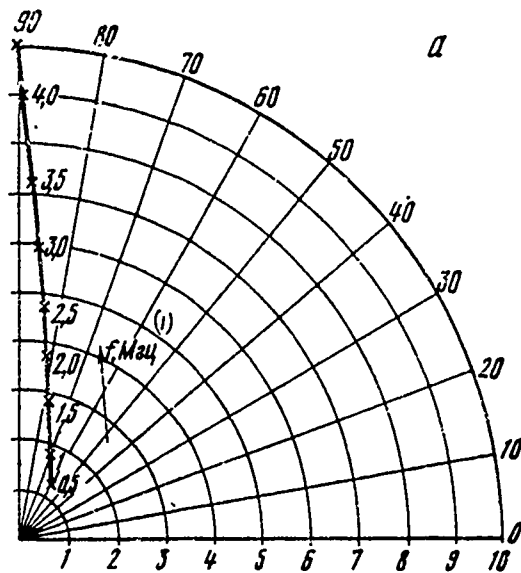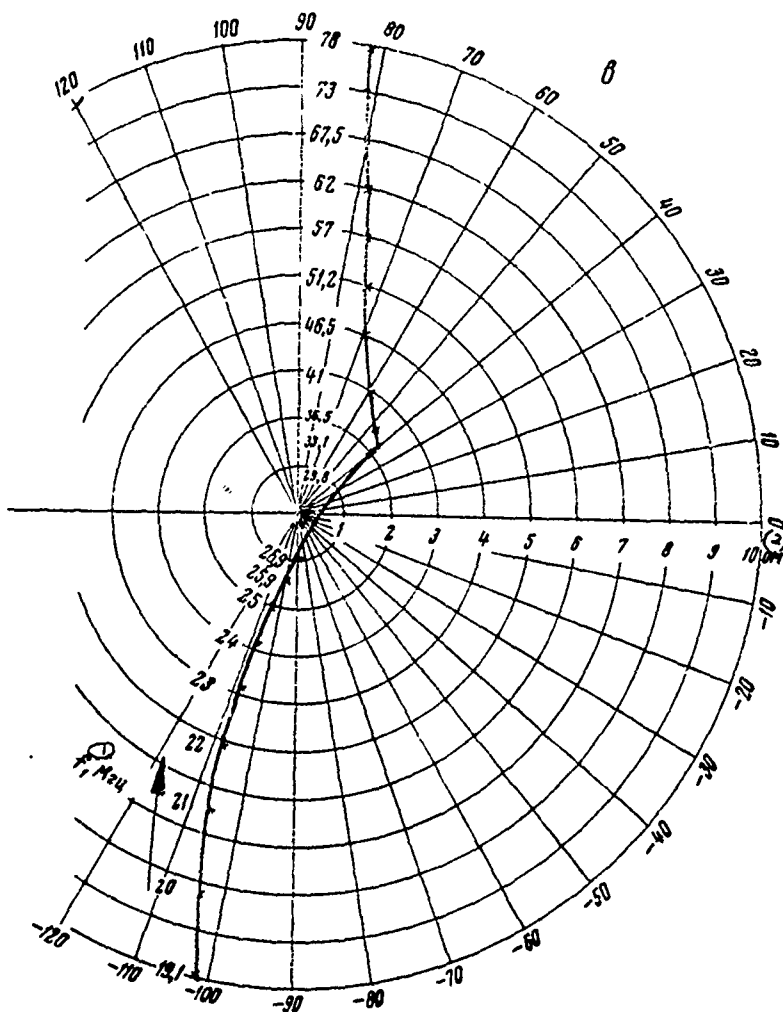
Fig. 3. Impedance of resonator in the function of frequency (MHz). a) 0.5-4.5; b) 5-17; c) 19.1-78.

Key: (1). MHz. (2). ohm.

5. System of the missing separatrix.

As it was noted earlier, it is necessary to take measures so that would not occur blurrings of separatrices in the phase space, until they were filled with protons of the injector. Therefore HF system must create high-frequency gate. making it possible to shape chain/network of 20 full waves wnich follows the dead time of 10 full waves.

Page 132.

The maximum voltage which can be obtained from the power amplifier in this mode/conditions, is limited to the maximum current of output tube and to ratio R/Q of resonator. Taking into account that the 1st and 2nd separatrices can somewhat be distorted with inclusion/connection and disconnection of voltage, system must create trigger pulse with an amplitude of 250-500 V of on one revolution.
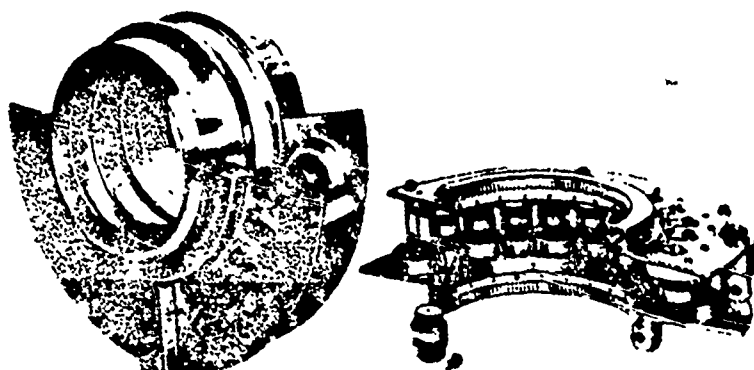
Fig. 4. The general view of tne elements/cells of tuning capacitor.

REFERENCES.

1. H.G. Hereward, K. Johnsen, A.Schoch, C.J.Zilverschoon. Proc. Internat. Conf. on High Energy Accelerators, 1961, p. 265–271.

2. K.Johnsen, W.C.Middelkoop, B.de Raad, L.Resegotti, A. Schoch, K.R. Symon, C.J.Zilverschoon. Proc. Internat. Conf. on High Energy Accelerators, 1963, p. 312–325.

3. O. Bayard. CERN–MPS/69/8 and 69/10, 1969.

4. K.Johnsen. Private communications.

5. W. Schnell. Stacking in proton storage rings with missing buckets. CERN–ISR–RF/67–38, 1967.

6. D.A.Swenson. CERN–AR/Int. – SR/61–19, 1961.

7. E.Keil, A.Nakach. CERN–66/9, 1966.

8. V.K. Neil, A.M.Sessler. Rev. Scient. Instr., 1965, v. 36, p.429–436.

9. A.M.Sessler, V.G. Vaccaro. CERN–67/2, 1967.

10. A.G.Ruggiero, V.G.Vaccaro. CERN–ISR–TH/68–33, 1968.

11. B.Zotter. Paper presented USSR II Nat. Conf. on Particle Accelerators, 1970.

12. E.Keil, W.Schnell. CERN–ISR–TH–RF/69–48, 1969.

Discussion.

V. A. Sichev. Was not examined in CERN for dealing with load by
beam the version of the construction of the final stage on the
diagram of cathode follower?

F. Ferger. Yes, but we arrived at the conclusion that this is
much less economical than the use of a deep negative feedback. With
the output on the cathode follower it is necessary 2 times of more
electron-tube power how there is, since cathode follower operates
furthermore with the high input voltage, which composes virtually
110o/o of voltage, which we want to transmit through it. Moreover,
cathode follower with such large voltages it is difficult to
stabilize, and it greatly easily converts/transfers into the
mode/conditions of generation.

I. I. Sulygin. Say, if you please, in the hall of circular
accumulator/storage in you are left all elements/cells of HF
generators or only output stages?

F. Ferger. In the circular hall only 3 cascades/stages: exit,
exciting and preexciting. All cascades/stages are carried out on the
hard tubes. We tried to avoid the use/application of semiconductor

and integrated circuits in these devices/equipment. On the other

hand, we hope that the intensity of radioactivity in the ring must be

very small, since the ring relied on the minimum of the losses of

beam in vacuum chamber, and we will not suffer from the radiation.

A. A. Komar. Is it possible it will change energy of protons in

the rings in order to trace the energy dependency of the measured

sections?

F. Ferger. Energy can be will be changed from 10 to 28 GeV, and

then from 3.5 to 28 GeV, which will make it possible to overlap

entire range of the available energies.

A. A. Kolomenskiy. How is explained the selection of energy 15

GeV for the works on the adjustment of rings?

F. Ferger. In this region of energies it is not necessary to

introduce magnetic field.

Page 133.

130. On the identification of the parameters of the accelerating system of large electronic circular accelerator.

S. A. Heifetz.

(Yorevan physical institute).

One of the main difficulties which must be overcome during the creation of large electronic circular accelerator (BEKU), is the compensation for energy losses to the synchrotron radiation. The value of these losses by particle in one revolution ΔE_{um} is proportional, as is known, the fourth degree of energy E of particle and first degree of the curvature ρ^{-1} of its trajectory. The accelerating system must ensure both covering these losses and strictly acceleration. An energy gain in one revolution U is determined by the relationship/ratio

$$U = f_u T_0 \bar{U} = 2\pi f_u T_0 E_0 \sqrt{1 - \delta^2 + 2\delta E/E_0 - E^2/E_0^2} \ , \quad (1)$$

where $E_0 = \theta H_0 \rho$, $(1-\delta) H_0$ - maximum value of magnetic field; f_u -
frequency of magnet power supply; δ - ratio of the constant component
of current in the magnet windings to amplitude of
variable/alternating, $T_0 = L_0/C$ - time of the access of resonant
particle; L_0 - length of its orbit. The total amplitude of
accelerating field on revolution $V_0 = (\Delta E_{u \cdot m} + U) \theta \cdot \cos \varphi_c$ defines both the
required power of high-frequency system and magnitude of losses of
particles for the time of acceleration. Its value, and also values
f_u, φ_s, frequencies of accelerating field f_u and number of
accelerating gaps k must be selected most optimally, so that for the
prescribed/assigned (small) fraction/portion of the lost particles
the average power $<P>$ of high-frequency oscillator would be as less
as possible.

Let us leave aside the asserting itself immediately output,
which consists in the creation of system with the large porosity and
not so much due to a reduction in the average/mean intensity of the
accelerated particles, as keeping in mind the desirability of the use
of a diagram with multiplication [1]. With the large porosity the
work in the mode/conditions of multiplication would become very
complex problem, since secondary particles it would be necessary long
time to somewhere "store".

The basic parameters of BEKU, which will be utilized for the

numerical estimations subsequently, are given below.

Maximum energy - 50 GeV.

Radius of curvature - 720 m.

Orbit circumference - is 7.55 km.

Logarithmic derivative α - $4.4 \cdot 10^{-4}$.

Number of accelerating gaps - 28.

Permissible relative energy dissipation (as a result of the correction of dependence Q_ν on E) - 1o/o.

Permitted of the field of the lost particles - 5o/o.

1. Estimation of the losses of particles.

The losses of particles in the phase oscillations occur in essence as a result of quantum fluctuations of radiation/emission. Precise calculations of losses are complex problem, in particular for the nonlinear vibrations. Such calculations in general can be carried out only numerically, which impedes the use of results of calculation

for the selection of the optimum parameters of the accelerating system. Obtained in this case precision/accuracy of estimations is hardly better than obtained with the aid of the approximation analytical formulas. For this reason we will utilize the simplest approximation formula for fraction/portion n of remaining in acceleration mode particles [2]:

$$n(t) = \exp\left\{-\frac{4(1+\beta)}{T_0}\int_0^t \frac{\Delta E_{uss}}{E}\frac{A^2_{gon}}{\bar{A}^2}\exp x \times (-A^2_{gon}/\bar{A}_2)\,\overline{dt}\right\}.$$

(2)

Here $A_{gon}, \sqrt{\bar{A}^2}$ - permissible and root-mean-square amplitudes of phase oscillations; β - coefficient, which considers the redistribution of the decrements of damping oscillations due to radial-phase connection/communication. In the strong-focusing synchrotron without the attenuation $\beta=0$. This value let us accept for the estimations.

Formula (2) is valid only when velocity losses it is small, i.e., when bulk of particles is located on the bottom of deep potential pits. Formally this condition is observed with fulfillment of inequality $A^2_{gon}/\bar{A}^2 \gg 1$. Furthermore, it is obtained for the linear oscillations, for which only and has sense $\bar{A}^{-2}$.

As shown in work [2], formula (2) can be utilized, also, for the large nonlinear vibrations, if only for A^2_{gon} to accept the value, which is obtained by the linearization of potential well,

$$\left(A^{(0)}_{gon}\right)^2 = 4(1-\varphi_s\,ctg\,\varphi_s).$$

(3)

However, are possible conditions, with which A^2_{qon} is determined not by phase oscillations. For example, this situation appears, when the effective boundary of the amplitude of phase oscillations is determined by the allowed value of the deviation of the frequency of transverse vibrations due to the divergence of their energy from the equilibrium.

Let us find the values of the equilibrium phases for which the permissible square of amplitude, determined by transverse vibrations

$$(A^{(M)}_{qon})^2 = 2\overline{\varphi^2}/\Omega^2 = 8\pi^2 f_y^2 \alpha^2 (\Delta E/E)^2_{qon}/\Omega^2 \qquad (4)$$

(where $\Omega^2 = 2\pi f_y \alpha (\Delta E_{usn} + U) tg\, \varphi_s / T_0 E$ — frequency of phase oscillations), becomes equal to $(A^{(\delta)}_{oon})^2$ (see (3)).

Page 134.

After equating relation $(A^{(M)}_{qon}/A^{(\delta)}_{qon})^2$ — to unit, let us find that for the values of phases less φ_{s} determined to the transcendental equations

$$tg\,\overline{\varphi}_s - \overline{\varphi}_s = \frac{f_y \alpha (\Delta E/E)^2_{qon}}{2f_u [\varpi(1-\cos\varpi)^3 + ctg\, \varpi/2]} \qquad (5)$$

$(A^{(M)}_{qon})^2 > (A^{(\delta)}_{qon})^2$. entering in (4) and (5) value $(\Delta E/E)_{qon}$ is determined by

the standard deviation of number Q_τ of radial betatron oscillations and is proportional $\Delta Q_\tau / Q_\tau$. For the parameters of the accelerator in the high-energy region $tg\,\bar{\varphi}_s - \bar{\varphi}_s = 0{,}01/(f_u/50)$ accepted (for the standard deviation of a number of radial oscillations $\Delta Q_\tau = 0{,}1$ and without the account to the correction of the dependence of frequencies on the energy). For $f_u = 50$ Hz this gives $\bar{\varphi}_s = 0{,}2$. However, for 90o/o of correction of the dependence of frequency on the energy (for $(\Delta E/E)_{gon} \approx 0{,}02$) $\bar{\varphi}_s = 1{,}08$.

In equation (5) $x = (\Delta E_{uam})_{E=E_0}/2\pi f_u T_0 E_0$, and $\bar{x} = 2\pi f_u t$.

The root-mean-square amplitude of phase oscillations for the accelerator without the attenuation is approximately equal to [3]:

$$\bar{A^2} = 255\, f_y\, T_0\, \alpha\, e^2 (E_0/mc^2)^3 / tg\,\varphi_s\, \rho (\Delta E_{uam})_{E=E_0}. \quad (6)$$

For evaluating the losses of particles let us accept in accordance with (5), which A_{gon} is determined $(\Delta E/E)_{gon}$. In this case we consider that $\Delta E_{uam} \gg U$):

$$(A_{gon}^{(m)})^2 / \bar{A^2} = a/(1-\cos x)^3,$$

where

$$a = \pi mc^2 (\Delta E/E)_{gon}^2 \,\sigma\rho/255 e^2 (E_0/mc^2)^2.$$

βAfter substituting this expression in (2) and after passing in to integration for x, we will obtain the following estimation of the fraction/portion of the remaining after particle acceleration:

$$n = \exp\left\{ -\frac{64 e^2 (E_0/mc^2)^3}{3mc^2\, \rho\, f_u\, T_0} \sqrt{\frac{\pi a}{24}}\, \exp(-a/8) \right\}$$

As is evident, in this case of loss they depend neither on $\varkappa_{y}$, from φ_{s}. For parameters ($\Delta E/E = \Delta Q/Q$) accepted n=0.28 for $f_{u} = 50$ Hz; n=0.73 for $f_{u} = 200$ Hz and n=0.85 for $f_{u} = 400$ Hz.

It is interesting to also find the estimation of losses for the case when the losses of particles define the boundaries themselves in the phase oscillations (i.e. $A^{2}_{qon} = (A^{(\delta)}_{qon})^{2}$.

In this case

$$(A^{(\delta)}_{qon})^{2}/\overline{A}^{2} = (tq\,\varphi_{s} - \varphi_{s})/\delta f_{y}, \qquad (7)$$

where

$$\delta = 255\,T_{0}\alpha e^{2}(E_{0}/mc^{2})^{3}/mc^{2}\rho(\Delta E_{uan}/mc^{2})_{E=E_{0}} \qquad (8)$$

it does not depend on energy.

The fraction/portion of the remaining particles is equal to

$$n = \exp\left\{-\frac{5(\Delta E_{uan})_{0}}{f_{u}T_{0}E_{0}}\,\frac{A^{2}_{qon}}{\overline{A}^{2}}\exp\left[-\frac{A^{2}_{qon}}{\overline{A}^{2}}\right]\right\}. \qquad (9)$$

Table 1 gives the results of estimation according to formula (9) of the fraction/portion of the remaining particles ($\delta = 0.335 \cdot 10^{-11}$ Hz^{-1}).

As can be seen from (9), the losses of particles in this case depend

on relation $(\eta \varphi_s - \varphi_s)/f_u$ and therefore, from the point of view of
losses, to it is more advantageous select the smallest possible
frequency of accelerating field. Having in mind also an increase in
shunt resistance R_w, with an increase in frequency ($R_w \sim \sqrt{f_u}$ [5]), it is
easy to understand that in this case are optimum values f_u and $\langle \cdot \rangle$
providing as the minimum of the power of oscillator, so also
retention/preservation/maintaining the prescribed/assigned
fraction/portion of particles in the mode/conditions of acceleration.

The decreases of fraction/portion of the lost particles it would
be possible to attain by an increase in the repetition frequency, but
this leads to an increase in the power of HF oscillator (appropriate
results for the brevity we omit). Output could be also an increase α
(decrease Q_+). However, in this case can become substantial the
effects of the discreteness of acceleration [4].

Table 1.

f_y, ru (1)	f_u, ru (1)		
	50	200	400
$1.2 \cdot 10^9$	0,32	0,75	0,87
$0.6 \cdot 10^9$	0,95	1,0	1,0

Key: (1). Hz.

2. Estimation of the optimum frequency of accelerating field.

Above it was shown that in the case when the losses of particles define the boundaries themselves in the radial oscillations, i.e., $(\Delta E/E)_{oon}$, these losses do not depend on the frequency of accelerating field f_y. Since $R_w \sim \sqrt{f_y}$ [5], it is more advantageous to select as possible more the high frequency of acceleration.

However, in the case of compensation Q_y from E, which can be required for decreasing the losses of particles, effective boundary can prove to be $(A_{oon}^{(o)})^2$ (4). In this case increase f_y of higher than certain optimum value again leads to an increase in the power of oscillator (for the prescribed/assigned fraction/portion of the remaining particles).

Optimum frequency f_y^o and phase ψ_s^o in this case can be found

from following relationships/ratios [6]:

$$tg\,\varphi_s^0 = 4\varphi_s^0/3, \qquad \varphi_s^0 = 0,85 .$$
$$f_y^0 = \varphi_s^0\,\overline{A}^2/3b(A_{gon}^{(6)})^2,$$

where B is determined by relationship/ratio (8), and $(A_{gon}^{(6)})^2/\overline{A}^2$ is determined from relationship/ratio (9) through the prescribed/assigned fraction/portion of the remaining particles n.

Table 2 gives the optimum values of the frequency of accelerating field and its wavelengths, found for the values $\alpha=4.4\cdot10^{-4}$ and n=0.95 (B=0.335$\cdot10^{-11}$ Hz^{-1}). The obtained wavelengths are too small in order to think about their practical use. However, this it indicates, in what range to it is more advantageous select the frequency of acceleration.

Page 135.

3. Given above considerations, in particular that that optimum wavelength of accelerating field proves to be so/such small, suggest, that should be thoroughly studied possibility of design BEKU as waveguide synchrotron [6]. The definite advantage of this solution is the decrease of orbit circumference by 30o/o ($\approx$5 km instead of 7.5 km) or, at the same length, an increase in the curvature (and, consequently, the decrease of the emitted energy) to 50o/o. Furthermore, in this case drop off all effects of the discreteness of acceleration.

Table 2.

f_u, ru(1)	$A^2_{pon}/\overline{A^2}$	$f^0_y \cdot 10^{10}$, ru②	λ^0_y, см
25	7,83	1,08	2,8
50	7,03	1,20	2,5
100	6,21	1,36	2,2
200	5,37	1,58	1,9
400	4,50	1,88	1,6

Key: (1). Hz.

REFERENCES

1. A. I. Alikhanyan, et al. International Conference on Accelerators of Charged Particles of High Energies, Vol. II, Izd-Vo Academy of Sciences of Armenian SSR, 1970, p. 103.

2. S. A. Kheyfets, Yu. F. Orlov, G. V. Gendzhoyan, ZhTF, Journal of Technical Physics, 1961, No. 7, 824.

3. S. A. Kheyfets. Losses of particles in modern cyclic accelerators. Candidates disertation, Yerevan, 1960.

4. S. F. Kheyfets. News of AS of Armenian SSR, Physics, 1968, 3 No. 4, 265.

5. K. W. Robinson. IRE Trans. Microwave Theory and Techn., 1960, 8, 593.

6. A. A. Vorobyev, et al. Waveguide synchrotrons, Moscow, 1966, Atomizdat, p. 79.

Discussion.

A. L. Mints. To me seems doubtful the advisability of positioning/arranging the accelerating structure within the small-aperture chamber/camera. This chamber/camera is singularly advisable. Therefore I think that to it is more right place the accelerating structures in gaps between the magnets.

S. A. Heifetz. The estimations of the optimum wavelength of accelerating field lead to the such low values, that there is the hope to place the accelerating structures within vacuum chamber without an increase in magnet opening.

A. N. Didenko. I would want to make the following observations.

1. Examining question about use of septate waveguides as accelerating systems of cyclic accelerators, it is necessary to investigate question about effect of all components of high-frequency field, in general case which are changed concerning radius and height of waveguide, to stability of action of particles. The calculations, given by us for the project of cybernetic accelerator on 1000 GeV, showed that if we utilize the waveguide systems of the t_pe of Shnell, which are double-row staircases in the circular waveguide, then the presence of the transverse components of high-frequency field leads to movement of operating point in the process of acceleration within the limits of the selected rhomb of stability. This shift can be such, that in the process of acceleration the operating point can the secants, which correspond to the resonances of the 3rd and the higher orders. This effect can be strongly weakened, if adjacent waveguide sections are turned relative to each

DOC = 80069311   PAGE 56 7

other on 90°.

2. Unfortunately, S. A. Heifetz's report does not contain
concrete/specific/actual data, but his conclusions are too
general/common/total and diffuse. I consider that data on the
development of the waveguide accelerating systems for the cyclic
accelerators, obtained at the present time in NII [
Scientific Research Institute] nuclear physics TPI and NIFI, even now
make it possible to make the more substantiated confirmations apropos
of advantages and disadvantages in one or the other system and
shortly to develop the design of the waveguide accelerating system
for the proton or electronic cyclic accelerator to the completely
specific energy.

Yu. F. Orlov. The conducted investigation shows that the use of
vacuum chamber within the magnetic clearance as the waveguide in the
large electronic circular accelerator to the energy 100 GeV is
completely inexpedient. I will indicate main reasons.

1. In version of magnet accepted we obtain large reduction of
prices of project due to small clearance (2-4 cm), small thickness of
framework and total light weight and reserved magnetic energy. Cannot
be indicated the version of the retarding structure, which would not
lead to a considerable increase either in the clearance or the length

of magnet, or reserved energy.

2. In version accepted vacuum chamber within magnet is absent. The chamber/camera, carried out as waveguide, will cost too dearly.

3. In version accepted is not required fine vacuum within magnet (it is sufficient $10^{-4}-10^{-3}$ mm Hg). chamber-wave requires obtaining vacuum $\sim 10^{-6}$ mm on the very large longth, which will also very raise in price project.

4. At wavelength ~ 10 cm optimum length of accelerating section taking into account beam load would be ~ 1 m, that many times of less than length of magnet. It would be necessary to introduce HF power on each meter of the length of magnet, which by itself will reduce magnetic length.

5. In version accepted we wanted to forego or almost to refuse tunnel for magnetic system. If we utilize chamber-waveguide, then hopes for the magnet, which has the form of cable (magnet-cable), prove to be unrealizable.

6. In version accepted overall length of accelerating gaps is 3 km at length of magnets 17 km. Power, which exits with the radiation/emission, the order of the half entire power of HF system.

Therefore chamber-waveguide gives actually advantage neither in the length of ring nor in power of HF system. Transition to the superconducting linear accelerators gives the overall length of HF gaps/intervals ~100 m (3 GeV/revolution) and will increase efficiency.

Page 136.

131. Selection of the fundamental characteristics of the accelerating system of proton synchrotron in the waveguide sections.

O. A. Val'dner, Yu. A. Khlestkov, A. V. Shal'nov.

(Moscow physical engineering institute).

The identification of the parameters of the accelerating system depends on the series/row of the competing factors. Such parameters, as radio-frequency, synchronous phase, equilibrium energy gain per revolution, etc., affect the characteristics of the processes, occurring both in the ring and in the accelerating system. In this work is made the attempt to sum up the basic laws, which are of interest. As the accelerating system is selected the broadband nonreadjustable system in the waveguide sections, which makes it possible to obtain high efficiency in the range of frequency rearrangement [1].

1. Large ring.

Let us examine some characteristics of the large ring of proton

synchrotron to the superhigh energy, which must be taken into consideration during the determination of the parameters of the accelerating system.

The maximum number of particles in orbit, determined by permissible Coulomb frequency shift of betatron oscillations (in the case of equality the frequencies of the booster and ring and full/total/complete filling of orbit with clusters)

$$N^{\delta}_{max} \sim |n|^{\frac{1}{2}} R^{-1} \gamma^1 a^2 \varphi_s^1 , \qquad (1)$$

where $|n|$ - index of decrease, a - radius of beam upon the injection. Let us note that N^{δ}_{max} does not depend on oscillator frequency ω and most strongly it depends on a radius of beam upon the injection (as a^2).

Number of synchrotron oscillations per revolution [2]:

$$\nu_{so} \sim V_s^{\frac{1}{2}} R^{\frac{1}{2}} \beta^{-\frac{1}{2}} \gamma^{-\frac{1}{2}} K^{\frac{1}{2}} \varphi_s^{\frac{1}{2}} \omega^{\frac{1}{2}} , \qquad (2)$$

where

$$K = -\frac{\alpha\gamma^2 - 1}{\gamma^2 - 1} .$$

Permissible energy and radial scatter of particles [2]:

$$\frac{\Delta p}{p_s} \sim V_s^{\frac{1}{2}} R^{-\frac{1}{2}} \beta^{-\frac{3}{2}} \gamma^{-\frac{1}{2}} K^{-\frac{1}{2}} \varphi_s^{\frac{3}{2}} \omega^{\frac{1}{2}} , \qquad (3)$$

$$\Delta \tau_c \sim |n|^{-1} V_s^{\frac{1}{2}} R^{\frac{1}{2}} \beta^{-\frac{3}{2}} \gamma^{-\frac{1}{2}} K^{-\frac{1}{2}} \varphi_s^{\frac{3}{2}} \omega^{-\frac{1}{2}} . \qquad (4)$$

It is most strong (3) and (4) depend on synchronous phase (as which can affect selection $\varphi_s^{\frac{3}{2}}$), from the point of view of the φ_s

agreement of phase volumes on syncarotron oscillations upon the injection.

The maximum intensity on the synchrotron oscillations, connected with the disturbance/breakdown of the mechanism of phase stability, depends on density distribution of space charge in clusters [3] for the even distribution

$$N^c_{max} \sim V^1_s \; \tau^1 \; \varphi^3_s \; a \qquad (5a)$$

and it does not depend on frequency, and for the sharply collapsible/dropped to the edges of cluster distributions

$$N^c_{max} \sim V^1_s \; \tau^2 \; \phi^4_s \; \omega^{-1} \qquad (56)$$

it does not depend on a radius of clusters and more strongly it depends on φ_s.

The optimum time of the phase correction must be of the order of the half the period of synchrotron oscillations [4]:

$$\Delta \tau_{\varphi a 3} \sim V^{-\frac{1}{2}}_0 \; K^{-\frac{1}{2}} \; R^{-\frac{1}{2}} \; \tau^{\frac{1}{2}} \; \rho^{\frac{1}{2}} \; \omega^{-\frac{1}{2}}, \qquad (6)$$

where V_0 - amplitude of accelerating voltage.

2. Accelerating system.

Efficiency $\eta = \dfrac{IV_i}{P_{0z}}$ and integral shunt resistance $x = \dfrac{V^2_s}{P_{0z} L_z}$, the characterizing effectiveness uses HF power and length of system [1]:

$$\eta \sim I^{-1} V_s^{-1} A^2(x,y) R_{cs}^{-1} L_{\Sigma}^2 n_c^{-1} \cos^2 \varphi_s \omega^2, \qquad (7)$$

$$\chi \sim A^2(x,y) R_{cs}^{-1} L_{\Sigma}^{-1} n_c^{-1} \cos^2 \varphi_s \omega^2, \qquad (8)$$

where R_{cs} - coupling resistance of the retarding structure, L_{Σ} - the total length of system, $A(x, y)$ - the parameter, depending on the full/total/complete fading (x) and the slip of particles (y) along the phase relative to wave at the length of section L [3], n_c - a number of sections in orbit. It is evident that η and χ most strongly depend on oscillator frequency (as ω^2), and χ does not depend on resistance of beam $\frac{V_s}{I}$ and on the total length of system.

The ohmic losses of HF power are determined by the parameter of fading $x: \frac{\Delta P_{\alpha}}{P_{0\Sigma}} \sim 2\pi n_c$. Taking into account that total required power $P_{0\Sigma}$ depends on the efficiency of section (7), for the ratio of total losses to the power of beam $P_s = IV_s$ we will obtain [1]:

$$\frac{\Delta P_{\alpha}}{P_s} \sim \eta^{-1} V_s^{-1} I^{-1} A^2(x,y) L^{-1} \cos^{-2} \varphi_s \omega^{-\frac{1}{2}}. \qquad (9)$$

It is interesting that with the fixed/recorded efficiency the losses decrease with an increase in the frequency.

Page 137.

The instability of the parameters of those accelerating sections (frequency ω of the arbitrary geometric dimension of section ℓ and

temperature t°) leads to a change in the amplitude of the
accelerating stress/voltage due to the appearance of supplementary
slipping and to the mixing of synchronous phase $\delta\varphi_s$. Counting
divergence $\delta\omega$, δl, $\delta t°$ mutually independent, for the case when in the
nominal rating they will achieve the synchronism (slip is absent), we
obtain:

$$\frac{\delta\omega}{\omega} \sim tg^{\frac{1}{2}}\varphi_s \delta\varphi_s^{\frac{1}{2}} \; L^{-1} \; R_{c8}^{-1} \; \omega^{-1} , \qquad (10)$$

$$\frac{\delta l}{l} \sim tg^{\frac{1}{2}}\varphi_s \delta\varphi_s^{\frac{1}{2}} \; L^{-\frac{1}{2}} \; R_{c8}^{-1} \left(\frac{1}{f_\theta}\frac{\partial f_\theta}{\partial l}\right)^{-1} \omega^{\frac{1}{2}} , \qquad (11)$$

$$\delta t° \sim tg^{\frac{1}{2}}\varphi_s \delta\varphi_s^{\frac{1}{2}} \; L^{-1} \; R_{c8}^{-1} \left(\frac{1}{f_\theta}\frac{\partial f_\theta}{\partial l}\right)^{-1} \omega^{-1} , \qquad (12)$$

where $\frac{1}{f_\theta}\frac{\partial f_\theta}{\partial l}$ - derivative of the frequency of the vibration mode θ of
the accelerating transmission mode according to size/dimension of l.
Let us note that relative tolerances in size and frequency are
proportional to $\omega^{\frac{1}{2}}$ and ω^{-1}, whereas absolute allowance $\delta\omega$ does not
depend on frequency, and $\delta l \sim \omega^{-\frac{1}{2}}$.

The effect of the "break of impulse/momentum/pulse" [5] can
occur by asymmetry strength of beam or accelerating section. The
multisectional character of the accelerating system, the large
duration of acceleration impulse and the recurrence of passage by the
beam of the accelerating sections are favorable reasons for the
development of this lateral instability. However, the presence in the
proton synchrotron of the focusing magnetic system, automatic control
on the beam they can preve to be the positive factors, which decrease

the effect of the multisectional character.

For the single accelerating section the value of the threshold intensity at which the increment of build-up/growth is equal to zero [5], is proportional:

$$N_{\text{nup}} \sim E_0^1 \, \tau^1 \, L^{-3} \, R_{CB}^{-1} \, \omega^{-3}. \tag{13}$$

In the multisection accelerator the divergence of the center of gravity of clusters in the field of the induced or transverse wave can build up until clusters hit to the walls of vacuum chamber (critical current). "Effective length", at which in the cyclic accelerator will be the break, is, obviously, the length, which corresponds to the half the period of synchrotron oscillations (time of the correction of the position of beam). From the qualitative considerations:

$$I_{\text{kp}} \sim E_0^1 \, \tau_{max}^1 \, n_C^{*-1} \, L^{-2} \, R_{CB}^{-1} \, \omega^{-2}, \tag{14}$$

where n_C^* - number of sections at "effective length" of accelerator.

Those enumerated and series/row of other factors, which are determining the identification of the parameters of ring and waveguide accelerating system, are assembled in the table. Is especially isolated φ_s and ω, since they most strongly affect the properties of accelerator. Points and circles designated the factors, which require increase φ_s and ω (next-to-last column) and decrease φ_s and ω (latter/last column). For example, from the point of view

of maximum intensity and allowances to the parameters of accelerating
sections φ_3 is desirable to increase, and for decreasing radial and
energy of scatter of particles, increase in efficiency and integral
shunt resistance of the accelerating system - to decrease φ_3. An
increase ω is desirable from the point of view of an increase in the
frequency of synchrotron, the decrease of scatter in a radius and
impulses/momenta/pulses, increase in the efficiency and shunt
resistance, decrease of transverse size of sections, ohmic losses and
increase in the relative allowances for the precision of
manufacturing the accelerating sections.

Page 138. Table. Basic factors, determining the identification of the parameters of the accelerating system.

(1) Факторы	(2) Параметры			●↓○ ω φ_s	●↓○ ω φ_s
Предельная интенсивность, определяемая бетатронными колебаниями	N^δ_{max}	$|n|^{1/2} R^{-1}$ $\quad \tau^1 \quad$ α^2	φ_s^1	— $\quad$ ○	
Частота синхротронных колебаний	ν_{so}	$R^{1/2} \beta^{-1/2} \tau^{-1/2} \kappa^{1/2} V_s^{1/2}$	$\varphi_s^{1/2}$	$\omega^{1/2}$ $\quad$ ◉	
Допустимый разброс по импульсам	$\dfrac{\Delta p^c}{p}$	$R^{-1/2} \beta^{-3/2} \tau^{-1/2} \kappa^{-1/2} V_s^{1/2}$	$\varphi_s^{3/2}$	$\omega^{-1/2}$ $\quad$ ●	○
Допустимый радиальный разброс	$\Delta \tau^c$	$|n|^{-1} R^{1/2} \beta^{-3/2} \tau^{-1/2} \kappa^{-1/2} V_s^{1/2}$	$\varphi_s^{3/2}$	$\omega^{-1/2}$ $\quad$ ●	○
Амплитуда бетатронных колебаний, соответствующая эмиттансу	$\Delta \tau_i^\delta$	$|n|^{1/4} R^{-1/2} \partial^{1/2}$ $\quad$ α^2	—	—	—
Аксептанс ускорителя	A	$|n|^{1/2} R^{-1}$ $\quad \alpha^2_{max}$	—	—	—
Амплитуда ускоряющего напряжения при инжекции	V_{oi}	$|n|^2 R^{-1} \beta^3 \tau^1 \kappa^1$	φ_s^{-3}	ω^1 $\quad$ ○	●
Время фазовой синхронизации при инжекции	$\Delta \tau_{фаз}$	$R^{-1/2} \beta^{1/2} \tau^{1/2} \kappa^{-1/2} V_{oi}^{-1/2}$	—	$\omega^{-1/2}$	●
Адиабатическое затухание синхротронных (радиально-фазовых) и бетатронных колебаний	Ψ_m	$\beta^{1/2} \tau^{-1/4} \kappa^{1/4} V_s^{1/4}$	$\varphi_s^{-1/4}$	$\omega^{1/4}$ $\quad$ ○	●
	$\Delta \tau^c$	$\beta^{-1/2} \tau^{-1/4} \kappa^{-1/4} V_s^{1/4}$	$\varphi_s^{1/4}$	$\omega^{-1/4}$ $\quad$ ●	○
	$\Delta \tau^\delta$	$|n|^{-1/2} R^1 \beta^{-1} \tau^{-1/2}$	—	—	—
Предельная интенсивность, определяемая синхротронными колебаниями:					
равномерное распределение плотности	N^c_{max}	$\tau^1 \quad V_s^1 \quad \alpha^1$	φ_s^3	— $\quad$ ○	
резко спадающее распределение плотности	N^c_{max}	$\beta^1 \tau^2 \quad V_s^1$	φ_s^4	ω^{-1} $\quad$ ○	●
К.п.д. ускоряющей системы	η	$\Gamma^1 A^2(x,y) R_{св}^{-1} n_c^{-1} L_\Sigma^2 V_s^{-1}$	$\cos^2 \varphi_s$	ω^2 $\quad$ ●	○
Интегральное шунтовое сопротивление	χ	$A^2(x,y) R_{св}^1 n_c^{-1} L_\Sigma^1$	$\cos^2 \varphi_s$	ω^2 $\quad$ ●	○
Апертура пролетного канала	a_{max}	$R_{св}^{-\kappa}$ $(\kappa \sim 1)$		ω^{-1}	●
Поперечный размер секции	φ			ω^{-1} $\quad$ ●	
Омические потери в.ч. мощности	$\Delta P_\alpha/P_s$	$\tau^{-1} \Gamma^{-1} A^2(x,y) \quad L_\Sigma^{-1} V_s^1$	$\cos^{-2} \varphi_s$	$\omega^{-1/2}$ $\quad$ ●	○

Key: (1). Factors. (2). Parameters. (3). Maximum intensity, determined by betatron oscillations. (4). Frequency of synchrotron. (5). Permissible variations along impulses/momenta/pulses. (6). Permissible radial scatter. (7). Amplitude of betatron oscillations, which corresponds to emittance. (8). Acceptance of accelerator. (9). Amplitude of accelerating voltage upon injection. (10). Time of phase synchronization upon injection. (11). Adiabatic damping of synchrotron (radial-phase) and betatron oscillations. (12). Maximum intensity, determined by syncarctron oscillations. (13). uniform density distribution. (14). sharply collapsible/dropped density distribution. (15). Efficiency of accelerating system. (16). Integral shunt resistance. (17). Aperture of span channel. (18). Transverse size/dimension of section. (19). Ohmic losses of HF power.

(20) Попуски на стабильность параметров ускоряющей секции							
(21) относительные	$\delta\omega/\omega$	R_{cB}^{-1}	L^{-1}	$\delta\varphi_{s}^{1/2}$	$(tg\,\varphi_{s})^{1/2}$	ω^{-1}	○
	$\delta l/l$	$\left(\frac{1}{f_0}\frac{\partial f_0}{\partial l}\right)^{-1}R_{cB}^{-1}$	$L^{-1/2}$	$\delta\varphi_{s}^{1/2}$	$(tg\,\varphi_{s})^{1/2}$	$\omega^{1/2}$	◉
(22) абсолютные	$\delta\omega$	R_{cB}^{-1}	L^{-1}	$\delta\varphi_{s}^{1/2}$	$(tg\,\varphi_{s})^{1/2}$	ω^{0}	○
	δq	R_{cB}^{-1}	$L^{-1/2}$	$\delta\varphi_{s}^{1/2}$	$(tg\,\varphi_{s})^{1/2}$	$\omega^{-1/2}$	○
	δt°	$\left(\frac{1}{f_0}\frac{\partial f_0}{\partial l}\right)^{-1}R_{cB}^{-1}$	L^{-1}	$\delta\varphi_{s}^{1/2}$	$(tg\,\varphi_{s})^{1/2}$	ω^{-1}	○
(23) Пороговая интенсивность из-за "обрыва импульса" в одиночной секции	$N_{пор}$	E_0^{1} $R^{1}R_{cB}^{-1}\tau^{1}L^{-3}$			—	ω^{-3}	
(24) Критическая интенсивность в многосекционном ускорителе	$N_{кр}$	E_0^{1} n_c^{-1} $R_{cB}^{-1}\tau^{1}L^{-2}$			—	ω^{2}	
(25) Длительность переходных процессов	$\tau_{пер}$	R_{cB}^{1}	L^{1}		—	—	—
(26) Вакуумный объем и вес металла ускоряющей секции	$V,\,G_{мет}$	L^{1}			—	ω^{-2}	●

(20). Allowances for the stability of the parameters of the

accelerating section. (21). relative. (22). absolute. (23). Threshold

intensity due to "break of impulse/momentum/pulse" in single section.

(24). Critical intensity in multisection accelerator. (25). Duration

of transient processes. (26). Vacuum volume and weight of metal of

accelerating section.

REFERENCES.

1. O. A. Val'dner, A. V. Shal'nov, Yu. A. Khlestkov, V. P. Zubovskiy. Transactions of the All-Union Conference on Accelerators of Charged Particles. Moscow, 1968, Izd-Vo VINITI, 1970, Vol II, p. 149.

2. A. A. Kolomenskiy, A. N. Lebedev. Theory of Cyclic Accelerators. Moscow, Fizmatgiz, 1962.

3. Yu. A. Khlestkov, Yu. M. Tereshchkin. ZhTF. Journal of Technical Physics, 1971, 41, No. 2, 339. See also present collection. Vol. II.

4. 200BeV Accelerator Design Study, LRL, VIII-2, June, 1965.

5. G. V. Voskresenskiy, Yu. N. Serebryakov. Transactions of the All-Union Conference on Accelerators of Charged Particles. Moscow. 1968. Moscow VINITI, 1970, Vol. II, p. 442.

Page 139.

132. Los Alamos meson-producing cyclotron.

E. A. Knapp.

(California university, USA).

1. Introduction.

The construction of new experimental installations for obtaining the information about the nucleus and the elementary particles pursues the target of the expansion of experimental possibilities in two completely different directions. On one hand, the construction of accelerators to ever higher energies brought fruitful results, after making it possible to reveal/detect many new phenomena which thus far still remain incomprehensible. Another possibility of expanding the boundaries of the region of investigations, determined by the intensity of beam, available for the experiments on the accelerators, begins to be utilized only now. Only practice will make it possible to give response/answer to a question, will expand an increase in the intensity of the beams of the possibility of obtaining the new information about the nucleus and the elementary particles to the

same degree as an increase in the energy. Higher intensities can be
utilized for the investigation in the regions of physics,
unattainable with the less intense flows, by two different methods.
First, the higher intensities of beam make it possible to attempt to
observe the very rare events whose probability at the smaller
intensities proves to be too small for their observation. In the
second place, high intensities can be used for increasing the
resolution in the experiment, which has as a goal the detection of
the effect of the fine structure which can contribute to more a
fundamental understanding of the phenomenon being investigated. An
increase in the intensity to the greatest extent expands the
possibilities of experimentation, in which are utilized secondary
beams, for example, beams π - mesons. At Los Alamos meson-producing
cyclotron (LAMF) the intensity of proton beam with the energy 800 MeV
will be increased to four orders. Energy is selected from the
considerations that along with the intense primary beam to obtain the
intense flows of secondary particles, namely pi-mesons, μ- mesons,
which are formed as a result of their decomposition/decay, and also
neutrons. Average/mean intensity of proton beam in 1 mA was selected
on the basis of the following considerations. First, contemporary
level of development of technology and available experiment make it
possible to work with such intensities in the sense that heating
target, induced radioactivity and requirements, presented to the
protection, do not represent serious problems.
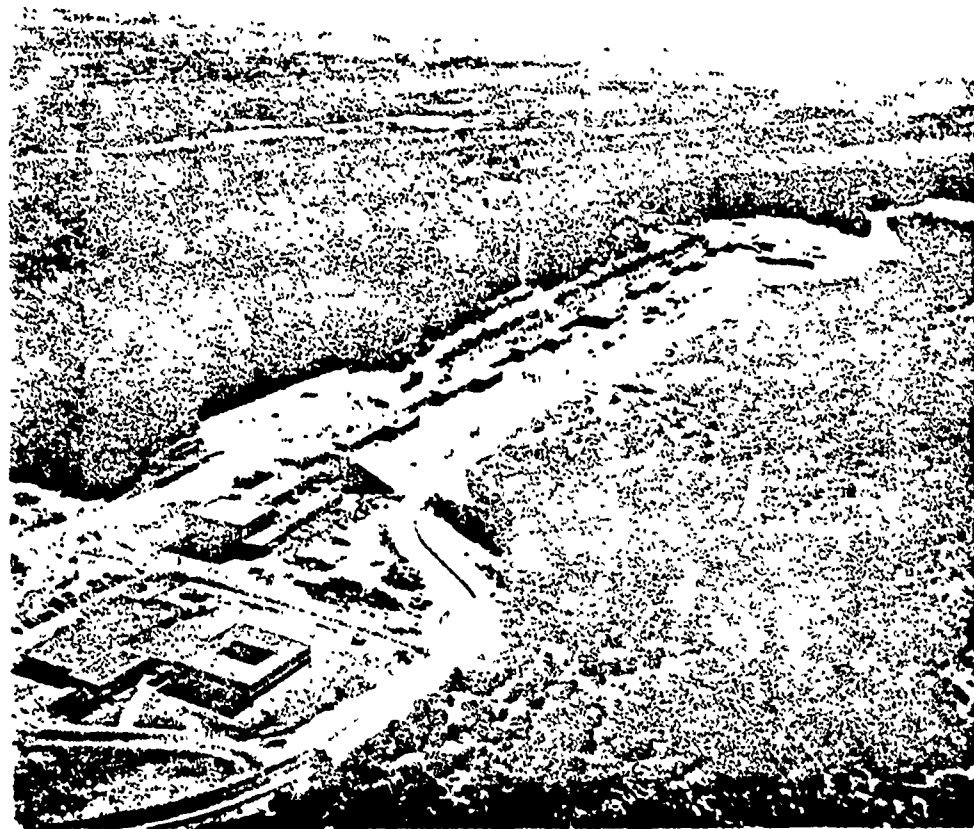
Fig. 1. Aerial photograph of construction of LAMF.

Page 140.

In the second place, this intensity of beam, from the point of view

of the opened/disclosed possibilities of experiment, they are

completely new region. Another being of large interest parameter is

macroscopic duty factor whose increase from 6 to 12o/o corresponds to

improvement almost to two orders in comparison with the possibilities

cf contemporary linear accelerators both proton, and electronic and
provides exceptional universality from the point of view of
experiment. The basic parameters of linear accelerator LAMF are given
on page 148.

2. General/common/total description of the construction/design of
accelerator LAMF and state of its construction.

Main accelerator LAMF consists of three parts: injector on 750
keV; the supplied of it drift-tube linac (of Alvarez's type), of the
worker at frequency 201, 25 MHz and linear accelerations with the
variable/alternating energy to 100-800 MeV, working at the frequency
805 MHz. The overall length of accelerator is 840 m. Fig. 1 shows
aerophotography of construction, taken/removed during June 1970.

The complex of injector will consist Cockroft-Walton's their
three accelerators whose sources will give the positive ions of
hydrogen (H^+), negative icns of hydrogen (H^-) and polarized negative
ions of hydrogen [1]. Provision is made for the system of
transportation and bunching of beam, which ensures the possibility of
simultaneous injection into the section of the type of Alvarez of the
beams of positive and negative icns or positive and polarized
negative ions; the construction/design of linear accelerator provides
for simultaneous acceleration of both beams and their separation by

the beam-separation system. The possibility of the simultaneous
acceleration of positive and negative hydrogen ions provides the high
universality of accelerator in the sense of the possibility of
simultaneous experimentation in several beam areas. the magnetic
separation of the beams of positive and negative ions, and also
use/application by correspondingly of the mixed foil for the
stripping of the negative ions, which are determining the emittance
of the obtained positive ion beam or which create several
supplementary proton beams, makes it possible to ensure the wide
selection of the conditions for experiment. Fig. 2 shows the
plan/layout of injection complex and system of the transportation of
beams, intended for the accomplishment of this objective. At present
the high-voltage rectifier of Cockroft-Walton, ionic source and
system of the transportation of the positive ion beam of hydrogen are
found in running order; satisfactorily moves work on the equipment
installation for obtaining the beam of negative hydrogen ions. At
present are conducted measurements for the purpose of the
determination of the emittance of beam and its energy uniformity. As
a result of preliminary measurements were obtained very satisfactory
characteristics. At the entrance into the first tank of a section of
Alvarez's type were obtained the values of emittance less 1π cm mrad.
The difficulties, connected with the limited service life of source,
it was not noted. In Fig. 3 it is shown photograph of injector -
Cockroft-Walton's accelerator.

The drift-tube linac on 100 MeV has the new construction/design, which promises to be considerable improvement in comparison with the accelerators of such type, constructed several years ago. In this new system, developed in recent years in Los Alamos laboratory [2], for stabilization of the magnetic field and elimination of the phenomena, connected with the beam load, transition effects and detuning of resonators, are utilized resonance dowels.
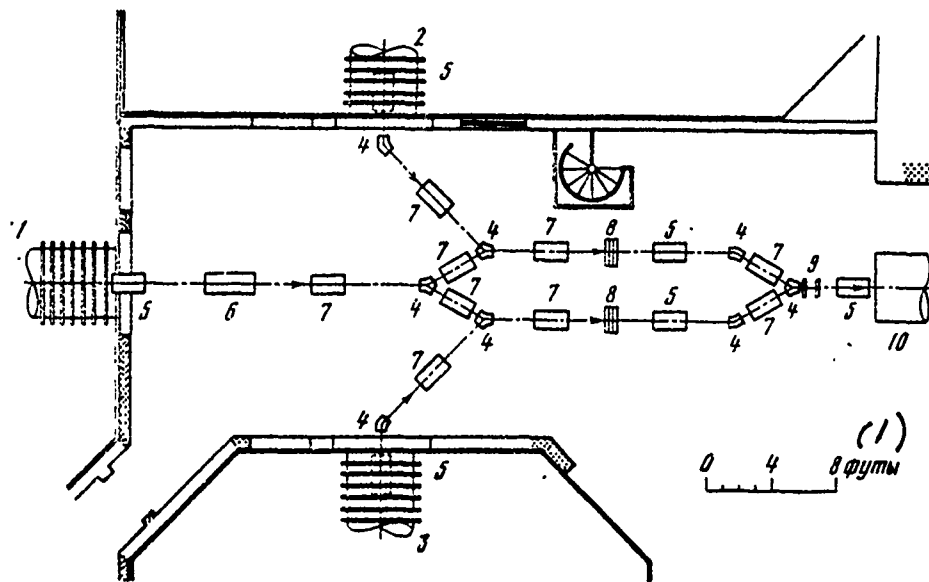
Fig. 2. Injector and system of the transportation of the beam: 1 -
source of the polarized ions; 2 - source H^+; 3 - source H^-; 4 - the
deflecting magnet; 5 - quadruplet; 6 - magnet for rotating the
direction of polarization; 7 - triplet; 8 - shaper of beam; 9 -
buncher; 10 - section of accelerator with the drift tubes.

Key: (1). In the feet.

Page 141.

They provide a change of the characteristics of the propagation of
the accelerating wave in the resonator due to an increase in the
group velocity from zero to high values, as a result of which, for

example, the sensitivity of field distribution to the detuning of
resonators descends more than 200 times in comparison with the
sensitivity of usual resonators. The high group velocity provides
also the uniform build-up of field in the resonators upon the
inclusion/connection or during other transient processes. The linear
accelerators of old construction/design were distant from
satisfaction of this condition.

the supply of these resonators is accomplished/realized from the
triode amplifiers RCA7835, which work at average/mean power 430 kW,
also, at the peak power of 3.0 MW. The peak power, indicated above,
is completely usual. However, average/mean power consumption is
completely unusual, and for the satisfaction of the stated
requirements was required the careful studying of construction/design
[3]. The unique special feature/peculiarity of the high-frequency
amplifier, arranged/located in the tank accelerator, is very precise
amplitude control and phase of field, provided by the
construction/design of system. Theoretically because of the very good
characteristics of the propagation of energy in the tank of
accelerator field measurement at one point makes it possible to
determine its amplitudes and phases in the entire system. The
thoroughly thought-out construction/design of the system of the
feedback, intended for the control of field by means of a change in
amplitude and phase of excitation, to ensure dynamic control of these

parameters during the high-frequency pulse with the
precision/accuracy is better than one percent in the amplitude and
one degree on phase [4].

The first section of section with the drift tubes to the energy
5 MeV is already led to the working order; on 10 June, 1970, is
obtained proton beam with the energy 5 MeV. At present this section
is utilized for the tests of the high-frequency power-supply system
and injector in process of which slowly are removed technical
defects. The first tank of linear accelerator to the setting up of
covers/caps is shown in Fig. 4. Fig. 5 shows the same tank, installed
together with the system of the transportation of beam. To the autumn
of 1970. it is proposed to obtain the large part of the data about
the characteristics of this system. the plans/layouts of construction
provide for obtaining proton beam with the energy 100 MeV during July
1971, and at present not evidently any obstructions and to their
execution.

The section of linear accelerator LAMF, which provides the
acceleration of protons from 100 to 800 MeV, it has the unique new
construction/design which, as they assume/set, it will ensure
exclusively good characteristics both in the sense efficiency during
the conversion of high-frequency energy into the energy of beam and
in the sense of the precision/accuracy of timing adjustment of

electromagnetic field in accelerator [5, 6]. At the basis of the
construction/design of linear accelerator LAMF lies/rests the system
of resonators with the lateral coupling elements, shown in Fig. 6. In
this system the sequence of the accelerating cavities,
arranged/located along the axis/axle of bundle, is connected with the
coupler cavities, arranged/located beside the axis/axle of bundle. In
the operational conditions (mode $\pi/2$) these coupling elements are
excited very weakly, which provides the insignificant dissipation of
high-frequency energy, but is formed the mechanism, which ensures the
very rapid energy transfer with the transient processes in the system
or the emergence of the imbalance of field. The action of such
resonators is analogous with the action of resonance dowels in the
drift-tube linac, and stabilization is compared with attained at the
use of dowels. The measurements of their shunt resistance showed that
in this case is reached the gain in the efficiency almost four times
in comparison with the resonance wave-guide system, loaded with
diaphragms, and an increase in the stability of field 200-500 times.

590
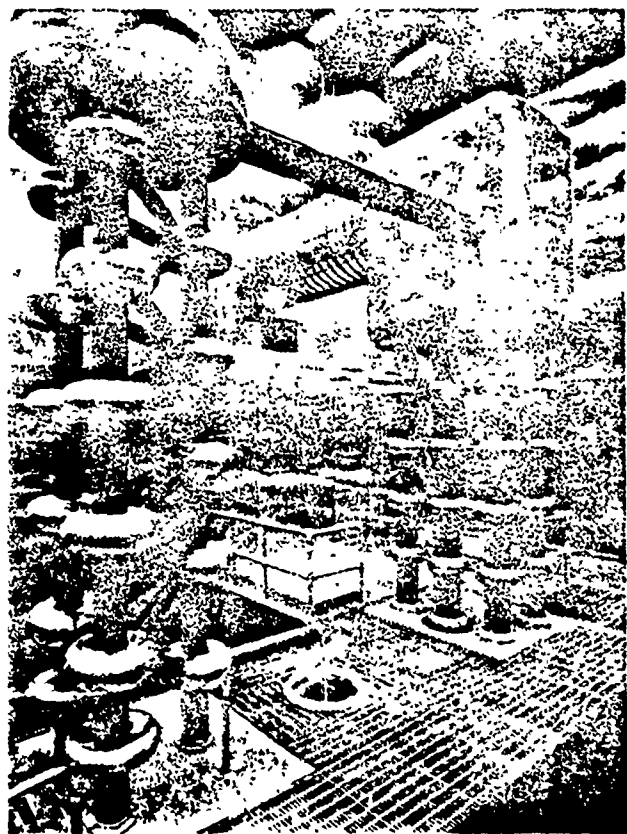
Fig. 3. Injector of Cockroft-Walton's type.
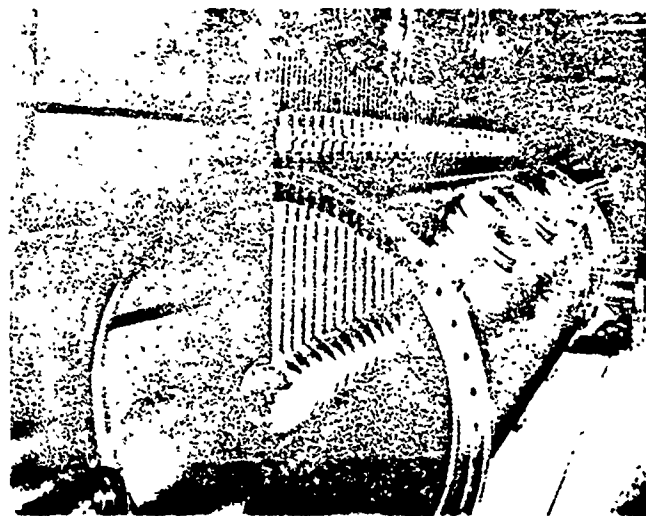
Fig. 4. First tank of accelerator of Alvarez's type before setting up of covers/caps.

Page 142.

Fig. 5. First tank of accelerator of Alvarez's type in installed
state with line of transportation of beam.
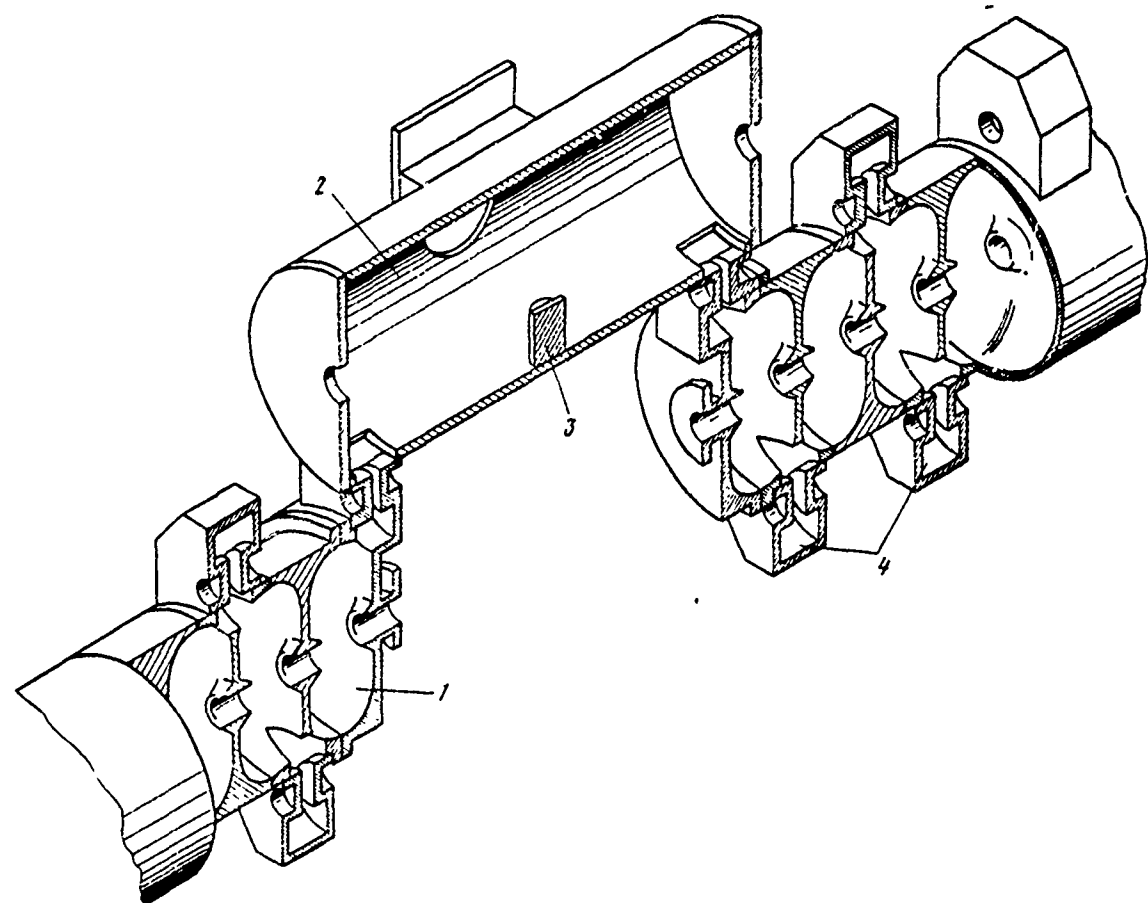
Fig. 6. Structure of accelerator with lateral connection/communication: 1 - accelerating cavity; 2 - coupling resonator; 3 - resonance dowel; 4 - resonator of connection/communication.

Page 143.

The high-frequency system, utilized for the supply of this part of the linear accelerator LAMF, is also unique development. Its basic part is klystron with power 1.25 MW with the modulating anode in power 160 kW, which is the greatest achievement in the region of developing the high-power tubes for the supply of linear accelerators. This lamp works in the mode/conditions of linear amplifier, moreover the modulating anode is utilized only for including of lamp and its disconnection, but not for the control. Fine adjustment of power output and phase is accomplished/realized due to modulation of radio-frequency drive. Were made the very careful measurements of the characteristics of these amplifying tubes, which makes it possible to optimize the construction/design of the feedback of the control system. Conducting these measurements required the developments of the precision high-frequency measuring meter which was not produced by industry [8].

At present the production of resonators with the lateral coupling elements of that initiated of approximately 25o/o of their total number is already prepared, and is conducted their assembly in the tunnel of accelerator. Fig. 7 shows the photograph of the tunnel of accelerator with the installed part of the linear accelerator. The delivery of the first series samples/specimens of klystrons is expected during September 1970. Is completed the production of two prototypes of high-frequency systems; is initiated the production of

the systems of modulation. it is assumed that the series
sample/specimen of high-frequency system will be finished/prepared
for the tests in the fall of 1970. The prototypes of high-frequency
systems were used for the longevity tests of klystron amplifiers. at
present 10 klystrons studied under high voltage 22000 hours without
the emergencies; for one of them during 7000 hours of work it was not
noted any signs/criteria of deterioration in the characteristics.

The development of the convenient for the mass use method of the
adjustment of resonators and the subsequent tests of. these resonators
with the high loads were the most labor-consuming work on the
investigation of accelerative systems, carried out in the course of
the latter/last six months. Although the allowances for the systems
of resonators with the lateral coupling elements are not too rigid,
is required the very fine tuning of general/common/total frequency
and the very precise knowledge of the medium frequency of the
matching elements/cells. The general/common/total leading principle,
accepted by the autumn of last year, lies in the fact that for
achievement of the reproducible results during the adjustment of
10000 resonators of which consists the system, is necessary the
method of the adjustment of individual resonators, which ensures the
appropriate precision/accuracy.

Fig. 7. Tunnel of linear accelerator LAMP with the established/installed sections of accelerator.

Page 144.

Was completed the development of equipment for the adjustment and the corresponding procedures, and after several false starts was begun

the series adjustment of resonators in the tunnel of accelerator
which continues already somewhat acre than month. The uniformity of
the distribution of electric field, attained with the aid of these
methods of adjustment, apparently, satisfies the requirements, which
escape/ensue from the dynamics of beam.

Were initiated the tests of accelerative system with the high
loads. The first measurements were carried out for the target be
convinced of the fact that accelerating field does not depend on the
average/mean power level in the individual tanks of accelerator. For
explaining this question were developed some unique instruments with
the aid of which it is possible to conduct the measurements of a
difference in the frequencies of accelerating cavities and coupling
elements with the precision/accuracy of above 10 kHz at the peak
power of 1 MW and relative change in the amplitudes with the
precision/accuracy approximately 1o/o. The results, obtained up to
now, show that the amplitudes of field are changed less than by 2o/o
with a change in the average/mean power of excitation from 9 to 90 kW
at the peak power of approximately 750 kW. Continue further
investigations for the purpose of determining the tuning precision of
individual resonators. In the near ones several months will be
carried out measurement at the high power for the purpose of checking
the transient responses, calculated theoretically, the investigation
of the characteristics of feedback loops for amplitude control and

phase in the final construction/design of accelerator and attempt at
revealing the possible problems, connected with the reliability of
the systems as a whole, which can require attention subsequently.

Besides these investigations, conducted on the serially produced
nodes/units of final construction/design, during more than two years
at present already continues the operation of the electronic
prototype of accelerator [9] in process of which were obtained
exclusively good results. this accelerator was intended for a strict
and precise checking of automatic control systems of amplitude and
phase which will be utilized in the linear accelerator LAMF, and also
for the common checking of the characteristics of the waveguide
system of accelerating cavities with lateral
connection/communication. The advantages of the linear accelerators
in which can be utilized the automatic control system with feedback,
visually become apparent in the measured characteristics of beam at
output of accelerator. Addition of the system of the transportation
of beam with the magnetic analyzer made it possible to measure the
characteristics of beam at output with the high current. Passage
90o/o of accelerated beam through the system of slots, which ensures
momentum resolution +-0.25o/o with the energy 25 MeV, is standard,
and the instability of energy of the accelerated beam comprises less
than 0.1o/o. These numerals characterize the precision/accuracy of
the work of automatic control system with the feedback and confirm

that the characteristics of accelerator are actually/really such,
that make it possible tc utilize for the supply the systems of the
feedback of field measurement at one point. It is proposed to conduct
further tests of this accelerator for the purpose of the more
detailed investigation of its characteristics.

In the system of control LAMP is utilized average/mean TsVM [
- digital computer], which accomplishes/realizes check of all systems
of setting up and control by them [10]. Were designed couplers for
collection and transmission of the corresponding information; the
prepared prototypes of this equipment successfully worked under
conditions of the high noise level in immediate proximity of the
high-frequency amplifiers. Is obtained the controller and at present
is conducted work on scftware of system. Is posed the problem during
the winter of 1970-1971 cf checking the control system in the
operation on the injector complex and the first tank of an
accelerator of Alvarez's type. Will further carried out the tests of
system as a whole for the purpose of checking its ability fulfill the
entrusted to it functions. At present the degree of the readiness of
entire complex of accelerator ccmprises more than 50o/o.

3. Investigations in physics of nucleus and elementary particles at
Los Alamos meson-producing cyclotron.

Which best way of using the provided by LAMF fantastic increase
in the intensity for obtaining new data in the region of physics of
nucleus and elementary particles? This question is sufficiently
complex and to it it is not possible to give immediate
response/answer. The author will attempt to help listeners to
understand some considerations, which served as basis/base for the
construction of this setting up. For this purpose will be examined
some experiments which were proposed or they are prepared for the
conducting on LAMF. At the basis of these experiments li. ~/rests the
use of high intensity of beam either for increasing the statistical
precision/accuracy during the observation of very rare events and
processes, which have small sections, or for an improvement in the
experimental resolution.

Two most important systems of experimental installations are
intended for a considerable increase in the general/common/total
resolution with which it is possible to carry out different
experiments. Such systems are the complex of the proton spectrometer
of high resolution (PSVR) and the channel of spectrometry of those
scattered $\mathcal{K}$.- mesons (KSRM). Stimulus for the development of these
programs were faster consideration the expansions of the experimental
possibilities of nuclear physics, than the interests of physics of
elementary particles.

At the basis of the selection of construction/design PSVR
lie/rest following considerations [11]. With the energies, which
exceed several hundred MeV, mean free path of nucleons by the nuclear
substance is maximum, the probability of their multiple scattering in
the nucleus minimum, the De Broglie wavelength is lower than average
distance between the nucleons and it is possible to consider that the
bombarding protons interact in the nucleus with the separate
nucleons. Because of this the experimenter falls into the completely
new region, than that that was investigated with the energies,
available with the aid of the accelerators of a Van de Graaf. In this
region can be set the experiments, which make it possible to
investigate the behavior of separate nucleons or nucleon associations
in the nucleus. For example, the observation of reactions of the type
(p,px),   where x designates any light nucleus, in particular, deutron
or alpha-particle, will make it possible to investigate the
correlations between the nucleons of nucleus. Is at present selected
the final version of construction/design PSVR, and will agree orders
for the delivery of many basic elements of this setting up. Is
selected the method of spectrometry on the energy losses of
particles. In other words, will be used such spectrometric system, in
which the degree of the inelasticity of reaction is measured with
considerably the higher precision/accuracy than the absolute values
of the impulses/momenta/pulses of the bombarding and scattered
particle.

Page 145.

This construction/design makes it possible to utilize considerably higher speed of count without a reduction in the precision/accuracy.

It is expected that PSVR will possess the following characteristics: 1) energy resolution 100 keV (full/total/complete width on the half height) for the protons with the energy 800 MeV, scattered on Mg^{2+} at angle of 45°. 2) the solid angle of 10 msr. 3) Angular resolution 2 mrad, minimum scattering angle by 10°.

4. Achromatic system of the transportation of beam.

Fig. 8 shows the beam-separation system at the output from the accelerator. The beam of negative hydrogen ions is deflected/diverted to the left, is recharged to abrasive device/equipment and is directed for beam area c, where is arranged/located the electromagnet of spectrometer.

(1) Масштаб в футах
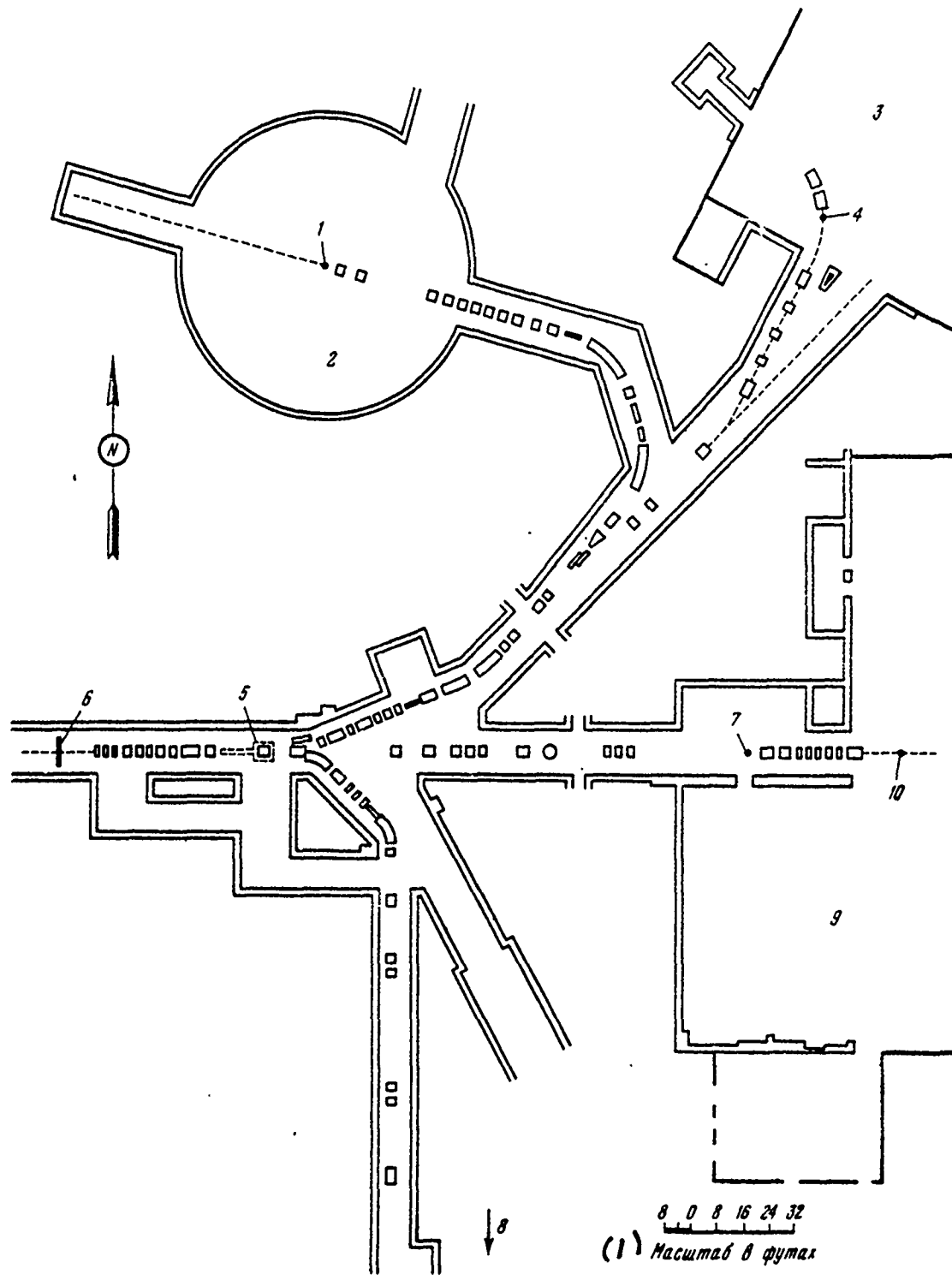
Fig. 8. The plan/layout of the beam-distribution system at the output of the accelerator: 1 - turntable of spectrometer and target; 2 - beam area S; 3 - beam area V; 4 - target from deuteride of lithium; 5 - device/equipment for the decontamination and monitors of beam (length - 1.5 m), that consists of carbon slots, ionic chamber/camera, monitor with the secondary emission, etc., 6 - output of accelerator; 7 - thin target; 8 - to beam area D; 9 - beam area A; 10 - target A-1.

Key: (1). Scale in feet.

Page 146.

In target region the beam undergoes dispersion in the vertical direction, and then is assembled in the spectrometer, so that the elastic scattered protons are focused into the point whose position does not depend on the position of source. Fig. 9 shows magnet PSVR and shielded chamber/camera of spectrometer. The characteristics of spectrometer indicated make it possible to raise momentum resolution 45 times in comparison with the achievement in the analogous experiments on the cosmotron and to observe processes with the sections to two orders lower than they were investigated earlier.

At the basis of construction/design of KSRM lie/rest analogous

considerations with the difference that here as the "projectiles" for
the nuclear bombardment are utilized the pi-mesons, but not protons
[12]: their use/application significantly simplifies the
interpretation of results. Since the spin of pion is equal to zero,
the amplitude of pion-nucleon scattering has considerably simpler
spin structure, than the amplitude of nucleon-nucleon scattering.
With the low energies the amplitude of pion-nucleon scattering also
is considerably weaker than the amplitude of nucleon-nucleon
scattering, and considerably more simply it depends on energy.
Therefore optical models, brought-out theoretically, and
conclusion/output, obtained in the approximation/approach of single
scattering, will very agree well with the data about the scattering
with the low energies of pi-mesons, but not nucleons.

Pions differ from nucleons in the mass, the isotopic spin and
the statistics by which they are subordinated. Because of this
difference connection/communication between the energy, the
impulse/momentum/pulse and the moment of momentum for the pi-mesons
another, than for the protons. A difference between spins and
isospins of these particles leads to the fact that during scattering
of pi-mesons by nucleus are soaked other nuclear states, than during
the scattering by the nucleus of nucleons. Dual overcharging can
serve as the characteristic example to the reaction, making it
possible to obtain the nuclei, unattainable with other methods of

study. Since the pi-meson is not identical to the particles, entering
nuclear composition, Pauli's principle does not create difficulties
with the interpretation of the corresponding experiments. The capture
of pi-meson by nucleus increases energy of nucleus on 140 MeV without
a change in its moment of momentum. The investigations of the capture
of pi-mesons can give information about the correlations between the
nucleons, their momentum distribution and existence in the nucleus of
nucleon associations.

Use both of positive and negative pi-mesons gives very
interesting to possibility obtainings of information about
differences of the distribution of protons and neutrons in the
nucleus as a result of the study of the full/total/complete inelastic
scattering cross section and differential elastic cross sections.

(1) Экспериментальная зона С

5 0 5 10 15 Футы (2)
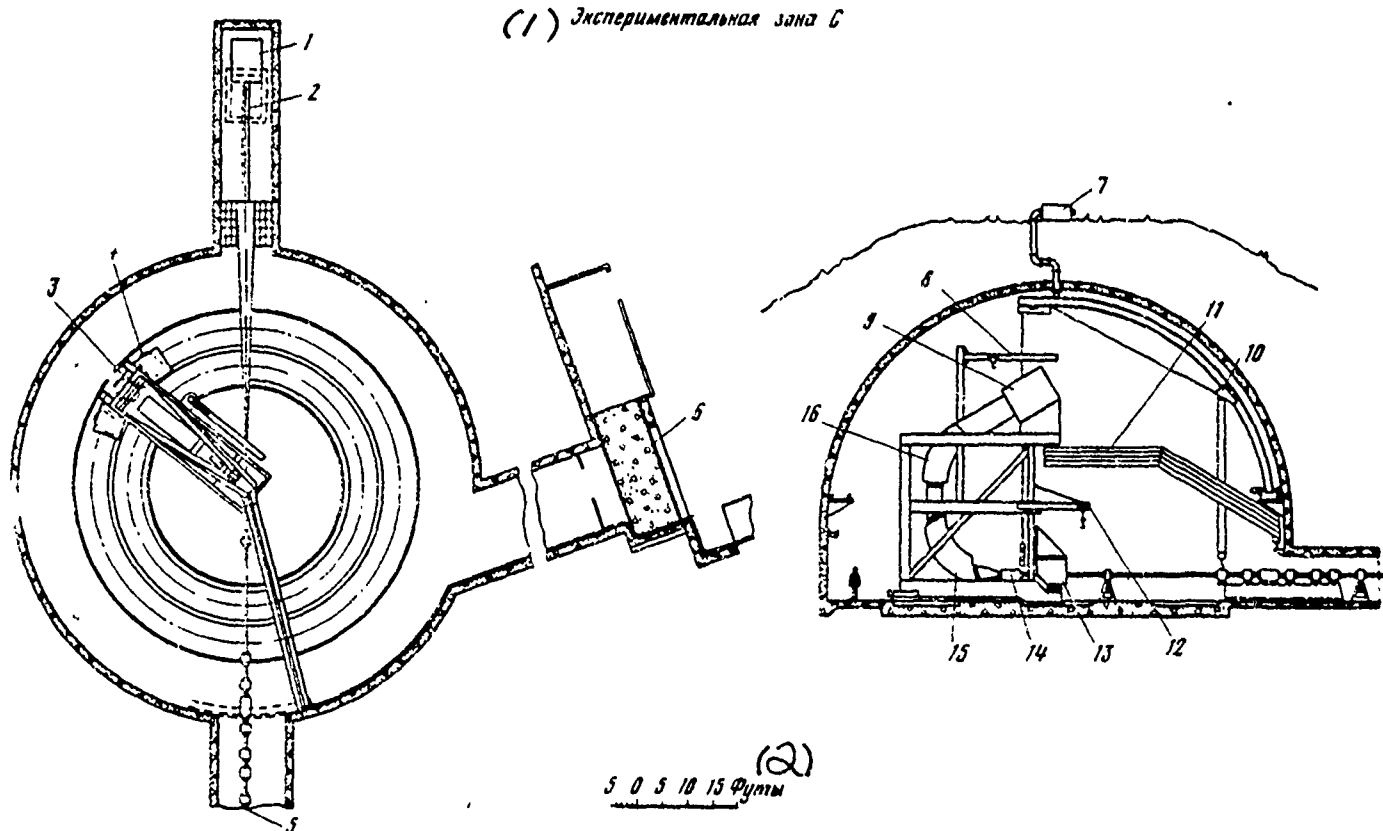
Fig. 9. Magnet and shielded chamber/camera of the proton spectrometer of the high resolution: 1 - water tank; 2 - beam plug (graphite with the water cooling); 3 - spectrometer of high resolution; 4 - air cushions; 5 - from the device/equipment of stripping; 6 - Screened door to air shock absorbers; 7- ventilation opening; 8- tap/crane; 9 - detectors; 10 - tap/crane which will be established/installed in the future; 11 - bridge for the cables and other communications; 12 - tap/crane of target; 13 - target; 14 - quadrupole lens L=0.77 m, R=12.25 cm, B=5.30 kg (on the surface of poles), weight 8.5 t; 15 - deflecting magnet (divergence on 75° of particles with the

80 10 29 102

impulse/momentum/pulse 1463 MeV/s in the field 13.94 kg); 16 - the

deflecting magnet (divergence of particles of 75° with the

impulse/momentum/pulse 1463 MeV/s in the field 13.94 kg, weight 127.5

t).

Key: (1). Experimental zone C. (2). Feet.

Page 147.

The comparison of the results of scattering experiments of pions and

nucleons is of large interest from the point of view both checking

the applicability of theoretical methods and obtaining of nuclear

physics information.

The establishment of difference and resemblance of these .

processes is very important from the point of view of the systematic

investigation of the properties of nuclei. The comparison of the data

about a radius of proton, obtained as a result of scattering of

pi-mesons and particles, which test/experience electromagnetic

interaction, is very important for checking the theoretical

approaches.

The system of proposed KSRM consists of the pion channel, in

which of pin, which appear in the target, arranged/located on the

path of intense proton beam, is formed/shaped the high(ly)-monoenergetic beam of pi-mesons, and the spectrometer which provides recording the scattered mesons with the high precision/accuracy. KSBM is "spectrometer on the losses", so and PSVR, where a change in the impulse/momentum/pulse is determined with considerably the higher precision/accuracy than general/common/total impulse/momentum/pulse. Initial system must have the following characteristics:

Meson channel.

Solid angle ... of 10 msr full/total/complete width.

Momentum acceptance ... 1o/o.

Momentum resolution ... $1 \cdot 10^{-4}$ with the sizes/dimensions of source 3x1 cm x of 1 mm.

The angular resolution ... of 10 mrad.

The range of energies ... from 100 MeV to E_{max} (which depends on assignments).

Scattering target ... 15x15 cm.

Spectrometer.

Solid angle ... of 10 msr.

Momentum acceptance ... 30o/o.

Momentum resolution ... $1 \cdot 10^{-4}$.

The angular resolution ... of 3 mrad.

Impulse/momentum/pulse ... of 100-750 MeV/s.

Since maximum energy of spectrometer and its aperture ratio determine the cost/value of system, study program was subjected to careful study for the purpose of the guarantee of a minimum cost/value.

KSRM is only one of several channels with the use of the secondary beams which are planned/glided on LAMF. Fig. 10 shows the plan/layout of the experimental zone, situated along the line of the transportation of intense beam. On it is shown the location KSRM, channel of slow mesons, channel of fast mesons, channel of retarded

μ-mesons, pion channel cf general purpose (having low cost/value) and channel of fast μ-mesons. Necessary for the construction of these all channels means at present are absent. However, some of these projects are located in the stage of serious study, and it is possible to expect that their construction will be begun in a year.

Most typical of these channels of secondary particles is the channel of slow pi-mesons. Was recently published the sufficiently full/total/complete study of the construction/design of this channel [13]. The configuration of magnet is shown in Fig. 11. Particle trajectories are bent in the vertical plane in order to ensure the minimum height of source and maximum resolution. Was selected the construction/design with four deflecting magnets, which provides excellent accessibility to equipment, its universality and convenience in the use, and are examined the following designed conditions:

1. Resolution. For some experiments, in particular, for the study of scattering pi-mesons on nuclei and capturing the pi-mesons, is necessary a good resolution ($\Delta p/p$ order 0.1o/o or less). For other experiments, for example, of investigation β - the decomposition/decay of pi-mesons, it is necessary to encompass the wide interval of the values of impulses/momenta/pulses.

2. It is desirable to have both positive and negative pi-mesons.

3. Sizes/dimensions of focal spot. Divergence of beam and corresponding sizes/dimensions of focal spot must be changed in the limits from 0.5x1.0 cm tc 5x5 cm.

4. Emittance. In scme experiments is required maximum intensity of flow and are permitted large emittances ($\Delta\Omega$>10 msr). In other experiments, in particular, on the scattering, the divergence of scattering must be +-10 mrad or less.

5. System must be achromatic, i.e., position of focal spot and angle of deflection beam at output must not depend on particle momentum.

6. Channel must be isochronal, which is necessary for retaining/preserving/maintaining time/temporary structure of beam of pi-mesons.

7. Length of channel must be small in order to decrease to minimum of loss of intensity, connected with decomposition/decay of pi-mesons low energy.

8. It is necessary to ensure minimum pollution/contamination of

beam.

The obtained sizes/dimensions of focal spot and the flows of pi-mesons are given in the table.

Энергия (1) π-мезонов	$\Delta p/p = \pm 0,05\%$ $\Delta\Omega=10$ мстерад (2)	$\Delta p/p = 1\%$ 20 мстерад (2)	$\Delta p/p = \pm 5\%$ 15 мстерад (2)
50	$4,0 \cdot 10^6$	$1,6 \cdot 10^8$	$6,0 \cdot 10^8$
100	$1,9 \cdot 10^7$	$7,3 \cdot 10^8$	$2,7 \cdot 10^9$
200	$3,3 \cdot 10^7$	$1,3 \cdot 10^9$	$5,0 \cdot 10^9$
(3) Размер фокусного пятна по горизонтали	$\pm 1,5$ см (4) ± 125 мрад	$\pm 1,5$ см (4) ± 125 мрад	$\pm 3,5$ см (4) ± 115 мрад
(5) Размер фокусного пятна по вертикали	$\pm 0,13$ см (4) ± 40 мрад	$\pm 1,0$ см (4) ± 40 мрад	$\pm 3,4$ см (4) ± 45 мрад

Notes: 1. Table shows the flows of positive pi-mesons (s^{-1}) in angle of 45° with carbonic/carbon target with a thickness of with a of 3 cm. 2. Sizes/dimensions of focal spots are calculated with an accuracy to corrections of second order and switch on 95o/o of total intensity of beam or more. Since the existing beams of pi-mesons have an intensity in the limits of 10^5-10^6 s^{-1}, the intensity of meson channel is the supplementary advantage of accelerator.

Key: (1). Energy of pi-mesons. (2). msr. (3). Size/dimension of focal spot on horizontal. (4). mrad. (5). Size/dimension of focal spot on vertical line.

Page 148.
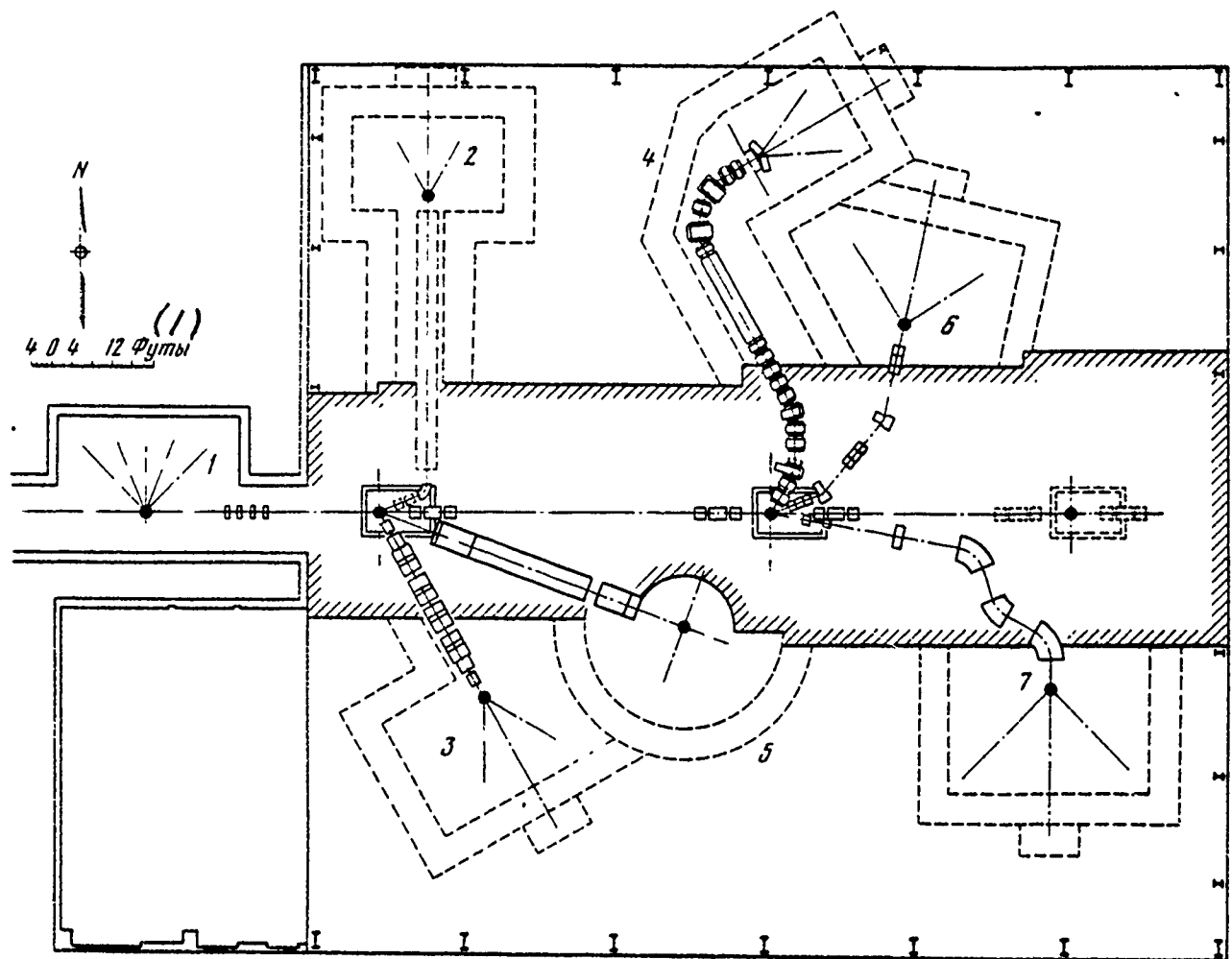
Fig. 10. Experimental zone A, arranged/located along beam of high intensity: 1 - zone of thin target; 2 - channel of fast μ-mesons (it is planned/glided in future); 3 - beam of pi-mesons low energy; 4 - channel of stagnation pi-mesons; 5 - beam of rapid pi-mesons and channel of spectrometry; 6 - ionic channel of general purpose; 7 -

beam of high-energy π-mesons.

Key: (1). Feet.
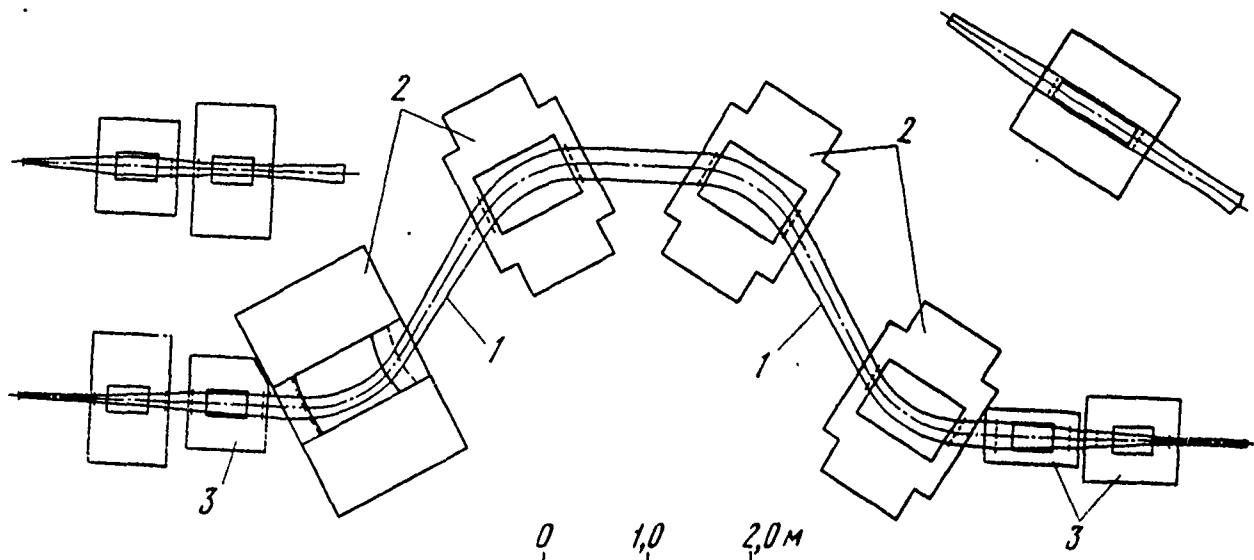
Fig. 11. Channel of slow pi-mesons of general purpose: 1 - envelope of particles ($\Delta p/p=+-5o/o$, $\Delta\Omega=15$ msr); 2 - deflecting magnets (clearance 15.2x61x86.4 cm, maximum intensity/strength of field 16 kg, curvature R1=2.17 m, R2=1.34 m, R3=5.71 m, R4=∞); 3 - magnets of quadrupole lenses (channel with a diameter of 25.4 cm, iron core with a length of 40.6 cm, maximum field 5 kg).

Page 149.

In conclusion should be made several observations relative to experiments in physics of elementary particles. First of all it

should be noted that in twenty years of the intense investigations of

the elastic scattering cf pions on the nucleons it is not yet

obtained the only system of phases, describing scattering amplitude.

The use of intense beams of pi-mesons in conjunction with the

polarized targets must provide the final and total determination of

these phases. The investigation cf reaction $\pi^- + p \rightarrow n + \gamma$ and reverse

reaction must ensure checking the invariance of electromagnetic

interaction relative to time reversal. For the more detailed study of

the scattering amplitudes of pi-mesons on the nucleons out of the

nuclear shells were proposed experiments in the measurement of the

bremsstrahlung of pi-mesons. Retention/preservation/maintaining

vector current (CVC) occupies central position in the contemporary

understanding of weak interaction. Based on this hypothesis

theoretical calculations of the speed of the β-decay of pi-meson

$\pi^+ \rightarrow \pi^0 + e^+ + \nu$ give the value, which has the precision/accuracy of higher

than one percent. The most precise experimental values of this value

are today determined with error $7 o/o$. The measurement of decay rate

for the freely moving/driving mesons on the almost parallel meson

beam LAMP of high intensity (10^9 particles in s) will ensure the

experimental check of this prediction of the theory with

precision/accuracy $\sim 1 o/o$.

The concept of the partial retention/preservation/maintaining of

axial current (RSAS), connected with this question, at present has

important value from the point of view of the analysis of the
bremsstrahlung of pions and reaction $\pi + n \rightarrow \pi + \pi + n$ near the threshold.
Is here involved also a question about the importance of the
contribution of meson-meson S- scattering (final-state interaction)
to the reaction of the generation of pions near the threshold and far
from it.

One of the greatest riddles of physics of elementary particles
is seemingly identity of electron and μ-meson in every respect, with
exception a more than hundredfold difference between masses and
nonidentities of muon and electronic neutrino. The intense flows of
muons and pions which will be obtained on LAMF, will make possible of
the precise measurement of the properties of μ- mesons. One of such
experiments, proposed for the purpose of checking the degree of the
resemblance of μ- mesons and electrons, is the precise measurement of
the relationship/ratio of the probabilities of two methods of
decomposing/decaying the pi-mesons $(\pi \rightarrow e + \nu)/(\pi \rightarrow \mu + \nu)$. The precise
measurements of the mass of muon and electronic neutrino also can
contribute to the resolution of this riddle.

Special experiments on LAMF will make it possible to obtain an
enormous quantity of new information both in the region of physics of
elementary particles and in the region of nuclear physics. There is a
confidence, that overcoming the boundary of experimental

possibilities, connected with the limited intensity of beam, during
the next several years will lead to many unexpected contingencies and
fundamental discoverys/openings.

Besides the program of fundamental studies in the region of
physics of nucleus and elementary particles, outlined for LAMP, is
developed/processed the very vast and intense program of applied
research on this setting up. The most captivating region of such
investigations is the use/application of negative pi-mesons for the
radiotherapy of cancer/crab. The beam of negative pi-mesons possesses
the properties which make it from a contemporary point of view with
almost ideal means for the radiotherapy. Because of a small mass fast
pion creates minimum ionization on the larger part of its path/range.
However, upon decay after dead lock it creates several heavy
fragments whose considerable energy remains localized near the point
of their formation/education. This makes it possible to reliably
localize large radiation dosages on the swellings, arranged/located
deeply in the body of man. The information about the possibility of
using the intense beams of negative pions for the radiotherapy caused
in the medical circles considerable reanimation, and at present is
conducted the active development of the program of the clinical
use/application of a beam of negative pi-mesons LAMP. Are intensely
developed/processed also other study programs, which have applied
directionality, in particular, the investigation of radiation

damages, obtaining isotopes with the aid of the beams of the
accelerated particles, obtaining intense neutron beams for the
investigations i. the region of solid state physics and others.

The more detailed description of the programs of the
experimental studies, planned/glided on LAMP, in which it is possible
to find full/total/complete bibliography, and the substantiation of
the planned/glide experiments is published earlier.

General,'common/total characteristics LAMP.

Energy of protons, MeV - 100-800.

Average/mean beam current on target, mA - 1.

Average/mean power of team, kW - 800.

Duty factor, o/o - 6-12.

Pulse repetition frequency, s^{-1} - 120.

Peak beam current, mA - 17.

Duration of pulse, μs - 500-1000.

DOC = 80069311   PAGE 6 620

Peak HF power, MW - 55.

Average/mean HF power, MW - 3.3-5.8.

Operating frequency of sections of the type of Alvarez, Mgts - 201.25.

Operating frequency of waveguide sections, MHz - 805.

The overall length of accelerator, m - 840.

Total required power in operational conditions, MW - 35-55.

Cost/value, millions of dollars - 55.

Predicted duration of construction - 4 years.

REFERENCES
1. P.W.Allison, Emigh C.R., R.R. Stevens, Jr.
   The Injector Complex for the LAMPF Accelerator.
   IEEE Trans. on Nuclear Sci., 1969, v. NS-1-6,p.135,
   Part I.
2. D.A.Swenson, E.A.Knapp, J.M.Potter, E.J.Schnei-
   der. Stabilization of the Drift Tube Linac by Operation
   in the π/2 Cavity Mode. Proc. 6th Internat. Conf. on
   High Accelerators, 1967, CEAL-2000,p. 167.
3. J.R. Faulkner, T.J. Boyd. LAMPF 200—MHz Power
   Sources. Proc. 1968. Proton Linear Accelerator Conf.,
   part I, p. 87.
4. R.A. Jameson. Automatic Control of RF Amplifier
   Systems. Proc. 1969. Proton Linear Accelerator
   Conf., p. 149.

DOC = 80069311   PAGE 621

5. D.E. Nagle, E.A.Knapp, B.C.Knapp. Coupled Resonator Model for Standing Wave Accelerator Tanks. R.S.I., 1967, 38, N 11, p. 1583–87.

6. E.A.Knapp, B.C. Knapp, J.M.Potter. Standing Wave High Energy Accelerator Structures. R.S.I., 1968, 39,N 7, p. 979–91.

7. D.C. Hagerman. 805–MHz Power Sources for the LAMPF Accelerator. Proc. 1968. Proton Linear Accelerator Conf., Part I, p. 76.

8. R.A. Jameson, W.J.Hoffert, D.I.Morris. Microwave Instrumentation for Accelerator RF Systems. – IEEE Trans. on Nuclear Sci., v. NS–16, Part I, N 3, p. 367.

9. E.A. Knapp, W.J. Shlaer. Design and Initial Performance of a 20–MeV High Current Side Coupled Cavity Electron Accelerator. 1968. Proton Linear Accelerator Conf., Part II, p. 635.

10. H.S. Butler, R.A. Gore, D.T. Van Buren. Computer Control of a Linear Accelerator. Proc. 1968 IFAC/IFIP Svmpos. on Digital Control of Large Industrila Systems, Toronto.

11. G.Igo et al. A Proposal to the Atomic Energy Commission for a High Resolution Spectrometer Facility for Studying Proton Induced Reactions near 800–MeV. Unpublished.

12. H.A. Thiesen et al. A proposal for EPICS. Unpublished.

13. J. Amato, R. Burman, H. Cowan, M.Jakobson. Properties of a Proposed Low Energy General Purpose Pion Channel Unpublished.

14. L. Rosen. Physics with Meson Factories, High Energy Physics and Nuclear Structure. North–Holland, 1967.

Page 150.

133. New accelerating structure on a π/2- wave for the proton linear accelerator to the high energies.

V. G. Andreev, V. M. Pirozhenko.

(Radio engineering institute of the AS USSR).

In the proton linear accelerators by the energy of higher than 100-150 MeV it is proposed to utilize the accelerating structure with alternating accelerating field in the mode/conditions of a π/2-wave. In the mode/conditions π/2 - the wave when phase displacement between electromagnetic fields in the adjacent cells of structure is equal to π/2, accelerating field possesses a small sensitivity to errors in the production and beam load. This is caused by the effect of the mutual compensation for the waves, excited in the structure by heterogeneities and maximum removal/distance in the frequency in the frequency of working from the adjacent types of oscillations. The use of alternating accelerating field when in the adjacent accelerating gaps fields are equal in magnitude, but they are opposite on the

sign, it makes it possible to most economically expend/consume high-frequency power for accelerating the proton beam.

1. Description of the accelerating structure and possible versions of its construction/design.

Let us examine the developed in RAIAN of the USSR structure with alternating accelerating field in the mode/conditions of a $\pi/2$-wave. The accelerating structure is the cylindrical cavity resonator with the conducting washers and the drift tubes, loaded into middle of the gaps/intervals between the washers with conducting diaphragm (Fig. 1A). The conducting washers are fastened in the resonator with the aid of two or more metallic rods, parallel to axis/axle and arranged/located in the rf node. Metallic rods are utilized also in the cooling system of the conducting washers. For this purpose within the metallic rods and the washers must be provided for the channels, on which circulates the cooling fluid. The use of through metallic rods, attached only on the bottoms of resonator, is inconvenient on a whole series of reasons. Actually/really, at the large length of resonator it is difficult to ensure the required stable position of the conducting washers in the resonator with the diameter of metallic rods 20- 0 mm (at frequency ~1000 of MHz the diameter of rods of more than 30 mm is undesirable due to the large losses in them). In the resonator of this construction/design it is difficult to also ensure

the heat removal from the conducting washers.

The hardness of the attachment of the conducting washers in the resonator can be improved due to the introduction of the cross connections between the rods and the diaphragms (Fig. 1b). Cross connections are located radially and are located in the plane, passing through the middle of the corresponding diaphragm. Within each cross connection is provided for the coolant passage. The resonator of this construction/design can be assembled from the separate moduli/modules each of which encompasses washer together with the relating to it diaphragm, the rods, the cross connections and the cut of cylider (Fig. 1b). The metallic rods of two adjacent moduli/modules are connected with the aid of the clamps, providing only electrical contact, since coolant passage within the adjacent rods can be excluded without the damage to the cooling system of washers. In the resonator of this construction/design it is possible to utilize metallic rods of smaller diameter (12-15 mm at frequency ~1000 of MHz) which will make it possible to raise the effectiveness of the use of high-frequency power for accelerating the charged/loaded particles due to the decrease of losses on the surface of metallic rods.

Page 151.

Construction/design and technology of the production of resonator even more will be simplified, if we exclude the cuts of metallic rods without the coolant passage (Fig. 1c); in this case are eliminated clamp connections, and the surface of metallic rods (with the permanent diameter) decreases doubly.

2. Determination of the geometry of the accelerating structure.

Greatly frequently under the dispersion formula is understood the dependence of resonance frequency of the excited in the accelerating wave structure on a number of variations in field along the sequence of cells or on the phase angle of electromagnetic field to one cell θ. In the accelerating structure from the uniform cells the dispersion formula in the region π/2 - wave is virtually linear and symmetrical, i.e., each pair of the oscillations, adjacent with π/2- wave and which differ from it in a number of variations in the field to one and the same number, equidistant in the frequency from π/2- wave. Dispersion formula for the structure being investigated in the form of the chain/network of the connected cells of two types (cell in the near-axial region - space between two adjacent washers, and cell on the periphery - space between two adjacent diaphragms) is very complicated, since it consists of two branches one of which relates to the resonator with the conducting washers, and the second - to the resonator with the diaphragms. On the basis of the theory of

electromagnetic field, it is possible to show that for agreeing these two branches into the overall dispersion formula, the linear and the symmetrical in the region of $\pi/2$-wave, it is necessary to tune for the operating frequency the sections of two types (see Fig. 2a and b) during their excitation in the mode/conditions $\pi/2$ -wave on the transverse magnetic oscillations with the axial symmetry. The calculated structure of electromagnetic fields for these oscillations is also given in Fig. 2a,b.

The calculation of the geometric dimensions of resonator r_0 and R was carried out cn tne computers in the following sequence: 1) with certain initial radius of resonator R from the calculation of section with the washer (Fig. 2a) is determined a radius of washer; 2) from the calculation of section with the diaphragm (Fig. 2b) is determined a radius of resonator R; 3) again are repeated operations/processes on parts 1. and 2. Radius R weakly affects the resonance frequency of section with the washer, while radius r_0 - for the resonance frequency cf section with the diaphragm. Therefore this process of successive approximations converges already in the second or third approximation/approach. The remaining sizes/dimensions of resonator are selected on the basis of the dynamics of beam, economical use of high-frequency power, dielectric strength of accelerating gap and design specifications.
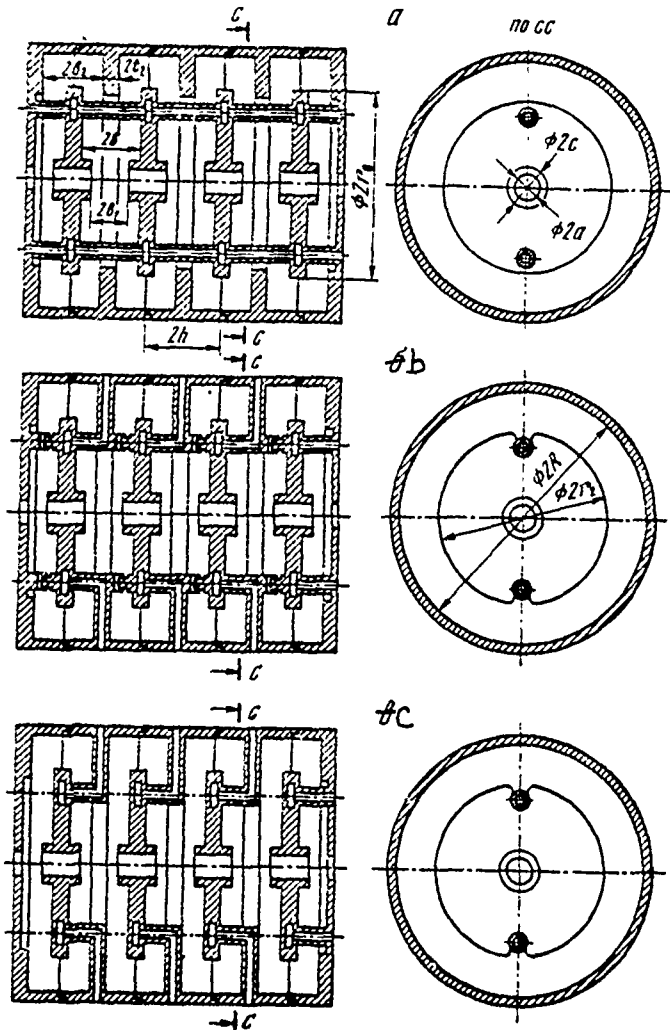
Fig. 1. Possible methods of the attachment of the conducting washers in the resonator. a) with the aid of the through rods; b) through rods, supported on diaphragms; c) half-rod, established/installed on the inflows/bosses of diaphragms.
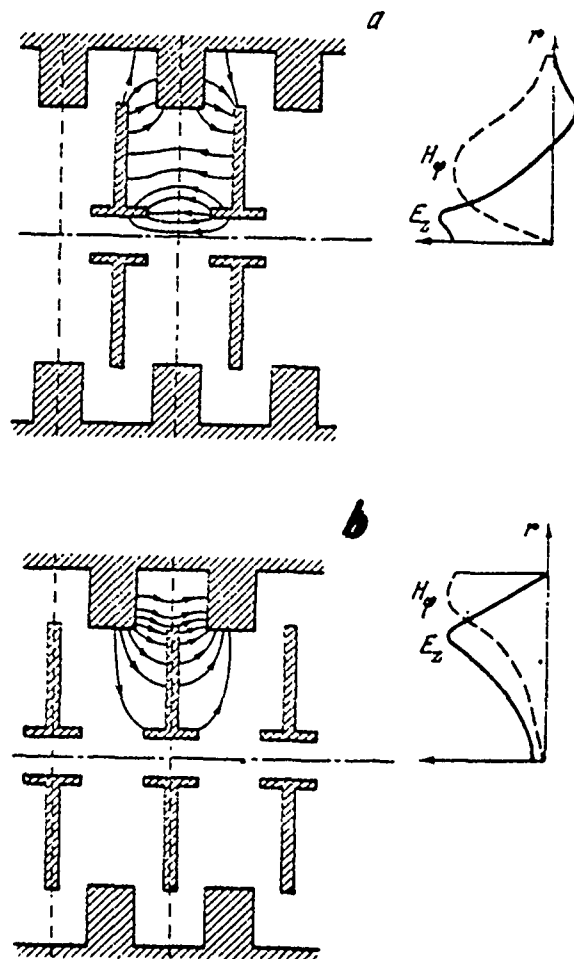
Fig. 2. Sections of resonator and field distribution in them.

Page 152.

The optimum value of gap between the drift tubes, with which high-frequency power is expended/consumed most economically, it is brought in Fig. 3a in the form of the dependence of the coefficient

of clearance $\alpha_1 = \delta_1/h$ on β. The diameter of opening/aperture in the diaphragms is lower than the diameter of washers, since otherwise appears the second branch of dispersive characteristic $(2\nu_0 - 2\nu_2 = 0.2$ cm). thickness of the diaphragms with small ones β weakly affects high-frequency losses in the resonator; with $\beta > 0.6$ are optimum values of the thickness of diaphragm, with which high-frequency losses are minimum. These values are shown in Fig. 3b depending on β. Fig. 3c and 3d gives the values of a radius of washer ν_0 and radius of resonator R for the optimum values of the accelerating clearance and thickness of diaphragm and frequency of 1000 MHz. During the calculation was considered the effect of two rods with a diameter of 2 cm, which rest on the diaphragms (Fig. 1c).

3. Radio engineering parameters of the accelerating structure.

Computed values of effective shunt resistance zT^2 and Q-factor of resonators at the frequency of 1000 MHz are given in Fig. 4. The basic fraction/portion of high-frequency losses falls to the washers (from 85o/o with $\beta = 0.4$ to 54o/o with $\beta = 1$). High-frequency losses can be somewhat lowered, if we to drift tube give conical shape.

Fig. 5 gives dispersion formula for the resonators, in which the washers are attached with the aid of two through metallic rods, placed in the rf node and which do not rest on diaphragm (curve 1),

or which rest on the diaphragms (curve 2). From the represented dependences it is evident that the dispersion formula for these resonators in the region of $\pi/2$-wave is virtually linear and symmetrical. Coupling coefficient K, which describes removal/distance in the frequency of an O-wave from π- wave, composes in this case K= (51-53) o/o.
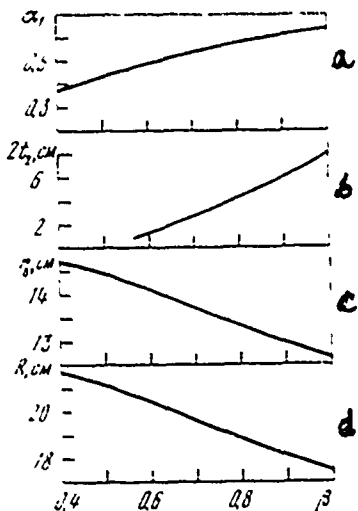
Fig. 3. Geometric dimensions of resonator (a - 2 cm; c - 2.7 cm; 2h-2B=1 cm) in the function β: A) the coefficient of clearance; b) the thickness of diaphragm; c) a radius of washer; d) a radius of resonator.
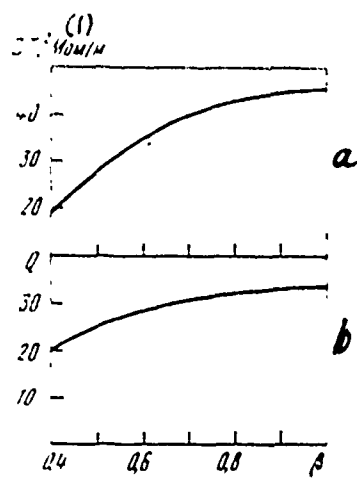
Fig. 4. Effective shunt resistance (a) and quality (b) of resonator (a=2 cm; c=2.7 cm; 2h - 2b=1 cm).

Key: (1). Mohm/m.
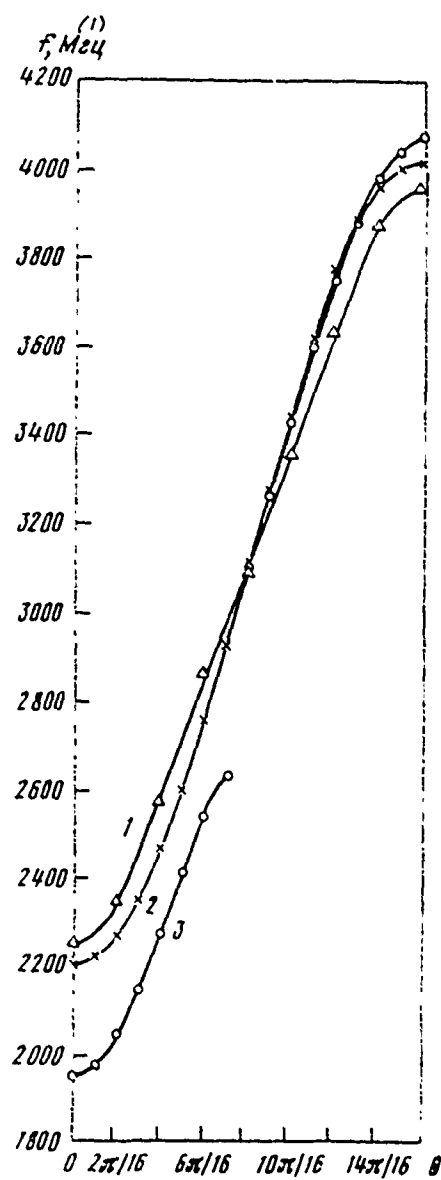
Fig. 5. Dispersion characteristics for the resonator with the different methods of the attachment of the conducting washers.

Page 153.

For the resonator with the washers, attached on the diaphragms (Fig. lc), the dispersion dependence (Fig. 5 curve 3) has a gap in the region of $\pi/2$-wave, and electrical field on the axis proves to be that decreasing in proportion to approximation/approach to that bottom of the resonator where is fastened washer. Thus, for the resonator of this construction/design the procedure of the determination of geometry with the aid of two separate sections (Fig. 2a and b) needs refinement.

Discussion.

A. I. Zykov. Which the quality of resonator?

V. M. Pirozhenko. 20-30 thousand.

B. P. Murin. Could not you give comparative characteristics of the investigated by you resonators for the range of energies of more than 100 MeV with the parameters of the resonators, used in Los Alamos linear Accelerators.

V. M. Pirozhenko. Structure with the conducting washers and the diaphragms possesses considerably larger coupling coefficient;

therefore resonators can be made longer (approximately/exemplarily 10 times). Shunt resistance of this structure by approximately 5o/o less than remaining having in mind structures, in which it is approximately/exemplarily equal. Structure with the circular resonators is simpler technologically and makes it possible to obtain 2 times higher coupling coefficient.

I. S. Sidorenko. How is explained an increase in the quality with an increase in the relative velocity of part? By smaller quantity of washers or by something other?

V. M. Pirozhenko. Yes, in the same stored energy high velocities correspond smaller losses, since in this case more rarely stand washers.

134. Study of the radic engineering characteristics of the stabilized accelerating structures with the standing wave.

V. G. Kuhlmann, V. M. Pirozhenko, V. B. Chistcv.

(Radio engineering institute of the AS USSR).

Recently in the linear accelerators of protons are applied the accelerating structures in which the resonance frequency of working oscillation it is arranged/located in the middle part of the dispersive characteristic. Such structures possess the high stability of accelerating field. Are given below some results of the theoretical and experimental investigations of the basic parameters and properties of the stabilized structures.

1. Conditions of the stabilization of field distribution.

In the long resonators the distortions of amplitudes and phase of field along the resonator occur due to the admixture to the working oscillation field component of adjacent with them oscillations. Applying perturbation method, it is possible to obtain the following expression for the nonuniformity of the amplitude of

accelerating field in steady state during the distortion of the volume of resonator to value Δv:

$$\Delta \varepsilon = \sum_{\nu} \varepsilon_{\nu} \frac{f_n^2}{f_n^2 - f_{\nu}^2} \frac{\int_{\Delta v} (H_n \cdot H_{\nu} - \varepsilon_n \cdot \varepsilon_{\nu}) dv}{\int_{v} H_n^2 dv} , (1)$$

where ε_n and H_n - the electrical and magnetic fields of working oscillation with frequency f_n; ε_{ν} and H_{ν} - the field of adjacent oscillations with frequencies f_{ν}; v - the volume of resonator.

The decrease of the field nonuniformity is achieved by an increase in the difference in the frequencies between the working and adjacent oscillations. Furthermore, if adjacent oscillations have frequencies, arranged/located on both sides from the operating frequency, then their effect on accelerating field can average out. For the full/total/complete compensation during the disturbance/perturbation in the arbitrary place of resonator, as it follows from formula (1), is necessary satisfaction of two conditions:

a) frequencies of adjacent must be symmetrical relative to operating frequency $(f_n^2 - f_{\nu_1}^2 = f_{\nu_2}^2 - f_n^2)$;

b) Field component of adjacent oscillations must be identical $(H_{\nu_1} = H_{\nu_2}; \varepsilon_{\nu_1} = \varepsilon_{\nu_2})$.

Strictly speaking, condition b) never is satisfied accurately, since for different oscillations always there is a region in the resonator where Field ccmponent are different. In the structures, which consist of the ccnnected cells and the workers on the standing $\pi/2$- wave (for example, in the structure with the circular resonators of connection/communication), field component of nonoperative oscillations they differ only near the coupling elements. Therefore the field nonuniformity in such structures is caused, in essence, by difference in the coupling coefficient between the cells and weakly it depends on errors in the adjustment of cells.

In the resonators, which work on an O- wave (of Alvarez's type) SOS by the tabulating resonance rods, field component of adjacent oscillations, as it will be shown below, can substantially differ. In this case the best stabilization can be achieved/reached during their partial compensation as a result of a compromise between conditions a) and b).

Page 154.

2. Parameters of structures with the circular resonators of connection/communication.

From a number of stabilized structures for accelerating high-energy in the region protons $(\beta=0.4-1.0)$ by us was investigated the structure with the circular resonators of connection/communication (Fig. 1A), which works on standing $\pi/2-$ wave [1]. Computed values of effective shunt resistance of structure ZT^2 in this range of energies at the frequency of 1000 MHz and diameter of aperture 4 cm compose 26-52 Mchm/m. Experiment showed that with the coupling coefficient between cells $K=5-10o/o$ real values ZT^2 for 20-25o/o lower than calculated ones due to the additional losses, caused by the state of the conducting surfaces and by the presence of coupling elements.

Fig. 2a gives dispersive characteristics of one of the models of resonator in the process of adjustment (curve 1), also, after the termination of adjustment (curve 2). The presence of the band of opacity Δf_H decreases the degree of the mutual compensation for nonoperative oscillations. The value of the nonuniformity of the amplitude of field in the i-th accelerating cell is determined in this case by the relationship/ratio

$$\frac{\Delta \varepsilon_i}{\varepsilon} = \frac{2N^2}{K^2 \pi^2} \frac{\Delta f_H}{f_n} \sum_{\nu} \frac{p_\nu}{\nu^2} \cos \frac{\nu \nu \pi}{N}, \quad (2)$$

where N - number of cells in the resonator; p_ν - generally accepted

coefficients of the expansion of "local" frequency in the Fourier series.

Errors in the adjustment of the cells of resonator lead to the appearance of a field in the cells of connection/communication, which causes a reduction in effective shunt resistance of resonator to value

$$\frac{\Delta Z T^2}{Z T^2} = 2 \frac{Q_\text{ч}}{Q_\text{c}} \left(\frac{N}{k \pi}\right)^2 \sum_\nu \left(\frac{p_\nu}{\nu}\right)^2, \qquad (3)$$

where $Q_\text{ч}$ and Q_c - quality of the accelerating cells and cells of connection/communication respectively.

From the calculations and the analysis of experimental data it follows that in the resonators with the coupling coefficient of approximately 10o/o, which contain on the order of 100 accelerating cells, are required comparatively light allowances for production and adjustment of cells (~0.02-0.05o/o in the frequency).

Fig. 3 shows the dismountable model of the section of the resonator of working at the frequency 1000 MHz.

The mutual compensation for adjacent oscillations can occur also with the work at other points of dispersive characteristic. Fig. 1b shows the accelerating structure with the circular resonators of

connection/communication, intended for the work on the the standing $2\pi/3$ - to wave, while in Fig. 2b - its dispersive characteristic, measured on the model of resonator. This structure is of interest because of a smaller number of cells of connection/communication, what is important structural/design advantage, especially in the region of comparatively low energies.
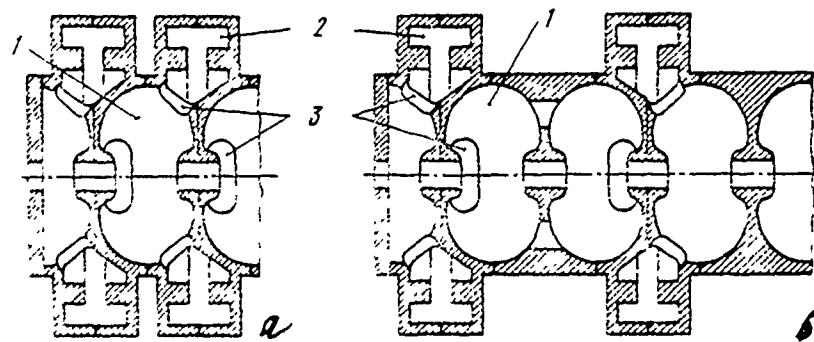
Fig. 1. Of accelerating structures with the circular resonators connections/communications with $\pi/2$- stink (a) and $2\pi/3$ - to wave (b): 1 - accelerating cells; 2 - cell of connection/communication; 3 - window of connection/communication.
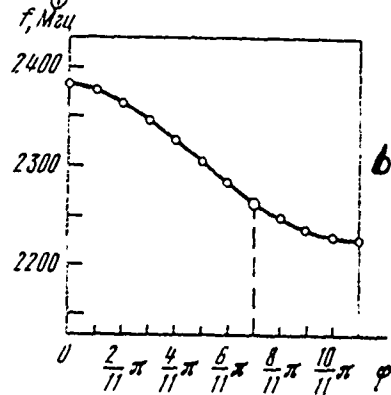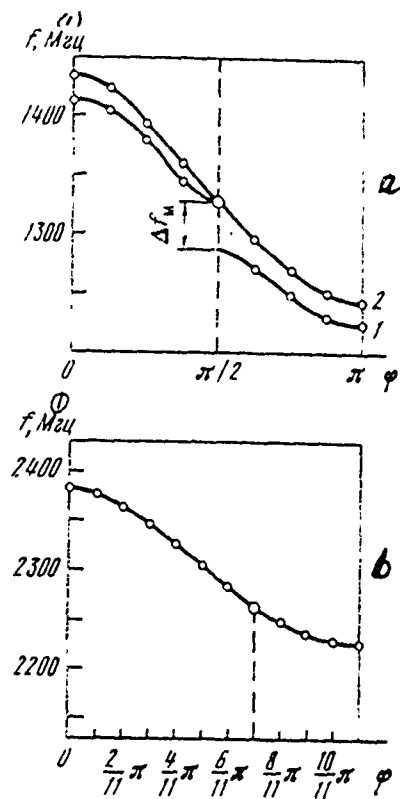
Fig. 2. Experimental dispersive characteristics of accelerating structures with circular resonators connection/communication a) with work on $\pi/2$ - to wave; b) with work on $2\pi/3$ - to wave.

Page 155.

3. On the stabilization of field in the resonator with the aid of the resonance rods.

Let us examine the operating principle of resonance rods based on simple example. let into midale of resonator be introduced one rod from the cylindrical wall perpendicular to axis/axle. In Fig. 4 solid lines showed the course of the natural frequencies of oscillation of the resonator of the type $TM_{01\nu}$ and the oscillation of a rod TS, which in the first approximation, can be considered as four-wave vibrator.

During the introduction of the rod between oscillations TS and TM_{011} appears intertype connection/communication, in consequence of which tuning curves these oscillations differ from initial course and do not intersect, but smoothly they convert/transfer into each other [2] (dotted lines in Fig. 4). Between oscillations TM_{010} and TS intertype connection/communication is absent. In the interaction region $(\ell_1 \div \ell_2)$ the newly formed vibrations are hybrid. The field of

each of them is the sum of the fields of oscillations TM_{011} and TS, the relationship/ratio between which depends on the position of operating point in the tuning curve. When $\ell = \ell_0$ the fields of hybrid oscillations have approximately identical structure; however, their resonance frequencies are asymmetric relative to frequency TM_{010}. Consequently, simultaneous satisfaction of the conditions a) and b) mentioned above is impossible.
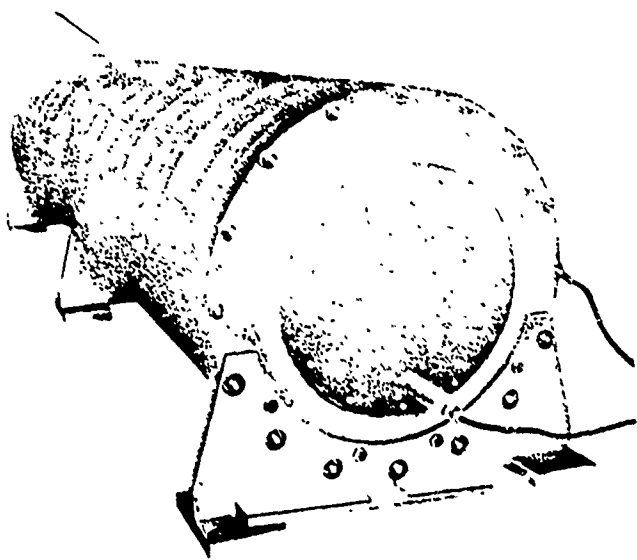
Fig. 3. Model of accelerating structures with the circular resonators connection/communication.
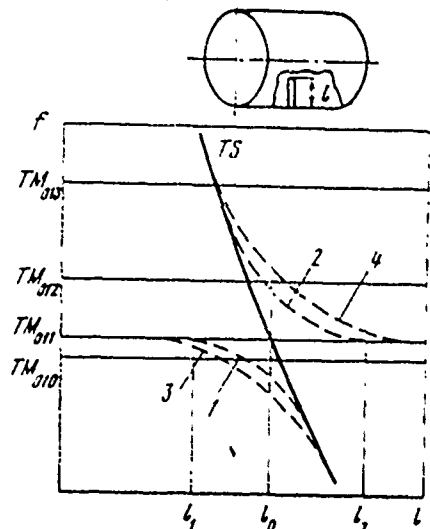
Fig. 4. Tuning characteristics of resonator with rod.
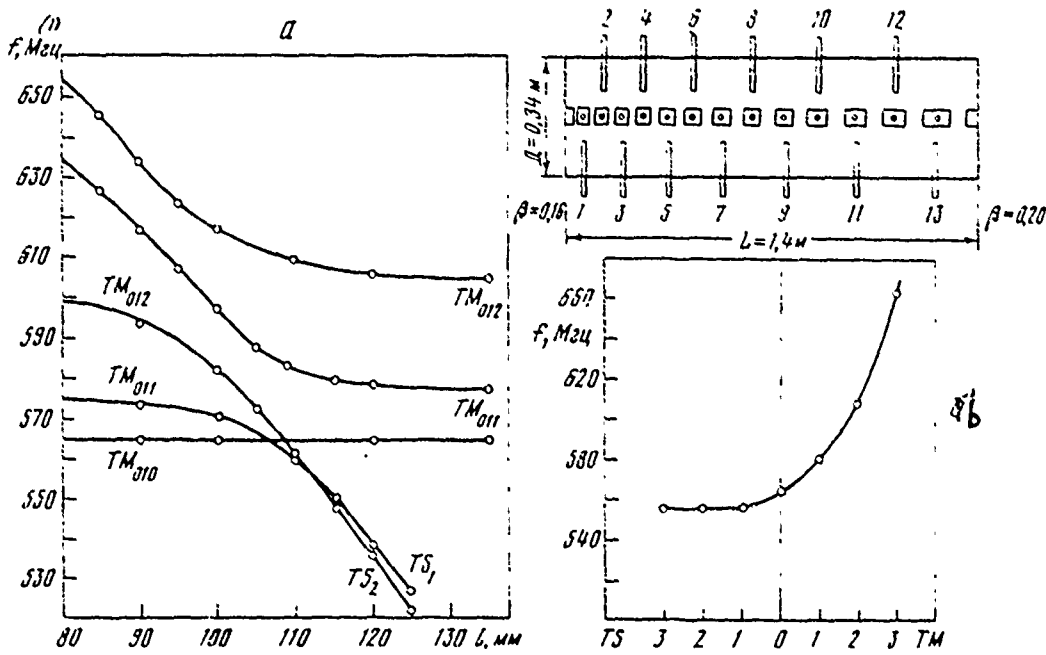
Fig. 5. Experimental tuning characteristics (a) and dispersion formula (b) of resonator with the rods.

Key: (1). MHz.

Page 156.

The degree of the compensation for nonoperative oscillations depends on the following factors. With an increase in the length of resonator oscillation TM_{011} approaches oscillation TM_{010} and is improved the symmetry of the frequencies of the nonoperative of

relatively working. An improvement in the symmetry of frequencies of the nonoperative occurs also with an increase of the quantity of rods in the resonator, since in this case is amplified interaction between oscillations TS and TM_{011} (curves 3 and 4) and increases the divergence of frequencies of the hybrid from the natural frequencies. The analogous phenomena occur also with other oscillations of the type $TM_{01\nu}$.

The behavior of tuning curves was investigated on the models of resonator in which it was simultaneously introduced 13 rods. Fig. 5a gives experimental tuning curves for several lowest oscillations. With $\ell = 116$ mm is satisfied the condition of the symmetry of nonoperative oscillations (condition a), see above); however, the structure of the fields of these oscillations is different (is not satisfied the condition b). With $\ell = 108$ mm is satisfied the condition b), but is not satisfied the condition a). Measurements showed that the best stabilization is achieved at $\ell = 112$ mm. The corresponding dispersive characteristic is given in Fig. 5b. The model of resonator is shown in Fig. 6.

For an improvement in interaction with any of the oscillations of the type $TM_{01\nu}$ rods it is necessary to arrange/locate in antinodes [loops] of field ε_τ of this oscillation. Based on this, it is possible to determine the optimum location of rods, which

ensures the compensation for a maximum number of harmonics, in the structure with the rods of connection/communication, located in the center-line plane, perpendicular to the rods of drift tubes when a number of rods is lower than the number of drift tubes.

REFERENCES.

V. G. Kul'man, E. A. Mironchik, V. M. Pirozhenko, PTE [Experimental Instruments and Techniques], 1970, No. 4, str. 56.

2. V. V. Shteynshleyger. Phenomena of the Interaction of Waves in Electromagnetic Resonators, Moscow, Izd-vo, Soviet Radio, 1955
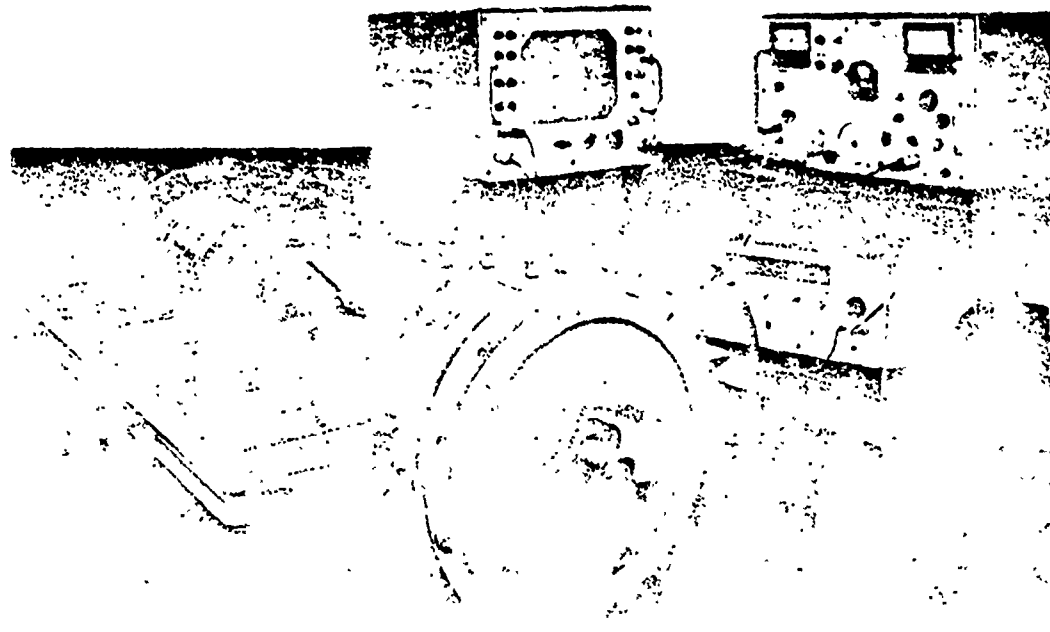
Fig. 6. Model of resonator with the rods.

Page 157.

135. Experiments of the compensation for decreases in accelerating field in the injector of Serpukhov synchrotron upon the acceleration of intense beams.

A. I. Kvash, A. V. Mishenko, B. I. Murin, B. I. Polyakov, Yu. S. Cherkashin.

(Radio engineering institute of the AS USSR).

For the purpose of preparation for experiments on the three-reverse injection on the accelerator I-100 - the injector of Serpukhov synchrotron [1] were tested the systems of the compensation for decreases high-frequency in the field upon the acceleration of proton beams with the current to 100 mA in the impulse/momentum/pulse by duration to 40 µs. Experiments were conducted to 1 and partially on the III resonators of accelerator, moreover on 1 resonator were established/installed two in parallel working terminal amplifiers (OU). Are given below short description and basic results of experiments.

The compensation for decreases in accelerating field at the beam

load was achieved by an increase in the power at the output of
terminal amplifiers at the moment of acceleration automatically or in
the program due to regulating of the anode voltage of terminal
amplifiers or combined regulating of their ancde voltage and
excitation. Field control was conducted by a change in the anode
voltage of powerful/thick exciter. In some experiments as the
actuating element of control system was utilized shunting lamp [2] in
others - supplementary modulator. Shunting output of modulator lamp
GI-27A was controlled cn the grid and it made it possible to change
voltage on the anodes of terminal amplifiers from 20 to 37 kV.
Control of anode lamp was accomplished/realized both according to the
program and in the diagram of automatic regulating.

Supplementary modulator is carried out on the diagram with the
forming line and the thyristor discharger analogous to basic
modulator [3]. The duration of its pulse is equal to the duration of
the current pulse of beam, and the output of supplementary modulator
is included parralel with base. The presence of the considerable
leakage inductance of the peak transformer of basic modulator
prevents closing/shorting short supplementary impulse/momentum/pulse
by output circuit of basic modulator, and is consistently with the
output of supplementary modulator connected diode key/wrench. Upon
the inclusion/connection or supplementary modulator occurs the
addition of the powers of basic and supplementary modulator on the

anodes of terminal amplifiers according to predetermined program.

a) the program regulating of anode voltage OU.

The program regulating of anode voltage OU was conducted with the aid of the shunting lamp or with the aid of the supplementary modulator. In both cases are obtained close results. The oscillograms, which characterize the work of the system of program regulating, are given in Fig. 1.
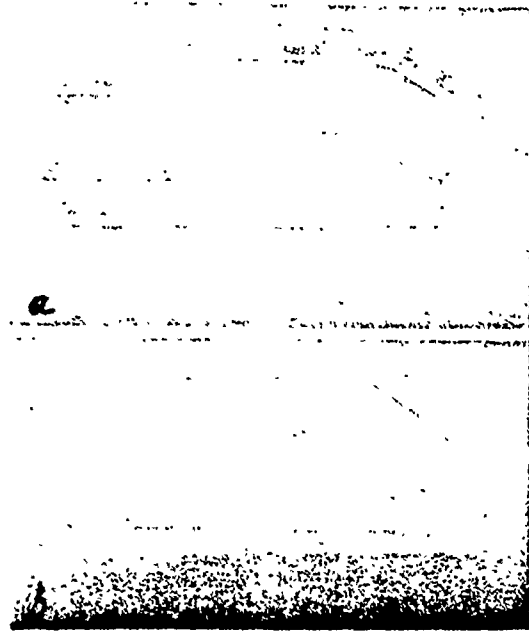
Fig. 1. Characteristic oscillograms in the presence of program regulating (a) and without it (b): 1 beam - anode voltage; II - ray/beam - apex/vertex of envelope HF in the resonator; the III ray/beam - beam current.

Table 1.

(1) Режим работы	(2) Параметры				
	(3) Анодное напряжение, кв	(4) Анодные токи, а	(5) Катодные токи, а	(6) Спад поля, %	(7) Спад импульса тока пучка, %
(8) До компенсации	18	101 / 105	145 / 135	8	67
(9) В момент компенсации	34	117 / 121	145 / 135	< 1	16

Key: (1). Operating mode. (2). Parameters. (3). Anode voltage, kV.
(4). Anode currents, A. (5). Cathode currents, A. (6). Field slope,
o/o. (7). Decrease in current pulse of beam, o/o. (8). Before
compensation. (9). At moment of compensation.

Page 158.

From the comparison of Fig. 1a and b it is evident that the anode
voltage on the lamps OU grows at the moment of acceleration more than
1.5 times. In this case a field slope at the moment of acceleration
decreases almost to zero, and the amplitude of beam current
grows/rises by 30-40o/o. The nonuniformity of the pulse apex of beam
current decreases more than triply. The basic parameters of the
mode/conditions of terminal amplifiers before the compensation and at
the moment of compensation are given in table 1. By the automatic
regulating of anode voltage OU.

Automatic regulating anode voltage OU was conducted with the aid
of the shunting lamp. For the control of lamp was utilized the
difference signal between the envelope HF voltage in the resonator
and the reference voltage. For eliminating the effect of the 1st
overtone of resonator the voltage from the resonator was
removed/taken with the aid of two loops, arranged/located in the
beginning and end/lead of the resonator respectively. After detection
the signals from the loops entered adding circuit, and the resulting
signal after comparison with the standard and necessary amplification
was supplied to the grid of the shunting tube. In this case the
effect of first and some higher overtones of resonator substantially
was weakened/attenuated. The characteristic oscillograms, obtained
with the work of this system, are given in Fig. 2. In this case a
field slope with the beam load with the current 80 mA in the
impulse/momentum/pulse by the duration of 40 μs decreased 3-4 times.
Amplitude and form of the current pulse of beam noticeably were
improved as in the preceding case. The basic parameters of the
mode/conditions of terminal amplifiers to and at the moment of
compensation are given in Tables 2.

c) the combined regulating of anode voltage and excitation of OU
according to the program.

Characteristic for this case oscillograms are given in Fig. 3. In this case are obtained approximately/exemplarily also the results, as in preceding/previous. However, here for achievement of the full/total/complete compensation for field slopes was required a somewhat smaller change in the anode voltage of OU. The basic parameters of the mode/conditions dF generators to and at the moment of compensation are given in Table 3. The measured total quantity of phase disturbances/perturbations in experiments did not exceed 2°.

Conclusion/output.

In experiments conducted is obtained the satisfactory compensation for decreases in accelerating field upon the acceleration of beam. Idle phase disturbances/perturbations with the work of stabilization systems are negligible. The introduction to the compensation for field slopes in all cases noticeably improved the form of the current pulse of beam at output of resonator.
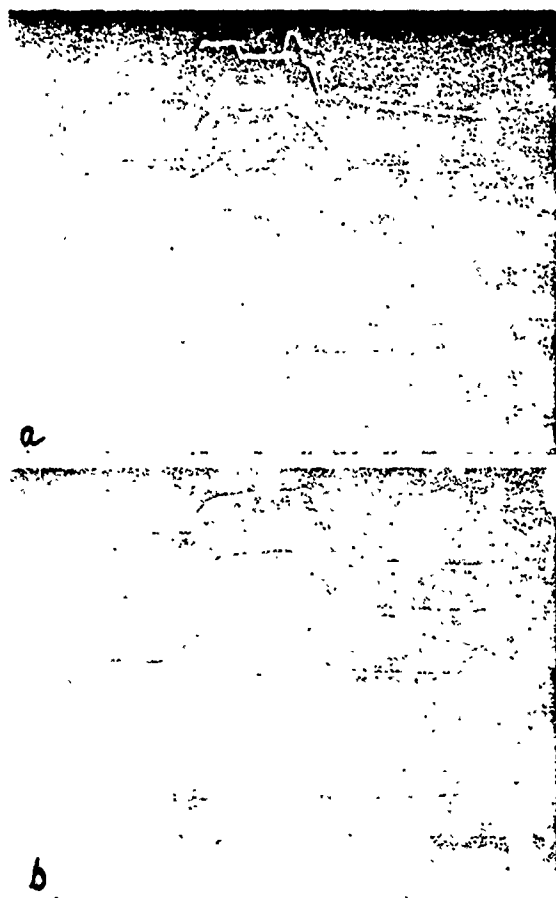
Fig. 2. Characteristic oscillograms in the presence of automatic control (a) and without it (b): 1 - beam- anode voltage; the II ray/beam - cathode current of lamp of OU; the III ray/beam - anode current; the IV ray/beam - apex/vertex of envelope of HF in the resonator; U - beam current.

Table 2.

(1) Режим работы	(2) Параметры				
	(3) Анодное напряжение, кв	(4) Анодный ток, а	(5) Катодный ток, а	(6) Спад поля, %	(7) Спад импульса тока пучка, %
(8) До компенсации	20	95 / 112	104 / 153	13	45
(9) В момент компенсации	32	114 / 134	114 / 168	4	25

Key: (1). Operating mode. (2). Parameters. (3). Anode voltage, kV. (4). Anode current, A. (5). cathode current, A. (6). Field slope, o/o. (7). Decrease in current pulse of beam, o/o. (8). Before compensation. (9). At moment of compensation.

Page 159.

BIBLIOGRAPHY

1.   A. L. Mints. Linear Accelerators of Protons. Trudy
Vsesoyuznogo soveshchaniya [Transactions of the All-Union, 1970, t. 1,
Conference on Accelerators of Charged particles, Moscow, VINITI, str 67.

2.   K. Batchelor, G. Gallagher-Daggitt. Accurate Field Level
and Phase Control and Monitoring for a Proton Linear Accelerator
IEEE Trans. on Nuclear Sci., J., 1965, v. NS-12, N 3, p. 195.

3.   L. V. Nikolayev, L. D. Runovskiy, Ya. S. Cherkashin, V. V.
Chirkov. Pulse Modulator of the System of HF Feed of Linear
I-100. Trudy Vsesoyuznogo soveshchaniya [Transactions of the
All-Union Conference on Accelerators of Charged particles,
Mosco , VINITI, t. 11, str 215.

Fig. 3. Characteristic oscillograms with combined regulating:

I ray/beam - anode voltage; II and III rays/beams - anode

currents OU; IV - apex/vertex of envelope HF in resonator; V ray/beam

- beam current.

Table 3.

(1) Режим работы	(2) Параметры			
	(3) Анодное напряжение, кв	(4) Анодные токи, а	(5) Катодные токи, а	(6) Спад поля, %
(7) До компенсации	20	95 / 97	95 / 110	13
(8) В момент компенсации	29	120 / 110	156 / 160	1,5

Key: (1). Operating mode. (2). Parameters. (3). Anode voltage, kV.

(4). Anode currents, A. (5). Cathode currents, A. (6). Field slope,

o/o. (7). Before compensation. (8). At moment of compensation.

136. Optimization of the initial part of the linear waveguide accelerator.

V. N. Petrov, S. I. Radin, A. V. Ryabtsov, Yu. A. Svistunov.

(Scientific research the institute of the electrophysical equipment im. D. V. Efremov).

D. A. Ovsyannikov.

(Leningrad state university im. A. A. Zhdanov).

The parameters of beam at output LUE in many respects are determined by the initial part of the accelerator. Depending on the requirements, imposed on the beam on the target, must be formulated the requirements for the parameters of initial part of LUE. It is almost always importan to have at the output of LUE a beam of part with the narrow energy spectrum. At the same time in the case of high-energys accelerator (LUE on 2 GeV in Kharkov, SLAC) waveguide buncher must provide the minimum phase width of cluster; in the case of accelerators to low energies (3-5 MeV) - the minimum of energy spread in part in the cluster. In medium-energys accelerator it is

important to minimize both these values. Questions of the
optimization of the parameters of waveguide buncher were examined in
works [1-3]. However, in this case discussion dealt with the
selection of the optimum laws of change along the length of the
accelerator of the voltage of field $\alpha = \frac{\theta \mathcal{E} \lambda}{m_0 c^2}$ and phase wave velocity
in waveguide $\beta_\phi = \frac{v_\phi}{c}$ from the narrow class of curves.

Page 160.

In the present work the class of permissible curves $\alpha^{(2)}$ and $\beta_\phi^{(2)}$
(subsequently we will call their controls) consists of the
piecewise-continuous functions, included in the rectangle

$$0 \le \alpha < \alpha_{max}, \qquad (1)$$
$$0 \le \beta_\phi < \infty .$$

Mathematically task is formulated as follows. The equations,
which describe longitudinal electron motion in the accelerator, take
the form:

$$\frac{du_m}{dz} = -\alpha(z) \sin \varphi_m = g_m(z),$$

$$\frac{d\varphi_m}{dz} = 2\pi \left(\frac{1}{\beta_\phi(z)} - \frac{u_m}{\sqrt{u_m^2 - 1}} \right) = f_m(z), \qquad (2)$$

where $m = 1, 2, \ldots, N$, N - number of particles which by hypothesis
determine the motion of cluster as a whole. Remaining designations
are obvious or universal. Variable/alternating u_m and φ_m satisfy
the initial conditions

$$u_m\big|_{z=0} = u_{m0}, \quad \varphi_m\big|_{z=0} = \varphi_{m0}. \qquad (3)$$

From the mentioned class of curves it is necessary to select such controls α and β_ϕ, in cruer to ensure the minimum of the functional

$$P = P_1 + P_2 = \sum_{i=1}^{N}\left(\frac{u_i}{a}-1\right)^2 + \beta \sum_{i=1}^{N}(\varphi_i - \bar{\varphi})^2, \qquad (4)$$

where a - total energy in the energy units of rest to which it is necessary to accelerate particles, at the fixed/recorded length of the initial part of the accelerator.

The search of optimum controls α and β_ϕ was accomplished/realized by several methods. The method of gradient, used to the problem, stated above, leads to the following formulas for the correction of controls α and β_ϕ in the s stage of step-type descent [4]:

$$\alpha^{s+1}(z) = \alpha^{(s)}(z) + \frac{\partial \alpha^{(s)}}{\partial \sigma}\Delta\sigma,$$

$$\beta_\phi^{(s+1)}(z) = \beta_\phi^{(s)}(z) + \frac{\partial \beta_\phi^{(s)}}{\partial \sigma}\Delta\sigma, \qquad (5)$$

where $\Delta\sigma$ - step/pitch of descent,

$$\frac{\partial \alpha'}{\partial \sigma} = -[P]_\alpha \equiv \sum_{m=1}^{N}\psi_m(z)\frac{\partial q_m}{\partial \alpha},$$

$$\frac{\partial \beta_\phi}{\partial \sigma} = -[P]_{\beta_\phi} = -\sum_{m=1}^{N}\psi_{m+N}(z)\frac{\partial f_m}{\partial \beta_\phi}, \qquad (6)$$

and functions $\psi_m(z)$, $\psi_{m+n}(z)$ are determined from the decisions of the system of equations, conjugated/combined with respect to system (2). Interconnected circuit, is closely related with the equations for variations δu_m and $\delta \psi_m$ and therefore gradient method gives extreme controls near some initial and knowingly non-optimal controls. Usually as the initial ones were taken $\alpha(z)$ and $\beta_\phi(z)$, those used in the calculations of the already existing accelerators. Despite the fact that the extreme values α and β_ϕ differed after several steps/pitches of gradient descent at the appropriate points from initial ones only by several percentages along α and β_ϕ, the decrease of functional and an improvement in the characteristics of beam was essential. For example, during the minimization of functional P_2 the phase width of cluster $\Delta \psi$ decreased 1.5-2 times during a simultaneous improvement in the energy spectrum.

The best results were obtained during the consecutive use/application of a method of the "averaged gradient" and a method of ravines [5]. Let us briefly describe the process of the search of extremum in this case. Is minimized functional
$P\left[x_1(L), x_2(L), \ldots, x_m(L)\right]$. Let us break region $0 \leq z \leq L$ on n sections and will write controls $\alpha(z)$ and $\beta_\phi(z)$ symbolically in the form of the vector of the controls:
$$v = (v_1, v_2, \ldots, v_n). \qquad (7)$$
Let us introduce the mutually orthogonal variations in the vector of

the controls

$$\Delta v_i = (0,\ldots,0,\Delta v_i,0,\ldots,0) \qquad (8)$$

and let us construct the matrix/die

$$\left\| \frac{\Delta x}{\Delta v} \right\| = \left\| \begin{array}{cccc} \dfrac{\Delta x_1}{\Delta v_1^{(0)}}, & \dfrac{\Delta x_1}{\Delta v_2^{(0)}}, & \cdots, & \dfrac{\Delta x_1}{\Delta v_m^{(0)}} \\ \cdots & \cdots & \cdots & \cdots \\ \dfrac{\Delta x_n}{\Delta v_1^{(0)}}, & \dfrac{\Delta x_n}{\Delta v_2^{(0)}}, & \cdots, & \dfrac{\Delta x_n}{\Delta v_m^{(0)}} \end{array} \right\| \qquad (9)$$

from n the rows and m columns. Rate of change in functional P with respect to a variation in the control in i section Δv_i exists:

$$P'_{v_i} = \sum_{j=1}^{m} \left. \frac{\partial P}{\partial x_j} \right|_{x_j = x_j^{(0)}} \frac{\Delta x_j}{\Delta v_i^{(0)}} , \qquad (10)$$

where $\left. \dfrac{\partial P}{\partial x_j} \right|_{x_j = x_j^{(0)}}$ — derivative of functional P on the initial vector of controls v. component change v_k can be written in the form:

$$v_k^{(1)} = v_k^{(0)} - \gamma_k^{(0)} \text{ sign } P'_{v_k^{(0)}} . \qquad (11)$$

Variations Δv_i can be undertaken large and this it is provided the nonlocality of method. In our calculations gap/interval $[0.8]$ was divided/marked off in 11 sections with the end-points: by 0; 0.2; 0.5; 0.8; 1.2; 1.6; 2.0; 2.5; 3.0; 3.5; 4.0; 8.0. Constants α and β were respectively equal to 9.8 and 1. Within each section the controls α and β_ϕ changed linearly. Thus, was a 22-dimensional vector of controls v, a number of variable/alternating x_i was also

equal to 22 (was examined the motion of 11 independent particles, evenly distributed in the interval of phases $-2.5 \leq \varphi_0 \leq 2.5$; energy of injection was equal to 80 keV). The simplifying fact was the possibility to utilize one matrix/die (9) several times. The initial controls and the controls, obtained after the triple construction of matrix/die (9), are given in Fig. 1 and 2. In this case functional P decreased from 1.72 to 0.162.

For further search was applied the method of ravines, proposed by Gelfand and Tsetlin [5] which made it possible to increase substantially the dimensionality of the vector of controls (interval [0.8] it was divided/marked off in 40 equal sections by length 0.2). In this case the functional decreased to value $P_{\text{кон}} = 0.06$.

Page 161.

Controls, which correspond $P_{\text{кон}}$, are shown in Fig. 1 and 2. An improvement in the characteristics of beam one can see well in Fig. 3. Let us note that the control, which differs from final control of several gradient descents, provides the phase width of cluster $\Delta\varphi = 6^\circ$ (phase motion for this case shown in Fig. 4). However, these controls it is difficult to realize in practice. Was produced "smoothing" curves 4 in Fig. 1 and 2 for the target attain a steadier change in controls $\alpha(z), \beta_\varphi(z)$.
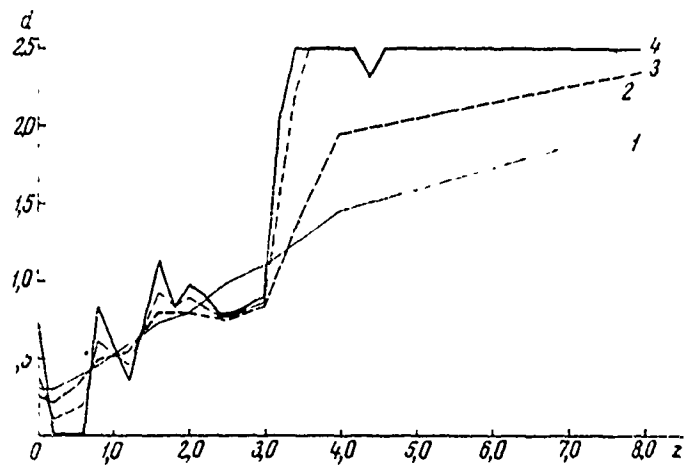
Fig. 1. Initial control $\alpha(z)$ of afterward several gradient ones it is lowering, and also control $\alpha(z)$, obtained by the method of the averaged gradient and by the method of ravines. 1 - the initial control of afterward several gradient ones it is lowering; 2 - control, obtained by the method of the averaged gradient; 3.4 - control afterward of the 10th and 30th ravine steps/pitches.
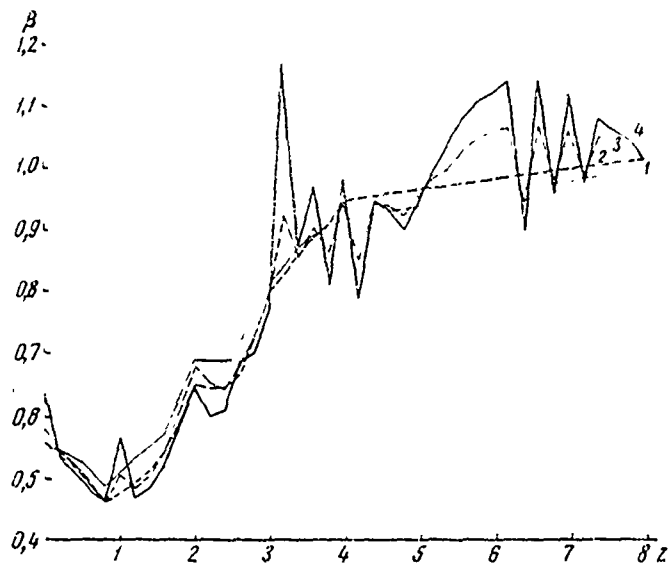
Fig. 2. Initial control $\beta(z)$ of afterward several gradient ones it is lowering, and also control $\beta(z)$, obtained by method of averaged gradient and by method of ravines.

Designations the same as in Fig. 1.
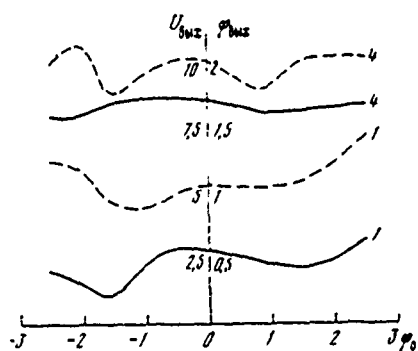
Fig. 3. Energy (dotted lines) and phase (solid lines) characteristics of beam during controls 1 and 4.

1, 4 – correspond to controls of 1.4 in Fig. 1.2.
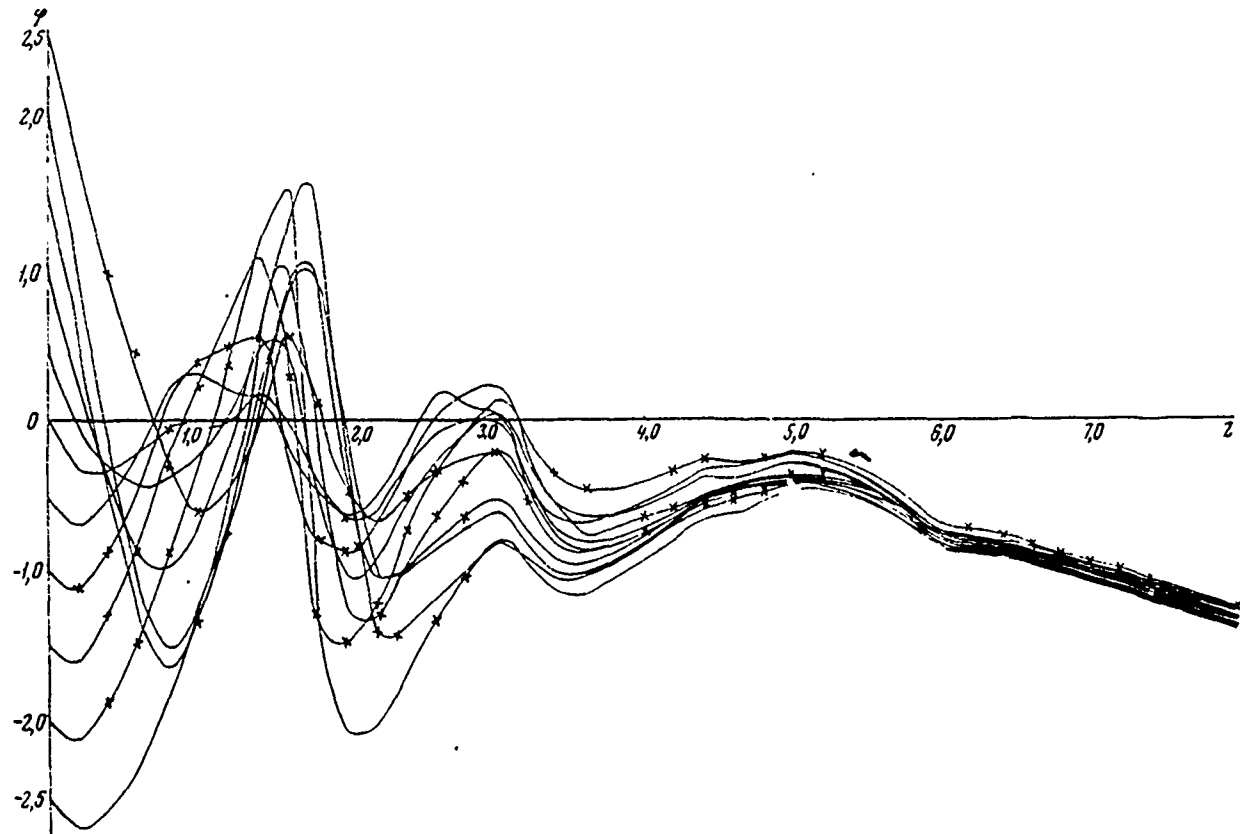
Fig. 4. Phase particle motion during controls by 4.

Page 162.

The smoothed controls are given in Fig. 5. They provide beam with $\Delta\varphi = 11,5°$, $\frac{\Delta\varepsilon}{\varepsilon} = \pm 4,5\%$ with $\varepsilon_{cp} \simeq 10$ MeV. As can be seen from Fig. 1 and 2, control α is in effect equal to zero in cut [0.2-0.6]. This means that the optimum system, which ensures the high coefficient of
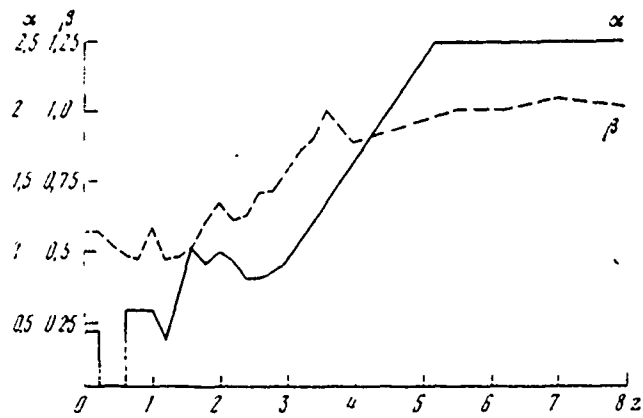
Fig. 5. Smoothed ravine control.

capture, must consist of resonator and waveguide bunchers. In this case the length of drift space proves to be substantially less in comparison with case, when both bunchers are considered independent variables. It is interesting to also note (Fig. 4) that change α and β_ϕ in the initial section contributes to the cophasality of the longitudinal oscillations of all particles.

In conclusion the authors consider as the pleasant duty to express appreciation to N. Ye. Kirin and V. Ya. Kotkovnika for useful advice and discussion of the questions, touched upon in the work.

REFERENCES.

1. A. V. Shal'now, S. P. Lomnev.   Lineynyye uskoriteli.[Linear Accelerators], 1959, p. 64.

2. S. P. Lomnev. Method of calculation of linear electron acceleratorsMoscow, VTs AN SSSR, 1962.

3. O. A. Val'dner, A. D. Vlasov, A. V. Shal'nov. Linear accelerators, Moscow, Atomizdat, 1969.

4. Method of optimization with approximations to the mechanics of space flight. Edited by Dzh. Leytman, Moscow, Izd-vo "Nauka", 1965.

5. I. M. Gel'fand, S. L. Tsetlin, UMN [Progress of Matematical Sciences], 1962, 17, No. 1.

137. Theory of the rescnators, loaded with spheroidal dielectric and metallic bodies.

V. A. Popov, N. A. Khizhnyak.

(physiotechnical institute of AS UkSSR).

The task about frequency shift and structure of the field of resonator, loaded with disturbing body, is of considerable applied interest and for the isotropic disturbing bodies it was up to now examined predominantly by the methods of perturbation theory.

In the present work on the basis of the equations of Maxwell in the integral form is posed analogous problem for the disturbing bodies with the arbitrary parameters of anisotropy. In a number of cases possible the exact solution of these equations, which makes it possible to define both the frequency shift and structure of the steady fields.

Initial are the following integral equations, equivalent to the equations of Maxwell and to boundary conditions on the surface of disturbing body [1,2]

$$\mathcal{E}(\imath,t) = \mathcal{E}_0(\imath,t) + \left(grad\ div - \frac{\varepsilon_1 \mu_1}{c^2} \frac{\partial^2}{\partial t^2}\right)\Pi^e - \frac{\mu_1}{c}\frac{\partial}{\partial t} rot\Pi^m; (1)$$

$$H(\imath,t) = H_0(\imath,t) + \left(grad\ div - \frac{\varepsilon_1 \mu_1}{c^2} \frac{\partial^2}{\partial t^2}\right)\Pi^m + \frac{\varepsilon_1}{c}\frac{\partial}{\partial t} rot\Pi^e; (2)$$

where $\mathcal{E}_0(\imath,t)$, $H_0(\imath,t)$ - fields, which existed in the resonator in the absence of disturbing body, ε_1 and μ_1 - permeability of medium, which fills resonator, Π^e and Π^m - the electrical and magnetic vectors of hertz. They are equal to:

$$\Pi^e(\imath,t) = \frac{1}{4\pi}\int_0^\infty dt'\int_V\left(\frac{\hat{\varepsilon}}{\varepsilon_1} - 1\right)\mathcal{E}(\imath',t')f(|\imath-\imath'|,t-t')d\imath';\quad (3)$$

$$\Pi^m(\imath,t) = \frac{1}{4\pi}\int_0^\infty dt'\int_V\left(\frac{\hat{\mu}}{\mu_1} - 1\right)H(\imath',t')f(|\imath-\imath'|,t-t')d\imath',\quad (4)$$

where $\hat{\varepsilon}$ and $\hat{\mu}$ - tensors of the dielectric and magnetic permeability of disturbing body; V - its volume, function f is determined by the nonhcmogeneous wave equation

$$\Delta f - \frac{\varepsilon_1 \mu_1}{c^2}\frac{\partial^2}{\partial t^2} f = -4\pi\delta(|\imath-\imath'|)\delta(t-t')\quad (5)$$

and the corresponding boundary conditions on the surface of resonator. During the determination of integration constants for each component of field are selected such sets of eigenfunctions, so that the electric fields would satisfy the required boundary conditions on the surface of resonatcr.

Page 163.

Let us introduce the system of its own orthonormalized function

$\chi_N(\tau)$ of resonator without the load, that satisfy the equation

$$\Delta \chi_n(\tau) + k_{0N}^2 \chi_N(\tau) = 0$$

(6)

and the condition for the standardization

$$\int_\Omega \chi_N^*(\tau)\, \chi_{N'}(\tau)\, d\tau = \delta_{NN'},$$

where k_{0N}- its own wave number of resonator, which depends from three indices, Ω - volume of resonator.

Then the decision of equation (5) we find in the form

$$f(|\tau-\tau'|, t-t') = \begin{cases} \dfrac{4\pi c^2}{\varepsilon_1 \mu_1 \Omega} \sum_n \chi_n(\tau)\chi_n^*(\tau') \dfrac{\sin \omega_{0N}(t-t')}{\omega_{0N}} & \text{при } t > t', \\ 0 & \text{при } t < t', \end{cases}$$ (7)

where $\omega_{0N}^2 = k_{0N}^2 c^2 / \varepsilon_1 \mu_1$ - natural frequencies of the unloaded resonator.

Let us assume, now, that after the introduction of exciting body into the resonator the natural vibration frequency changed and became equal to ω. Then in the steady-state mode/conditions of field in the resonator when τ outside V take the form

$$E(\tau, t) = E(\tau) \cos \omega t; \qquad H(\tau, t) = H(\tau) \sin \omega t. \quad (8)$$

Substituting (7) and (8) in (1) and dividing the components/terms/addends, that have the temporary/time dependence $\sim \sin \omega_{0N} \tau$, $\sin \omega t$ and $\sim \sin \omega_{0N} t$, we will obtain two groups of the equations:

$$E(\tau) = -\frac{c^2}{\varepsilon_1 \mu_1 \Omega} \sum_N \frac{1}{\omega^2 - \omega_{0N}^2} \left[(\text{grad div} + k_{0N}^2) \chi_N(\tau) \int_V \left(\frac{\hat{\varepsilon}}{\varepsilon_1} - 1 \right) E(\tau') \times \right.$$
$$\left. \times \chi_N^*(\tau') d\tau' + \frac{\mu_1 \omega}{c} \text{rot} \chi_N(\tau) \int_V \left(\frac{\hat{\mu}}{\mu_1} - 1 \right) H(\tau') \chi_N(\tau') d\tau' \right]; \quad (9)$$

$$E_0(\tau) = -\frac{c^2}{\varepsilon_1 \mu_1 \Omega} \frac{1}{\omega^2 - \omega_{0M}^2} \left[(\text{grad div} + k_{0M}^2) \chi_M(\tau) \int_V \left(\frac{\hat{\varepsilon}}{\varepsilon_1} - 1 \right) E(\tau') \times \right.$$
$$\left. \times \chi_M^*(\tau') d\tau' + \frac{\mu_1 \omega}{c} \text{rot} \chi_M(\tau) \int_V \left(\frac{\hat{\mu}}{\mu_1} - 1 \right) H(\tau') \chi_M^*(\tau') d\tau' \right]. \quad (10)$$

Equations for the magnetic field are obtained analogously. For points outside V equation (9) determines the excited field through the internal field in the disturbing body and frequency shift. Equation (10) determines frequency shift through the parameters of resonator itself and disturbing body. From (10) it is possible to obtain the known formula of slater and Mayer [3] for frequency shift of cylindrical cavity upon the introduction in it of isotropic dielectric ball/sphere, moreover for the internal field in the ball/sphere we will use the results of the quasi-static approximation/approach:

$$\frac{\Delta \omega}{\omega} = -\frac{3}{2} \frac{\varepsilon - \varepsilon_1}{\varepsilon + 2\varepsilon_1} \frac{V E_{02}(\tau_0)}{\int_\Omega E_0^2 \, d\tau}. \quad (11)$$

Here $E_{0z}(\tau_0)$ - undisturbed field in the location of ball/sphere. For the cylindrical cavity, loaded with spherical heterogeneity from the isotropic dielectric, arranged/located at point $(0, 0, Z_0)$ from (10) it is possible to obtain the following dispersion equation:

$$\omega^2 - \omega_{0N}^2 = -\frac{V}{\Omega}\frac{6c^2}{\varepsilon_1\mu_1}\frac{\cos^2 k_{3p}z_0}{J_1^2(\alpha_0^n)}\left(\frac{\alpha_0^n}{R}\right)^2\frac{\varepsilon-\varepsilon_1}{\varepsilon+2\varepsilon_1}, \quad (12)$$

where R - radius of resonator, $J_1(x)$ - the Bessel function on the order of 1, α_0^n - the n root of Bessel function zero order.

The structure of the excited field is described by equation (it is brought expression only for component E_z):

$$E_z = -A J_0\left(\alpha_0\frac{n\tau}{R}\right)\left(\frac{d^2W}{dz^2} + k^2W\right),$$

$$(13)$$

where $A = \frac{2}{\Omega J_1^2(\alpha_0^n)}\int\limits_V\left(\frac{\varepsilon}{\varepsilon_1}-1\right)E_z^{(0)}(\tau')d\tau';$

$$W(z,z_0)=\frac{c^2}{\varepsilon_1\mu_1}\sum_{\ell=0}^{\infty}\frac{\cos k_x z_0 \cos k_{3\rho} z}{\omega^2-\omega_{0n\ell}^2}=\begin{cases}\dfrac{L}{2}\dfrac{\cos k_3 z \cos k_3(L-z_0)}{k_3 \sin k_3 L}\text{ при } z<z_0;\\[2em]\dfrac{L}{2}\dfrac{\cos k_3 z_0 \cos k_3(L-z)}{k_3 \sin k_3 L}\text{ при } z>z_0;\end{cases}$$

$$\tag{14}$$

$$k_3^2=k^2-\left(\frac{\alpha_0^n}{R}\right)^2;$$

L - length of resonator.

For small disturbing bodies $(\alpha/\lambda\ll 1)$ frequency shift and change in the structure of field from the quiescent value is also small. However, in the case of small bodies from the materials with the high value of dielectric permeability or in the case of the metallic bodies whose sizes/dimensions are commensurated with the wavelength appear the resonance conditions whose essence can be illustrated by the following example. According to (12) the smallness of frequency shift is determined by the smallness of the ratio of volumes $\frac{V}{\Omega}$. In the case of sphere from the material with the large dielectric permeability formula (12) qualitatively remains valid; however, instead of value ε should be substituted value $\varepsilon_{\text{эфф}}=\varepsilon F(ka\sqrt{\varepsilon})$ [4], where

$$F(x)=\frac{2(\sin x - x\cos x)}{(x^2-1)\sin x + x\cos x}.\tag{15}$$

Analogous situation occurs also for other spheroidal configurations, although the function $F(x)$

takes more complicated form and depends not only on the absolute value of wave vector, also on the orientation of body.

Function $F(x)$ can take both positive and negative values; when $\varepsilon_{\perp\perp} + 2\varepsilon_\parallel \to 0$ frequency shift becomes large, in spite of the smallness of relation V/Ω, and field distribution becomes qualitatively different from the distribution in the undisturbed resonator. From (12) and (15) it is possible to find dependence ω on ε, i.e. as the final result, dependence k_3 on ε. But according to (13) and (14) k_3 is determined E_2- field component. In other words, changing ε disturbing body, it is possible to control the structure of field in the resonator. In particular, with continuous (adiabatic) change ε is possible continuous transformation, for example mode E_{011} into mode E_{010}.

DOC = 30069312 PAGE 678

REFERENCES.

1. N. A. Khizhnyak, ZhTF [Journal of Technical Physics], 1958, 28, No. 7, ctr. 1952.

2. N. A. Khizhnyak. Sb. "Radiotekhnika" [Radio Engineering], Issue 4, Izd-KhGU, 1967, str. 87.

3. L. S. Maier, I. S. Slater. J. Appl. Phys., 1952, 23, p. 68.

4. L. LEVIN. Sovremennaya teoriya volnovodov [Modern theory of waveguides]. Moscow, IL, 1954.

Page 164.

138. High-frequency system of the electron-positron ring VEPP-3.

V. G. Veshcherevich, E. I. Gorniker, N. N. Ioshchenko, M. M. Karliner, V. M. Petrov, V. V. Petukhov, I. K. Sedlyarov, M. N. Tarshish, I. A. Shekhtman.

(Institute of nuclear physics of SO AN USSR   [Siberian Department of the Academy of Sciences of the USSR]).

The high-frequency system of ring VEPP-3 encompasses two accelerating cavities and high-frequency oscillators for power supply of these resonators. One of the resonators operates at a frequency of 4 MHz (1st harmonic of the frequency of revolution of electrons and the positrons), another - at the frequency of 76 MHz (19th harmonic).

On accelerating resonator gap on 4 MHz is developed the voltage in amplitude to 10 kV, necessary in the mode/conditions of the accumulation of positrons for obtaining one cluster. After the

accumulation of particles is included the second resonator on
clearance of which is created the voltage to 750 kV at the required
power of approximately 100 kW. This voltage makes it possible to
achieve maximum energy of the particles of 2-2.5 GeV, determined by
losses to the synchrotron radiation.

Subsequently are intended to supplement system with two
resonators and generators at the frequency of approximately 160 MHz,
which will make it possible to achieve the calculated maximum energy
VEPP-3-3-3.5 GeV with the total voltage on the clearances to 3.8 MV
and power of generator to 1 MW.

System consists of accelerating cavities, power amplifiers and
units of control and check. The schematic of resonator for the
frequency of 4 MHz (it is more precise than 4.03 MHz) is represented
in Fig. 1. Resonator is the short-circuited cut of coaxial line,
loaded to the capacity/capacitance with the value of 6000 pF, from
60 ceramic capacitors K15U1 100 nF, 130 kVa. Resonator is comprised
on the axial plane of two parts which
cover the ceramic insulator, sealed in in vacuum chamber of
accumulator/storage. Insulator separates/liberates chamber/camera
from the filled with air interior of resonator and is located in the
accelerating clearance. The adjustment of resonator is
accomplished/realized by the rotating copper framework. Resonator has
the following electrical parameters: quality 2000, characteristic

impedance of 5.7 ohms, shunt resistance of 11 kiloohm, maximum
amplitude of voltage on the clearance 10 kV. Cooling resonator -
forced, air. The large part or the power (about 4 kW with the maximum
voltage) is scattered in the capacitors/condensers which require
intense ventilation.

Resonator for the frequency of 76 MHz (76.6 MHz) in the
construction/design (see Fig. 2) is analogous to the resonator of
accumulator/storage VEPP-2 [1], but has somewhat larger
sizes/dimensions, also, in connection with this
approximately/exemplarily 3 times larger shunt resistance.
Furthermore, two accelerating clearances are increased from 3 to 8 cm
each, that allows the total voltage on two clearances to bring to
800-900 kV.
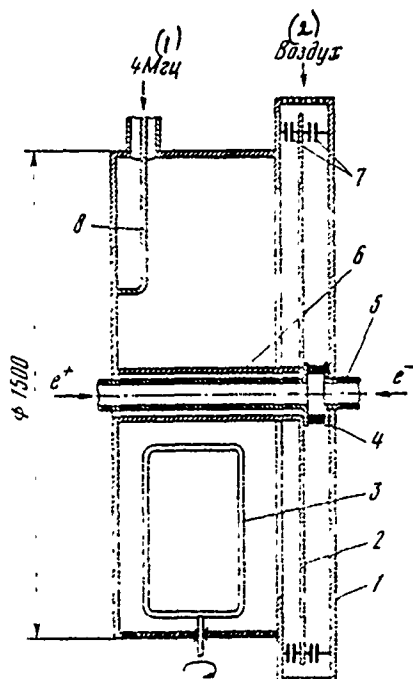
Fig. 1. Accelerating cavity by the frequency of 4 MHz. 1 - housing; 2 - disk; 3 - adjusting framework; 4 - ceramic insulator; 5 - vacuum chamber of accumulator/storage; 6 - internal conductor of coaxial line; 7 - ceramic capacitors; 8 - loop of the introduction/input of power.

Key: (1). MHz. (2). Air.

Page 165.

Within the vacuum housing of rescnator from the rod is suspended/hung copper duct with the disks ("coil"). Rod is isolated/insulated by

ceramic insulator from the housing; on it to the coil is supplied the

voltage - 20 kV for the depression of resonance electron discharge.

Bypass capacitors serve for closing/shorting of HF voltage, which

appears at the rod as a result of the residual/remanent asymmetry of

coil relative to housing. The electrical parameters have the

following values: quality 20000, characteristic impedance of 150

ohms, shunt resistance of 3 MΩ, maximum amplitude of accelerating

voltage 750 kV. The adjustment of resonator is accomplished/realized

by an elastic deformation of the end walls of the resonator, placed

into the external vacuum snell. Is cooled resonator by the distilled

water, which takes place through the rod into the hollow walls of

coil, and also on the tubes, soldered to the housing of resonator.

The HF supply of resonators is accomplished/realized from two

power amplifiers. One of them for the frequency of 4.03 MHz is

intended for the supply of resonator for this frequency. Its exit

two-cycle cascade/stage on two lamps GU-22 develops power to 50 kW.

Power amplifier at the frequency of 76.6 MHz in the

construction/design is analogous to the generator of

accumulator/storage VEPP-2 [2]. Its final stage - two-cycle on two

tetrodes GU-53A; power output - 150 kW.

The block diagram of high-frequency system is given in Fig. 3.

HF system is excited by the master oscillator at the frequency of

1.34 MHz. Exciter is reconstructed in limits of ±0.34o/o from the
medium frequency. The voltage of the master oscillator enters the
entrance of frequency tripler; from its output the voltage of the
frequency of 4.03 MHz is supplied to the entrance of channels 4.03
and 76.6 MHz. At the entrance of the first channel there are the
electrically controlled phase inverter and amplifier with the
adjustable amplification factor. In second channel series-connected
the electrically controlled phase inverter, frequency multiplier to
19, electrically controlled phase inverter and adjustable amplifier.
Amplifiers are controlled by the modulators that provide
inclusion/connection and disconnection of HF power, automatic control
of amplification for voltage regulation on the resonators, and also
disconnection of HF power in the emergency modes.

The controlled phase inverters are connected with the diagram,
which ensures the automatic agreement of phases in two channels. With
the aid of this diagram the voltage on both resonators is cabled on
the phase to the reference voltage. The latter is obtained as
follows. The voltage of the frequency of 3.68 MHz, removed from the
output of frequency doubler, enters the shaper, which forms
impulses/momenta/pulses with the repetition frequency 2.68 MHz, of
amplitudes of 0.5 V and the duration on the half-height of
approximately 5 ns. These impulses/momenta/pulses are supplied to the
mixers, to one of which enters also the voltage from resonator 4 MHz

through the phase inverter A, and on another - the voltage of the
frequency of 76.6 MHz from the multiplier output of frequency on 19.
If the centers of gravity of impulses/momenta/pulses coincide with
zero radio-frequency voltage, then on the output of mixer the
amplitude of the voltage of the intermediate frequency of 1.34 MHz is
equal to zero.

But if HF voltage is displaced on the phase, then the amplitude
of the voltage of intermediate frequency on the output of the mixer
is proportional to the amount of phase shift, and its phase changes
on 180° with sign change of phase shift. From the outputs of mixers
the voltages of intermediate frequency enter the synchronous
detectors.
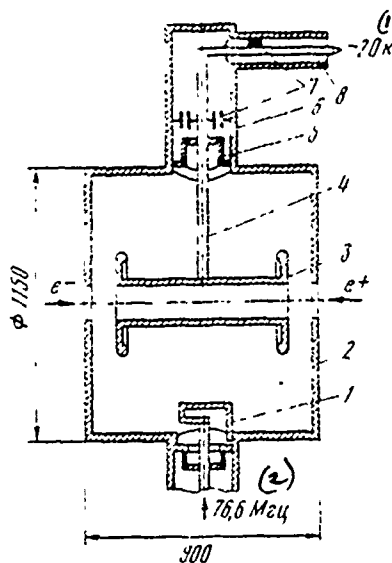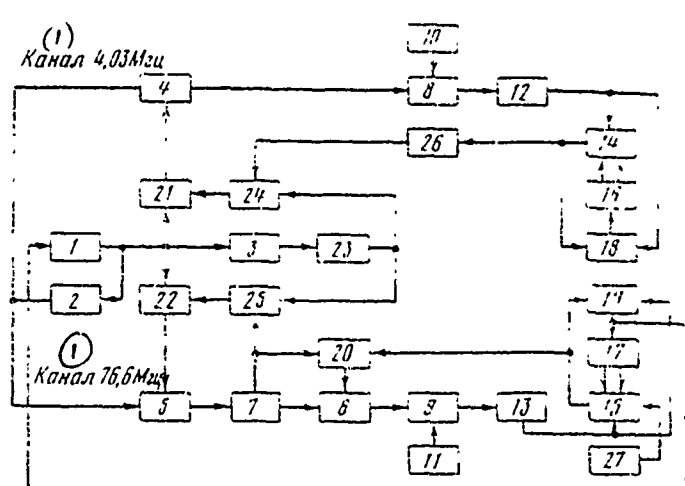
Fig. 2.   Fig. 3.

Fig. 2. Accelerating cavity by frequency of 76 MHz. 1 - loop of the
introduction/input of power; 2 - housing; 3 - duct with the disks
(coil); 4 - rod; 5 - ceramic insulator; 6 - housing of the node/unit
of high-voltage introduction/input; 7 - bypass capacitors; 8 -
busbar/tire of the application of voltage of displacement.

Key: (1). kV. (2). MHz.

Fig. 3. Functional diagram of HF supply of accumulator/storage
VEPP-3. 1 - master oscillator 1.34 MHz; 2 - frequency tripler; 3 -
frequency doubler; 4, 5 and 6 - controlled phase inverters; 7 -
frequency multiplier to 19; 8 and 9 - modulated amplifiers; 10 and 11

- modulators; 12 and 13 - power amplifiers; 14 - resonator 4.03 MHz; 15 - resonator 76.6 MHz; 16 and 17 - servodrives of resonators; 18, 19 and 20 - phasemeters; 21 and 22 - synchronous detectors 1.34 MHz; 23 - impulse shaper 2.68 MHz; 24 and 25 - mixers; 26 - phase inverter A; 27 - rectifier of mixing.

Key: (1). Channel 4.03 MHz.

Page 166.

The reference voltages of detectors by the frequency of 1.34 MHz are removed/taken from the master oscillator. The exit voltages of synchronous detectors control phase inverters in such a way that the output pulses of shaper coincide with zero exit voltage of phase inverter A of the frequency of 4.03 MHz and with zero exit voltage of frequency multiplier on 19. Resonator voltage 76.6 MHz cables itself on the phase to the exit voltage of frequency multiplier on 19 with the aid of the phasemeter, which affects controlled phase shifter. The setting up of necessary phase displacement of accelerating voltages on the resonators is accomplished/realized by a phase inverter A.

A difference in the clamping circuits of the phase of accelerating voltages of frequencies 4.03 and 76.6 MHz to pulse

voltage of the frequency of 2.68 MHz is connected with the large range of changes in the resonator voltage 76.6 MHz.

Resonators are equipped with devices/equipment for the automatic tuning of natural frequencies. Into each of the devices/equipment enters the phasemeter, which measures a phase difference between the voltage on accelerating resonator gap and the current of the feeder of resonator. Signals from the outputs of phasemeters are supplied to the servodrives which reconstruct the natural frequencies of resonators.

Resonators on 4.03 and 76.6 MHz and blocks of the control system are prepared, tested and work in the accumulator/storage VEPP-3.

689

REFERENCES

1. V. G. Veshcherovich, M. M. Karliner, V. M. Petrov,
   I. K. Sedlyarov, I. A. Shekhtman. Trudy Transactions of the
   All-Union Conference on Accelerators of Charged Particles.
   9-16 October 1968. Moscow. VINITI, 1970, Vol II, p. 143.

2. E. I. Gorniker, M. M. Karliner, V. M. Petrov, V. V. Petukhov,
   I. A. Shekhtman. Trudy Transactions of the All-Union
   Conference on Accelerators of Charged Particles. Moscow,
   9-16 October 1968. Moscow VINITI, Vol II, p. 139.

Page 139.

Discussion.   -

A. V. Mishchenko. In what mode/conditions (continuous or pulse) does work the generator?

V. M. Petrov. In the continuous.

A. Ya. Belyak. Is included resonator in the vacuum container? Are such the exemplary/approximate dimensions of resonator on 76 MHz?

V. M. Petrov. Resonator is included in the vacuum container. Sizes/dimensions of the resonator: the diameter of 1150 mm, the length of 900 mm, the accelerating clearances on 80 mm.

A. A. Glazov. Which the precision/accuracy of phasing?

V. M. Petrov. The precision/accuracy of the phasing of accelerating voltage with the frequency of 4 MHz relative to voltage with the frequency of 76 MHz corresponds to $\Delta t=0.5 \cdot 10^{-9}$ s.

V. Ya. Stepanyuk. What is the controlled phase inverter?

V. M. Petrov. The controlled phase inverter consists of the stepped phase inverter, which changes phase irregularlyly on 45°, the steady phase inverter, which is the resonance single-stage amplifier, included by ARU. In the latter the phase smoothly changes on ±45° due to the rearrangement of contour/outline.

V. I. Bobylev. In what limits it is possible to reconstruct the frequency of resonator on 76 MHz due to the elastic deformations of walls? From what material is prepared the resonator and which face wall thickness?

V. M. Petrov. The thickness of walls is ~10 mm, material - copper. Rearrangement composes ±1o/o.

139. Precision system of the high-frequency supply of spectrometric cyclotron.

G. A. Vasil'yev.

(Physical institute of the AS USSR).

M. S. Davidov, I. I. Pinkel'shteyn.

(Scientific research institute of the electrophysical equipment im. D. V. Efremov).

The accelerating system of spectrometric cyclotron consists of two basic resonators in angular extent on 45°, excitable in the range frequencies of 10-15 MHz, and two supplementary resonators by angular extent of 15°, excited on the third harmonic of the frequency of basic resonators. The amplitude of accelerating voltage in the basic resonators 125 kV, and supplementary 15 kV [1]. Both both bases and supplementary resonators are united in pairs so that each pair is actually one resonator of the type of "eight". Therefore from a radio engineering point of view each pair can be considered as one resonator. This makes it possible for their excitation to use only

two generators - basic with power on the order of 200 kW and supplementary (third harmonic) with power output on the order of 15 kW.

Basic difficulties during the development of the system of HF supply are connected with the need for the stabilization of amplitude in the basic resonator with the precision/accuracy not worse $\pm 3 \cdot 10^{-5}$, or phase difference between the HF voltages of fundamental frequency and third harmonic with precision/accuracy of $\pm 0.03°$.

Page 167.

System block diagram is given in the figure. The master oscillator ZG encompasses the synthesizer of frequencies with the stability of frequency on the order of $\pm 1 \cdot 10^{-7}$ and the auxiliary stabilization system of the amplitude of exit voltage, which ensures the constancy of exit voltage ZG with the precision/accuracy not worse than $\pm 10^{-4}$.

HF voltage of ZG through the control unit, the broadband power amplifier and the final stage excites basic resonator R1. The final stage is installed directly on the resonator and excites the latter without the use/application of intermediate circuits and feeder line.

The final stage and the power amplifier work in the understressed mode/conditions and, for the purpose of an increase in the stability of amplification and phase responses, they are included through the resonator by feedback in the high frequency.

The presence in feedback loop of high-Q resonator makes it possible to carry out sufficiently deep (K on the order of 50-100) feedback without the destabilization of system. In this case the stabilization factor in the first approximation, is equal to the coefficient of feedback. This stabilization of HF voltage on the accelerating clearance of basic resonator is accomplished/realized by an artificial stability installation (ASA1).

As the measuring element of system (sensor) is utilized the photoelectric comparator, which ensures the precision/accuracy of the comparison of the average/mean value of HF voltage with standard constant stress of order 10^{-5}. The precision/accuracy of this order it is at present obtained in the comparators, developed in by Tomsk polytechnic institute [2].

The introduction of the integrating component/link makes the system of ASA astatic, due to what it is provided, in particular, a sufficient range of regulating.

However, in connection with the use/application of an inertia comparator and the introduction of integration ASA basic system becomes slow. For eliminating the rapid fluctuations of amplitudes is applied the support system of ASA. Support system static (K on the order of 50) with the limited range of regulating. The work of support system can be considered as the correction of basic system with derivative control.

It is assumed that this combination of ASA systems will make it possible to obtain the acceptable transient responses (operating speed) with the range or regulating and prescribed/assigned precision/accuracy reached. The system of ASA of channel on the third harmonic is analogous tasic.

For the stabilization of tne phase relationships/ratios between the oscillations in the basic and supplementary resonators is utilized the artificial stability installaticn of phase (ASF).

The basic difficulty of developing this system consists in the creation of the measuring device (indicator), which fixes the divergences of a phase difference of multiple frequencies from the given one with the precision/accuracy not worse than $\pm 0.02°$ in the fundamental frequency).

At present is conducted the development of this measuring device. Works are conducted in two directions: are investigated diagrams with intermediate frequency multiplication and heterodyning of signal, and also diagram of the direct comparison of phase at the multiple frequencies. Structurally system ASF is carried out (as ASA system) in the form of the combination of wide-range astatic system with the high speed statistical (with the limited range of regulating).

Besides the basic stabilization systems (ASA and ASF) the HF supply encompasses the series/row of auxiliary stabilization systems: in particular, the system of the self-alignment of the natural frequency of resonators (APCh). Systems APCh of basic and supplementary resonators are carried out on the phase principle. The signals of detuning are developed by the phase sensors, which compare with respect to the phase excitation voltage with the voltage in the resonator. After the appropriate amplification and conversion they act on tuning elements. Systems APCh are astatic. Precision/accuracy in phase on the order of 0.5-1°. The residual/remanent errors for systems APCh exceed the permissible error for the mutual phasing of resonators, but their value considerably less than the range of regulating systems ASF and ASA.

Therefore systems ASF and ASA easily remove the effect of the

errors for systems APCh cn the precision/accuracy of the
stabilization of accelerating voltages.

In connection with the extremely high requirements for the
precision/accuracy of the maintenance of the prescribed/assigned
parameters at the development of the system of HF supply are accepted
the measures for a maximally possible reduction in the value of the
destabilizing effects. All supply voltages are stabilized with the
precision/accuracy of crder $1 \cdot 10^{-4}$. Provision is made for
thermostatic control of the separate elements of the system of HF
supply, and also heat stabilization with the high precision/accuracy
of accelerating cavities.

At present are examined the possibilities of simplification in
the developed system and further increase in its precision/accuracy
and reliability. In connection with this are conducted investigations
of the possibilities of exciting the supplementary resonator directly
from the basis due to the introduction to connection/communication
between them through the nonlinear elements/cells.

DOC = 80069313   PAGE 698
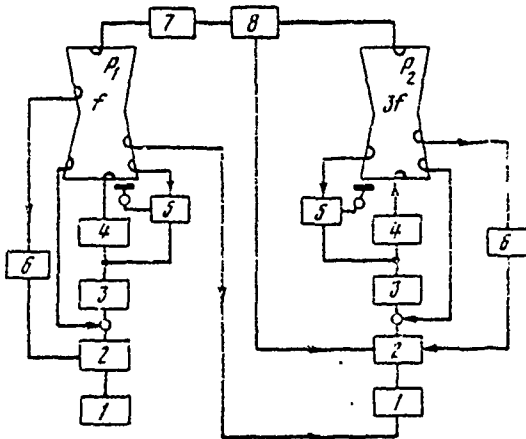
The system block diagram of HF supply: 1 - master oscillator; 2 - control units; 3 - broadband power amplifiers; 4 - the final stages; 5 - the automatic frequency control; 6 - the automatic tuning of amplitude; 7 - diagram of control of frequency; 8 - phase sensor; R_1 - resonator of fundamental frequency; R_2 - resonator of the third harmonic.

Page 168.

REFERENCES

1. I. Ya. Barrit, et al. Spectrometric Isochronous Cyclotron with Controllable Energy of the Particles. Trudy Transactions of VII International Conference on Accelerators of High Energies. Yerevan, 1969, Vol. 1, p. 324.
2. M. S. Poytman. A Stable Source of Calibrated Variable Voltage. Avtometriya, 1968, No. 3.

140.

HIGH-FREQUENCY SYSTEM OF HIGH-CURRENT F-M CYCLOTRON OF JOINT

INSTITUTE FOR NUCLEAR RESEARCH.

(Installation "F").

A. A. Glazov, V. A. Kochkin, L. M. Onishchenko, V. I. Peregud, M. M.

Semenov, I. V. Tuzov, M. N. Knarlamova.

(Joint Institute for Nuclear Research, scientific research institute

of the electrophysical equipment im. D. V. Yefremov).

In the high-current F-M cyclotron J.I.N.R. [1] the terminal

radius of acceleration is 2.7 m, magnetic field is formed/shaped in

such a way that the acceleration of protons before the energy 700 MeV

must be accomplished/realized with a change in the frequency of

accelerating voltage in the range $18.18 > f > 14.41$ MHz.

The introduction to variation and the growing with a radius

magnetic fields leads to the contraction of working frequency band;

however in this case sharply decreases by interpolar magnet gap, and

with the selected aperture of dee 100 mm the clearance between dee

and cladding of chamber/camera will be only 78.5 mm. With this
clearance accelerating voltage to avoid breakdowns and excessive
losses is selected equal to 50 kV.

As the modulating device/equipment it is decided to utilize the
mechanical rotating variable/alternating capacitor/condenser, which
is up to now represented by the best device/equipment for a variation
in the frequency of the accelerating system of F-M cyclotron. In all
projects of the reconstruction of accelerators in operation [2, 3]
also is provided for precisely this method of the rearrangement of
frequency. In connection with the relatively narrow operational
frequencies band for the resonance system in this case it proves to
be possible to utilize a cut of uniform line so that the voltage on
the bunchers would be always less than accelerating voltage.

The ratio of the maximum capacity/capacitance of bunchers to the
minimum has a minimum at the length of resonance line, close to 6.5
m. However, in connection with the fact that in the minimum of
relation C_{max}/C_{min} the value of capacity/capacitance C_{max} is very
great, and the minimum sufficiently flat/plane, by optimum length it
will be 7.3-7.5 m. This length is optimum and for the design
considerations, since it makes it possible to remove bunchers and
high-frequency oscillator behind the radiation shielding.

Thus, the accelerating high-frequency system of installation "P"
is the rectangular in the plan/layout flat/plane half-wave uniform
line with a width of 6 m, with length of 7.3 m with the permanent
clearance 78.5 mm. The adjustment of system is accomplished/realized
by two identical capacitive punchers of frequency, carried out in the
form of capacitor/condenser with the rotating rotor whose axis/axle
is parallel to dee lip.

The results of calculating the electrical characteristics of
resonance line are given in the table (one-dimensional calculation).

In connection with the fact that the resonance line has
considerable width, was also produced its calculation in two
measurements. In this case it was assumed that on the contour/outline
the normal component of current is everywhere equal to zero with
exception of the places of the connection of the buncherss where it
was permanent.

(1) Одномерный расчет				(2) Двумерный расчет	
f, МГц (3)	$U_{бар}/U_{уск}$	$C_{бар}$, (4) пф	(5) P, квт	$U_{бар}/U_{уск}$	$C_{бар}$, пф (4)
18,6	0,055	1080	154	1,030	1000
17,5	0,891	1870	157	0,909	1670
16,5	0,813	2800	157	0,943	2400
15,7	0,713	4080	155	0,861	3380
14,3	0,572	6450	150	0,741	5060

Key: (1). One-dimensional calculation. (2). Two-dimensional

calculation. (3). MHz. (4). pF. (5). kW.

Page 169.

Under this hypothesis

$$Z_{18x} \simeq -j Z_0 \, ctg \, k\ell + j \frac{Z_0 k x^2}{\pi^2 A} \sum_{n=1}^{\infty} \frac{\sin \frac{n\pi A}{x}}{n^2} ,$$

$$U_{бар}/U_{уск} \simeq \cos k\ell - \frac{k x^2}{\pi^2 A} \sin k\ell \sum_{n=1}^{\infty} \frac{\sin \frac{n\pi A}{x}}{n^2} ,$$

(1)

where 2x - width of resonance line; A - length of bunchers, equal to

1.333 m; the centers of bunchers are located at a distance of x/2

from the edges of line. Results of calculating also are presented in

the table (two-dimensional calculation).

The use/application of mechanism for the rearrangement of the

resonance frequency of system automatically is assumed the presence

of the back stroke, during which the frequency of system returns from
its finite value to the initial. If one assumes that the time of
acceleration is equal to the duration of foreward stroke, then with
the angular extent of stator plates, approximately/exemplarily equal
to $\theta - \theta_p$, the effectiveness of cycle will be

$$\eta = \frac{\theta - \theta_p}{\theta}. \qquad (2)$$

where θ_p is angular of the extent of the blades of rotor; $\theta = 2\pi/N$ -
angular distance between them (N - number of blades of rotor).

On the lower voltage frequency on the bunchers in accordance
with the data of calculation must be approximately 30 kV. In this
case four-millimetric clearance is completely sufficient from the
point of view of dielectric strength and reliability. As showed
preliminary estimations, the necessary maximum capacity/capacitance
with this clearance can be obtained in the bunchers with the
seven-degree moving vanes with a length of 12-13 cm with the diameter
of rotor about the meter and two stator packages. The effectiveness
of the cycle of bunchers is sufficiently high, and when selecting of
a number of blades of rotor the determining factor it must be the
rotational speed.

Velocity the rotation of rotor is determined by the expression:

$$\omega = \frac{60\eta}{N t_\psi} \quad [об/мин.] \qquad (3)$$

Key: (1). r/min.

where the time of acceleration t_4 for the selected law of a change
in the magnetic field and set of energy per revolution is 1038 μs.
From (3) and values η for the bunchers with seven-degree blades it
is evident that, if we are not oriented on the use of a reducer or
the development of special engine, bunchers must have 10-12 blades.
In connection with the fact that with N=10 the bunchers has a
somewhat larger value η and smaller sizes/dimensions, this version
it was accepted as the worker.

The calculation of the profile/airfoil of stator plates was
based on assumption about a linear change in the capacity/capacitance
from the angle of rotation, which corresponds well to the necessary
law of a change in the frequency. Was assumed also a linear change in
the working clearance from 7 to 4 mm in the dependence on the angle
of rotation of rotor, which provides the exemplary/approximate
constancy of electric intensity in the bunchers.

The profile/airfoil of stator plates (submersion depth of rotor
plates into the stator) $Y(\varphi)$ was determined from the expression for
the capacity/capacitance of the parallel-plate capacitor:

$$C(\varphi) = \frac{n\,S(\varphi)\,(a+\delta\varphi)}{3,6\pi\,h(\varphi)} \simeq \frac{n\left[R - \frac{1}{2}Y(\varphi)\right]Y(\varphi)\,\theta_p\,(a+\delta\varphi)}{3,6\pi\left[h_0 - \varkappa\varphi\right]}, (4)$$

where the coefficients α and β characterize the apparent increase in rotor plate due to edge effect [4]; h(#) - working clearance; 2R - diameter of rotor; n - number of clearances, undertaken by the equal to 116.

As the device/equipment, which grounds rotor in the high frequency, was accepted lamellar collector capacitor/condenser with the angular extent of plates of 284°. In this case in it simultaneously are found 8 moving vanes of each disk, and with the clearance in the collector capacitor/condenser, equal to 1.5 mm, its capacity/capacitance is 3200 pF.

For the final selection of the characteristics of HF system of accelerator after conducting of the number of model investigations was prepared its full-scale mock-up, schematically shown in Fig. 1. The same figure shows section/cut and are given the basic dimensions of the bunchers of frequency.

For facilitating the production of stator plates their profile/airfoil, obtained with the aid of expression (4), was approximated by circular arc with radius 535 mm.

Section/cut in the line is intended for a frequency division of the closest idle mode of vibration on 2-3 MHz in entire operating range.
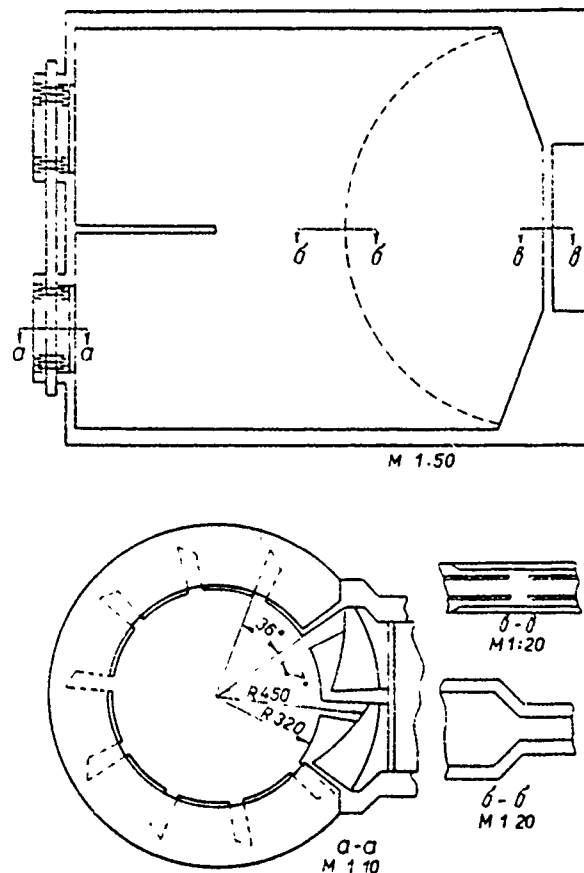
Fig. 1. Mock-up of HF system of installation "F".

Page 170.

    The basic experimental results, obtained in the mock-up, are

given in Fig. 2, where are constructed dependences on the angle of

rotation of the total capacitance of bancherss, operating frequency

and relation $U_{\text{бар max}}/U_{\text{уск}}$, and also voltage distribution on the

bunchers for different frequencies. It is evident that the system provides obtaining operating frequencies with the considerable supply: η_{max} composes 0.723, that sufficiently close to maximally possible, and the experimental results coincide sufficiently well with the calculated ones.

A voltage drop along the accelerating slot to the edge of tapers varies from 5o/c at the lower frequency to 12o/o on the upper.

The obtained dependence $f(\phi)$ was used for calculating phase acceleration mode with U_{yck}= 50 kV and $\cos \varphi s$ = 0,4. The results of calculation are given in Fig. 3. Certain increase $\cos \varphi s$ at the medium frequencies must not lead to the phase losses in view of angular damping.

DOC = 80069313   PAGE 34
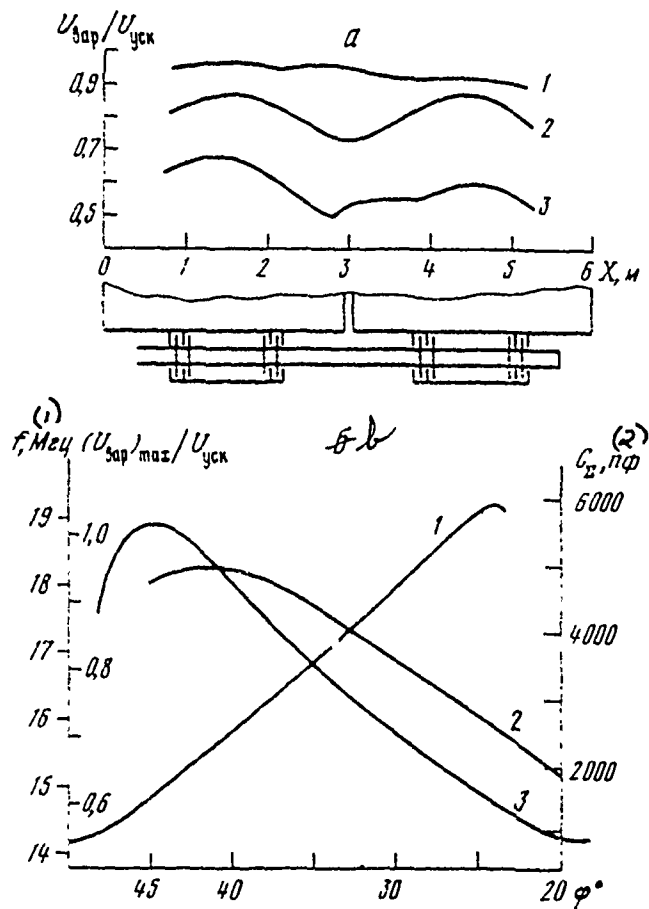
Fig. 2. Results of experimental investigation of the mock-up of RF system. a) voltage distribution on buncherss $U_{бар}/U_{уск}$ at different frequencies: 1 - f=18.88 MHz, 2 - f=16.21 MHz, 3 - f=14.2 MHz; b) dependence on the angle of rotation of the rotor: 1 - total capacitance of bunchers; 2 - ratio of maximum voltage on the buncherss to accelerating voltage $(U_{бар})_{max}/U_{уск}$, 3 - the operating frequency f.

Key: (1). MHz. (2). pF.

709
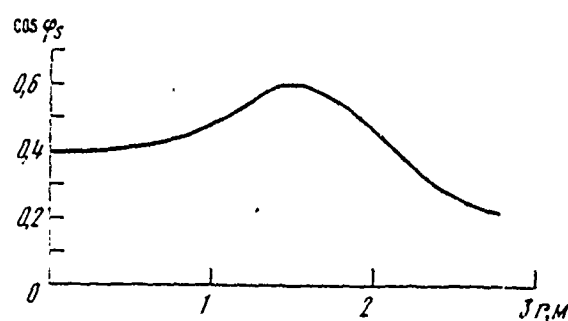
Fig. 3. Dependence $\cos \varphi_s$ on a radius.

REFERENCES

1. A. A. Glazov, Yu. N. Denisov, V. P. Dzhelenov, V. P. Dmitriyevskiy, et al. Atomic Energy, 1969, Vol. 27, issue 1, p. 16.
2. R. Cohen, E. Martin, J. Rainwater, et al. Nevis Synchrocyclotron Conversion Project. International Conference on Cyclotrons Oxford, 1969.
3. K. Mackenzie. The Berkeley Synchrocyclotron Improvement Programme International Conference on Cyclotrons, Oxford, 1969.
4. V. Smayt. Electrostatic and Electrodynamics. Moscow. IL 1954, 1954.

141. Debuncher of the injector of synchrophasotron the J.I.N.R. with modulation of energy of the accelerated beam.

L. P. Zinov'yev, R. B. Kadyrov, N. N. Plyashkevich, V. A. Popov, I. N. Semenyushkin, V. L. Stepanyuk.

(Joint Institute for Nuclear Research).

One of the effective methods of increasing the intensity of synchrophasotron of J.I.N.R. is reducing to the minimum of the losses of particles in the process of injection and acceleration. It is possible to obtain a considerable increase in the intensity of the accelerated particles, if we decrease the energy spread of the beam of injector and to select the optimum mode/conditions of injection into synchrophasotron [1, 2]. Virtually this can be carried out, if on the output of linear accelerator to establish/install the device/equipment (resonator), which makes it possible to change energy of the injected into the synchrophasotron beam in accordance with an increase in the magnetic field. With the correctly selected distance from the linear accelerator this resonator will be able besides modulation of energy also substantial to decrease the energy spread of the injected beam, fulfilling the functions of so-called

debuncher.

Page 171.

This installation is at present created and launched in high-energy laboratory of J.I.N.R. In this work are given the basic results of calculating the effectiveness of injection into the synchrophasotron of J.I.N.R. during modulation of energy and contraction of the energy spread of the beam of injector, the short description of debuncher and the basic experimental results, obtained in the process of its adjustment and field testing on the synchrophasotron.

If energy of the particles, injected into the synchrophasotron, is changed in such a way that the instantaneous equilibrium orbit to which are injected the particles, has the fixed/recorded radius and it passes in immediate proximity of the internal inflector plate, then, obviously, injection into the synchrophasotron can be continued until the instantaneous equilibrium orbit of the particles, injected at first, as a result of turning in the building up magnetic field achieves internal chamber wall. In this case the particle injection will occur always with a small amplitude of radial betatron oscillations. In contrast to this, in the case of permanent energy of injection a radius of instantaneous equilibrium orbit, to which are injected the particles, in connection with an increase in the

magnetic field always decreases and occurs an increase in the
amplitudes of radial betatron oscillations. In this case the
injection continues until the instantaneous equilibrium orbit of the
injected particles achieves the middle of chamber/camera, but the
amplitude of radial betatron oscillations will stop to the equal
radial half-width of chamber/camera.

Thus, with the variable/alternating energy of injection it is
possible to twice increase the time of injection and, furthermore, to
carry out injection with small amplitudes of radial betatron
oscillations. This is made it possible, first of all, to twice
increase a quantity of injected into the chamber/camera of
synchrophasotron particles, in the second place, it is essential to
decrease the losses of particles in the initial period of synchrotron
acceleration.

The calculation of the effectiveness of injection during
modulation of energy of injector and contraction of its energy spread
with the aid of the resonator of debuncher was performed by the
method of numerical integration and it was reduced to the
maximization of the function

$$\tau_{эф} = \sigma_\beta\, \sigma_s\, \tau_u ,$$

where $\tau_{эф}$ - effectiveness of injection; σ_β - coefficient of the
capture of particles into the betatron acceleration mode; σ_s -

coefficient of capture into synchrotron acceleration mode; τ_u - duration of injection pulse. Calculation was performed for the existing injector with the energy 9.4 MeV and the current 1.2 mA. The necessary depth of modulation of energy of this injector m=3o/o, for which it is necessary to change the phase of voltage on accelerating resonator gap with -45° to $+45^\circ$ with the voltage on the clearance 200 kV (amplitude value). During the location of the resonator of debuncher at a distance of 3 m from the output of linear accelerator it will produce contraction of the energy spread of the injected particles from $\frac{\Delta W_m}{W_0} = 2,3\%$ to $\frac{\Delta W_m}{W_0} = 0,6\%$. For calculating the effectiveness of injection were undertaken the real distributions of the injected particles according to the angles γ, the section of cluster g and energies W whose maximum values for the existing injector are $\Delta\gamma_m = 6\cdot10^{-3}$ rad, $\Delta q_m = 3,5$ cm, $\frac{\Delta W_m}{W_0} = 0,6\%$. The basic results of calculation are given in the table.

Thus, during the use/application of debuncher with modulation of energy should be expected increase in the intensity of synchrophasotron from $Q_{yck} = 1,0\cdot10^{11}$ the particles in the cycle of acceleration to $Q_{yck} = 5,0\cdot10^{11}$ the particles, moreover 2 times due to an increase in the duration of injection τ_u from 300 to 625 μs and 2.5 times due to an increase in the general/common/total coefficient of capture σ from 0.12 to 0.3 ($\sigma = \sigma_\gamma \sigma_q$).

The block diagram of debuncher is given in Fig. 1. Basic node/unit is the resonator which creates the high-frequency electric field, which affects the beam of particles of the injector. High-frequency power enters resonator from the unit of HF oscillators which together with the preamplifier amplify HF power up to the value, necessary for the supply of resonator. The modulator of phase serves for modulation of the phase of entering the resonator of HF voltage relative to the phase of voltage in the resonator of linear accelerator (LU). For the tuning of initial phase is provided for mechanical phase inverter. The modulator of phase is controlled with the aid of the voltage, developed by the oscillator of control voltage. Pulse anode voltage for the unit of HF oscillators and preamplifier creates the pulse modulator, that encompasses the assembly of artificial line. For the tuning of the natural frequency of resonator is utilized the element/cell of steady tuning. Phase bridge serves for the comparison of the phases of signals from the resonator and the unit of HF oscillators. The synchronization of entire installation is accomplished/realized with the aid of the delay unit, by trigger pulse of the beginning of injection.

Режим [1] инжекции	$\frac{\Delta W_m}{W_0}$	$\tau_u \cdot$ [2] мксек	σ	$\tau_{эф}$, [2] мксек	$Q_{уск}$, част. [3] имп.
[4] $W_0 = 9,4$ Мэв, без дебанчера	$2,3 \cdot 10^{-2}$	300	0,12	36	$1,0 \cdot 10^{11}$
[5] $W_0 = 9,4$ Мэв, с дебанчером	$6,0 \cdot 10^{-3}$	300	0,21	63	$1,7 \cdot 10^{11}$
[6] $W_0 = 9,4$ Мэв, с дебанчером и модуляцией	$3 \cdot 10^{-2}$	625	0,3	191	$5,0 \cdot 10^{11}$

Key: (1). Mode/conditicns of injection. (2). μs. (3). part./pulse.
(4). MeV, without debuncher. (5). MeV, with debuncher. (6). MeV, with
debuncher and modulaticn.

Page 172.

The resonator of debuncher (Fig. 2) is a quarter-wave cut. of
coaxial line with the round cross-section. The length of accelerating
resonator gap $d = 5$ см was selected from the condition of obtaining
the factor of time of flight $G=0.9$ with the intensity/strength of
field 40 kV/cm. The quality of resonator $Q_0=12800$, shunt resistance
$R_\omega = 1200$ to kiloohm, self-resonant frequency is equal to the
frequency of the resonator of linear accelerator (143 MHz). For
obtaining on the slot cf resonator 200 kV it is necessary to feed to
it 50 kW.

Fig. 3 depicts the photograph of resonator within vacuum

envelope.

The modulator of phase 2 (in Fig.) is carried out in the form of ten-component artificial line. As the capacities/capacitances of line are utilized the semiconductor diodes whose capacity/capacitance is controlled by bias voltage, which comes from the oscillator of control voltage.

At present the debuncher is installed, fixed and is located in the stage of field testing on the synchrophasotron of J.I.N.R.
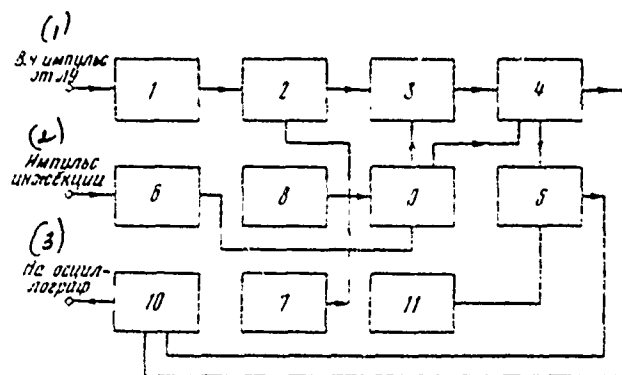
Fig. 1.
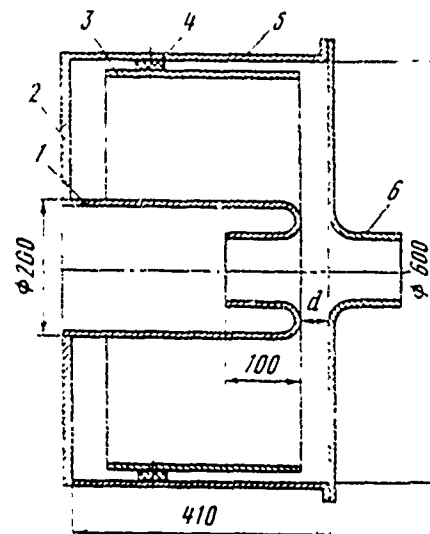
Fig. 2.

Fig. 1. Block diagram of debuncher. 1 - mechanical phase inverter, 2 - the modulator of phase; 3 - preliminary HF amplifier; 4 - unit of HF oscillators; 5 - resonator; 6 - delay unit; 7 - oscillator of control voltage; 8 - artificial line; 9 - pulse modulator; 10 - phase bridge; 11 - element/cell of tuning.

Key: (1). HF pulse from LU. (2). Impulse/momentum/pulse of injection. (3). To oscillograph.

Fig. 2. Schematic of resonator: 1 - center conductor; 2 - end-type disk; 3 - internal electrode for depression of high-frequency resonance discharge; 4 - insulators for attachment of electrode; 5 -

external conductor; 6 - screens for decreasing radiation/emission of HF power from resonator.

Fig. 3. Resonator within vacuum envelope.

REFERENCES

1. A. B. Kuznetsov. Preprint. J.I.N.R. P-2266, Dubna, 1965.
2. N. Myers and S.Abraham. IEEE Transactions on
   Nuclear Science, June, 1967,p.666-669.

1. 2. Powerful/thick peak transformer.

O. S. Bogdanov, Yu. P. Vakhrushin, V. G. Zhitenev, N. I. Kolesov, A. V. Orlov.

(Scientific research institute of the electrophysical equipment im. D. V. Efremov).

For the electron gun of the linear induction acceler... .s (see for example, [1]) is required the source of the high-voltage power supply with the voltage 300-500 kV, the current of load 250-300 A for the duration of pulses $\tau_{0.95}=0.5$ μs and at the frequency of messages to 50 s^{-1}. Possible decision is the use of a modulator, analogous to the main modulator of the system of the pulse supply LIU [2] in combination with the powerful/thick peak transformer, which consists of the series/row of the annular magnetic circuits each of which is covered by the primary windings, connected in parallel; secondary windings are connected in series one way or another [3-5].

Page 173.

We tested the mock-up of the version of the peak transformer which is intended to utilize in LIU-30/250.

The schematic diagram of peak transformer is given in Fig. 1. It consists of the circular magnetic circuits whose quantity is selected on the basis of the necessary voltage on secondary winding. Each magnetic circuit is covered by the turns which are connected in parallel and they form the primary winding of transformer. Secondary winding covers all magnetic circuits and voltage on it it is determined by the equality

$$U_2 = N U_1,$$

where U_1 - voltage on the primary winding; N - number of magnetic circuits; U_2 - voltage on secondary winding.

In contrast to conventional diagrams [6] in this diagram it is possible to realize the construction/design of transformer, during which is accomplished/realized a good transmission of the shape of pulse and at the same time easily are solved questions of insulation/isolation of secondary winding, application of voltage on the preheater of electron gun and cooling of magnetic circuits.

For the purpose of the unification of the assemblies of accelerator for the peak transformer it is expedient to utilize inductors of the accelerating system. Fig. 2 shows the construction/design of the peak transformer in which are used the

inductors of the accelerating system LIU-30/250.

Cores are performed from the strip/film of alloy 50NP with a thickness of 10 μ with insulation/isolation between the turns from magnesium oxide, applied by the method of cathophoresis. Cores are included in the electrical insulating frameworks/bodies of glass-mica which insulate cores from the primary winding and they at the same time protect them from the mecnanical effects. Cores with the framework/body are secured in the water-cooled housing from the aluminum alloy.

Inductors are collected into the column with the aid of the stud bolts, which are simultaneously the exterior of secondary winding. Between the inductors are placed packing layers.

Along the axis of assembled thus column passes the tube which on the one hand is secured on the flange, and with another on the insulator. Thus, tube together with the flange and the stud bolts forms secondary winding. In order to ensure a sufficient electro-insulation between the central tube and the housings of inductors, the internal cavity of column is filled with transformer oil. For supplementary insulation/isolation between the inductors it is not required, since the busbars/tires of adjacent inductors are shifted along the azimuth.

7 2 ²
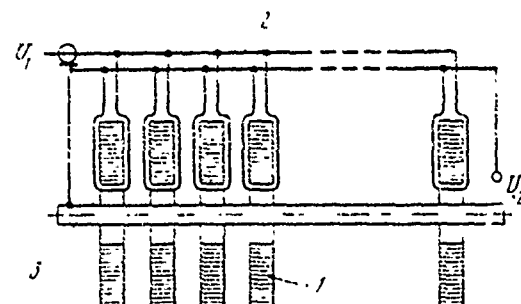
Fig. 1. Schematic diagram of peak transformer. 1 - circular magnetic circuits; 2 - turns of primary winding; 3 - secondary winding of transformer.
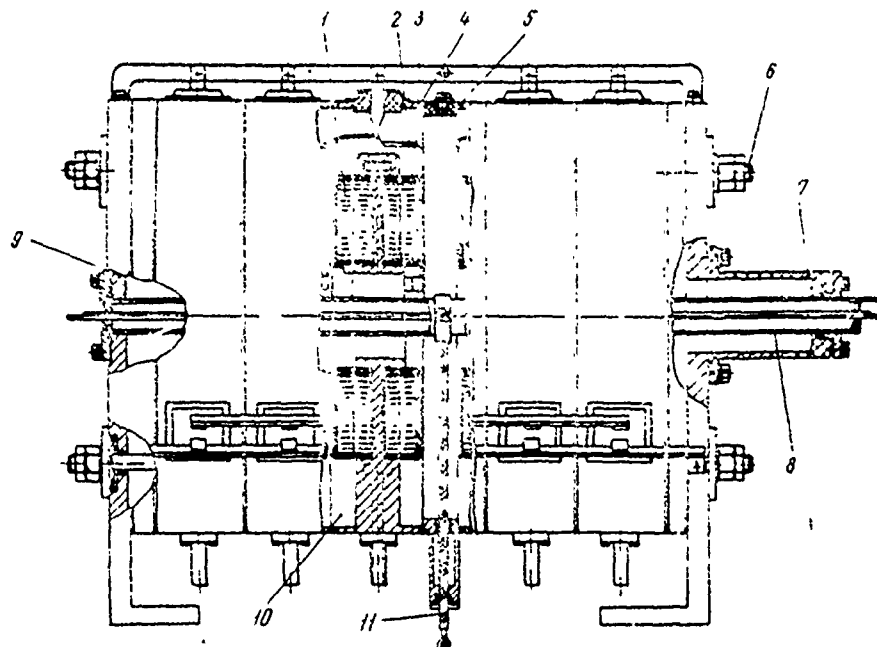
Fig. 2. Construction/design of peak transformer. 1 - circular cores; 2 - electrical insulating frameworks/bodies of cores; 3 - primary winding; 4 - housing, water-cooled; 5 - packing layers; 6 - stud bolt; 7 - insulator; 8 - tube; 9 - flange; 10 - volume, filled with

transformer oil; 11 - intermediate conclusion/output.

Page 174.

The supply leads of the preheater of gun are placed within the central tube, which makes it possible to forego isolation transformer. During the use of a transformer for the supply of three-electrode gun from the central tube is done the diversion/tap, voltage on which will be proportional to a number of included inductors.

For the mock-up of peak transformer were utilized eight inductors, carried out with the use of epoxy trowelling compound [2]. Of the photographs of mock-up it is given in Fig. 3. The schematic diagram of the supply of transformer and change in its parameters is given in Fig. 4. In the modulator is utilized a thyratron of the type TGI-1-2500/50 and a heterogeneous forming line on the capacitors/condensers PKGI-50-25000. Modulator makes it possible to obtain voltage to 23 kV and commuted current to 15 kA. Voltage from the modulator is supplied with the aid of the cables of the type RK-50-11-13 to the primary winding of transformer. During the first stage of testing the load was imitated ·y resistances of the type TVO-60-51. The selected rating of resistances corresponded to beam current 400 A. In the second stage to the transformer was connected

the three-electrode electron gun from cathode of which drew current
to 700 A. In this case to the grid of gun was supplied the voltage
from the diversion/tap of transformer, equal to 5/8 from the total
voltage. The supplies of the preheater of gun it was
accomplished/realized from the filament transformer with the aid of
the conductor, that passed within the central tube of transformer.
Demagnetizing cores was accomplished/realized by alternating current
with voltage $u_p = 12$ V and current ≈ 160 A with the aid of the special
system of demagnetizing.

In the measurements was utilized two-beam oscillograph of the
type DSO-1. While conducting of tests were measured the voltages on
the primary winding of transformer with the aid of the divider, the
current through the thyratron with the aid of the Rogowski loop, the
voltage on secondary winding with the aid of the divider and the
current of gun with the aid of the measuring system of the secondary
current of transformer and Rogowski loop.

Fig. 5a gives the oscillograms of the pulses of the voltage of
primary and secondary windings of peak transformer. Upper oscillogram
is the pulse of voltage on the inductor (primary winding), lower -
the voltage pulse in secondary winding of transformer. Oscillograms
were removed/taken in the following parameters: charging voltage of
forming line $u_{\phi\Lambda} \approx 45$ kV, $U_1 = 19$ kV, $U_2 = 190$ kV. Sweep length 1.2 µs.

Duration of gauging markers 0.2 μs. Equivalent load corresponded to beam current 400 A.

DOC = 30069313   PAGE
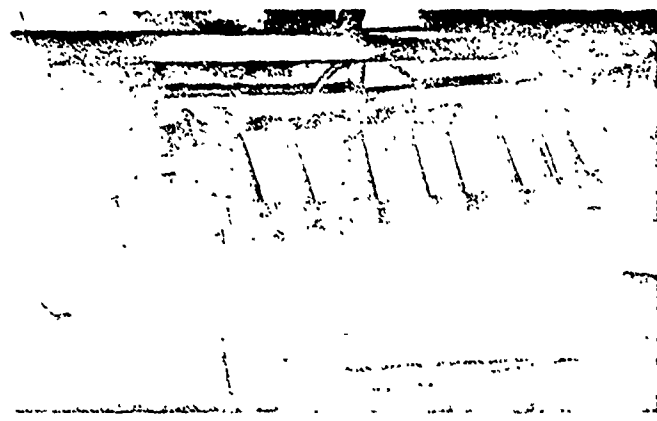
Fig. 3. Mock-up of peak transformer.
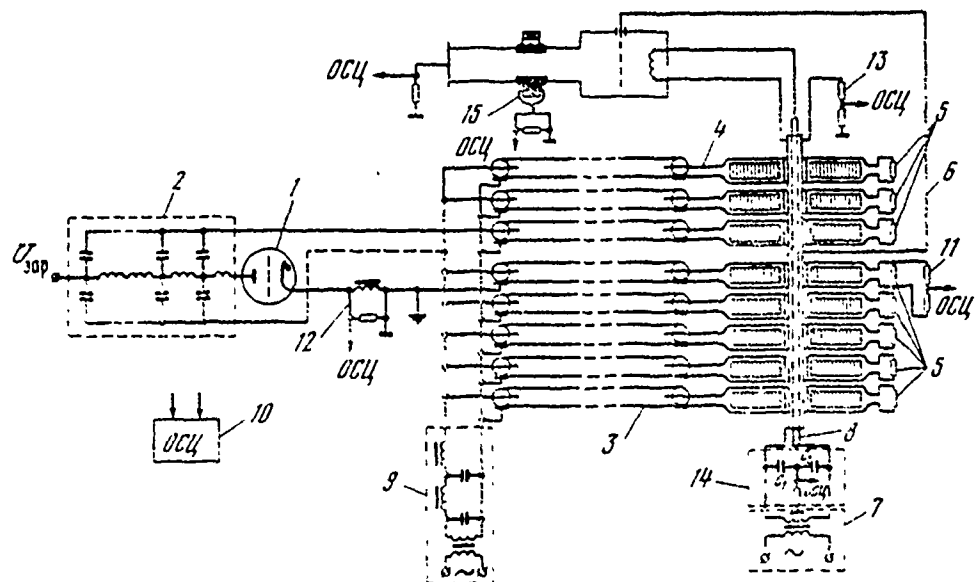
Fig. 4. Schematic diagram of supply of transformer: 1 - thyratron; 2 - heterogeneous forming line; 3 - transmitting cables; 4 - primary winding; 5 - load resistances; 6 - intermediate conclusion/output; 7 - filament transformer; 8 - conductor; 9 - system of demagnetizing; 10 - monitoring oscillograph; 11 - divider (resistances TVO-20,

coefficient of division 56); 12 - Rogowski loop (it is carried out on

ferrite, sensitivity of 0.16 V/A); 13 - divider (resistances TVO-10,

coefficient of division 343); 14 - measuring system of secondary

current of transformer; (chain/network RC, capacity/capacitance

$C_1-C_2=8$ μF, R=0.5 ohm); 15 - Rogowski loop (it is carried out on the

ferrite, the sensitivity of 0.26 V/A).

Page 175.

The analysis of oscillograms showed that the durations of the

flat/plane part of the impulses/momenta/pulses of primary and

secondary windings coincide and comprise at the level $0.95\tau_{0.5}=540$

ns. The analysis of leading impulse fronts also showed the good

coincidence: $\tau_\phi=200$ ns, in both impulses/momenta/pulses.

Fig. 5b gives the oscillograms of current pulses through the

thyratron (upper oscillogram) and the voltages on the primary

winding. Oscillograms were removed/taken in the following parameters:

$\bar{I}_{max} = 7.16$ kA, $U_1=19$ kV, $U_{c} = 5$ kV, sweep length 1.2 μs, the duration

of gauging markers 50 ns.

The prolonged work of transformer showed the high reliability of

oil insulation of secondary winding. Breakdowns within the

transformer were not observed. It was established/installed, that

filling of the cavity between the inductors by transformer oil does
not make the shape worse of the pulse of voltage on the primary
winding of transformer. In both cases the duration of pulse edge was
200 ns.

The results of testing the mock-up make it possible to recommend
transformer for the high-voltage supply of power of electron gun
LIU-30/250. It is necessary to note that it is desirable to reduce
the duration of the front/leading and trailing edges of pulse of
voltage since beam electrons whose energy differs from nominal, are
lost in the process of acceleration and only in vain load accelerator
tube Since the power of beam is enormous, too the great losses of
electrons can lead to the damage of accelerator tube. One of the
possible methods of shortening the duration of fronts is introduction
to the secondary circuit of the controlled key/wrench, for example,
of electron tube. In this case it is possible to expect that the
duration of fronts will be ≈ 30 ns.

In the preparation of mock-up for the testing and conducting of
measurements besides the authors participated V. I. Kornev and A. I.
Pavlov.
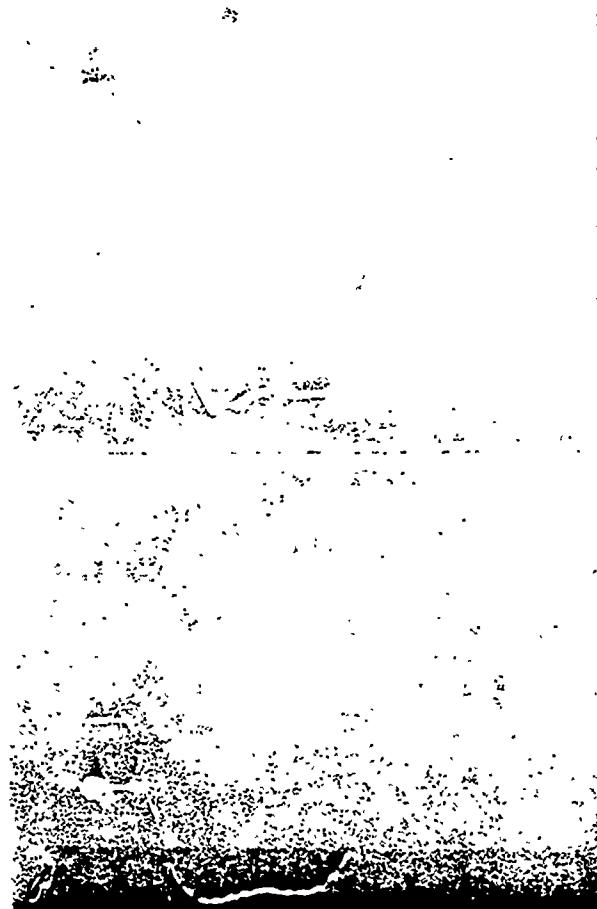
Fig. 5a. Oscillograms of the voltage pulses on the primary (upper curve) and on secondary windings of peak transformer (a), current through the thyratron (upper curve) and the voltages on the primary winding of peak transformer (b).

730

DOC = 80069313   PAGE 54

REFERENCES

1. V. D. Ananyev, et al. Pulse Reactor with Injector IBR-2, Preprint J.I.N.R. 13-4392, 1969.

2. A. I. Inatskiy, O. C. Bogdanov, et al. Atomic Energy, 1966, Vol 21, Issue 6, p. 439.

3. Christofilos, et al. Trudy Transactions of the International Conference on Accelerators of High Energies, Dubna, 1963, Moscow, Atomizdat, 1964, p.1073.

4. Yu. P. Vakhrushin, I. M. Matora, V. P. Sartsev, A. G. Sorokin, V. A. Suslov. Electron Gun. Author's certificate No. 256903, Bulletin of Inventions and Trade Marks, 1969, No. 35.

5. P. V. Bukayev, A. I. Gryzlov. Pulse transformer, Author's certificate No. 233035, Bulletin of Inventions and Trade Marks 1969, No. 2

6. A. A. Bernshteyn, N. K. Rudyachenko. Pulse Radio Transmission Devices. Kiev, Gosidat of Technical Literature of the Uk.SSR, 1963.

Page 176.

143. COMBINATION 2-GAP BUNCHER WITH DRIFT TUBE FOR LINEAR ION ACCELERATORS.

Yu. D. Beznogikh.

(Joint Institute for Nuclear Research).

For increasing the effectiveness in the use of a beam of the preinjector between the linear accelerator and preinjector is established/installed high-frequency buncher - the single-gap resonator of klystron the function of density distribution of charge according to the cross section of the grouped beam has vividly expressed nonuniformity (it is maximum on the axis/axle of bundle and drops to zero when $r = r_0$, where r_0 - radius of beam), particle-velocity distribution in the section of the drift between buncher and entrance of linear accelerator with the high currents of beam ambiguously connected with the law of the phasing forces, prescribed/assigned in the clearance of buncher.

As a result appears certain uncertainty/indeterminancy in the selection of the position of buncher and amplitude of the phasing voltage on the clearance of buncher, which consists in the fact that the parameters indicated are dissimilar for the particles, arranged/located on different radii over the beam section. The uncertainty/indeterminancy indicated could be removed under the condition for the maximum approximation/approach of buncher to input part of the resonator of linear accelerator, but in this case for obtaining the optimum phasing of the grouped particles to the clearance of buncher it is necessary to feed so large a voltage, that the part of the particles can exceed the limits of the separatrix of linear accelerator due to the large spread along the impulses/momenta/pulses of the bunched particles.

The grouping of high-current beams showed a noticeable reduction in the effectiveness of single-gap buncher with the currents of grouping on the order of 300-400 mA [1, 2].

Works indicated give the experimental results which show that with the work with the buncher the current n the output of linear accelerator grows/rises in all by 30-35o/o. With the high currents of the grouped beam it is possible to expect an even larger reduction in the effectiveness in the work of klystron buncher.

Fig. 1 schematically depicts the double-gap buncher with the
drift tube and the diagram in coordinates $\varepsilon, \omega t$, which elucidates the
work of buncher (ε - electric intensity on the axis/axle of buncher).

Synchronous particle passes the electrical center of the first
clearance in phase $\varphi_{s,1} = -\frac{\pi}{2}$. Double-gap of the type. The effectiveness
of such buncher which is arranged/located usually at a distance on
the order of 1 m from the inlet of linear accelerator, depends,
generally speaking, on the intensity of the grouped beam. Since the
system of buncher is calculated in such a way that the second
clearance of buncher the synchronous particle passes in phase
$\varphi_{s,2} = +\frac{\pi}{2}$, after passing path from the electrical center of the first
clearance to the electrical center of the second clearance, equal to
$L = k\beta_{s\rho}\lambda$. Value k can take values of 1.5; 2.5, etc. For example, for
$\beta_{s\rho} = 0,03483$ ($W_{s\rho} = 570$ the keV) $\lambda = 2.08$ m and k=1.5 we obtain L=10.8 cm.

The behavior of the nonsynchronous particles (i.e., the
particles whose phase with the passage of the first clearance of
buncher it is different from $-\pi/2$) is shown in of the curves of Fig.
2 for one of the versions of 2-gap buncher.

Fig. 2 shows the curves of spread the impulses/momenta/pulses of
the grouped particles in coordinates $\frac{\Delta\rho}{\rho_{s\rho}}\%, \varphi_2$ where φ_2 - phase of
particle in the second clearance of buncher.

Curve $\Delta p_1 = f_1(\phi_2)$ characterizes scatter along the particle momenta after the passage of the first clearance of buncher in the function of their position in the second clearance of buncher.

Curve $\Delta p_2 = f_2(\phi_2)$ characterizes scatter along the impulses/momenta/pulses of part after the passage of the second clearance of buncher.

In the curves is not shown the second region of phases, which in effect is mirror image relative to the origin of coordinates.

In of the curves of Fig. 2 in the degrees are shown the phases of particles with the passage by them the electrical center of the first clearance of buncher.
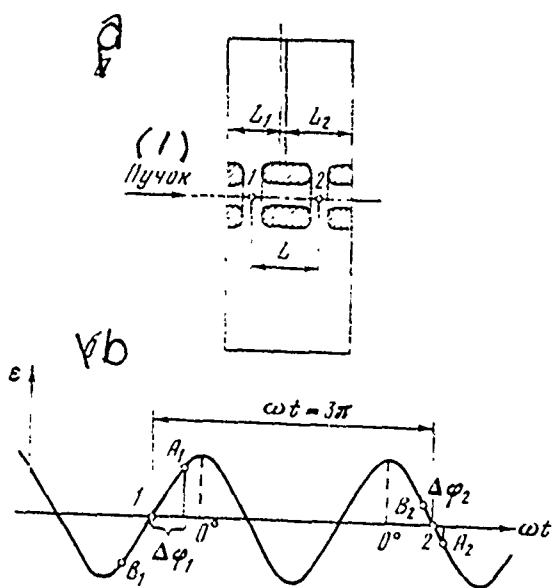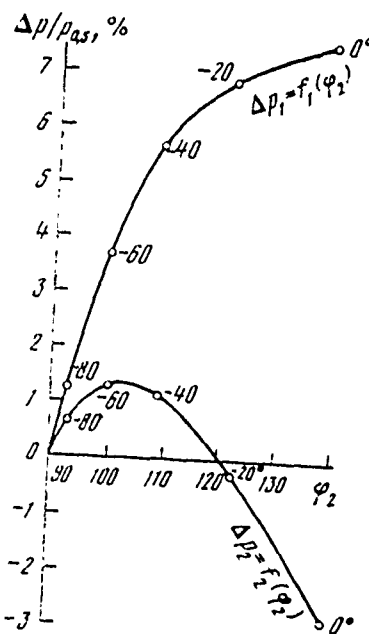
Fig. 1.   Fig. 2.

Fig. 1. Schematic diagram of 2-gap buncher (a) and diagram $\varepsilon(\omega t)$ (б)

Key: (1). Beam.

Fig. 2. Curves of scatter along impulses/momenta/pulses of grouped particles afterward of first and second clearances of buncher (ε_0 = 20 kV/cm; L_1=8.4 cm; L_2=11 cm; L=10.8 cm; T_1=0.5; T_2=0.7; $\bar{\beta}_{sp}$ =0.0348).

Page 177.

Thus, the particles whose phase with the passage of the first clearance of buncher is not equal to $\frac{\pi}{2}$, obtain in the first clearance a large supplementary energy gain (positive or negative), in consequence of which the more phasing forces confine their phase to the synchronous phase in the second clearance of buncher, whereas with the second the clearance of buncher produces the specific equalization of energies of all grouped particles to the energy of synchronous particle, leaving their phase of constant/invariable in the plane of the electrical center of the second clearance of buncher.

Consequently, a 2-gap buncher with the drift tube makes it possible to substantially decrease the space of the free drift of the grouped particles between the buncher and the linear ion accelerator. (This space it is determined by the structural/design possibilities of the approach of buncher with the input part of the resonator LU). This raises the effectiveness of grouping with the high currents of the grouped beam, since the Coulomb forces, which block the phasing of particles, act at a comparatively small distance, and the phasing forces, which appear in the clearances of a 2-gap buncher, are substantially more than the phasing forces in the clearance of klystron buncher.

But a 2-gap buncher with the drift tube as single-gap klystron

buncher, possesses that deficiency/lack, that
structurally/constructurally it is carried out as separate
device/equipment and therefore for its work it requires the separate
supply of power, separate phasing device/equipment and separate
introduction/input of high-frequency power into the resonance volume
of buncher.

If we a 2-gap buncher structurally/constructurally fulfill as
unit with the resonator of the linear accelerator whose accelerating
structure is a usual structure of the type of Alvarez-Blyuetta, then
it is possible to arriv at the diagram of the combination buncher,
depicted in Fig. 3.

In Fig. 3 section 1 is a 2-gap buncher with the drift tube, and
section II is the accelerating structure of proton linear
accelerator. Thus, the accelerating structure of linear accelerator
is the natural continuation of 2-gap buncher, since the buncher and
the accelerating structure of linear accelerator are placed in one
resonator. In this case, naturally, there is no need for in the
separate supply and the phasing cf buncher, since this is performed
automatically during the excitation of resonator on the wave of the
type E_{010}.

On the synchrophasotron of the J.I.N.R. at present is realized

the method of accelerating of deuterons and α-particles [3, 4]. As
the injector is utilized the proton linear accelerator with grid
focusing which upon the acceleration of deuterons and α-particles is
transferred/translated into the mode/conditions of the dual
multiplicity of the drift of the accelerated particles, moreover
voltage on accelerator tube of preinjector is reduced upon the
acceleration of deuterons 2 times, i.e., to 285 keV. With this
voltage sharply deteriorate the parameters of the injected beam, as a
result deuteron output current of linear accelerator also descends.
With the voltage 285 kV on accelerator tube of preinjector at the
output of linear accelerator was obtained deuteron current on the
order of 200 μA in the impulse/momentum/pulse. In connection with the
fact that in this case there is specific possibility to raise voltage
on accelerator tube of preinjector, were realized two versions of the
combined 2-gap buncher.

     Version I.

     Injection into the third clearance of the accelerating
structure. In this case the first two drift tubes were taken/removed
and replaced by new ones calculated so that two first clearances
would fulfill the functions of a 2-gap buncher. The required voltage
of injection increased to 400 kV. In this case the injected input
current in the aperture of LU increased two times, and the

accelerated output current of LU increased 4 times (800 μA). Thus, the expected effect of an increase of the accelerated current 2 times from the action of buncher was confirmed experimentally.

Version II.

Injection into the fifth clearance of the accelerating structure. The first four tubes of the accelerating structure were taken/removed and replaced new so that the third and fourth clearances would fulfill the function of buncher, and for the first two clearances the factor or transit time was equal to zero. Therefore the first two clearances of particle passed without the change their wave energy, in the third and fourth clearances they were grouped, and resonance acceleration began from the fifth clearance. The required voltage of injection in this case increased to 525 kV, input current in the aperture of LU - 2.5-3 times, and the accelerated output current of LU 6 times (1200 μA).
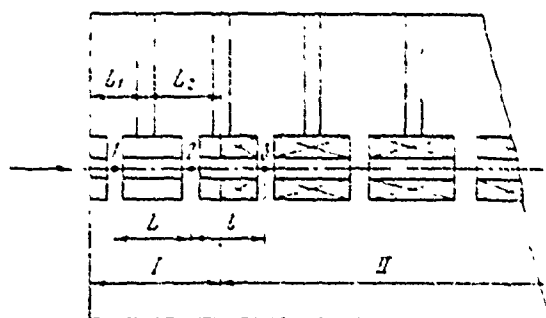
Fig. 3. Combination 2-gap buncher.

REFERENCES.

1. Л.М.Капчинский, В.К.Плотников. Линейный ускоритель И-2. Характеристики продольного и поперечного движения. ПТЭ, 1967, № 5.

2. В.А.Батаиин и др. Линейный ускоритель И-2. подготовка форинжектора к пуску и основные характеристики пучка на выходе форинжектора. ПТЭ, 1967, № 5.

3. Ю.Д.Безногих, Л.П.Зиновьев и др. Об одном режиме ускорения d — и α-частиц в синхрофазотроне ОИЯИ до импульсов 11 и 22 Гэв/с соответственно. Препринт ОИЯИ Р9—4214, Дубна, 1968.

4. Ю.Д.Безногих, Л.П.Зиновьев и др. Режим ускорения d — и α-частиц в синхрофазотроне ОИЯИ до импульсов 11 и 22 Гэв/с. ПТЭ, 1969, № 4.

Page 178.

144. MULTICHANNEL SYSTEM OF CHARGING AND STABILIZATION OF POWERFUL PULSE GENERATORS.

A. P. Baydak, I. Ye. Zhul', A. P. Panov, G. I. Silvestrov.

(Institute of nuclear physics of SO AS USSR).

The task of the charge of storage battery C_H and voltage regulation on it is not new and successfully solved by series/row by the author [1], but for the case of supply from the individual single-phase full-wave rectifier and at the maximum repetition frequency of cycles the "charge-discharge" of the unit of the hertz.

During the development of the power-supply system of the elements/cells of electron-optical channel on the complex VEPP-3 it was decided to supply without pulse generators from one general/common/total powerful power supply. For this purpose was developed multichannel system of charge and voltage regulation on the storage capacities/capacitances of all pulse generators. In this case essential attention was given the possibility of the work of system from the source of permanent high voltage with any degree of

pulsations.

Technical specifications of system.

1. Number of supplied oscillators (channels) $n=16$.

2. Value of voltage on storage batteries (independently for each capacity/capacitance) any in interval $u_{c_H} = (0,5 \div 10)$ kV.

3. Maximum repetition frequency of cycles charge-discharge C_H $F_u = 10$ Hz.

4. Values of storage capacities/capacitances in oscillators $C_H = (2 \div 1000)$ μF.

5. Maximum energy content of each oscillator $W_{max} = 30$ kJ with general/common/total energy content of all oscillators $W_{\Sigma} = 100$ of kJ.

6. Stability of maintenance of voltage $\Delta u_{c_H} = 5 \cdot 10^{-4} u_{c_H}$.

7. Supply of power — rectifier on transformer $P = 400$ of kVA $E_u = 10$ kV on diagram of Larionov on diodes VKDL-150 - 9 kl.

Block diagram of channel.

The operating principle can be examined on the block diagram Fig. 1. From the common source into the rectified voltage through charging resistor and high-voltage part of diagram C, C_m it charges storage capacity/capacitance $c_н$.

Voltage $u_{вх}$, proportional $u_{c_н}$, removed from the lower part of the divider UD, enters comparator - comparator 2 in the electronic control unit ЭБ, where it is compared with reference voltage u_{on} from the special source.

By the impulse/momentum/pulse from the external synchronizing unit, which comes the trigger through the shaper and the thyristor amplifier is opened/disclosed the passage device/equipment, through which occurs rapid charge $C_н$. At the moment of the comparison of the voltage of divider with the supporting/reference the comparator puts out pulse train on amplifier 3 (see Fig. 1). By the first impulse/momentum/pulse is inverted trigger and impulse/momentum/pulse through the thyristor amplifier it starts the quenching circuit of passage device/equipment. Quenching circuit instantly ceases rapid charge $C_н$.
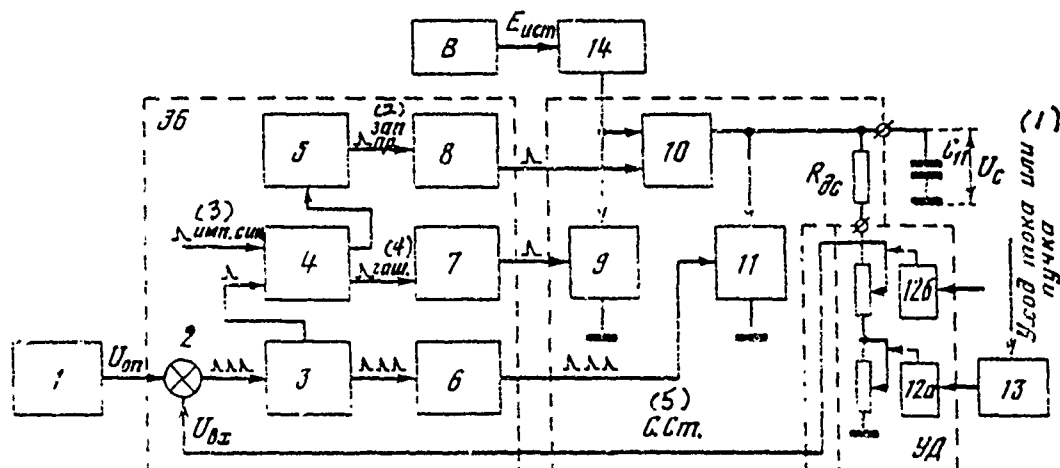
Fig. 1. Block diagram of channel. 1 - reference-voltage source; EB - electronic component; 2 - comparator; 3 - amplifier; 4 - trigger; 5 - shaper; 6-8 - thyristor output amplifiers; $C \cdot C_m$ - is high-voltage the strut of stabilization; 9 - quenching circuit; 10 - passage device/equipment; 11 - contour/outline of the discharge/break; UD - controlled divider; 12a, 12b - electromechanical devices/equipment of the rotation of potentiometer and switch; 13 - device/equipment of parametric stabilization; 14 - charge water resistance; V - rectifier.

Key: (1). Departure/attendance of current or beam.

Page 179.

Pulse train from comparator comes through the amplifier the
starting/launching of the device/equipment of discharge/break, which
accomplishes/realizes voltage regulation u_{c_H} by the method of the
portion discharge/break of excessive charge [1].

High-voltage part of the system.

The schematic diagram of the high-voltage part of the channel of
stabilization is shown in Fig. 2. the rapid charge of
capacity/capacitance is conducted through the passage
device/equipment - a thyratron of the type TB1-6/15 (L_1), which by
trigger pulse, which enters from thyristor amplifier EB through the
joint R2.

The principle of extinguishing is characterized by simplicity
and reliability in operation; it permits implemention of
extinguishing L_1 with any value $\Delta u_A = E_u - u_{c_H}$ on the anode of passage
thyratron.

At the moment of time t_1 (see Fig. 3) through joint R_1 enters
the trigger pulse of quenching circuit, which ignites at
moment/torque t_2 lamp L_2. Since the voltage on capacitor C_1 is equal
to zero, point A (anode L_1) proves to be under the potential, which
falls in the gap/interval the anode-catnode L_2 which for the case of

thyratron TR1-6/15 is ~30 in. Thus, at the moment of time t_2 point V (cathode L_1) proves to be actually under voltage u_{c_M}, applied in the opposite direction. Logically, the current through L_1 ceases (moment/torque t_2, Fig. 4). The time of extinguishing $t_{zaw} = t_2 - t_1 \simeq 200$ ns is determined in essence by the time of ignition L_2.

At moment/torque t_3 the anode L_1 proves to be under the potential of cathode. Further the potential of the anode L_1 becomes more than the potential of cathode and extinguishing condition ceases to be performed. Consequently, for the reliable extinguishing of passage thyratron it is necessary that the time $\Delta t = t_3 - t_2$ would be more than the deionization time t_{geuw}, which for TR1-6/15 depending on taking place through it at the moment of extinguishing current is 500-100 ms.

Thus, time t, determined from the condition

$$u_{c_1} = \mathcal{E}_u \left[1 - e^{t/\tau_1} \right] = u_{c_M}, \qquad (1)$$

must be greater than t_{geuoh}:

$$\frac{t}{\tau_1} = \ln \frac{u_{c_H}}{E_u} , \qquad (2)$$

$$t = \tau_1 \ln \frac{u_{c_H}}{E_u} > t_{geuoh} , \qquad (3)$$

where $\tau_1 = 3R_3C_1$.

From (3) it is evident that the value

t is directly connected with value C_1. For the reliability we take

$t = 2t_{geuoh}$; then

$$3R_3C_1 \ln \frac{u_{c_H}}{E_u} = 2t_{geuoh} \qquad (4)$$

or

$$C_1 = \frac{2t_{geuoh}}{3R_3 \ln \frac{u_{c_H}}{E_u}} . \qquad (5)$$
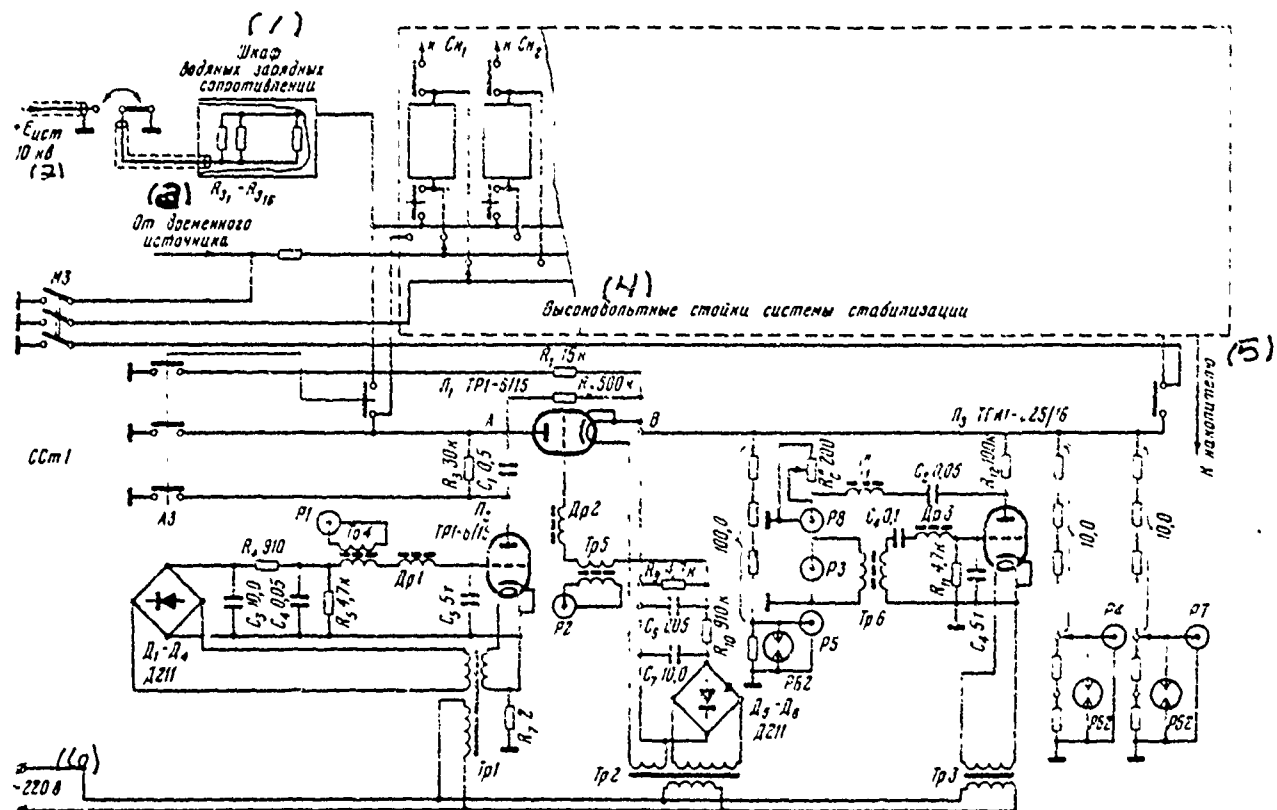
Fig. 2. Schematic diagram multichannel system of charge and stabilization of powerful/thick pulse generators. R1 - inlet "starting/launching of quenching circuit"; R2 - inlet "starting/launching" of passage; R8 - inlet "discharge/break".

Key; (1). Cabinet of water charge resistor. (2). kV. (3). From temporary source. (4). High-voltage rack of stabilization system. (5). To storage. (6).v.

Page 180.

In order to ensure efficiency of diagram in entire range of regulating u_{c_H} relatively E_u, in condition (5) it is necessary to

substitute $u_{c_H\,min}$ and $t_{geuoH\,max}$. Finally

$$C_1 = \frac{2t_{geuoH.\,max}}{3R_3\,\ell n\,\dfrac{u_{c_H\,min}}{E_u}}.$$ (6)

Shunting of C_1 by resistor R_3 is conducted for the discharge between the cycles of charge. Value R_3 we select from the conditions so that C_1 would manage to be discharged between the cycles and at the same time current $J = \dfrac{E_u}{R_3}$ was less than the current of combustion L_2 (on the order of 50 Ω). Value R_3, or more precisely time

$$t' \simeq 3\tau_2 = 3R_3 C_1$$ (7)

determine the maximum operating speed of the entire high-voltage circuit as a whole:

$$F_{u.\,max} = \frac{1}{t_{3ap} + t'}.$$ (8)

In the presence of recuperation the diagram works with $F_u = 25$ Hz to accumulator/storage $C_H = 150$ μF. But on sufficiently great capacities C_H and levels u_{c_H}, considerably less for prescribed/assigned frequency E_u, can cease to be satisfied the F_u condition (8). Then it is necessary to replace R_3 with chain/network from the necessary resistance and key/wrench (thyratron). Thyratron L_2 goes out when $u_{c_1} \simeq E_u$. After this it is possible to open/disclose key/wrench. Now value R_3 will be limited only by the permissible current through the key/wrench.

Schematic diagram of electronic component.

The full/total/complete schematic diagram of electronic

component is given in Fig. 5. Besides the basic nodes/units, isolated
on the block diagram, it contains the series/row of ancillary
circuits (protection circuit T_4, T_5, check, etc.). One should
somewhat stop in the diagram of comparison and its functions. As the
element/cell of comparison is used a diode-regenerative comparator to
T_1 [2] with the threshold of functioning $u_{n.c} = 5 \cdot 10^{-3}$ in $u_{n.c}$ it changes
to $2 \cdot 10^{-3}$ V in the range of temperatures of 10-60°C. As is known,
work θ-R of comparator is based on the blocking process in the
presence $\Delta u_{\delta x} = u_{\delta x} - u_{0n} \geqslant u_{n.c}$. After comparison the comparator puts
out the sequence of impulses/momenta/pulses as function from value
$\Delta u_{\delta x}$ in the range of frequencies from the unit of the hertz to
certain $F_{u.max}$ with that determined $\Delta u_{\delta x} \gg u_{n.c}$. Latter/last property
made it possible to utilize a comparator as the assigning pulse
generator for the starting/launching of the key/wrench (L_3) of the
contour/outline of discharge/break.

Dependence of $F_k = f(\Delta u_{\delta x})$ and wide frequency band $F_k = (1 \div 1000)$ Hz
made it possible simply to carry out stabilization u_{c_H} in entire
range E_u.

Reference-voltage source.

Relation $\dfrac{\Delta u_{c_H}}{u_{c_H}}$ is equivalent to relation $\dfrac{u_{n.c}}{u_{0n}}$. On the basis of
permissible instability $\dfrac{\Delta u_{c_H}}{u_{c_H}} = 5 \cdot 10^{-4}$, we find

$$u_{on} \geqslant \frac{u_{n.c}}{5 \cdot 10^{-4}} = \frac{5 \cdot 10^{-3}}{5 \cdot 10^{-4}} = 10 V.$$

Taking into account the series/row of the destabilizing factors, accepted $u_{on} = 100$ V. Reference-voltage source is carried out in the form of two-stage parametric stabilizer with the output stage on 12 stabilitron tubes D818Ye.

The high-voltage part multichannel stabilization system is structurally/constructurally carried out in the form of the separate interchangeable struts. The supply of accumulators/storage from the common source made it possible to combine the inputs of all charging resistors, and use as the active element/cell of usual industrial water ($\rho = 3$ kΩ/cm^3) made possible to replace the set of bulky struts with compact cabinet. Structurally, separate resistance is made in the form of beaker from fiberglass. Contact is accomplished/realized through the metallic flanges. Resistance by the method of commutations easily is changed in the range from R_0 to $4R_0$ through the unit, and by the method of the introduction of inserts/bushings to beaker into dozens of times. The continuous current of water makes it possible to scatter the order 50 kW of active power on the separate resistance.
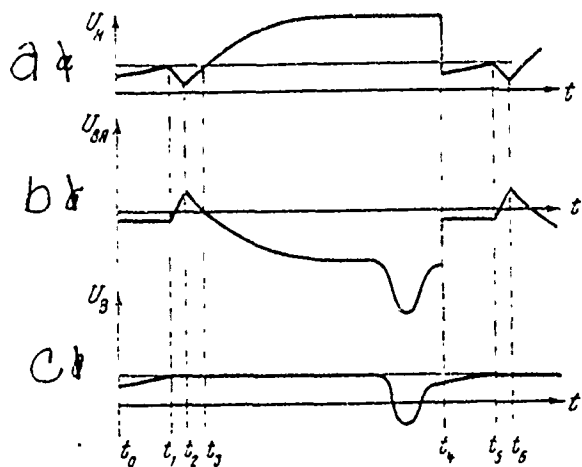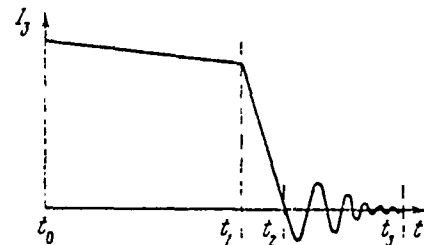
Fig. 3. Time graphs of electrode voltages of passage thyratron L_1: a) voltage of anode; b) voltage cathode-anode; c) voltage of cathode.

Fig. 4. Time graph of charging rate.

Page 181.

Although during operation all components/links of system are connected together, their functions are clearly demarcated, which is especially important with the large multichanneled effect.

The tests of stabilizer showed that in the static behavior the

instability of voltage on capacity/capacitance $\frac{\Delta u_{c_H}}{u_{c_H}} = 5 \cdot 10^{-5}$ in 12 hours. The drift of voltage within this time comprised $-5 \cdot 10^{-4}$. During the cyclic discharge of capacity/capacitance $\frac{\Delta u_{c_H}}{u_{c_H}} = 5 \cdot 10^{-4}$. Time of the output of system to the mode/conditions $\simeq 1$ hours.
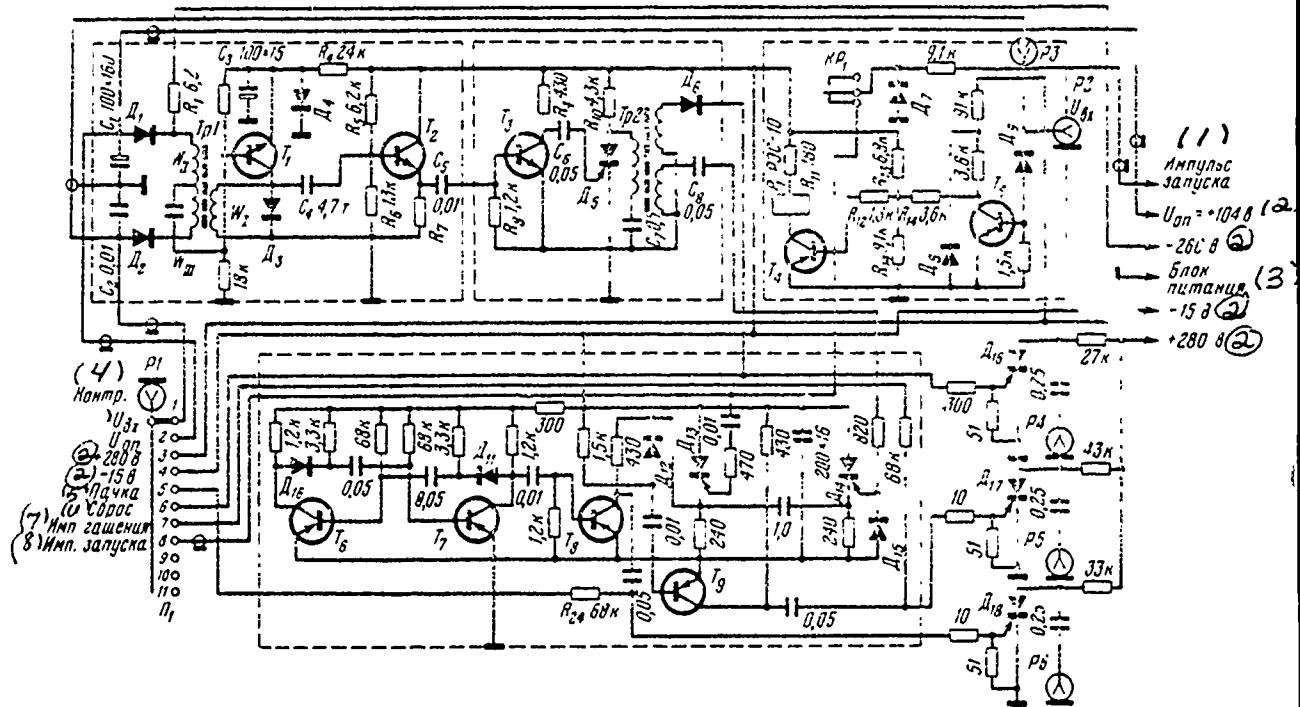
Fig. 5. The schematic diagram of electronic control unit R4 - output "discharge/break"; R5 - output "extinguishing"; R6 - output the "starting/launching" of passage.

Key: (1). Trigger pulse. (2). V. (3). Power supply unit. (4). Cont. (5). Packet. (6). Discharge/break. (7). Pulse extinguishing. (8). Pulse starting/launching.

Refrences.

1. V. F. Romanovskiy and et. al. "Charging Device". Author's Certificate No. 251078.
Byull. izobret. i tov. znakov [Bulletin of Inventions and Trademarks]. 1969, No. 27.

2. A. P. Stakhov. Study of a Balance Diode - Regenerative Voltage Comparator with Transformer Feedback. Voprosy radio elektroniki [Questions of Radio Electronics]. 1965, vyp. 6, seriya VII, str. 82.

Page 182.

Session XI.

Targets, separation and transportation of beams. Input and output.

145. OUTPUT OF THE PROTON BEAM OF THE SYNCHROCYCLOTRON OF THE PHYSICOTECHNICAL INSTITUTE OF THE ACADEMY OF SCIENCES USSR WITH PROTON ENERGY OF 1 GeV.

N. K. Abrosimov, V. A. Volchenkov, V. A. Yeliseyev, G. A. Ryabov, N. N. Chernov.

(Physiotechnical institute im. A. F. Joffe of the AS USSR).

The output unit of synchrocyclotron on 1 GeV [1] is nonlinear regenerative system [2]. During the design of leading-out system was taken into consideration the real spectrum of the amplitudes of radial and bouncing, which made possible to design for computers the emittance of beam at the inlet into magnetic pipe and to design channel as optical circuit under the prescribed/assigned emittance of beam.

On the basis of the calculations conducted for an increase in the effectiveness of conclusion/output was accepted the number of the measures: was selected the optimum inclination/slope of the inlet of channel, are considerably expanded the apertures of channel, all sections of channel - focusing, and value and sign of the gradients of channel were selected from conformity condition for the radial and vertical emittances of beam with the acceptance of channel. Furthermore is increased the effective aperture of the magnetic field of regenerator, which led to the decrease of the losses of particles due to the heterogeneity of field on the vertical line. The schematic of output unit is represented in Fig. 1. Magnetic pipe consists of five curvilinear sections which are fastened to the C-shaped frame. Frame can remotely/distance be moved within the acceleration chamber without the deterioration in vacuum. The position of each section within the frame can be regulated on +-25 mm, also without the deterioration in vacuum. In cross section of the basic plates of sections and the magnetic field of sections are represented in Fig. 2.

The calculation of the emittance of beam was conducted employing procedure, analogous that described in works [3, 4]. For it is tenth and the values of the amplitudes of radial oscillations with the aid

of the computers was located the radius or energy of particle, after
which ceases the precession and begins the building up of radial
oscillations with the fixed/recorded node/unit whose position is
determined by regenerator. Consecutive trajectory calculation with
different amplitudes of radial and bouncing from a radius of
regeneration to the inlet into magnetic pipe gives radial and
vertical phase beam areas at the duct inlet. The account of the
distribution of a number of particles according to the amplitudes of
betatron oscillations makes it possible to obtain besides phase area
even and density distribution of particles in the phase space.
Density distribution of particles in the radial phase space was
obtained taking into account the vertical motion. This made possible
to determine the direction of the radial motion of basic part of the
particles and, in accordance with this, to select the optimum
inclination/slope of the inlet of channel to the final circular
orbit. For the axial particle for magnetic pipe was accepted the
point by the phase area, which corresponds to maximum particle
density in the radial phase space. Selected thus axial particle of
channel has in the process of acceleration the betatron radial
oscillations, different from zero.
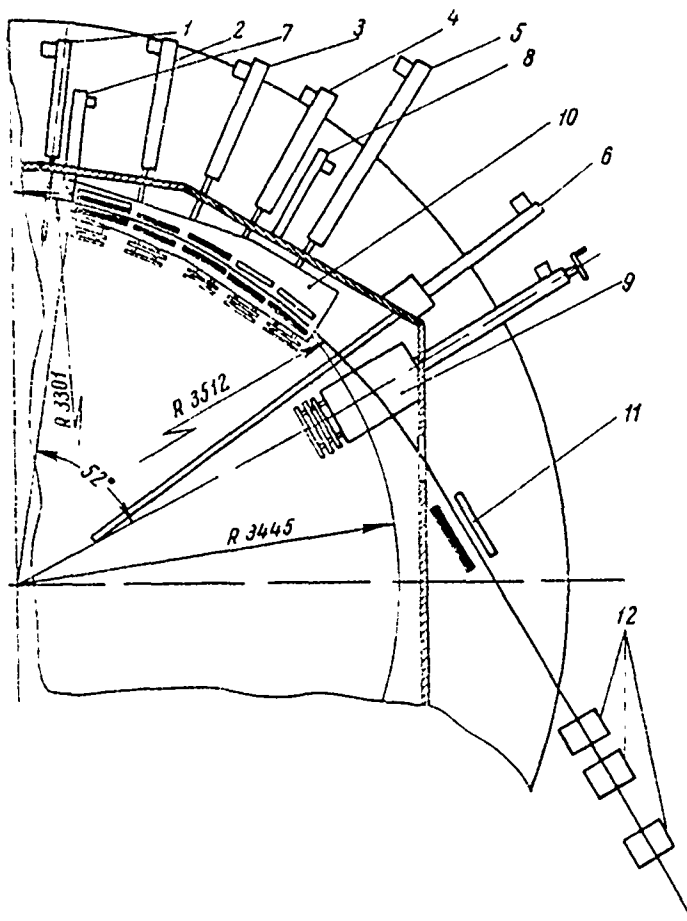
Fig. 1. Schematic of output unit. 1 - tester with small ionization chamber; 2, 5 - tester between the sections of magnetic pipe; 6 - thermocouple tester; 7, 8 - drives of channel; 9 - regenerators; 10 - frame of magnetic pipe; 11 - supplementary to a horizontal-focusing section; 12 - triplet of lenses ML-ZA; F - intermediate focus.

Page 183.

Bulk of particles is derived/concluded with the incomplete energy and with the radial inlet velocity into magnetic pipe of larger (~1.5 times), than for the particle, which does not have radial oscillations. Because of this channel it must be arranged/located at large angle to the final circular orbit, which makes it possible to utilize within the channel smaller field weakenings. The introduction to axial trajectory of channel makes it possible to linear approximation/approach to separately examine the deflecting and focusing properties of channel and respectively weakening and focusing gradients of sections.

Field weakenings within the sections are selected by such that the axial trajectory of beam of particles at the output of channel would acquire radial coordinate and velocity, necessary for the incidence/impingement particles after the passage of the scattered field at the center of the sergeant of the relief of magnet. During the analysis of the focusing properties of magnetic pipe was examined entire circuit of wiring the bundle which consists of magnetic pipe, stray field of accelerator, supplementary radial-focusing section of the stray field out of accelerator chamber and triplet of lenses ML-2A. Value and sign of the focusing gradients, and also necessary apertures of sections were selected by program TRAMP. The focusin,

sections were represented in the form of lenses, and the optical properties of stray field near the axial trajectory were approximately assigned by sequence of eight quadrupole lenses. As a result of these calculations for an increase in the channel capacity there were increased the radial and vertical apertures of channel and was introduced focusing into all sections (Fig. 2).

The expansion of the geometric aperture of regenerator, i.e., an increase in the region of uniform in the vertical line field, leads to the identical radial motion of particles with different bouncing. An increase in the smallest aperture of regenerator to 80 mm with the preservation of value $\int \Delta B d\theta$ was ontained due to the selection of the adequate/approaching configuration of iron and increase in the azimuthal length of regenerator to 0.2 rad (Fig. 3). The law of a change of the field of regenerator in the dependence on a radius can be approximately represented in the form $\frac{R_0}{R_0}\int \Delta B d\theta = 0.23(R-R_0) + 0.054(R-R_0)^2$.
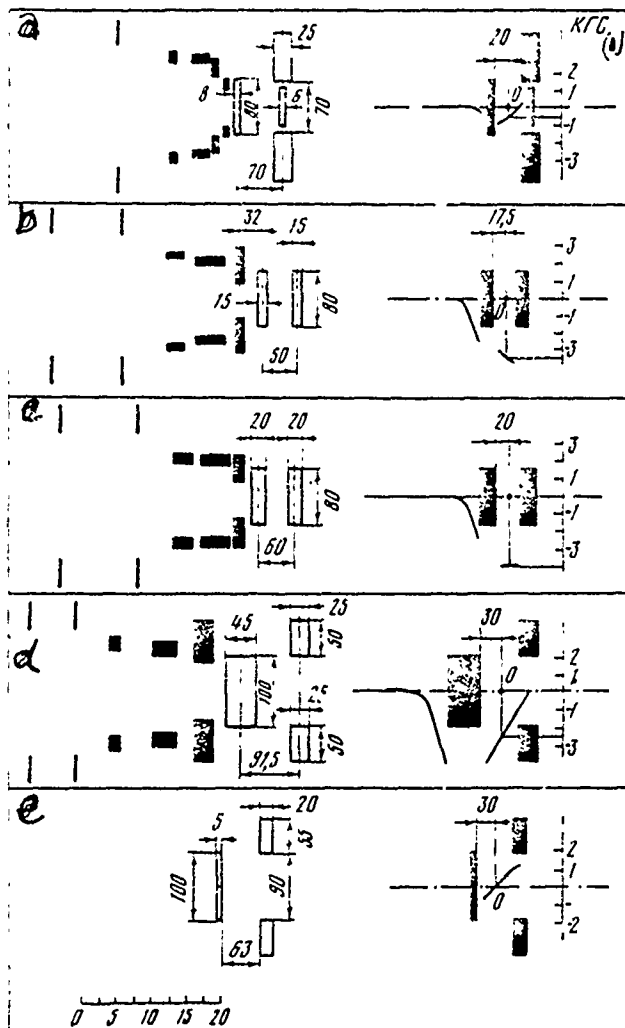
Fig. 2.
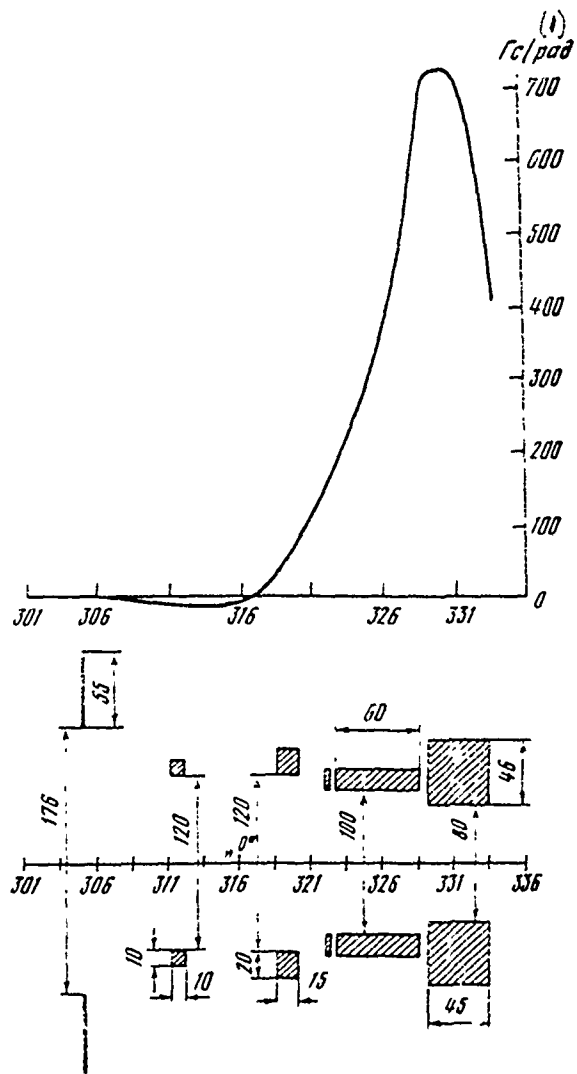
Fig. 3.

Fig. 2. Cross section of sections and magnetic field in sections. a) the first; b) the second; c) the third; d) the fourth and fifth sections; e - supplementary section. Point O - the optical axis of section. Weakenings in the sections are respectively equal to 650,

3470. 4000, 2600, 0 (G). Gradients of sections 540, 150, 0.800, 400 (G/cm). Total gradients in the field of accelerator 450, -250, -225, 540, 360 (G/cm).   KEY: (1) kG.

Fig. 3. Section of magnetic elements/cells of regenerator and magnetic field of regenerator $\int \Delta B d\theta$ (G•rad).   KEY: (1) G/rad.

Page 184.

The expansion of the apertures of channel with the retention/preservation/maintaining of weakening and gradients within the sections is possible only due to an increase in the sizes/dimensions of the plates of channel, which caused supplementary difficulties during the compensation for the action of channel in the region of normal acceleration. Magnetic measurements were performed with the aid of the equipment, which made it possible to carry out the automatic installation of sensors and recording the results of measurements [4]. Field measurements were made by nuclear magnetometer and magnetcmeter on the basis of the thermostatically controlled Hall pickup. Median measurements were made with the aid of two vertically oriented Hall pickups. During the first stage each section was shimmed separately. After the assembly of the separately shimmed sections and exposure of channel with the aid of the filament with the current along the axial trajectory was conducted the

shimmering of channel as a whole with the aid of the shims, which lie on the magnet poles for the compensation for formed failure/dip/trough of field by value to 300 G all over length of channel. The region of shimmering occupied along azimuth of 90° and on a radius from 200 to 325 cm. As a result of shimmering the fundamental harmonic of field comprised 2-3•10⁴ to a radius of 325 cm, i.e., to the radius, distant on 2 cm behind the plate of the first section.

For the adjustment of the system of conclusion/output on the beam was utilized the following equipment: tester with small ionization chamber for the study of the throw/excess/overshoot of particles into the channel, four testers between the sections for obtaining the radio-signatures of the beam within the channel, thermocouple tester for beam measurement within the chamber/camera and at the output of channel, icnization chamber with a diameter of 15 cm, arranged/located at a distance of ~5 of m from the chamber/camera, luminescent screens for the visual observation with the aid of the television equipment. Was observed critical dependence of conclusion/output on the current in the supplementary winding, which makes it possible to regulate the position of median plane. The radio-autographs of beam are shown in Fig. 4.

The obtained at present coefficient of conclusion/output

composes 25o/o at the intensity of the emitted beam of 6.10^{11} part./s. The density of beam in intermediate focus 2.10^{11} part./cm^2s., divergence 0.1^o.
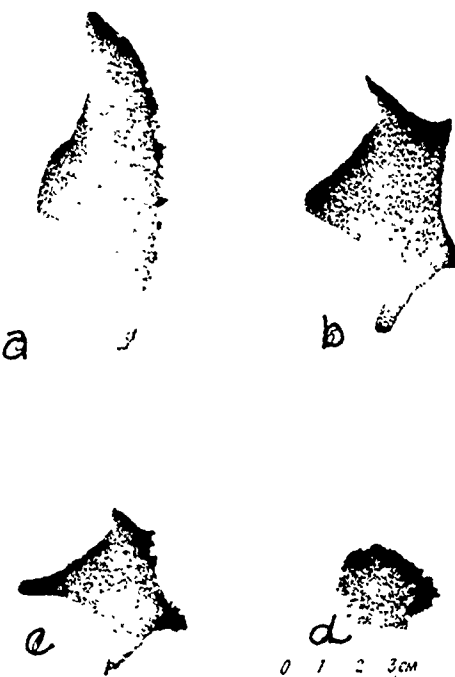
Fig. 4. Radio-autographs of beam. a) on tester 2; b) on tester 4; c)
on tester 5; d) in the intermediate focus.

REFERENCES.

1. N. K. Abrosimov, D. G. Alkhazov, S. P. Dmitriyev and et. al.
Synchrocyclotron of FTI AS USSR on the energy of Accelerated
Protons of 1 GeV.

2. G.T.Kruiff, N.V. Verster. The Orsay 160 Mev
Synchrocyclotron with Beam-Extraction System. Phys.
Techn. Rev., 1961/62, 12, 381.

3. A. C. Paul. Study of the Regenerative Extractor for
the Berkeley 184 inch Synchrocyclotron UCID-3142, 1968.

4. V. I. Dannlov, V. B. Mukhina, E. A. Polferov. Calculation
of a System for Extraction of a Synchrocyclotron. Preprint
OIYAI R9-4102, Dubna, 1968.

5. V. A. Yeliseyev, G. A. Ryabov, I. I. Tkach. Apparatus
for Magnetic Measurements on a Synchrocyclotron of the
Physical - Technical Institute of the USSR Academy of
Sciences for air energy of Protons of 1 GeV. See Russian
Collection, Vol. II.

Page 185.

146. SYSTEM OF RAPID BEAM DROPPING ON THE TARGET IN THE ACCELERATOR
OF THE INSTITUTE OF HIGH-ENERGY PHYSICS WITH ENERGY OF 70 GeV.

V. I. Gridasov, B. A. Zelenov, C. V. Kurnayev, E. A. Merker, K. P.
Myznikov, N. M. Tarakanov. (Institute of high-energy physics).

On the accelerator of the IFVE the generation of short-term
particle momenta for the experimentation with bubble chambers is
accomplished/realized with the aid of the rapid discharge/break of
the accelerated beam to internal target. For these purposes is
utilized known method [1], which consists of the creation of a
rapidly growing through time magnetic field in the special deflecting
magnet, arranged/located in straight section. The special
feature/peculiarity of the described system lies in the fact that in
it is used the slow iron magnet with rise time of magnetic field of
approximately 1 ms. Since for the works with the chambers/cameras is
required the very small intensity of secondary particles, it proves
to be sufficient to aim at the target only the part of the
accelerated beam. Guidance to the target ceases on the signal of
reverse from the band, that corresponds to the prescribed/assigned
number of particles in bubble chamber. Combination relative to slow

kicker with the dosing apparatus makes it possible to obtain a stable from one cycle to the next number of particles in the chamber/camera during the time interval by duration into several hundred microseconds. On the other hand, this decision considerably simplifies the design concept of system and its electrical diagram.

The dependence between the deflecting force of magnet and the beam displacement on the azimuth of target relied on computers taking into account the objective parameters of the magnetic field of accelerator employing the procedure, presented in work [2]. As an example Fig. 1 gives the form of the distorted orbit in the region of target location with the connected kicker by the force of 1.5 kOe•m. Fig. 2 shows the dependence of the amount of beam displacement on the azimuth of target from the frequency of radial betatron. Utilizing two magnets, the shifted along the azimuth relative to each other distance, multiple of quarter-wave length betatron oscillations, it is possible by the appropriate selection of currents in them to obtain the necessary divergence for any azimuthal target location.

The operating range of targets on a radius in the accelerator of IFVE is +-5 cm. In order to reduce to a minimum the necessary force of the kicker, rapid beam spill to the target is accomplished/realized into two stages. During the first stage the

accelerated beam is fed to the target with the aid of the slow system
of the excitation of local magnetic bump in the boost clusters [3].
This system is switched cn it in advance and creates the necessary
beam displacement on the azimuth of target. Then with the aid of the
kicker is created rapid orbit distortion and beam is discarded to the
target. For obtaining the necessary intensity in the chamber/camera
it proves to be sufficient to produce rapid displacement to the value
smaller than the diameter of beam, which composes several
millimeters. The remaining part of the beam consistently is aimed at
other targets, with the aid of which are conducted the experiments,
which use a calculating procedure.

The pulse C-shaped magnet with a length of 1 m is glued from the
sheets of transformer steel with thickness of 0.5 mm. The
measurements conducted showed that during the location in magnet gap
of vacuum chamber of the stainless steel with wall thickness of 0.4
mm the magnetic field within it at the frequency of 1 kHz is
weakened/attenuated not more than by 5o/o. These data will agree well
with the calculations, carried cut employing procedure [4]. On this
basis/base the magnet was placed out of vacuum chamber, which made it
possible to avoid complicated constructive solutions.

The schematic of the power-supply system of the kicker is given
in Fig. 3. It encompasses the stabilized controllable rectifier.

Energy storage occurs in the gap/interval between the cycles of acceleration in capacitor bank C_1. From the impulse/momentum/pulse, accurately synchronized with the accelerator, proceeds the discharge of the battery through key/wrench T_4 to the winding of magnet. The special feature/peculiarity of diagram is the possibility of the inclusion of current in the magnet with the aid of the device/equipment, which doses the intensity of the particles, discarded to the target. As the sensors of intensity are utilized counters C_1, C_2, C_3 (Fig. 2), established/installed in the channel focusings of secondary particles.
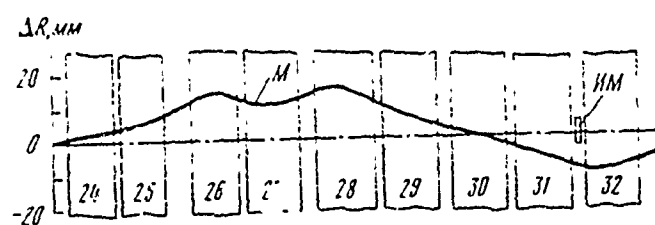
Fig. 1.
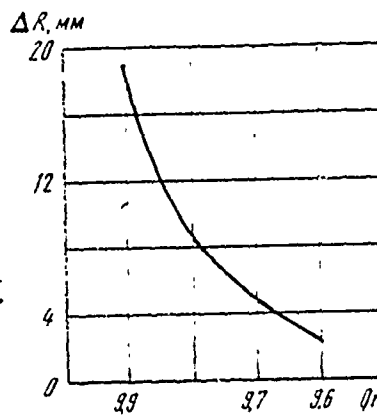
Fig. 2.

Fig. 1. Section of disturbed orbit of IM - kicker; M - target.

Fig. 2. Dependence of beam displacement in region of location of target on value Q_z
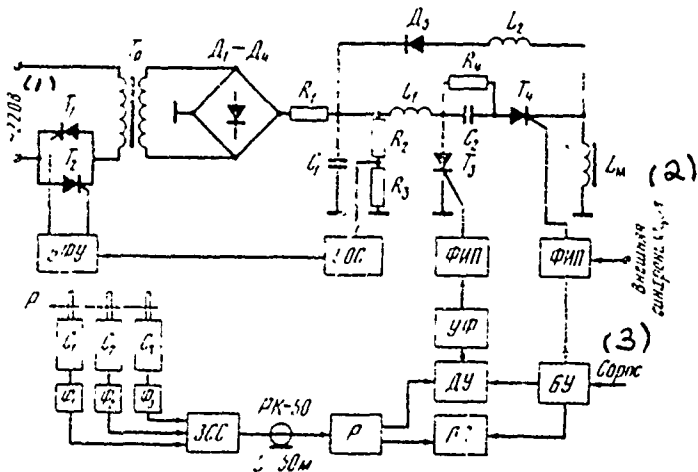
Fig. 3. The system block diagram of the supply of the winding of magnet with dosing apparatus C_1, C_2, C_3 - scintillation particle counters; Φ_1, Φ_2, Φ_3 - shapers; 3 cc - triple coincidence circuit; P - fan-out; PS - conversion system; DU - dosing apparatus; BU - control unit; UF - amplifier-shaper; BIP - unit of the impulses/momenta/pulses of ignition; BFU - unit of phase control; UOS - feedback amplifier.

Key: (1). V. (2). External synchronization. (3). Discharge/break.

Page 186.

They are connected through the shapers P with the triple circuit of coincidence 3 cc, from output of which the impulses/momenta/pulses enter the fan-out R. All units of rapid electronics are carried out

on the standard moduli/modules, accepted in IFVE [5]. From one output
of fan-out R the impulses/momenta/pulses enter the scaler PS with the
maximum speed of count 10 MHz, as which is utilized an industrial
instrument of the type PP-9. From the second output of fan-out the
impulses/momenta/pulses enter the dosing apparatus which consists of
input unit of shaper and three decades/ten-day periods, constructed
according to system 1-2-4-8. Potential outputs from the triggers are
brought out to the switch for the establishment of the threshold of
limitation according to count [6]. Impulse/momentum/pulse, that
corresponds to the prescribed/assigned level of count, is
differentiated, is amplified and is formed/shaped with the unit of
UV. The unit of control BU accomplishes/realizes setting of the
necessary time interval of functioning units DU and PS, and also a
discharge/break of readings of the scalers of these units.
Impulse/momentum/pulse from the output of the dosing apparatus
through the unit of UF enters the unit of the ignition of thyristor
key/wrench T_3 and are opened/disclosed it. In order to decrease the
decay time in the current in the magnet, with its circuit is
connected the additional capacity/capacitance C_2. This measure made
it possible to increase the velocity of the removal/diversion of the
accelerated beam from the target and led to the clearer work of the
system of dosage.

Were carried out the experimental tests of the described system

together with bubble chamber. Fig. 4 shows the oscillogram of current
pulse in the magnet (lower ray/beam) and the current pulse of
particles on internal target (upper ray/beam). It is evident that
after the ignition of key/wrench T_3 on the signal from the dosing
apparatus proceeds a sharp decrease in the current in the magnet. As
a result the trailing edge of pulse of current on the target is
obtained sufficiently to steep/abrupt ones. The pulse duration does
not exceed 500 µs. Out of this interval of the background of
particles it was not observed. Fig. 5 depicts the histogram of
loading bubble chamber from the counter readouts,
established/installed directly before the chamber/camera.
Measurements are carried out during the long time. It is evident that
a basic number of events corresponds to 4 particles with the scatter,
which does not exceed ←3 particle. The idle background of particles
in the chamber/camera within the time of discharge/break it was not
observed. This mode/conditions proved to be satisfactory for the
experimentation with bubble chamber.
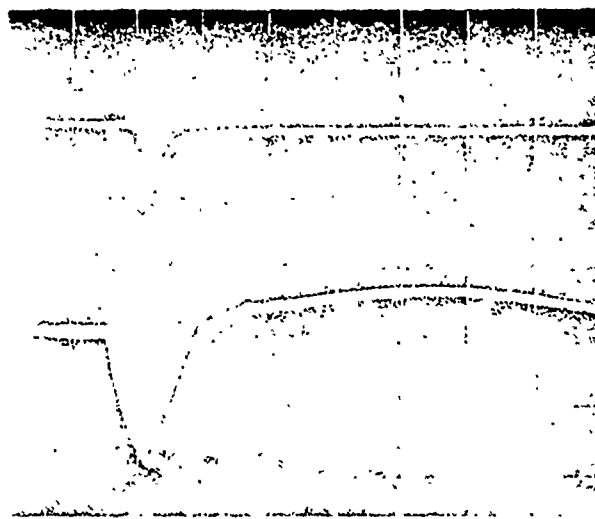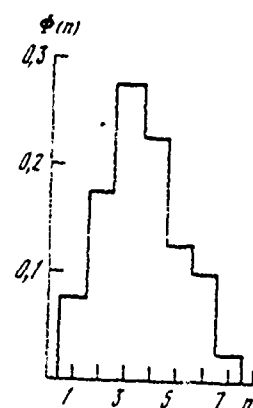
Fig. 4.

Fig. 5.

Fig. 4. Oscillogram of signal from monitor of particles (upper ray/beam); oscillogram of current pulse in magnet (lower ray/beam). Time/temporary scale - 500 μs/cell.

Fig. 5. Histogram of loading bubble chamber. Along the axis of abscissas is deposited/postponed a number of particles, which record from the cycle to cycle, along the axis of ordinates, the standardized/normalized density of the appearance of this number of particles.

REFERENCES.

1. O.C. Rahm. Rev. Scient. Instr., 1961, 32, 1116.

2. V. I. Gridasov, K. P. Myznikov. Preprint of IFVE 68-60, Serpukhov, 1968.

3. V. I. Gridasov, A. A. Kardash and et. al. Methods for the Generation of Secondary Particles on Internal Targets of IFVE Accelerator for Energy of 70 GeV. Trudy VII Mezhd. konf. po uskoritelyam [Proceedings of 7th International Conference on Accelerators, Yerevan, 1969, Vol. 1, p. 509.

4. Yu. F. Orlov, S. A. Kheyfets. PTE, 1959, No. 1.

5. Yu. B. Bushnin, A. F. Dunaytsev, V. A. Sen'ko. Functional Modules of Logic Electronics with Maximum Counting Rate of 100 MHz. Materialy Simpoziuma po nanosekundnoy yadernoy elektronike B-3700, [Materials of Symposium on Nanosecond Nuclear Electronics V-3700, Dubna, 1967.

6. A. G. Grachev, S. S. Kirillov. Preprint OIYAI, 1962.

Page 187.

147. System of the conclusion/output of electrons from the Yerevan synchrotron.

R. O. Abramyan, L. A. Ananova, G. V. Badalyan, A. A. Dallakkyan, G. M. Daniyelyan, S. K. Yesin, I. P. Karabekov, V. I. Kovalenko, A. A. Markaryan, M. A. Martirosyan, Ya. D. Nersisyan, Yu. F. Orlov, A. G. Sal'man, Kh. A. Simonyan.

(Yerevan Physical Institute).

O. A. Gusev, B. N. Zhukov, V. K. Zagaynyy, A. P. Lebedev, V. I. Sesnikov, B. S. Mingalev, N. A. Monoszon, B. G. Mud'yugin, V. P. Nadgornyy, A. G. Nechaev, N. S. Bezchikova, B. V. Rozhdestvenskiy, Yu. P. Sivkov, A. S. Sudarushkin, M. M. Suvorov, P. A. Pefelov.

(Scientifically research institute of the electrophysical equipment im. D. V. YEfremov).

The removal of electrons from the Yerevan synchrotron is accomplished/realized cu the quadratic resonance at the frequency of betatron $Q_\nu = 51/3$ [1 - 5]. For the creation of the quadratic nonlinearity of field and for frequency shift of betatron oscillations are utilized respectively sextupole and quadrupole lenses (Fig. 1). As a result of the resonant step-up the electrons are thrown into a septum-magnet (SM) and removed by them beyond the limits of the aperture of chamber/camera. The divergence of beam to the electron conductor is accomplished/realized by the deflecting magnet (OM). Beam focusing on the route of electron conductor is conducted by quadrupole lenses L_1 and L_2. The distributive magnet (RM), supplied by direct current, makes it possible to guide emitted beam along five different channels into the experimental hall.

The calculation of resonance of build-up was conducted both by the method of averaging [6, 7] and by numerical on the computers "Razdan-3". On the basis of calculation were selected the necessary values of disturbances/perturbations. Specially was investigated the effect of a comparatively rapid passage of betatron frequency through the resonance value. It was explained that at the selected values of the nonlinearity of field and duration of conclusion/output $\approx(1.0-3.0)$ ms only the insignificant part of the electrons (namely those which they have amplitudes of betatron oscillations of less than several ten millimeters) it can pass resonance without having

swung. Divergence from the stability virtually does not affect the step/pitch of driving.

During all calculations the motion in undisturbed field was considered linear. Fig. 2 gives the calculated distribution on the phase plane of the particles, neglect/deserted for the septum with the different field distortions. The calculated size/dimension of the emittance of emitted beam is equal to (1-3) π, mm- mrad. Real throws/excesses/overshoots due to the natural nonlinearity of field can noticeably differ from calculated ones. Therefore is provided for the possibility of amplitude control and phase of nonlinear field distortion. Phase is regulated discretely on +-41° by method of the changeover of the polarity of some sextupoles. As can be seen from Fig. 1, phase shift between sextupoles on 16 harmonic of disturbance/perturbation is multiple $2\pi/3$. In combination with continuously variable control of the current of septum this regulating of phase is sufficient for obtaining the optimum mode/conditions of conclusion/output.

In order to localize along the azimuth the place of the throw/excess/overshoot of particles into a septum-magnet, not cutting to deeply into aperture of chamber/camera, and, furthermore, to decrease the effect of its own nonlinearity of the field of accelerator, in the location of septum is created local orbit

perturbation.

The calculations of routes from a septum-magnet to the output of
beam from the accelerator show [8] that the location of septum from
the outer side from the orbit leads to the passage of beam in the
nonlinear field and the strong distortion of its phase volume.
Although the location of a septum-magnet from inside leads to certain
reduction in the effectiveness of conclusion/output, it was
acknowledged by preferable. To the divergence of beam in a
septum-magnet it is 3-5 mrad depending on the phase of nonlinear
disturbance/perturbation. Supplementary divergence to OM is -30 mrad.
After passage in the stray field of basic electromagnet the beam
emerges by sufficiently strongly diverging on the horizontal.
Therefore lens L_1 is arranged/located as close as possible to
accelerator.

Let us pause in somewhat more detail at the separate elements of
the system of conclusion/output. A septum-magnet has the laminated
core, the thickness of sheets 0.5 mm. The overall length of magnet on
the iron 500 mm. Resistance of single-turn winding 3.10^{-3} ohm,
inductance 4.10^{-3} H magnetic intensity 1600 e in clearance 7330 mm^2.
The cross section of a septum-magnet is shown in Fig. 3a. Frontal
conductor (septum) is made from the copper strip/film with a
thickness of 0.7 mm. Heat withdrawal is conducted through the copper

lobes/lugs, which envelope the water-cooled tube ∮ 10x2. Tube and current conductor are isolated/insulated from the housing by poliamide film.

Fig. 1. Overall diagram of the system of the conclusion/output of electrons from the Yerevan synchrotron.

Key: (1). Magnet block. (2). target. (3). Septum- magnet. (4). Deflecting magnet.

Page 188.

Runnin-water supply is carried out by two coaxial conclusions. Decoupling with the vacuum tank is accomplished/realized through the bellows. Are accepted special measures for the protection of magnet under the load in the case of the sudden cessation of water supply.

Radial field distribution in SM given in Fig. 4.   Effective

thickness of septum is somewhat increased due to a reduction in the field in operating region near it. This reduction was the result of the location of current conductor out of the clearance SM.

The deflecting magnet (see Fig. 3b) has a thickness of current conductor 6 mm and screened outside by plate made of the carbon steel with a thickness of 1 mm. The construction/design of magnetoconductor and running-water supply of the deflecting magnet is analogous the construction/design of a septum-magnet.
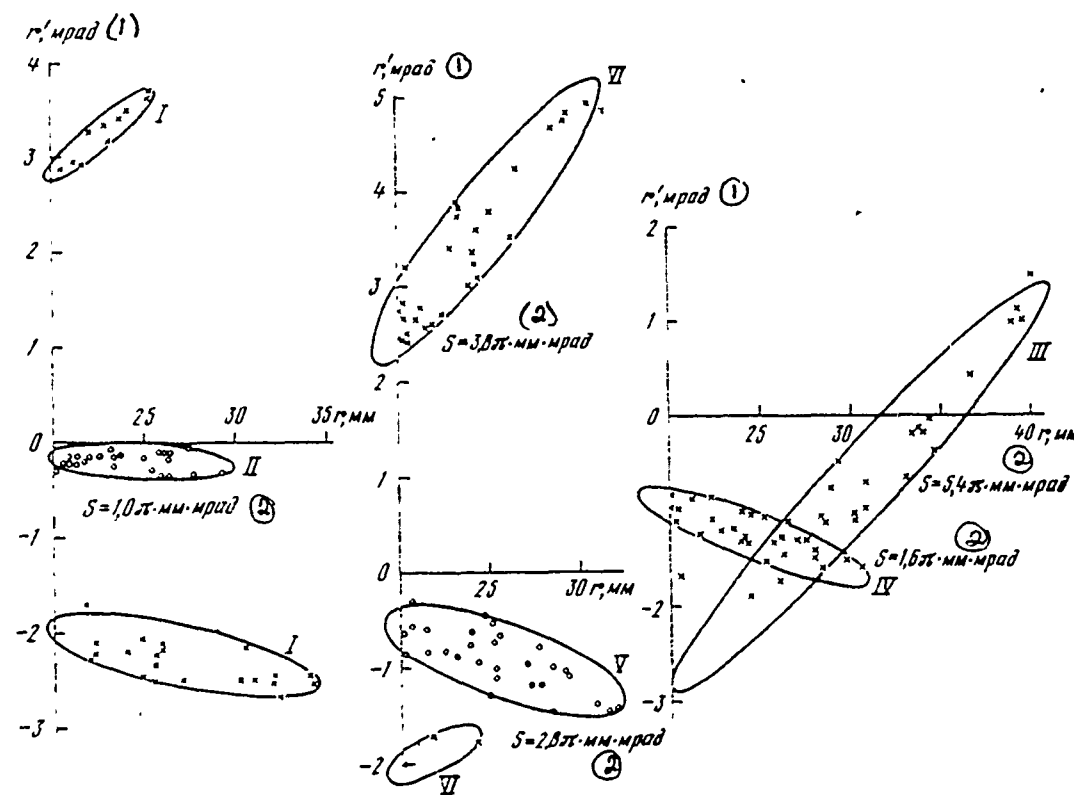
Fig. 2. The calculated distribution of the particles on the phase plane, neglect/deserted to the septum for six versions of the inclusion/connection of sextupoles (LSh -lens six-pole, LK - lens quadrupole).

Key: (1). mrad. (2). mm·mrad.

DOC = 80069315   PAGE # 784

Варианты :	Промежутки				Примечание
	26–27	40–41	42–43	10–11	
I	–	–	+	–	2 ветви
II	+	+	–	+	
III	+	–	–	–	
IV	–	+	+	+	
V	–	+	–	+	
VI	+	–	+	–	2 ветви

Key: (1). Versions. (2). Gaps/intervals. (3). Note. (4). branch.
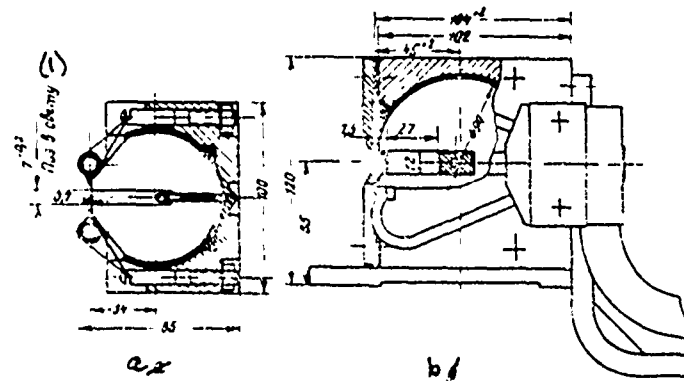
Fig. 3. Leading-out magnets. a) a septum-magnet SP-139; b) - the deflecting magnet SP-138.

Key: (1). Pos. in the light/world.

Page 189.

Current pulses in the devices/equipment of the system of conclusion/output are switched on with certain lead/advance in

comparison with the maximum energy (Fig. 5). During the
conclusion/output the energy of electrons continues to change;
therefore for guaranteeing the permanent angle of deflection in SM
and OM currents in them must change approximately/exemplarily
according to the same law. The quantum building up of the
oscillations under the action or synchrotron radiation does not
permit implemention of a conclusion with the energies 5-6 GeV after
the maximum magnetic field. This limits the duration of
conclusion/output by the value of 1.5-2 ms. A change of the energy of
electrons in the process of conclusion/output makes it necessary to
approach achromaticity of the focusing system and requires the
careful adjustment of the synchronization of output units.

In the power-supply systems of quadrupole and sextupole lenses
the formation of pulses is conducted with the aid of dipoles, which
consist of the parallel-connected series circuits. Stability of
impulses/momenta/pulses at the apex/vertex to worse than +-0.5o/o.

A septum-magnet is supplied from the pulse generator, which
consists of the storage capacity/capacitance with the aid of which
are formed/shaped the pulse edges, and stairs type artificial lines
for the compensation for ohmic losses in the load. For the purpose of
obtaining the best shape of pulse storage capacity/capacitance and
artificial line are corrected consecutive system it makes it

possible to obtain impulses/momenta/pulses with the pulsations at the apex/vertex not more than 10o/o with respect to the duration of fronts to the apex/vertex not more than 0.25.

In the power-supply system of the deflecting magnet where the porosity of periodic process is equal to 1.4, the recharge of the capacity/capacitance, which forms front, is conducted through the buffer capacity/capacitance, which makes it possible to ensure the stability of the charge of basic capacity/capacitance and the uniform loading of the phases of charging rectifier. For guaranteeing the recurrence of current in the magnets from one impulse/momentum/pulse to the next is developed the sampled-data system of the stabilization of the charge of capacities/capacitances, based on the current cutoff in the charge inductance upon reaching of voltage on the capacity/capacitance of desired value. The selection of the final versions of supply was conducted in the analog computers.
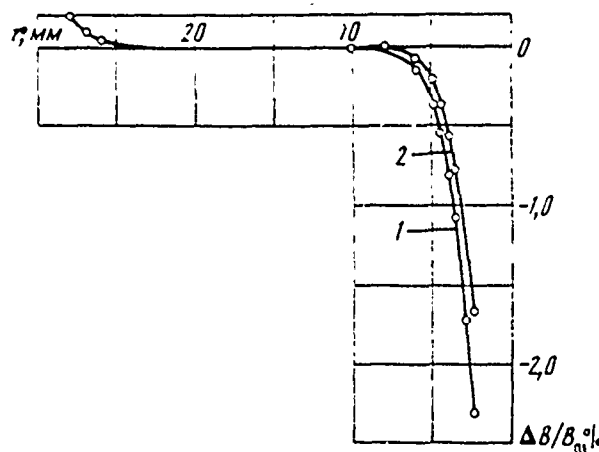
Fig. 4. Distribution of magnetic field according to a radius within the clearance of a septum-magnet in the center of the gap/interval between the gashes. the "step/pitch" of gashes. 1 - 15 mm, 2 - 75 mm, $B_0 = 1600$ vs ($r = 15$ mm, r -distance from the septum).

(1) Система питания	(2) Форма импульса и временная привязка	(3) Параметры импульсов	(4) Схема системы питания
(5) Цикл ускорения		(6)	
(7) Локальное возмущение орбиты	(6)	$J_m = 15\,a$ (6) $t_u = 11\,мсек$ $L_н = 20 \cdot 10^{-3}\,гн$ (8) $R_н = 0,4\,ом$ (9)	(10) К контуру
(11) Линза вывода a) квадруполи б) секступоли	(6)	a) $J_m = 200\,a$ $L_н = 9,5 \cdot 10^{-3}\,гн$ (8) $R_н = 0,3\,ом$ (9) б) $J_m = 250\,a$ $L_н = 4,8 \cdot 10^{-3}\,гн$ (8) $R_н = 0,2\,ом$ (9) $\tau = 2\,мсек;\ t_ф = 2\,мсек$ $T = 6\,мсек$ (6)	(10) К контуру
(12) Септум-магнит		$J_m = 1050\,a$ (6) $\tau = 3\,мсек$ (6) $t_ф = 0,5\,мсек$ (6) $T = 4\,мсек$ (6) $L_н = 4 \cdot 10^{-6}\,гн$ (8) $R_н = 4 \cdot 10^{-3}\,ом$ (9)	(13)
(14) Отклоняющий магнит		$J_m = 14000\,a$ (6) $t_u = 14\,мсек$ (6) $L_н = 2,5 \cdot 10^{-6}\,гн$ (8) $R_н = 0,5 \cdot 10^{-3}\,ом$ (9)	(13)

Fig. 5. Power-supply systems of leading-out lenses and magnets and time characteristics of impulses/momenta/pulses.

Key: (1). Power-supply system. (2). Shape of pulse and timing. (3) The parameters of impulses/momenta/pulses. (4). Diagram of power-supply system. (5). Cycle of acceleration. (6). ms. (7). Local disturbance/perturbation of (8). H. (9). ohm. (10). To circuit. (11). Lens of conclusion/output a) quadrupoles, b) sextupole. (12). Septum-magnet. (13). Is true. charge. (14). That deflecting magnet.

Page 190.

For observation of beam and adjustment of output to the external route of electrons were established/installed the following instruments:

a) a gauss-quantameter, which gives absolute intensity of emitted beam;

b) slotted ionization chamber, which gives the radial center-of-gravity location of beam [9];

c) the small low-quality resonator, tuned to a frequency of the accelerating system of synchrotron (132.8 MHz);

d) scintillation counter with FEU;

e) the glass plates, which give the image of beam.

At the same time was provided the distance observations of the phosphorescent glow, plotted/applied to the surface of septum, turned to the equilibrium orbit.

DOC = 80069315   PAGE <s>790</s>

On 13 March, 1970, was fixed the emitted beam of electrons with
the energy 3 GeV by the duration of 1 ms. Fig. 6 depicts the
transverse size/dimension or beam on the exhaust duct (3.5 m for OM).
The effectiveness of conclusion/output in the first performances was
approximately 10o/o.

At present is conducted work on an increase in effectiveness and
duration of conclusion/output.

References!

1. U. Bizzarri. et al. Nuovo cimento, 1966, 42, p. 639.
2. F.W. Brasse et al. 1963. CEAL-1006.
3. Barton M.Q.et al. VII Internat. Conf. on High Energy
   Accelerators, Yerevan, 1969.
4. W.Schmidt. DESY 65/18, 1965.
5. K. P. Myznikov, A. D. Artemov, et al. VII International Conference
   on High Energy Accelerators, Yerevan, 1969.
6. D. G. Koshkarov, Yu. A. Globenko. PTE, 1967, No. 2.
7. A. V. Gal'chuk, Kh. A. Simonyan, et al. VII International Conference
   on High Energy Accelerators, Yerevan, 1969.
8. G. V. Badalyan, Yu. P. Sibkov, et al. All-Union Conference on Charged
   Particle Accelerators. Moscow, 1968, Preprint EFI - UFT -8 (69), 1969
9. G. A. Arakelyan, G. S. Vartyanyan, et al. Instruments and Methods for
   Measuring Three-Dimensional Characteristics of External ARUS Beams.
   See this collection, Vol. II.

Discussion.

K. A. Belovintsev. Which the required precision/accuracy of power
supply of quadrupole and sextupole lenses?

G. V. Badalyan. Required stability of current at the pulse apex $\pm$

0.5o/o, the permissible amplitude of the pulsation of the same order.

A. A. Vorobyev. What effectiveness of conclusion/output it is
possible to achieve with the aid of your system?

G. V. Badalyan. As is known, the effectiveness of conclusion/output
$K = 1 - \frac{\delta}{\Delta \nu}$, where δ - effective thickness of septum, $\Delta \nu$ - step/pitch
of the resonant step-up of the amplitude of oscillations near the
septum. For the Yerevan synchrotron $\delta = (1-2)$ mm, $\Delta r = (5-10)$ mm and the
respectively expected effectiveness of conclusion/output comprises
(60-80)o/o.

L. L. Gol'din. You carried out both the analytical and numerical
calculations of the building up of the oscillations of outgoing
particles. Did make it possible numerical calculation to obtain any
new data in comparison with the analytical data?

G. V. Badalyan. Generally the method of averaging works well, when a
change in phase and amplitude of betatron oscillations with the
passage of one nonlinear field distortion is small. On the
latter/last revolutions before the throw/excess/overshoot of -
particles into a septum-magnet this assumption ceases to be valid.
Therefore the study of particle motion on the latter/last revolutions
and, in particular, the determination of the phase volume of emitted

beam must be produced with method of numerical calculations. The result of calculations by ETsVM, nevertheless, is conclusion about the fact that the driving of the amplitude of betatron oscillations will agree sufficiently well with the forecasts of the method of averaging.

The method of averaging was utilized for obtaining the initial data, and the future calculations were conducted with the aid of ETsVM.

CM

Fig. 6. Photograph of brought-out electron beam to focusing.

Page 191.

148. Channel of the separated particles for 2-meter liquid hydrogen
     J. I. N. R.
bubble chamber ~~of IHEP~~ (calculation data).

A. V. Samoilov, Yu. M. Sapunov, A. M. Frolov.

(Institute of high-energy physics).

Channel is designed for the irradiation on the accelerator IFVE
                                                    J.I N.R.
of 2-meter liquid hydrogen bubble chamber of ~~IHEP~~ in pure/clean

beams $K^\pm, \bar{p}, p, \pi^+$ of particles in the range of pulses p~10-25 GeV/s. The

optical diagram of channel, represented in Fig. 1, and high-frequency

separator are analogous utilized in the acting in CERN [1],

Brookhaven [2] and installed in IFVE [3] channels of the separated

particles. Separator consists of three waveguide-deflectors, excited

on the hybrid wave EN_{11}, and works together with the rapid

conclusion/output of accelerated protons [4]. The basic calculated

parameters of separator, undertaken work [5], and the parameters of

channel gives below:

Sizes/dimensions of external target (vertical line $\times$ horizontal

$\times$ length) ... 2x2 of 100 mm^3.

Material of the target of ...to copper.

Angle of particle production ... ₁ 0°.

Acceptance angle of particles from the target into the channel:

the horizontal ...   +-1.8 mrad.

the vertical line ...   +-4.6 mrad.

The solid angle of the capture of channel ... 33 μerased.

Relative pulse interval in the channel ... +-0.25o/o.

Quantity of quadrupole lenses ... 17 (with a length of 2 m).

Quantity of the deflecting magnets ... 2 (by length 4 m) +1 (with a length of 3 m).

Quantity of collimators ... 10.

The linear magnifications: horizontal vertical line.

first pulse collimator ... 0.50 -.

the centers of deflectors ... 1.42 5.70.

intermediate images after separator ... 0.46 12.00.

the second pulse collimator ... 0.71 -.

Dispersion of the image of the target:

the first pulse collimator ... $5\text{MM}/\dfrac{\Delta p}{p}$ $=1\%$

the second pulse collimator ... $11\text{MM}/\dfrac{\Delta p}{p}$ $=1\%$

Full length of the channel (target - chamber/camera) ...   194.2 m.

Quantity of LF deflectors ... 3.

distances between deflectors:

L_{12} ... 28 m.

L_{23} ... 42 m.

Length of deflector ...   4 m.

Aperture of deflector ... 2a=46 mm.

Working wavelength ...   10.7 cm.

Transverse pulse in the deflector at power 20 MW ... 23.7 GeV/s.

The use of any two deflectors makes it possible to derive of the beam either one undesirable type of particles (single-particle rejection), or two types two-particle rejection) at the values of pulses of those given in the table.
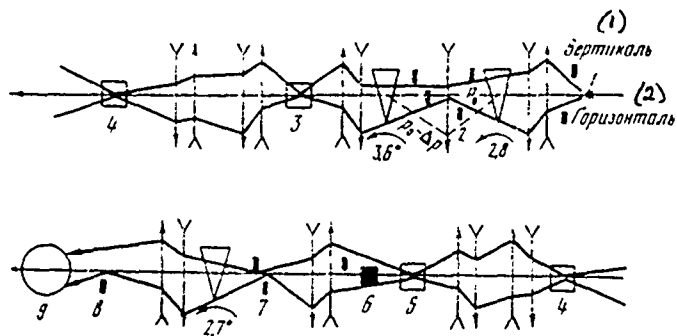
Fig. 1. The optical diagram of channel. 1 - external target; 2 - first pulse collimator; 3 - deflector I; 4 - deflector II; 5 - deflector III; 6 - cluster absorber; 7 - intermediate images; 8 - second pulse collimator; 9 - bubble chamber.

Key: (1). Vertical line. (2). Horizontal.

The values of the impulses/momenta/pulses of the separated particles with the two-deflector separation (region p>7 GeV/s).

(1) Режекция	(2) Частицы	L_{12}= 28м (3) p, Гэв/с	$(\delta v)_2/(\delta v)_1$	L_{23}= 42 м p, Гэв/с	$(\delta v)_2/(\delta v)_3$	L_{13}= 70 м p, Гэв/с	$(\delta v)_2/(\delta v)_3$
(4) Одночастичная	K±	7,2-7,8 9,8-11,6		7,2-7,7 8,8-9,6 12,0-14,2		7,3-7,6 9,4-9,9 11,4-12,3 15,5-18,4	
	П+	8,4-9,8 22,0-25,0		7,7-8,3 10,3-12,0		7,1-7,3 8,1-8,2 9,9-10,6 13,3-15,4	
	p, p̃	13,0-25,0		7,7-8,3 10,3-12,0		7,0-8,1 8,6-9,4 21,0-25,0	
(5) Двухчастичная	K±	7,5 10,6	1,3 1,0	7,5 9,2 13,0	0,8 1,0 1,0	7,5 8,1 9,7 11,0 16,8	1,1 0,7 1,1 1,0 1,0
	П+	9,1	1,0	7,9 11,2	1,0 1,0	7,2 8,3 10,2 14,4	1,0 0,7 1,0 1,0
	p, p̃	—	—	—	—	8,6	0,9

Key: (1). Rejection. (2). Particles. (3). GeV/s. (4). Single-particle. (5). Two-particle.

Page 192.

For the comparison of effectiveness of two and three-deflector version of separator in the table they are given relationship of the corresponding to versions angular deflections of the separated particles at one and the same value of the maximum power, introduced

into the deflector. In this case the angular deflections of the separated particles are given to angular divergence $\pm\delta_v$ of the undeflected beam in the first deflector, providing the condition of optimum separation [1]. Fig. 2 depicts separative curves for the isolation/liberation of one type of particles on the basis of of three-deflector diagram (two-particle rejection) optics of channel is optimized from the point of view of the possibility of the realization of the maximum divergence of beam, permitted by the geometry of deflector.

The relative composition of the unseparated beam and the absolute flows of negative particles on the chamber/camera with the energy of acceleration $\bar{z}_0 = 70$ GeV were evaluated on the basis of experimental data, obtained in IFVE [6], and for the positive particles - on the basis of calculations according to Trilling [7] they were represented in Fig. 3 and 4.
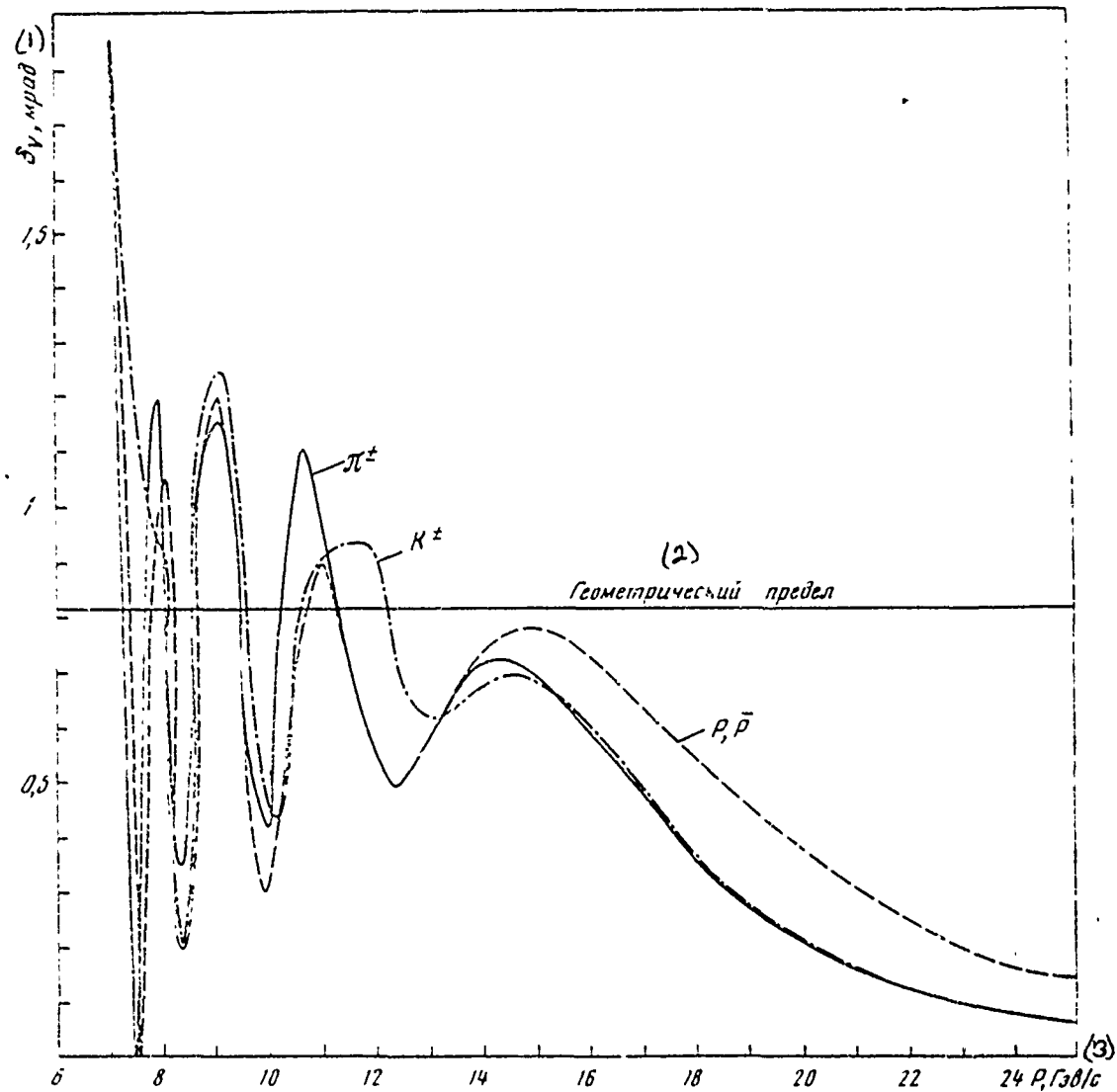
Fig. 2. Three-deflector separation of particles (acceptance of channel on vertical line $\pm\alpha_v = \pm 5,7\delta_v$). $z_{12}=28$м, $z_{13}=70$м, $\lambda=10.7$ см, $P_1=23.7$ GeV/s.

Key: (1). mrad. (2). Geometric limit. (3). GeV/s.
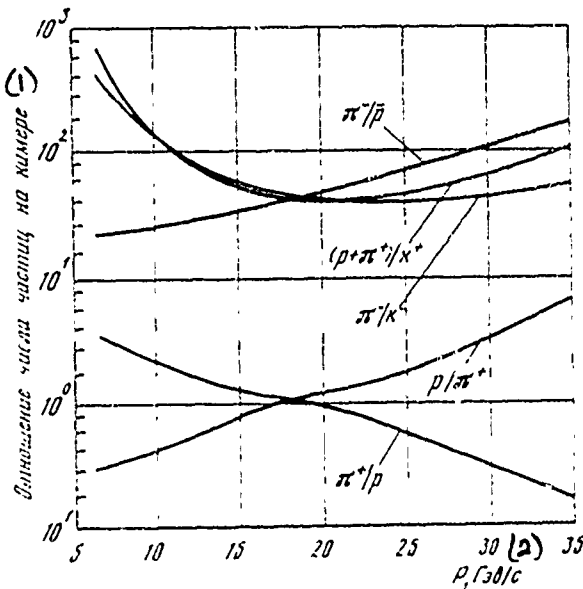
Fig. 3. Relative composition of unseparated beam on bubble chamber with energy of acceleration of 70 GeV.

Key: (1). Relation of the number of particles on the chamber/camera.
(2). GeV/s.

Page 193.

These estimations and expected coefficient of the depression of undesirable particles ~1500 [1] make it possible to rely on the possibility of separation $K^{\pm}, \bar{p}, p, \pi^{+}$ of particles in the whole range of pulses p~10-25 GeV/s. The expected μ- meson pollution/contamination of separated beams $K^{\pm}$ and $\bar{p}$ compose $\leqslant 15o/o$. Channel makes it possible to also transport to chamber from external target the beams

of unseparated particles of both signs of charge and from internal

target of accelerator - beam of the elastic scattered primary protons

with pulse in both cases of p < 35 GeV/s. Furthermore, is in principle

possible transportation from internal target to the chamber/camera

cleaned by the magnetic field of the accelerator of the beam of

positrons with pulse p ~ 35 GeV/s ($E_0 = 70$ GeV).

REFERENCES

1. P. Bernard et al. CERN 68-29, 1968,
2. H.W.J.Faelsche et al. Rev.Sci. Instr., 1967, 38, 879.

3. Z. M. Galyayev, P. Bernard, et al. High Energy Separated Beam
   and HF Separator for IFVE Accelerator. Proceeding of VII
   International Conference on Accelerators, Yerevan, 1969 CERN/
   D.Ph. II Sept. 69-4, 1969.
4. K. P. Myznikov, et al. Preprint. IFVE SKU 68-57, Serpukhov,
   1968; B. Koyper. et al. Systems for the Rapid Extraction of the
   Serpukhov Accelerator. VII Internation Conference on Accelerators.
   Yerevan. 1969. Vol. 1, p. 549.
5. V. M. Levin, et al. Deflecting System of HF Separator for IFVE
   Proton Synchrotron. Vol. II.
6. F. Binon, S. P. Denisov, et al. Preprint IFVE SEF 69-78,
   Serpukhov, 1969.
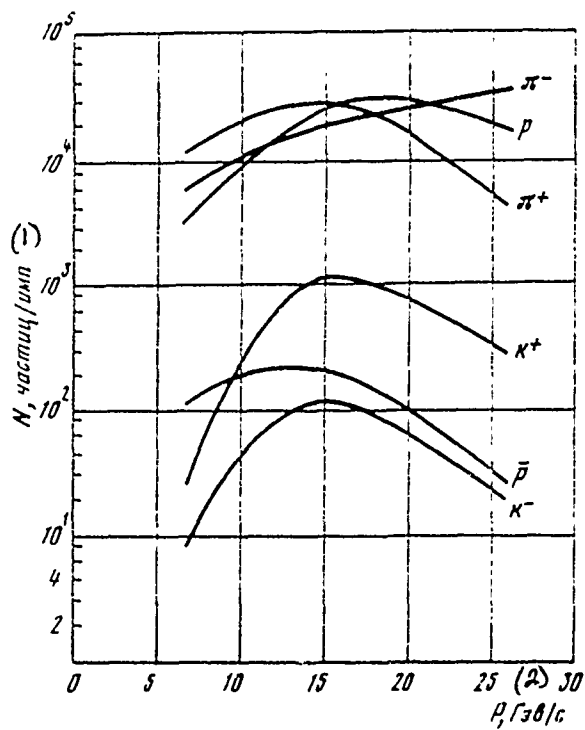
Fig. 4. Expected flows of the separated particles on the bubble
chambers/cameras with the energy of acceleration 70 GeV (flow of
primary protons 10^{11} pulses^{-1}, efficiency of target 0.1
$\Delta p/p = +-0.25o/o$, coefficient of the transmission of cluster absorber
0.5: for π^- they are given maximum flows without the separation).

Key: (1). particles/pulse. (2). GeV/s.

149. On some possibilities of the formation of the muon beams of high energies.

I. A. Aleksandrov, Yu. P. Dobretsov, B. A. Dolgosheni, A. V. Samoilov, V. A. Titus, A. M. Frolov, I. A. Shukeylo.

(Institute of high-energy physics).

With the formation of the muon beams of high energies becomes possible the use/application of the magnetized iron for purposes of braking and focusing simultaneously, which can considerably simplify the creation of matching systems.

Let us examine the limited applications of a lens, which is the cut of the metallic cylinder, along which flows current I, evenly distributed over the section with a density of $j=\frac{I}{\pi R^2}$ (R - a radius of lens). The magnetic induction B within the cylinder has only azimuthal component and in the case of unsaturated iron is proportional to the radius: $B(r)=B_\varphi(r)=\mu\frac{2\pi}{c}jr=Gr$ (μ - magnetic permeability). This lens focuses or defocuses simultaneously in all transverse directions.

Let the particle momentum during the motion in the substance of lens change as $(p_0 - \varepsilon z)$, that correctly with

$$\varepsilon z \ll p_0 , \qquad (1)$$

where ε - ionizing losses at the radiation length, z - longitudinal coordinate in cylindrical system (τ, φ, z), τ and z they are measured in the radiation lengths. Then in the case of focusing equation of motion in the plane $\varphi = \text{const}$ takes the form

$$\tau''_{zz} = - \omega^2 \frac{\tau}{1 - \frac{\varepsilon z}{p_0 c}} , \qquad (2)$$

where $\omega^2 = \frac{eGt^2}{p_0 c}$, t - radiation length. Its solutions are Bessel function of the 1st kind the 1st order z_1:

$$\tau = \sqrt{1 - \frac{\varepsilon z}{p_0 c}} \; z_1 \left(2 \frac{p_0 c \omega}{\varepsilon} \sqrt{1 - \frac{\varepsilon z}{p_0 c}} \right) .$$

Page 194.

Under the assumption (1) this decision with an accuracy to the 1st order in $\frac{\varepsilon z}{p_0 c}$ can be presented in the form:

$$\tau = \cos(\omega z + \beta) - \frac{\varepsilon z}{4 p_0 c} \left[\omega z \sin(\omega z + \beta) + \cos(\omega z + \beta) \right] , \qquad (3)$$

where β is determined from the initial conditions. To account for multiple scattering was utilized the function of distribution [1]

$$F(z, \tau, \theta) = \frac{1}{2\pi B} \exp\left(- \frac{\theta^2 A_2 - 2\tau\theta A_1 + \tau^2 A_0}{4 A_0 B} \right) ,$$

where

$$A_0 = \frac{E_s^2 z}{4 p_0 (p_0 - \varepsilon z)}; \quad A_1 = \frac{E_s^2}{4\varepsilon^2}\left[\ell n \frac{p_0}{p_0 - \varepsilon z} - \frac{\varepsilon z}{p_0}\right];$$

$$A_2 = \frac{E_6^2}{4\varepsilon^2}\left[2z - \frac{z^2 \varepsilon}{p_0} - 2\frac{p_0 - \varepsilon z}{\varepsilon}\ell n \frac{p_0}{p_0 - \varepsilon z}\right];$$

$$B = (A_0 A_2 - A_1^2)^{1/2};$$

$E_s = 21.2$ MeV, θ - projection of angle $(p_0' z)$ on the plane of motion $\phi = const.$

The account of ionizing losses (ε) and scatter in the mean free path was conducted according to known experimental data (for example, see [2]). The numerical calculation of the parameters of muon beams was carried out according to the method of Monte Carlo. Let us examine some versions of the use of such lenses for the formation of muon beams.

1. Inhibiting muon channel.

According to the conditions for experiment it is necessary to take into the channel a maximally possible flow of muons with the impulse/momentum/pulse $p_0 = 22.66$ GeV/s and without the considerable losses to bring them to the detector, after inhibiting to the energy 200-500 MeV. Let us compare the transportation possibilities of two inhibiting muon channels. Isotropic- the consisting of 13.6 m

unmagnetized iron, and the anisotropic, consisting of the layer 0.8 m unmagnetized iron and muon lens with a diameter of 20 cm with a length of 12.8 m. Induction in the lens is considered as the linearly increasing with a radius and its maximum value on the edge is undertaken equal to 15000 G. Fig. 1 gives the envelopes of beams in both channels. A root-mean-square radius in the lens is everywhere less than in the isotropic iron. It reaches maximum on first 2.5 m and further nowhere it exceeds this its value. On inset of Fig. 1 is given the effectiveness of circuits E (relation of a number of particles, which fell to the infinitely thin detector, to a total number of particles, leaving from the target) in the dependence on a radius of detector R_q. It is evident that the use of a lens of the instead of unmagnetized iron makes it possible with the identical count to decrease the section of detector 30-40 times. Aperture ratio of anisotropic channel ≥ 4000 μster which is two orders higher in comparison with the case when for these purposes it is utilized any of the acting pion channels IVFE (for example, see [3]).

2. Beam of pure/clean muons.

Usually for obtaining the energetic muon beam utilize the decay pion channels, which consist of 15-20 quadrupole lenses. For the isolation/liberation of the muons before the detector is placed nuclear filter of the iron or another substance, following it - the

focusing objective. Use as the filter of muon lens makes it possible to get rid of subsequent objective (doublet or more complicated system of quadrupole lenses) and to directly focus beam to the detector.

Let on the filter with a thickness of 8 m fall the parallel beam from the impulse/momentum/pulse 30 GeV/s, shaped with the preceding/previous magneto-optical system. The diameter of beam let us accept equal to 20 cm. Fig. 2 gives envelope of particles in the case of filter from the unmagnetized iron, its combination with the doublet of quadrupole lenses and in the case of the lens with a diameter of 20 cm with gradient $G = 1500$ G/cm. During the replacement of the unmagnetized filter with the doublet by one muon lens it is possible to completely preserve the parameters of beam.
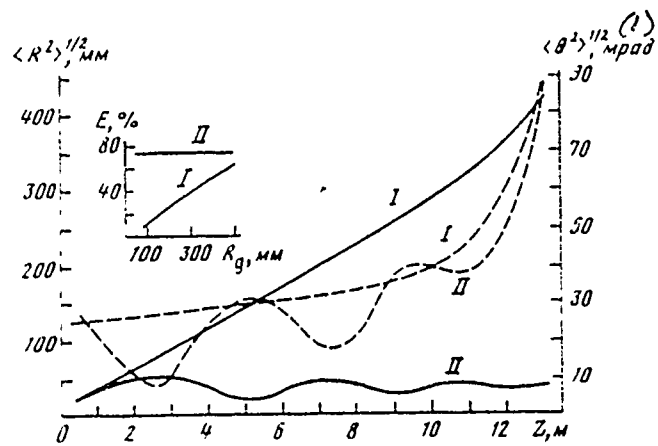
Fig. 1. Envelope of particles (solid line) and root-mean-square angle
(dotted line) in the isotropic (1) and the anisotropic (II)
inhibiting muon channels. On the fitting - effectiveness of channels
with different radii of detector R_q

Key: (1). mrad.
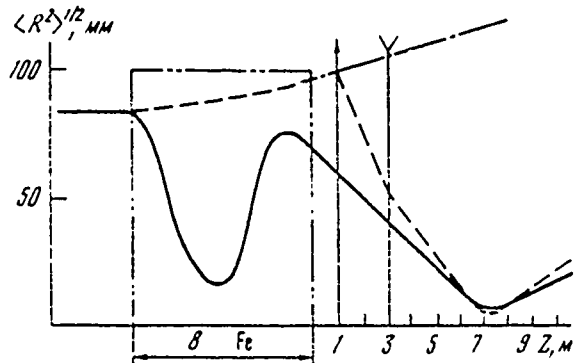
Fig. 2. Envelope of particles in muon channel; unmagnetized iron
(prime dotted line); unmagnetized iron and doublet of quadrupole
lenses (dotted line); muon lens (solid line).

Page 195.

3. Beam of pure/clean muons without the pion channel.

Large muon lens can combine the function of capture and beam shaping, nuclear protection and subsequent objective. Fig. 3 gives envelope of particles in the channel, which is of the target, the decay gap/interval the length of 200 m and muon lenses with a diameter of 2 m with the induction on 15000 G edges. Is given the position of crossover for the partial beams p_0=20, 30, 40 GeV/s, and nonmonochromatic beam with uniform spectrum (30+-10) GeV/s. Evidently that crossover clearly is observed not only in partial bundles, but also in polychromatic beam with considerable pulse scatter $(p_0$+-33o/o).

4. Focusing target.

Target for studying muon interactions with the large transmission of impulse/momentum/pulse represents the iron cylinder with a diameter of 10 cm and with a length of L. Fig. 4 depicts the case when to the target gives the parallel beam of muons $(p_0$=30 GeV/s). Unbroken curve is represented the decrease of flow Π along

the unmagnetized target due to the escape through side walls. The same dependence for the magnetized target with linearly building up on a radius induction B shows that the lens "holds" beam considerably better. A change of the flow in this case is clearly correlated with a change in the envelope - in the maximum of the envelope the greatest losses.

At the high values of $B(r)$ the iron of lens in the the peripheral range is saturated. This case was approximated in the calculations by the law of the build-up of field in the form of trapezoid. From the calculation it follows that the transition into the mode/conditions of saturation can somewhat raise flow.

Fig. 5 gives the effectiveness of target in the dependence on the length. It is evident that the use of the lens with a length ~10 of a raises effectiveness in comparison with the unmagnetized target approximately 2 times.

REFERENCES

1. L. Evges. Phys. Rev., 1918, 74, 10, 1534.
2. R.M. Sternheimer. Phys. Rev., 1960, 117, 485: 1959, 115, 137.
   J.A.Gerbel, J.Ranft. Nucl.Instr.and Methods, 1965, 32,65; J.Ranit,CERN,1964,64-47.

3. I. A. Aleksandrov, M. I. Grachev, K. I. Gibriyenko, et al. Preprint IFVE OP 69-36, 1969.

Discussion.

L. L. Gol'din. What value currents must be passed through your lenses?

I. A. Aleksandrov. If we are restricted to fields 12-13 kg on the edge, then currents on the order of 1 kA. With further increase in the field the required currents sharply grow/rise. Thus, if field on the edge 15-16 kg, then currents already on the order of 3 kA.
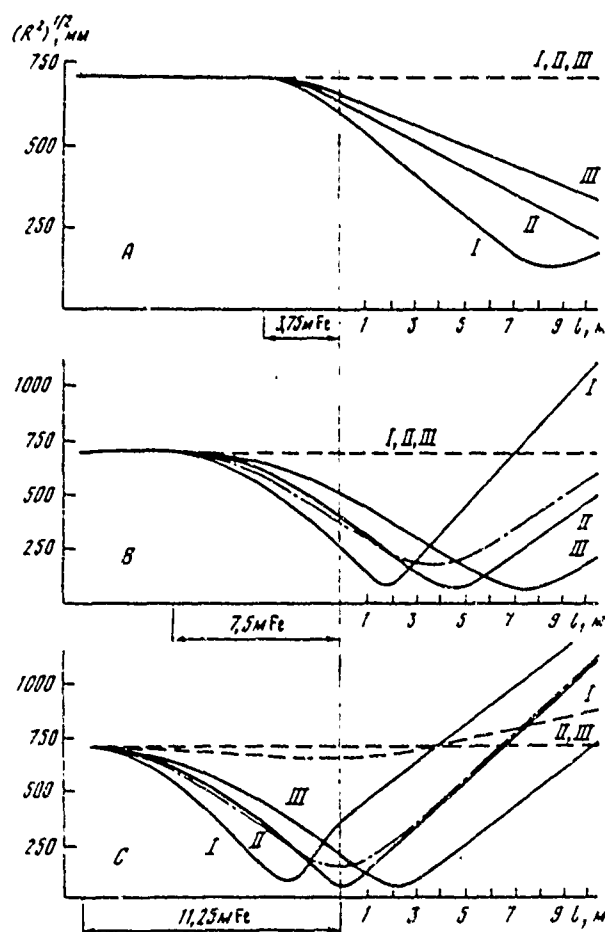
Fig. 3. Envelopes of partial and polychromatic beams in the muon channel with the lens with a diameter of 200 cm. a) the length of lens is 3.75 m; b) the length of lens 7.5 m; c) the length of lens 11.25 m; I - 20 GeV; II - 30 GeV; III - 40 GeV; polychromatic beam (30+-10) GeV.
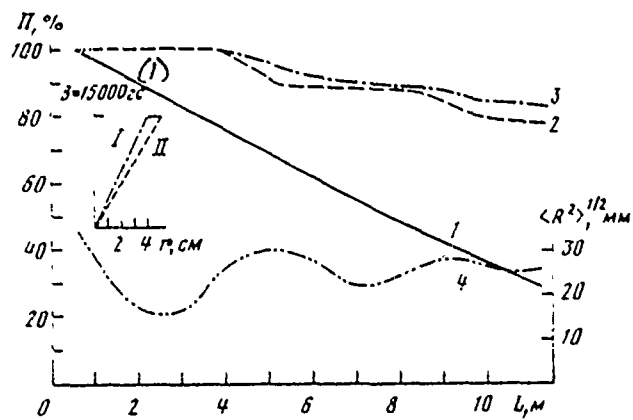
Fig. 4. Change in flow cf muons n along the length of muon target.
1 - isotropic detector: 2 - lens with a linear increase in the
induction from a radius; 3 - saturated lens; 4 - envelope of
particles in the unlimited in transverse direction of lens with the
linear build-up/growth of induction. On the fitting: the
build-up/growth of induction on a radius of that extra-saturated (I)
and saturated (II) lenses.

Key: (1). G.
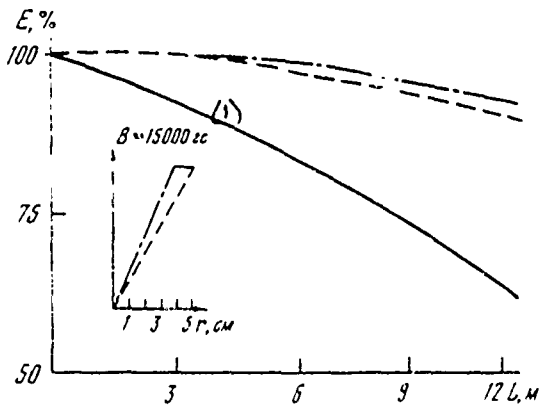
Fig. 5.

Fig. 5. Dependence of effectiveness of muon target E on length. Designations the same as in Fig. 2.

Key: (1). G.

Page 196.

150. Diagram of obtaining antiprotons on an installation with opposing proton-antiproton beams.

G. I. Budker, T. A. Vsevolozhekaya, G. I. Silvestrov, A. N. Skrinskiy.

(Institute of nuclear physics of the Siberian Department of the AS USSR).

The project of obtaining the intense beam of antiprotons for the experiments on the opposing proton-antiproton beams with the energy 2x25 GeV in the installation VAPP-NAP assumes the accumulation of antiprotons by the method of electronic cooling [1] with the energy 1.8 GeV in the intermediate accumulator/storage NAP.

The actualization of project requires the development of the series/row of the complicated impulses/momenta/pulses of the magneto-optical devices/equipment, what is by partly developing in

with Novosibirsk the institute of nuclear physics of program on the use of strong and ultrapowerful (megagauss) pulse magnetic fields in the accelerative technology.

In the present work are examined questions of formation and introduction/input into the accumulator/storage of the bundle of antiprotons with the energy 1.8 GeV and the focusing to the target of primary protons.

Antiprotons are obtained in external target with the aid of the proton beam, accelerated to 25 GeV in the basic ring VAPP and then released and focused to the target. In this case the selected relationship/ratio of energies of antiprotons and primary protons close to the value, which corresponds to the maximum of the generation of antiprotons in the case of target from heavy substance, as it is possible to conclude from the experimental data for Pb, given in work [2].

The angular distribution of antiprotons with the energy 1.8 GeV according to the data of this work, extrapolated into the region low energies of secondary particles, can be expected by close one to the Gaussian with root-mean-square angle $\sqrt{\bar{\vartheta}^2}$ 0.15 rad.

Total number of antiprotons at the output of target on the

assumption that entire path to its end/lead they pass to target materials, depends on the length of target as $P(\ell) \sim \rho_0 \cdot \frac{1}{\sigma_{in}n}$ and reaches maximum $P_m = \frac{1}{e} \frac{d\bar{\sigma}}{dp} \frac{\Delta p}{\sigma_A}(\rho_A$ - the section of inelastic interaction of protons and antiprotons with the target nuclei, $\frac{d\bar{\sigma}}{dp} \Delta p$ - production cross section of antiproton with the impulse/momentum/pulse in the assigned time interval (p, p+Δp) n - number of nuclei into 1 cm^3) when $\ell = \frac{1}{\sigma_A n}$, to the length of inelastic nuclear interaction.

The root-mean-square emittance of antiprotons $\bar{\phi}$ under the assumption of infinitely thin proton beam, increases with the length of target proportional to unit $(\bar{\phi} = \bar{\theta}^2 \rho)$ also, with the dyne l=10 cm, which is approximately/exemplarily equal to the length of inelastic nuclear interaction in the tungsten, it is 225 mrad cm and has a form, shown in Fig. 1. It is obvious that with this emittance the anti-proton beam cannot be effective seized in the accumulator/storage.

For increasing the capture efficiency in IYaF of SO AN USSR is developed/processed the method of the beam shaping of secondary particles directly on the target by the method of the transmission on it of large (~10^6 A) current. The appearing magnetic field does not make it possible for particles to be driven out from the axis/axle of system, forcing them to oscillate within size/dimension $v_{max} = \theta_{max}\sqrt{\frac{pc r_0}{e H_0}}$, where v_0 - radius of target, H_0 - field on its surface,

as θ_{max} it is possible to take the rms value of the angle of the generation of antiprotons.

The emittance of beam in this case does not depend on the length of target and is determined only by the gradient of magnetic field and by the width of the angular distribution of antiprotons.

DOC = 80069316   PAGE 820
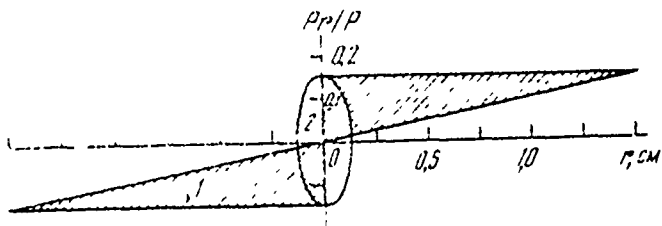
Fig. 1. Emittance of the beam of antiprotons at the output of the
target with a length of 10 cm. 1 - without the field in the target; 2
- in the field in the target with gradient $\nabla H = 1,3.10^7$ Oe/Ω.

Page 197.

In comparison with the target without the field occurs the decrease
of the emittance of beam, that it does not contradict Liouville
theorem, since secondary particles are born directly in the magnetic
field effect of which on the primary protons can be
disregarded/neglected (in the first approximation,) in view of the
large difference in the energies and the smallness of the phase
volume of proton beam, which makes it possible to focus it into a
small size/dimension at the entire length of target.

In the case in question the root-mean-square emittance of
anti-proton beam decreases to ~50 cm mrad during the creation in the
target of magnetic field with gradient $\nabla H = 1,3.10^7$ Oe/Ω. This it
requires current density in the target into 220 kA/mm², with which

the repeated use of a target is impossible.

Therefore it is proposed to utilize a target once with the automatic replacement cf its new for the time between the cycles, which is determined by the rate of "electronic cooling" and is ~100 s. It is essential only so that the decomposition of target would cccur after the first maximum of current, which can be achieved/reached for the sufficiently short duration of the half-period of current, since the development of strains in the target is iteration prccess.

From the results, achieved/reached by us at the present time, should be noted obtaining rield into 1.3 MOe on the surface of rod from tungsten with a diameter of 2 mm for the duration of the half-period of current in 1.35 μs. In this case occurred the full/total/complete evaporation of target, which began, however, after the maximum of current, as it is possible to conclude from the type of oscillogram. In the field into 1 MOe it was observed only the partial decomposition cf target in the bearing edge.

The short duration of the half-period of current unavoidably advances a question about the heterogeneity of current distribution according to the section of target. Actually/really, for the duration of ~1 μs the thickness cf skin-layer in the tungsten is ~0.2 mm.

However, heating targets to the temperature, close to the melting point, leads to an increase in the specific strength of materials of target, so that skin-layer becomes comparable with its radius.

The task of the focusing of protons to the target into a small size/dimension at entire its length in the case of target with the current becomes complicated by the defocusing of proton beam in the target and requires for its execution sufficiently strong lens. In our case the proton beam with emittance $\varphi = 5 \cdot 10^{-4}$ rad cm can be focused into the root-mean-square (along the length of target) size/dimension of $+-0.35$ mm with lens in focal length approximately 25 cm.

With the energy of protons 25 GeV this lens can be based only on the axisymmetric focusing with the field of forward current, with the possessing maximum focusing force. The developed/processed by us lens is rod with the current from beryllium or titanium with a diameter of 1 cm and with a length of 6-8 cm, with the field on the surface to 300 kOe.

For the collection from the target of the beam of antiprotons with the angular divergence $+-0.15$ rad and the scatter along the impulses/momenta/pulses in several percent is required the lens not only high-aperture, but also sufficiently short-focus, that the

angular scatter at its output, caused by chromatic aberration, would not exceed phase angles in the beam. For this purpose is developed/processed explosive parabolic lens with focal length of ~20 of cm, with the current ~1.5•10⁰ A and the field to 600 kOe. The current surfaces of lens serve simultaneously as the electrodes of discharger/gap, moreover explodes only the exit surface of lens, which has the form of plane and therefore easily changed [3].

The accumulator/storage of antiprotons is a racetrack with four long straight sections (length ^{7} m with a radius of quadrants R=3 m), cne of which it is abstracted/removed for injection and conclusion/output of antiprotons, and the others for the electronic cooling and the resonator. The magnets of quadrants have zero gradient and edge focusing, symmetrical relative to the centers of quadrants, what provides constancy ψ - to function in the linear gaps/intervals, necessary for the successful "cooling" of antiprotons.

The aperture of accumulator/storage $A_z \times A_R = 4 \times 32$ cm^2 makes it possible to seize beam of particles with the emittance to 70 mrad cm and scatter along the impulses/momenta/pulses $\Delta p/p = +-2.5•10^{-2}$.

The conditions for "electronic fading" require the minimum energy scatter of particles at each point; therefore admitted beam

undergoes chromatic dispersion in accordance with values ψ - function in the linear gap/interval of accumulator/storage. As a result the scatter on the impulses/momenta/pulses at each point does not exceed $\Delta p/p = \pm 0.60/c$.

The chromatic dispersion of the admitted beam is accomplished by the rotary magnet M_1 (see Fig. 2) and following after it lens L_1 whose focal length is connected with the angle of rotation φ and the index of a field slope n of magnet and   with the ψ-function of accumulator/storage by relationship/ratio $F = \psi \frac{\sqrt{1-n}}{\sin\psi\sqrt{1-n}}$.

The introduction/input of particles into the accumulator/storage is conducted in the beginning of intake gap/interval on the vertical line from below by magnets M_2 and M_3 (Fig. 2), upper playing the role of a septum-magnet in thickness of wall of less than 1 cm. Admission at the entrance into the quadrant, optimum for the stress/voltage on the inflector, would require the duplication of the vertical aperture of accumulator/storage, since the emittance of the admitted beam is virtually equal to the admittance of accumulator/storage [1].

FOOTNOTE [1]. The capture of beam with this emittance is feasible with the pulse sinchronization of inflector with the moment/torque of passage by its previously stacked beam, so as to the latter would not fall in the field of inflector. ENDFOOTNOTE.

The presence of long gap/interval makes it possible to inject beam at small angle to the median plane directly into the inflector, arranged/located in the same gap/interval. in this case the shock of inflector it must be increased approximately 1.7 times in comparison with the optimum diagram of injection [4]. Furthermore, the distance between the plates of inflector must be equal to the doubled aperture of path/track, which even more increases stress/voltage on the plates, namely of up to approximately +-500 kV in the contrary traveling wave.

For decreasing this value it is proposed to carry out an injection through the plate of inflector as follows: space between the plates can be divided into two fields - field of the aperture of the accumulator/storage where livas the seized beam and the field of inflector must be created in the form of impulse/momentum/pulse with the duration smaller than the period of revolution, and by steep wave fronts, that also present basic difficulty, and the region, which is located lower than the aperture where it is possible to create quasi-permanent magnetic field into ~300 e, that ensures the corrective turn of the lower part of the beam.

Page 198.

These regions are separated by current partition by the thickness
into several the tenths of millimeter, through which the beam is
passed virtually without the losses. This partition is the upper part
of the volumetric plate of inflector and the "knife" of unusual
septum-magnet, which is located within the plate. This method of
injection substantially decreases the difficulties of designing of
high-voltage oscillator for the inflector.

The described diagram of obtaining and injection of antiprotons
will make it possible to gather all particles in the root-mean-square
angle of generation in the prescribed/assigned momentum range and to
bring the coefficient of capture into the accumulator/storage to
$\cdot 10^{-3}$.
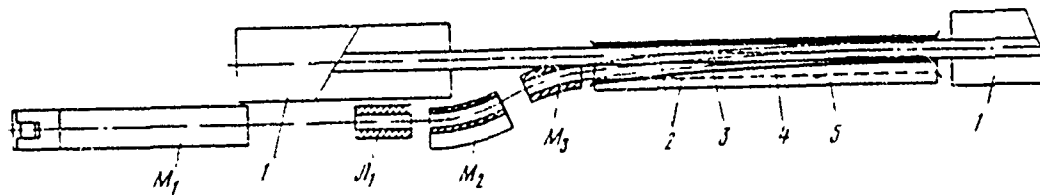
Fig. 2. Diagram of the injection of antiprotons into the accumulator/storage. M_1 - rotary magnet; L_1 - lens; M_2 and M_3 - intake magnetic 1 - magnetic accumulator/storage; 2 - upper plate of inflector and position of lower (dotted line) with the admission with that doubled distance between the plates; 3 - separating current foil; 4 - current busbar/tire of septum-magnet; 5 - volumetric lower plate in the case of the admission through the foil.

REFERENCES.

1. G. I. Budker. AE, 1967, 22, No. 5.
2. D. Dekkers, et al. Phys. Rev. Ser. 2. 1765, 137, N 413, p. 962.
3. T. A. Vsevolozhskaya, L. L. Danilov, V. N. Marasvuk, G. I. Sil'vestrov. Parabolic Lensis for the Focusing of Secondary Particles with an Energy of Several GeV. See this Collection, Vol. II
4. T. A. Vsevolozhskaya, G. I. Sil'vestrov. A. N. Skrinskiy. Trudy All-Union Conference on Charged Particle Accelerators, M. 1968. p. 495.

151. Aberrations and allowances in the system of the
monochromatization of the external beam of isochronal cyclotron.

Yu. G. Basargin, V. I. Bogdanova, O. A. Minyaev, Yu. P. Severgin.

(Scientific research institute of electrophysical equipment im. D. V.
Efremov).

N. I. Venikov, N. N. Posel'siy, Ya. M. Khodakov.

(Institute of atomic energy im. I. V. Kurchatov).

The description of system earlier was given in work [1], where
also are contained the results of the ion-optical calculations,
carried out in the linear approximation/approach, whence follows the
possibility of the tenfold decrease of energy scatter, if the phase
width of monoenergetic ion clusters does not exceed 6° at the
entrance into debuncher. The present communication/report supplements
work [1] by the results of the calculations of the longitudinal and
transverse aberrations of the second order, which appear with wiring
of the bundle through longitudinal separator-achromatic rotary system
(see figure). Furthermore are evaluated allowances.

Calculation method.

Was integrated the system of three equations, which describes with an accuracy down to the terms of the second order of smallness particle motion in the curvilinear system of coordinates [2]

$$x'' + (1-n)h^2 x = h\delta + (2n-1-\beta)h^3 x^2 + h'xx' +$$
$$+ \frac{1}{2}hx'^2 + (2-n)h^2 x\delta + \frac{1}{2}(h'' - nh^3 + 2\beta h^3)z^2 +$$
$$\cdot h'zz' - \frac{1}{2}hz'^2 - h\delta^2 + f_x^* ;$$
$$z'' + nh^2 z = 2(\beta - n)h^3 xz + h'xz' - h'x'z + hx'z' +$$
$$+ nh^2 z\delta + f_z^* ;$$
$$\sigma + \frac{1}{\gamma^2}\delta = -hx - \frac{1}{2}(x'^2 + z'^2).$$

Page 199.

Here x and z - horizontal and verticals deflection from the basic orbit; σ - the longitudinal deflection of particles from the center of gravity of cluster; a - curvature of basic orbit; δ - relative heterogeneity of impulses/momenta/pulses; n and β - respectively generalized the field index and the coefficient of its quadratic nonlinearity; γ - relativistic factor; f_x^* and f_z^* - functions, which consider the divergences of the parameters from the ideal ones; differentiation is produced on the arc of basic orbit.

Reference point for the horizontal and longitudinal motions was
undertaken at a distance of ~3.0 m before magnet m_1 (see figure); for
the vertical motion this distance is equal to ~3.6 m. At the points
indicated is assumed the distribution of initial conditions on the
phase rolling planes within the rectangles with the sides

$$2x_0 = 0.2 cm; \quad 2z_0 = 0.5 cm; \quad 2x_0' = 2 \cdot 10^{-2} rad,$$
$$2z_0' = 8 \cdot 10^{-3} rad.$$

The heterogeneity of impulses/momenta/pulses is assumed to be equal
to $\delta = +-10^{-3}$. In the calculations were utilized the geometric and
magnetic parameters of system, indicated in [ ]. Coefficient β in
270- degree magnets is accepted equal to 0.69 (conical of pole).

Quadratic corrections for the focusing by the fringing field of
sector magnets were introduced under the assumption of "rigid" edge.
With the bent boundary of rotary magnet with field B_0 in basic orbit
the effect of a radius of bending R is equivalent to effect from the
sextupole lens of length 1 with the "gradient" $\frac{1}{2} \frac{\partial^2 B}{\partial x^2}$, if is
fulfilled the relationship/ratio:

$$\frac{1}{2} \frac{\partial^2 B}{\partial x^2} \ell = -\frac{B_0}{2R} \sec^3 \varepsilon.$$

2. Axial motion.

Longitudinal divergence of particles relative to the center of
gravity of cluster is calculated at the output of system after magnet

m¦in the point, the symmetrical initial. With an accuracy down to the terms of the second order of smallness this divergence (in the centimeters) is expressed by the dependence

$$\sigma = \sigma_0 - 75104\delta + \begin{vmatrix} -13.8\cdot10^6 \\ 0 \end{vmatrix}\delta^2 + \begin{vmatrix} 4.16\cdot10^5 \\ 0 \end{vmatrix}\delta\cdot x_0' +$$

$$+\begin{vmatrix} -11.4\cdot10^3 \\ 0.09\cdot10^3 \end{vmatrix}\delta\cdot x_0 + \begin{vmatrix} -55.2 \\ -3.03 \end{vmatrix}x_0^2 + \begin{vmatrix} -3.6\cdot10^3 \\ -0.35\cdot10^2 \end{vmatrix}x_0'^2 + \begin{vmatrix} 139 \\ -46.4 \end{vmatrix}x$$

$$\times x_0 x_0' + \begin{vmatrix} 4.42 \\ -5.8 \end{vmatrix}z_0^2 + \begin{vmatrix} 0.199\cdot10^3 \\ -0.5\cdot10^4 \end{vmatrix}z_0'^2 + \begin{vmatrix} 25.5 \\ -112 \end{vmatrix}z_0 z_0'.$$

The second term corresponds to the efficiency of the longitudinal separation of particles on the impulses/momenta/pulses, which reaches +-75 cm. The upper values of coefficients correspond to the connected corrective sextupola lenses. In this mode/conditions the maximum aberrational broadening (shift) of clusters reaches 26 cm, which corresponds to the broadening of monoenergetic clusters to inadmissibly high value of 13°. The greatest contribution introduce in this case the terms, proportional to δ_2 and $\delta x_0'$. The parameters of sextupole lenses are selected for the purpose of becoming zero appropriate coefficients. For lenses SP_2 and SP'_2 dimensionless parameter $\frac{1}{2}\frac{\partial^2 B}{\partial x^2}\frac{\ell^3}{B\rho}=0.0475$; for lenses SP_3 and SP'_3 it is equal to 0.0454 (length of lenses l=40 cm). In the compensated mode/conditions (lower coefficients maximum aberrational broadening is 0.6 cm or 0.3° on the

phase.

3. Transverse motion.

At the output of system the parameters of transverse horizontal motion with the connected sextupole lenses are determined by the expressions:

$$x = -x_0 - 2,57 \cdot x_0^2 - 1,04 \ 10^3 x_0'^2 + 58,1 \ x_0 x_0' + 62,2 \delta x_0 +$$
$$+ 1,3 \delta x_0' - 2,95 z_0^2 - 5,5 \cdot 10^3 z_0'^2 - 133 \cdot z z_0' - 0,13 \cdot 10^5 \delta^2;$$

$$x' = 6,97 \cdot 10^{-2} x_0 - x_0' - 0,76 \cdot 10^{-2} x_0^2 + 41,1 \cdot x_0'^2 + 0,33 x x_0' +$$
$$+ 1,34 \delta x_0 - 187 \delta x_0' - 8,4 \ 10^{-3} z_0^2 + 99,9 \cdot z_0'^2 - 0,06 z_0 z_0' -$$
$$- 0,13 \cdot 10^3 \delta^2.$$

From these expressions it is evident that at the point of horizontal focus the aberrational broadening composes not more than 0.8 cm and aberrational angle not more than 3•10⁻³ rad. Similarly the calculated aberrational broadening z at the point of vertical focus is not more than +-0.4 cm and the aberrational angle z¹ is not more than +-2•10⁻³ rad.
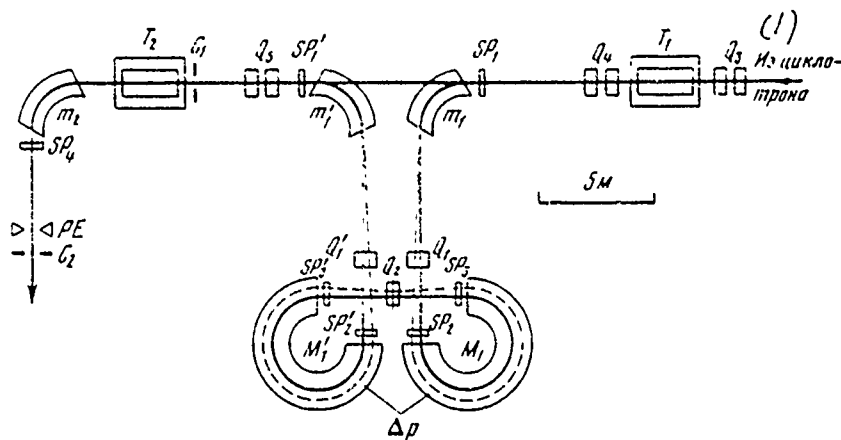
system of monochromatization.

Key: (1). From the cyclotron.

Page 200.

The optimization of the aberrations of transverse motion is possible by the selection of the parameters of the six-pole lenses SP_1 and SP^1_1, which do not affect longitudinal motion. From the estimations conducted it follows that the start of these lenses decreases the linear and angular aberrations approximately/exemplarily doubly.

4. Allowances.

Were carried out the calculations of the

disturbances/perturbations, caused by the imperfection of the geometry of system and by the temporary/time instabilities of magnetic fields.

The inadequacy of geometry leads in limits of accuracy of calculations only to the stationary longitudinal shift/shear of center of gravity of cluster and it does not affect the resolution of the diagram of monochromatization. However, it gives the lateral misalignment of beam at output of system. Geometric allowances were estimated, on the basis of the maximum root-mean-square disturbance/perturbation of the angle of axial trajectory, equal to $+-10^{-3}$ rad. Allowance for the transverse displacement of the magnetic axes of the quadrupole lenses Q_1, Q'_1 and Q_2 is $+-0.1$ mm, the longitudinal displacement of these lenses must be not more than $+-2$ mm and rotation relative to center is not more than $+-10^{-3}$ rad. Allowances for transverse displacements 270- and 90-degree magnets are $+-0.5$ mm, longitudinal displacements $+-2$ mm and angular $+-10^{-4}$ rad. Allowance for the value of the index of a field slope in 270-degree magnets composes $+-0.1$o/o. The geometric allowances indicated can be provided with both the use/application of means of geodesy and with use of the corrective windings in the lenses and in 270- degree magnets.

The temporary/time instabilities of the fields of rotary magnets

lead both to the instability or the longitudinal position of clusters
and to the unsteady lateral misalignment of beam at output of system.
To the latter/last effect it leads also an inaccuracy in the setting
up of fields in the magnets with the control of energy. If four
rotary magnets are excited from the independent power supplies, then
with the stability of field in each magnet (M, M'_1, m_1, m'_1) +-$2 \cdot 10^{-5}$
and the same precision/accuracy of the setting up of field will occur
instability of +-0.6° phase of cluster in debuncher and instability
+-$2 \cdot 10^{-3}$ rad of the inclination/slope of the axis/axle of beam at
output of system. With the series feed of the excitation windings of
all four magnets from one source in view of achromaticity of system
generally is absent the lateral misalignment of beam at output of
system. In this case the instability +-$2 \cdot 10^{-5}$ of field current leads
to instability of +-0.8° phase of cluster; is permitted the
precision/accuracy of +-10^{-4} settings up of current with the control
of energy. The stabilization or coil current of quadrupole lenses
with precision/accuracy +-10^{-4} is more than sufficient.

Allowance for the phasing of resonators of +-1°; allowance for
the amplitude of stress/voltage - +-$2 \cdot 10^{-3}$.

5. Conclusion.

Results of the calculations of aberrations and allowances

confirm the possibility of the tenfold decrease of the energy scatter of cyclotron beam with phase width of 5° and with the transverse emittance 30÷40 mm mrad. Upon the start of sextupole lenses the aberrational broadening of clusters does not exceed 0.5° and effective transverse emittance is not more than twice. Allowances for the geometry of the elements of system and for the stabilization of magnetic fields are virtually fulfilled.

REFERENCES.

1. Yu. G. Basargin, V. I. Bogdanova, M. I. Vesikov, F. N. Korol', N. N. Posel'skiy, Yu. P. Severgin. Atomnaya Energiva. 1970, No. 8.
2. V. I. Kotov, V. V. Miller. Focusing and Fission for Masses of High-Energy Particles. Moscow. Atomizlat, 1963.

152. Procedure of beam extraction on the accelerator of "Nimrod".

D. Grey, M. Harold, R. Morgan, N. Knig, M. O'Konnel.

(Rutherford high-energy laboratory, England).

tav introduction.

The proton synchrotron of "Nimrod" to the energy 7 GeV with the intensity $2.5 \cdot 10^{12}$ protons per pulse has three lines of beam extraction (Fig. 1). Two of them (X1 and X2) work from one deriving/concluding magnet. At the flat/plane pulse apex the current of magnet they change over, providing rapid beam spill for line X1 and slow discharge/break for lines X2. Third line (X3) services/maintains new experimental hall and it emerges at angle of 90° relative to line X1. Until June 1970 for both channels was utilized the achromatic method of conclusion/output [1] without the energy losses and the effectiveness of conclusion/output were usually approximately 30o/o. For each channel, except the deriving/concluding magnet, is necessary plunger quadrupole lens. Since more than 80o/o circulating beam utilize for the conclusion/output, were developed the test plans of other two methods which must increase the

effectiveness of conclusion/output.

Page 201.

The first of these methods, named "Piccioni's diagram with the
thin shielding partition" [2], were developed to January 1970 and was
utilized on line X3. The second method "resonance conclusion/output"
[3] was also tested, but for its optimization were necessary further
investigations.

Piccioni's diagram with the thin shielding partition.

As it follows from the name, this method requires the use of
plunger deriving/concluding magnet (XM10) with the thin shielding
partition which in practice has a thickness of 11 mm (Fig. 2). Beam
they guide to beryllium target with a length of 1.85 cm, the most
probable energy loss in which is 5.1 MeV. Due to an abrupt change in
the closed orbit the large part of the beam enters in XM10 for one
revolution later and is deflected/diverted in the direction of
half-quadrupole XHQ2, located in the fringing field "Nimrod" (Fig.
3). This quadrupole partly removes the large radial divergence of
beam, introduced by fringing field. Further protons enter into the
first elements of the line of beam extraction.

The starting/launching of diagram with the thin shielding partition was considerably entreated by the use of a system of cybernetic control, put into operation six by months earlier. Was first introduced current ramp in XHQ2, which made it possible, to accelerate normal beam with the intensity $2 \cdot 10^{12}$ protons per pulse to the energy 7 GeV. The fears that this will prove to be difficult operation/process due to the interaction between "Nimrod" and quadrupole lens, proved to be unsubstantiated. From the very beginning it became possible to accelerate normal beams, supplying XHQ2 by direct current. However, because the attracting forces force quadrupole lens strongly to be shifted/sheared with each impulse/momentum/pulse of "Nimrod", it it was necessary to displace relative to nominal position by 2.5 cm. Possibly, this causes certain loss of beam. At present is developed/processed the more durable holder for the quadrupole lens, which will make it possible to set it in the optimum position. The observation of beam is produced with the aid of the scintillators, placed before and after XHQ2. The results of observations confirm the conclusion that XHQ2 will cost not in the best position, since the beam interferes the far end of the neutral pole.

However, after the optimization of the length of beryllium target first time it was possible to derive of "Nimrod" $1.0 \cdot 10^{12}$ protons per pulse with the effectiveness only below 50 %. After

this on entrance XHQ2 they set coil irradiation by which showed that the beam has an expected form and a size/dimension and corresponds to 66o/o of circulating beam. Thus, the gear ratio of the line of beam extraction, which switches on XHQ2, composed 76o/o. It is known that XHQ2 turns the beam approximately/exemplarily on 3 mrad. This rotation they compensate by the supplementary quadrupole lens XHQ3, which ensures further focusing. However, can prove to be sufficient set instead of XHQ3 the small deflecting magnet, which will be that more moving rapidly, cheap and less complicated. It is assumed that this will make it possible to raise the effectiveness of conclusion/output to 60o/o.

Resonance conclusion/output.

Theoretical studies showed that it is possible to derive/conclude beam along the existing lines X1 and X3, utilizing resonance with Q_x-2/3. Realization of this became possible after the setting up of the deriving/concluding magnet with the thin shielding partition for Piccioni's modified diagram. Vertical-plunger magnet on the field 2 kHz is arranged/located to one octant before XM10, and it has the shielding partition with a thickness of 2.5 cm (Fig. 4). With the emergence of resonance the protons, which passed through this shielding partition, are deflected/diverted to inlet XM10 and then they will be ejected normally.
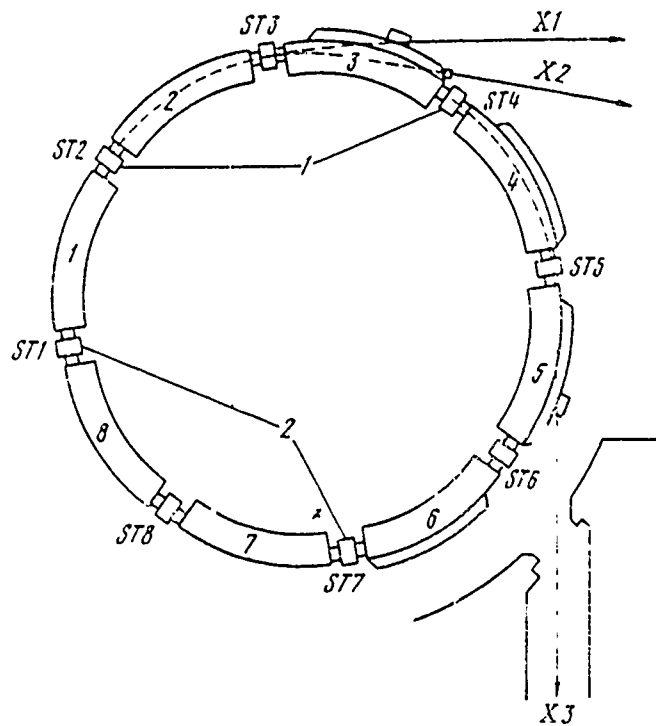
Fig. 1. The diagram of the layout of the sections of the conclusion/output of the accelerator: 1 - plunger magnets; 2 - plunger quadrupole lenses; X1, X2, X3 - channels of emitted beam.
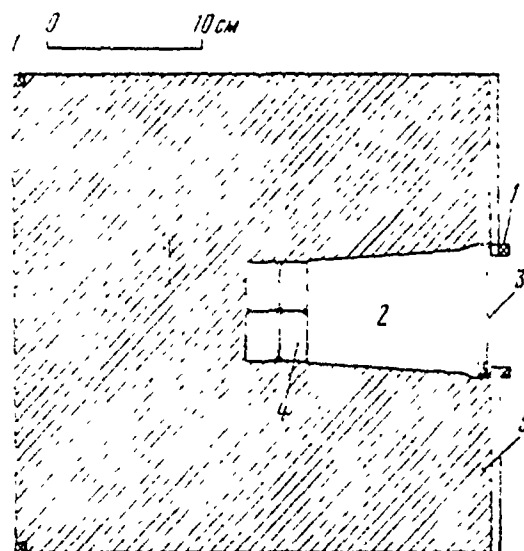
Fig. 2. Plunger deriving/concluding magnet XM10. 1 - winding for the compensation for magnetic resistance; 2 - aperture; 3 - shielding partition; 4 - winding for the compensation for external magnetic flux; 5 - magnet yoke.
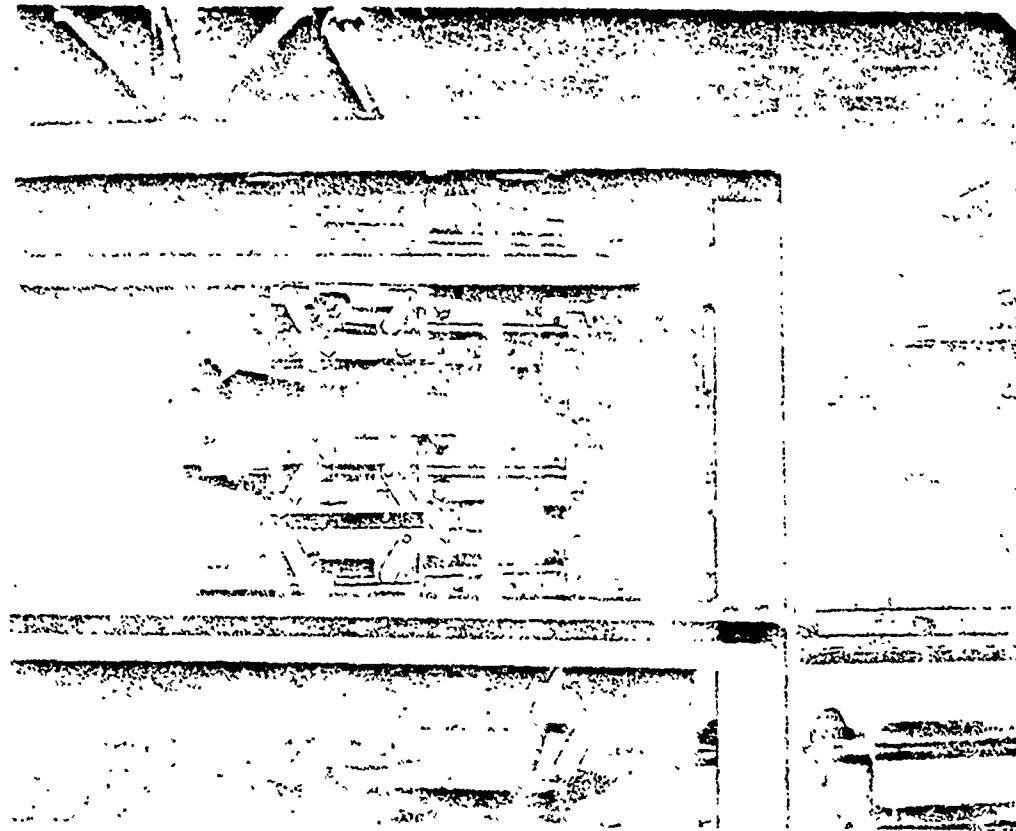
Page 202.

Fig. 3. Semiquadrupole XhQ2.

Fig. 4. Vertical-plunger magnet in field 2 kg.

Page 203.

Since "Nimrod" is accelerator with the large aperture, for the control of field gradient and for obtaining the necessary sextupole component of the second harmonic utilize the pole windings. Field gradient in the aperture of "Nimrod" with the intensity/strength 14 kg is shown in Fig. 5. On radius R_0 the field index n is equal to

0.7, which considerably exceeds the resonance value of $n_{2/3}=0.647$. With the approach to the resonance from the side of the higher values of n an increase in the amplitude is limited to the large octupole component of field (Fig. 6), in connection with which before beginning conclusion/output it is necessary to bring value of n approximately/exemplarily to 0.6. With the approach to resonance from the side of this lower value n for the protons affects the average/mean field gradient, which approaches $n_{2/3}$ in proportion to an increase in the amplitude, so that resonance is unconfined by useful aperture. With the approximation/approach to an external part of the aperture gradient they suppress, utilizing another pole winding, which creates the small purely sextupole component of field. This allows as one of the possible methods of discharge/break to direct beam into the unstable region. Another method of discharge/break in question consists in holding of beam on the circumference of a permanent radius and in an adjustable manner to increase n to value of $n_{2/3}$ for the elongation/extent of flat/plane pulse apex.

The width of the circulating beam varies from 12 to 15 cm. Since the region of a good field comprises the majority of the cases of altogether only of 20 cm, remains little place for the beam displacement. Furthermore, it is not possible to allow the penetration of protons too far into first magnet (RX3), since the nonlinear leading field on these small radii will distort the

characteristics of phase space upon transfer from RX3 to XM10. For
this reason RX3 they establish/install close to inward flange of
beam. As a result the compression in three revolutions on a radius of
the shielding partition is changed in the process of discharge/break
over wide limits with the decrease of size of stability region (Fig.
7). Another deficiency/lack is a large change in the divergence of
the concluded beam with the discharge/break (Fig. 8).

The first tests of this diagram were moderately encouraging. The
method of discharge/break consisted in the confining of beam on the
circumference of a permanent radius and increase n to $n_{2/3}$. The time
of discharge/break was approximately 100 ms. As it was expected,
proved to be to difficult control beam at the flat/plane pulse apex
without the premature losses; however, from 50 to 60o/o of
circulating beam it was possible to transmit to external target where
was obtained the spot of a good quality. The measured
sizes/dimensions of spot composed a total of several millimeters in
both directions. The foil, irradiated at the entrance into XMQ2,
recorded 70o/o of beam, but it detected the divergence of beam from
the horizontal axis (Fig. 9).
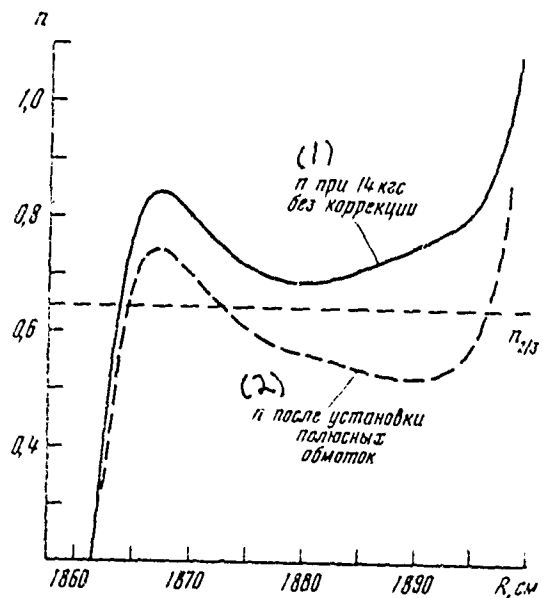
Fig. 5.
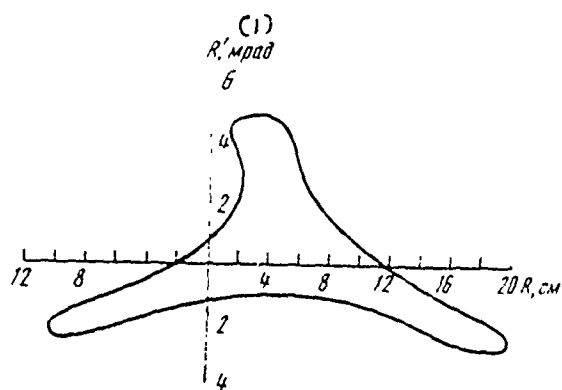
Fig. 6.

Fig. 5. Field gradient in accelerator of "Nimrod".

Key: (1). n with 14 kg without the correction. (2). n after setting up of pole windings.

Fig. 6. Octupole component of field.

Key: (1). mrad.
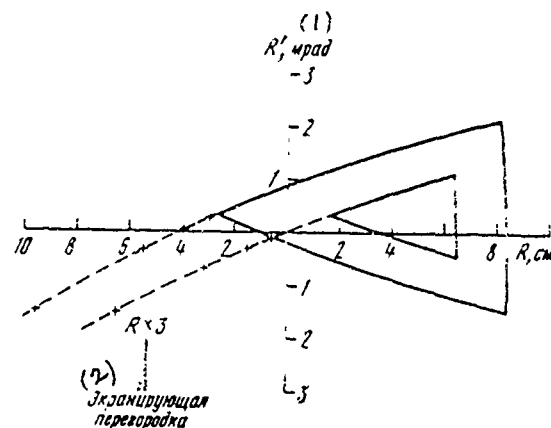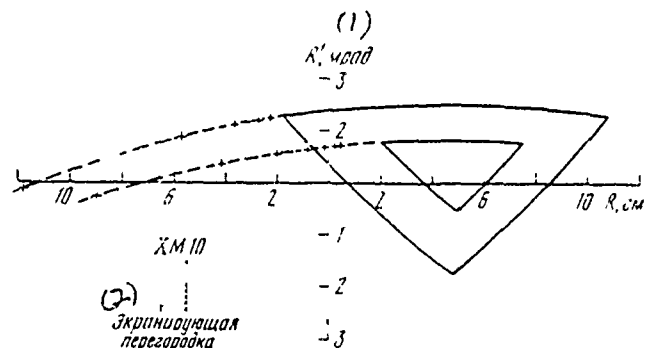
Fig. 7.   Fig. 8.

Fig. 7. Decrease of winding of stability during compression.

Key: (1). mrad. (2). Shielding partition.

Fig. 8. Change in divergence of concluded beam with discharge/break.

Key: (1). mrad. (2). Shielding partition.

Page 204.

The detailed laying out of the protons through the line of beam
extraction thus far it was not carried out, so that it cannot be
said, it does lead this divergence to the serious losses of beam.
Divergence is explained either by the errors for the leading field in

the median plane or by connection/communication with nearest

resonance $2Q_v - Q_\tau = 1$. Further program provides the detailed studies of

different methods of discharge/break, optimization of currents in the

pole windings and the control of the radial position of plunger

magnets. Is planned/glued to also replace RX3 with the magnet, which

contains the cooled on the periphery shielding partition by the

thickness of altogether only of 1.2 mm. In this stage it is not

possible to predict final effectiveness - for this it is necessary to

fulfill still much work.

Diagram with the energy losses on the thin shielding partition

in essence justified authors' expectations. It is assumed that after

the setting up of the mentioned above deflecting magnet will be

achieved/reached the effectiveness of order 60o/o. Since in this case

will not be required the plunger quadrupole lens, is decreased time

to the maintenance, will rise reliability and it will prove to be

possible to divide the circulating beam with external targets. If

this diagram was accepted for complex X1/X2, not only would increase

the effectiveness of these beams, but it would be possible to forego

the supplementary plunger mechanism.

Resonance conclusion/output requires supplementary plunger

mechanism and possesses known deficiency in the form of modulation of

discharge/break due to the presence of the pulsations of field. It is

difficult also to ensure the separation of beam with external
targets. Furthermore, the uncommonly high currents, consumed by pole
windings, remaining within the limits of allowances, indicate the
determination structural/design deficiencies and radiation damages,
which appear in the end connections. This led to the considerable
time losses in the period of starting/launching. Even if thes·
mechanical deficiencies/lacks it is possible to overcome, the
mentioned above difficulties in combination with the success,
achieved during the use of a diagram with the thin shielding
partition, will mean that the resonance method makes sense to accept
only upon reaching of effectiveness not less than 80o/o.
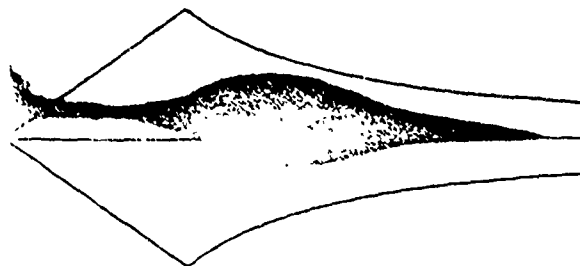
Fig. 9. Photograph of beam at entrance HXQ2.

REFERENCES.

1. R.G.T.Bennett, J.W.Burren. An achromatic system
   for extraction from proton synchrotrons. J. Nuclear
   Energy, part C, 1961, 3.
2. A.G.A.M. Armstrong et al. Energy–loss system with
   thin–septum plunged magnet at Nimrod. IEEE Trans. on
   Nuclear Sci., VS–16, No.3.
3. M.R. Harold. A resonant extraction system for Nimrod.
   RHEL, Nov. 1968, R/173.

153. Strong-focusing elements/cells for the beam steering in the systems of the transportation of beam.

S. Ya. Yavor, L. P. Ovsyannikova.

(Physiotechnical institute im. A. F. Joffe of the AS USSR).

Ye. Koltai, G. Sabo.

(Institute of nuclear research, Hungary).

In the literature is examined the series/row of different electron-/electronic- optical systems, utilized as the devices/equipment of beam steering in the systems of the transportation of beam. From experiment of practical work on the accelerators it is known that the position and the direction of beam at output of accelerator are subjected during the work of the accelerator to random changes For obtaining the stable conditions of irradiating the target it is desirable to create the systems of beam steering, capable of correcting such oscillations of beam. Among different known systems it is possible to indicate the magnetic and electrostatic deflection fields of different configurations.

Several years ago two of the authors of this work proposed the new elements/cells, based on the principle, experimentally checked in the institute of Nils Bohr in Copenhagen. In the literature these elements/cells are mentioned as "asymmetric quadrupole lenses". In the earlier work of the authors it was shown that during the new feed mode of the quadrupole lenses, available on each accelerator, it is possible to achieve beam steering without the introduction to the system of the transportation of the beam of new elements/cells.

Page 205.

As a result of the continuous operation, connected with the electron-optical description of such asymmetric lenses, was developed the electron-optical treatment of the first and third orders, and are also brought out and calculated the supplementary aberrations, called asymmetrization. Were simultaneously obtained experimental results for different systems on the accelerators in the institute of nuclear research in Debrecen (Hungary) and on van de Graaf's oscillator in the Joint Institute for Nuclear Research in Dubna. This latter/last work was carried out in the collaboration with I. Osetinskiy's group.

Will summed up below some enumerated above results for the

target convince scientists, who work on the accelerators, of the usefulness of asymmetric quadrupole lenses. For simplicity will here deal the question with electrostatic lenses, although the obtained results are real for the magnetic quadrupole lenses. Authors' experimental results were obtained on the electrostatic high-voltage accelerators; however, the same systems can successfully be used on other types of accelerators, switching on accelerators with the topmost energies.

The idea of asymmetrization is illustrated on given below figures. Fig. 1 shows normally symmetrical quadrupole field; generated by four cylindrical electrodes, moreover in electrodes are shown stresses/voltages, expressed in the percentages. Points were obtained with the aid of the electrolytic bath, and curves show calculated equipotential lines. Fig. 2 depicts the case of asymmetrization along the horizontal axis. Here the voltages of electrodes are changed from -100 on -140 and from -100 to -60o/o respectively, i.e., along the horizontal axis/axle is introduced 40-percent asymmetry. The character of equipotential lines clearly shows that asymmetrization leads in essence to the shift of initial field to the electrode with the lower voltage, without the special distortion of the structure of field. In Fig. 3 it is depicted asymmetrization to 40-40o/o in two directions. In this case the center of field will be mixed on layers x and y in accordance with

the potentials, indicated on the electrodes. The quantitative
charactaristics, given in Fig. 3, make it possible to assume that
field distribution in the first approximation, can be written in the
simple form, which corresponds to shift/shear along the axes:

$$\Phi = -\frac{V}{\tau_E^2}\left\{(x-x_0)^2-(y-y_0)^2\right\}+C,$$

where x_0 and y_0 designate the shift of the center of field. Utilizing
principle of superposition and method of conformal mapping, the
formula of the potential distribution of the third order was obtained
in the following form:

$$\Phi = -2Vk\left\{\frac{1}{2}\tau_E^2(x^2-y^2)-\tau_E^{-1}(p_1x-q_1y)+\right.$$
$$\left.+\frac{1}{3}\tau_E^{-3}\left[p_3x(x^2-3y^2)-q_3y(3x^2-y^2)\right]\right\}.$$
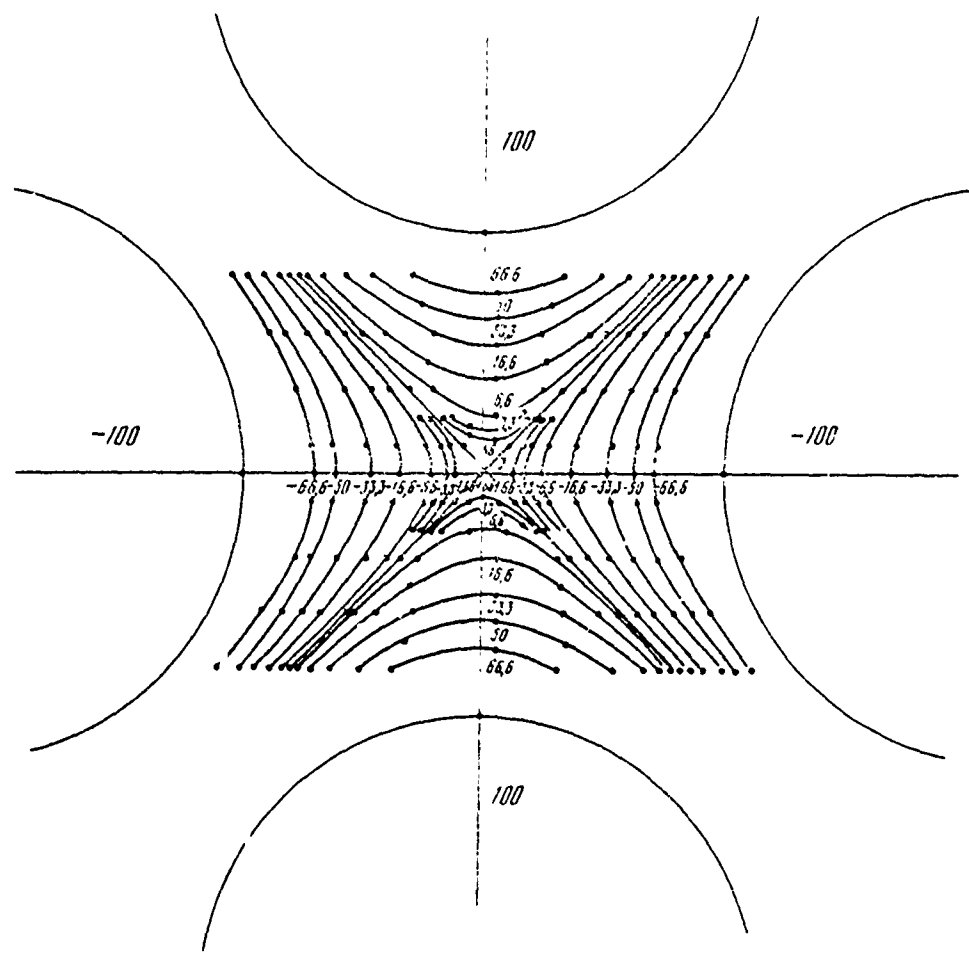
Fig. 1. Symmetrical quadrupole field (δ=0).

Page 206.

Fig. 2. Asymmetric quadrupole field (δ=40o/o).
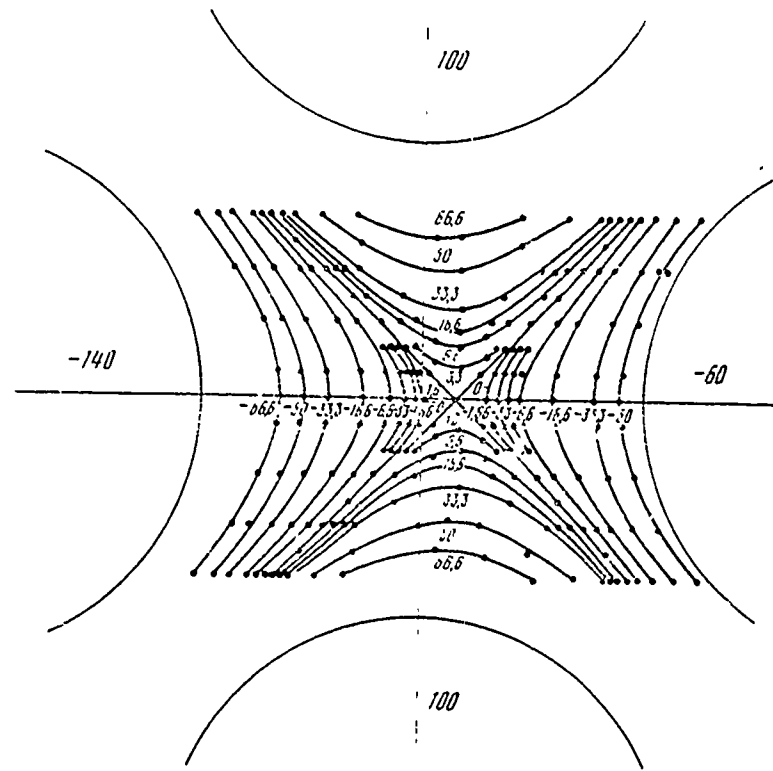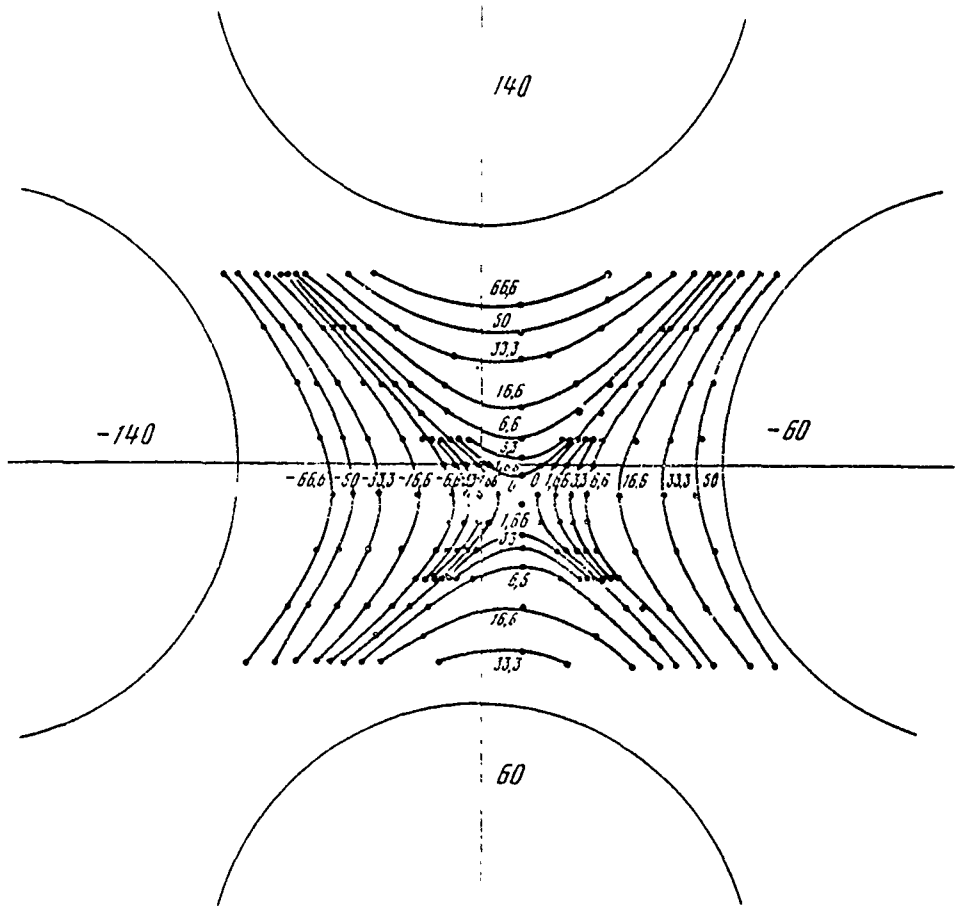
Fig. 3. Asymmetric in two directions quadrupole field (δ=40o/o).

Page 207.

Here p_i and g_i - different functions of potential asymmetries and geometric location. Consequently, the shifts of center x_0 and y_0,

entering first-order formula, prove to be equal to $\frac{1}{2\sqrt{2}}\frac{\Delta V_1}{V}\tau_E$ and $-\frac{1}{2\sqrt{2}}\frac{\Delta V_2}{V}\tau_E$ respectively for the case of cylindrical electrodes. This means that the relative mixing of center is connected with the relative asymmetry with coefficient $\frac{1}{2\sqrt{2}}$.

On the basis of the formula of potential distribution of first-order it is possible to describe the focusing properties through the usual matrix formalism and by the use of a matrix/die of transfer 3x3, which contains four elements/cells of the symmetrical case and other two elements/cells, connected with the parameters of asymmetry.

From this examination it follows that the focal length of asymmetric lens is equal to focal distance of symmetrical, but as a result of asymmetrization of the current of focus it is displaced in the transverse direction in the distance, equal to the shift of the center of field. Therefore image will be located on the axis/axle of lens only in the case if object is displaced with respect to the axis/axle.

Fig. 4 depicts the behavior of the shift of the beam of asymmetric singlet as the function of asymmetry of potential. From the experimental points and the calculated solid lines it follows that the beam is displaced in the transverse direction with respect

to the axis/axle in the distance, proportional to asymmetry. Fig. 5
depicts the same properties for the asymmetric doublet. In the case
of doublet it is possible to select four parameters of asymmetry in
accordance with concrete conditions for the entrance; two on the
first lens and two on the second, in both cases for x and y axes. It
is obvious that these four independent parameters make it possible to
correct four independent variables - coordinates x and y angles x^1
and y^1 at the entrance of lens so that the beam after lenses would
emerge along the axis/axle. This means that the image, created by the
effect of the focusing of quadrupole doublet, can be obtained on the
axis/axle of lens even in the case when beam does not enter along the
axis/axle of doublet, when four parameters of asymmetry have the
appropriate values.

By considering the field of asymmetric lens as the superposition
of the fields, which belong to the usual symmetrical lenses
(quadrupole component) and the asymmetrizing potential difference
(dipole component), it is possible to expect that the fringing field
of these two components has different character. This means that, as
a rule, effective length of symmetrical (focusing) components differs
from effective length of asymmetric (deflecting) components. The
results of measurements and calculations showed that effective length
of the deflecting component is greater than focusing one. In
accordance with these investigations among the studied configurations

was selected the quadrupole lens, which consists of the concave
cylindrical electrodes, since it had the smallest difference between
symmetric and asymmetric effective lengths. However, this difference
of effective lengths also can be taken into consideration in the
formalism of the matrix/die of the transfer.

Fig. 6 depicts typical case or the use/application of an
asymmetric quadrupole lens for the focusing and the beam steering.
Here beam enters to the right and is focused by doublet on the
entrance slit of magnetic sector. The second astigmatic image is
arranged/located on exit slit of the same magnet. Thus, beam passes
through the entrance slit at the very high intensity, undergoing at
the output the double focusing.
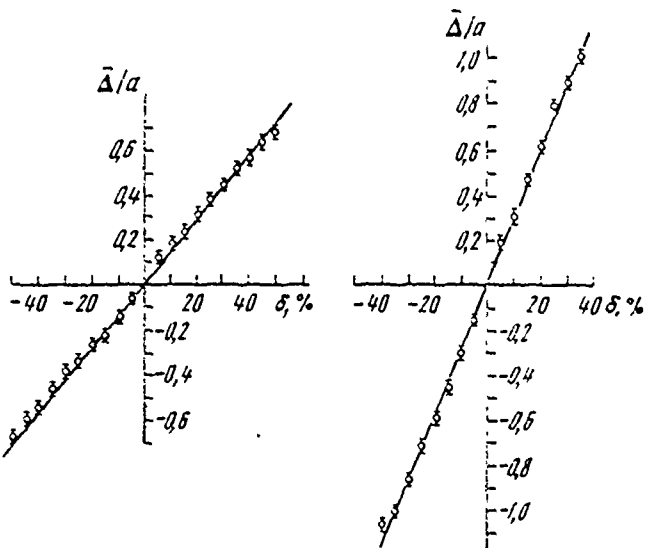
Fig. 4. Shift of beam in the asymmetric singlet in the function of asymmetry of the potential

$a - L/\alpha = 7.1, \quad \alpha/t = 0.16, \quad \Phi/\Phi_0 = 0.025;$
$\delta - L/\alpha = 7.1, \quad \alpha/t = 0.07, \quad \Phi/\Phi_0 = 0.05$
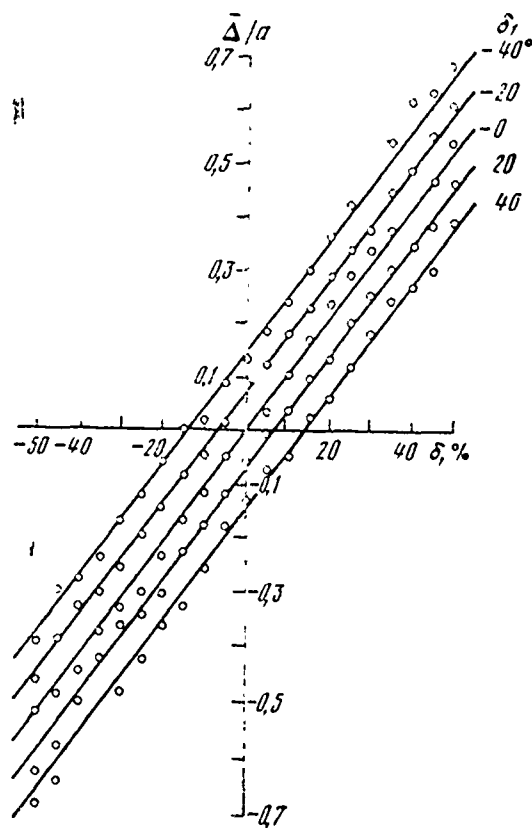
Fig. 5. Shift of beam for the asymmetric doublet

($L/\alpha=7,1$; $\alpha/t=0,18$; $\Phi_1/\Phi_0 = \Phi_2/\Phi_0 = 0,03$)

Page 208.

The properties of beam steering for the doublet allow/assume the same precise focusing, virtually not depended from position and direction of beam at the entrance of lens. The authors created also systems for three different high-voltage accelerators in the sections of the mating of accelerator tubes with the magnetic analyzers and it turned

out that the intensity of beam during the use of the focusing effect
cf doublet can be increased 1.5-5 times, moreover this high intensity
is attained independent of the conditions for the introduction/input
of beam.

From the point of view of practical uses/applications is very
important a question, do appear due to the distortions of field as a
result of asymmetrization strong supplementary aberrations. The
theory of the third order, developed by the authors for the focusing
properties of asymmetric lenses, gives response/answer to this
question.

As illustration of the results of analytical calculations Fig. 7
depicts the curved aberrations, calculated for the electrostatic
quadrupole singlet with a length of 150 mm with concave cylindrical
electrodes $(2\varepsilon = 45°)$ and by aperture 15 mm. Distances from the
object and from the image were 1000 mm respectively from the intake
planes and output. Curves are the envelopes of aberration for the
radius of entrance, equal to the half aperture, moreover in both
planes of asymmetrization it varied from 0 to 40o/o. As a result of
the smallness of effect the scale along the axis x is increased 10
times. Numbers by the curves show beam spreading due to
asymmetrization.
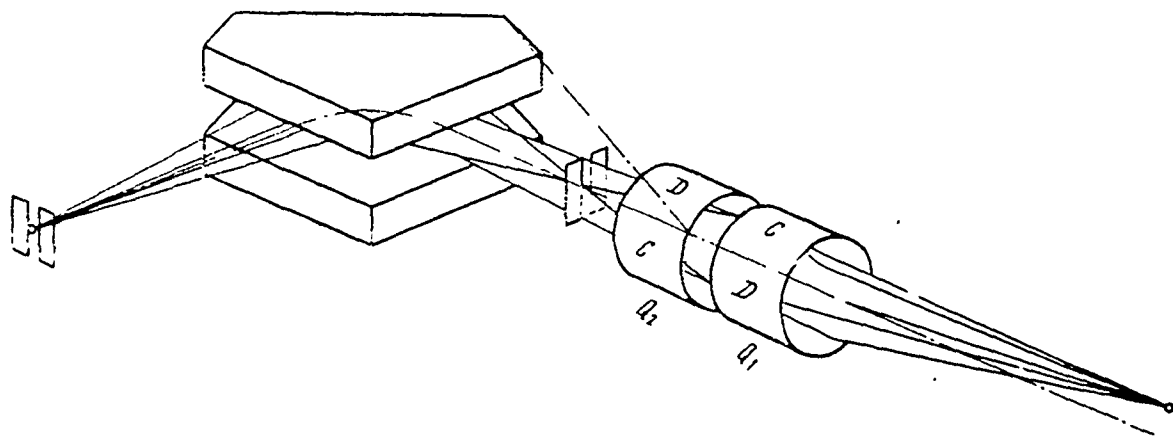
Fig. 6. Schematic of the use of an asymmetric quadrupole lens.
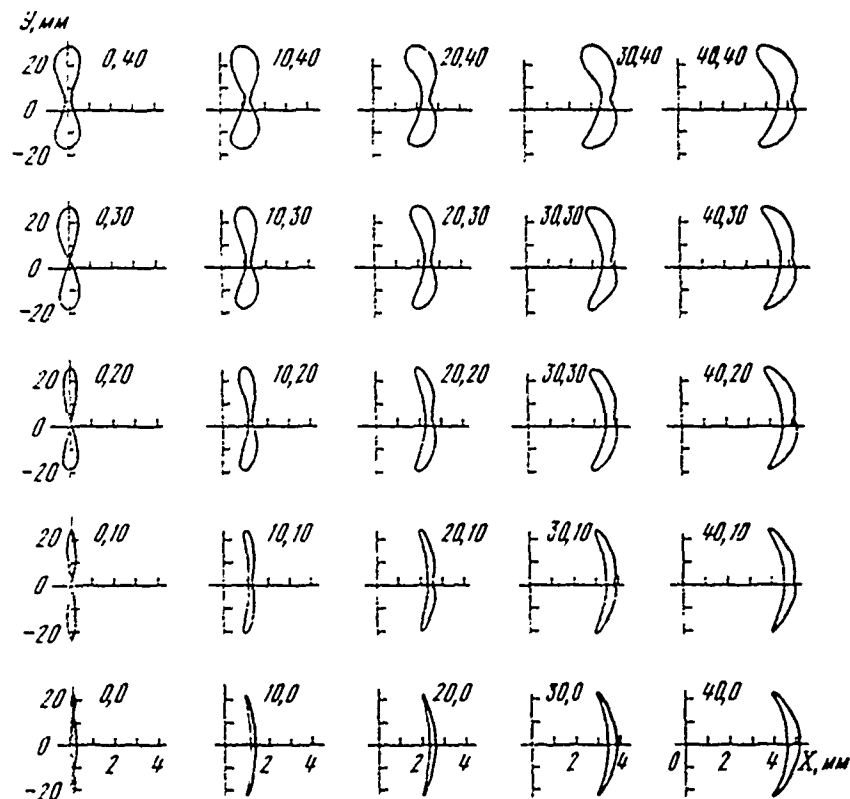
Fig. 7. Curved aberrations for quadrupole singlet in measurement of

asymmetrization in both planes from 0 to 40o/o.

Page 209.

However, this effect does not significantly affect the operating
conditions of the system of transportation during the use of low
values of as_nmetry and nearness to the paraxial beam.

Fig. 8 gives curved aberrations for different entrance apertures
in the case of the object, displaced from the axis/axle at distance 5
mm. For the shift of image to the axis/axle was used 40- percant
asymmetry. Scale along the axis x is increased ten times, and on the
fitting is represented the spot of beam on the true scale.

The programs of computers were written also for the
full/total/complete case of asymmetric quadrupole doublet. The
curves, calculated for the electrostatic quadrupole corrector who is
intended to set to van de Graaf's oscillator with the energy 5 MeV in
Debrecen, are given in Fig. 9 and 10 for the full/total/complete
positional errors and direction respectively. Here also the scale of
the scale of the perpendicular of image is increased ten times. The
curves of the increasing area correspond to the increasing by
steps/stages in 0.05 ₁ apertures input radii. Density distribution
of current in the spot of beam on the entrance slit of magnetic

analyzer is represented in Fig. 11, for the beam with the Gaussian

distribution, concentrated to 90o/o on one half the aperture of len_

at the entrance. Taking into account scale distortions, from Fig. 11

it follows that the large part of the beam is concentrated on the

narrow line near the axis/axle.
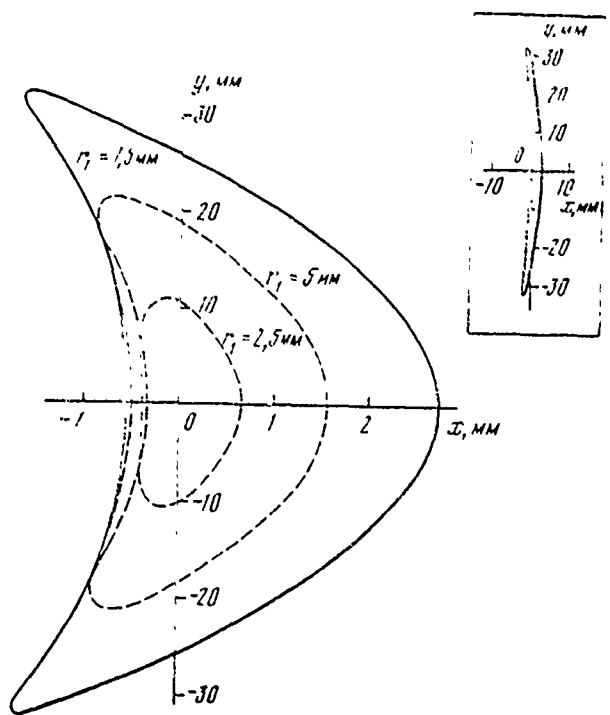
Fig. 8. Curved aberrations for different entrance apertures.
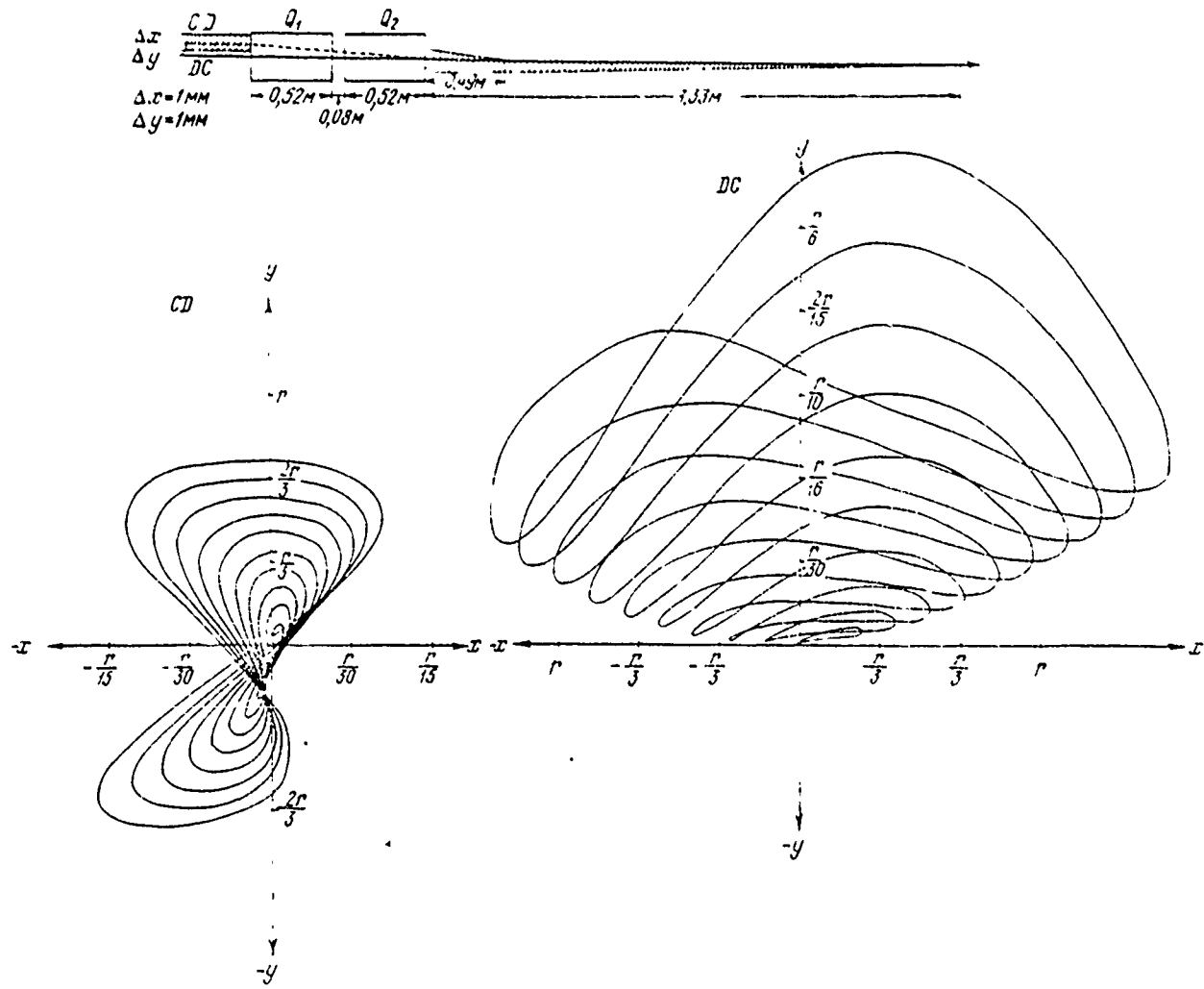
Fig. 9. Curves of the full/total/complete positional error of beam.

Page 210.
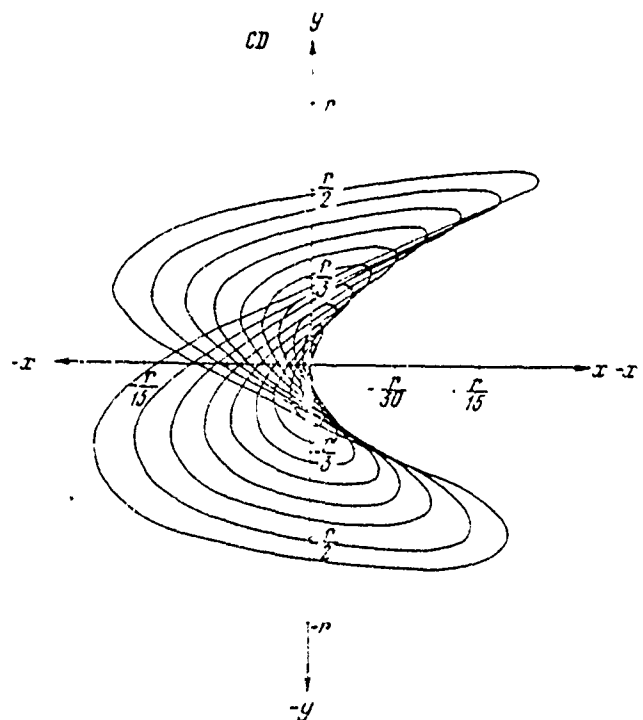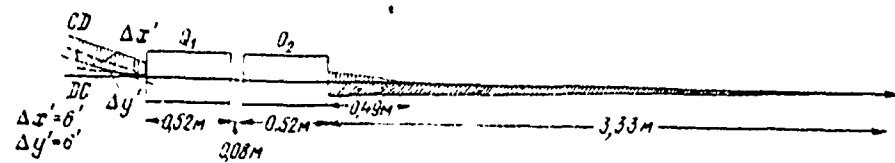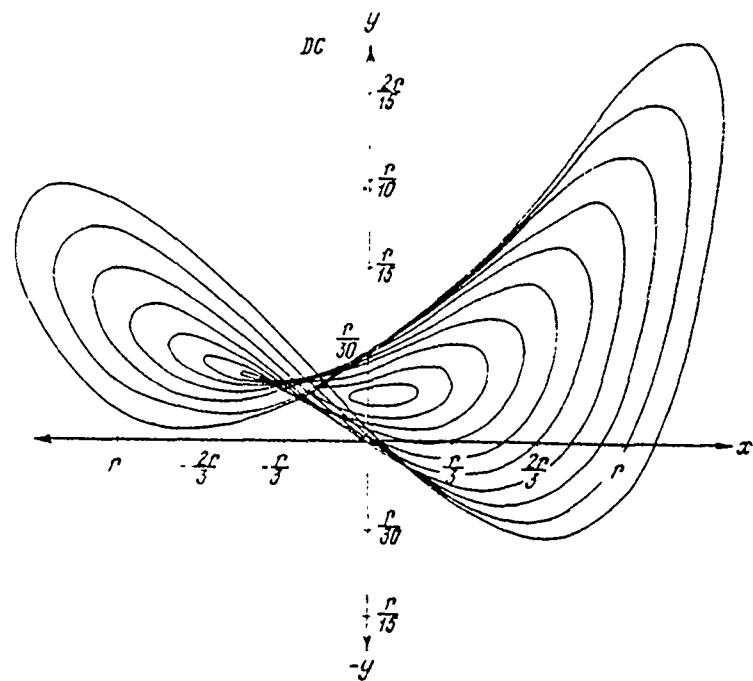
fig 10. Curves of the total error for the direction of beam.
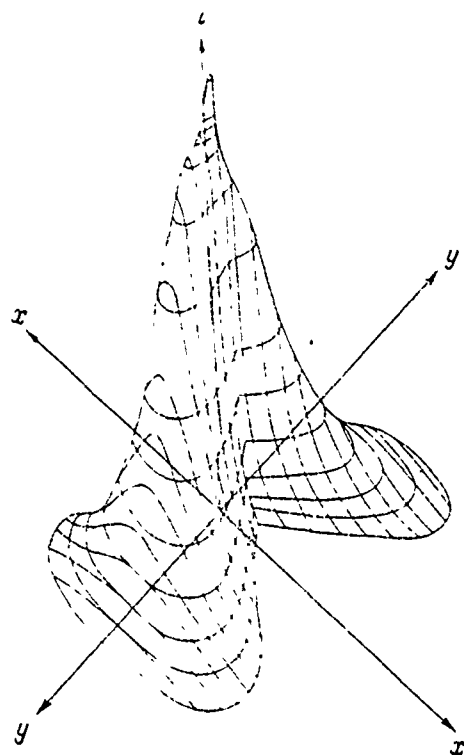
Fig. 11. Density distribution of beam current.

discussion.

Ye. Regenshtreyf. What difference between your method and method, which uses a superposition of dipole and quadrupole fields?

Ye. Koltai. Yes, this method is actually/really equivalent to the superposition of dipole and quadrupole fields and all calculations were carried out on the basis of this superposition.

Ye. Regenshtreyf. In what then does consist the advantage of your method?

Ye. Koltai. Advantage of method - simplicity of realization. We utilize usual quadrupoles and we only change a little power-supply system.

Ye. Regenshtreyf. I doubt, that in this case you do not lose degree of freedom in the compensation for aberrations.

Ye. Koltai. In the case of asymmetric quadrupole doublet are four parameters, which it is sufficient for the adjustment of position and direction of beam. They make it possible for us to obtain the necessary four degrees of freedom.

V. G. Davidovskiy. You took usual quadrupole and they supplied pole by the current of different force. In this case to the basic quadrupole field are added dipole and highest multipole fields. However, in the calculations were taken into consideration only dipole and quadrupole fields. Do intend you to prepare and to investigate the system, which forms the superposition only of these two fields?

Ya. Koltai. With the aid of this system we in practice obtained the sufficiently good quality of focusing. Therefore any further research we did not conduct.

Page 211.

154. Calculation of the optical characteristics of the system of the transportation of the beam of linear electron accelerator to the energy 60 MeV.

Yu. G. Basargin, V. P. Belov, A. M. Kokorin.

(Scientific research institute of electrophysical equipment by them. D. V. Efremov).

The economical utilization of an accelerator requires the creation of the system of the transportation of beam, which ensures work by several independent targets. The beam-separation system in question is calculated and designed in NIIEFA. It must accomplish/realize transportation of beam from LUE to five to target devices/equipment (Fig. 1) with the minimum losses and provide beam focusing on the targets into the spot with a diameter of 2-3 cm. Energy of electrons E_{HOM} = 60 MeV, in this case not more than 10o/o all electrons have an energy of less than $0.9E_{HOM}$, current in impulse/momentum/pulse 1 a. Frequency of accelerator pulses into the separate channels from 10 to 1500 Hz with the duration of flat/plane pulse apex from 0.5 to 6 μs. The geometric parameters of beam at the

entrance into the system: diameter - 2 cm, divergence 1.10^{-3} rad.

To the system are presented the requirements of pulse-by-pulse beam allocation, which leads to the use of the kickers. This, in turn, it imposes the restriction on the maximum angle of rotation. The wide energy spectrum of electrons and the large distances between the targets cause the need for the selection of the achromatic system of the rotation of beam. If system ensures the passage of electrons in the range of energies $+-0.1$, in the worse case of loss in the intensity they will comprise 20o/o of the full current. With the energy of electrons 60 MeV the isolatable heat output will be ~12 kW, in this case appear intense γ and neutron fluxes and the protection of equipment from radiations/emissions is represented by the problem of paramount importance. Obviously, under such conditions must be created the system, which consists of a small number of interchangeable radiation stable elements/cells, equipped with the means of check of the position, with form and beam current of the accelerated electrons.

1. Description of system of transportation of beam.

General/common/total beam layout is represented in Fig. 1. Beam allocation along channels 1-3 is accomplished/realized with the aid of the kickers IM which compose together with magnets $M_1-M_2-M_1$ the

achromatic system of rotation on 90°. Lenses L_9-L_{10} focussed beam on the target. All three channels are identical. The translation/conversion of beam into channel 4 is accomplished/realized with the aid of the achromatic system of almost parallel translation. This channel is comprised of the magnets, different from magnets M_1, M_2, but they all are selected so that they are characterized by only angles of rotation (windings of all magnets are standardized). Straight/direct channel 5 is comprised of the magnetic lenses and the corrective magnets. Magnetic lenses, besides the exit lenses L_9, L_{10}, and lenses L_3, L_4, which use for the correction of beam shape in channel 4, are established/installed by quartets, forming the so-called "single elements/cells". This structure of straight/direct channel because of a small angular divergence provides close initial entrance conditions of each of the channels.
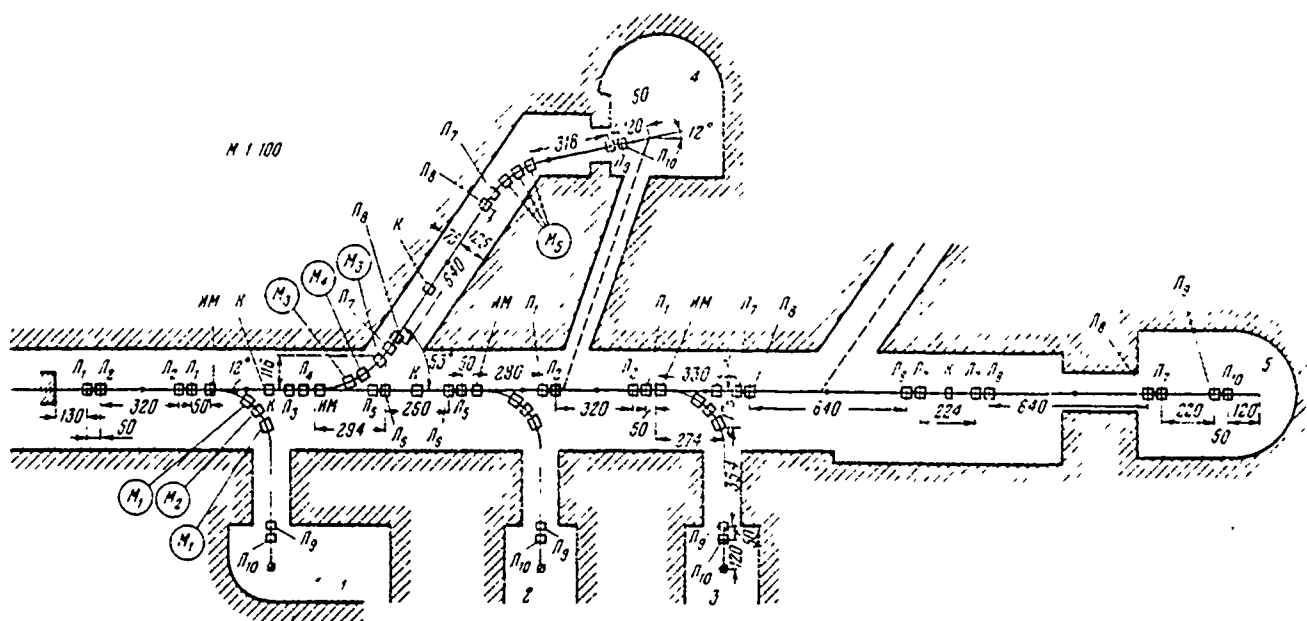
Fig. 1. Beam layout (l, cm):

$l_0 = 120$; $l_1 = 20,4$; $l_2 = 46,9$; $l_3 = 30,4$; $l_4 = 67,4$; $l_5 = 53,5$; $l_6 = 31,7$

Page 212.

2. Calculated parameters of elements of system of transportation of beam.

The achromatic system of rotation into channels 1-3 and initial rotation of beam into channel 4 they were calculated from the formulas, given in [1]. In this case were selected such values of the angles of rotation of magnets and their radii, so that the distances between the magnets would be sufficient for the setting up of

collimators and instruments of observation of beam. The parameters of the kicker φ, R were selected from the conditions of the minimum input power, independence or the work of channels 5 and minimal sizes of beam. The basic parameters of the magnets of the system of the transportation of beam are given in the table.

Note. h - width of working path/track; δ - pole gap, R - radius of central trajectory; φ - angular solution/opening of the field of magnet taking into account the stray field.

The gradients of lenses in the quartets were determined from the condition of dual focusing in the middle quartet in the approximation/approach of thin lenses and then they were more precisely formulated with the aid of the nomograms, described in [2]. Lenses have an aperture 11 cm, a length of pole 10 cm and gradients ~100 of Oe/cm. In view of the smallness of gradients are utilized the lenses with the rectangular aperture (of type of Panov [3]. The same lenses upon other start of windings are utilized as the corrective magnets. Envelope of particles and matrix elements in channels 1-5 are given in Fig. 2a, b and 3.

For guaranteeing the stability of the position of beam on the targets with the permissible root-mean-square shift by $|\Delta x| \leq 1$ cm the supply of the kicker must be stabilized with precision/accuracy

+-1.5o/o, magnets and lenses +-0.1o/o.

	H_{max}, э	R, см	φ, град (1)	δ, см	h, см
M_1	3080	65	53	5	15
M_2	5500	36,4	28	5	15
M_3	4300	46,7	35	5	10
M_4	4300	46,7	27	5	10
M_5	4300	46,7	43	5	10
ЯМ	1500	134	12	1	4÷7

Key: (1) deg.
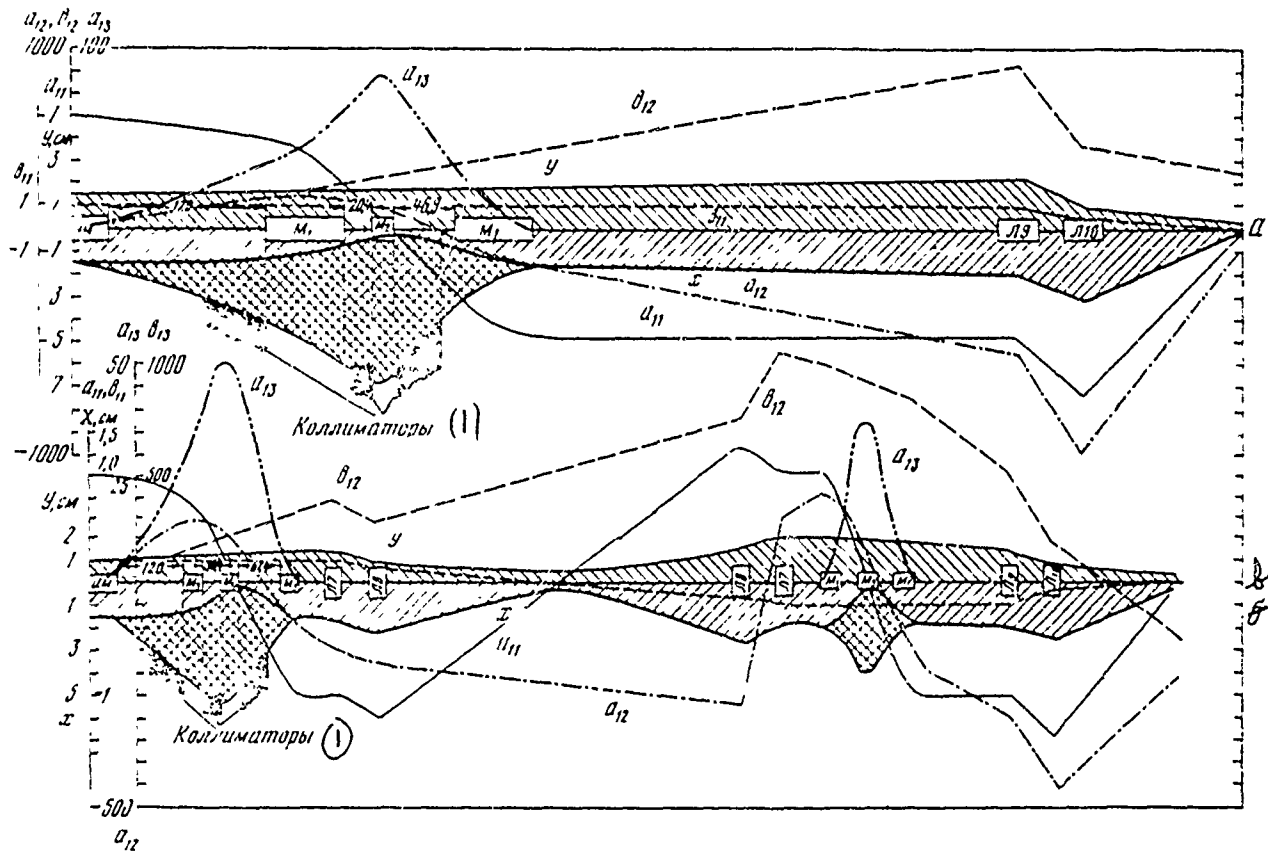
Fig. 2. Envelope of particles |x|, |y| and matrix elements a_{ik} and b_{ik} for horizontal and vertical motions in channels: a — channels

1-3. Initial conditions: $\tilde{x}_0 = \pm 1,5$ см, $y_0 = \pm 1,5$ см, $\frac{\Delta E}{E_0} = \pm 10\%$; b - channel 4.
$$x_0' = 1 \cdot 10^{-3}, \quad y_0' = 1 \cdot 10^{3},$$

Initial conditions: $\tilde{x}_0 = \pm 1,5$ см, $y_0 = \pm 1,0$ см, $\frac{\Delta E}{E_0} = \pm 10\%$;
$$x_0' = \pm 1 \cdot 10^{-3}, \quad y_0' = \pm 1 \cdot 10^{-3}$$

Key: (1). Collimators.
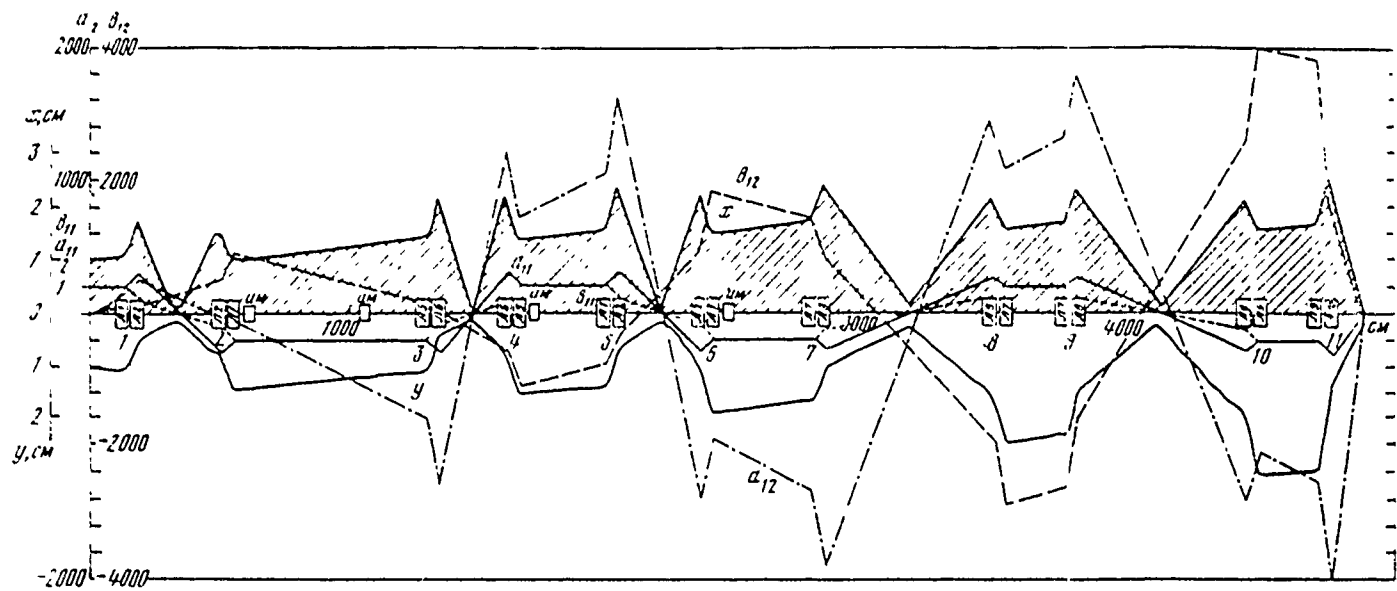
Fig. 3. Envelope of particles $|x|, |y|$ and matrix elements a_{ik} and δ_{ik} for the horizontal and vertical motion in channel 5 for the initial conditions $x_0 = +-1.0$ cm, $y_0 = +-1.0$ cm, $x'_0 = +-0.5 \cdot 10^{-3}$, $y'_0 = +-0.5 \cdot 10^{-3}$.

REFERENCES

1. V. P. Belov, A. M. Kokorin. ZhTF, 1969, Vol. 39, p. 2018.
2. Yu. G. Basargin, L. Ye. Korolev. ZhTF, 1969, Vol. 39. p.1478.
3. L. H. Haud, W.K.H. Panofsky. Rev. Scient. Instr., 1959, 30, p. 927.

Page 213.

155. Channel design of the transportation of the beam, formed by magnets S by axial symmetry.

P. A. Vodop'yanov, A. A. Kalinin.

(Radio engineering institute of the AS USSR).

In a large number of problems, which appear during the construction of the superconducting magnetic systems of charged particle accelerators, the problem of ponderomotive forces and the problem of the precision/accuracy of shaping of magnetic field with the prescribed/assigned configuration relate to the most complicated ones. The problem of forces appears in the large/coarse superconducting electromagnets - rotary magnets and focusing lenses of contemporary accelerators and magnetic pipes of the transportation of the accelerated particles. In the dipoles with the magnetic intensity H the linear force density of the pushing apart of windings is of the order

$$F \sim 5 \cdot 10^{-7} a H^2 \, \frac{\text{кг}}{\text{см}} \, ,$$

where a - width of the working zone of field. With H=60 kOe, a=10 cm value F composes ~20 t/cm. The thickness of the confining banding

must be ~10 cm.

For screening and retention of windings it was proposed [1] to
conclude them into the iron cylindrical screen with a thickness ~15
of cm. In this case for the screening ~1 m of magnet it is necessary
to ~2 t of iron, so that for the accelerator with a length of 1500 m
(Serpukhov accelerator to the energy 70 GeV) the consumption of steel
is 3000 t.

During the location of screen in helium Dewar for his cooling
down to temperature of $4.2^{\circ}K$ is required to consume 0.5 l/kg of
liquid helium or ~1000 l on 1 m of the length of magnet. The location
of screen out of the cryostat creates the serious problem of the
transmission through its walls of large attracting forces.

The problem of the precision/accuracy of shaping of magnetic
field is especially serious in the accelerators with the stationary
field and alternating gradient. Here for guaranteeing
prescribed/assigned field distribution with the turns, which form
protuberances and projections of the field of spiral form, it is
necessary to place superconductors with the precision/accuracy 10 μm.
The task of guaranteeing this precision/accuracy of the position of
superconductors is complicated with cooling of coils down to the
temperature of liquid helium.

The problems indicated can obtain simpler resolution with the execution of magnetic systems and channels from a large number of electromagnets with the axial symmetry - in the form of Helmholtz's coils.

Page 214.

In Fig. 1 are illustrated examples of execution with such coils of rectilinear magnetic beam-transport corridor, spiral channel for the accelerator of the type COK and the multi-spiral channel for the accelerator of the type of circular F-M cyclotron.

The high precision/accuracy of shaping of field with its prescribed/assigned distribution is provided in these systems due to a precise location of elementary coils in the previously located places; the scatter of the sizes/dimensions of coils can be lowered to the minimum during the use/application of a machine method of production. The problem of forces here becomes simpler, because, in the first place, ponderomotive forces become apparent as interruption strengths of the winding of separate elementary coils, the not exceeding strengths to the interruption/discontinuity of superconductors with the voltage of field to 100 kOe, in the second

place, the forces of interaction between the elementary coils are
easily maintained/withstood by the plates/slabs, on which are
installed these coils.

During the design of different magnetic systems from many
elementary coils with the axial symmetry of magnetic field appears
the task of determining the law of their three-dimensional/space
location, and also relationship/ratio of the current of their supply.
This task did not thus far yet obtain full/total/complete resolution
and for its solution is necessary conducting the series/row of
intermediate calculations.

In the present work is given the result of calculating the
equivalent field of elementary coil. The dependence of the vertical
component of the strength of the field of a coil of Helmholtz's type
in the median plane is shown in general form in Fig. 2. It is
identical for the vertical sections of coil with respect to all
azimuths. The presence of negative sections in the curve, that
stretch theoretically to infinity, requires during the calculation of
particle motion in this coil of the calculation of the fields of
adjacent coils. However, for the tentative calculations it is useful
to replace the real coil of equivalent, in which the magnetic field
is constant along the outside diameter and it is equal to zero in the
entire remaining region. For calculating the strength of the field of

equivalent coil should be calculated the integral

$$H_э = \frac{1}{\mathcal{D}_{бнеш}} \int_{-\infty}^{\infty} H_z(x)\,dx,$$

in which x - way of integration, determined by the trajectory of particle motion.
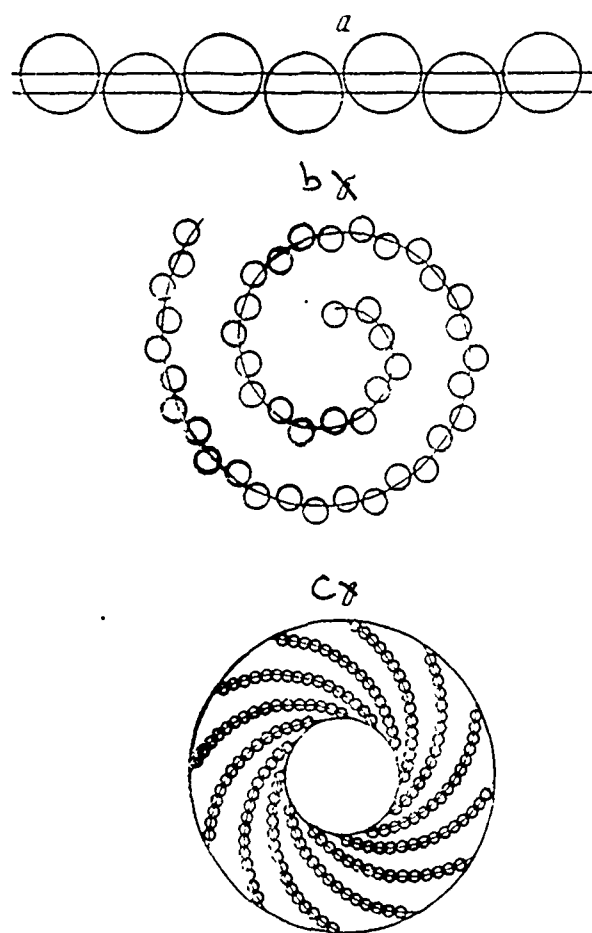
Fig. 1. Examples of the execution of rectilinear magnetic
beam-transport corridor (a), spiral channel for the accelerator of
the type COK (b) and the multi-spiral channel for the accelerator of
the type of circular F-M cyclotron (c).
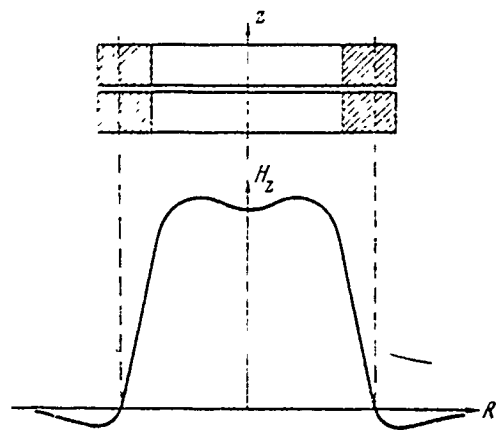
Fig. 2. Field of a coil of Helmholtz's type.
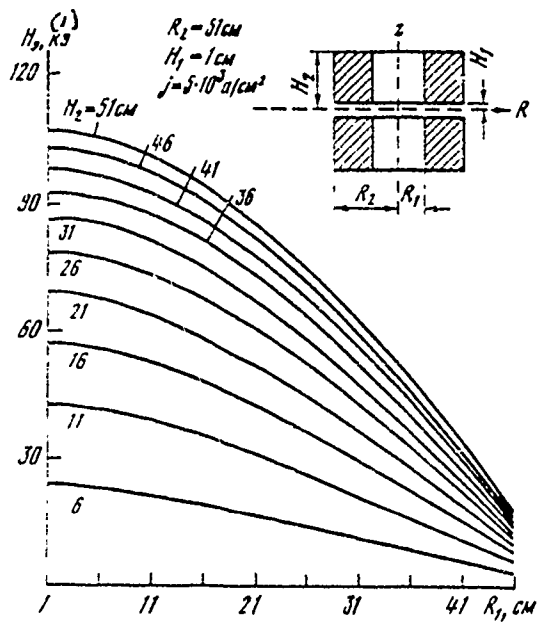
Fig. 3. Dependence of equivalent to intensity/strength coil on thickness and height of coil/winding.

Key: (1) kOe.

Page 215.

Fig. 3 depicts the calculated on the computers "Mir" family of curves, which express dependence H_3 on the thickness of winding for the case of particle motion along the diameter in the median plane of coil. The parameter is the height of coil/winding. Calculation is produced in connection with the sizes/dimensions of the superconducting electromagnet, planned in the radio engineering institute of the AS USSR [2], at the current density 5000 A/cm² (inside radius of electromagnet 34 cm).

In the case of using the magnets with the axial symmetry in the magnetic systems of accelerators it is necessary to perform the calculation of repeated particle motion along the closed orbits.

REFERENCES

1. J. P. Blewett. Iron Shielding for air corl magnets. Proc. 1968 Summer Study on Superconducting Devices and Accelerators, Part III. Brookhaven Nat.Lab., 1969, 1042.

2. F. A. Vodop'yanov, V. V. Yelyan, V. N. Litvinov. Experimental Superconducting Electromagnet with Diameter of Thermal Field 600 mm. VII International Conference on Accelerators. Yerevan. Vol 2. 1969, p. 710.

156. Conditions for existence of beam during the resonance
conclusion/output.

Zh. *For,* A. Khilar, P. Strolin.

(CERN).

1. Introduction.

For holding of induced radioactivity at the tolerance level in
the proton synchrotrens of next generation to the high energies must
be provided the very high effectivenesses of conclusion/output.
Besides the minimization of the losses of particles in the output
unit, it is necessary to know, is retained in the accelerator the
part of the beam after the end of the process of conclusion/output
and as is great this part. The preserved beams whose loss is not
admitted, can be brought out later with the use, for example, of a
system of rapid conclusion/output.

In the present work are represented analytical and digital
calculations, relating to possibilities and degrees of the
retention/preservation/maintaining beam during the conclusion/output

on the full/total/complete resonance and in the presence of the
resonance of the third order. Numerical examples relate to the
investigations of the project of proton synchrotron CERN for the
energy 300 GeV.

2. Conclusion/output on resonance of third order.

During the conclusion/output on the resonance of the third order
accomplish/realize a reduction in area of phase plane the stability
for each monochromatic line of beam so that finally this area when
intersects resonance value ν, it becomes equal to accurately zero. At
the moment of intersection all particles of beam are unstable.
However, the theory shows whereas that immediately after this the
stable region is begun to increase, moreover with the same rate, with
which it at first decreased. Thus, especially in the case of rapid
discharge/break, the significant part of the beam is seized and again
it falls into the stability region.

During a precise estimation of the emittance of the seized beam
in the principle it is necessary to consider changes in the
configuration of the phase plane, which occur, when particles fall
outside separatrix. Instead of this will be here used the following
simple criterion. Particle will be seized, if for the
elongation/extent of three revolutions after transition through the

resonance of the amplitude of its oscillations r it does not increase
over the limits of stability region. The jump of amplitude r in three
revolutions on curved separatrix (Fig. 1) composes Δr, expressed as

$$\Delta \tau = \frac{3}{4} K_S \tau^2, \qquad (1)$$

where K_8 - standardized/normalized sextupole force of
disturbance/perturbation [1]. For the same speed the limit A of
stable region is displaced in the same direction on [1]

$$\Delta \tau_A = \sqrt{3} \; \frac{(4\pi)^2}{K_6} \; \frac{d\nu}{d\theta}, \qquad (2)$$

where θ - azimuthal angle in the circumference of accelerator.

According to the prescribed/assigned above criterion, particle P
is seized, if $\Delta \tau \ne \Delta \tau_A$. In this case for the area of phase stability
region (capture) is obtained the expression:

$$S_t = 36 \left(\frac{2\pi}{K_S} \right)^2 \; \frac{d\nu}{d\theta}. \qquad (3)$$
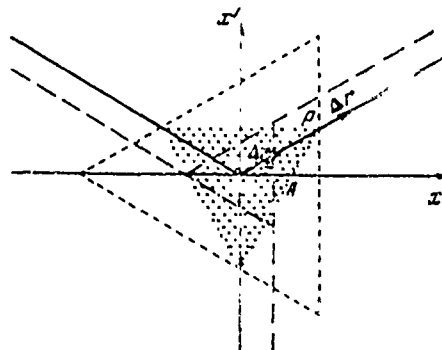
Fig. 1. To the determination of the jump of the amplitude of particle during the resonance conclusion/output.

Page 216.

The initial emittance of beam S_i is connected with initial ν- with shift $\Delta\nu_i$ from resonance value ν [1]:

$$S_i = 12\sqrt{3}\left(\frac{2\pi\Delta\nu_i}{K_6}\right)^2. \qquad (4)$$

Consequently, the ratio of the emittance of the seized to the emittance initial beam can be rated/estimated as follows:

$$\frac{S_t}{S_i} = \sqrt{3}\ \frac{d\nu/d\theta}{(\Delta\nu_i)^2}\ . \qquad (5)$$

Within the seized region of phase plane, as it is possible to expect, will prove to be the particles, arranged/located along the separatrices, which are displaced in the external direction in the presence of the resonance. Proposing sufficiently arbitrarily that

the captured particles are arranged/located only within the shaded triangle on Fig. 1, we obtain

$$\frac{N_t}{N_{i_0}} = \frac{d\nu/d\theta}{\sqrt{3}(\Delta\nu_i)^2} \ . \qquad (6)$$

Maschke and Simon [2] give the formula whose derivation is unknown to the authors of article, for s_t/s_i. This formula coincides with (5), with exception of the fact that instead of coefficient in the numerator in it is a coefficient of $\sqrt{3}$ in the denominator.

In order to check the validity of the given above formulas, was written program for the computer, in which for the elongation/extent of the process of conclusion/output were outlined $N_i = 2000$ monoenergetic particles. Were undertaken the parameters of proton synchrotron CERN with the energy 300 GeV [3]. The initial value of emittance $S_i = 0.7$ of mrad mm, corresponds to beams 50 GeV; ν - shift is assigned by the quadrupole lenses, which excite resonance process. With the standard work is expected the conclusion of the monochromatic line of beam in 2000 revolutions, i.e., in 50 ms. Taking into account energy dissipation in the beam, the corresponding total time of conclusion/output is 500 ms.

Table gives the results of numerical and analytical calculations, obtained for three different times of discharge/break. The analytical formulas, in particular led in this work are in the

satisfactory agreement with the numerical results, in spite of their

approximate conclusion/output.
Preservable part of beam in the case of output on third order
resonance from the 300 GeV CERN synchrotron (% of initial beam)
3. Conclusion/output in the presence of full/total/complete

resonance.

It is usually assumed that for the conclusion/output in the

presence of the full/total/complete resonance the stability region in

the phase plane exists exclusively for positive (or negative, for

this specific case) changes in the impulse/momentum/pulse with

respect to the equilibrium orbit. In other words, the axis/axle of

impulses/momenta/pulses is the semi-infinite "instability line", on

which all particles are unstable. In such a situation also it is

possible to expect the retention/preservation/maintaining the part of

the beam in orbit. Shown below that with an increase in the energy of

synchrotron assumption indicated above becomes ineffective. For

example, instability line during the conclusion/output from the

proton synchrotron CERN with the energy of 300 GeV becomes comparable

in the width with the scatter of impulses/momenta/pulses in the beam.

This in work [4] theoretical analysis, used to the model of

Hereward [5], by one quadrupole and one sextupole to the lenses,

arranged/located it is diametrically opposite on the ring, it shows

that the stability region in the phase plane is proportional to value

1.

$$\Delta = \Delta_1 + \Delta_2 = -2 K_L K_S \, x_L \left[(1-h) \cos \frac{\mu_0}{2} + \right.$$
$$\left. + K_L \sin \frac{\mu_0}{2} \right] + (1-h)^2 \qquad (7)$$

and what the necessary condition for existence stability region is $\Delta > 0$.

FOOTNOTE 1. The authors do not consider a small normal member, proportional to the shift of the undisturbed equilibrium orbit in the sextupole lens. ENDFOOTNOTE.

In given above equation $\nu_0 = \mu_0 / 2\pi$ - quiescent value ν; K_L and K_S - the standardized/normalized focusing forces of quadrupole and sextuple; x_L - standardized/normalized shift of the undisturbed equilibrium orbit in the quadrupole lens and $h = (\cos \mu_0 + \frac{K_L}{2} \sin \mu_0)$ - half-spur of the matrix/die of the transfer in one revolution in the accelerator, agitated only by the quadrupole lens ($h = 1$, if quadrupole it adjusts slightly value ν accurately to the near integer).

We select reference orbit, such, that for the particles, oscillating relatively it, $h = 1$. We determine

$$\alpha_p = \frac{dx_L}{dp/p} \quad \text{и} \quad \alpha_\nu = \frac{d\nu_0/\nu_0}{dp/p} \, . \qquad (8)$$

Taking into account the dependence of forces of lenses and retaining in the momentum error dp/p from the reference orbit only the member of

lowest order, we will obtain

$$\Delta_1 \simeq -8\alpha_p \, K_S \sin\frac{\mu_0}{2} \, tg^2 \frac{\mu_0}{2} \left[\frac{\Delta p}{p}\right]; \qquad (9)$$

$$\Delta_2 \simeq (\mu_0 \alpha_\nu + \sin\mu_0)^2 \, tg^2 \frac{\mu_0}{2} \left[\frac{\Delta p}{p}\right]^2, \qquad (9a)$$

where all coefficients they are calculated in reference orbit.

In the previous uses/applications was considered only the term Δ_1 (antisymmetric on $\Delta p/p$). This led to unique final solution ($\Delta p/p \approx 0$) of the equation of the limits or instability line ($\Delta = 0$) and, therefore, to the semi-infinite instability line.

Время вывода пучка (моноэнергетические частицы) (1)	Числовые расчеты (2)		Аналитические расчеты (3)		
			Машке и Саймон (4)	Настоящая работа (5)	
	S_t/S_i	N_t/N_i	S_t/S_i	S_t/S_i	N_t/N_i
50 мсек (6) (2000 оборотов) (7)	41	1,7	1,3	6,9	2,2
25 мсек (6) (1000 оборотов) (7)	5,9	4,6	2,6	13,8	4,6
5 мсек (6) (200 оборотов) (7)	34	20	13	69	23

Key: (1). Time of beam extraction (monoenergetic particle). (2). Numerical computations. (3). Analytical calculations. (4). Maschke and Simon. (5). This work. (6) ms. (7) revolutions.

Page 217.

If we examine also term Δ_2 (symmetrical on $\Delta p/p$), is obtained the final width of instability line

$$\left| \frac{\Delta p}{p} \right|_{неуст} = \frac{8\alpha_p K_S \sin\frac{\mu_0}{2}}{(\mu_0 \alpha_\nu + \sin\mu_0)^2} . \qquad (10)$$

In practical case $\nu_0 \approx$ to integer $+-1/4 \gg 1$ and $\alpha_\nu \approx -1$, then, replacing the bulk factor of orbits α_p in the quadrupole by average value

$\langle\alpha_p\rangle \approx R/\nu_0^2$ and introducing the average value of the amplitude of

betatron oscillations $\langle\beta\rangle \approx R/\nu_0$, where R - radius of accelerator, we

obtain

$$\left| \frac{\Delta p}{p} \right|_{неуст} \approx \frac{\sqrt{2} K_S \langle\beta\rangle}{\pi^2 \nu_0^3} . \qquad (10a)$$

For those obtained above expressions is characteristic strong inverse dependence on value ν, from the size of accelerator.

In the case of the acting proton synchrotron CERN, accepting $\nu_0 = 6.25$, $\alpha_p = 2.23$ m and $K_s = 0.0068$ mm^{-1}, we obtain $|\Delta p/p|_{\text{Heycm}} \simeq 5 \cdot 10^{-2}$. During the comparison with the scatter of impulses/momenta/pulses in the beam this width of instability line can be considered infinite.

In the case of the projected/designed proton synchrotron CERN to the energy 300 GeV, assuming/setting $\nu_0 = 27.75$, $\alpha_p = 0.262$ m and $K_s = 0.003$ mm^{-1} [3, 6], we obtain from (10a) $|\Delta p/p|_{\text{Heycm}} \simeq 1.4 \cdot 10^{-4}$. Curve Δ in Fig. 2 was obtained on the basis of the numerical calculations of the dynamics of the particles, carried out as a result of applying the program of computers, described in [1], to the system of the conclusion/output of accelerator on 300 GeV. The width of instability line is forecast according to formula (10a) correctly. Curve Δ_1 is obtained by the method of changing the scale of curve Δ with the coefficient $\Delta_1/\Delta = [1 + (\Delta p/p)(\Delta p/p)_{\text{Heycm}}]^{-1}$. Δ_2 not only is determined the finiteness of the width of instability line, but also it changes the dependence of stability region on the particle momentum. The width of instability line in this case has the same order of

magnitude, as the shift of impulse/momentum/pulse, necessary for the conclusion/output of monochromatic beam ($\sim 10^{-4}$) or the scatter of impulses/momenta/pulses in beam ($\sim 3 \times 10^{-4}$).

Numerical computations were carried out, just as during the conclusion/output on the resonance of the third order, for the case of proton synchrotron CERN to the energy 300 GeV. Calculations show that if we discharge/break control by means of the creation of the heterogeneity of the closed orbit, a retention/preservation/maintaining beam must not have the place even for such short durations of discharge/break as 60 μs (3 revolutions).

During the conclusion/output on the resonance of the third order the part of the beam is retained in the synchrotron. The value of this part can be sufficiently accurately rated/estimated analytically. Conclusion/output on the full/total/complete resonance makes it possible to avoid the retention/preservation/maintaining beam, even with the very short times of beam extraction. Thereby is confirmed the advantage of full/total/complete resonance from the point of view of use for the beam extraction.
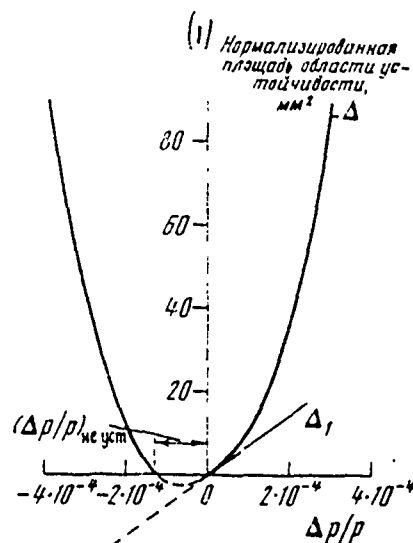
fig 2. Dependence of the area of stability region on the particle momentum for the proton synchrotron CERN on the energy 300 GeV.

Key: (1). Normalized area of the stability region, mm².

REFERENCES

1. P. Strolin. Resonant Extraction from the CERN Intersecting Storage Rings. CERN Report, 69–6, 1969.
2. A.W. Maschke, K.R. Symon. Extraction System for the 200 GeV Accelerator. NAL Report, August 5 1968.
3. E.J.N. Wilson. Missing Magnet Lattice MR 29 complete with L1 straight sections. CERN Internal Report MC/13, October 22 1969.
4. P. Strolin. Integral resonance slow extraction from alternative gradient synchrotrons. CERN Divisional Report, ISR-TII/66-41, 1966.
5. II.G. Hereward. The Possibility of resonant extraction from the CPS. CERN Internal Report, AR/Int. CS/61-5, 1961.
6. A.Laisné, P.Strolin. Integral resonance extraction from the MR 29 lattice. CERN Internal Report, EJ/6, January 29 1970.

Page 218.

157. Project of slow conclusion/output from the proton synchrotron ITEF.

L. Z. Barabash, Yu. G. Glovenko, L. L. Gol'din, I. P. Kleopov, D. G. Koshkarev, V. V. Miller, L. I. Sokolov.

(Institute of theoretical and experimental physics).

V. Ye. Kornakov, B. S. Mingalev, N. A. Monoszon, Yu. P. Sivkov, P. M. Spevakova, A. M. Stolov.

(Scientific research institute of the electrophysical equipment im. D. V. YEfremov).

A slow conclusion from the proton synchrotron ITEF can be carried out with the aid of resonance $3Q_z = 28$ or resonance $4Q_z = 37$. A deficiency/lack in the second of them is the rapid decrease of the width of the resonance in the region of small amplitudes, in connection with which substantially decreases the effectiveness of conclusion/output. The only reason, which can be given against the use of resonance of the 3rd order, consists in the fact that the

magnetic structure of the reconstructed proton synchrotron ITEF
contains 8 superperiods. Therefore between the identical
gaps/intervals of adjacent superperiods are placed 3.5 oscillations
of 28 harmonics of disturbance/perturbation. This it forces for the
possibility of the selection of the optimum phase of quadratic
disturbance/perturbation to utilize other free gaps/intervals of the
superperiod where the modulus/module of the function of floquet is
considerably less.

The system of conclusion/output in question consists of three
sextupole lenses and motionless septum- magnet (Fig. 1). Since the
septum is moved into the aperture of chamber/camera, at the beginning
of the cycle is created local orbit perturbation with field weakening
in three blocks/modules/units of electromagnet. Shift to the
resonance is accomplished/realized by a gradual change of the
gradient in the corrective quadrupole lenses.

During the calculation of the resonant step-up of oscillations
were considered the peculiarities associated with the discontinuous
distribution of quadratic field distortion. As is known [for 1, 2],
in this case are possible both the build-up/growth the amplitudes on
some azimuths, more rapid than on the azimuth of the location of
septum and the appearance of the supplementary quasi-stable points on
the phase plane, about which an increment in the amplitude of

oscillations is very small.

Examination is conveniently produced in the smooth approximation/approach on phase plane $\frac{\tau'}{\bar{\omega}}, \tau$ (Fig. 2), where $\bar{\omega} = \frac{2\pi Q}{L} \approx 0,235 \text{ м}^{-1}$.

We will consider first that the disturbance/perturbation is created with the aid of one thin sextupole lens. We will examine particles, in which the frequencies satisfy a precise resonance condition $Q = n + 1/3$. If we arrange septum-magnet in the place of maximum divergence, then lens will be located from septum-magnet on angle $\varphi_s = \frac{\pi}{6}$.

With the n flight/span through the thin sextupole lens the particle obtains an increase in the angle

$$\Delta \tau'_{n+1} = \alpha \tau_n^2, \qquad (1)$$

where $\alpha = \frac{1}{2BR} \frac{\partial^2 B}{\partial \tau^2} \ell$. In three revolutions the particle three times will traverse the lens, moreover each subsequent passage will be cut of phase of relatively of preceding/previous on $2\pi/3$.

If $\Delta a < a$ (a - the amplitude of oscillations, Δa - its increase), then increases in amplitude and phase of oscillations are equal to respectively

$$\frac{\Delta a_{n+1}}{a_0} = \frac{\Delta \tau'_{n+1}}{a_0 \bar{\omega}} \sin \left(\varphi_s + \frac{2\pi}{3} n \right); \quad (2)$$

$$\Delta \varphi_{n+1} = \frac{\Delta \tau'_{n+1}}{a_0 \bar{\omega}} \cos \left(\varphi_s + \frac{2\pi}{3} n \right). \quad (3)$$

Thus (see Fig. 2) a resonance increase in the amplitude in three revolutions will be

$$h = 2\Delta a = \frac{\Delta z'}{\omega} \sin \psi_s + \frac{\Delta z'}{\omega} \sin\left(\frac{2\pi}{3} + \psi_s\right) = \frac{\Delta z'}{\omega}, \quad (4)$$

and an increase in the phase will be close to zero.

Since an increase in the phase in each lens increases approximately/exemplarily as r^2 (see (1) and (3)), then for the sufficiently large amplitudes it it can exceed $\pi/6$, and then particle can hit the mode/conditions of the amplitude reduction with the following passages of lens. This is possible, if $\frac{\Delta z'}{a_0 \omega} > 0.5$. Therefore the maximum value of the step/pitch of driving near the septum must be several times of less than the amplitude of the oscillations before the septum (distance from the orbit to the septum).
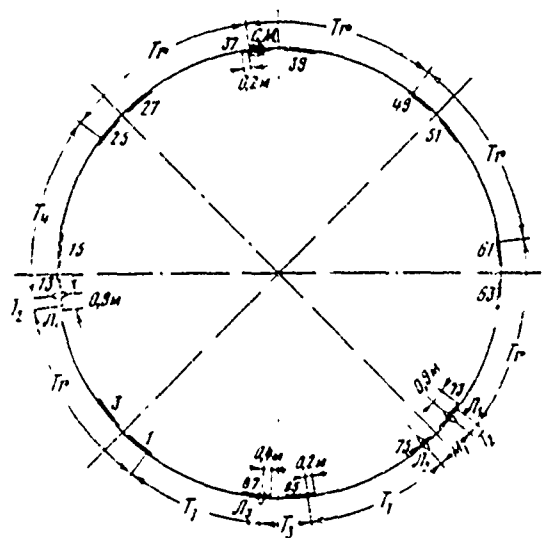
Fig. 1. Ring layout with the leading-out elements,'cells c.m. - septum-magnet; Π_{1-4} - predicted places of the arrangement/position of nonlinear lenses.

Of course strength of resonance must provide driving with this step/pitch. In our case condition $\Delta a < a$ is satisfied by the correct selection of the initial parameters of the system of the conclusion/output h=1.6 cm, a=2.2 cm, a number of lenses 2. The absence of sufficient quantity of long free gaps/intervals in our case does not make it possible to realize precisely this version. Nevertheless, since examination in the smooth approximation/approach showed that the resonance step/pitch weakly depends on the phase, it is possible to make a dual septum- magnet (Fig. 3). First septum - electrostatic with a width gap of Δ=4 mm and thickness of knife ~0.1

mm and combined with it along the azimuth of the second
septum-magnetic with a width gap 25 mm and thicknesses of knife of
$\Delta_1 = 3$ mm. The angle of deflection of the first septum must be such so
that the combined action of sextupole lenses and this septum would
give divergence $\sim \Delta + \Delta_1$. The first septum in this case works as the
supplementary strongly nonlinear lens which is switched on beginning
from some amplitudes (in our case when $r \geqslant 2.2$ cm).

The trajectory calculation, produced for the slow
conclusion/output with the use of a dual septum- magnet, it showed
fundamental possibility of the realization of this version. With
$r \geqslant 2.2$ cm was switched on the first septum, giving $\Delta r' = 1.3 \cdot 10^{-3}$ rad.
Fig. 4 gives dependence of r on r' in septum-magnet, beginning with
$r = 1.5$ cm up to the incidence/impingement into the clearance of the
second septum- magnet. The parameters of the first electrostatic
septum: the value of working clearance - 4 mm, thickness of knife
~ 0.1 mm, fields in the clearance 60 kV/cm the length of plate is 20
cm, the required stability of field +-1 kV/cm.

One of the most complicated technical tasks, which appear during
the development of slow conclusion/output with a comparatively large
duration (order 0.5 s) - shaping of the flat/plane part of the
impulse/momentum/pulse of magnetic field. Requirements for the
permissible value of the amplitude of the pulsations of magnetic

field depend on the conditions of limiting modulation of the intensity of emitted beam, that leads to the need of reducing the amplitude of the pulsations of the voltage of the converter of power-supply system of up to values on order of 0.1o/o of maximum rectified voltage, while the existing filter gives the values of the order of several percentages.
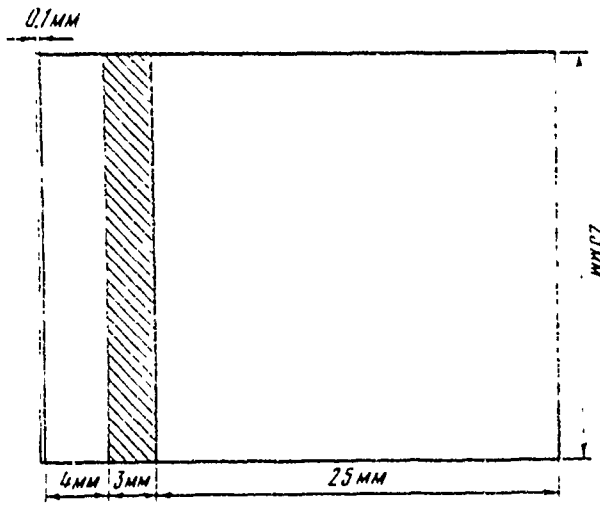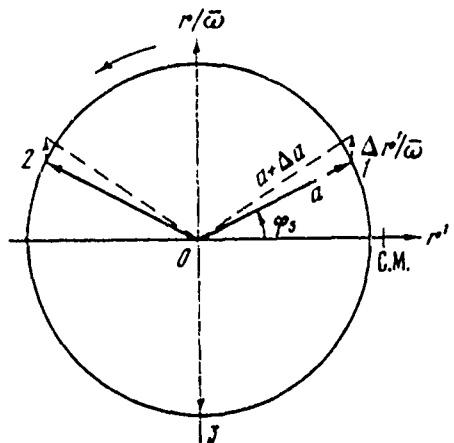
Fig. 2. On the calculation of a resonance increase in the amplitude.

Fig. 3. Section of aperture of combined septum- magnet.
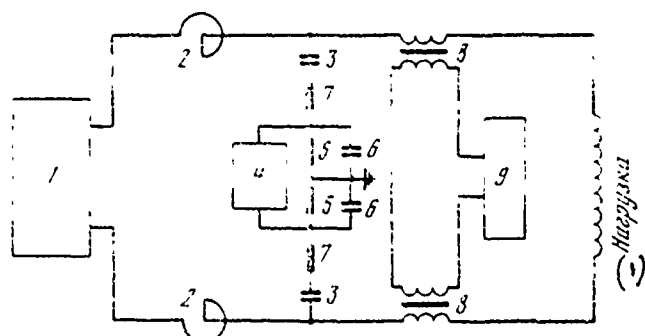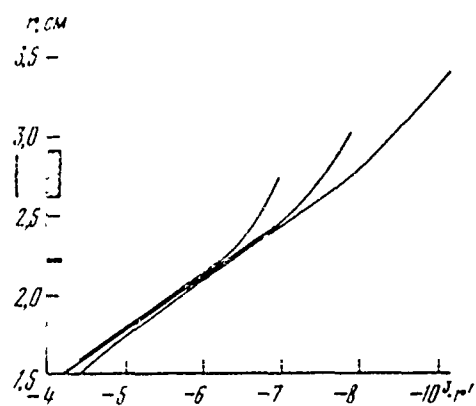
Fig. 4. Form of the function r(r') in septum-magnet.

Fig. 5. System block diagram of filtration: 1 - converters of power-supply system; 2 - filter choke; 3 - buffer capacitor banks; 4 - device/equipment of changeover of filter; 5 - attenuating resistances; 6 - filter capacitors; 7 - resistance of filter; 8 - series transformers of active filter; 9 - low-frequency amplifier.

Key: (1). Load.

Page 220.

The task of the realization of filters with the filtration factor on the order of 500-1000, that ensure the fulfillment of allowances, becomes complicated by the need of obtaining the frequency characteristics of the filtering devices/equipment, which satisfy the conditions of limiting the transit time, and also values of the ejections of voltages and currents of magnet winding during the transient processes, caused by the pulse character of the work of power-supply system. The work experience of power-supply systems with the valve converters showed the practical impossibility of guarantee in the curve of the rectified voltage only of harmonic components with the frequency, equal and to multiple conversion frequency. The harmonics of low frequencies (25, 50 Hz and multiple by them), as a rule, compose significant part in the general/common/total spectrum of the harmonics of the voltage of converter. This fact substantially complicates filtration system. Apparently, is most expedient the realization of the system of the depression of pulsations by the method of the combination of the passive aperiodic filter whose characteristics for obtaining the satisfactory transient process are reconstructed in the process of exciting the electromagnet, and the active filter, intended mainly for the depression of the low-frequency part of the spectrum of harmonics.

The system block diagram of filtration is given in Fig. 5.

REFERENCES

1. R. Alison, Kh. Gluider, G. L. Lambertson. Use of Nonlinearities
   of a Field for Resonance Extraction from a Besatron.
   Proceedings of VII International Conference on Accelerators.
   Yerevan, 1969, Vol. 1, p. 675.
2. Zh. Erb. Some Properties of a Phase Plane of a Simple
   Extraction System. Proceedings of VII Internation Conference
   on Accelerators. Yerevan, 1969, Vol. 1, p. 592.

158. Method of increasing the effectiveness of conclusion/output and improvement in the energy nomogeneity of ion beam, concluded from the cyclotron.

L. N. Katsaurov, Ye. M. Moroz, L. P. Nechaeva.

(Physical institute im. P. N. Lebedev of the AS USSR).

The problem of an improvement in the effectiveness of the beam extraction of the accelerated ions is very important for the cyclotron. With the approximation/approach of the effectiveness of conclusion/output to 100o/o disappears the difficulty, connected with the radioactivity of the walls of vacuum chamber and dees, induced by the accelerated ions, scattered to the walls during the beam extraction from the cyclotron. Scattering ions occurs during their incidence/impingement to splitter. Heating splitter by the falling to it ions is also the important reason, which establishes/installs the limit of cyclotron current. For eliminating this reason it is possible to change the construction/design of deflector. (Let us note that the proposed modernization can prove to be effective, apparently, only for such cyclotrons in which the energy scatter of

ions in each cluster is noticeably less than the energy gain of ions in one revolution). Longitudinal gash full length of the knife of electrostatic deflector will allow beam freely to pass inside the deflector. Analogously in the case of applying the electromagnetic deflector longitudinal gash in the septum will allow ion beam with the unwinding along the spiral trajectory freely to pass inside the deflector. (As it will be clear from the following presentation, iron electromagnetic deflector in the cyclotron with the proposed modernization it is expedient to replace with iron free pulse).

The discussed modernization of cyclotron is not limited one gash alone of knife or septum of deflector. It is easy to see that the presence of gash by itself does not solve posed problem. Is eliminated only heating knife, but not the dispersion of ion beam, which will be conducted by the scattered deflection field in the small region of knife or septum. The size/dimension of the region of stray field is approximately/exemplarily equal to the height of slot in the knife or the septum. It is necessary to increase several times the radial distance between the adjacent clusters of ions in the cyclotron, so that when the concluded cluster is located in the deflection field of deflector, the nearest to it cluster of ions would be even beyond the limits of the stray field of deflector. Satisfaction of this condition makes it possible to solve another problem, not less important than the guarantee of 100-o/o

effectiveness of conclusion/output. Discussion deals with an increase
in the energy homogeneity of the concluded ion beam.

At present in the series/row of the acting cyclotrons the large
energy scatter of ions is caused by the poor separation of clusters.
The radial size/dimension of the cluster of ions is compared with the
distance between the adjacent clusters on the latter/last turns of
spiral trajectory. Therefore into the output unit together with the
concluded cluster falls the part of the ions from the following after
it cluster, which did not yet pass the complete cycle of
acceleration. Energy of the ions, which prematurely fall into the
deflector, by several hundred kiloelectronvolts lower than nominal
energy of the concluded beam. This undesirable phenomenon is removed
with an increase in the distance between the clusters, and the energy
scatter of ions in the concluded beam can be reduced to the value of
the energy scatter of ions in one cluster.

If in the cyclotron is utilized external injection, then an
increase by several times of the radial distances between the
clusters is provided with the pulse modulation of the density (
bunching) of the injected beam, produced with the frequency Ω, into
the integer of times of the smaller frequency ω of accelerating
voltage.

Upon the internal injection it is possible to
intercept/detach the series/row of clusters and to pass necessary
clusters by pulse electrostatic or electromagnetic inflector and slit
diaphragms, established/installed on the initial turns of trajectory
in the central region of cyclotron.

The enumerated changes, as can easily be seen, do not provide
the solution of all stated problems. It remains to still remove the
harmful effect of the stray field of deflector directly to the
concluded cluster with its approximation/approach to a deflector. For
this purpose it is necessary to use the pulse supply of deflector
with the frequency Ω, to the equal frequency of bunches, and with the
duration of each pulse it is less than the period of revolution of
ions into cyclotron. Pulses of the supply of deflector, which
accomplish/realize a beam extraction of the cyclotron, they are
synchronized with the impulses/momenta/pulses, which pass the
clusters through the inflector in the central region of cyclotron (or
with the impulses/momenta/pulses of injection), and, therefore, and
with accelerating voltage, so that the deflection field of deflector
would be absent when cluster, completing several latter/last
revolutions, is passed through the dangerous region, situated before
the deflector. The deflecting pulse field appears for the time of the
latter/last revolution of the concluded cluster and it reaches the
prescribed/assigned value up to the moment/torque of the passage of

the cluster through the deflector.

At first glance it can seem that the modernization in question
will lead to a reduction in the average/mean intensity of cyclotron
beam, since from the beam is cut out the series/row of clusters.
However, reductions in the intensity will not occur. In the game
enter the more powerful/thicker factors: the elimination of the
limits of intensity, caused by heating knife or septum of deflector
and by induced radioactivity of walls, as a result of which it is
possible to increase a quantity of ions, accelerated in each cluster.

The Coulomb stability limit of betatron oscillations lies/rests
sufficiently far, and the longitudinal Coulomb effect, which leads to
an increase of the energy scatter of ions in each cluster, is
connected only with the net charge of the ionic sector of disk, which
turns into the cyclotron, and greatly weakly it depends on number of
the clusters, which compose this sector [1].

Each of three changes (gash in splitter, modulation of density
upon the injection and replacement of constant stress of deflector by
pulse ones) examined does not solve the problems, stated in this
report. Only the realization of all three changes gives the required
positive effect.

The modernization examined does not affect the bases of the construction/design of cyclotron and can be realized on any acting cyclotron.

REFERENCES

1. M.M. Gordon. The Lingitudinal Space Charge Effect
   and Energy Resolution. Oxford Cyclotron Conf., Sep-
   tember, 1969.

159. Acceptance phase range of the alternating-gradient doublet,
carried out on the quadrupole lenses with different apertures.

Ye. Regenshtreyf.

(France).

1. Introduction, adopted designations and assumptions.

Alternating-gradient doublet is in corpuscular optics basic
element/cell during compiling of the lines of the transportation of
beam, accelerators, matching devices and large number of other
devices/equipment. Therefore better understanding of its properties
is expedient not only from a theoretical point of view, but also
taking into account the practical uses/applications.

The purpose of this work is obtaining simple formulas for the
properties of the transmission of the beam of the
alternating-gradient doublet: acceptance phase range, for the case,
when the lengths of the quadrupole lenses, which form doublet, and
also their gradients and apertures are different. After developing

jeneral theory, it is easy to give quantitative response/answer to
the question: "which must be a radius of the second quadrupole lens,
so that entire the four-dimensional phase space, seized by the first
quadrupole lens, would be passed also through the second lens"?

Let s_1, s_2 - respectively length I compose their quadrupole
lenses, G_1 and G_2 - corresponding gradients, $2R_1$ and $2R_2$ -
corresponding apertures, and L - effective distance between the
lenses.

Let us accept the following designations:

$$k_1^2 = \frac{G_1}{p/q} , \qquad k_2^2 = \frac{G_2}{p/q}$$

and

$$\theta_1 = k_1 s_1 , \qquad \theta_2 = K_2 s_2 ,$$

where p - particle momentum, and q - their charge.

As the assumptions is accepted $\theta_1 < \frac{\pi}{2}, \theta_2 < \frac{\pi}{2}$, and examination is
limited to linear theory, and therefore by uncoupled motions. It is
further assumed that vacuum chamber has square section, beam is
monochromatic, and also is not considered possible
decomposition/decay in flight. Finally, energy of beam is assumed
sufficiently high so that it would be possible to disregard/neglect
the effects of space charge. Are not done any assumptions, which
concern density distribution of particles in the beam, us interests

only the overall trapping range of doublet, determined by its geometry and magnetic characteristics.

2. Acceptance phase range with focusing-defocusing in X- plane.

The possible forms of the phase contour/outline: let E_1 - over-all aperture ratio, superimposed by the entrance of the first quadrupole lens; I_1 - over-all aperture ratio, superimposed by the internal part of the first quadrupole lens; S_1 - over-all aperture ratio, superimposed by the output of the first quadrupole lens; E_2 - over-all aperture ratio, superimposed by the entrance of the second quadrupole lens, and S_2 - over-all aperture ratio, superimposed by the output of the second quadrupole lens.

The possible forms of the contour/outline of acceptance are given below:

$$E_1 I_1 S_1 S_2 \qquad\qquad E_1 I_1 E_2 S_2$$
$$E_1 I_1 S_1 \qquad\qquad E_1 E_2 S_2$$
$$E_1 I_1 S_2 \longrightarrow E_1 I_1 S_2$$
$$I_1 S_1 S_2 \qquad\qquad I_1 E_2 S_2$$
$$E_1 S_2 \longrightarrow E_1 S_2$$
$$I_1 S_2 \longrightarrow I_1 S_2$$
$$E_2 S_2$$

The left column where is absent E_2, corresponds to the cases when the aperture of the first lens is less than the aperture of the

second lens, i.e., $R_1 < R_2$ whereas the second column, in which is absent S_1, corresponds to the cases, with the inverse relationship/ratio, i.e., $R_1 > R_2$. When $R_1 = R_2$ there are only three possibilities, namely $E_1 I_1 S_2$, $I_1 S_2$ and $E_1 S_2$, general/common/total for both columns. With $R_1 = R_2$ are possible ten different cases of the form of phase contour/outline.

Partial matrices/dies and important values of ratio R_2/R_1. Let us define the "matrix/die of entrance", examining the first lens with its drift space as

$$
m_e = \begin{Vmatrix} a_e & \beta_e \\ c_e & d_e \end{Vmatrix} = \begin{Vmatrix} 1 & L \\ 0 & 1 \end{Vmatrix} \times \begin{Vmatrix} \cos\theta_1 & \frac{1}{k_1}\sin\theta_1 \\ -k_1\sin\theta_1 & \cos\theta_1 \end{Vmatrix},
$$

"exit matrix/die", examining the second lens with preceding it drift space as

$$
m_s = \begin{Vmatrix} a_s & \beta_s \\ c_s & d_s \end{Vmatrix} = \begin{Vmatrix} \mathrm{ch}\,\theta_2 & \frac{1}{2}\mathrm{sh}\,\theta_2 \\ k_2\mathrm{sh}\,\theta_2 & \mathrm{ch}\,\theta_2 \end{Vmatrix} \times \begin{Vmatrix} 1 & L \\ 0 & 1 \end{Vmatrix},
$$

and the matrix/die of entire doublet:

$$
M = \begin{Vmatrix} A & B \\ C & D \end{Vmatrix} = \begin{Vmatrix} \mathrm{ch}\,\theta_2 & \frac{1}{k_2}\mathrm{sh}\,\theta_2 \\ k_2\mathrm{sh}\,\theta_2 & \mathrm{ch}\,\theta_2 \end{Vmatrix} \times \begin{Vmatrix} 1 & L \\ 0 & 1 \end{Vmatrix} \times \begin{Vmatrix} \cos\theta_1 & \frac{1}{k_1}\sin\theta_1 \\ -k_1\sin\theta_1 & \cos\theta_1 \end{Vmatrix}.
$$

There are nine important values of parameter R_2/R_1, which can be utilized for determining the separatrices between ten times the

configurations of the phase space:

$$\frac{R_2}{R_1} = -A, \quad \frac{R_2}{R_1} = A, \quad \frac{R_2}{R_1} = \alpha_e, \quad \frac{R_2}{R_1} = \alpha_s, \quad \frac{R_2}{R_1} = \rho,$$
$$\frac{q_2}{R_1} = \sigma_1, \quad \frac{R_2}{R_1} = \sigma_2, \quad \frac{R_2}{R_1} = \tau_1, \quad \frac{R_2}{R_1} = \tau_2.$$

In the given above relationships/ratios it is placed:

$$\rho = \frac{A\beta_s + \alpha_s B}{B - \beta_s};$$

$$\sigma_1 = \frac{\alpha_e B - A\beta_e}{\sqrt{(B-\beta_e)^2 + \frac{1}{k_1^2}(A-\alpha_e)^2}}; \quad \sigma_2 = \frac{\alpha_e B - A\beta_e}{\sqrt{(B+\beta_e)^2 + \frac{1}{k_1^2}(A+\alpha_e)^2}};$$

$$\tau_1 = \frac{\alpha_e B - A\beta_e}{B - \beta_e}; \quad \tau_2 = \frac{\alpha_e B - A\beta_e}{B + \beta_e}.$$

Form of the contour/outline of acceptance. Is expediant to examine three basic cases of $R_2/R_1 < -A$, $R_2/R_1 < A$ and $\frac{R_2}{R_1} > |A|$, and to isolate within each case all possible subcases (see the Table).

$\frac{R_2}{R_1} < -A$		$\frac{R_2}{R_1} < A$		$\frac{R_2}{R_1} > |A|$	
(1) условие на $\frac{R_2}{R_1}$	(2) тип фазового контура	условие на $\frac{R_2}{R_1}$	тип фазового контура	условие на $\frac{R_2}{R_1}$	тип фазового контура
$\frac{R_2}{R_1} > a_s$	$I_1 S_1 S_2$	$\frac{R_2}{R_1} < \tau_1$	$E_1 S_2$	$\frac{R_2}{R_1} > \rho$	$E_1 I_1 S_1$
$a_s > \frac{R_2}{R_1} > \sigma_1$	$I_1 S_2$	$\tau_1 > \frac{R_2}{R_1} > \tau_2$	$E_1 E_2 S_2$	$\rho > \frac{R_2}{R_1} > a_s$	$E_1 I_1 S_1 S_2$
$\frac{R_2}{R_1} < -A$		$\frac{R_2}{R_1} < A$		$\frac{R_2}{R_1} > |A|$	
$\sigma_1 > \frac{R_2}{R_1} > \sigma_2$	$I_1 E_2 S_2$	$\tau_2 > \frac{R_2}{R_1}$	$E_2 S_2$	$a_s > \frac{R_2}{R_1} > \sigma_1$	$E_1 I_1 S_2$
				$\sigma_1 > \frac{R_2}{R_1} > a_e$	$E_1 I_1 E_2 S_2$
$\sigma_2 > \frac{R_2}{R_1}$	$E_2 S_2$			$a_e > \frac{R_2}{R_1} > \tau_2$	$E_1 E_2 S_2$
				$\tau_2 > \frac{R_2}{R_1}$	$E_2 S_2$

Key: (1) condition on. (2) the type of phase contour/outline.

Page 223.

Areas of acceptance. In order simply to write the formulas, which give the area of acceptance, let us determine first three angles α, β and α_e:

$$A \cos \alpha + k_1 B \sin \alpha = \frac{R_2}{R_1};$$

$$A \cos \beta + k_1 B \sin \beta = -\frac{R_2}{R_1};$$

$$a_e \cos \alpha_e + k_1 B_e \sin \alpha_e = \frac{R_2}{R_1}.$$

After designating new through A the area of acceptance, we get for ten cases, contours/outlines of different types:

(1) для $E_1 I_1 S_1$:
$$A = k_1 R_1^2 \left(\theta_1 + 2 \operatorname{ctg} \frac{\theta_1}{2} \right).$$

(2) для $E_2 S_2$:
$$A = \frac{4 k_2 R_2^2}{\operatorname{sh} \theta_2}.$$

(3) для $E_1 S_2$:
$$A = \frac{4 R_1 R_2}{B}.$$

(4) для $I_1 S_2$:
$$A = k_1 R_1^2 (\alpha - \beta) + R_1 R_2 \frac{\cos \alpha + \cos \beta}{B}.$$

(5) для $E_1 I_1 S_2$:
$$A = k_1 R_1^2 \left(\alpha + \frac{B}{B} \right) + R_1 R_2 \frac{2 + \cos \alpha}{B}.$$

(6) для $E_1 E_2 S_2$:
$$A = R_1^2 \left(\frac{B}{B} - \frac{a_e}{B_e} \right) + 2 R_1 R_2 \left(\frac{1}{B} + \frac{1}{B_e} \right) + R_2^2 \frac{\left(\frac{1}{B} - \frac{1}{B_e} \right)^2}{\frac{A}{B} - \frac{a_e}{B_e}}.$$

(7) для $I_1 S_1 S_2$:
$$A = R_1^2 \left[k_1 (\theta_1 - \beta) - \frac{a_s}{B_s} \right] + R_1 R_2 \frac{2 + \cos(\theta_1 - \beta)}{B_1}.$$

① для $I_1E_2S_2$:

$$A = k_1 R_1^2(\alpha_e - \beta) + R_1 R_2\left(\frac{\cos\beta}{\beta} + \frac{\cos\alpha_e}{\beta_e}\right) + R_2^2\left[\frac{1}{AB} + \frac{\left(\frac{1}{\beta} - \frac{1}{\beta_e}\right)^2}{\frac{A}{\beta} - \frac{\alpha_e}{\beta_e}}\right].$$

② для $E_1I_1S_1S_2$:

$$A = R_1^2\left(k_1\theta_1 + \frac{A}{B} - \frac{\alpha_s}{\beta_\theta}\right) + 2R_1R_2\left(\frac{1}{\beta} + \frac{1}{\beta_s}\right) - \frac{R_2^2\sin\theta_1}{k_1 B\beta_s}.$$

③ для $E_1I_1E_2S_2$:

$$A = R_1^2\left(k_1\alpha_e + \frac{A}{B}\right) + R_1R_2\left(\frac{2}{B} + \frac{\cos\alpha_e}{\beta_e}\right) + R_2^2\frac{\left(\frac{1}{\beta} - \frac{1}{\beta_2}\right)^2}{\frac{A}{\beta} - \frac{\alpha_e}{\beta_e}}.$$

Key: (1) for.

Examined below one of the possible uses/applications of theory.

Which must be a radius of the second quadrupole lens, so that the phase space in X- plane, seized by the first quadrupole lens, would be passed also by the second lens?

Of the given above formulas by very simple form follows the condition:

$$\frac{R_2}{R_1} \geqslant ch\,\theta_2 + ctg\frac{\theta_1}{2}\left(k_1 L + \frac{sh\,\theta_2}{k_2}\right).$$

3. Acceptance phase range with focusing-defocusing in Y- plane.

For the recording of the corresponding relationships/ratios in Y- plane it is sufficient simple exchange of indices 1 and 2 and observance of the elementary rules of the execution of operations/processes. One should, however, consider that the form of the seized area at the entrance of doublet is completely different in two planes.

SUBJ CODE 125D MT VERSION- PROG 18 APR 80 DICT 132--01-22-80

Page 224.

160. Parabolic lenses for the focusing of secondary particles with the energy V of several GeV.

T. A. Vsevolozhskaya, I. L. Danilov, V. N. Karasyuk, G. I. Silvestrov.

(Institute of nuclear physics of the Siberian Department of the AS USSR).

For obtaining the intense beams of secondary high energy particles, which are born, as a rule, in the large solid angle, are required electron-optical systems with the large aperture ratio and the sufficiently small focal length. Relatively small particle scattering of high-energy with the passage of substance makes it possible to utilize for their focusing the magnetic field of forward current, which possesses axial symmetry and maximum focusing force. An example of such optical systems are parabolic magnetic lenses to 120 kOe, developed in .YaF Siberian Branch AN in 1963 [1] and used for the collection of positrons with the energy 125 MeV in solid

angle of ~0.04 sterad (linear angle θ~0.1 of rad). The idea of
parabolic lens lies in the fact that for achievement of linear
focusing in the field form $H = \frac{H_0 R_0}{\imath}$ the particle must pass along the
axis/axle of current path, proportional $\imath^2$, i.e. the region of field
it must be limited by paraooloids of revolution with generatrices
$z = a\imath^2$, the focus distance of lens exists $F=B/2a$, where $B=pc/eH_0R_0$,
H_0 - field at a distance of R_0.

Since the field of lens cannot virtually exceed the values of
200-250 kOe, for the particles with the energy in several GeV the
necessary focal length are obtained due to an increase in the
constant of the parabola or "a", which for the angles of collection
θ~0.1-0.2 rad indicates the large length of trajectory in the field,
compared with the focal length. This requires attentive examination
of the optical properties of lens and construction of its surfaces of
the optical properties of lens and its construction of surfaces in
accordance with the exact solution of the equations of motion of
particles in field H~$1/\imath$. In this case the lens with the parabolic
surfaces detects considerable spherical abberation at the angles,
which do not correspond to the condition of thin lens $B\alpha^2/2 \ll 1$ (Fig.
1A).

In case of point source spherical abberation are removed
completely, if the generatrices of the surfaces of lens are connected

with the relationships/ratios

$$\tau_2(\alpha_0) = \tau_1(\alpha_0) e^{\delta(1-\cos\alpha_0)};$$

$$z_2(\alpha_0) = z_1(\alpha_0) + \delta\tau_1(\alpha_0) \int_0^{\alpha_0} \cos\alpha\, e^{\delta(\cos\alpha - \cos\alpha_0)}\, d\alpha,$$

where $(\tau_1(\alpha_0))$ and $(\tau_2(\alpha_0))$ - parametric equation of the generatrices of surfaces, input (1) and exit (2); α_0 - flight path angle of particle to Z-axis at the entrance into the lens.

The form of exit surface can be prescribed/assigned arbitrarily. However, in this case the input coordinate of particle in general nonlinearly depends on angle α_0, which indicates the dependence of the focal length of lens F from α_0, although the position of the principal focus is prescribed/assigned independent of α_0.

With the beam focusing the different from zero transverse phase volume (from the nonpoint source) this nonlinearity leads to the distortions of the emittance or beam, nonremovable with the aid of the subsequent linear focusing as, for example, in the case of lens with the parabolic input surface (Fig. 2a).

Lens is linear, if its input surface is assigned by the equations

$$\tau_1(\alpha_0) = F \sin \alpha_0 e^{-\delta(1-\cos\alpha_0)};$$

$$z_1 = F\left(\cos\alpha_0 \, e^{-\delta(1-\cos\alpha_0)} - 1\right),$$

so that exit coordinate depends on α_0 as $\tau_2(\alpha_0) = F \sin \alpha_0$. In this case there is a large region of angles and coordinates, in which the emittance of beam is transferred virtually without the distortions (Fig. 2b).

An interesting example of the lens in question is lens with the flat/plane exit surface, $z_2(\alpha_0) \equiv 0$. The coordinates of input surface are connected in it with the relationship/ratio

$$z_1(\alpha_0) + \delta\tau_1(\alpha_0)\int_0^{\alpha_0} e^{\delta(\cos\alpha - \cos\alpha_0)} \cos\alpha \, d\alpha = 0,$$

besides obvious from the geometric considerations relationship/ratio $(F + z_1) \, tg\,\alpha_0 = \tau_1$.
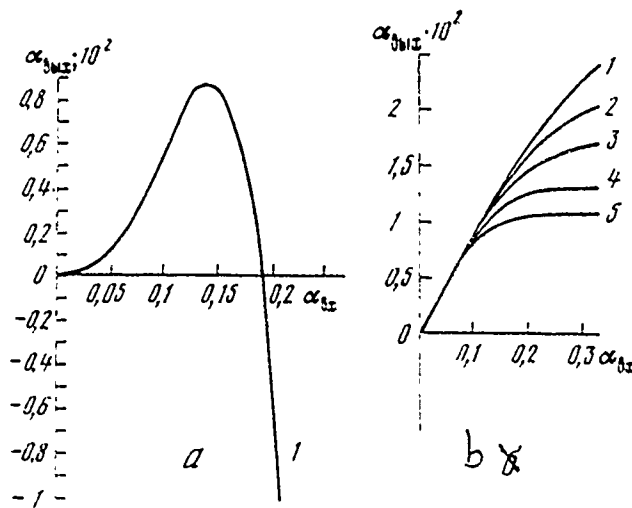
Fig. 1. Spherical of aberation of parabolic lens with the defective profile/airfoil with B=30, F=60 cm, a=0.25 (a) and the chromatic aberration of lenses with the different profiles/airfoils (b): 1 - half lens; B=12, F=60, a=0.1; 2 - linear lens B=12; 3 - parabolic lens (with the corrected profile/airfoil) B=12; 4 - linear lens B=30, F=60, a=0.25; 5 - parabolic lens B=30.

Page 225.

System of two such lenses, connected by planes, serves for the beam focusing from the point into the point. The surfaces of each "half lenses" are constructed in accordance with their focal lengths of f_1 and f_2 and fields H_1 and H_2.

With the equality fields in each half it is possible to combine them,

after removing the dividing surface of z=0.

With the particle focusing from nonpoint source it is in general necessary to consider ϕ - particle speed in contrast to point source where the motion occurs in plane (x,z). However, there is practical interest in source in the form of the thin cylinder whose axis/axle coincides with Z-axis - this case it can occur with the focusing of secondary particles, if the primary beam, which possesses, as a rule, a small phase volume, was focused optimally. In this case ϕ - the rate can be considered equal to 0 for all particles.

The figures Fig. 2 refer exactly to this source and show the conversion of the emittance of the beam, which has rectangular initial (in the first focal plane) emittance, on the passage lenses (in the second focal plane). Along the axis of abscissas is plotted the coordinate of particle referred to the focal length, along the axis of ordinates - the transversa impulse, in reference to the full/total/complete particle momentum. In this form the given results are valid for any values of focal length at one and the same value B. The calculations of trajectories were conducted on the computers with precision/accuracy $\sim 10^{-6}$.

Chromatic aberration of lens, i.e., angular scatter at its output depending on the scatter of impulses/momenta/pulses, can be

expressed by relationship/ratio $\Delta\alpha = \alpha_0 \varepsilon(\alpha_0)\frac{\Delta p}{p}$, where $\varepsilon = 1$ at the angles, which correspond to the approximation/approach of thin lens, and then decreases with the increase α_0. Dependence $\varepsilon(\alpha_0)$ differs somewhat for different types of lenses and different values B (Fig. 1b).

At present in IYaF is conducted the development of two types of parabolic lenses. The first lens will be used in the unit of the target of a proton-antiprotonnoyo accumulator/storac. VAPP-4 for the collection fr the target of antiprotons with the impulse/momentum/pulse 1.8 GeV and the angles of generation +-0.15 rad [2]. It is linear lens in focal length less than 20 cm and by maximum field on the neck (point of connection of current shells) $H_{max} = 200 + 450$ kOe. Fig. 3 gives the section of lens with the set of tires. the housing of lens is made fr natural titanium; wall thickness on the input surface which the particles pass at minimum angle, it reaches on an outside radius of 0.5 mm and it increases in the neck so that in the field on inside radius $H_{max} = 200$ kOe maximum mechanical stresses in each section are $\sigma \approx 3500$ kg/cm². The path of particle in the walls of lens is 6-8 mm. The construction/design of set of tires is made by such, that with attachment of both contact surfaces of lens appears no axial of loads of its housing. The coaxial set of tires of lens halfway converts/transfers into two wide flat/plane busbars/tires for the supply of current. Two halves sets of tires, which are located under the different potentials, are

isolated/insulated by the glass cloth, saturated with epoxy resin under the pressure 30 atm., to the voltage to 15 kV. Lens has an inductance 30 cm and it will be supplied by sinusoidal current pulse with the duration on the basis/base 3-5 μs and by amplitude of 500-700 kA. Lens is fed by current from the oscillator, which is high-voltage storage capacity/capacitance and system of vacuum dischargers/gaps, through the matching current transformer with the transformation ratio 4 and a small scattering (led to load $L_p \approx 2$ cm), designed for the voltage in the primary circuit to +-50 kV.

The second type of lens is developed/processed for the use/application in the focusing system of neutrino circuit IPVE [3]. From six such lenses it is proposed to assemble the objective which must accomplish/realize an acromatic focusing of mesons in the large momentum range. Since in this system of lens they do not have the specific focal length, they all have parabolic surfaces. Fig. 4 gives the section/cut of mock-up of one of the lenses with the set of tires.
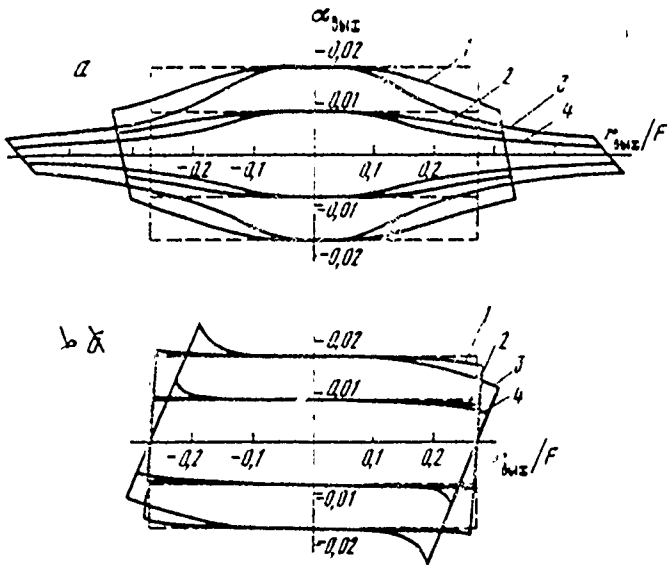
Fig. 2. Geometric of aberrations of lenses with the different
profiles/airfoils; in the first focal plane source has rectangular
emittance with the sizes/dimensions of 1.3-+-1 cm, 2.4-+-0.5 cm; and
by the maximum angles of entrance α_{0max}" 0.27 rad in all cases: a)
parabolic lens (1.2 - E=12; 3.4 - E=30; b) linear lens 1.2 - B=12;
3.4 - B=30.
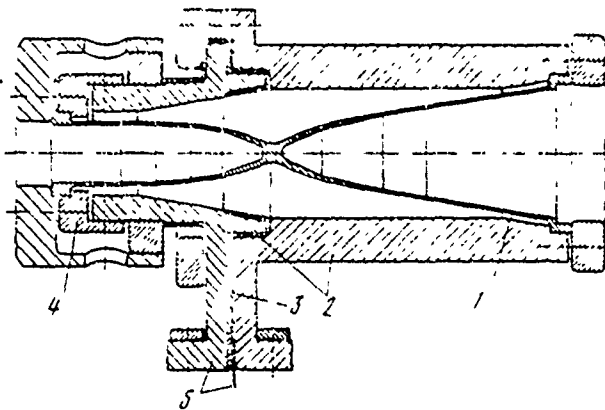
Fig. 3. Linear lens for the collection of antiprotons 1 - the housing of lens, 2 - set of tires; 3 - insulation/isolation; 4 - clamp contact; 5 - flat/plane current input.

Page 226.

Lens has maximum radius $R_{max} = 16$ cm and length $2z=32$ cm. Set of tires is also carried out in the form of the coaxial, which converts into two flat/plane current-conducting busbars. One side of the housing of lens is rigidly attracted/tightened to the set of tires by clamping ring, the second side has clamp attachment for eliminating the axial loads with the attachment. Inductance of system $L_H \simeq 40$ cm. Lens is supplied from the low-induction current transformer by semisinusoidal current pulse by duration in the basis/base 100 μs and the amplitude to 1000 kA [4]. Lens will be supplied by the doubled current pulses of arbitrary polarity, separated by the interval of

0.25 s with the frequency of the messages of 1 times in seconds. The
first mock-up of the housing of lens is prepared from the dural D-16
without the heat treatment. A radius of neck $r_{min} = 1.5$ cm, of wall
thickness is made such, that in the direction in parallel to the
axis/axle of ray/beam the particles pass to substance less 2x0.5 cm.
This lens was tested by currents 750 kA, which corresponds to maximum
field $H_{max} = 100$ kOe. At present is developed/processed technology of
the heat treatment of the duralumin housings of lenses, which will
substantially increase maximum permissible mechanical stresses in the
walls and will make it possible to ensure the reliable work of lens
with the currents 1000 kA. Another method of an increase in the
reliability of lens is the production of its housing from titanium.
Is prepared and is prepared for with tests the welded titanium lens:
the middle of lens in the region of neck is grooved from the natural
material, to which are welded rolled from the sheet of cone,
processed then along necessary profile/airfoil. This lens possesses
substantially best mechanical properties; however, complication in
its use they can be caused by the increased thermal condition,
connected with high specific resistance of titanium.
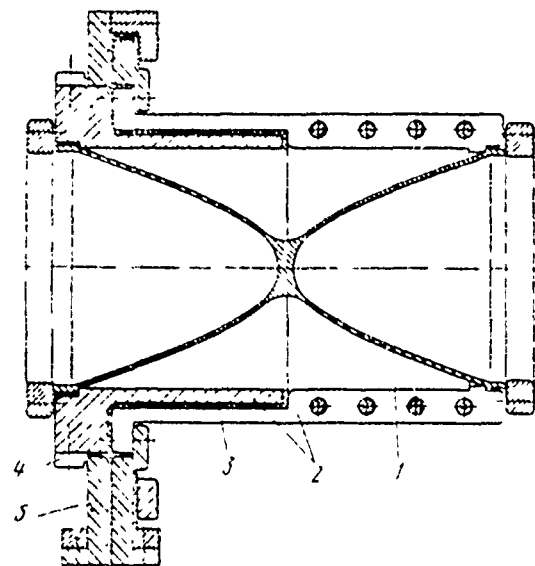
Fig. 4. The parabolic lens of neutrino circuit 1 - the housing of lens; 2 - set of tires; 3 - insulation/isolation; 4 - clamp contact; 5 - flat/plane current input.

REFERENCES

1. L. L. Danilov and et. al. ZhETF,[Journal of Experimental and Theoretical Physics] Vol. 37, p. 914, 1967.

2. G. I. Budker and et. al. Scheme for obtaining antiprotons on an apparatus with counter protron-antiproton beams of IYaF [Institute of Nuclear Physics], of the AS of USSR. (See present collection, Col. II).

3. A. V. Samoylov and et. al. Focusing device for netron experiments. (See present collection, Vol. II).

4. L. L. Danilov and et. al. Pulse generator with a reactive power of 1.5-2 TW on magneto controllable valves. (See present collection, Vol. II).

161. Focusor for the neutrino experiments (design characteristics).

V. I. Voronov, I. A. Danil'chenko, R. A. Rzayev, A. V. Samoilov.

(Institute of high-energy physics).

In the series of problems of physics of elementary particles, in particular, in the experiments with the neutrino, appears the need for converting the divergent charged particle beam into the parallel or the close one to it, moreover this formation it must undergo maximally wide energy and angular ranges. With fulfilling of these requirements the neutrino flux, originated during the decomposition/decays π and κ-mesons, will be maximum. Supplementary important requirement is the need for conducting the beam shaping of particles on possibly the shorter basis so that in the fraction/portion of the shaped beam would remain the significant part of flight path.

At the present time for the accomplishment or this objective they were applied or were examined "magnetic horn" [1], "magnetic fingers/pins" [2], plasma lens [3] and "crucible" with one-two supplementary reflectors [4].

Page 227.

The focusing properties of such systems and neutrino flux from them it is accepted to compare with the spectrum of neutrino from so that called "neutrino parents' ideally focused" beam (NR), under which we understand parallel and infinitely pencil NR. If we accept as the initial parameters energy of the proton beam, which forms beam NR, $E_p = 76$ GeV and distance from the target of generation NR to detector the neutrino flux whose spectrum is shown in Fig. 1 (curve 1). Under the same conditions magnetic horn with one supplementary reflector will give neutrino flux with the spectrum, shown in Fig. 1 (curve 2) [5]. From the comparison of curves it is evident that the real focusing gives neutrino flux into 2-3 smaller than ideal (without taking into account losses in the walls of system).

All above mentioned systems are pulse with the duration of the pulse of field of approximately 2-5 µs. In the systems of the type crucible/horn, horn[crucible]+ reflector and magnetic fingers/pins the axisymmetric magnetic field is created by the current, which flows along the axisymmetric shells; field length is determined by the set of the conical surfaces, which assign the profile/airfoil of shell. In the plasma lens this field is initiated by the high-voltage

discharge in the plasma, which gives current with an approximately/exemplarily permanent density of j. In this case the deflecting force of plasma lens is approximately/exemplarily proportional to distance from its axis/axle.

The characteristic feature of all devices/equipment of the described types is the fact that value

$$F = \alpha_{\delta b i x} / \alpha_{\delta x}, \qquad (1)$$

describing the focusing properties of system, is either the function of particle momentum or by the function : the angle of its entrance into system $\alpha_{\delta x}$ and the impulse/momentum ($\alpha_{\delta b i x}$ - angle at which the particle leaves the system), while for the ideal focusing is required the equality zero relations (1) in as possible more the broad band of the angles of the entrance and impulses/momenta/pulses.

Let us examine a question about the possibility of the formation of parallel beam NR by different combinations of current parabolic lenses (PL).

In PL [6] (Fig. 2) the components of magnetic field in the cylindrical coordinate system ρ, z, ϕ are equal to:

$$B_\rho = 0, \quad B_\varphi = \frac{\alpha}{\rho}, \quad \alpha = const \qquad (2)$$

and, since the length of the lens

in approximation of thin lenses the deflecting force of the parabolic lens is proportional to the radius on which the particle falls into the lens:

$$B_x = c\rho, \quad c = const. \qquad (4)$$

Matrix/die single PL can be presented in the form

$$M = \begin{bmatrix} 1 & 0 \\ -x/p & 1 \end{bmatrix}, \qquad (5)$$

where x - focusing force of the lens

$$x = \infty I ; \qquad (6)$$

I - the current, which goes through the lens; x - parameter, which describes the profile/airfoil of lens and which switches on dimension factors; p - particle momentum.

let the distance from a target-source NR to PL be equal s=1. Then the curve of dependence of F on the particle momentum will be IMET [- Institute of Metallurgy im. A. A. Baykov] the form

$$F(p) = \frac{\alpha_{\delta bix}}{\alpha_{\delta x}} = M_{22}(p). \qquad (7)$$

It is given for one PL in Fig. 3 (curve 1). For the two-lens system where each of PL we have deflecting forces of x_1 and x_2 and it is located at a distance of ℓ_1 one from another, requirement of the parallelism of beam gives the relationship/ratio

$$M_{22} = 1 - \frac{1}{p} \left[x_1 + (1 + \ell_1) x_2 \right] + \frac{1}{p^2} \ell_1 x_1 x_2 = 0, \qquad (8)$$

that reducing to the equations

$$\begin{cases} x_1 + (1 + \ell_1)x_2 = p_1 + p_2, \\ \ell_1 x_1 x_2 = p_1 p_2, \end{cases} \qquad (9)$$

where p_1 and p_2 - those impulses/momenta/pulses, with which the beam is strictly parallel. Form $M_{22}(F)$ is shown in Fig. 3 (curve 2) for case of $p_1/p_2 = 3$.
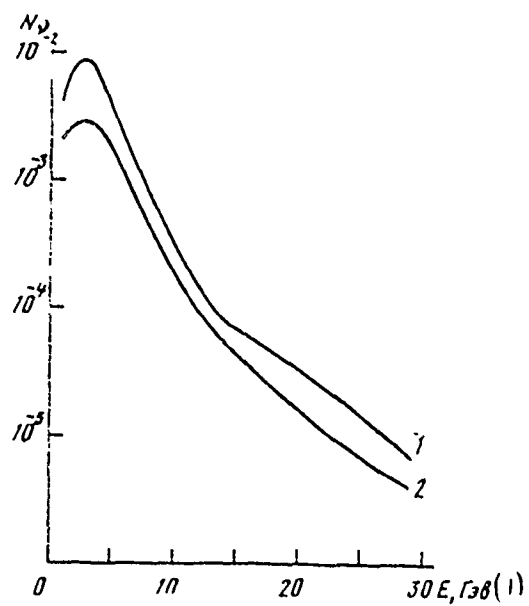
Fig. 1. The spectra of neutrino with "ideal" (1) and real focusing (2) of the neutrino parents (is given the output of neutrino to one interacted proton).

Key: (1). GeV.
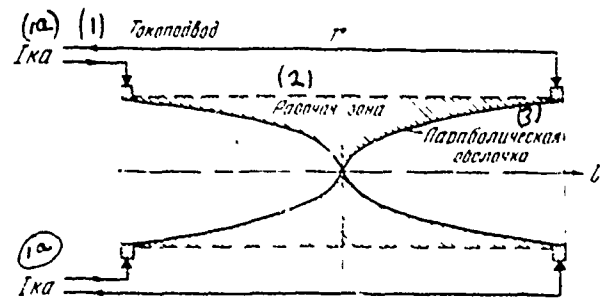
Fig. 2. Schematic of parabolic lens.

Key: (1A). kA. (1). Current input. (2). Working zone. (3). Parabolic

shell.

Page 228.

In the three-lens version where the forces are equal to x_1, x_2, x_3, and distances with respect 1, ℓ_{x_1}, ℓ_{x_2}, requirement of parallelism gives

$$M_{22} = 1 - \frac{1}{p}\left[x_1 + (1+\ell_1)x_2 + (1+\ell_1+\ell_2)x_3\right] + \frac{1}{p^2}\left[\ell_1 x_1 x_2 + (\ell_1+\ell_2)x_1 x_3 + \ell_2(1+\ell_1)x_2 x_3\right] - \frac{1}{p^3}\ell_1\ell_2 x_1 x_2 x_3, \quad (10)$$

whence we have equations for the particle momenta and forces of the lenses:

$$\begin{cases} x_1 + (1+\ell_1)x_2 + (1+\ell_1+\ell_2)x_3 = p_1 + p_2 + p_3, \\ \ell_1 x_1 x_2 + (\ell_1+\ell_2)x_1 x_3 + \ell_2(1+\ell_1)x_2 x_3 = p_1 p_2 + p_1 p_3 + p_2 p_3; \\ \ell_1\ell_2 x_1 x_2 x_3 = p_1 p_2 p_3. \end{cases} \quad (11)$$

Form $M_{22}(P)$ for three-lens system when $P_{max}/P_{min} = 3$ is shown in Fig. 3 (curve 3).

Finally, for the four-lens system with the forces of lenses x_1, x_2, x_3, x_4 and with distances or 1, ℓ_{x_1}, ℓ_{x_2}, ℓ_{x_3} condition $M_{22}=0$ gives the following equations:

$$\begin{cases} x_1 + (1+\ell_1)x_2 + (1+\ell_1+\ell_2)x_3 + (1+\ell_1+\ell_2+\ell_3)x_4 = p_1 + p_2 + p_3 + p_4, \\ x_1 x_2 + (\ell_1+\ell_2)x_1 x_3 + (\ell_1+\ell_2+\ell_3)x_1 x_4 + (1+\ell_1)\ell_2 x_2 x_3 + \\ \quad + (1+\ell_1)(\ell_2+\ell_3)x_2 x_4 + (1+\ell_1+\ell_2)\ell_3 x_3 x_4 = \\ \quad = p_1 p_2 + p_1 p_3 + p_1 p_4 + p_2 p_3 + p_2 p_4 + p_3 p_4, \\ \ell_1 \ell_2 x_1 x_2 x_3 + \ell_1(\ell_2+\ell_3)x_1 x_2 x_4 + \ell_3(\ell_1+\ell_2)x_1 x_3 x_4 + (1+\ell_1)\ell_2\ell_3 x_2 x_3 x_4 = \\ \quad = p_1 p_2 p_3 + p_1 p_2 p_4 + p_1 p_3 p_4 + p_2 p_3 p_4, \quad \ell_1 \ell_2 \ell_3 x_1 x_2 x_3 x_4 = p_1 p_2 p_3 p_4. \end{cases}$$

In general for the systems, which consist of the n lenses

$$M_{22} = \frac{1}{p^n} \prod_{i=1}^{n}(p - p_i), \qquad (13)$$

where p_i - those values of the impulses/momenta/pulses, with which the beam is strictly parallel (see Fig. 3, curve 5).

Thus, combinations of three or four parabolic lenses, which have the deflecting forces, determined by the systems of equations of type (11) or (12), make it possible to form beam NR, close to the parallel over a wide range of impulses/momenta/pulses in the absence of the dependence of the character of focusing on entrance conditions into the system: for the comparison Fig. 3 shows the appropriate system characteristics the "crucible", used in CERN [7] (see Fig. 3, curves 6 and 7).

Fig. 4 shows fundamental optical diagram of one of the versions of two-lens system for case of $\zeta = 4$, $P_{max}/P_{min} = 3$ and one of the versions of three-lens system for case $P_{max}/P_{min} = 6$, $\ell_1 = 2$, $\ell_2 = 6$.

The overall length of three-lens system with S=1.2 m has a value
of 11 m, i.e., occupies 5.5o/o of flight path 200 m. For the
comparison let us point out that the system, described in work [8],
forms/shapes beam for elongation/extent 60o/o of flight path.

Let us examine a question about the absorption of particles by
multilens systems. In order to deflect particles with
impulse/momentum/pulse P_{max} on angle $\alpha_{\delta x}$, is required one lens or
system of lenses with the total deflecting force

$$B_z = B(\rho)\delta\rho^2 = \sum_{i=1}^{n} B(\rho_i)\delta_i\rho_i^2, \qquad (14)$$

where $\sum_{i=1}^{n}\delta_i = \delta$, if $\rho = \rho_i$. $\qquad (15)$
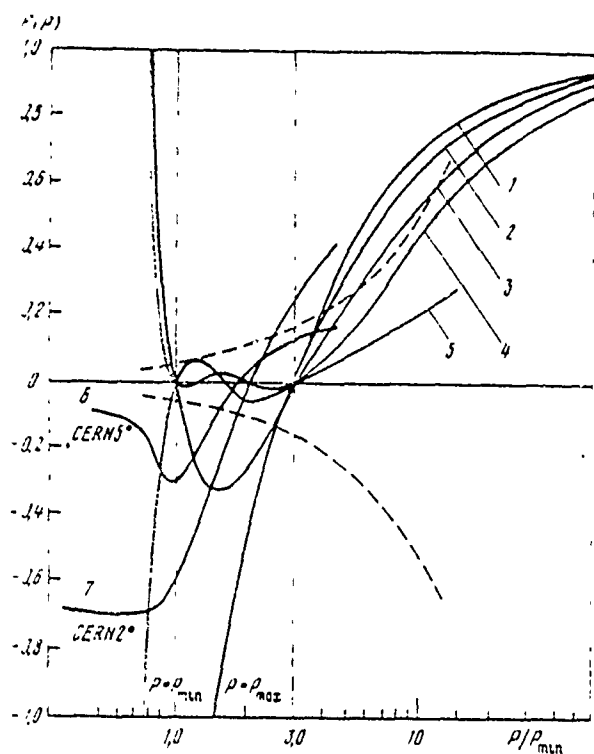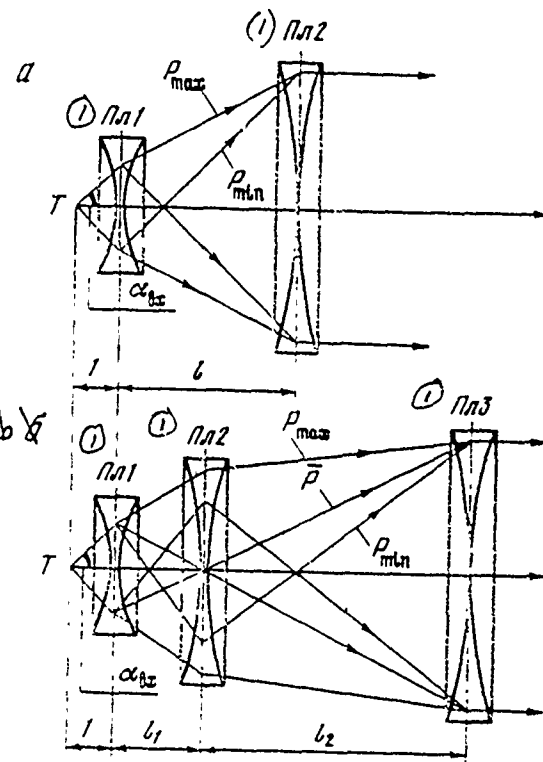
Fig. 3.

Fig. 4.

Fig. 3. Focusing properties of different systems by multiplicities.

Fig. 4. Fundamental optical diagrams of one of versions of two-lens system (a) and one of versions of three-lens system (b).

Page 229.

The path of particle in the wall of lens is lengthened in

accordance with the relationship/ratio

$$\frac{dz}{d\rho} = 2\beta\rho = 2\sum_{i=1}^{n} \delta_i \rho_i, \qquad (16)$$

i.e. during the separation of one lens on somewhat shorter lenses the absorption of particles changes it unessentially and depends only on the radial position of particle. Therefore each lens of the focusing system of one or the other multiplicity can be presented in the form of the objective, which consists of the series/row of shorter lenses.

It is clear, the the systems, constructed according to the described principle, can decide other tasks - to focus parallel beam with the large scatter along the impulses/momenta/pulses into the image of small sizes/dimensions, or to transfer to the required image distance of the source of the particles (in this case the necessary equations obtain, equalizing to zero matrix coefficient M_{12}).

The calculations outlined above, executed in approximation of thin lenses, were checked by a precise calculation on the computers; agreement in all cases was not more badly 15-20 %.

References.

1. S. van der Meer. CERN, 61-7, 1961.
2. R.B.Palmer. Sympos. on Neutrino Physics, CERN,
   1965.
3. E.B.Forsuth, L.M.Ledermann. J. Sunderland.
   CERN, 65-32, 1965.
4. A.Asner, Ch. Iselin. CERN, 65-17, 1965.
5. G.C.Sacerdotti, E.Fiorini, A.Pullia,
   C.Conta, C.Franzinetti. High Energy Neutrino
   Beam for the Serpukhov Accelerator. Milano,
   1969.

6.   L. L. Danilov, S. N. Rodionov, G. I. Sil'vestrov,
AhTF [Journal of Technical Physics], Vol. 37, p. 914,
1967.'

7. S. van der Meer, K.M.Vahlbruch. CERN, 63-37,
   1963.
8. G.Grüber, R. Grüb, B. Langeseth. CERN NPA/Int,
   69-13, 1969,

162. Deflection system $\overset{HF}{\text{+. ¬.}}$ of separator for the proton synchrotron
IFVE.

V. M. Levin, V. A. Meringol, V. L. Smirnov, Yu. A. Sokolov, A. K.
Orlov.

(Scientific research institute of the electrophysical equipment im.
D. V. Efremov).

V. N. Alferov, M. A. Bulgakov, A. M. Vishnevskaya, M. B.
Vladimirtsov, V. I. Kotkov, B. V. Prosin, V. G. Rogozinskiy, I. R.
Yampol'skiy.

(Institute of high-energy physics).

In the high-frequency separators of the charged/loaded particles
as the deflectors are applied the diaphragm waveguides, which work in
the mode/conditions of the traveling hybrid wave EH_{11} [1-3]. Such
systems have much in common with the accelerating sections of
electronic linear accelerators. However, the use of the asymmetric
wave EH_{11} causes the series/row of the supplementary requirements,
connected with the need for the stabilization of the plane of

polarization and the selection of the operating modes with the
maximum electric fields for the large durations of pulses (to 10 μs).
The parameters of deflectors were selected employing the procedure,
described in work [4], and were given below.

(1) Параметры   (2) Величина   (n) Длина волновода ℓ, м 4
(3) Рабочая частота f_0, Мгц 2797,2   (13) Максимальная мощность в импульсе P, Мвт 20
(4) Внутренний диаметр диафрагм 2a, мм . .46   (14) Напряженность отклоняющего поля
(5) Диаметр полости   волновода, 2в,мм . . 119,8 E_0,кв/см 74
(6) Толщина диафрагм t, мм 6   (15) Максимальная напряженность электри-
(7) Шаг ячейки d, мм 26,8   ческого поля E_{max}, кв/см 240
(8) Сдвиг фазы на ячейку . . . . π/2   (16) Длительность   импульса τ, мксек   10
(9) Групповая скорость $\beta_{гр}$ . . . . −0,0327
(10) Отношение шунтового импеданса
   к добротности $\frac{R}{Q}$, ом/м $1,2.10^3$
(11) Коэффициент затухания α, нп/м   0,091

Key: (1). Parameters. (2). Value. (3). Operating frequency f_0, MHz.
(4). Bore of diaphragms 2a, mm. (5). Diameter of cavity of waveguide,
2V, mm. (6). Thickness of diaphragms t, mm. (7). Step/pitch of cell
d, mm. (8). Phase displacement to cell. (9). Group velocity. (10).
Ratio of shunt impedance to quality, R/Q, Ω/m. (11). Attenuation
factor α, np/m. (12). Length of waveguide. (13). Maximum power in
impulse/momentum/pulse R, MW. (14). Deflecting field strength E_0,
kV/cm. (15). Maximum electric intensity E_{max} kV/cm. (16). Duration of
pulse τ, μs.

Work examines the design features of deflector and are given the
results of the measurements of the parameters of one-meter

experimental section at the low and high power levels. Experimental
section is completely soldered construction/design from the separate
cells and the matchers, prepared with the allowances +-5 μm (2V) and
+-10 μm (remaining sizes/dimensions). Section is equipped with jacket
made of the stainless steel for the thermostatic control. In the
center of section is provided for the coupling element with crosstalk
attenuation 60 dB, which makes it possible to measure the averaged
phase of the strength of field. To avoid the rotation of the plane of
polarization of wave in the loading disks are made the slots (see
Fig. 1).

Page 230.

In this case the dispersive characteristic of the wave, polarized in
the plane of the divergence of particles, virtually is not distorted
(curve I), but in the perpendicular plane it is displaced on 40 MHz
(curve II), which corresponds to the decrease of phase change to the
call on 23.5° in the operating frequency. Natural frequencies $\pi/2$ -
the vibration mode of separate cells were measured by the method of
wave resonator [5]. In order to exclude the accumulation of
reflections along the length of section, cell they are assembled by
way of a steady change in their natural frequencies. Matcher contains
movable diaphragm which makes it possible to compensate for the
reflections, connected with the possible with the damage of structure

in the process its rations.

For determining the parameters of section at a small power level was developed the measuring unit, based on the principle of nonresonant disturbance/perturbation [6]. The basic results of measurements are given in Table 1. Are there for the comparison shown computed values [1] and results, obtained by the method of resonance disturbance/perturbation to models [4, 7]. From the comparison of given data it is evident that they coincide in the limits of several percentages.
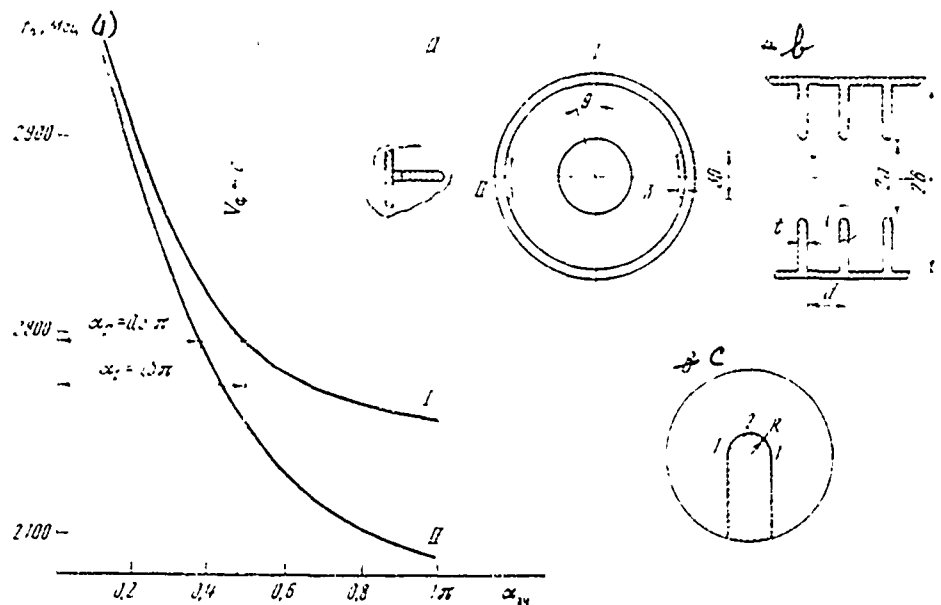
Fig. 1. Basic dimensions and dispersive characteristic of the section: a) wave is polarized in the plane of divergences (1) and in the plane, perpendicular to the plane of divergence (11); b) the location of slots for the stabilization of the plane of polarization; c) place with a maximum quantity of breakdowns (1) and point of the maximum value of electric field (2).

Key: (1). MHz.
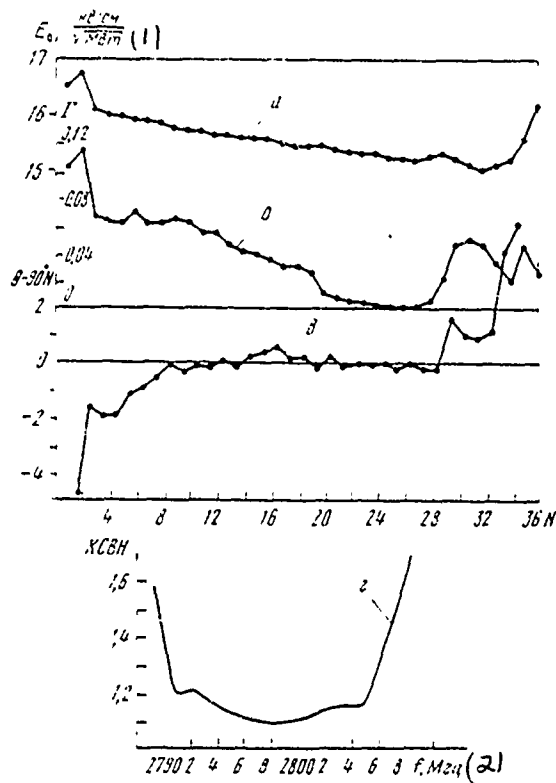
Fig. 2. Fundamental characteristics of the section: a) the distribution of the standardized/normalized deflecting intensity/strength along the section; b) the distribution of reflection coefficient along the section; c) change of the phase of field along the section; d) band characteristic at the entrance of section in the presence of ceramic windows.

Key: (1). kV/cm//MW. (2). MHz.

table 1.

(1) Параметры	(2) Метод нере-зонансного возмущения	(3) Метод резо-нансного возмущения	(4) Расчетные величины
(5) Отношение шунтового импеданса к добротности, Ом/м	$1,47.10^3$	$1,50.10^3$	$1,59.10^3$
(6) Относительная групповая скорость	$-0,0326$	$-0,0327$	$-0,0329$
(7) Коэффициент затухания	$0,036$	$0,092$	$0,090$
(8) Нормированная отклоняющая напряженность поля $\frac{E_0}{\sqrt{P}}$, кВ/см(4)/ V Мвт	$15,9$	$16,3$	$16,8$

Key: (1). Parameters. (2). Method of nonresonant

disturbance/perturbation. (3). Method of resonance

disturbance/perturbation. (4). Calculated values. (5). Ratio of shunt

impedance to quality, Ω/m. (6). Relative group velocity. (7).

Attenuation factor. (8). Standardized/normalized deflecting strength

of field. (9). kV/cm//MW.

Page 231.

The measurements of field distribution in the section showed

that the reflection coefficient does not exceed 0.12 and phase change

it differs from calculated not more than on +-2° (see Fig. 2). It must be noted that the strength of the field of the incident wave builds up to the input and exit matchers by approximately 5o/o. In this case phase changes in the appropriate cells differ significantly from calculated ones. More detailed measurements showed that, apparently, this is connected with the mechanism of the regeneration of wave TE_{01} in the conductive waveguide and the matcher into the hybrid wave EH_{11} in the section. KSVN [99sp04 - VSWR], measured from entry side of section at the operating frequency in the presence of separating ceramic windows, does not exceed 1.1 (see Fig. 2). The divergence of the plane of polarization from the vertical was determined by the method of the comparison of field distributions along Z-axis (in each section fields were measured at several points according to the azimuth) and proved to be $\leqslant 2°$.

For testing the experimental section at the high power level it was connected to klystronKIU-12, ensuring power 20 MW for the duration of pulse of 10.3 µs (see Fig. 3). The excitation of klystron was accomplished/realized by the master oscillator with frequency stability $\Delta f/f=10^{-6}$ and by amplifier stage on the travelling-wave tube. Power measurement was made by the calorimetric absorbing load (see [8]). Breakdowns in the section were recorded by FEU, established/installed in inspection window, and to the reflected wave. For the evacuation of section was utilized the aggregate/unit

the era 300 (two celite and one titanium pumps NEM-300), the ensuring vacuum at the entrance into the section $2 \cdot 10^{-7}$ torus, and at the output $-6 \cdot 10^{-7}$ torus. The composition of residual gas is given in Table 2.
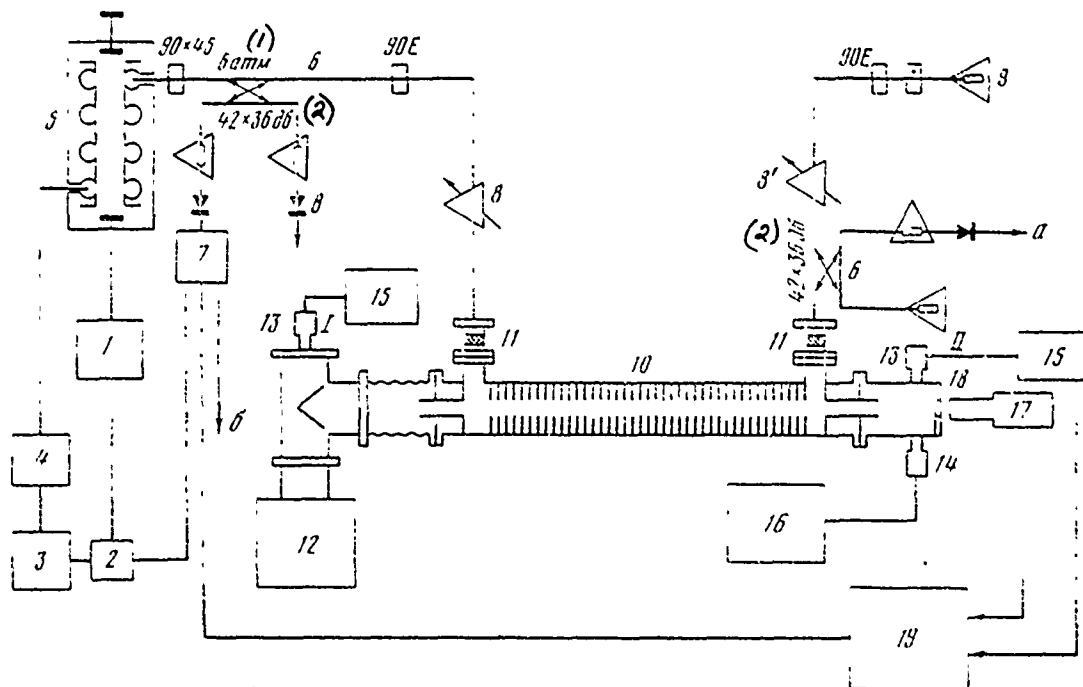
Fig. 3. Block diagram for the test run at the high power level 1 - the modulator of klystron (U=300 kV, P=70 MW, τ_u =10 μs); 2 - discriminator and impulse shaper of rapid protection; 3 - master oscillator; 4 - amplifier on the travelling-wave tube; 5 - test klystron KIU-12; 6 - the directional couplers; 7 - the emitter follower; 8,8' - transformers agreeing, waveguide; 9 - calorimetric load; 10 - experimental section; 11 - ceramic separating windows; 12 - vacuum aggregate/unit ERA 300; 13 - manometric lamp IM- 12; 14 - sensor of RMO-4 ; 15 - vacuum gauge VI-12; 16 - meter of partial pressures IPDO-1; 17 - FEU-27; 18 - window for observing the breakdowns; 19 - automatic recorder N320-5; a, b, c, to the oscillograph.

Key: (1). atm. (2). dB.

Table 2.

Режим (1)	Суммар-ное дав-ление, тор (2)	Газовые компоненты, % (3)					
		H_2	H_2O	$CO+N_2$	O_2	Ar	CO_2
(4) До ввода мощности	6.10^{-7}	26	34	27,4	2,7	3	2,3
(5) В.ч. трени-ровка до прогрева секции	3.10^{-7}	15,6	22,6	45,3	2,2	7,3	3,2
(6) После прогрева (1)	$8,4.10^{-8}$	15,2	33	41	1,7	—	4,2
(7) В момент пробоя (2)	$2,8.10^{-7}$	24	12,5	43	2	—	16,5
(8) Отношение режима (2) к (1)		5,2	1,24	3,4	4	—	13

Key: (1). Mode/conditions. (2). Total pressure, torus. (3). Gas components, %. (4). Before introduction/input of power. (5). V. h. aging/training to warm-up of section. (6). After warm-up. (7). At moment of breakdown. (8). Relation of mode/conditions.

Page 232.

In the beginning of aging/training it was explained that the breakdowns, which appear at power ~5 of MW, lead to a sharp reduction in dielectric strength as a result of disturbance of the surface of structure with the large energy of breakdown. For decreasing the output energy was introduced protection (see Fig. 3), which lowers

the excitation 0.2 μs after the emergence of the wave reflected. Simultaneously was disconnected voltage from the klystron and then during 20 s exponentially it neaved to the previous level. In this case it was possible during 20 hour to raise the introduced power to 20 MW with the frequency of breakdowns ~15 hour. Further aging/training did not lead to an essential improvement in dielectric strength. The warm-up of section to temperature of 390°C made it possible to improve vacuum despite the fact that after warm-up in the section was short-term admitted the atmosphere. However, in this case a number of breakdowns decreased insignificantly. The latter fact gives grounds to assume that the effect of aging/training consists not so much in degassing or the walls of section, as in removal (burning-out) of microheterogeneities.

For the purpose of the acceleration of aging/training in the section transformers 8 and 8' established/installed mode/conditions $KSVN=1.7$ that it corresponds to the strength of field on the edges of diaphragms $E_{max} = 330$ kV/cm instead of 250 kV/cm in $KSVN=1.1$ (corresponding field distributions on the diaphragms, measured by the method of nonresonant disturbance/perturbation, are given in Fig. 4). After aging/training in this mode/conditions during 7 and 4 hour with the shift of the maximums of intensities/strength to the adjacent diaphragms it was possible to virtually exclude breakdowns in the nominal rating. The examination/inspection of surface condition of

section after aging/training snowed that the traces of breakdowns are on all diaphragms and there is no clear correlation between the value of the strength of field and the place of breakdown. For example, the traces of breakdowns are discovered in the places where the intensity/strength fields by above 100 kV/cm (point 1 with $\theta=66^{\circ}$, Fig. 1c), and are not discovered at points with the intensities/strength 330 kV/cm (point 2 with $\theta=0$, Fig. 1c). In this case substances the places of breakdowns with the low strength of field the quality of finish of the surface of diaphragms is noticeably worse. Thus, with a good quality of finish of the surface of section it is possible to rely on the achievement of the maximum intensities/strength of fields 330 kV/cm in the modes/conditions with the pulse duration to 10 μs.
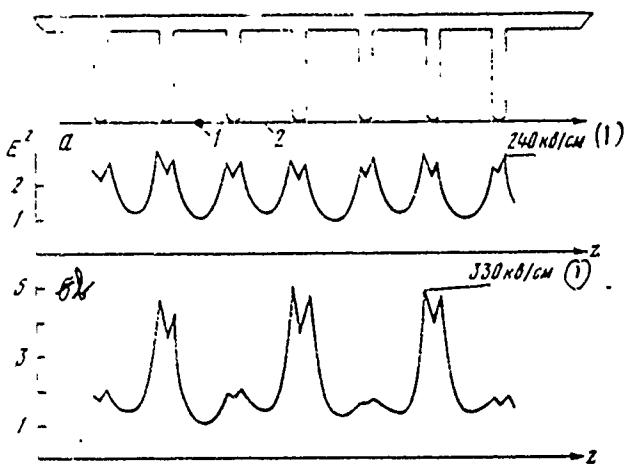
Fig. 4. The field distribution according to the roundings of
diaphragms, during the nominal rating - KSVN=1.1 (A) and during the
training mode/conditions KSVN=1.7 (b) 1 - measuring probe (sphere
from the teflon with a diameter of 2.5 mm); 2 - nylon filament (ϕ =
=0.13 mm).

Key: (1). kV/cm.

REFERENCES

1. P. Bernard, H. Lengeler, V.Vaghin. CERN Preprint, CERN.68-30, 1968.

2. H.Hahn, H.I.Halama. Rev. Scient. Instr., 1965, 36, p.1733.

3. R.R.Larsen, O.A.Altenmuller, G.A.Loew.   Mezhdu-narodnaya konferentsiya po uskoritelyam,[International conference on accelerators], (Dubna, 1963). Atomizdat, 1964, p. 804.

4. V. I. Kotov, I. R. Yampol'skiy. ZhtF, 1968, Vol. XXXVIII, Issue 1, p. 143.

5. V. L. Smirnov. In collection: "Elekronfizicheskaya apparatura", Issue 8, 1969, p. 164.

6. Ch. W.Steele. IEEE Trans. MTT-14, N 2, p.70, 1966.

7. I. R. Yampol'skiy. ZhtF, 1966, Vol. XXXIX, Vo.7, p.1300.

8. V. M. Alferov and et. al. ZhTF [Electronic technology ser es I. Electronics of SHF], 1969, Issue 6, p. 37.

163. Method of automatic electromagnetic separation into the energy
in the resonator accelerator.

V. G. Bagramov, G. R. Basman, D. V. Iremashvili.

(Sukhumi physiotechnical institute).

For conducting the number of investigations in the field of
laser technology, radiation chemistry, studying the questions of
plasma-beam interactions, etc. were required high-current electron
beams. Depending on specific physical problem can be produced
different requirements for the energy homogeneity, the focusing and
the duration of front and snear/section of the make pulse of electron
beam [1].

In 1963 in the Sukhumi physiotechnical institute was developed
high-current electron accelerator "EU" of the resonator type
(frequency f=6.5 MHz) with by accelerating voltage to 1.3 MV at the
eyepiece of beam to 1000 and also the frequency of messages 0-5 Hz
[2].

Page 233.

The investigations of the current-response characteristics of accelerator showed that the specific special features/peculiarities of the work of plasma spark electron source lead to the appearance at the output of the package of make pulses (5-10 pcs) in one cycle of acceleration, moreover the amplitude of make pulses unguided is changed both in the package and from one impulse/momentum/pulse to the next [3]. For expanding the experimental possibilities of accelerator is developed and place in operation second channel, which makes it possible to obtain the single stable make pulse of the separated electrons. As the electron source is utilized the thermionic-emission gun with the hexaboridelanthanum cathode, designed for obtaining of electron beams with the current 500-1000 A. Gun is developed by the authors [4]. For obtaining the prescribed/assigned energy spread of electrons the accelerated beam, which possesses continuous energy spectrum (accelerating voltage has sinusoidal form), it is necessary to subject to separation. The analy is of the existing methods of the separation of electrons - magnetic, electrodynamic, temporary/time - showed that in the cavity-type accelerator most promising is the method of automatic electromagnetic separation. The final adjustment of the method of separation was conducted on the electron gun, which makes it possible to obtain electron beams with the current ~50 A.

The method of automatic electromagnetic separation consists in the use of mutually perpendicular electrical and magnetic fields, which are changed in the time and the space in the coaxial region of the cap/filling of accelerator (Fig. 1). In the middle part of the cap/filling of accelerator the electric field has only radial, and magnetic - only azimuthal constituting. In the range of change in question of the fields in the time occurs according to the sinusoidal law, the maximum of the amplitude of magnetic field advancing on 90° maximum of the amplitude of electric field. The electron, which starts in zero phase ($\phi\sim0$) of accelerating voltage, supplies into the perpendicular to its rate magnetic field of maximum intensity/strength which strongly deflects/diverts trajectory from the rectilinear. The electron, which starts in phases of $0<\phi<90°$, falls into the collapsible/dropped magnetic field and the increasing electrical and therefore is tested/experienced smaller divergence. Electron path, which starts at $\phi=90°$, will be almost rectilinear, since at this moment magnetic field is absent. With further increase in the phase of the start of electron ($90°<\phi<180°$) the divergence will occur in the opposite direction. Consequently, in the process of acceleration electron beam scans on the target. With a change in the distance of the target occurs the capture of different sections of scanning beam and, thus, a change in the duration of make pulse and

energy spectrum of electrons, impinge on target. Fig. 2 gives the photograph of the trace of electron beam with current ~30 while at a distance of 260 mm from the anode opening/aperture.

In the structure of field in question the electron motion occurs in plane xz (cm Fig. 1). Disregarding space-charge effect, let us write the equation of the trajectory of relativistic electron taking into account field component in the following form:

$$\dot{p}_x = -eE_x - eB_y\dot{z};$$

$$\dot{p}_z = eB_y\dot{x}, \tag{1}$$

where p_x, p_y - components of pulse, e - electron charge,

$$E_x = \frac{U_m \sin(\omega t + \varphi)}{x \, \ln R/v_0} \quad \underline{u}$$

$$B_y = \mu_0 \frac{U_m \cos(\omega t + \varphi)}{2\pi \rho \, x}$$

Key: (1). and the components of electrical and magnetic field in the coaxial part of the cap/filling of the accelerator; U_m - the amplitude of accelerating voltage; ρ=33 ohm - the characteristic impedance of resonator; $v_0 = 0.625$ - radius of cap/filling; R=0.7 a m-radius of jacket of resonator; $\omega = 2\pi f$; $\mu_0 = 4\pi \cdot 10^7$ H/m. A change of the relativistic mass of electron in accelerating gap/interval is determined by the expression

$$m = \frac{m_0}{\sqrt{1-\beta^2}} = m_0\left[1 + \frac{eU_m}{m_0c^2} \; \frac{\ln x/v_0}{\ln R/v_0} \times \right.$$

$$\left. \times \sin(\omega t + \varphi)\right], \tag{2}$$

where m_0 - is mass of the rest of electron

$$\beta = \frac{v}{c}.$$
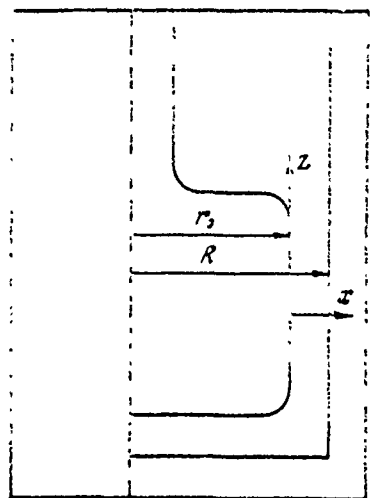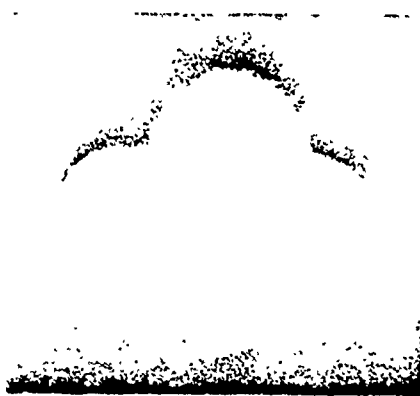
Fig. 1.   Fig. 2.

Fig. 1. Geometry of nozzles of accelerator.

Fig. 2. Photograph of electron beam.

Page 234.

To analytically solve system of equations (1) is impossible. However, in the in practice utilized interval of phases ($60°<\phi<120°$) and voltages ($U>0.5$ MV) by a change in the value of strength of electrical and magnetic fields for the electron transit time of accelerating gap can be disregarded/neglected. In the interval indicated the system of equations (1) is solved with a sufficient for the practical targets approximation/approach. On the basis of the

solutions of the system of equations (1) and geometry of electron
beam for the fixed values of the amplitude of accelerating voltage
were constructed the graph/diagrams of the dependence of the duration
of make pulse (or energy of the electrons, impinge on target) from
the distance between the anode opening/aperture of accelerator and
the target for different diameters of cathode and target. Fig. 3
gives one of the characteristic graph/diagrams of the dependence of
the duration of make pulse not target from the distance to the anode
with accelerating voltage, equal to 0.9 MV, and the diameter of
cathode and target 16 mm. points on the graph/curve showed the
experimental values of the durations of make pulse. From the
graph/curve it follows that the coincidence between computed values
of duration and experimental data of current pulse can be considered
satisfactory and lying/horizontal at margins of error in measuring
equipment +-5o/o.

It should be noted that the method of automatic electromagnetic
separation is based on the use of its own structure of the field of
resonator and therefore it does not require supplementary systems and
power supplies.

Thus, experimental results snowed that in the resonator
accelerator the method of automatic separation is optimum.
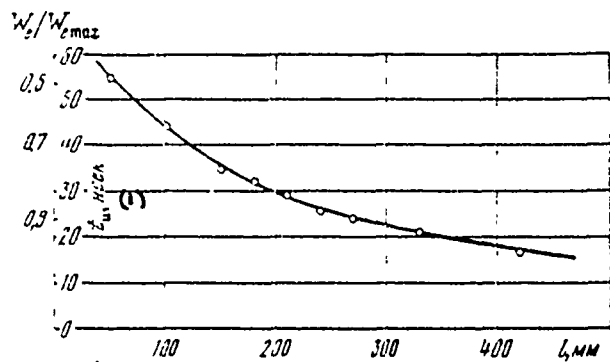
Fig. 3. Dependence of the duration of make pulse on the target from the distance to the anode.

Key: (1) ns.

REFERENCES

1. N. G. BASOV, Yu. M. Popov, B. M. Vul. ZhETF, 1959, Vol. 37, p. 587.

2. D. V. Iremashvili, N. N. Leont'yev, A. A. Plyutto. PTE [Experimental Instruments and Techniques], 1967, No. 2.

3. D. V. Iremashvili. Kand. dissert. [Candidate's dissertation], Sukhumi, 1967.

4. V. I. Perevodchikov, A. L. Fedorov, K. A. Yumatov. Theses of reports. Trudy Ukrainskoy respublikanskoy konferentsii po elektronnoy optike, nosvyashchennoy 100-letiyu so dnya rozhdeniya V. I. Lenina [Transactions of the Ukrainian Republic conference on electron optics devoted to the 100th Anniversary of the Birth of V. I. Lenin], Kiev, 1970.

164. System of control of the synchrocyclotron of FTI of the AS USSR.

R. P. Davyaterikov, A. V. Kulikov, V. V. Lavrov, G. F. Mikheev.

(Physiotechnical institute im. A. I. Joffe of the AS USSR).

The system of control, synchronization and check of the work of the high-frequency accelerating system of the synchrocyclotron of FTI of the AS USSR - SUF - fulfills the following basic functions:

1. Are given the intervals of manipulation, controlling the work of the manipulator of the anode supply of the basic oscillator HF accelerating system. With the run of job of accelerator as the input pulses, which assign the interval of manipulation, are utilized the impulses/momenta/pulses of the angle of rotation of the rotor of buncherss, generated by photodiodes. This interval of manipulation seizes with certain supply entire operational frequencies band HF program from 30 to 13 MHz. With the aid of the auxiliary timing pulses the porosity and the period of manipulation can be changed in the dependence on the requirements of the mode/conditions of work of the accelerator [1].

2. It permits implementation of control and synchronization of auxiliary of accelerator: oscillator of brace of duration of pulse of ac 'lerated protons, oscillator of discharge/break of protons of internal target, devices/equipment of pulsing of ionic source, etc. [2].

3. Is accomplished/realized synchronization of entire complex of physical equipment, which requires joint operation with accelerator.

4. It provides protection of HF system of accelerator from breakdowns and during closings/shortings. With the rare (single) breakdowns the device/equipment of protection removes/takes anode voltage from the basic oscillator to the preset time, then smoothly it are reduced. In case of repeated breakdowns with the low voltage and vacuum deterioration high voltage is disconnected entirely.

SUF has a control device of the noise in the bearings of buncherss, which produces the cutoff/disconnection of HF system with the increase of noise level of higher than the permissible limit.

5. It permits implementation of control of work of all devices/equipment of HF system of accelerator.

Page 235.

For the removal of information about the voltages at different points of HF system are arranged/located divider-sensors and detector caps/knobs. For the control, the measurements and the adjustment together with SUF is utilized broadband dual-trace oscillograph and scaler with the numerical indication.

For executing the first three functions SUF develops a large number of standardized timing pulses the time of generation of which can be changed over wide limits. Synchropulses can have the controllable/controlled/inspected joining to any instantaneous value of the frequency of accelerating voltage and be shifted/sheared with the aid of the delay circuits.

Functional possibilities of SUF make it possible to obtain different modes/conditions of work of the accelerator: the mode/conditions of the accumulation of accelerated protons [3], the mode of successive operation to internal and external targets, etc. With the work in the mode/conditions of control and adjustment the system can work from its own oscillator, which imitates the input pulses of photosensitive devices. Furthermore, SUF has a series/row of auxiliary, which make it possible in all modes/conditions to realize recalculation, passage and distribution of the cycles of

acceleration over wide limits, and to also accomplish/realize external resolutions exclusions to any number of cycles of acceleration or to any time interval of work of the accelerator.

Block diagram and principle of operation SUF.

1. Manipulation and isolation/liberation of basic modulation cycle. Block diagram of SUF is represented in Fig. 1. Pulses from two sensors 1, which correspond to beginning and end/lead of the basic modulation cycle of the accelerating frequency of synchrocyclotron, come the entrances of two channels "launching/starting" and "reams/feet". Preliminarily shaped in units 2 impulses/momenta/pulses of both channels fall to powerful/thick shapers 3, which develop pulses of synchronization. These and similar to them shapers are constructed according to the uniform diagram on the thyristors. Each such shaper has 5 outputs with output resistance of 75 ohms. The signals of all shapers are standardized and are the impulses/momenta/pulses of negative polarity with the amplitude 10V and rise time 1 μs. One of the impulses/momenta/pulses of shaper 3 in the channel "launching/starting" enters the gate 4, through which pass the impulses/momenta/pulses only in the presence of enabling pulse from the channel "stop" or from the terminal "external launching/starting". Further this signal, passing through scaling circuit 5, delay unit 6 shaper 7, enters the entrance of trigger 8.

Analogously by form the signal of "stop", passing through the
unit of summator 24 whose designation/purpose will be explained
below, delay unit 6 shaper 7, it enters the second entrance of
trigger 8, which develops square-wave signal, which corresponds to
the duration of modulation cycle.

Since all elements/cells of manipulator 14, who ensures the
manipulation of anode voltage on basic oscillator 15, are found under
the high potential relative to the earth/ground, the control by
manipulator is achieved through isolation transformer 13 at the
carrier frequency of 550 кHz. The signal of the carrier frequency, is
developed by oscillator 9 and is formed/shaped in the duration in the
modulator circuit 10. Further this signal is intensified by terminal
amplifier 11 and through that adjusted $\lambda/2$ the cable enters
preamplifier 12, which is located in high-voltage manipulator's
location 14. After traversing isolation transformer 13, signal is
detected and is controlled by manipulator.

2. Obtaining timing pulses and realization of different
operating modes.

For the control of work of auxiliary of synchrocyclotron and

obtaining of the timing pulses of joining to the instantaneous value
of the frequency of accelerating voltage is utilized the set of the
devices/equipment whose basis compose frequency selectors [4]. HF
voltage from capacitive divider-sensor 17, located near accelerating
dee lip 16, through the matched cable, shaper 18 and fan-out 19
enters the entrances of frequency selectors 20-23. Each of the
selectors develops the timing pulse, cabled to any instantaneous
value of the frequency or accelerating voltage. With connection of
one of the selectors, for example 22, to summator 24 its timing pulse
enters the channel of "stop" and is produced the removal/taking high
voltage from oscillator 15 upon reaching of the prescribed/assigned
frequency of modulation cycle. Remaining selectors are utilized for
obtaining other modes/conditions of work of the accelerator. Thus,
for instance, with the aid of selector 21 can be organized the
mode/conditions of accumulation. For this the timing pulses of
selector 21 are established/installed for the frequency, which
corresponds to the selected radius of accumulation, and within
spacing device/equipment 25, controlled by scaling circuit 5, they
enter summator 24 and further into the channel of "stop",
accomplishing/realizing a cessation of the acceleration of protons on
the prescribed/assigned radius. Scaling circuit 5 makes it possible
to select any relationship/ratio of a number of cycles of
accumulation and conclusion/output.

For the control of the work of the jettison system of protons on internal target is utilized selector 23. Synchronizing pulse from this selector, passing through the gate 26, controlled also by scaler 5, enters the control of the oscillator of the discharge/break of protons of internal target.

The functional check of diagram can be realized with the aid of control oscillator 27, connected to the entrances of shapers 3 instead of sensors 1.

On the block diagram of device/equipment pf SUP given above are not shown the units of the control of noise and measurement of the revolutions of variations, the shielding blocks of HF system from the breakdowns, the units of the beam monitoring of the accelerated protons.
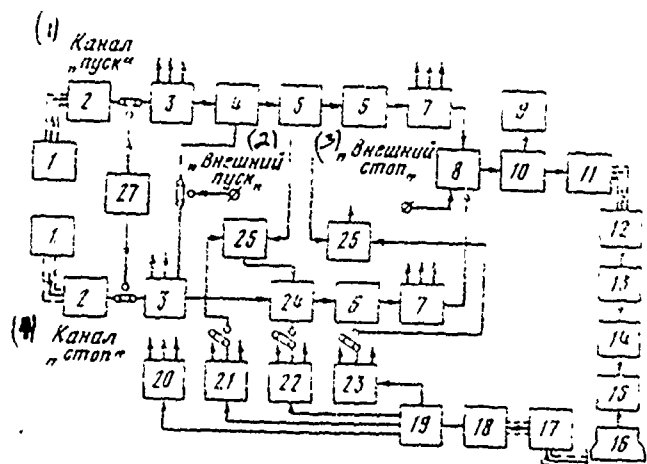
Block diagram of SUF.

Key: (1). Channel "launching/starting". (2). External "launching/starting". (3). External "stop". (4). Channel of "stop".

REFERENCES

1. V. I. Danilov and et. al. Preprint OIYAI, 2136, Dubna, 1965.

2. T. N. Tomilina and et. al. Preprint OIYAI, 1637, Dubna, 1964.

3. V. I. Danilov and et. al. Preprint OIYAI, R-2811, Dubna, 1966.

4. S. M. Rubchinskiy and et. al. "Radiotekhnika i elektro-nika" [Radio Engineering],
No. 7, pp. 986-1000, 1956.

Page 236.

165. Internal oil target for proton Synchrotron.

N. I. Nachatyy, K. K. Onosovskiy.

(Institute of theoretical and experimental physics).

Introduction.

In the proton synchrotron on 7 GeV the experiments are
accomplished/realized on the beams of secondary particles, obtained
on internal targets in vacuum chamber.

Depending on objectives of mission are required the short or
expanded in the time beams of secondary particles.

The ideal substance which gives the maximum output of secondary
particles, is hydrogen; however, the production of target from
hydrogen represents great technical difficulties.

As target it is possible to utilize the stream from diffusion oil of brand VM-1, which during the intersection with the beam will interact with it. With the beam interact each time the new portions of oil; therefore such target is mechanically not destroyed with beam, as this occurs, for example, with the target from polyethylene.

Mineral oil consists of saturated hydrocarbons, the percentage of hydrogen molecules is sufficiently great and, therefore, the output of secondary particles can be let us compare it with output on polyethylene. Furthermore, mineral oil under the beam forms only the short-lived isotopes; therefore it is safe with the work. Arrangement/position of oil target in vacuum chamber will lead to vacuum deterioration due to heating and radiolysis of oil of target. However, as showed calculation and experimental data, this deterioration unessentially and work of the accelerator does not affect.

Construction/design of oil target.

Fig. 1 shows the general view of target. The piston, to which is supplied the pressure of the compressed air, is created a pressure of oil in the cylinder of nozzle on the order of 270 atm. The nozzle entry is constantly overlapped by the locking needle which is pressed by spring.

Upon reaching of the specific pressure in the cylinder of nozzle locking needle heaves, opening of access to oil to the nozzle. Changing the effort/force of spring, it is possible to be given the necessary value of the pressure of locking needle. The jet of oil escapes through nozzle φ 0,15 мм at a rate of 100-170 m/s, intersecting in this case beam.
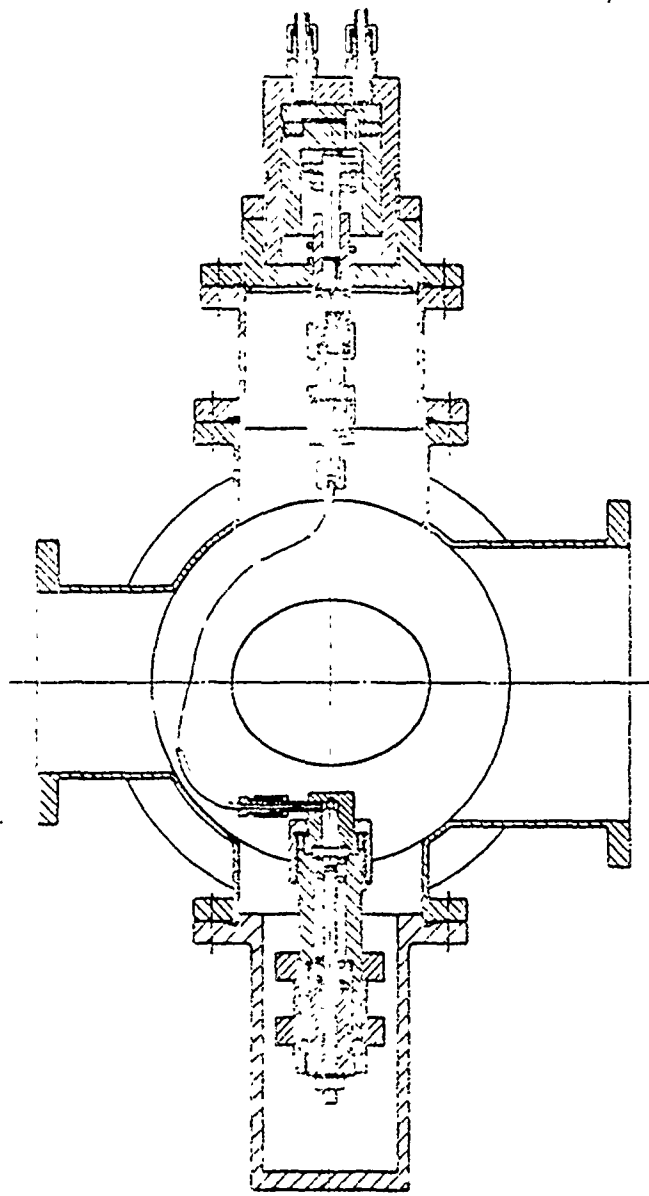
Fig. 1. The general view of oil of target.

Page 237.

After the pressure relief of air the oil pressure in front of
the nozzle will fall, and locking needle under the action of spring
will begin to close nozzle, but oil piston cannot instantaneously
leave back/ago due to inertia and friction; therefore is possible
outlet from the nozzle at a smaller pressure. This fact leads to the
"inflow of oil", on outlet is formed the drop of oil. For the
liquidation of the phenomenon indicated along the axis of piston is
bored the opening/aperture which is connected with the annular groove
on the piston.

After extrustion by the piston of oil from the cylinder (piston
is located in the upper position), the annular groove of piston is
connected with the openings/apertures in the cylinder and oil from
the conduit/manifold through ball valve, oblong hole in the piston,
neck and openings/apertures in the cylinder pours into the reservoir,
as result of what the pressure in front of the nozzle sharply falls.
Furthermore, for a rapid pressure drop in conductor oil filter is
carried out floating.

For the creation of pulse pressure is utilized the system of
magnetic valves, used on bubble chambers.

Translation of motion to the vacuum is accomplished/realized
through the ground/wiped stock/rod which continuously lubricated by

oil.

The construction/design of this target makes it possible to begin the injection of oil with given speed and the drop of oil, if it even appears, at the rates above 100 m/s no longer is changed the position of jet; therefore target can be fixed.

Works of target.

Since at the rates above 100 ms jet is stable, and changes from one cycle to the next are insignificant, it it is possible to utilize as the target (stability of jet was studied by the method of photographing jet at the different moments of time).

At high rates occurs jet disruption due to the inequalities in nozzle and viscosity of oil; however, this phenomenon strongly depends on the pressure of the medium, in which flies the jet of oil, and it is characteristic for the positive pressures. Under conditions of high vacuum this phenomenon becomes apparent more rarely.

In obtaining of the curves of scatter of particles to the oil target it was not noticed the nonuniformity of jet structure; obtaining jet velocity more than 200 m/s we did not succeed in. By us was carried out comparative estimation of the discharge/break of

particles to the different targets. Fig. 2 gives the oscillogram of the discharge/break of particles to the oil target with the aid of the three-dimensional/space shift of orbit by a change of distributing the magnetic field according to the ring.

The upper ray/beam of oscillogram shows the output of secondary particles, recorded by the monitor, arranged/located opposite the branch pipe in which is established/installed the target; lower the value of primary proton beam.

Fig. 3 gives the oscillogram of the discharge/break of particles, obtained by the same method, also, under the same conditions, from the usual flag target (aluminum foil).

Deficiencies/lacks in target.

1. Target is not point: its image on radius is 0.13 mm, but on height it corresponds to size/dimension of beam.

2. Construction/design of oil target is more complicated than flag one.

3. Developed construction/design cannot be replaced through standard sluices.

Fig. 2.   Fig. 3.

Fig. 2. Oscillogram of discharge/break of particles on oil target.

Fig. 3. Oscillogram of discharge/break of particles on flag aluminum target.

Conclusion.

Is experimentally shown the possibility in principle of using the oil target on strong-focusing accelrator. Oil target makes it possible to increase in the output of secondary particles with the same current of primary beam, which increases the effectiveness of accelerator, decreases the radiation danger for the personnel and is decreased background in the experimental locations.

Page 238.

Discussion.

G. V. Vadalyan. What is oil header in your system? It is possible whether thus to make a liquid hydrogen jet-edge target?

K. K. Onosovskiy. The receiver of oil is the reservoir, arranged/located at a distance of 150 mm lower than orbit and which has the special device/equipment, which prevents oil from the sputtering.

As far as target is concerned liquid hydrogen, then this is fairly complicated task. With this will substantially deteriorate vacuum. During the evaporation of oil from the walls appear the reaction forces, which will bring down jet direction, since to you from all sides it is impossible to ensure identical coefficient of reflection and identical heat withdrawal.

V. I. Kovalenko. Which the maximum frequency of functioning the oil spray nozzle?

K. K. Onosovskiy. Accelerator works with the frequency one cycle 4 s. Respectively works oil target. The temporary/time extent of jet is approximately equal to 500 ms.

Page 239.

Session XII.

CONTROL AND DIRECTION OF ACCELERATORS WITH THE AID OF THE COMPUTERS.

166. Main principles of the automation of Serpukhov accelerator.

A. A. Vasil'yev, Yu. S. Ivanov, A. A. Kuz'min, S. M. Rubchinskiy.

(Radio engineering institute of the AS USSR).

The considerable cost/value of the operation of Serpukhov accelerator, a continuous increase in the volume of physical experiments, further development of accelerative complex and connected with this complication of control of complex leads to the need for the automation of diagnostics of its systems and control by them.

When selecting of the principles of the automation of Serpukhov accelerator was used Soviet [1, 2] and foreign experiment [3-6].

On the basis of the conditions, which exist on the Serpukhov

accelerator, was selected the functional principle of the
construction of the diagram of automation, which makes it possible
utilize the existing communications and to gradually automate the
separate functional systems of accelerator without the
disturbance/breakdown of its operation with their subsequent
association into the single controlled complex. The diagram accepted
must provide the possibility of rapid transition to the manual
control of functional systems from the local control panels.

All devices/equipment of accelerator it is possible to divide
into two groups: 1) the workers synchronously with the cycle of
acceleration even 2) the devices/equipment whose work is not
connected with the cyclic character of the process of acceleration.

Some systems of accelerator completely consist of the
devices/equipment, which relate to the second group. These systems
require only incidental control and virtually they do not need
control by operational personnel after inclusion/connection. By such
the systems of overall designation/purpose are vacuum system, systems
of water cooling and general/common/total power delivery and
series/row of measuring systems, such, for example, as radiation
monitoring. All systems of this group can be united under the overall
diagram of the centralized control and direction with the wired
program of external units and under the simple program of data

processing. Other systems contain devices/equipment and assemblies of both types, but as a whole they are characterized by the cyclic character of works.

They include: a) linear accelerator, b) the introduction/input of beam, c) the system of radio electronics, generation of accelerating field and measurement of the parameters of beam, d) the power-supply system of electromagnet, e) the system of the correction of magnetic field, f) the beam extraction, g) the channels of the transportation of beam.

At present all devices which ensure cyclic work of the accelerator, are program and the part of the devices/equipment is supplemented by analog feedback. Programs can be corrected by operators on the basis of experiment or calculations. The programs of the work of the series/row of devices/equipment change with a change in requirements of experimental physicists' on the part. This readjustment occurs through many cycles of acceleration and in a number of cases in this case is required accelerator shutdown. The more number of controllable/controlled/inspected parameters it can be processed for a minimum number of cycles, the more operational there will be the control by accelerator.

All informational signals, existing on the accelerator, it is

possible to subdivide into 3 groups in form of the signal: time, state, voltage. The signals of state and voltage are divided into the signals, which appear periodically with the cycle of acceleration (dynamic), and the signals, emergence and change in which it is not connected with the cyclic recurrence of work of the accelerator (static).

Furthermore, dynamic signals can change within the cycle of acceleration with different speed (dynamic rapid and dynamic slow).

And finally, signals it is possible to subdivide according to the degree of the importance: the signals of subsystem, system, group of systems and accelerator.

In accordance with the data of classifications, given below, a quantity of informational signals of accelerator following:

(1) Вид сигналов	(2) Количество
(3) Состояние	
(4) статическое 17400	
(5) динамическое 1600	
(6) статическое 4000	
(7) Аналоговые	
(8) медленные 900	
(9) быстрые 400	
(10) Временные	
(9) медленные 130	
(4) быстрые 15	
(11) Общее число машинных слов (2 байта) . 8000	
(12) Число машинных слов в каждом цикле 1700	

Key: (1). Signal aspect. (2). Quantity. (3). State. (4). static. (5). dynamic. (6). static. (7). Analog. (8). slow. (9). rapid. (10).

Temporary/time. (11). Total number of information words (2 bytes).
(12). Number of information words in each cycle.

It is logical what a large quantity of signals is must be worked
with the aid of the computers.

Page 240.

However, even the best computers cannot work with the accelerator in
real time. On the other hand, the operating speed of the
information-control system, which contains computers, they are to a
considerable extent determined by the limited capacity of
communicating systems and by the inertness of actuating elements.

One of the special features/peculiarities of the control system
in question is the relatively weak synchronization of the work of
computers with the accelerator. In this case are observed only the
conditions: 1) all required information enters computers for the
time, multiple to the cycle of acceleration; 2) all control signals
enter the actuating elements into pause between the cycles; 3) the
information, which enters each cycle, it is analyzed in the same
cycle.

For the realization of this operating mode must exist the buffer

devices/equipment, matching the rate of the emergence of information
with the speed of the admission of data into the computers and the
devices/equipment, which make it possible to match the rate of the
delivery of the computers of signals with the numerous ones, the rate
of the delivery of the computers of signals with the numerous but
slow actuating elements.

Fig. 1 gives the block diagram of the collection of information
and control of one of the systems of accelerator. This diagram
contains the converters of different signals into the digital form
and the buffer storage. The synchronization of the moments/torques of
measuring of signals and writing into the buffer storage is
accomplished/realized by the special synchronizers whose programming
is conducted by operator or computer. Addressing to the
devices/equipment and the memory is accomplished/realized with the
aid of the digital code of sent EVM or from the panel for operator
into the control unit of addressing.

The part of the analog signals, necessary for the direct
observation, they are transferred by the wide-band cables and are
connected up to the independent equipment for representation; input
of these signals into the computers can be accomplished/realized with
aid of the converters which equipped computer. All remaining signals
are transferred literally with the aid of the commutator, controlled

by computers or operator of system (or accelerator). Controling
channel of subsystem contains inverters: code- state, the code
analog, code- shaft.

All signals from the accelerator and to the accelerator are
relayed to the computers through panel for operator.

With the aid of the devices/equipment on the panel the operator
can follow the information, which enters in the computers, and
accomplish/realize autonomously collection of information and manual
control of the devices/equipment of system.

Into equipment for panel enters the storage unit, which has the
limited number of cells (~10). In the mode of automatic control the
recording of information into the cell is accomplished/realized only
under the condition of coinciding the address, which comes from
computers, with the address, collected on the panel of manual
control. Recording occurs through the commutator with the aid of the
control unit of recording, then digital signal will be decoded and is
reproduced on the display devices/equipment of panel. Transition from
the automatic control to the manual local is conducted with the aid
of the control unit by the kind of work. During the manual control
the operator of system must collect on the panel of the manual
control of the address of informational and actuating

devices/equipment, and also the codes of the values of the control pressures. Transmission and reception of signals must be synchronized with the cycles of acceleration.
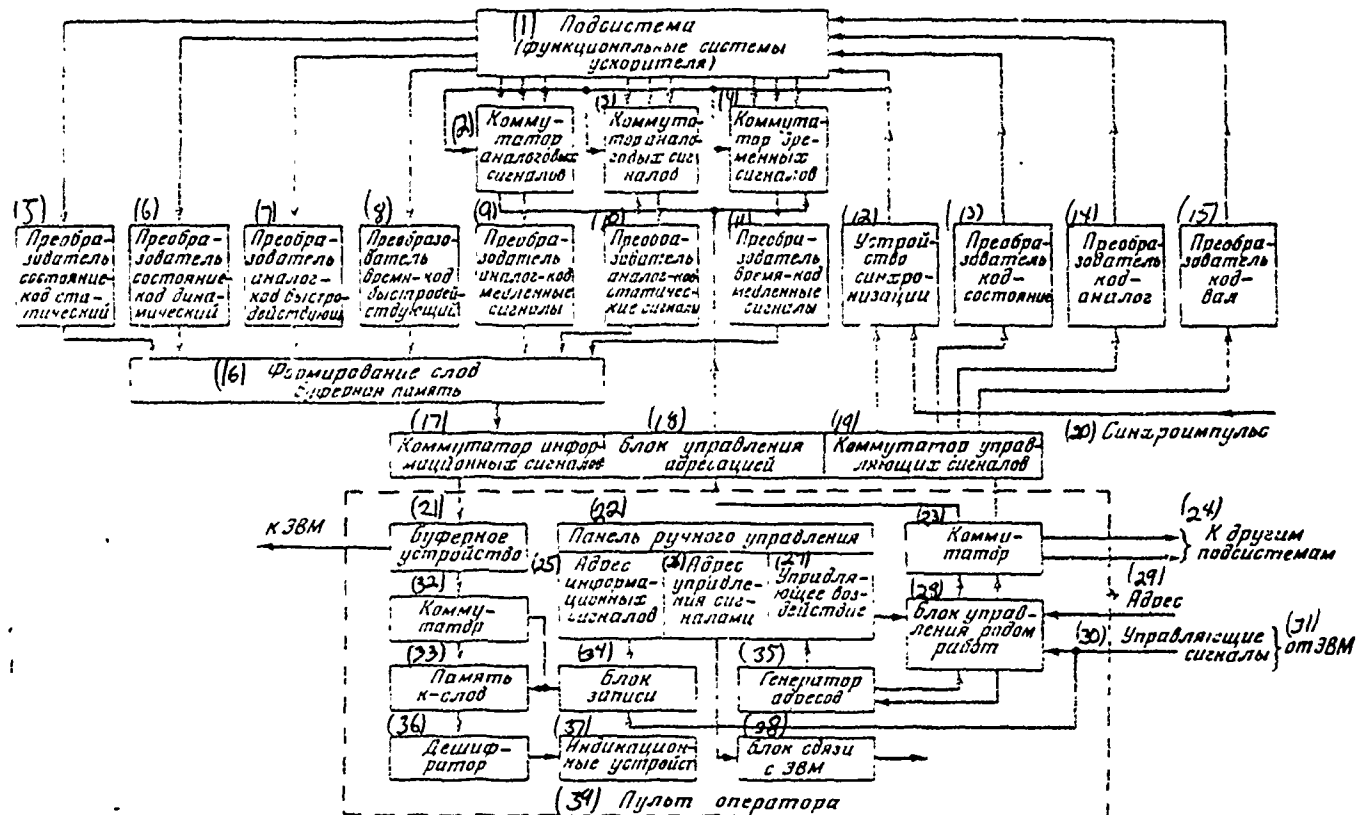
Block diagram of the collection of information in the control of the system of accelerator.

Key: (1). Subsystem (functional systems of accelerator). (2). Commutator of analog signals. (3). Commutator of analog signals. (4). Commutator of temporary/time of signals. (5). Converter of state-code (static. (6). Converter of state-code (dynamic. (7). Converter of analog-code high-speed. (8). Converter time- code high-speed. (9). Converter analog-code (slow of signal) (10). Converter analog-code

static signals. (11). Converter a time- code slow signals. (12).
Synchronizer. (13). Converter code- state. (14). Converter analog
code. (15). Converter code- shart. (16). Formation of words buffer
storage. (17). Commutator of informational signals. (18). Unit of
control of addressing. (19). Commutator of control signals. (20).
Timing pulse. (21). Buffer device/equipment. (22). Panel of manual
control. (23). Commutator. (24). To other subsystems. (25). Address
of informational signals. (26). Address of control of signals. (27).
Controlling effect. (28). Control unit by kind of works. (29).
Address. (30). Controlling signals. (31). from. (32). Commutator.
(33). Memory of k- words. (34). Recording unit. (35). Oscillator of
addresses. (36). Decoder. (37). Indicative device. (38). Coupling
unit s. (39). Panel for operator.

Page 241.

This operation/process during the manual control is produced the
oscillator of addresses.

    Address signals, both arriving from without and formed during
the manual control, partially will be decoded in the unit of control
by the kind of work and control the commutator of subsystems, which
connects the appropriate address and controlling channels.

Block of connection/communication of the panel for operator with the computers and the central control desk, makes it possible to check the actions of operator, and it also makes it possible for operator TO systematize setting up in the computer memory and to request the required programs. In the series/row of the panels for systems it will be necessary to set the indicative devices/equipment, controlled of the computers, and which supply the operator of system by the data, obtained on the basis of information analysis. Central accelerator frequency can be constructed according to the same diagram.

The block diagram of the collection of information and transmission of the control pressures is suitable both during the use by one computer for the control of entire accelerator and during the use of several computers, united into the hierarchical system from the computers of the highest and of lower level.

During the use of cheap and reliable small computers the use/application of a multimachine version is more preferable, since in this case the step by step possible conducting of automation along the functional systems with the consecutive insertion of means into the equipment and the communications. The analysis of the informational and control signals taking into account the use of the proposed block diagram they make it possible to make the conclusion

that in control of Serpukhov accelerator there is no need for applying computers with the the large high-speed. So for the single-machine version is necessary computer with the operating speed of 50-100 thousand operations/processes per second and in volume of working storage ~64 k. In the multimachine version the operating speed of the computers of the lower level can be limitedly 20 thousand operations/processes per second. Volume of working storage 4 and 32 to cells for the computers of lower and upper level respectively. In any event central computer must have interchangeable disks and strips/films with the informational capacity/capacitance not less than 500 k, display on the cathode-ray tube, ATSPU and unit of selection of programs from the lasting computer memory teleprinter or electrified macine.

During the first stage of automation must be accomplished the checking of the parameters of accelerator and the presentation of information of the analysis of its work in the edited form. In the second stage must be introduced into the computer memory the routines of control; they must be caused by the operator on the basis of data, represented to computers. Third stage - direct control of computers by the accelerator on the basis of data, obtained from it. The introduction of the programs of this type will be it occurs only after the careful analysis of the accumulated experience.

Tha effectiveness of automation and the correctness of the selected principles and methods is intended first to approve on one or two functional systems of accelerator.

Use of computer for the automation of Serpukhov accelerator must as a result increase the reliability of the functioning of accelerator and a number of conducted on it physical experiments, and also improve the parameters of the accelerated beam.

REFERENCES

1. E. L. Burshteyn, A. A. Vasilyev, A. L. Mints, V. A. Petukhov, S. M. Rubchinskiy. DAN USSR, 1961, 141, 590: Atomnaya Energiya, 1962, 12, III.
2. A. A. Vasil'yev, N. I. Kuz'mina. et al. Doklady. Reports of VII International Conference on Accelerators. Yerevan. 1969.
3. R. Frankei. IEEE Trans. on Nuclear. Sci., 1967, NS-14. n3,p.1042.
4. H. Van der Beken, A. Remmer. CERN Report. MPS computer 69-2, 9 May, 1969.
5. E. Asseo et al. Internat. Conf. on Remote data Proc. Paris 24-28 Mars 1969.
6. R. Keyser. CERN Report, ISR-Co/69-45, July 1969.

Discussion.

V. G. Sukhov. There were any assumptions relative to the type of the machines, to which you are oriented?

A. A. Kuz'min. If we speak about the machines of low level, then we are oriented toward the machines of the type "βarameter".

167. To a question about the overall automation of linear accelerator on energy of ⬛ 2 GeV.

I. A. Grishaev, Yu. I. Dobrolyubov, V. M. Kobezskiy, V. I. Kolosov, V. D. Krasnikov, V. V. Mel'nichenko, V. I. Myakot.

(physiotechnical institute of AS UkSSR).

Linear electron accelerator to the energy 2 GeV is put into use in 1965 [1]. Control of accelerator at present is conducted of three points. The initial part of the accelerator, which consists of 10 sections, copes with the panel for operator. The others of 40 accelerating sections cope with the central control desk for dispatcher, and output units and the system of beam shaping - from the panel for conclusion/output.

Page 242.

On the panel for operator are arranged/located 50 control devices and 54 monitoring and measuring instruments, 200 controlling also about 220 monitoring and measuring instruments on central control desk for dispatcher and on the order of 20 controlling and

monitoring and measuring instruments to the panel for output. On the

local control panels are about 250 monitoring and measuring

instruments, on which is conducted the estimation of the state of

work of the accelerator. Local control panels are arranged/located in

the klystron hall, having length of 250 m.

In the course the operation of the accelerator of the

characteristics of individual systems is improved and at present the

series/row of the output parameters of beam significantly exceed

designed. Usually the energy dissipation of the accelerated electrons

in the operating range of energies does not exceed 0.7o/o at the

level $0,5J_{max}$ and 1.9o/c at the level $J.10_{max}$ and the best values

respectively - 0.15 and 0.55o/o.

Work of the accelerator in the modes/conditions with the close

tolerances, and also increase in the requirements for the beam lead

to considerable complication of its control. During the operation of

accelerator in 1969   about 20o/o of time left to the tunings and a

change in the mode/conditions. Among other things to the

rearrangement of accelerator with a change in the parameters of beam

in the demand of experimenter are spent about 8o/o, to the tuning of

accelerator with the insignificant divergence of the parameters of

beam - about 6o/o and to the search of malfunctions with the

divergence of the parameters of beam from the given ones - about

60/0.

For an improvement in the effectiveness of control of accelerator, reduction of the unproductive expenditures of time and guarantee of maximally possible stabilities of the parameters of beam is developed the program of the overall automation of accelerator.

The basis of overall automation is the use of the electronic digital controlling system "Dniepr-2", with the aid of which it is proposed to solve the following problems: a) the automatic check of the parameters of beam and the important parameters of support systems; b) the retention of energy of the accelerated particles with the precision/accuracy $+-(0.1-0.01)$o/o, the guarantee of divergence in limits $(1-5) \times 10^{-5}$ of rad and necessary size/dimension of beam for the target, limiting the drift of the center of charge not more than $+-0.25$ mm, or the retention of the intensity of beam within limits of $+-1$o/o; c) a change in energy and intensity of the accelerated particles in the demand of experimenter; d) are more distant near forecasting of parameters of beam and technical diagnostics of the systems of accelerator; e) the optimization of control of accelerator.

For our accelerator it is proposed to utilize the information-control system whose block diagram is shown in Fig. 1a.

The selection of mode/conditions and the setting up of the necessary
parameters of beam are conducted by experimentor and with the aid of
the input unit it is transferred to the system "Dniepr-2". In the
dispatcher of accelerator on by indicator device are reflected the
required parameters of beam and the operating mode. With the aid of
the special commutators of control and measurement the machine
automatically controls equipment component and automatically are
measured the parameters of beam and systems. The dispatcher of
accelerator controls remotely intermediate systems and is checked the
part of the parameters of systems. Connection/communication with the
computer dispatcher produces with the aid of the teleprinter.

Retaining the principle of additivity, a program of the overall
automation of accelerator it is proposed to carry out into several
stages.

I stage. Introduction of the central control of systems, the
start of local regulators to the basic parameters of beam, automatic
control the output parameters of beam and efficiency of main systems
with the aid of the computational controlling complex "Dniepr-2",
testing of program of consultant.

II stage. Preparation and inclusion into the control of the
accelerator of the electronic digital controlling system "Dniepr-2"

into the mode/conditions of the retention of the parameters of beam, the testing of the program of forecasting and technical diagnostics.

III stage. Gradual transition to full-automatic control for the self-teaching program.

From the point of view of control linear electron accelerator is system with a large quantity of input and disturbing effects, which determine in the final analysis the output parameters of beam and their stability. To the most important output parameters should be carried: the parameters of the energy spectrum of the accelerated particles; the position of the center of the charge of beam in the accelerator and to the target, the emittance of beam; average/mean and pulse intensity.

The investigation of the instabilities of beam shows that in terms of the character and conditionally it is possible to divide them into somewhat sufficient clearly chosen groups: instability to (2-3) o/o with characteristic periods (0.5-2) s (Fig. 2a); instability of approximately 5o/o with period (10-20) s; to instability (10-20)o/o with the periods more than 1 min (Fig. 2b, c); short-term short duration failures (Fig. 2b).
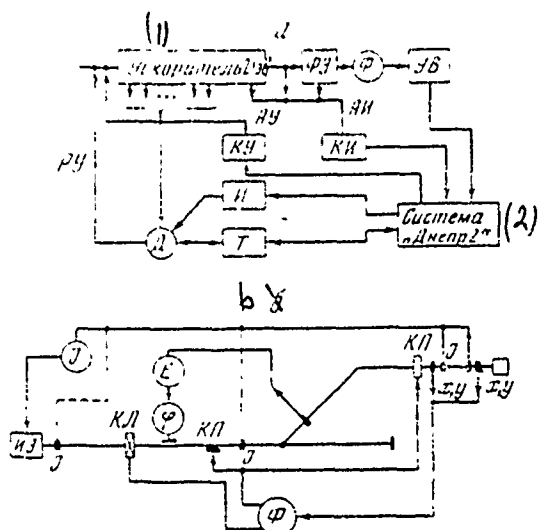
Fig. 1. The block diagram of the information-control system (a), the basic control loops of accelerator (b) D - dispatcher of accelerator; F - experimenter; KI, KU - commutators of the measuring and controlling channels; AU, RU - automatic and manual control; UV - input unit; FE - equipment for physical experiment; I - indicator signal panel of dispatcher; T - teleprinter; E, U, F - circuits of control; by energy; by the intensity of particles and by beam shaping; ϕ - phase inverter; KP - magnetic corrector; IE - electron source; J_{ky} - sensors or intensity, position and sizes/dimensions of beam; KL - quadrupole lenses.

Key: (1). Accelerator 2 GeV. (2). System "Dniepr 2".

Page 243.

Data on the analysis of stability of accelerator [2, 3] show that in the control system it is possible to isolate three bases of the contour/outline: control loop of energy of the accelerated particles, the contour/outline of the beam shaping and control loop of the intensity of beam. The block diagram of accelerator with such contours/outlines is shown in Fig. 1b.

The work of control loops it is possible to describe by the functionals:

$$W = f(E_{0i}, \varphi_i),$$

$$\Phi_{xy} = \varphi(W_i, J_{\Phi k}, J_{xi}, J_{yi}, W),$$

$$J = \psi(P_{3n}, J_{H}, E_{uc}),$$

where i=1, 2, 3 ... 50; k=1, 2, 3 ... 18; W — output energy of accelerator; E_{0i} — amplitude value of accelerating field i of section; φ_i — phase of accelerating field; Φ_{xy} — form and position of beam; W_i — energy, acquired by electron in section; $J_{\Phi k}$ — current of the focusing solenoid, J_{xi}, J_{yi} — magnetic correctors' currents; J — intensity of particles at the output of accelerator, P_{3n} — power of electronic preheating, J_{H} — filament current of gun; E_{uc} — intensity/strength of accelerating field of injector section.

For simplification of the adjustment of accelerator the part of

the independent variables in functionals $(E_{0i}, W_i, J_{\Phi k}, J_{x i}, J_{y i}, J_H, E_{u c})$ is

assembled into the standard sets of values and for this mode is

supported by constant. The introduction of such standard

modes/conditions made it possible to bring together a quantity of

control pressures to 60-70 instead of 250, which led to the

considerable facilitation of control of accelerator.
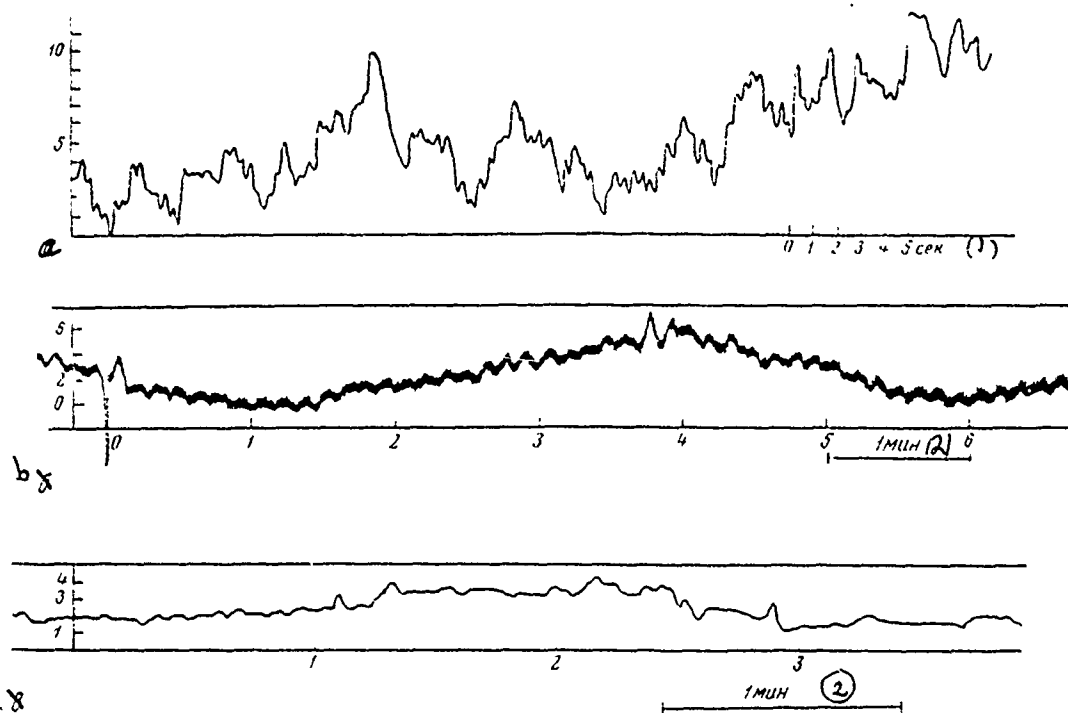
Fig. 2. Some characteristic recordings of instabilities. a) signal from the quantameter (target crystal); b) signal from the quantameter (target amorphous); c) signal from the monitor.

Key: (1). s. (2). min.
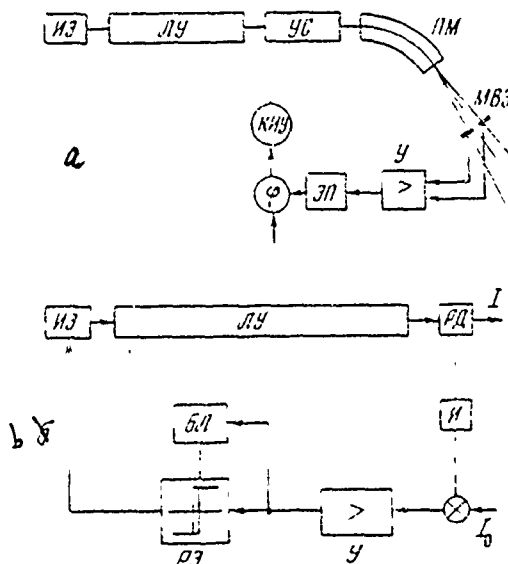
Fig. 3. Block diagram of the stabilization of energy (b) and current control at the output of linear accelerator. IE - electron source; LU - linear accelerator; RD - resonator sensor; I - integrating unit; BL - block of logic; RE - unit with the relay characteristic; U - amplifier; US - accelerating section; MVE - monitor of the secondary emission; φ - phase inverter; EP - electromagnetic drive; KIU - klystron pulse amplifier; PM - rotary magnet SP-82; T - current of accelerator.

Page 244.

For the adjustment of energy in the small limits it is utilized by one of the latter/last accelerating sections, and position and beam shape - magnetic corrector and quadrupole lens. The control of

intensity of beam is conducted by the changing of the mode/conditions of the electronic preheating of the gun of injector.

For an improvement in the stability of energy of the accelerated particles is used the stabilization system [4] (Fig. 3a), which makes it possible to compensate disturbances/perturbations (20-25)   MeV with precision/accuracy 0.2o/o as the sensor with use of monitors of the secondary emission, difference signal from which is amplified and is supplied to the control phase-inverter with electromagnetic actuator. A change in the phase of accelerating field leads to a change in the energy of particles. Differential circuit makes it possible to eliminate in some limits the effect of current.

In the control loop of the intensity of part is used the control system whose block diagram is shown in Fig. 3b. For reducing the mutual effect of the regulator of intensity on the work of the stabilization system of energy is used the unit with the relay characteristic (RE). Deadband is selected as being equal to 2o/o. With an abrupt change in the intensity of particles the block of logic (BL) disconnects regulator and shields from the damage electron source. As the sensor of intensity is utilized span type standard resonator.

This combination of regulators made it possible to obtain the

independence of the work of regulators in the mode/conditions of the

retention of the parameters of beam. In the process of the

realization of plan/layout, probably, will be introduced corrections

and supplements taking into account inventions in experience of

control of accelerator. Basic task is the introduction of a

program-adviser.

REFERENCES

1. A. K. Val'ter, I. A. Grishayev, Ye. V. Yeremenko, et al.
   Transactions of the International Conference on Accelerators.
   Dubna, 1963, Atomizdat. 1964, p. 420.
2. I. A. Grishayev, G. K. Dem'yanenko, K. S. Pubtsov, ZhTF. 1970,
   40, 1, 149.
3. I. A. Grishayev, N. A. Kovalenko, V. I. Kolosov, V. V. Petrenko,
   ZhTF, 1969, 396 1, 197.
4. V. J. Kuzilov, L. A. Makhnenko, V. A. Skubko. Electron Accelerators.
   Trudy Transactions of the VI International University Conference
   on Accelerators. Tomsk, 1966, Izd-vo "Energiya" 1968, p.221.

Discussion.

V. V. Tsyganov, is assumed plotting of the mathematical model of

linear accelerator?

V. I. Kolosov. Thus far this it was not done, but after the execution

of the 1st stage of works we will begin the construction of this

model.

168. Data transmission and use/application of means of computer technology in the project of the intersecting rings.

By P. Uolstenkholy.

(CERN, Switzerland).

1. Project of intersecting rings (PNK) [1].

The actualization of the project of the intersecting rings in CERN was begun in 1966; the beginning of experimental investigations on this installation up is planned for July 1971. Proton beams they will circulate in two opposite directions in two separate rings, arranged/located in the general/common/total tunnel (see Fig. 1). Into each ring will be injected a large number of impulses/momenta/pulses from the proton cyclotron on the energy 28 GeV and as a result of the accumulation of particles they will be achieved/reached current on order of 20a. The intersection of beams is possible at eight points; however, in the first experiments will be used only four of them.

PNK differ from other installations for the investigations in high-energy physics in terms of two special features/peculiarities: large area, occupied by this installation and by an enormous quantity

of accessory equipment. For example, vacuum system contains more than
700 pumps and vacuum manometers and represents already itself very
complicated object from the point of view of control and direction.
There are approximately 300 separate circuits of power supply of the
magnets which require control and control, and also large number of
devices/equipment for monitoring the beam.

The electronic circuits of control and the sources of power
supply cannot be established/installed in the circular tunnel as a
result of the high amounts of radiation; therefore they are arranged
in eight buildings for the equipment, erected in the circumference of
ring. Ninth building is located near the beginning of system for the
translation/conversion of beam. Finally, very large tenth building is
oc⁻ ied with the central equipment of the system of power supply and
cooling; in one end/lead of this building is arranged/located
console.

Equipment for data collection and control system they are
concentrated in these buildings for the equipment; the signals
between these buildings and console are transferred usually by the
multiplex channels for the purpose of the savings of cables.

Page 245.

2. Control system with computer [2].

The system of control of ENK with the computer was planned as observation system (control), but not for the automatic control. Computer functions consist of ensuring of transmission and indication information to the service personnel and to transfer the commands of operator to different equipment components. At present primary attention is concentrated in providing functions which can prove to be useful during launching/starting of rings; however, in future year will be turned larger attention to the automation of control. Up to now program any cybernetic elements/cells, and all operations/processes of control are fulfilled by operators; however, at the same time are examined several diagrams of automatic control with closed circuit, which fulfill the functions of optimization. One should emphasize that the most complicated problem in the case of any control system with the computer concerns the input units and conclusion/output. Only after it is established/installed, that the machine has an access to the reliable information, it is possible to examine the mathematical problems of closed circuits of correction.

'n order to ensure the maximum accessibility of the system of computer, it was decided to set two identical computers of modular construction/design. One of them is utilized as the basis, the worker "on line", whe has the second serves as the source of different

blocks/modules/units for the replacement (ZU magnetizing cores, the digital units of input and output, etc.) and is utilized as the computer "off line". Both machines are connected the lines of the transmission of information, which makes it possible to utilize the second machine for the solution of some problems on real time, too complicated for one basic machine. Up to now the presence of two computers having inestimably Contributed to acceleration of the development of system, ensured the possibility of the parallel development of equipment and program of software. In the period of operation PNK during use by one of the machines "on line" this will ensure the possibility of continuing the development of system without the limitations and the difficulties, which may arise during the attempt to combine that and other functions in one machine.

Each computer has ZU on the disks, is conducted assembly ZU on the magnetic tape. The latter will be utilized for the recording of data in the operating cycles of computer and for the recording of data in the usual order, and they will be also useful in the process of development of software (see the block diagram Fig. 2).

In the system with the external control most important element/cell is connection/communication of machine with the operator. Although the data extraction of computer will be accomplished/realized with the aid of several fixed/recorded

annunciators, and control of it with the aid of the fixed/recorded

control switches, important value for all new or special fucntions of

machine has its flexibility. Therefore computer will be equipped

besides the teleprinters with powerful/thick display system with the

electron tubes and with keyboard. with the aid of teleprinter or

keyboard of display system it will be possible to turn to any

programs and cause them in any sequence. During at least the the

nearest to twelve months the majority of programs will be utilized

thus such.

    All programs and arrays of information are equipped with the

designations, which contain to four letters. For addressing the

program on the keyboard is collected/composed its designation, and

then, if necessary, the table of the values of the parameters. The

conditions, which are not necessary, make it possible to launch

program into the specific moment/torque either the time interval or

to synchronize it with the moments/torques of injection in PNK, or to

cause the specific external unit.
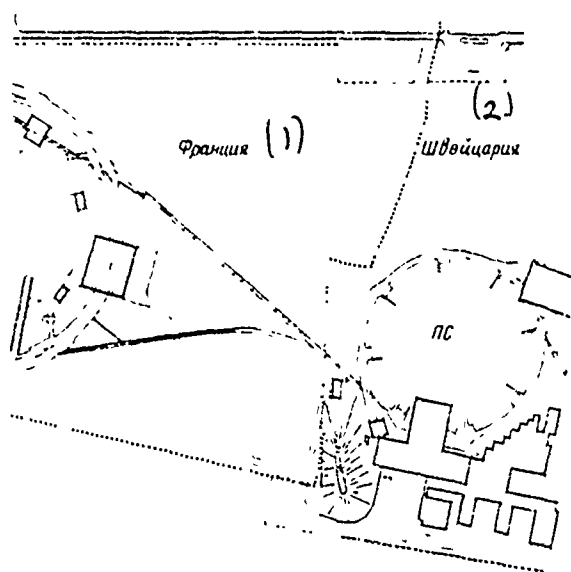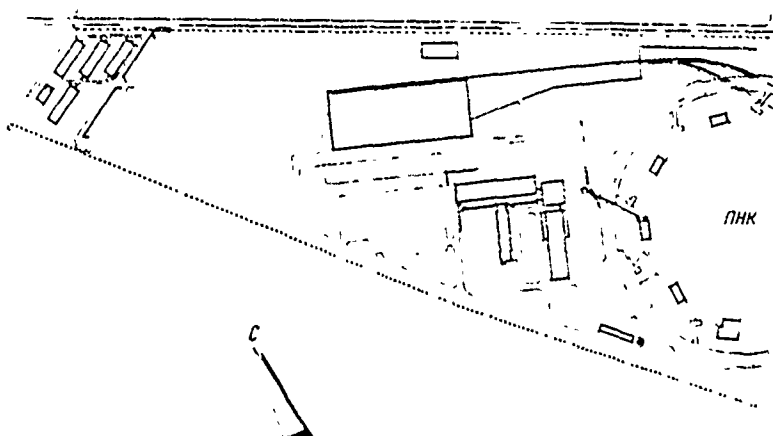
Fig. 1. Plan/layout of construction site of PNK.

Page 246.

To each command is given the marker which either is

collected/composed by operator or it is appropriated by machine.
Marker can be utilized to terminate the work of program. Are given
below some examples of the commands:

VTVR - indexes/identifies the position of beam;

MSET (246T, 1) - feed mode of the magnets of section 1 to set in
accordance with the Table 246T;

TEST; ASCN, IN=5S(2), 25(2, 34, 2) - test program; is studied analog
interrogating unit 2, introduction/input 34, after every 2 s, prints
10 references. Marker "TEST";

L PEMOVE TEST - ceases the work of preceding/previous program
(ASCN).

Program-dispatcher switches on the means of multiprogramming for
seven users each of whom has available the separate panel (keyboard),
the means of memory allocation in ZU on the magnetic cores and on the
disks between programs and arrays of the data, and also the memory
buffer ZU of display system.

Fundamental sets of input and output, connected with PNK, are
considered as external units and are controlled also by supervisory

program. This makes it possible to utilize them more than in one simultaneously called program, which is substantial for such elements of system as the analog interrogating unit.

Programs usually are stored in ZU on the disks in the moving binary form in the state of readiness for the call for any field ZU on magnetic cores.

The time of days is assigned through every 10 ms with the aid of the pauses from the central synchronizing system of PNK, and the operating time of all programs caties itself either to these pauses or to the impulses/momenta/pulses of device/equipment for the particle injection, accelerated on the synchrotron.

In another computer is utilized another program-dispatcher. It contains more complicated operators of the arrays of information and allows/assumes the possibility of composition and use in the line of programs in the language FORTRAN. Programs can be stored in ZU on the disks, being they are written, if this is necessary, in the input language, the accumulating language, in the mixed or absolute binary code. Since the plotter requires the larger library of routines in the language FORTRAN and the larger capacity of storage (ZU on the magnetic cores), it is connected with the second computer.

When this is convenient, with the programming is utilized the possibility of the "conversation" of machine with the operator. For example, if command incomplete, machine puts out the information about the missing element/cell and the correction method of error.
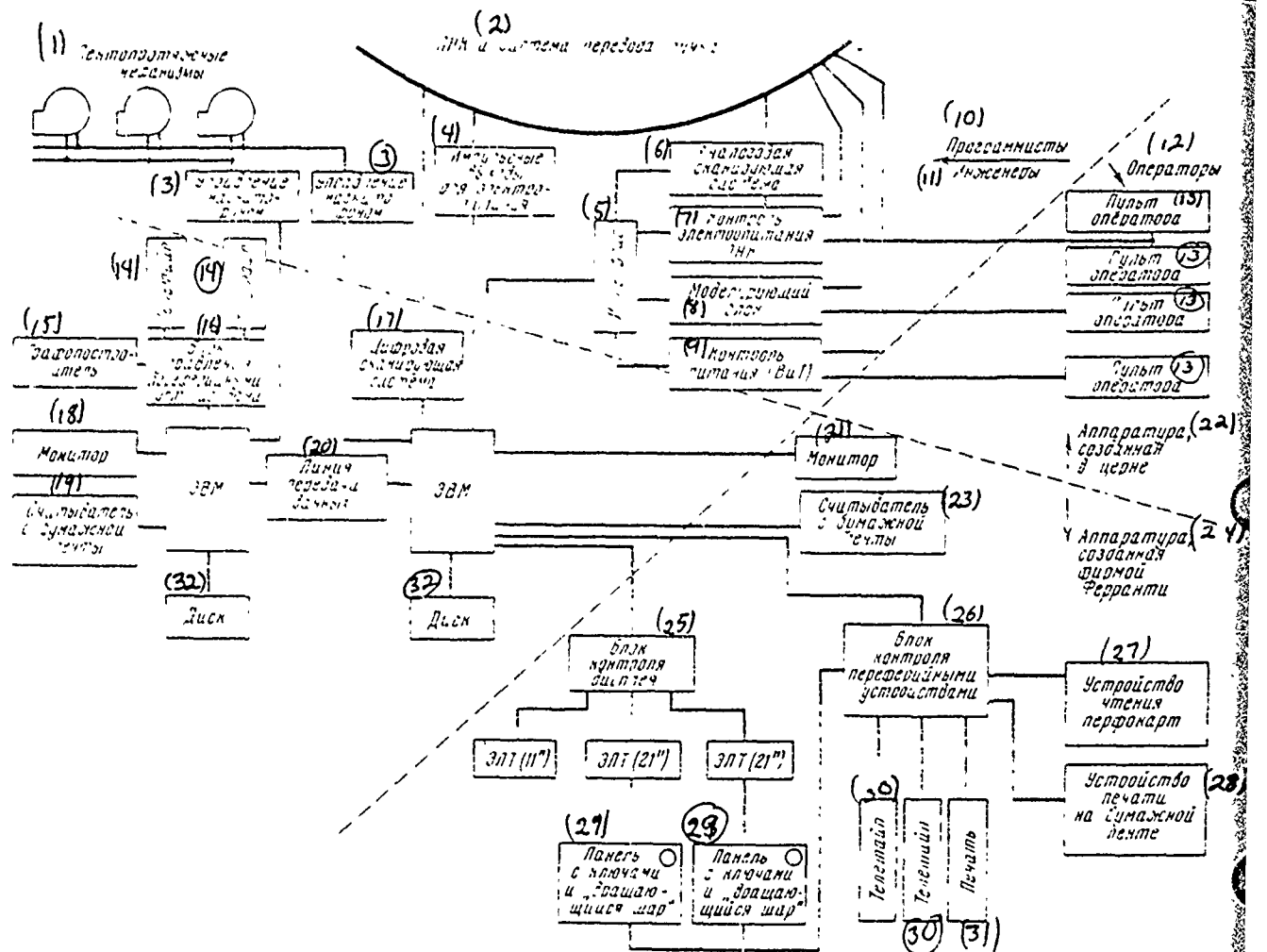
Fig. 2. System block diagram of control of PMK with use of two controlling computers.

Key: (1). Tape-drive mechanisms. (2). and system of of beam transfer. (3). Control of magnetic recorder. (4). Pulse outputs for electric power supply. (5). Interface. (6). Analog scanning system. (7).

Control of electric power supply. (8). Simulating block/module/unit.
(9). Control of power supply (it is twisted). (10). Programmers.
(11). Engineers. (12). Operators. (13). Panel for operator. (14).
Teleprinter. (15). Graph plotter. (16). Control unit of peripheral
devices (17). Digital scanning system. (18). Monitor. (19). Read out
from paper tape. (20). Line of data transmission (21). Monitor. (22).
Equipment, created in CERN. (23). Counter from paper tape. (24).
Equipment created by firm Ferranti. (25). Unit of control of display.
(26). Unit of control by punch devices/equipment. (27).
Device/equipment of reading or punch cards. (28). Device/equipment of
press/printing on paper tape. (29). Panel ◯ with keys/wrenches and
"rotating sphere". (30). Teleprinter. (31). Press/printing.

3. Data collection.

Slowly changing numerical data, for example signals about the
position of valves/gates and the state of the control equipment, and
also signals about the malfunctions in the power-supply system, are
collected by the continuously working interrogation device/equipment
with the control on transistors [4], which simultaneously requests
groups of 24 contacts and it introduces directly into ZU on the
magnetic cores of word of 24 bits, which describe their state. Every
112 ms in ZU on the magnetic cores is supplied the perfect
information about the state of 8064 contacts, which replaces the

previously entered information.

Readings of the analog instruments of are gathered by
interrogating unit on the relay, and then enter integrating digital
voltmeter [5, 6]. This instrument has a somewhat unusual
construction/design and consists of the converter of voltage into the
frequency, path of impulses/momenta/pulses from which they are
supplied to the counter in the console. Usually measurements are
conducted with the time of integration 20 ms, but for each reading it
is possible to assign the time of integration 10, 100 or 200 ms.
Although this system can seem by slow, because of the presence of two
converters in each of 12 centers of data collection the total rate of
measurement can reach several hundred readings 1 s.

Several subsystems are connected with the computer by rapid
lines of transfer of digital information.

4. Data transmission.

PNK contains very diverse equipment. Some of its elements/cells
are connected with the machine, others are not depended; the part of
this equipment is constructed in CERN, and part is prepared with
industry. Therefore the unavoidably simultaneous use of several
transmission systems of signals. It was at the same time necessary as

far as possible ensure the savings of cables and not to supply all
signals directly to the equipment in the console. Therefore for the
transmission of information to the buildings for the control
instruments frequently are utilized the multiplex communication
channels. In the systems or data collection from control system by
power supplies on the wide scales is utilized the matrix method with
the use of diodes, which makes it possible to transmit MxN signals on
M+N to leads/ducts.

As far as possible in the lines of transmission of signals to
the buildings for the equipment are utilized the high levels of
signal and narrow frequency bands. Standard multicore cables of PNK
consist of the woven pairs of strands of the common screen; it was
established/installed, that they are very convenient for the balanced
transmission of synchronizing signals. The special four-wire cables,
containing each 2 veins/strands for the video frequency and the low
frequency, proved to be excellent for the balanced transmission of
signals at the more high frequencies and with the distinct results
they are utilized in the closed-circuit television systems. The
use/application of long coaxial cables is limited by the cases when
is required broad frequency band or precise knowledge of delay time.

In many lines of control for the vacuum systems is used the
system of carriplex [7], which makes it possible to combine 400

channels for the transmission of control signals or measurement data
with the frequency by band 10 Hz in one cable. In this system there
are separate receivers and transmitters, which can be
established/installed in any place, which makes it possible to ensure
extreme decentralization. Thus, basic designation/purpose of this
system in PNK there will be the guarantee of temporary/time,
experimental either urgent lines of communications when the packing
of special cables is uneconomical, or unrealizable fast enough.

The leading idea during the design of the control systems
consisted of concentrating of complicated equipment in the console,
and to utilize simple multiplex methods of the transmission of
commands from the console to the distant objects of the controls
which also must be possibly simpler. Where this is possible, the
computer is connected with the multiplex line in parallel with the
panel for manual control. One should emphasize that PNK are not the
pulsed accelerator, but by the machine, which works in the continuous
duty, which after starting/launching continues to work without the
supplementary injection. Therefore the frequency band of control
signals is small, and the frequency band of the system of monitoring
equipment also could be small, if it is not required to provide
access to the large quantity of information for guaranteeing the
successful launching/starting of this new machine. The large part of
pilot signals is connected with the pulse nature of the process of

injection.

5. Control of the sources of feed.

Power supplies in the system for the translation/conversion of beam are equipped with digital-analog converters of the type of catenary with relay changeover [8]. Majority of them has the resolution of 5 decimal points and short-term stability about 2.10^{-6} h^{-1}: their control is accomplished/realized on the basis in parallel collected information.

The basic sources of power supply of each ring PNK by full/total/complete with power of o.9 MW are equipped with the analogous converter, modified with the calculation of stepped control instead of the straight/direct parallel control.

In the power supplies for the auxiliary magnets of PNK are utilized digital-analog converters [9], in which resistance catenary is equipped with semiconductor switches. In the control system is utilized the reversible binary counter by capacity/capacitance 12 bits. It is the electronic analog of potentiometer with the step-by-step motor as the drive.

Control channels of the sources of power supply of different

types are not depended. In parallel entering data from 95 supplies power of the system of the translation/conversion of beam alternately are supplied to the converter. The full/total/complete setting up of currents in the entire line of the translation/conversion of beam is accomplished/realized by a computer in 1-2 s.

Page 248.

The tuning of the sources of power supply of PNK, the need for which can arise in the presence of the circulating beam, and which frequently requires the matched change in the series/row of currents, it is reached in the control system with the computer with the aid of a 320- channel pulse generator [10] and binary multiplier with the distributed time, that ensure the independent frequencies for all channels in the range 0-255 Hz. Control is accomplished/realized with the aid of the table, calculated by computer each second and by that storing in small ZU on the magnetic cores. Supplementary manual control is limited by the slow and rapid adjusting of two power supplies simultaneously.

The programs of installation of the modes/conditions of power supplies are constructed in such a way that is provided the indication of the conditions, which block the execution of command. For this purpose all sources are connected with the digital

interrogating unit for the checking of their state.

6. Observation of beam.

Rings and channels of beam transfer are equipped with HF
electrostatic electrodes for measuring the orbital parameters. These
electrodes are connected by the circuit of coaxial cables with the
switches, which makes it possible to derive signals from two of any
pairs of electrodes to the broadband oscilloscopes in the console
[11]. This system makes it possible to observe the structure of
clusters and a change in the orbital parameters.

In addition to this broadband system, which makes it possible to
observe readings of one _ two monitors; it is provided for the
system of processing signals [12], which transmits in the narrow
frequency band on the computers the information, from which
simultaneously are extracted data for all 52 measuring electrodes
rings. Is possible two regimes of the work: the measurement of the
orbital parameters on any one revolution immediately after injection
(in the limits of ten revolutions) and the measurement of the
parameters of the closed orbit with the higher precision/accuracy
after the dephasing of betatron oscillations. For processing of
signals from translation/conversion system of bundle are used the
entreated devices/equipment for calculating the orbital parameters in

one orbit. Very character of these calculations, in combination with the errors for calibration and the drift of electronics, requires use for calculating the position of the beam precisely TsVM, if results it is proposed to utilize for the immediate orbit trim. It is planned/glided to construct the display unit on the cathode-ray tubes, which will give the image of orbit in two projections and the press,'printing its parameters.

The results, obtained up to now, show that at intensity 10^{12} protons per pulse the precision/accuracy of measuring in the channel of the translation/conversion of beam will be $+-0.5$ mm.

7. the inspection of vacuum system.

Vacuum system of PNK is very extended [13], contains an enormous number of pumps and vacuum manometers. Polecat it does not require the frequent operations/processes of control, it is necessary to ensure regular control for the purpose of the timely detection of failures and checking of the general state of vacuum.

TsVM is utilized for guaranteeing the operator with the almost entire necessary information. Complex problem is the operation of the vacuum gauge of Bayard -Alpert with the modulated supply with the vacuum 10^{-11} torus.

8. Conclusion.

The problems, stated on the first phase of construction PNK, are very diverse. By computers it is utilized for installation of modes/conditions, for the high-speed indication of results on the real scale of time and for the recording of data when there is a hope to set the more effective method of their use. In this region there are great possibilities of further development, in particular, development of cybernetic methods of control by machine and the guarantee of aid to physicists. The ways of this development will depend on the experience, acquired on the first phase. Results, obtained up to now, very heartening. The author must note the productive efforst of all colleagues of the subdivision of automation and aid and support from side of many other colleagues of division of PNK.

REFERENCES

1 K.Johnsen. The CERN Intersecting Storage Ring
Project, ISR-DL 67-63. (Paper presented to the VIth
International Conference on High-Energy Accelerators,
Cambridge, Mass.).

2. D.A.G.Neet, P. Wolstenholme. Proposal for Use
of a Digital Computer for Data Handling and Control
in the ISR Project, ISR-CO/68-6, 1968.

3. R.Kevser. The Dual Argus 500 Control Computer Sy-
stem for the ISR, ISR-CO 69-45, 1969.

4. Ferranti M.L.D. 5 and 7.

5. B.Sagnell and P.Wolstenholme. Remote Data Col-
lection Systems for the ISR, ISR-CO 55-24, 1968.

6. P. Wolstenholme. Input and Output Systems for the
ISR Control Computer, ISR-CO 69-24, 1969.

7. B.Sagnell. The Carryplex System as Applied to the
ISR, ISR-CO/70-40, 1970.

8. J.G.Pett. A Digital to Analogue Converter. ISR-BT,68-9,
1968.

9. P.Campiche. Etude d'un Convertisseur Numerique Ana-
logique, ISR-PO/70-22, 1970.

10. P.Wolstenholme. Controls for ISR Auxiliary Power
Supplies, ISR-CO 69-54, 1969.

11. W.de Jonge. The Wide-Band Beam Position Measu-
rements System, ISR-RF/69-74. 1969.

12. J. Borer and R. Scholl. The Beam Position Monitoring
System for the ISR ISR-RF,CO/69-55, 1969.

13. O.Gröbner. Procosed Computer Control for the ISR
Vacuum System, ISR-CO/70-6, 1970.

Discussion.

S. A. Heifetz. What principle is laid as the basis of your control

system: the principle of the maintenance of the prescribed/assigned

values of the parameters or the principle of the optimization of the

parameters, i.e., the search of the best solution in this situation?

P. Uolstenkhol'm. We have two rings, injection in which is

accomplished during the half-nour. All parameters, which ensure the

circulating beams, must have high stability during entire time of experimentation (24 hours). To this was made special detent. By the task of the optimization of processes we did not thus far yet deal.

DOC = 30069320   EAGE *1038*

249.

169. Automatic complex rcr control of the model of cybernetic accelerator.

V. Ye. Abadzhidi, N. I. Andryusncnenko-Lutsenko, G. I. Batskikh, A. A. Basil'yev, Yu. S. Ivanov, N. K. Kaminskiy, V. N. Kudin, A. A. Kuz'min, Yu. S. Kuz'min, N. I. Kuz'mina, V. A. Mironos.

(Radio engineering institute of the AS USSR).

Advance all to the high energies of the accelerated particles necessitated the developing/processing of proton synchrotrons to hundred, and in the future also to thousands of GeV [1-4]. The tendency to decrease the cost/value of the circular accelerators by the superhigh energies into hundred and thousands of GeV led to the idea of the construction of small-aperture cybernetic accelerators [6-8], steering of beam in which is accomplished/realized with the aid of the control computers.

For gaining of the experience of development and construction of

cybernetic accelerators in the radio engineering institute of the AS

USSR is created the model of cybernetic accelerator [9] - the

small-aperture cybernetic proton strong-focusing synchrotron, which

has the mean diameter of 17 m.

The test of experimental works for the model of cybernetic

accelerator showed that particle acceleration in the small-aperture

accelerator, and similar it is possible to call the accelerator, in

which the mixings of beam as a result of errors in the magnetic field

are the values of the order of the aperture of vacuum chamber, it is

connected with a whole series of special features/peculiarities.

If we briefly describe these special features/peculiarities,

then it is possible to say that all effects, including usually

considering secondary, connected with the beam displacement from the

axis/axle of chamber/camera, under the effect of the various kinds of

the changing in the time disturbances/perturbations acquire

considerably greater sharpness, and the adjustment of the separate

modes of operation of an accelerator-process of injection, the

mode/conditions of the first revolution of transition from the

mode/conditions of the first revolution to the mode/conditions of

circulation - it requires considerably larger thoroughness, which

cannot be carried out without the use of UEVM.

To us it seems that in spite of the increasing spread/scope of mathematical simulation with the aid of computers, the experimental final adjustment of the algorithms of control on the model of cybernetic accelerator, that giving possibility to correctly and convincingly consider the actual conditions for the work of the complex of equipment together with beam of accelerated particles, will allow henceforth to obtain important data, necessary for development and starting/launching of the projected/designed and planned accelerators for the superhigh energ.   in which it is proposed to widely use the methods of the automatic control (see also [9 - 12, 14, 15]).

At present for the control of the model of cybernetic accelerator it is utilized JEVM of the type "Dnepr", connected with the equipment for accelerator with the aid of electronics of connection/communication. In preceding/previous work [17] were described some algorithms of the adjustment of beam in the accelerator. In the present work is described the block diagram of the projected/designed automatic complex of the model of the cybernetic accelerator which it is planned to construct on the basis two UEVM "Dnepr" with the accumulators/storage on the magnetic tapes, moreover it is provided for the possibility of the exchange of information with the computers "BESM-6", and also works on the creation of the composite/compound algorithm, which permits

implemention of an adjustment of the position of beam from the injection to the acceleration.

The block diagram of the projected/designed automatic complex for the control of the model of cybernetic accelerator is represented in Fig. 1. Into automatic complex enter two control computers "Dnepr-1" (UEVM-1 and UEVM-2) and universal digital computer BESM-6 (computers). Directly control and direction of the modes/conditions of work of the accelerator accomplish/realize the machines "Dnepr", which work in parallel. Discrete/digital and analog input and output units of both machines through the switching devices/equipment are connected to different elements/cells of equipment for accelerator.
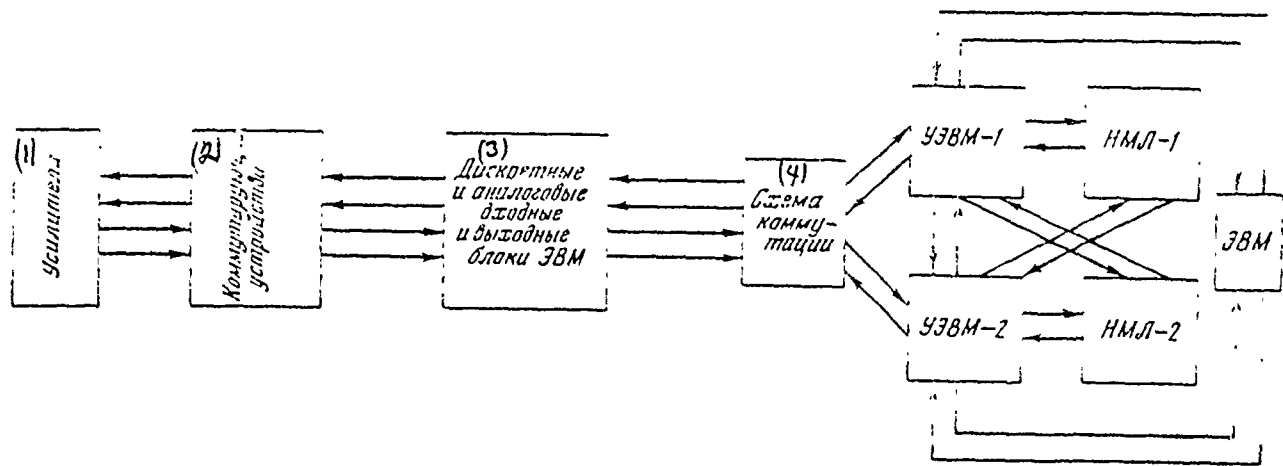
Fig. 1. Block diagram of automatic complex for the control of the model of cybernetic accelerator.

Key: (1). Amplifiers. (2). Switching devices/equipment. (3). Discrete/digital and analog input and output units of computers. (4). Switching circuit.

Page 250.

To UEVM these units also are connected through the switching circuit so that any UEVM can work with any input and output units. During this construction of the control system in the case of breakdown of one of the machines another can partially take the execution of its function for itself. In the process of the work through the special device/equipment UEVM they are exchanged between themselves

information. The synchronization of computer operation with the work of the accelerator in the time is accomplished/realized through the channels of interruption by signals of the timer device/equipment of control system by the processes of accelerator.

Algorithm of the work of entire automatic complex is determined by general routine - dispatcher, placed in working storage one of the machines "Dnepr". All programs on completion of the separate operations/processes of control and direction are stored in the accumulator/storage on the magnetic tape (NML) and are transferred/translated into the working storage of UEVM as needed. UEVM can turn to any of two NML. The information, obtained from the accelerator, is preliminarily worked by machines "Dnepr" and is introduced in NML, whence periodically, if necessary, it can be transferred to the machine BESM-6 for more full treatment.

In last two years on the model of cybernetic accelerator conducted experimental work on the creation of the algorithms of control and control of the separate working processes in the accelerator, which subsequently must enter as composite/compound component parts into the general routine of the work of automatic complex.

The general/common/total algorithm of control and control of

cybernetic accelerator encompasses the algorithm of position control of beam in the modes/conditions of the first revolution, circulation and accelerations, and also algorithm of the functional inspection of the basic systems of accelerator (Fig. 2).

The composite/compound algorithm of the control of position of beam in the mode/conditions of the first revolution in turn, switches on in itself the algorithms of the setting up of the value of the magnetic intensity, which corresponds to energy of beam, selection of the optimum conditions for the introduction/input of beam and adjustment of the divergences of beam from the axis/axle of vacuum chamber, caused by an azimuthal error in the magnetic field.

Before the adjustment of the divergences of beam in the mode/conditions of the first revolution the initial conditions for the introduction/input of beam into the accelerator preliminarily are established manually so that the divergences of beam, measured according to the established/installed along the accelerator fluorescing screens, would be mini um.

Time of execution of the algorithm of the adjustment of the divergences of beam from the axis/axle of chamber/camera 10-15 min.

After the adjustment of the divergences of beam from the

axis/axle of chamber/camera on the first revolution is fulfilled into
the mode/conditions of circulation the automatic refinement of the
initial conditions for the introduction/input of beam from readings
of the device/equipment, which records a difference in the positions
of beam with the first and second revolutions at two initial points
of ring, spread on the perimeter to 1/4 lengths of betatron
oscillations. Algorithm accomplishes/realizes changes with the aid of
the correctors of position and angle of the introduction/input of
beam from the ion guide into the accelerator and it reduces to zero
differences in readings of these sensors; those measuring the
divergence of beam on the first and second revolutions. The execution
of the algorithm of the control of the initial conditions for the
introduction/input of beam occupies 4-5 min.

After the refinement of initial conditions should be again
carried out an adjustment of the divergences of beam from the
axis/axle of chamber/camera in the mode/conditions of the first
revolution. After this it is possible to transfer/translate
accelerator into the mode/conditions of circulation.

During the circulation it is possible to accomplish the
adjustment of the divergences of beam from the axis/axle of
chamber/camera both in the mode/conditions of magnetostatic field and
in the mode/conditions with the growing magnetic field. Measurement,

and if necessary the correction of the divergences of beam during the circulation in the mode/conditions of magnetostatic field is desirable from the point or view of the control of the preceding/previous stages of control. The correction of the divergences of beam in the mode/conditions of circulation upon the injection in the growing magnetic field allows, furthermore, to consider the errors in the magnetic field, which appear in the growing magnetic field.

For controlling the divergences during the circulation were finished two algorithms. In one of them was determined and automatically was established/installed the average/mean relative to the boundaries of aperture, position of beam. In this case as the indicator of bundle was utilized the sensor of the intensity of beam current, and as the performing systems - organized in "triplet" corrective magnets (20 pcs), which make it possible to obtain the shift of orbit during the excitation of the correctors, who belong to one "sets of three" only in the limits of this "set of three". Control occupies 10-12 min. Precision/accuracy of control - 0.5 mm.

Another algorithm is based on the depression of the dangerous azimuthal harmonics of magnetic field. In this case as the indicator of bundle is utilized the sensor of the intensity of beam current, and as the performing system - system of the corrective magnets which

on the commands from UVM excite 5, 6 and 7 azimuthal harmonics. The
control of the position of beam with the depression of three
harmonics lasts by 1.5-2 min.

1048
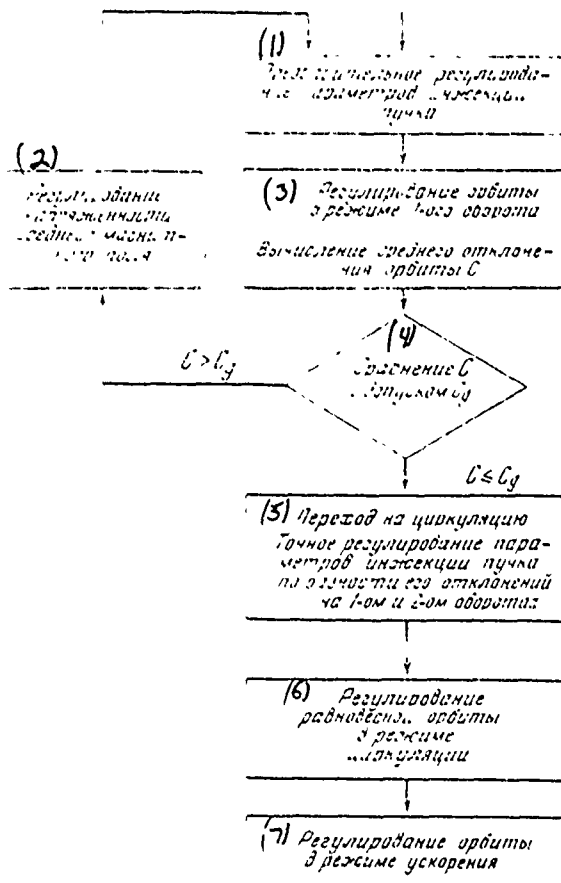
Fig. 2. Block diagram of algorithm of the control of orbit.

Key: (1). Preliminary control of parameters of the injection of beam.
(2). Control of intensity/strength of middle magnetic field. (3).
Control of orbit in mode/conditions of 1st revolution. Calculation of
average divergence of orbit C. (4). Comparison C to allowances. (5).
Transition for circulation precise control of parameters of injection
of beam on difference in its divergences on 1-ohm and the 2nd

revolutions. (6). Control of equilibrium orbit in mode/conditions of circulation. (7). Control of orbit in acceleration mode.

Page 251.

For orbital correction maneuver in acceleration mode to the corrective magnets with the aid of UVM "Dnepr" are put out the currents, which have piecewise-linear form. For this the step voltages, generated by UVM, are converted into the linearly changing current by the smoothing operational amplifiers. Broken curves have to eight sections with different slope/transconductance.

The search of optimum currents is conducted consecutively/serially on the sections. As the criterion of optimum character in each section is selected the minimum of a decrease in the intensity of beam in this section.

It is possible to correct the zero harmonic of magnetic field, for which to all correcting magnets are put out the currents with the identical slope/transconductance. Optimum inclination/slope in this section is selected by the method of change from the cycle to the cycle of the slope/transconductance of the build-up of current.

For the adjustment of azimuthal errors the currents into the

corrective magnets are put out with such inclinations/slopes so as in accordance with the position of the correctors on the ring of accelerator to reproduce one of the dangerous three-dimensional/space harmonics with the amplitude, which grows in the time. Changing the phase of harmonic and the rate of the increase of its amplitude, find the optimum values of these parameters consecutively/serially for 6th, 7th and 5th harmonics.

Besides the described here algorithms, are realized the algorithms for the functional inspection of the series/row of the systems of accelerator.

The authors express gratitude to academician A. L. Mints, Cand. of tech. sciences A. I. Dzergach, Candidate of Technical Sciences. To N. L. Sosenskiy, Yu. A. Vasinoy, G. I. Klenov and other colleagues of radio engineering institute, and also to colleagues of the department of electronic computers MFTI, which participated in the discussion of the described above works.

REFERENCES.

1. Design study for 300-1000 BeV accelerator, August 28 1961. Brookhaven Nat. Lab.
2. Report on the Design Study of a 300 Gev proton Synchrotron AR/Int SG/64-15, v.I, II, 19 November 1964.

3. Kibernsticheskiy Uskoritel' Protonob na energiye [Cybernetic proton accelerator at energy of 1000 GeV]. RAIAN, N.T. 925- 148 Moscow, 1967.

4. Design Report National Accelerator Laboratory. January 1968.

5. J. B. Adams, E.J.N. Wilson, 300 GeV Accelerator, CERN 70-60, 1970.

6. E. L. Burshteyn, A. A. Vasil'yev, A. L. Mints, et al., DAN SSSR [Report of Academy of Sciences of USSR], 1961, 141, 590.

7. E. L. Burshteyn, A. A. Vasil'yev, A. L. Mints, et al, Atomnaya Energiya, 1962, 12, III.

8. E. L. Burshteyn, A. A. Vasil'yev, A. L. Mints. Mezhd. Konf. po uskoritelyam [International conference on accelerators], Dubna, 1963, Moscow, Atomizdat, 1964, p. 67.

9. A. A. Vasil'yev. Mezhd. konf. po uskoritelyam [International conference on accelerators] [Dubna, 1963), Moscow Atomizdat, 1964, p. 87 p. 871.

10. A. I. Dzergach, V. A. Karnov. Mezhdunarodnaya Konferentsiya po uskoritelyam [International conference on accelerators] (Dubna, 1963, Moscow Atomizdat, 1964, p. 867.

11. N. L. Sosenskiy. Mezhdunarodnaya konferentsiya po uskoritelyam [International conference on accelerators], (Dubna, 1963), Moscow, Atomizdat, 1964, p. 878.

12. G. R. Lambertson, L. Jackson, Laslett, V. Internat. Conf. on High Energy Accelerators. Frascati, 1965, p. 26.

13. E. L. Burshtein, A. A. Vasiliev, A. I. Ozergach. V Intermat. Conf. on High Energy Accelerators. Frascati, 1965, p. 34.

14. L. Resegotti. CERN AR/Int. SG/62-8, July 31, 1962.

15. G. Bronka, A. Kart'ye, C. Neyre et al. VII Mezhd. konf. po uskoritelyam vysokikh energiy [Seventh international conference on accelerators of high energies], Yerevan (Tsakhkadzor), 27 August- 2 September 1969 (Session N.).

1052

16. A. A. Vasil'yev, N. I. Kuz'mina et al. VII Mezhd. konf. po
uskoritelyam vysokikh energiy. [Seventh international conference
on accelerators of high energies], Yerevan (Tsakhkadzor),
27 August-2 September 1969 (Session N.).

17. A. A. Vasil'yev, N. I. Kuz'mina et al. Trudy Raiotekhn.
in-ta AN SSSR, NTD-691, [Transactions of radio engineering
institte of AS of USSR, NTD-691], 1969.

Discussion.

S. A. Heifetz. Say, if you please, which scope of the program of

correction on the harmonics?

Yu. S. Kuz'min. This is one of the shortest programs; it occupies

about 700 storage cells.

Page 252.

170. Correction of the ncnlinear magnetic distortions of proton synchrotron with the aid of the computers.

G. V. YEfimov, YE. B. Liubimov, O. A. Obraztsov, V. I. Savvateyeva, N. L. Sosenskiy.

(Radio engineering institute of the AS USSR).

1. Introduction.

The development of tecnnology of proton synchrotrons is at present characterized by explicit tendency toward the amplification of the requirements, presented to the magnetic field of accelerator. This is connected, first of all, with the tendency toward an increase in the ratio of the emittance of the injected beam to the admittance cf accelerator. Apparently, tnis tendency even more will be enforced with the introduction into the accelerative technique of the superconducting coil electromagnets, in which is very high the cost/value of the unit volume of a precise magnetic field. Furthermore, special requirements for the precision/accuracy of magnetic field appear with the realization of the various kinds of

DOC = 80069320   PAGE 1054

the special modes/conditions of work of the accelerator, such, for

example, as the passage of some resonances in the process of

acceleration, connected with the high intensity of beam, and slow

conclusion/output. In connection with this should be expected the

amplification of the role of the systems of the correction of

magnetic field both in the existing accelerators in proportion to an

increase in their intensity and in the accelerators of the near

future. In this case to be restricted to the correction only of the

dipole components of the fields which determine the closed orbit,

apparently, no longer be managed.

The complexity of the correction of arbitrary (among other

things nonlinear) magnetic distortions of accelerator is determined,

first of all, by a large number of parameters, which characterize the

corrective field. Most reasonably this task can be solved with the

use of the computer, which works together with the accelerator in

accordance with the special algorithm.

Recently in the radio engineering institute of the AS USSR were

conducted works [1] on the creation of this type of system. The

developed algorithms are fairly complicated; therefore their initial

investigation was carried out by the method of simulation on

computers. In the report is briefly described the system of the

correcting lenses of the accelerator RTI of the AS USSR, are

presented the basic ideas, which lie at the basis of the algorithm of

correction, and are also given some results of simulation on the

computers BESM-6.

2. System of correction.

System is intended for the creation of the azimuthal harmonics

of dipole, quadrupole, sextupole, and octupole components of magnetic

field. The system of the correction of accelerator (Fig. 1) consists

of 20 multipolar lenses, in each of which can be created any

combination from the multipoles. The formation of the necessary

azimuthal harmonics provides UVM "Dnepr".

3. Algorithm.

Let the cycle of acceleration be broken into the series/row of

the time intervals, for each of which the corrective field of

accelerator is determined by certain quantity of parameters. The

result of the work of the algorithm of correction are many parameters

of the corrective field, which correspond to all time intervals. In

the process of the realization of the algorithm of correction into

the accelerator is injected the beam, limited on the current density

and according to the transverse sizes/dimensions. Algorithm utilizes

the information against the motions of beam, which is determining by

three values: by frequencies of horizontal and vertical betatron, and
also by interval of the existence of beam. Latter/last value is the
time interval during which the transverse divergence of the part of
the beam does not exceed the prescribed/assigned value.

The algorithm (see Fig. 2) is the sequence of the stages, for
each of which is conducted the determination of the parameters of the
corrective field, which correspond to one of the time intervals. In
each stage by the method of changing the frequencies of transverse
vibrations of beam, and also initial conditions of its injection are
consecutively/serially created resonance conditions, under which a
basic effect on the motion of beam has only small part from a total
number of azimuthal harmonics of errors in the field. With the aid of
a variation in the corresponding azimuthal harmonics of the
corrective field is conducted the maximization of the interval of
existence. If a consecutive variation in all azimuthal harmonics,
which are subject to correction (one iteration), does not lead to the
assigned magnitude of the sum of the intervals of existence on all
resonances, then the process of correction is repeated. The assigned
magnitude of the interval of existence increases, until is
achieved/reached the required degree of correction.

Fig. 3 gives the diagram of resonance lines on the plane of
frequencies of the betatron, on which as an example are shown the

points, which correspond to the sequence of resonance conditions for the correction for the purpose of the creation of the possibility of passage through the whole resonance in the process of acceleration.
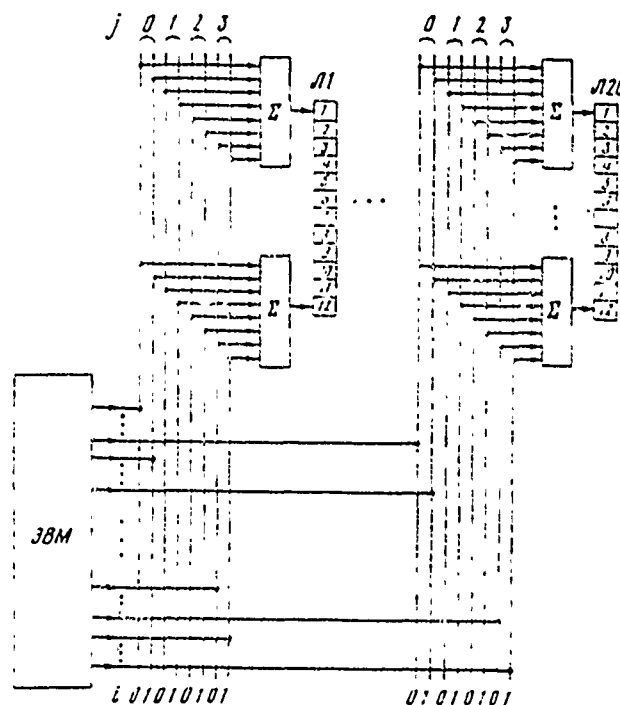
Fig. 1. Block diagram of the system of correction. Σ - summing amplifier; Л1...Л20 - correcting lenses; 1, 2... 12 - winding of lenses; j - order of multipole (j=0 - dipole; j=1 - quadrupole; j=2 - sextupole; j=3 - octupole; i - index, which is determining the attitude of multipole (i=0 - it corresponds to angle ϕ between the plane of the zero potential of multipole and the horizontal plane equal to zero; i=1 - corresponds to the angle ϕ, equal to $\frac{\pi}{2(j+1)}$). Computers - control computer "Dnepr".

Page 253.

4. Results of simulation.

In the process of the adjustment of algorithm its action was investigated for the case when errors in the magnetic field of accelerator are determined by the simultaneously present two quadrupole components, which excite parametric and sum resonances. Both components were the uncorrelated random functions of azimuth. Root-mean-square magnitudes of error were determined by the values with which resonance bands do not exceed value 0.02. Simulation was conducted for different realizations of random functions.

The process of correction was conducted at the level of injection and it ceased, when resonance bands reached value on the order of 0.001. The averaged on 10 realizations of random functions number of cycles of acceleration, necessary for achievement of the required degree of correction, proved to be equal to ~40 that it corresponds to the time of order 2 min.

The developed algorithm gives possibility, with some limitations to carry out a correction of the random errors in the field, which contain the set of multipole components. At present is conducted work on the improvement of algorithm.

The authors hope that the work experience with this system of

correction will prove to be useful not only for an improvement in the parameters of the existing accelerators, but especially for the future accelerators in which will be utilized the superconducting coil electromagnets.

Fig. 2. Block diagram of the algorithm of correction. 1 - assignment of stage; 2 - assignment of the interval of existence; 3 - establishment of resonance conditions; 4 - maximization of the interval of existence; 5 - determination of the sum of the intervals of existence from all resonances; 6 - determination of the sufficiency of the degree of correction; a) a next variation in the harmonic; b) transition to the following harmonic; c) transition to the following iteration; d) an increase in the intervals of existence; e) transition to the following stage.
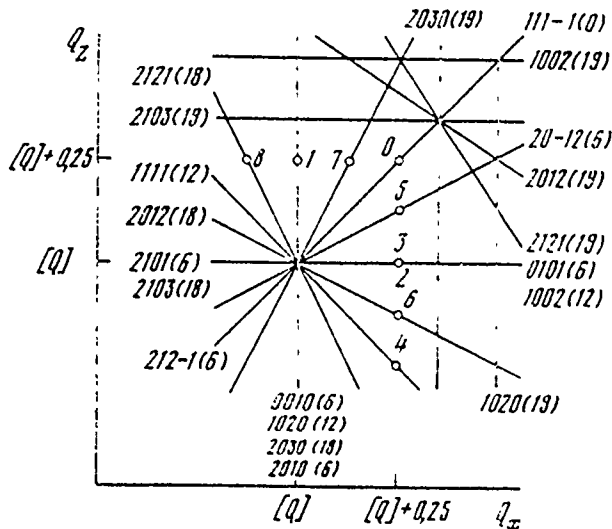
Fig. 3. The follower of resonance conditions Q_x, Q_z — frequency of horizontal and vertical betatron; [Q] - whole syllable Q; j - order of multipole (j=0 - dipole; j=1 - quadrupole; j=2 - sextupole; i - index, which is determining the attitude of multipole (i=0 - it corresponds $\phi=0$; i=1 - corresponds $\psi = \frac{\pi}{2(j+1)}$); τ - the number of the azimuthal harmonic of multipole; $pQ_x + \ell Q_z = \tau$ - equation of resonance line; $j \, i \, p \, \ell (\tau)$ - code of resonance line 1, 2... B - point; corresponding to resonance conditions; 0 - the operating point of accelerator.

REFERENCES.

1. N. L. Sosenskiy. Dynamics of particles in a highly focusing magnetic system with correction of the nonlinear distortions of the field according to information on the beam. Trudy Vsesoyuznogo Sovetsaniya po Uskoritelyam [Transactions of the all union conference on accelerators], 1968, Vol. II, p. 315

Page 254.

171. Measuring system of the parameters of the electron beam of the high-current accelerator.

Ye. V. Armenskiy, A. I. Borodulin, V. M. Rybin.

(Moscow physical engineering institute).

Linear electron accelerator to 60 MeV, developed by RAI of the AS USSR, is a six-section machine with a length of 30 m with the following parameters of pulse electron beam at the output of the accelerator:

maximum energy of the accelerated electrons - 60 MeV;

minimum pulse current - 100 mA;

maximum pulse current - 3 A;

the pulse duration is changed in the limits from 0.25 to 5.5 μs;

a decrease in the apex/vertex and the leading impulse front of

beam current comprise not more than 15c/o respectively from amplitude and pulse duration;

pulse repetition rate of beam current in the operational conditions is changed from 50 to 150 Hz for the duration of pulses 5.5 µs and from 50 to 1500 Hz for the duration of pulses 0.25 µs. In the setup mode/conditions the frequency of sequence comprises with respect 5 and 10 Hz;

the diameter of beam on half-decay of current is not more than 2 cm.

The measuring system of the parameters of beam, developed for this accelerator, permits implemention of continuous control of current and position of beam in five inter-section gaps/intervals and at the output of accelerator. The block diagram of this system is shown in Fig. 1.

Measuring equipment is placed in the special struts in the console hall at a distance of 50 m from the accelerator. Information from the current-sensing devices and position of beam comes the cathode followers which are carried out on the diagram with the dynamic load, they possess high(ly)-linear characteristics in the range of amplitudes to 10 *in* [1] and make it possible to transfer the

pulse signals of negative polarity by the lines
connections/communicaticns (coaxial cables of the type RK 100-7-21
with the wave impedance cf 100 ohms) to the struts of measurement and
observaticn.

As the current-sensing devices of beam are utilized
magnetic-induction senscrs [2-4], which with the work in the
aperiodic mode/conditicns give the possibility not only to measure
the beam current, but also to ouserve the form of the current pulses
of beam. The schematic cf current-sensing device is represented in
Fig. 2, where W_1 - measuring winding, W_2 - winding of the
calibrations which are arranged/located on the ferrite toroidal core.
For obtaining the aperiodic mode/conditions of the work of sensor it
is necessary to satisfy the ccndition $R_H \ll \frac{\rho}{2}$, where ρ - wave
impedance of measuring winding. In this case the sensitivity of
current-sensing device $S_I = \frac{R_H}{W_1}$ and virtually can reach 10 V/A with a
decrease in the apex/vertex and the leading impulse front of exit
voltage it is less than 10o/o.
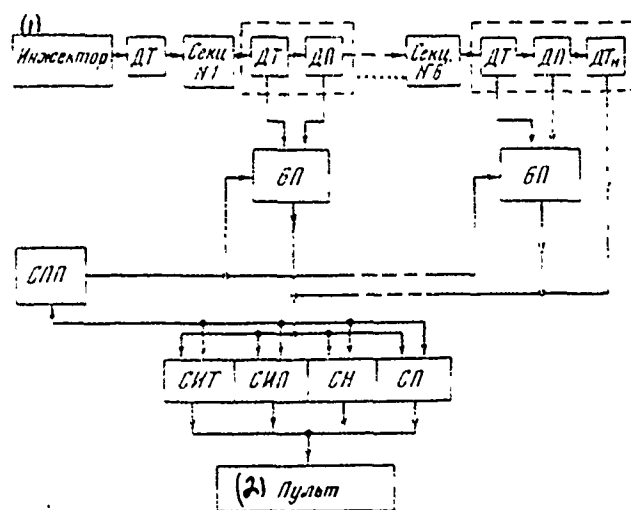
Fig. 1. System block diagram of the measurement of the parameters of the electron beam of linear high-current accelerator on 60 MeV RAI of the AS USSR. DT - current-sensing devices of beam; DP - beam-position sensors; BP - units of cathode followers; SPP - rack of measurement of beam current; SIT - rack of measurement of the position of beam; SI - rack of the observation of the form of the current pulses of beam; SP - power frame of measuring circuits.
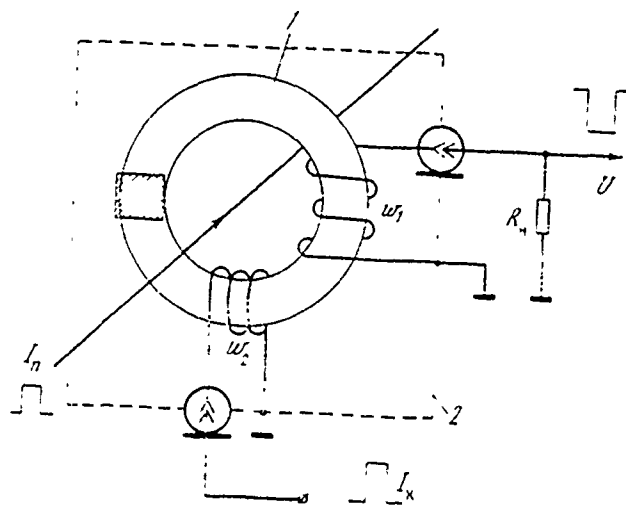
Fig. 2. The schematic diagram or the magnetic-induction current-sensing device of beam I_n - the pulse beam current of electrons; I_k - pulse current of calibration; u - exit cue voltage of current; R_H - the effective resistance of load; 1 - ferrite toroidal core; 2 - screen and protective jacket.

Page 255.

The winding of calibration serves for the adjustment, the functional test and calibration of entire channel of the measurement of beam current. For this through it is passed the pulse current of known value I_k (from the special pulse generator of calibration), which is equivalent to passage through the impulser of beam current with an amplitude of $I_n = W_2 I_k$. The current-sensing devices of beam in the

developed system have tne following parameters: outer diameter of

toroidal core from the ferrite 3000HM with magnetic permeability 3000

is equal to 95 mm, internal - 75 mm, height - 20 mm; W_1=50 turns,

W_2=15 turns (coil/winding uniform, lead/duct PEV with a diameter of 1

mm). For convenience in tne measurement the range of the measured

currents is broken into two: the first - with the limit to 1.5 A, by

the second - to 3 A. The selection of the necessary range of

measurement is accomplished/realized by a remote/distance change in

the effective resistance of tne load of sensor.

In the first range cf measurement the sensitivity of

current-sensing device is equal to 4 V/A (R_{H_1} =200 ohm), the secondly

- 2 V/A (R_{H_2} =100 ohm).

The block diagram of tne channel of the measuring system of beam

current is shown in Fig. 3. From tne current-sensing device after

cathode follower, after passing along the cable line, the pulses of

the voltages which in form and amplitude correspond to the current

pulses of beam, they enter the measuring circuit of the pulse

amplitude, which is compensative type pulse voltmeter [5], output of

which is a dial instrument of the type M4200. Simultaneously it is

possible to observe the form of the current pulses of frame on the

oscilloscope face of the type C1-20, established/installed in the

strut of observation (SN), in any of six

controllable/controlled/inspected points (by choice of operator). The
control unit of the measuring system of beam current
accomplishes/realizes an automatic selection of the ranges of the
measurement of current, provides the independence of the work of the
measuring circuit of the pulse amplitude from the recurrence
frequency of the current pulses of the beam (for this is utilized
signal from the timer of accelerator) and it makes it possible to
produce the calibration of channel with the aid of the pulse
generator of calibration, as which is utilized the pulse generator of
the type G5-15. A relative error of measurement of the amplitude of
the current pulses of beam after adjustment and calibration of the
channel of measurement is approximately 0.5o/c, absolute error ~5o/o.
An error in the reproduction of shape of the current pulses of beam
lies/rests within limits of 5-10o/o.

As the beam-position sensors are also used magnetic-induction
sensors [2-7], distinctive special feature/peculiarity of which is
the presence of quadrature winding. The schematic of this sensor,
which makes it possible to conduct the measurement of the position of
beam relative to electron conductor on one coordinate (on the
horizontal), is given in Fig. 4, where W_1 and W_2 - concentrated
windings which are arranged/located on ferrite toroidal core 1;
moreover one of them depending on the position of the contacts of
transfer relay short-circuited, and the second is loaded to the input

rasistance of cathode follower (active resistance R_H and capacity/capacitance C_H). For obtaining the larger sensitivity the position detector works in the oscillatory mode/conditions, i.e., $R_H \gg \frac{\rho}{2}$, where ρ - wave impedance of the nonshort-circuited winding, and diode D separates/liberates the first half-wave of the exit voltage of this winding whose amplitude bears information about the position of beam. Position detectors have the following parameters: outer diameter of toroidal core from ferrite 3000 HM with magnetic permeability 3000 is equal to 95 mm, internal - 75 mm, height - 15 mm; $W_1 = W_2 = 10$ turns (winding concentrated and they are arranged/located symmetrically, lead/duct PEV with a diameter of 0.47 mm). With one quadrature winding the signal amplitude u, which enters from the second winding position detectors the cathode follower, can be represented as follows:

$$U = S_I \, I_n + S_{\Delta x} \cdot I_n \, \Delta x,$$

where I_n - amplitude of the current pulses of beam, A;

S_I - sensitivity of position detector on the current, V/A;

$S_{\Delta x}$ - sensitivity of position detector on the beam displacement, $V/A \cdot mm$;

Δx - beam displacement relative to the geometric center of electron conductor, mm.
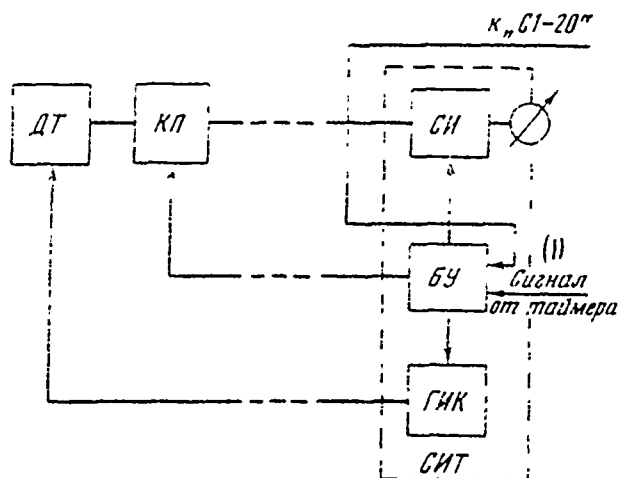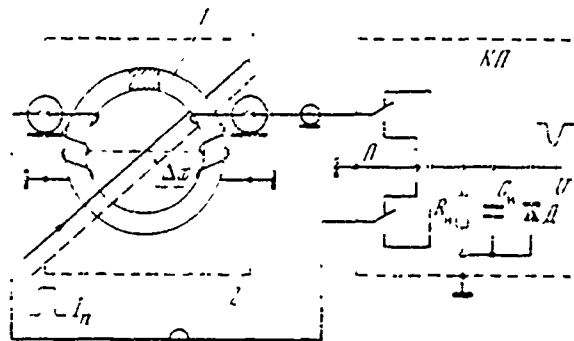
Fig. 3.   Fig. 4.

Fig. 3. Block diagram of channel of measuring system of beam current.
DT - current-sensing device; KP - cathode follower; SI - measuring
circuit of the amplitude of pulses of voltage; BU - contro' unit of
the measuring system of beam current; GIK - pulse generator of
calibration; SIT - strut of the measurement of beam current.

Key: (1). Signal from the timer.

Fig. 4. Schematic of magnetic-induction beam position detector. I_n -
pulse electron beam; ΔX - beam displacement; u - exit cue voltage of
position R_H - the effective resistance of load; C_H -
capacity/capacitance of load; D - diode, which releases first

half-wave of exit voltage; 1 - ferrite toroidal core; 2 - screen and protective jacket; KP - cathode follower; P - contacts of transfer relay of quadrature winding.

Page 256.

For the developed position detectors current sensitivity $S_I = 6$ V/A, and sensitivity on mixing $S_{\Delta x} = 0.12$ V/A·mm. Voltage pulses, which come the cathode follower from position detector, have funnel-shaped form, amplitude to 10 $\frac{v}{A}$ the duration of approximately 0.25 µs (on the basis/base). The possibility of the successive closing/shorting shortly of the windings of the position detector, accomplished by an operator by hand with the aid of the contacts of special transfer relay, makes it possible to fix/record the coincidence of the position of electron beam with the geometric center of electron conductor with the error +-0.2 mm with the beam current not less than 0.4 A in the impulse/momentum/pulse. The measurement of beam displacements on another coordinate (along vertical) is accomplished/realized by the analogous sensor whose windings are arranged/located along the vertical axis/axle.

The system block diagram of the measurement of the position of beam is given in Fig. 5. From the position detectors ($\Delta n_{1x} - n_{6x}$ and $\Delta n_{1y} - \Delta n_{6y}$) after cathode followers and cable line the pulses of the

voltages whose amplitude depends on the position of beam, enter the commutator of the strut of the measurement of the position of beam. The commutator, hand-operated, gives the possibility to operator by choice to take the measurement of the position of beam on two coordinates ("X" and "Y") simultaneously in one of six controllable/controlled/inspected points. For measuring the pulse amplitude are utilized the measuring circuits, analogous to the diagrams, established/installed in the channels of the measurement of beam current. At the output of measuring circuits are established/installed the dial instruments of the type M4200 according to the scale of which, that has zero in the middle, is taken a reading the amount of beam displacement. In the system is utilized the manual compensation for readings of the meters of the position of beam, which depend on the value of beam current (for this serves the special unit of compensation). Furthermore, in the system is provided for the calibration they are measuring circuits, which is accomplished/realized periodically by an operator. For this is utilized the special gauging signal (u_k). An error of measurement of the position of beam during the periodic calibration of measuring circuits and timely compensation or with the direct beam current is +-0.5 mm with the beam current not less than 0.5 A in the impulse/momentum/pulse.

Structurally/constructurally the current-sensing devices and

position of beam at each controllable/controlled/inspected point are
united and have common screen and protective housing. Electron
conductor in the site of installation of sensors has nonconducting
gap/interval, for which are sealed in special ceramic insets. The
setting up of sensors is accomplished/realized with the error +-0.5
mm relative to the geometric center of electron conductor.
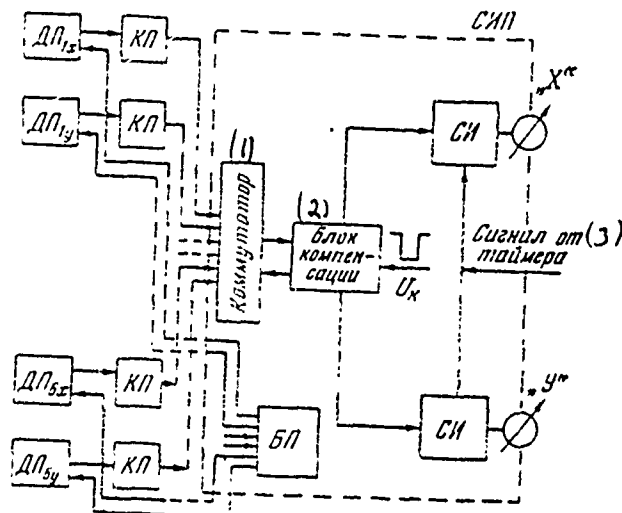
Fig. 5. System block diagram of the measurement of the position of

beam. $\Delta\Pi_{1x} \div \Delta\Pi_{6x}$ - beam-position sensor on the horizontal; $\Delta\Pi_{1y} \div \Delta\Pi_{6y}$

- beam-position sensors on the vertical line; кп - cathode followers;

cu - measuring circuit of the amplitude of pulses of voltage; ВР -

unit of the changeover of quadrature winding of sensors; u_k -

calibration impulse/momentum/pulse; SIP - the strut of the

measurement of the position of beam. Key: (1). Commutator. (2). Unit

of compensation. (3). Signal from timer.

REFERENCES.

1. A. M. Lozhnikov, Ye. K. Sonin. Kaskadnyye Usiliteli [Cascade amplifiers], GEI, 1961.

2. I. A. Grishayev, N. I. Mocheshnikov, V. F. Ivanov. Measurement of position and current of the transit pulse beam of charged particles. PTE, Nr. 4, 1960.

3. R. Bergere et al. 1962, NIM, 15, N 4, p. 327

4. R. Yamada. Japan. J. Appl. Phys. 1962, N 1, N 2, p. 92.

5. Ye. V. Kamenskiy, V. F. Zhirkov, V. M. Rybin. Semiconductor meter of the amplitude of pulses. Izmeritel'naya tekhnika, 1964 No 10, p. 35

6. K. Johnson et al, 1961, NIM, 14, N 2, p. 125.

7. L. Dorikens - Van Praet et al. NIM, 1967, 17, N 1, p. 58.

Discussion.

F. Ferger. Are such the ranges of the measurement of the divergences of beam in the horizental and vertical planes?

A. I. Borodulin. The ranges of measurements are +-5 mm.

F. Ferger. Which the bandwidth of the display of the position of beam?

A. I. Borodulin. The bandwidth makes it possible to measure the pulse durations to 0.1 μs.

G. Kumpfert. Are such the limits of the measurement of pulse beam current in your accelerator?

A. I. Borodulin. We change the peak values of current within the limits from 100 mA to 3 A in the impulse/momentum/pulse.

Page 257.

172. System for the control of injection in VEPP-3 and the synchronizations of the elements/cells of channel.

V. I. Nifontov, B. M. Peslyak.

(Institute of nuclear physics of SO AN USSR).

In the accelerative complex ELIT-3, B-4, VEPP-3, where the majority of elements/cells operate on a pulsed basis, vital importance has the synchronization of the moments/torques of the starting/launching of the working nodes/units of complex. The basic task of resolver of the unit of preliminary synchronization lies in the fact that to produce the timely start of the exhaust magnets of synchrotron B-4, rotary magnets and lenses of channel B-4 - VEPP-3 and to carry out control of issue from synchrotron B-4 at that moment/torque when energy of the accelerated particles achieves rating value. In the device/equipment is provided for the automatic tuning of time/temporary delay for adjusting of the register of the moment/torque of injection with the establishment of the maximum values of pulse magnetic fields in the elements/cells of channel. The stability of the energy level or particles at the moment of injection

is checked with the aid of the unit of control with digital reading.
The block diagram of device/equipment and the elucidating time graphs
are given in the figure.

Unit of the solution.

As the signal, which characterizes energy of particles in B-4,
is selected the value of the accelerating magnetic field in the
synchrotron. Sensor of magnetic field - inductive loop, which covers
cne of the quadrants of accelerator. The voltage from the sensor,
proportional dH/dt, enters precise integrator 1 (Fig. 1). Output
signal from the integrator through scale resistances proceeds with
the entrance of amplitude comparator. The reference voltage, U_{on}
(Fig. 1.8) proportional to energy of the produced particles, is
assigned by potentiometer and through the operational amplifier also
enters the working entrance of comparator. The form of pulse field in
synchrotron B-4 takes the form of half sinusoid $H(t) = H_m \sin \omega t$.
According to the working conditions of accelerative complex the issue
of particles occurs on the rear slope of pulse field.

With the coincidence of stress level on the integrator with the
level of reference voltage is formed/shaped the output signal, which
turns off/disconnects high-frequency accelerating voltage on the
resonator of synchrotron. From this point on, the energy of the

accelerated particles, without taking into account losses to the synchrotron radiation, remains constant and with further field slope the cluster of the accelerated particles is shifted/sheared to the external wall of the accelerative chamber/camera where is arranged/located deflector. Signal to the inclusion of deflector is formed/shaped into that moment/torque when is satisfied the condition

$$\frac{\Delta H}{H} = \frac{\Delta R}{R},$$

where ΔH - field change from the cutoff of high frequency to the moment/torque of issue; H - field value at the cutoff of high frequency; R - working radius of the equilibrium orbit of synchrotron B-4; ΔR - distance on the chamber/camera from the equilibrium orbit to the center of deflector.

Signal for the inclusion/connection of deflector is formed/shaped with second comparator 5 (Fig. 1), where a change in the scales of the addition of input signals, which assign a necessary radius of issuing, is accomplished/realized by stepped changeover of supplementary resistance.

For the specific time before the impulse/momentum/pulse of issue must be obtained the supplementary control signals for the preparation of exhaust magnets and pulse elements/cells of channel for the work. The time/temporary interval between the impulse/momentum/pulse of issue and the supplementary driving pulses

must with the specific precision/accuracy remain constant/invariable with the departure/attendance of the amplitude of accelerating field cf synchrotron within limits (2-3) o/o.
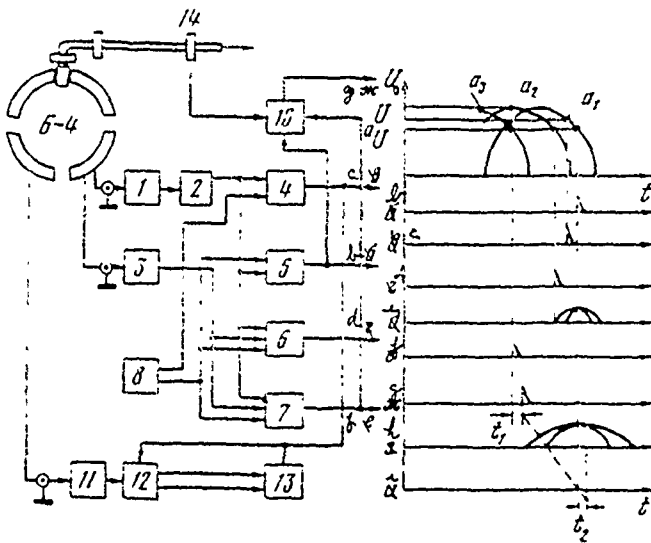
Fig. 1. Block diagram and time graphs of control system by injection in VEPP-3. 1, 11 - integrators; 2, 3 - scale units; 4 - comparator of the disconnection of high(ly)-scale oscillator; 5 - comparator of the issue of particles from B-4; 6 - comparator of the inclusion/connection of the exhaust elements/cells B-4; 7 - comparator of the start ˄ the exhaust elements/cells of channel; 8 - amplifier of reference voltage; 10 - tuning unit; 12 - unit of control; 13 - scaler; 14 - element/cell of channel; u_H - voltage, proportional to field B-4; u_{on}, u'_{on} - reference voltage; a_1 - voltage, proportional to the floor/sex B-4; a_2, a_3 voltage for the anticipating/leading solution; 6 - impul   ntum/pulse of the issue of particles of B-4; c) the impulse/momentum/pulse of the disconnection of HF oscillator; d) the impulse/momentum/pulse of the inclusion/connection of the exhaust elements/cells B-4; e) the field

of the exhaust elements/cells B-4; f) - the reference pulse of the
start of the elements/cells of channel; g) the operating pulse of the
start of the elements/cells of channel; h - field of the exhaust
elements/cells of channel; Δt_1 - adjustable time/temporary interval
between the reference and operating pulses; Δt_2 - the time interval
between the moment/torque of issue and the maximum of the field of
the elements/cells of channel.

Page 258.

Such control signals are obtained during the supplying to the working
outputs of comparators 6, 7 (Fig. 1) the signal of the form

$$U'(t) = Um \sin[\omega(t + \Delta t)],$$

i.e. the voltage, which anticipates/leads the voltage, proportional
to accelerating field of synchrotron to the prescribed/assigned
time/temporary interval. With the sinusoidal form of field $U(t) = U_m \sin \omega t$
this voltage can be obtained by the addition of function itself and
first derived this function in the specific scale relationship/ratio.
Actually/really, in the expansion of this function according to
Taylor are present only the members, who contain $\sin \omega t$ and $\cos \omega t$;
therefore in signal $U'(t) = U m m_1 \sin \omega t + U m m_2 \cos \omega t$ is sufficient to select
coefficients of m_1 and m_2 for obtaining the prescribed/assigned value
Δt, moreover first term in this expression is obtained from the
integrator, and second - is direct from the inductance pickup of

field. Scale factors are assigned by summing resistances in the comparators. Reference voltage corresponds to voltage on the comparator of issue U'_{on} (Fig. 1).

Comparator 6 (Fig. 1) is utilized for the control of the exhaust elements/cells B-4. Comparator 7 (Fig. 1), with the high value Δt controls the "long" magnetic elements/cells of channel.

The decisive unit provides the precision/accuracy of joining to the energy level on the order of 5.10^{-4}. The time/temporary interval between issue and inclusion/connection of the exhaust elements/cells B-4 is stable with the precision/accuracy $+-10^{-6}$ s; between issue and start of the elements/cells of channel - $+-5.10^{-6}$ s. Comparators are constructed on the basis of operating accelerators with the nonlinear feedback.

Tuning unit 10 (Fig. 1).

In the system of the preliminary starting/launching of the elements/cells of channel can appear large error due to the departure/attendance of the parameters (L and C), which are determining the duration of the pulse magnetic fields of these elements/cells. In this case the issue will occur not accurately at the apex/vertex and the quality of the transportation of the

accelerated particles sharply deteriorates. For the automatic tuning
of system according to this sign/criterion in the tuning unit is
separated/liberated the impulse/momentum/pulse, which coincides with
the moment/torque of the peak or field in the element/cell of channel
14 (Fig. 1) and with its departure/attendance to that or other side
relative to the impulse/momentum/pulse of issue t_1 (Fig. 1) is
separated/liberated the corresponding signal to the reverse counter.
The state of counter is converted into the analog signal, which
corrects the starting time of this element/cell of channel t_2 (Fig.
1). In the device/equipment is used the resolving diagram on the
dynistors, bidirectional counter is combined with the register of the
converter of code-analog, and as the time-assigning elements/cells
are used diode- regenerative comparators. Discrete/digital step/pitch
of tuning - 2.10^{-6} s. Range of tuning - $+-30.10^{-6}$ s.

Unit of control.

For the operational control of the energy level of issue is
developed the unit of control by 12 (Fig. 1). It consists of a
precise integrator, two keys/wrenches and comparator with the
shapers. At the cutoff of high frequency on the integrator is
memorized the analog signal, proportional to energy of the
accelerated particles and then it is converted into the time
interval. The significant figure of time interval, obtained on

decimal counter 13 (Fig. 1) induces to scale the level and the stability of energy of the produced particles. An error in the unit of control is not more than 10^{-4}.

Discussion.

I. P. Karabekov. Which the precision/accuracy of the maintenance of the mutual location of synchronizing pulses?

V. I. Infontov. The precision/accuracy of tuning in the time comprises: for the long element/cell – 5 μs, for the short element/cell – 2 μs.

173. Construction of the mathematical model of synchrotron to 1.5 GES and investigations on the model of some algorithms of control.

E. G. Voronin, V. V. Zakharov, V. A. Kochegurov, V. I. Naplekov, N. M. Filipenko, V. V. Tsygankov.

(Scientific research institute of nuclear physics, electronics and automation with by Tomsk polytechnic institute).

At present there was determined the following diagram of conducting of experiment with the use of accelerators (Fig. 1). As can be seen from figure, in the diagram there are two autonomous control systems. Problems of control of physical experiment, processing physical information entering on the computers widely are solved in all physical laboratories. However, they are solved in all physical laboratories. However, important role in the experimentation on the accelerators is the guarantee of effective control in the process of experiment accelerator itself. Control of accelarator represents very complex problem. in general accelerator can be considered as certain multiparametric dynamic system, which is located under the effect of the internal and external perturbing forces with the random change in the time

$$y = y(x, x_0(t), z(t)), \qquad (1)$$

where y - vector quantity, which characterizes the parameters of the accelerated beam (intensity, energy, duration); x - controlling parameters; $x_0(t)$, $z(t)$ - the random uncontrollable interferences, additive with x and y.

Page 259.

From the point of view of control of accelerator there is the greatest interest in the creation of the system, which ensures the continuous maintenance of the maximum value of intensity with the simultaneous stabilization of energy of the accelerated beam. For this purpose it is necessary, first of all, to create as far as possible more than the sensors of information about the state of accelerator; in the second place, to conduct the detailed investigation of accelerator as the object of automatic optimization, since the effectiveness of different algorithms of the search of the extremum of the functions of many variable/alternating in essence is determined by the type of the surface of the function of response, limitations, superimposed on the controlling parameters and, etc.

Are examined below questions of development and construction of

the mathematical model of synchrotron to 1.5 GeV TPI, and also
results of experimental check on the model of some algorithms of
optimization.

In general synchrotron cn 1.5 GeV can be presented in the form
of the block diagram, depicted in Fig. 2. The intensity of the
accelerated beam in the synchrotron in essence is determined by its
parameters at the injection, time of injection, by parameters of
accelerating voltage, and also by sizes/dimensions of the useful
region, in which occurs the accumulation and particle acceleration.
In connection with this let us examine beam shaping only in the
mode/conditions of accumulation (capture during the first stage of
injection) and in the initial stage of acceleration
(inclusion/connection of HF accelerating voltage and capture into the
acceleration). For the particles, injected for a period of time from
t to $t+dt$, condition for acceptance during the first stage takes the
form:

$$\rho(\vartheta) \le \min \begin{cases} s(\vartheta) + u + \dfrac{\vartheta}{2\pi} \Delta R, \\[2mm] 2u_1 - u - \dfrac{\vartheta}{2\pi} \Delta R, \end{cases} \qquad (2)$$

where $0 < \vartheta < 2\pi K, k = 1,2,\ldots;$ u_1 - half-dimension of operating region; ΔR
- compression of instantaneous orbit per revolution (miss); $s(\vartheta)$ is
considered collision either with inflector (s=0) or with the internal
wall of chamber/camera (s=s_1) or with target (s=3_2); $\rho(\theta)$ - solution

of the differential equation of the betatron oscillations of the
injected particles in the system, connected with the instantaneous
orbit, which is located at a distance of u from the internal plate of
inflector. For the particles with the initial conditions $\rho_0 = g+u$,
where g - distance from the internal plate of inflector to the
particle, and for the case of the linear equation of betatron
oscillations taking into account the distortions of the closed orbit
expression for the boundaries of the region of the initial parameters
of the injected beam, which satisfy inequality (2), will be written:

$$g(\vartheta) = \frac{1}{\cos\sqrt{1-n}\,\vartheta}\left\{\left[\sum_i \frac{1}{(1-n)}\frac{\delta_i}{(1-n)-i^2} - \frac{\gamma R}{\sqrt{1-n}}\right] \times \right.$$
$$\times \sin\sqrt{1-n}\,\vartheta - \sum_i \frac{1}{(1-n)-i^2} \times$$
$$\left. \times(\delta_i \sin i\vartheta + a_i \cos i\vartheta) + \alpha\right\} - u - \sum_i \frac{a_i}{(1-n)-i^2},$$

where α - the right side of inequality (2); a_i, δ_i - coefficients of
the harmonics of the distorted orbit; γ - angle of injection.

Let us introduce the designation of the minimum region between
the plates of inflector, from which is feasible the capture during
the first stage of the injection:

$$g_1(u,\gamma) \geq 0, \quad g_2(u,\gamma) \leq g_0, \qquad (4)$$

where g_0 - distance between the plates of inflector.

Then during the even distribution of the injected particles

according to u and τ particle charge, seized during the first stage of injection, can be determined from the expression:

$$Q_1 = \frac{Q_0}{g_1 u_1 (\tau_2 - \tau_1)} \int_{\tau_1}^{\tau_2} \int_0^{u_1} \int_{g_2(u,\tau)}^{g_1(u,\tau)} dg\, du\, d\tau,$$

(5)

where Q_0 - the net charge of the injected particles into the chamber/camera; $(\tau_2 - \tau_1)$ - angular scatter of beam.

From (2)-(4) it follows that Q_1 is the function of the currents of the corrections of orbit $(a_i, \delta_i), n, \Delta R$, of moments/torques of injection (τ_i) and the inclusion/connection of HP field (τ_v), since the range of integration for u is linearly connected with τ_i and τ_v.

The charge, seized into the acceleration taking into account two stages of injection, can be presented in the form [1]:

$$Q_2 = \frac{Q_0}{g_0 u_1 y_{0max} (\tau_2 - \tau_1) y_1} \frac{\varphi_{u\tau} - \varphi_{01}}{2\pi} \times$$

(6)

$$\times \int_{\tau_1}^{\tau_2} \int_{y_{01}}^{y_{02}} \int_{|y_0|}^{min} \left\{ \begin{matrix} y_1 \\ u_1 - (-y_0 \geq 0) \end{matrix} \right\} \int_{(-y_0 \geq 0)}^{u_1 - y} \frac{y}{\sqrt{y - y_0}} \times$$

$$\times \int_{g_2(u,\tau)}^{g_1(u,\tau)} dg\, du\, dy\, dy_0\, d\tau ,$$

where $(\varphi_{0\tau} - \varphi_{01})$ - azimuthal size/dimension of separatrix; y_1 - radial size/dimension of separatrix; $y_{0max} = \frac{R}{\rho^2(1-n)} \frac{\Delta E_{max}}{E_{max}}$, ΔE_{max} - energy scatter of beam.
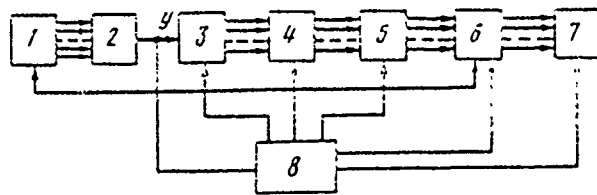
Fig. 1. Diagram of experimentation on the accelerator. 1 - control of accelerator; 2 - accelerator; 3 - experimental installation; 4 - detectors; 5 - accumulator/storage; 6 - processing; 7 - output of results; 8 - control of experiment.
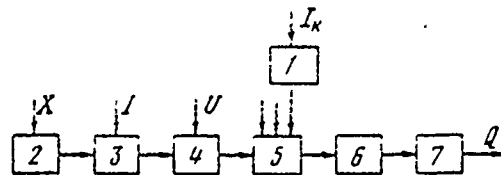
Fig. 2. Block diagram of synchrotron 1 - correction of magnetic field; 2 - injection; 3 - injection channel; 4 - inflector; 5 - 1st injection stage; 6 - 2nd injection stage; 7 - acceleration stage.

Page 260.

The order of integration in (5) can be decreased, if to utilize a property of the piecewise linearity of function $q(u,\tau)$.

Fig. 3 depicts dependence $\eta(\tau=0)=Q_1/Q_0$ on n and ΔR. Fig. 4 shows capture region (4), also, in Fig. 5 admittance of synchrotron for different moments of time. Calculation according to formula (5) showed that for the beam with the angular scatter the character of extrema was expressed not so/such not sharply.

As first approximation $q(u,\tau)$ it was approximated by plane, which made it possible to obtain from expression (6) the mathematical model of capture $J=J(x_1,x_2,x_3,x_4,x_5)$, where $x_1 \sim \tau_i$, $x_2 \sim \tau_v$, $x_3 \sim \Delta E$, $x_4 \sim \Delta w_0$, $x_5 \sim \Delta \rho$, Δw_0

- drift of the initial frequency of the accelerating HF field; $\Delta\rho$ - loss of operating region due to orbit distortion. During this function was conducted the investigation of the algorithms of the search of extremum.

Were compared two search circuits of maximum $J(x), x=(x_1,...x_s)$ - fastest descent [2] and random search [3]. In the diagram of the fastest descent were used three methods of calculating the gradient motion: the simple gradient, calculated as usual, by the method of difference quotient $J(x)$ to the interval of variations δ_k of certain variable/alternating x_k, statistical gradient and integral gradient whose calculation formulas take the form:

$$\delta_k \approx \delta_k^m = \delta_k^0 + \delta_k^{m-1} - \frac{1}{\tau_k}\left(\frac{1}{N_{2k}}\sum_{s} y_s^{m-1} - \frac{1}{N_{1k}}\sum_{\tau} y_\tau^{m-1}\right),$$
$$\delta_k^0 = \frac{1}{\tau_k}\left(\frac{1}{N_{2k}}\sum_{s} J_s - \frac{1}{N_{1k}}\sum_{\tau} J_\tau\right), \quad (7)$$

where $m = 1,2,...$; δ_k - component of the vector of gradient; δ_k^m - its approximation/approach, which is obtained on the m-th iteration; $\tau_k = (\beta_k - \alpha_k)\frac{t}{t+1}, t=1, (\alpha_k,\beta_k)$ - interval, in which were observed signs x^j of vector x and corresponding to them values $J_j = J(x^j); Y_j^m = \sum_{k=1}^{K} \delta_k^m x_k^j$.

Index τ marked N_{1k} the values of functions $T(x)$, k-variable/alternating of which will hit interval $(\alpha_k, \alpha_k + \delta_k)$, by index s N_{2k} of values $T(x)$, which have $x_k \in (\beta_k - \delta_k, \beta_k)$, where $\delta_k = \frac{\beta_k - \alpha_k}{j+1}, N_{1k} + N_{2k} = N$ to

a total number of observations $T(x)$. With $t \geqslant 10$ the components of gradient direction, calculated according to these formulas, are estimated with the error, smallest in the sense of linear orthogonal planning/gliding [4].

The algorithms of search were compared on model $T(x)$ under conditions of the interferences which were superimposed both on the entrance and on the output. As the interference was assigned the normally distributed random variable whose level was varied from zero to the values, 3 times which exceed value of $T(x)$ in the modulus/module.

As a result of experiments it was explained that the hypersurfaces of the level of model take the "ravine" form. Essential variable/alternating, search on which is especially hindered/hampered, they are: x_1 — change in the moment/torque of injection; x_2 — change in the moment/torque of including of the HF field; x_3 — drift of energy of injection.

As a result of this form of the function $T(x)$ most effective proved to be the method of random search. The accumulating interferences only increased interruption/discontinuity in the effectiveness between the method of the random search and the method of steepest descent. In this case even refinement of the components

of the vector - gradient according to formulas (7) did not lead to the substantial improvement in the diagram of the fastest descent. Thus, during 200 observations T(x) method of steepest descent gave 4.5 times the smaller value of intensity, and recommended as to optimum point was located 10 times further from the true point of maximum, rather than corresponding data of the method of the random search. In this case on the entrance was superimposed the interference with the dispersion, equal to 0.01, which at initial point composed approximately/exemplarily 1/3 from the value of entrances, and in the final stage of search 2-3 times it exceeded the values of entrances.
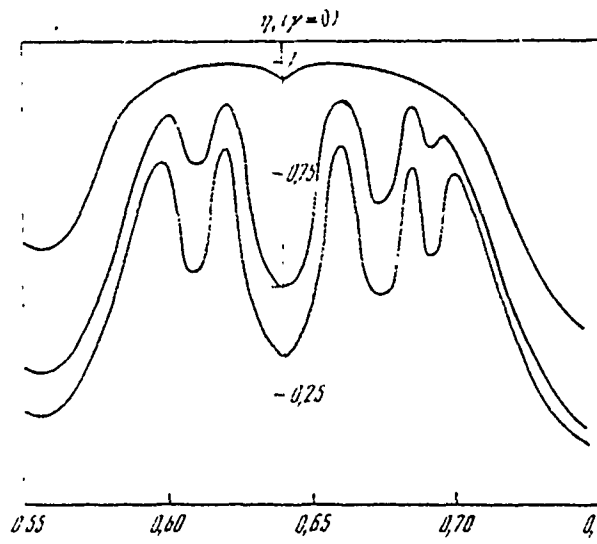
Fig. 3.   Fig. 4.
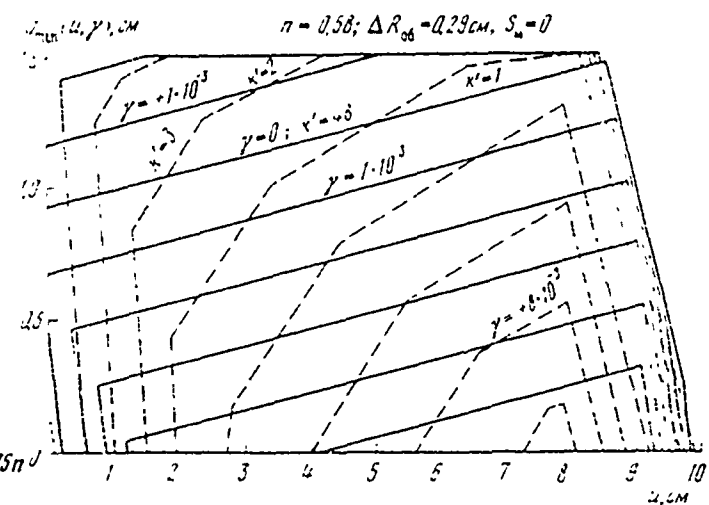
Fig. 3. Dependence of coefficient of capture on field index.

Fig. 4. Dependence of capture region on time of injection.

Fig. 5. Admittance of synchrotron.

DOC = 30069320   PAGE /1098
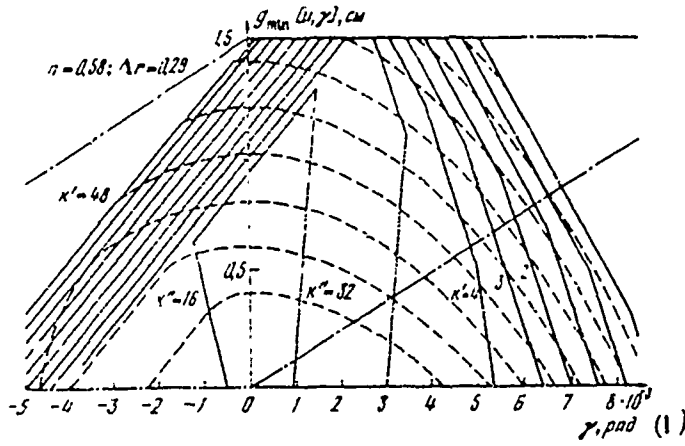
Key: (1). rad.

REFERENCES.

1. V. V. Tsygankov. Mathematical model of the capture of particles in a synchrotron. Izv. Tomskogo Politekhn. In-ta [News of the Tomsk polytechnical institute], 156, Izd. of Tomsk State University, 1969.

2. B. T. Polyak. Methods of the minimization of functions of many variables. Ekonomika i Matemat. Metody [Economics and mathematical methods], 1967, III, Issue 6, 881-902.

3. L. A. Rastrigin. Sluchynyy Poisk [Ramdom search], Riga, Izd-vo "Zinatne", 1965.

4. V. V. Nalimov. N. A. Chernova. Statisticheskiye Metody Planirovaniy Ekstremal'nykh Eksperimentov [Statistical methods of the planning of extremal instruments] Moscow, Izd-vo Nauka, 1965.

Page 261.

174. Measurement of the emittance of beam with the aid of the computers "Dnepr".

G. P. Ivanova, V. V. Kurasov.

(Radio engineering institute of the AS USSR).

For the realization of the optimum mode/conditions of the injection of beam into the chamber/camera of the model of cybernetic accelerator to the energy 1 GeV it is proposed to produce wiring the bundle through ion guide and agreement of the phase volume of the injected beam with the acceptance of accelerator automatically with the aid of computers "Dnepr". The process of optimization is broken into two stages. First computer measures the parameters of beam at output from the injector and according to them calculates the nominal rating of the work of the focusing and corrective elements/cells of the channel of transportation, and then from the information about the value of betatron oscillations and about the position of orbit in

accelerator chamber optimizes the calculated mode/conditions. As the
first stage of these works was realized the automatic measurement of
the emittance of beam at output of injector with the aid of the
computers "Dnepr". For measuring the emittance is utilized the method
of two slots [1]. By the first slot is cut out the part of the beam,
which corresponds to the specific value of Cartesian coordinate, and
then with the aid of the second slot, parallel to the first, and
induction current-sensing device is measured the width of the cut out
part of the beam and density distribution of current. Knowing the
distance between the slots, it is possible to determine the angular
separation of beam. The block diagram of system for the automatic
measurement of emittance is depicted in Fig. 1. Horizontal 1.3 and
vertical slots 2.4 have a width 2, 1.5, 1.5 and 1 mm respectively.
Control of the displacement/movement of slots is
accomplished/realized with the aid of devices/equipment 9-12. With
the displacement/movement of slot on 0.1 mm these devices/equipment
develop the impulse/momentum/pulse, which enters the analog input of
USO. By means of the counting of these pulses of computers it
determines they conducted to the rank of the displacement/movement of
slot. Selection and inclusion/connection of slot for the motion with
the specific step in any direction are conducted on the commands with
the aid of the induction current-sensing devices 5 and 6. The range
of the measurement of current from 1 μA to 5 mA is divided into 3
sub-ranges. The selection of necessary sub-range and the connection

of current-sensing device are conducted with the aid of decoder 8,
controlled by commands with the computers through the unit R, and
also with the aid of diagram 7, controlled through the unit A. With
the equality beam current to reference signal diagram 7 develops the
impulse/momentum/pulse, which enters the channel of the system of
interruption SP. 13 - decoder tor including one of four slots; UVM -
control computer "Dnepr"; AU UU - arithmetic unit and control unit;
PZU - passive memory unit; OZU - core storage.
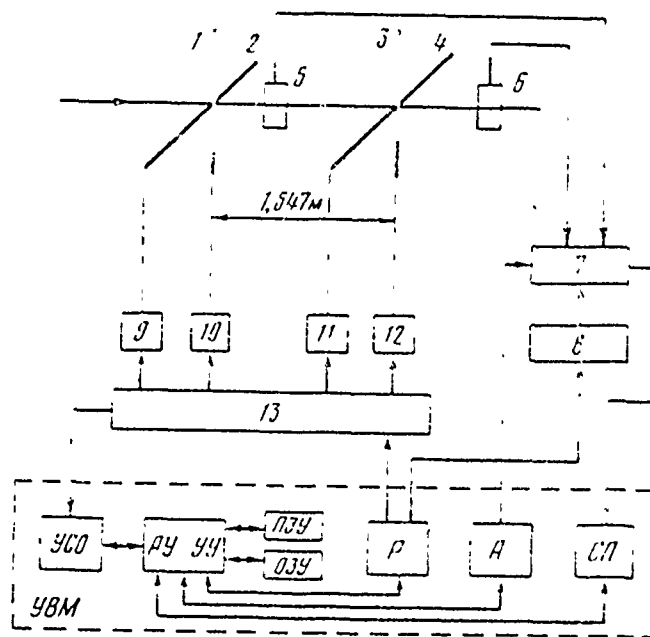
Fig. 1. System block diagram for measuring the emittance.

Page 262.

The algorithm of the measurement of emittance consists of two parts. First part - algorithm of the determination of boundaries of beam (Fig. 2). This algorithm is auxiliary for the algorithm of the direct measurement of emittance (Fig. 3) and makes it possible to determine interval and boundaries of the movement of slots in the process of measurement. The preliminary determination of beam boundaries considerably shortens the time of the measurement of emittance. Entire algorithm is constructed so that the work in the basic building blocks of program occurs in the interval between two adjacent impulses/momenta/pulses of the movement of slot, and results

are printed in parallel with the measurement. The current of the cut
cut part of the beam is measured only in that part of the
chamber/camera where there is a beam.

The request of current-sensing devices is synchronized with the
impulses/momenta/pulses of injector, and the results of measurement
are averaged. This allowed to bring the lower limit of measurement to
1 μA, and thereby to raise the accuracy of the measurement of
emittance.

At present the results of measurements are derived/concluded to
the press/printing in the form, convenient for graphing. Fig. 4 shows
the phase portraits of beam at output of injector in the horizontal
(X, X^1) and the vertical (Y, Y^1) phase planes, obtained with the aid
of the computers "Dnepr". Coordinates count off relative to center
the chambers/cameras of ion guide. The lines of the identical
current, measured in μA, show density distribution of particles on
the phase plane. As can be seen from figure, in the measurement plane
the center of beam has small coordinate and angular displacement
relative to the axis/axle of the chamber/camera of ion guide,
furthermore, beam has large angular separation in the vertical plane.

At present is conducted work on automatic processing of the
results of measurement and calculating the nominal rating of the work
of the channel of transportation.
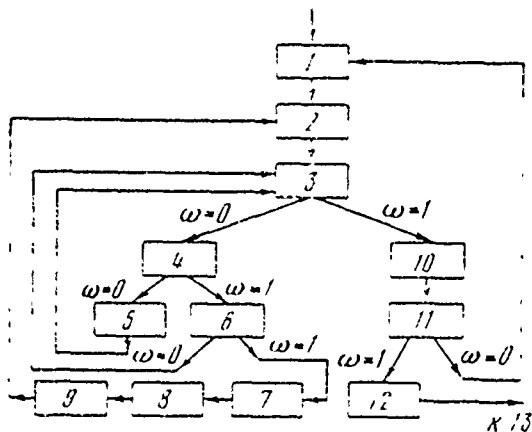
Fig. 2. Block diagram or the algorithm of the determination of beam boundaries. 1 - selection of the number of slot and dispatching of initial data; 2 - disconnection of slot: 3 - subroutine for recording the position of slot; 4 - subroutine for the determination of the presence of beam; 5 - determination of the moment/torque of the disappearance of beam: 6 - determination of the onset of a beam; 7, 10 - disconnection of slot; 8 - subroutine for the measurement of beam current; 9 - press/printing the value of current at the control point, vernier of control point and the dispatching of the vernier of control point for the storage into the memory; 11 - press/printing beam boundaries, analysis the number of the moved slot; 12 - determination of the interval of the movement of slots.
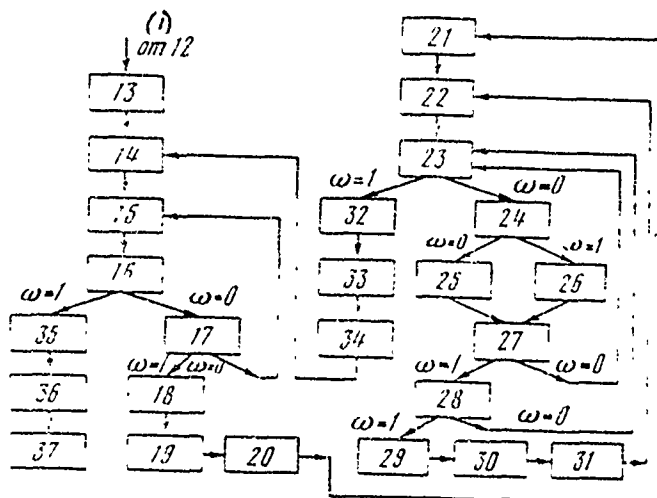
Fig. 3. The block diagram of the algorithm of the measurement of the emittance: 13 - dispatching of initial data into the working cells · OZU; 14 - start of current-sensing device 5 (Fig. 1); 15 - inclusion/connection of the slot, which is determining coordinate; 16, 23 - subroutine for recording the position of slot; 17 - measurement at the control points, press/printing of the result of measurement, analysis of the displacement/movement of slot; 18, 29, 32, 35 - disconnection of slot; 19 - disconnection of current-sensing device 5 (Fig. 1); 20 - press/printing the vernier of the position of the slot: (Fig. 1); 21 - start of current-sensing device 6 (Fig. 1); 22 - inclusion/connection of the slot, which is determining angle; 24 - subroutine for the determination of the presence of beam; 25 - determination of the mcrent/torque of the disappearance of beam; 26 - determination of the onset of a beam; 27 - analysis of the step/pitch of the displacement/movement of slot; 28 - checking the presence of

beam; 30 - subroutine for the measurement of beam current; 31 -
determination of angle; 33 - disconnection of current-sensing device
6 (Fig. 1); 34 - press/printing results and preparation for the next
cycle of measurements; 36 - press/printing the sign/criterion of the
termination of the measurement of emittance; 37 - stop of program.

Key: (1). from.
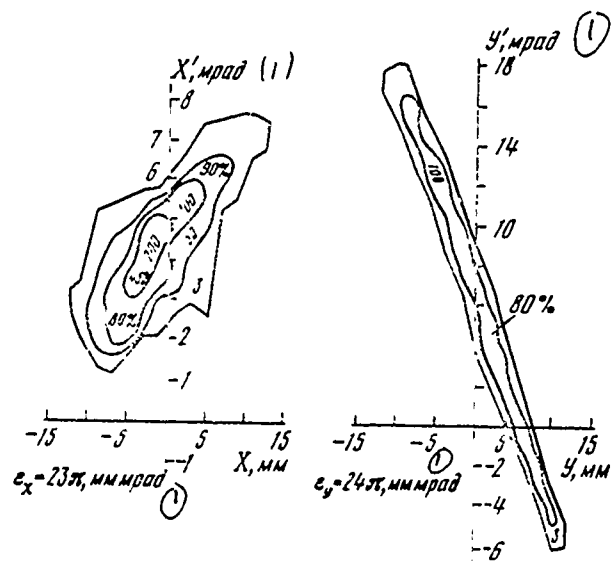
Fig. 4. Results of measuring the emittance of beam at output of the injector of the model of cybernetic accelerator to the energy 1 GeV.

Key: (1). mrad.

REFERENCES.

1. A. van Steenbergen. Nuclear Instr. and Methods, 1967, 51, 2

Page 263.

175. New systems of radio electronics and control of proton synchrotron IFVE.

A. A. Vasil'yev, F. A. Vodop'yanov, O. S. Gorchakov, A. M. Grishin, A. I. Dzergach, Yu. F. Dushin, V. V. Yelyan, Yu. S. Ivanov, N. K. Kaminskiy, A. A. Kuz'min, G. F. Senatorov.

(Radio engineering institute of the AS USSR).

K. F. Gertsev, Ye. S. Nelipovich, V. V. Osip, P. T. Pashkov, V. Ye. Pisarevsky, I. I. Sulygin, B. K. Shembel', K. A. Yakovlev.

(Institute of high-energy physics).

V. P. Gerasim, O. A. Gusev, V. A. Titus, V. G. Tsvetkov.

(Scientific research institute of the electrophysical equipment im. D. V. YEfremov).

An increase in the intensity of proton synchrotron by the energy 70 GeV to 5.10^{13} by method of the introduction of booster [1]

requires the development of the new systems of radio electronics,
control and monitoring of the beams of basic synchrotron and booster,
and also development of equipment for the translation/conversion of
particles from the booster into the basic synchrotron.

In the present report are given the results of the preliminary
development of the systems indicated.

In the project of an increase in intensity [1] is used "rapid"
booster. This fact together with others causes the series/row of
essential differences in the described systems from the systems of
radio electronics of the proton synchrotron of CERN,
developed/processed in connection with an increase in its intensity
[2].

Accelerating stations of basic synchrotron.

Acceleration at the enhanced intensity provide those existing of
54 accelerating cavities under the condition of increasing the power
of the final stages from 5 to ~15 kW. Such cascades/stages can be
constructed on the lamps GU-36B1. The cascades/stages of preliminary
amplification it is expedient to remove beyond the limits of the
tunnel of accelerator. For reducing the power of the signal of the
excitation of the final stages is developed the reconstructed in the

range of frequencies step-up transformer, connected between the grid
of output tube and the cable.

Remaining equipment for the system of the generation of
accelerating field of basic synchrotron is not changed, since is
provided for the possibility of work also with the old injector to
the energy 100 MeV.

System of radio electronics or booster.

Fig. 1 depicts a temporary/time change in accelerating voltage
of booster V_y of synchronous phase φ_s, frequency of revolution of
particles f and rate of its increase $\dot{s}$. For the particle acceleration
are applied 10 accelerating stations two of which stand-by.

Special feature/peculiarity of acceleration mode of booster -
low level of its accelerating voltage in the beginning and end/lead
of acceleration ($\frac{V_{ymax}}{V_{ymin}} \approx 45$) and the respectively small supply of
reactive energy in the resonators in comparison with the energy,
selected/taken by beam. Under these conditions stresses by beam -
insertion reactance and induced voltage - become extremely large. In
order to ensure allowances for the parameters of accelerating field,
it is necessary to take measures for weakening of these effects: to
introduce negative feedback in the high frequency in the system of

the excitation of accelerating voltage or controlled symmetrical

misphasing of resonators with the appropriate increase in the

amplitude of their minimum voltage 10-15 times.
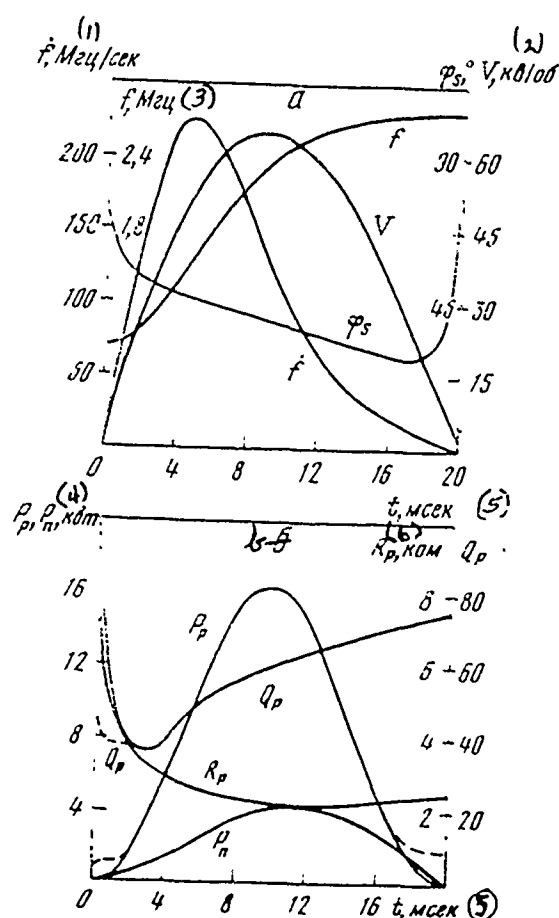
Fig. 1. Change in the time of the basic parameters of booster.

Key: (1). MHz/s. (2). kV/rev. (3). MHz. (4). kW. (5). ms. (6). kiloohm.

Page 264.

For weakening of requirements for the control systems of the

parameters of accelerating field it is expedient to introduce into the systems the program signals, which depend on the intensity of beam. The accelerating device/equipment is intended to fulfill in the form of two coaxial cavities which work in the antiphase on the general/common/total clearance and are reconstructed in the frequency by the magnetic biasing of ferrite. During the use of ferrite of the type 300 NNA, the lengths of resonator ~1.1 m its capacity/capacitance, in reference to the clearance, is 1850 pF.

The expected temporary/time change in the parameters of this resonator: quality Q, shunt resistance R_p, the power of losses P_b and power P_n, selected/taken by beam of particles, it is shown in Fig. 1b. Dotted lines show the course of the corresponding curved with the dephased supply resonators in the beginning and end/lead of the acceleration.

The system block diagram of the generation of accelerating field is depicted in Fig. 2. The voltage of induction coil 1 is integrated by integrator 2, which modulates the frequency of master oscillator 3, in composition of which is contained nonlinear function generator. In polyphase amplifier-distributor 4 is contained the phase smasher, which ensures phase displacement of voltages in 10 channels on 22.5°. Wideband amplifiers 6 and final stages 7 excite resonators 8. The programmer of amplitude 5 develops control voltage for changing the

amplitude of accelerating field.

The system of the correction of frequency on the beam contains pick-up-electrode 9, input unit 10, converter 11, summator of accelerating voltages 12, amplitude detector 13, programmed phase inverter 14, phase discriminator 15 and summing amplifier 16. It is similar to the analogous system of basic synchrotron 3. Supplementary block-programmed phase inverter 14 is introduced because of the need of changing the equilibrium phase in accordance with a change in the rate of the build-up/growth of magnetic field and amplitude of accelerating field (Fig. 1).

Control system by booster.

It is assumed that all technical functional systems of booster (16 systems) will be united under the single information-control diagram into which will enter terminal devices with the local panels (terminals), the line of communications, the central assembly of signals, small computer and central control panel. The total number of informational points on the booster (one informational point gives two bytes of information), according to the roughest estimates, order 2000. Number of information words (2 bytes), which enter each cycle, on the order of 200. A number of control signals will not exceed 1000. All control signals (changes in the settings of different

programmers) will be put out during the nonoperative section of
cycle. The synchronization of the work of computers and all systems
of accelerator will be accomplished/realized through synchronizing
circuit, entering the diagram of control.

Each terminal, as a rule, will service/maintain one functional
system. It must contain the signal-data converters of different form
into the code (analog, states, time), the commutators, encompass the
units of temporary/time selection, the small buffer storage (32-64
bytes) and the devices/equipment, which make it possible to produce
manual control and collection of information, passing computers.

Entire technological equipment for systems must have the
actuating elements, controlled by the binary code (analog code,
code-shaft, code-state).

The operating speed of computers is not less than 20 thousand
operations/s, the memory is not less 8K words, external ZU on NML or
disk. Provision is made for connection/communication of this computer
with the computers of higher level. Central control desk must contain
display to CRT, controlled by computers, the device/equipment of the
independent representation, the unit of the call of routines and the
devices/equipment, which make it possible to request information and
to transfer control signals with the adjustment and the breakdown of

computers.

The final goal of automation - increase in the reliability of the accelerating complex and improvement in the parameters of the accelerated beam (increase in intensity and stability of the parameters of beam). As the final result as a result of the consecutive development of automatic complex it is proposed to carry out the necessary cybernetization (in the plan/layout, developed with the work of the Radio Engineering Institute of the AS USSR [4] and with other accelerative centers [5]) accelerative complex.
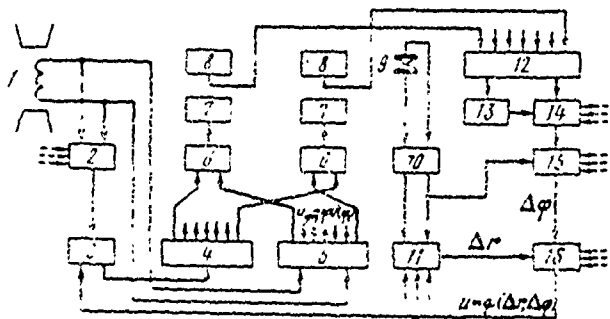
Fig. 2. Block diagram of equipment for generation and regulating of the amplitude of accelerating field with the control system for beam.

Dotted lines showed control signals.

Timing mechanism of the translation/conversion of beam from the booster into the basic synchrotron.

As a result of the analysis of the described earlier systems of this kind [6-8] and study of possible versions for further studying are selected two of them. In the first version due to the appropriate selection of the length of booster the frequency of revolution of its clusters at the moment/torque when particle momentum reaches the prescribed/assigned value, it differs on Δf relative to frequency $\frac{1}{2}qf_{oc}$, where q - harmonic order (30), f_{oc} - frequency of revolution of particles in the basic synchrotron.

At the moment of passage Δf through the rating value the
particle momentum differs from the given one not more than by 5.10⁻⁴.
Necessary phase displacement between the clusters and accelerating
voltage of the basic synchrotron, to which cables itself the
operation/process of translation/conversion, it is determined by the
moment/torque when voltage with frequency Δf passes for the first
time through zero after the moment/torque of the comparison of
impulses/momenta/pulses.

Page 265.

In the second version the master oscillator of booster with the
aid of the phase discriminator is seized in the frequency by
accelerating voltage of basic synchrotron with the difference in the
frequencies Δf, which does not call the disturbance/breakdown of
acceleration mode with the cutoff/disconnection of control for beam.
At this moment the amplitude of accelerating voltage is raised to
maximally possible in order to reduce to the minimum the time during
which phase displacement between the clusters of booster and
accelerating voltage of the basic synchrotron reaches the
prescribed/assigned value, with which is accomplished/realized the
matched translation/conversion of particles.

In both versions is possible the filling of separatrices with

bunches of booster in the prescribed/assigned sequence.

Monitoring beams in booster and circuits of translation/conversion.

Monitoring system, intended for the indication of the basic
parameters of beam (position, energy, intensity, profile/airfoil,
emittance, scatter along the impulse/momentum/pulse), and also
distribution of losses in the sections from the preinjector to the
point of introduction/input into main accelerator, is calculated for
the operating range of intensity $5.10^{10}-5.10^{12}$.

Besides the usual screens and the induction sensors the system
contains combined type electrostatic pickups for the simultaneous
measurement of shift d two planes (x and z), placed on the ring of
booster in the aperture of correcting lenses, and also ionizing
profilometers, placed in the circuits of translation/conversion also
on the ring of booster. The continuous measurement of
impulse/momentum/pulse at the output of linear accelerator proposes
to use phase-transit method. For the indication of the losses of
intensity and their localization is provided for the system of
monitors. The information, put out by monitoring system, is converted
to the form, convenient for the automatic collection and the
processing with the aid of computers.

Profilometer.

Profilometer, adjusted on the ring of main accelerator, ionizing type with independent obtaining of two orthogonal projections of distribution of charge in cross section [9]. The extraction of ionic image is accomplished/realized with the aid of the parallel electrical and magnetic fields, which ensure obtaining resolution 1 mm under conditions of the high intensity of beam [10]. Conversion of image into the visible and its transmission to the hall of control with the aid of the luminescent screens and the television equipment of the type PTU 101 (on one to each projection). The time of scanning of image - about 50 μs, makes it possible to observe the image, averaged on several revolutions.

REFERENCES.

1. Yu. M. Ado et al.   Increase in intens... .. the proton synchrotron
to energy of 70 GeV by means of increasin.. the injection energy.
Doklad, predstavlennyy na II vsesoyuznoy- -ovesnaniye po uskoritelyam
earyazhennykh chastits [Report presented to the II all-union
conference on accelerators of charged pa...cles], (Moscow, September,
1970).

2. U. Biliani et al.   Calculation of the intensity of a beam in
the design of a booster of the protron synchrotron.   Doklad
na VII mezhd, konf. po uskoritelyam zary..heennykh chastits
vysokikh energiy [Report to the VII inte...tional conference on
accelerators of charged particles of high energies], Yerevan, 1969.

3. F. A. Vodop'yanov et al.   Trudy Mezhd. konf. po uskoritelyam,
[Transactions of the international confe..nce on accelerators],
Dubna, 21-27 August, 1963, 932, 1964.

4. A. L. Mints et al.   Modern state of the development of the
proton synchrotron to 1000 GeV.   Doklad .. VII Mezhd. konf. po
uskoritelyam zaryazhennykh chastits vysokikh energiy [Report to
the VII internal conference on accelerators of charged particles
of high energies], Yerevan, 1969.

5. Computer in control. CERN Courier, 13.9, 9, p. 21.

6. L. Hesegotti, W. Schnell. Synchronization between a 300 GeV
Synchrotron and its Booster Injector, CERN 64-20 Accelerator
Research Division, April 23, 1964.

7. 200 BeV Accelerator Design Study. Lawrence Radiation Lav. Univ.
California, June 1965.

8. Protron synchrotron - injector (booster).   Edited by F. A.
Vodop'yanov.   Nauchnyye trudy rediotekhnicheskogo instituta AN SSSR.
[Scientific transactions of the Radio Engineering Institute of the
AS of USSR], Moscow, n.t., 9267-148, 1967, p. 167.

9. F. Hornstra and W.H. DeLuca, Proc. 6th Intern. Conference on
High Energy Accelerators, Cambridge, Mass., 1967, p. 374.

10. V. V. Yelyan. The effect of a space charge on the efficiency
of the ionization method of measurement of the ion beam in
accelerators.   Doklad, predstavlennyy na II vsesoyuznoye soveshaniye
po uskoritelyam zaryazhennykh chastits [Report presented to the
II all-union conference on accelerators of charged particles],
(Moscow, September, 1970).

Page 266.

FINAL WORD.

Chairman of organization committee academician A. L. Mints.

Respected comrades, associates, ladies and gentlemen !

Before coverage of the II All-Union conference on charged particla accelerators and oefore saying good-bye to you, solve to me to say several words in order to total of the work, done by conference.

Took place 12 sessicns of the plenum of the conferences, at which were made 110 repcrts. Furthermore, for the detailed discussion of most urgent/most actual tnemes were carried out seven seminars.

Began we the work of conference, in accordance with the steady tradition, from the pcsing of the question, that expect the theoretical physicists from the experiments, conducted on the charged particle accelerators, A very meaningful and interesting report on this question made Dr. A. A. Komar at the first session.

On the classical accelerators with the fixed target and the prospects for the creation of cybernetic proton synchrotrons to the energy into hundred and thousands of GeV reported Dr. A. A. Vasil'yev on behalf of the colleagues of the radio engineering institute of the AS USSR.

Should be especially noted extremely interesting and full/total/complete report of professor R. Nile from Stanford, who expanded/developed the picture of the state of works on SLAK and outlined path of his mcdernization, and also about experiment of the use/application of cryogenics to the linear electron accelerators.

Large interest called the report to Dr. Yu. M. Ado and his colleagues about the work of proton synchrotron to 76 GeV, established/installed near Serpukhov. This greatest in the world accelerator, because of the timely and careful preparation for experiments, made possible of obtaining the substantially new results. Moreover, and the coefficient of the use of time for the physical experiments proved to be very high, it which indicates the large reliability of this accelerator as a whole and of the numerous systems, entering it.

Me it was especially desirable to note that in addition to the Lenin prize, sentenced during April 1970 for the bases of the

development of this accelerator, several days ago our government
noted by two state prizes the creation of the largest in the world
proton linear accelerator - injector on 100 MeV at intensity 120 mA
in the impulse/momentum/pulse and the creation of the injector
complex of accelerator - its electromagnet with system of supply,
vacuum system, system of radio electronics, general/common/total
project and construction. Since the majority of the laureates of
these premiums are located in this hall, I would want on behalf of
our conference to warmly congratulate them with the high
acknowledgement of their merits.

Due to disease of academician Budker interesting report about
experiments in electronic cooling read his colleague R. A. Salimov.

On some possibilities of accelerating the protons in the
isochronal cyclotron reported L. A. Sarkisyan.

The second session of conference (chairman of the corresponding
member of the AS USSR A. A. Naumov) was dedicated to the
survey/coverage of the state of the accelerators of different types,
to the designs of new ones and reconstruction of the acting
installations.

To the electronic circular accelerator "DEZ1" in Hamburg (FRG)

dedicated his communication/report Dr. G. Kumpfert.

On the project of continuous microtron on behalf of the developers of this project reported Dr. V. A. Slobodyanyuk. This microtron, which gives the accelerated electrons with the energy 12 MeV and beam current 1-2 mA is very simple on the device/equipment and it will be very useful for studying the structure of atomic nucleus and for the investigations in radiation physics.

Dr. E. A. Myaye on behalf of the colleagues of the number of institutes made a report about the methods and the project of an increase in the intensity of the beams of particles of the Serpukhov proton synchrotron due to an increase in the energy of injection and use/application of an intermediate booster accelerator. At the special seminar under the management/manual by the corresponding member of the AS USSR A. A. Naumova were examined different aspects of the development of booster for these purposes. The series/row of interesting considerations on this question was expressed by professor R. Martin (USA) et al.

To the state of works on the linear electron accelerator to Sakle (France) dedicated his meaningful report professor P. Netter. Accelerator in Sakle relates to the class of the high-current accelerators of electrons and is characterized by the high parameters

for conducting the precision experiments.

G. S. Kazanskiy in his communication/report threw light on some questions, connected with the translation/conversion of Dubna proton synchrophasotron into the acceleration of deuterons.

The third session (leader Prof. Ye. G. Komar) was dedicated to direct voltage accelerators, to ionic and electronic sources. In the reports of M. A. Abroyan, B. P. Ad'yasevich, V. P. Yakushev and A. N. Serbinov, Ye. A. Abramyan and S. B. Wasserman et al. were examined questions of obtaining intense ion beams, obtaining of the polarized ions, modes/conditions of high-voltage discharge tubes, and also study of intense electron beams. On these reports at the conference was expanded/developed the lively discussion.

The fourth session (leader Dr. N. A. Monoszon) dedicated its work to questions of the development of the electromagnets of accelerators, systems of their supply and magnetic measurements.

Considerable interest generated the reports of professor N. A. Monoszon, I. P. Karabekov, Yu. R. Nazryadn, V. S. Panasyuk, B. A. Baklakov. The communication/report of N. I. Doynikov and A. S. Simakov was devoted to the mathematical simulation of three-dimensional magnetostatic fields.

The fifth session (chairman Dr. V. P. Sarantsev) was dedicated to one of the most fashicnable questions of accelerative science - to collective methods of acceleration. Proposed by academician V. I. Wexler and continued by Dr. V. P. Sarantsev method of the acceleration of the electronic ring-carriers of protons during the last few years became the coject of close attention and study not only in the USSR, where was proposed this method, but also in the laboratories of USA and Western Europe.

Page 267.

V. P. Sarantsev made an interesting report "collective ion accelerator - the new instrument in physics of elementary particles", in which he described about its latter/last works.

A. A. Kolomenskiy and I. I. Logachev gave the basic conclusions of developed by them the theory of the acceleration of ions by the scanning of electron beam.

Very meaningful was the communication/report of Zh . Peterson (USA) about the program Lawrence laboratory (Berkeley) on the accelerators with the electron rings. This report generated large

interest and so, as very interesting report of Khaynts about the works in Karlsruhe was accompanied by the numerous illustrations which showed the essential advance of construction of both installations.

Some theoretical considerations about the synchrotron radiation in the accelerator of electron rings and about the resonances of connection/communication of transverse vibrations of two circular beams reported K. Pellegrini (Frascati), D. G. Koshkarev and P. R. Zenkevich.

Should be noted communications/reports to N. G. Anishchenko, N. S. Repalova, I. N. Ivanov, A. S. Bonch-Osmolovskiy and O. A. Val'dnera, connected with the thematics of the 5th session. However, in participants in the session remained a feeling of dissatisfaction, since exchange opinions was not to sufficiently complete ones. Therefore organization committee accepted proposition to continue discussion at the specially organized seminar which takes place on 13 November this year under V. P. Sarantsev's management/manual.

The sixth session (chairman of Prof. F. A. Vodop'yanov) was dedicated to the most important theme - the development of superconducting elements of accelerators.

The vast study program of Rutherford laboratory (England) on the creation of the elements/cells of the superconducting synchrotron was reported by N. D. Vest.

The analogous programs, which are conducted in France (Sakle), were reported by Dr. G. Bronk. Communication/report about the state of investigations in Karlsruhe (FRG) on the superconducting and cryogenic magnets for the synchrotron was conducted by Dr. V. Khaynts. In Karlsruhe were prepared small models of both types.

Very interesting report was conducted by Prof. R. L. Martin (USA) about superconducting high-energys accelerator. Is possible the achievement of intensities 10^{14}-10^{15} prot./pulse. In front is in pr pect extensive work, but in the case of the success which one ought not to doubt, views on the advisable construction/design and on the projects of high-energy accelerators will require serious review.

A series/row of Soviet authors (Yu. P. Batakov, N. I. Doynikov, A. I. Kostenko, L. I. Greben' and Ye. S. Mironov et al.) announc about their calculations and experiments, connected with the design of superconducting elements of electromagnets in stationary and pulsed magnetic fields taking into account the losses in them. Reports at the seventh session (chairman Prof. A. A. Kolomenskiy) and eighth sessions (chairman Dr. D. G. Koshkarev) were dedicated to

questions of particle dynamics in the accelerators, the
accumulators/storage and the installations with clashing beams. Here
should be noted the reports to V. V. Petrenko on behalf of the group
of the colleagues of FTI of AS UkSSR about the longitudinal
compression of clusters, V. A. Teplyakov about the system of the
quadrupole high-frequency focusing in the linear ion accelerators,
during the use by which it is possible to obtain acceleration and
strong focusing of ion beams in the linear accelerators of protons
without the use of the focusing magnetic fields. Are found the simple
forms of the electrodes, which ensure necessary field pattern in the
interaction region with the beam. Are dismantled/selected the types
of the resonators, most advantageous for this system of focusing.

To questions of the investigations of the longitudinal
instability of beam in the accumulator/storage was dedicated A. M.
Shenderovich's report.

E. A. Myaes et al. (IFVE) reported about the conducted
investigations on the passage of the region of parametric resonance
on the Serpukhov proton synchrotron.

To the studies of synchrotron motion in the presence of space
charge dedicated his communication/report K. Reich (CERN).

To calculations and measurements of connection/communication
between the synchrotron and betatron oscillations in the electronic
synchrotron dedicated very interesting communication/report N. S.
Krouli-Millin (England).

Considerable interest were of the reports of G. I. Dimov (USSR),
B. Tsotter (CERN), A. A. Kolomanskiy and A. P. Pateyev, A. I.
Dzergach, Ye. L. Kosarev, B. N. Sidel'nikov, Ya. S. Derbenev et al.

Especially should be noted the interesting report of M. K.
Barton and Ye. K. Rak (USA) about the instabilities in V. h. the
system of Brookhaven synchrotron, caused by beam load.

The series/row of reports (B. I. Bondaryev, V. V. Miller et al.)
was dedicated to the use/application of computers for study and
simulation of the depression of phase oscillations and to the
investigations of the alignment procedure of work of the accelerator.

To questions of particle dynamics it was devoted so many
reports, that it was necessary in accordance with the program of the
work of conference to hear them in two sessions.

IX session (chairman Dr. A. A. Kuz'min) was dedicated to
questions of radio electronics of accelerators and to measuring

systems of the parameters of beam.

Of the foreign reports it is necessary to note the large and very meaningful report ct K. D. Johnsen (CERN) about the methods of measuring the parameters of beam. Lecturer introduced participants in the conference to the very rich material, assembled in CERN within the time of the operation of 28 GeV accelerators of protons.

The series/row of the reports of the Soviet researchers (L. V. Reprintseva, O. A. Gusev, K. A. Sodoyan, V. V. Yelyan, V. A. Skuratov, A. N. Didenko and I. P. Karabekova et al.) was dedicated to general/common/total questions of radio electronics of accelerators, to measuring systems of the parameters of beam and to specially created measuring installations, realized on the Soviet electron accelerators, and protons.

On tenth session (chairman Cr. B. P. Murin) were heard the reports to A. V. Mishchcenko cn behalf of the colleagues of radio engineering institute about the project of linear accelerator on 38 MeV - injector of the future booster of Serpukhov proton synchrotron, Yu. A. Khlestkov and O. A. Val'dner about the selection of the accelerating system in the waveguide sections. The lively discussion and some observations caused the report of S. A. Heifetz (Yerevan) about the selection of the design of the parameters of the

accelerating system of the electron accelerator on 50-100 GeV.

Was of interest the communication/report of F. F. Ferger and V. Shnell (CERN) about V. h. to system for the rings with the intersecting beams. This report is especially important because the unique rings in CERN are found already in the starting/launching stage and obtained the first encouraging results.

Page 268.

V. M. Pirozhenko on behalf of the group of the colleagues of the radio engineering institute of the AS USSR announced about the new types of the accelerating structures, which are very adequate/approach for the largest proton linear accelerators, in particular, for meson-producings cyclotron.

V. M. Petrov reported about the HF system of ring VEPP-3 (Novosibirsk), while V. L. Stepanyuk on behalf of the group of the colleagues of J.I.N.R. described about the works on the creation of new debuncher of synchrophasotron J.I.N.R. with modulation of energy of the accelerated beam.

Finally, A. I. Kvasna, A. V. Mishchenko, B. P. Murin, B. I. Polyakov and Yu. S. Cherkashin reported about very successful

experiments on the compensation for decreases in accelerating field in linak-injector of Serpuknov synchrotron upon the acceleration of intense beams to 100 mA. The shown oscillograms convincingly testified about the successful solution of stated problem.

By questions about the targets, the transportation of beams, their input and output was occupied the eleventh session (chairman Prof. L. L. Gol'din).

To the conclusion/output of the proton beam of 1 GeV synchrotron of the physiotechnical institute of the AS USSR was devoted the communication/report of G. A. Riadov et al. Were dismantled/selected the methods of calculation of magnetic pipe, was described its construction/design. The effectiveness of conclusion/output achieved 25o/o with divergence of 0.1°.

V. I. Gridasov reported the principles of construction and the technical special features/peculiarities of the system of the rapid induction of the accelerated beam to internal targets, which is applied on the Serpukhov synchrotron.

G. V. Badalyan et al. the colleagues of Yerevan physical institute in its communication/report reported about the method of the slow conclusion/output of electron beam from the synchrotron

"ARUS". Were given the parameters of emitted beam at the duration of
trace 2.5 ms. The communication/report of Prof. Regenshtrayf
(France), made partially in the Russian language, was devoted to
phase-space acceptance of the doublet, comprised of the quadrupoles.
It was listened with the considerable attention, and for the Russian
part of the report to Prof. Rejenshtrayf it was rewarded with
applause of auditorium.

Yu. G. Basargin et al. reported the results of the calculations
of the longitudinal and transverse aberrations of the second order
for 2.4-meter isochronal cyclotron of IAE im. I. V. Kurchatov.

The communication/report of M. R. Harold (England) was devoted
to the methods of beam extraction from the accelerator of NIMROD, and
in the communication/report of Zh. For were given the conditions for
existence of beam during the resonance processes of his
conclusion/output from the synchrotron.

T. A. Vsevolozhskaya on behalf of the group of the colleagues
academician G. I. Budker gave the diagram of obtaining antiprotons on
the installation, intended for the clashing proton-antiproton beams
in Novosibirsk.

Finally, at the twelfth final session (chairman Dr. A. A.

Vasil'yev) were examined questions of control and direction of accelerators with the aid of computers. On the automation of Serpukhov accelerator announced A. A. Kuz'min, while about the automation of Kharkov of 2 GeV electronic linak - V. I. Kolosov. On the use/application of computers on the rings of CERN made very interesting communication/report P. Uol'stenkhol'm. On the automatic complex for the control of the model of cybernetic accelerator described Yu. S. Kuz'min.

The appearance of these and other reports on the thematics of the 12th session for the first time so representatively began to sound at our conference.

My final survey/coverage, of course, is incomplete and I please apology in the lecturers whose names I did not mention. This does not in any way mean that their reports are less important or uninteresting.

Summing up the results of our conference, I would want to note that it passed successfully and fruitfully. I do not undertake to confirm that the most valuable occurred in this large hall or seminar rooms. Frequently the most interesting conversations occurred at the tables of halls and lobbies of the house of scientists, and sometimes also during the journeys. In a word, the most valuable were the

scientific contacts between the scientists of different institutes
and different countries.

On behalf of gathering at the conference I would want to thank
the colleagues of technical committee, its translators and workers of
the house of scientists, whose modest work aided our work and made
its effective.

Large appreciation to all lecturers and participants in the
conference for their creative contribution.

Solve to wish to all to you to preserve the good memory about
this II All-Union conference on charged particle accelerators, about
our capital - Moscow and about our great socialist native land. To
the meeting through two years.

Pages 269-282.

No typing.